R. Malcolm Brown, Jr.
Inder M. Saxena (Eds.)

Cellulose: Molecular and Structural Biology

Selected Articles on the Synthesis, Structure, and Applications of Cellulose

Springer

Cellulose: Molecular and Structural Biology

Cellulose: Molecular and Structural Biology

Selected Articles on the Synthesis, Structure, and Applications of Cellulose

Edited by

R. Malcolm Brown, Jr. and Inder M. Saxena

The University of Texas at Austin, Austin, Texas, U.S.A

Springer

A C.I.P. Catalogue record for this book is available from the Library of Congress.

ISBN-10 1-4020-5332-0 (HB)
ISBN-13 978-1-4020-5332-0 (HB)
ISBN-10 1-4020-5380-0 (e-book)
ISBN-13 978-1-4020-5380-1 (e-book)

Published by Springer,
P.O. Box 17, 3300 AA Dordrecht, The Netherlands.

www.springer.com

Printed on acid-free paper

TABLE OF CONTENTS

PREFACE

Cellulose was first described by Anselme Payen in 1838 as a "resistant fibrous solid that remains behind after treatment of various plant tissues with acid and ammonia." In its simplest form, cellulose is composed of β-1,4-linked glucan chains that can be arranged in different ways giving rise to different forms of cellulose. In nature, cellulose is produced in a hierarchical manner with the glucan chains associating with each other to form crystalline and noncrystalline regions that are assembled into higher-order structures such as the microfibril. Depending on how the glucan chains associate, different crystalline forms of cellulose may be observed within the same microfibril. In nature, cellulose is generally obtained as the cellulose I crystalline form in which the glucan chains are aligned parallel to each other. Two forms of the native crystalline polymer, cellulose, Iα, and Iβ, have been shown to be present in differing amounts obtained from different sources. Other crystalline and noncrystalline forms of cellulose have also been identified, and many of these forms can be converted from one form to the other form by chemical or physical treatments. Although much is known about the structure and properties of the different forms of cellulose and these studies are still continuing, only recently has it been possible to understand the molecular basis of cellulose biosynthesis.

The chapters in the present volume highlight the wide range of topics that deal with not only the structure and biosynthesis of cellulose, but also some of the more exciting and novel applications of cellulose. Since the first identification of genes for cellulose biosynthesis in the bacterium *Acetobacter xylinum* in 1990, significant progress has been made in identifying similar genes in a large group of organisms. Polymerization of glucose residues into the β-1,4-linked glucan chains is catalyzed by cellulose synthase, and genes encoding this protein have been identified not only in most of the cellulose-producing organisms, but also in a number of other organisms suggesting that cellulose biosynthesis may be much more widespread than previously thought. Analyses of the cellulose-synthesizing genes and specifically the cellulose synthase genes has led to interesting views on the evolution of cellulose biosynthesis and the cellulose synthase gene family, and this is discussed in the chapters by Nobles and Brown, Roberts and Roberts, and Youngs et al. In plants, a large number of genes encoding cellulose synthases have

been identified by sequence and mutant analyses. Mutant, sequence, and expression analyses have provided information on the role of specific synthases during cellulose biosynthesis in the primary and the secondary cell wall in a number of plants. The significance of these studies is discussed in the chapters by Taylor and Turner (Arabidopsis), Barreiro and Dhugga (maize), and Blomqvist et al. (*Populus*). Whereas, the role of cellulose is well understood in plants, it is not as well understood in the other organisms where cellulose biosynthesis genes have been identified. In bacteria, cellulose is secreted as an extracellular polysaccharide, and in some cases it is shown to be associated with other components as part of bacterial biofilms. The organization of genes and regulation of cellulose biosynthesis is well understood in bacteria belonging to the pathogenic *Enterobacteriaceae*, and this is summarized by Römling.

One of the major challenges in understanding cellulose biosynthesis in plants is the biochemical characterization of the cellulose synthase. Although some success has been achieved in synthesis and characterization of cellulose *in vitro* using membrane fractions from plants, purification and structural characterization of the cellulose synthase from plants is still far from complete. In the present volume, Bulone discusses steps in the characterization of cellulose synthase and other glycosyltransferase activities. At the same time, a number of other proteins are involved in regulating cellulose synthesis in plants; Haigler covers the role of substrate supply during cellulose synthesis in the cotton fiber.

Among the more interesting aspects of cellulose biosynthesis is the phenomenon of coupled polymerization-crystallization, and it is a matter of faith in the field that the parallel arrangement of glucan chains in crystalline cellulose I result because of an organized arrangement of cellulose-synthesizing sites in the membrane. Determining how these sites are organized is a major goal for a complete understanding of cellulose biosynthesis. A perspective on how the cellulose-synthesizing complexes may be assembled in plants and the role that the membrane-bound endoglucanase (KORRIGAN) and microtubules may have in the assembly of this complex and the cellulose microfibril is discussed by Saxena and Brown. Emons *et al*. review a few hypotheses and a theory to explain the assembly of cellulose microfibrils and the architecture of the cell wall in plants. While it is not clear as to how the cellulose-synthesizing sites are assembled, these complexes are being identified in many more organisms. Okuda and Sekida report on the identification of cellulose-synthesizing complexes in a dinoflagellate and some unique algae and discuss the diversity and evolution of these complexes. Among animals, tunicates are unique in synthesizing cellulose. Cellulose-synthesizing complexes have been observed in a number of organisms within this group. The cellulose-synthesizing complexes and the function of cellulose in tunicates is described by Kimura and Itoh. Although cellulose-synthesizing complexes could be identified in membranes by freeze-fracture analysis, it was not possible to identify the components of these complexes. The breakthrough that led to the localization of cellulose synthases to these complexes in plants and associated proteins in bacteria came

about with freeze-fracture labeling of replicas using antibodies. This technique and its application with respect to understanding the composition of the cellulose-synthesizing complexes is discussed by Itoh *et al*.

The structure of cellulose is closely tied to its synthesis, and although many of the chapters discuss the synthesis of cellulose, the nature of the cellulose product is always kept in mind. A comprehensive account of the structure of cellulose and its polymorphism is provided by French and Johnson, and the structure and properties of a novel form of cellulose (nematic-ordered cellulose) is described by Kondo. Cellulose is the most abundant biomacromolecule in nature, and it is used in a variety of applications. In almost all cases, the applications of cellulose as an industrial material are dependent on its physical and chemical properties. Two chapters discuss novel applications of cellulose. Czaja *et al*. describe the use of microbial cellulose for applications in wound care and Kim discusses the usefulness of cellulose as a smart material, specifically the production of cellulose-based electroactive paper.

The field of cellulose research spans the interests of molecular biologists to industrial chemists, and we are pleased to provide this collection of articles to a broad audience with a central interest in cellulose. Cellulose has always been an important product for human endeavors, and we predict that with novel approaches in molecular and structural biology, the uses of this invaluable biomaterial will diversify and grow.

Cellulose has been used for centuries as an industrial material, but for the first time, this product is being seriously considered as an alternative source of energy for biofuels. The use of plants and other sources of cellulose for producing ethanol will change not only our perspective of how we look at cellulose as a natural product but also how it can be used to satisfy humankind's appetite for energy!

We are grateful to all the authors for their excellent contributions and their patience during the assembly of this volume.

R. Malcolm Brown, Jr. and Inder M. Saxena
August, 2006

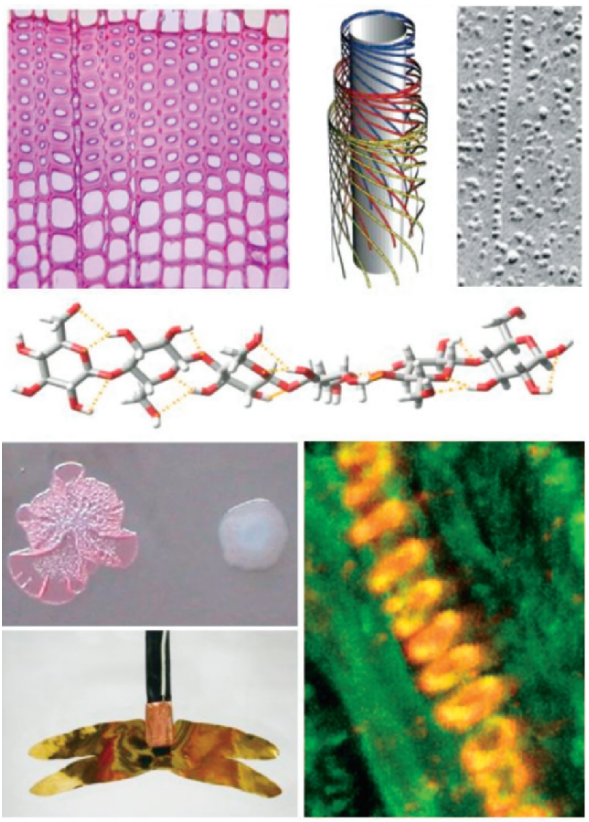

Multiple representations of cellulose (selected from chapter articles in this book)

CHAPTER 1

MANY PATHS UP THE MOUNTAIN: TRACKING THE EVOLUTION OF CELLULOSE BIOSYNTHESIS*

DAVID R. NOBLES, JR. AND R. MALCOLM BROWN, JR.**

Section of Molecular Genetics and Microbiology, The University of Texas at Austin, Austin, TX 78712

Abstract

Available evidence supports a common ancestry for all cellulose synthases. These enzymes appear to have been a bacterial invention acquired by various eukaryotes via multiple lateral gene transfers. However, the proteins associated with regulation of cellulose biosynthesis and polymer crystallization seem to have evolved independently. Sequence divergence of eukaryotic cellulose synthases and the presence of multiple gene clusters associated with bacterial cellulose synthases are discussed in relation to the possible evolutionary pathways of cellulose biosynthesis.

Keywords

bacterial cellulose, cellulose biosynthesis, cellulose synthase, cyanobacteria, lateral gene transfer, synteny.

1 INTRODUCTION

Cellulose biosynthesis is a phenomenon observed in bacteria (proteobacteria, firmicutes, and cyanobacteria) (Mühlethaler 1949; Deinema and Zevenhuizen 1971; Napoli et al. 1975; Brown, Jr. et al. 1976; Roberts 1991; Ross et al. 1991; Nobles et al. 2001; Zogaj et al. 2001, 2003; Spiers et al. 2002) and eukaryotes including plants (Glaucophyceae, Rhodophyceae, and Chlorophyceae) (Brown, Jr. 1985), animals (urochordates) (Kimura et al. 2001b), stramenopiles (Brown, Jr.

* Supported in part by grants from the Division of Energy Biosciences, Department of Energy Grant DE-FG03-94ER20145 and the Welch Foundation Grant F-1217.

** Author for correspondence: Section of Molecular Genetics and Microbiology, The University of Texas at Austin, Austin, TX 78712, Tel: 512 471-3364; Fax: 512 471-3573; e-mail: rmbrown@mail.utexas.edu

R.M. Brown, Jr. and I.M. Saxena (eds.), Cellulose: Molecular and Structural Biology, 1–15.

et al. 1969; Yamada and Miyazaki 1976) the myceteozoan *Dictyostelium discoideum* (Blanton et al. 2000), and *Acanthamoeba* spp. (Linder et al. 2002). The economical, ecological, and biological significance of cellulose production, as well as its widespread bacterial and eukaryotic distribution, have inspired a great deal of research into mechanisms of regulation and synthesis. The subject of this chapter is a much less researched area of cellulose research: specifically, the origins and evolutionary pathways of cellulose biosynthesis. In order to address this issue, it is first necessary to consider whether the trait of cellulose production among the wide range of organisms in which the process has been observed is a result of homology (similarity due to common descent) or homoplasy (similarity due to convergent evolution from independent origins).

Biosynthesis of the most common crystalline allomorph, cellulose I, requires the distinct processes of polymerization and crystallization (Benziman et al. 1980; Brett 2000; Saxena and Brown, Jr. 2005). These processes are coupled at highly ordered, membrane spanning, multienzyme terminal complexes (TCs) (Roelofsen 1958; Preston 1974). Such complexes have been observed in vascular plants (Mueller and Brown, Jr. 1980), algae (Brown, Jr. and Montezinos 1976; Giddings et al. 1980; Tsekos 1999; Schüaler et al. 2003; Okuda et al. 2004), *Gluconacetobacter xylinum* (synonym *Acetobacter xylinum*) (Zaar 1979; Kimura et al. 2001a), urochordates (Kimura et al. 2001b), and *Dictyostelium discoideum* (Grimson et al. 1996). A highly organized complex is believed to be necessary to produce the metastable parallel glucan chain orientation of the crystalline cellulose I allomorph and to prevent the biosynthesis of noncrystalline material and/or the folding of the nascent glucan chains into cellulose II – the most thermodynamically stable allomorph of cellulose (Brown, Jr. 1996).

The comparative morphology of TCs has been utilized as a tool for constructing an evolutionary history of cellulose biosynthesis of vascular plants and algae (Hotchkiss and Brown, Jr. 1988; Tsekos 1999). With regard to eukaryotic terminal complexes in general, it is not possible to know the validity of such inferences since the structural components of terminal complexes have not been identified. Although comparisons between such disparate groups as plants, stramenopiles, ascidians, and *Dictyostelium discoideum* are questionable, this methodology may have some merit when considering the evolution of eukaryotic TCs within related groups. The structural proteins comprising prokaryotic TCs are also unknown. However, the TC-associated proteins responsible for export and secretion of cellulose in bacteria with gram negative cell envelope architecture almost certainly have no relationship to their functional counterparts in eukaryotes. Therefore, the biosynthesis of cellulose I in bacteria and eukaryotes is in all likelihood a result of convergent evolution.

Polymerization of the β-1,4-glucan chain is catalyzed by cellulose synthase enzymes. All known cellulose synthases are family 2 processive glycosyltransferases, a ubiquitous family of enzymes which also includes chitin synthases, hyaluronan synthases, and NodC proteins (Saxena et al. 2001). Cellulose synthase sequences share a highly conserved catalytic region containing the D, D, D,

QXXRW (associated with regions U1, U2, U3, and U4, respectively), a motif characteristic of processive β glycosyltransferases (Saxena et al. 1995). Cellulose synthases undoubtedly share a common ancestry. Therefore, unlike the process of crystallization, synthesis of the β-1,4-glucan homopolymer in bacteria and eukaryota is a homologous process that forms an evolutionary link between all cellulose producing organisms.

2 SEQUENCE COMPARISONS

With the rapid growth of sequence databases, similarity searches such as BLAST have become integral tools for molecular biology and bioinformatics research. Although such searches are not suitable for inferring phylogenic relationships, they allow rapid identification of probable homologous sequences by utilizing pairwise alignments and give a statistical measurement of the significance of the similarity displayed by the two sequences. Pairwise alignments of cellulose synthase amino acid sequences yield interesting results. Although strong sequence similarity is displayed within related phyla (e.g., proteobacterial sequences are similar to other proteobacterial sequences and vascular plant sequences are similar to those of other vascular plants), cellulose synthases demonstrate little similarity when comparisons are made between more distantly related organisms (Blanton et al. 2000; Richmond 2000; Nobles et al. 2001). This is not necessarily surprising, as one might expect homologous sequences from *Arabidopsis thaliana* and *Escherichia coli* to display divergence. What is surprising, however, is that without exception, eukaryotic sequences display greater similarity to prokaryotic sequences than to their other eukaryotic counterparts (Table 1-1). Furthermore, in each case, the expectation values demonstrate that the similarity between eukaryotic and prokaryotic sequences is statistically significant. This is particularly noticeable in the results of pairwise sequence alignments of the

Table 1-1. Expectation values from pairwise BLAST alignments of eukaryotic and prokaryotic cellulose synthases

	IRX3	Ddis	Pram	Cint	Aory	N7120	Styp	Smel	Gxyl	Bthu
IRX3		8e-09	0.015	0.27	NSSF	***2e-28***	6e-06	0.27	0.35	0.006
Ddis	8e-09		4e-24	9e-24	2e-16	***9e-42***	2e-22	9e-19	3e-16	3e-23
Pram	0.015	4e-24		2e-13	3e-07	***3e-28***	3e-13	7e-10	3e-12	4e-14
Cint	0.27	9e-24	2e-13		7e-17	9e-33	8e-32	***9e-38***	3e-26	1e-36
Aory	NSSF	2e-16	3e-07	7e-17		2e-17	1e-19	***4e-24***	4e-20	3e-19

Results of alignments between two eukaryotic sequences are shaded. Expectations values from alignments involving bacterial sequences are unshaded. The expectation values demonstrating greatest sequence similarity are shown in bold and italicized. IRX3 – *Arabidopsis thaliana* (NP_197244.1), Ddis – *Dictyostelium discoideum* (AAF00200.1), Cint – *Ciona intestinalis* (BAD10864.1), Aory – *Aspergillis oryzae* (BAE64416.1), N7120 – *Nostoc* sp. PCC 7120 (NP_487797.1), Styp – *Salmonella typhimurium* (CAC86199.1), Smel – *Sinorhizobium meliloti* (NP_436917.1), Axyl – *Gluconacetobacter xylinus* (CAA38487.1), *Bacillus thuringiensis* serovar israelensis (ZP_00741731.1).

cellulose synthase from *Nostoc* sp. PCC 7120 with IRX3 (*A. thaliana* CesA) and the cellulose synthase from *Dictyostelium discoideum* (DcsA) in which expectation values of 2.5×10^{-20} and 2.25×10^{-18} times lower than the most similar eukaryotic sequences are obtained. Although no definite conclusions can be drawn from this data alone, it suggests that a mechanism other than vertical evolution is at work in the eukaryotic acquisition of cellulose synthesis.

3 EUKARYOTIC CELLULOSE SYNTHASES

3.1 The case for a cyanobacterial origin of plant cellulose synthases

Cellulose synthase amino acid sequences from various members of the Nostocales show striking similarity to plant cellulose synthase (CesA) and cellulose synthase-like protein (Csl) sequences (Nobles et al. 2001; Nobles and Brown, Jr. 2004). When a CesA (IRX3) from *A. thaliana* is compared with sequences from *Nostoc* sp. PCC 7120 (CcsA1), DcsA (the most similar nonplant eukaryotic sequence) and *Chloroflexus aurantiacus* J-10-fl (the most similar prokaryotic noncyanobacterial sequence), expectation values of 2e-28, 8e-09 and 7e-12 respectively, are generated. The significance of this similarity is augmented by multiple alignments of cellulose synthases which demonstrate sequence conservation within catalytic domains U1, U2, U3, and U4, but also reveal a large insertion region (first identified as the plant conserved and specific region or CR-P (Delmer 1999)) present in CesA, DcsA, and CcsA1 sequences that is absent in other prokaryotic sequences (Nobles et al. 2001; Roberts and Roberts 2004). Furthermore, protein trees generated by neighbor-joining, maximum likelihood, and maximum parsimony methods all demonstrate a sister grouping of cyanobacterial and vascular plant sequences similar to that observed with chloroplasts and cyanobacteria in 16s ribosomal trees (Olsen et al. 1994; Nobles et al. 2001; Nobles and Brown, Jr. 2004; Nakashima et al. 2004).

The primary endosymbiotic capture of an ancestral cyanobacterium, its subsequent evolution into a plastid, and concomitant transfer of genes to the host nucleus provide the most parsimonious explanation for the observed results. Gene transfers from organelles occur frequently and have had a profound effect on host genomes (Archibald et al. 2003; Huang et al. 2003). Indeed, it has been estimated that approximately 18% of the protein coding genes in *A. thaliana* are of cyanobacterial origin (Martin et al. 2002). Although xenologous transfer (lateral transfer from a free living organism) cannot be dismissed, gene transfer from the ancestral plastid (synologous transfer) seems the most probable pathway for the integration of a cyanobacterial cellulose synthase into an ancestor of vascular plants.

3.2 Lateral transfer of cellulose synthase in the urochordates

The urochordates are unique in that they are the only animals known to produce cellulose. This ability is especially curious given their position as basal chordates. In order to explain this, one must make one of three assumptions: (1) An early

diverging ancestor of animals possessed the ability to produce cellulose which was subsequently lost by all animals except the urochordates; (2) Cellulose biosynthesis in urochordates is the result of convergent evolution; or (3) The ability to produce cellulose was obtained via lateral gene transfer of one or more of the components necessary for cellulose biosynthesis. The occurrence of the scenario described by the first assumption would be extraordinary indeed! So extraordinary in fact, that it can likely be dismissed as far too improbable to occur. Furthermore, the identification of cellulose synthase sequences from *Ciona intestinalis* and *Ciona savignyi* as family 2 processive glycosyltransferases (Dehel et al. 2003) suggests that the process of synthesizing a β-1,4-glucan homopolymer by urochordates is homologous to that of other cellulose synthesizing organisms. Therefore, the second assumption is also rather unlikely. Further examination of *Ciona* cellulose synthase (Ci-CesA) sequences by BLAST alignment demonstrates that they have significantly greater similarity to cellulose synthase sequences from firmicutes, cyanobacteria, and proteobacteria than to other eukaryotic cellulose synthases. Unfortunately, differences in the expectation values generated by comparisons of Ci-CesAs with sequences from these distinct bacterial phyla are equivocal. Therefore, it is not possible to identify a likely a point of origin for Ci-CesA based on sequence similarities. To date, phylogenetic analyses have also been unable to demonstrate a clear relationship of Ci-CesAs to any group of bacterial cellulose synthases. Thus, based on analysis of the glycosyltransferase, the identity of the donor organism remains a mystery (Nobles and Brown, Jr. 2004; Nakashima et al. 2004).

However, there is another piece to the Ci-CesA puzzle. Ci-CesA sequences have a unique feature: the C-terminus displays sequence similarity to bacterial family 6 glycosylhydrolases. The glycosylhydrolase regions of *Ciona savignyi* and *Ciona intestinalis* cellulose synthases are degenerate and therefore, probably retain no enzymatic activity (Matthysse et al. 2004). While the presence of this region strengthens the case for lateral gene transfer, it poses a problem for the identification of the sequence donor(s). A gene fusion of this type is most likely to occur as a result of the simultaneous transfer of adjacent coding regions rather than from independent acquisition of sequences and subsequent fusion. Although some species of *Streptomyces* (Actinobacteria) possess gene clusters containing putative cellulose synthases and family 6 glycosylhydrolases (Nakashima et al. 2004), these sequences show comparatively little similarity to the N and C termini of Ci-CesA, respectively. Therefore, even though all available evidence indicates that urochordates acquired their cellulose synthase through lateral transfer(s) from bacteria, it is not possible to determine the phylum of origin at this time.

3.3 The cellulose synthase of *Dictyostelium discoideum*

The cellulose synthase sequence (DcsA) from *D. discoideum* is far more similar to cellulose synthase sequences from *Nostoc* spp. (CcsA1) than to any other sequences in the current databases. Additionally, DcsA branches as a sister clade to CcsA1 in protein trees (Nobles and Brown, Jr. 2004; Nakashima et al. 2004).

These observations suggest a lateral transfer of cellulose synthase from cyanobacteria to *D. discoideum*. However, while the primary and secondary endosymbiotic events that led to the evolution of plastids in plants and algae provide a clear mechanism for the transfer of a cyanobacterial cellulose synthase to photosynthetic organisms, such a mechanism is lacking for *D. discoideum*. Cyanobacterial genes are known to exist in eukaryotes which have secondarily lost plastids. However, there is no evidence for the existence of an endosymbiotic relationship between ancestors of *D. discoideum* and a cyanobacterium. Therefore, if a lateral transfer occurred, it was likely xenologous, possibly via a food ratchet mechanism (Doolittle 1998).

4 BACTERIAL GENE CLUSTERS

4.1 Introduction

A comprehensive phylogenetic analysis of bacterial cellulose synthases has not been performed to date. The few studies which include significant taxon sampling demonstrate that bacterial sequences included in cellulose synthase protein trees generally branch in a manner similar to that observed in species trees (Nobles and Brown, Jr. 2004; Nakashima et al. 2004). Unfortunately, phylogenetic studies have been unable to demonstrate the origin of cellulose synthase among the bacterial phyla (Nobles and Brown, Jr. 2004). However, the presence of cellulose synthases in firmicutes, actinobacteria, cyanobacteria, and proteobacteria indicates that the evolution of synthases cellulose likely predates the divergence of these groups.

The proliferation of complete genome sequences in public databases provides an additional means to track the evolution of cellulose in bacteria. Conservation of operons and/or gene clusters (synteny) can be used to trace not only the history of cellulose synthase, but also its associated proteins. The existence of a few these gene clusters has been well documented. In the sections below, I would like to give a brief review of the known gene organizations and introduce two novel ones which may be linked to the eukaryotic acquisition of cellulose biosynthesis.

4.2 Characterized gene clusters

Gene clusters responsible for cellulose biosynthesis have only been extensively characterized in proteobacteria. Three archetypal gene organizations encoding proteins required for the synthesis of cellulose in the α, β, and γ subdivisions have been identified. It should be emphasized that variations of these archetypes exist and as such, the examples given here are meant to serve as paradigms to simplify the discussion of the general characteristics of gene clusters associated with cellulose biosynthesis (for a comprehensive review of these gene organizations, see Römling 2002). Based on sequence conservation, the three archetypal organizations can be divided into two groups (Figure 1-1): the Group I cluster found in the α, β, and γ subdivisions, encodes a cellulose synthase – A (*bcsA*/*acsA*), as well as the B (*bcsB*/*acsB*) and C (*bcsC*/*acsC*) proteins within an

operon (Saxena et al. 1994; Zogaj et al. 2001). Additionally, a family 8 glycosylhydrolase, is encoded within or in close proximity to the cellulose synthase operon (Römling 2002). The Group II gene cluster is characteristically found in the α-Proteobacteria and has been most extensively studied in *Agrobacterium tumefaciens*. This organization consists of two adjacent directionally opposed operons. The first operon – *celABC* encodes homologs of the Group I *bcsA*/*acsA* (*celA*), *bcsB*/*acsB* (*celB*), and family 8 glycosyl hydrolase (*celC*). The second operon – *celDE* encodes proteins with no significant sequence similarity to the Group I proteins (Matthysse et al. 1995b). It should be noted however, that *celD* and *bcsC*/*acsC* share two conserved domains: COG3118 (thioredoxin containing proteins responsible for posttranslational modifications and protein turnover) and COG4783 (putative Zn-dependent proteases containing TPR repeats) (Marchler-Bauer et al. 2005) suggesting the possibility of a similar function.

Although all proteins encoded by Group I and II gene clusters are necessary for wild-type cellulose biosynthesis, only cellulose synthases have a known function.[1]

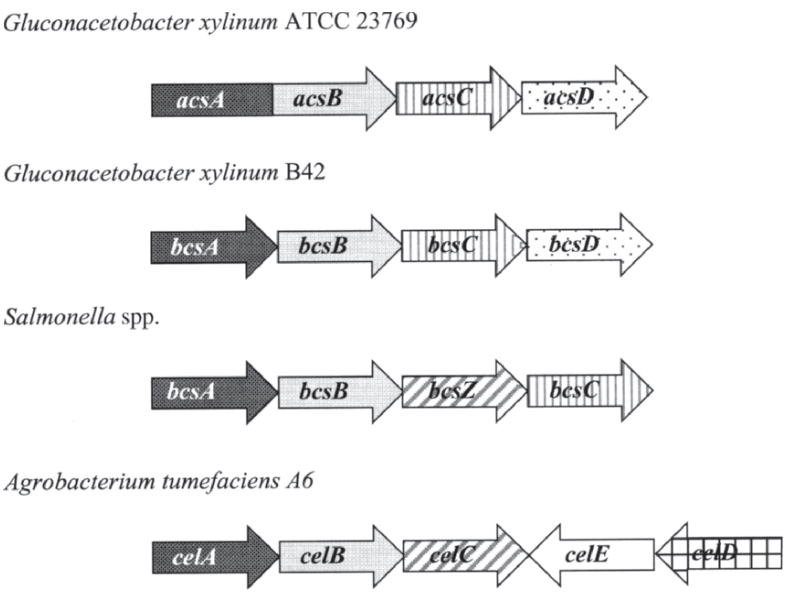

Figure 1-1. Characterized cellulose biosynthesis gene clusters of Group I (*Gluconacetobacter xylinum* ATCC 23769, *G. xylinum* B42, and *Salmonella* spp.) and Group II (*Agrobacterium tumefaciens* A6). Identical shades and patterns represent homologous sequences. Open reading frames are not drawn to scale. Note that *acsAB* comprises a single open reading frame in *G. xylinum* ATCC 23769 (synonym AY201). Although not shown here, fusions of *acsAB* are also observed in the cellulose synthesis operons of *G. xylinum* ATCC 53582 (synonym NQ5) (Saxena et al. 1994) and *Azotobacter vinelandii* AvOP

[1] Previous research suggested that AcsB/BcsB had the ability to bind c-di-GMP which led to a general consensus that the B subunit had a regulatory function in cellulose biosynthesis (Amikam and Benziman 1989; Mayer et al. 1991). However, based on recent data, a regulatory role for AcsB/BcsB is questionable (Amikam and Galperin 2006).

Organisms with the Group I gene organization are believed to carry out cellulose biosynthesis without the use of lipid-linked intermediates in a process which is upregulated by the allosteric activator cyclic diguanosine monophosphate (c-di-GMP) (Aloni et al. 1982; Ross et al. 1986; Saxena et al. 1994; Römling 2002; García et al. 2004). In the case of bacteria with Group II gene organizations, the presence of lipid linked intermediates and regulation by c-di-GMP are matters of some debate (Amikam and Benziman 1989; Matthysse et al. 1995a; Ausmees et al. 2001). Despite clear differences between the gene clusters of Groups I and II, the universal presence of a family 8 glycosylhydrolase and the positioning of the *acsB*/*bcsB*/*celB* genes adjacent to cellulose synthases suggests a common ancestry for these gene clusters and important roles for these proteins that transcend possible differences in mechanisms of synthesis.

5 NOVEL GENE CLUSTERS

5.1 Introduction

Although cellulose synthase sequences within closely related bacterial groups (e.g., within γ-proteobacteria or actinobacteria) generally display relatively high sequence conservation, they are often divergent when compared across phyla. Examination of sequenced genomes reveals the presence of alternative gene clusters that coincide with the sequence divergence of various groups of cellulose synthases. Such novel gene organizations exist in cyanobacteria, actinobacteria, chloroflexales, as well as proteobacteria and, unlike the Group I and II gene clusters described above, gene organizations are conserved across phyla. The characterization of novel gene organizations has the potential to inform current knowledge of the components necessary for cellulose biosynthesis, broaden our definitions of what constitutes cellulose, and ultimately provide a map of routes taken by organisms to utilize the β-1,4-homopolymer.

5.2 Group III

The Group III gene cluster is found in orders chroococales and nostocales of cyanobacteria and in the α and β subdivisions of proteobacteria. These clusters have not been experimentally shown to be responsible for cellulose biosynthesis and therefore, the designation of these glycosyltransferases as cellulose synthases is a putative one. Group III gene clusters encode a membrane fusion protein (MFP) of the AcrA/EmrA/HylD family adjacent and upstream of the cellulose synthase (Figure 1-2). This organization suggests the possibility of a three component system consisting of the cellulose synthase, a MFP, and an outer membrane protein OMP. In such a system, the cellulose synthase would be linked to an OMP pore by the membrane-bound periplasmic MFP and thus, form a continuous channel for export and secretion of the glucan polymer. Alternatively, some Group III clusters contain genes encoding ATP binding

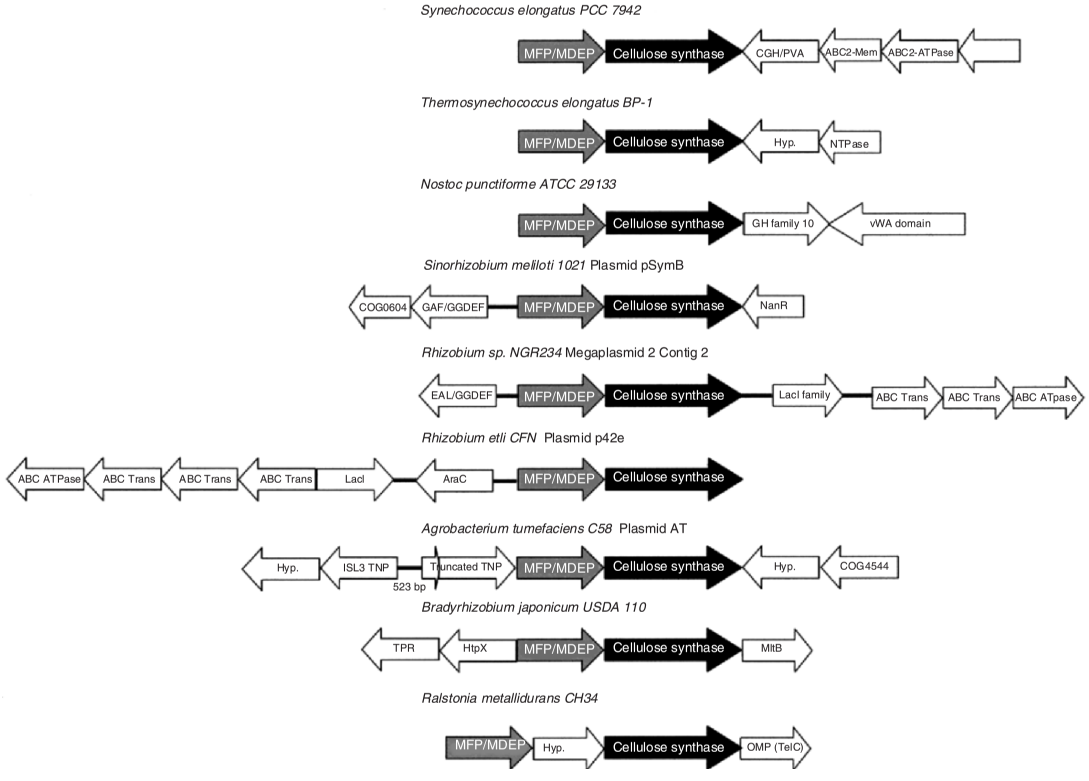

Figure 1-2. Group III gene clusters. MFP/MDEP–Membrane fusion protein/Multidrug efflux pump, CGH–Chololylglycine hydrolase, PIN–Nucleotide binding domain, GH–Glycosylhydrolase, vWA–von Willibrand factor, GGDEF–Diguanylate cyclase, NanR–NanR family transcriptional repressor, LacI–LacI family transcriptional repressor, AraC–AraC family transcriptional regulator, TNP–Transposase, TPR–TPR repeat region, HtpX – Heat shock protein, MltB–Lytic murein transglycosylase, Hyp.–Hypothetical protein, OMP–Outer membrane protein. The regions depicted here are not drawn to scale

cassette (ABC) transporter domains. This type of organization is characteristic of the bacterial ABC capsular polysaccharide exporter family (CPSE) in which secretion of polysaccharides is accomplished via the concerted actions of an ABC transporter, a membrane periplasmic auxiliary protein (MPA2 – analogous to the MFP associated with Type I bacterial secretion), an outer membrane auxiliary protein (OMA), and an as yet unidentified, outer membrane protein (OMP) (Silver et al. 2001). It is important to note that although the arrangement of bacterial genes in clusters is often indicative of components of a common pathway or mechanism (Korbel et al. 2004; Guerrero et al. 2005); this is by no means universally true. As such, in the absence of experimental data, any functional designation based on sequence organization must be considered speculative.

Although the presence of this gene organization in cyanobacteria and proteobacteria may indicate retention of key synthesis components from a common ancestor, lateral gene transfer cannot be ruled out. This is particularly true in the instances of *Rhizobium etli* CFN, *Rhizobium* sp. NGR234, and *A. tumefaciens* C58 where the Group III cluster is located on megaplasmids. Megaplasmids of the Rhizobiales have a significant propensity for recombination and transposition (Streit et al. 2004; Guerrero et al. 2005). Consequently, the sequences of these replicons are mosaic in nature – frequently shaped by lateral gene transfer (González et al. 2003).

In addition to the Group III gene cluster, the linear chromosome of *A. tumefaciens* C58 encodes a functional Group II gene cluster (Matthysse et al. 2005). The pNGR234 megaplasmid of *Rhizobium* sp. NGR234 also encodes an additional cellulose synthase (Streit et al. 2004) with significant similarity to the Group II cellulose synthase of *A. tumefaciens* C58 but does not possess the other conserved regions of the Group II cluster. The lack of sequence similarity between Group II and III cellulose synthases indicates that they are unlikely to be the products of gene duplication within these organisms. Rather, significant similarity with *Nostoc punctiforme* ATCC 29133 and *Synechococcus elongatus* PCC 7942 Group III cellulose synthase sequences (expectation values of 2e-56 – 1e-89 lower respectively, than observed when Group II and III sequences within the same organism are compared) indicates a possible lateral gene transfer.

5.3 Group IV

The Group IV gene cluster, found in nostocales, actinobacteria, and chloroflexales, encodes a cellulose synthase, an antisigma factor antagonist, and an antisigma factor. With the exception of those found in the chloroflexales, all Group IV clusters identified also contain an antisigma factor antagonist phophatase (Figure 1-3). The ancillary proteins surrounding the cellulose synthases in this group are homologous to SpoIIAA (antisigma factor antagonist), SpoIIAB (antisigma factor), and SpoIIE (antisigma factor antagonist phophatase) present in the regulatory clusters involved in the stage II sporulation of *Bacillus subtilis*.

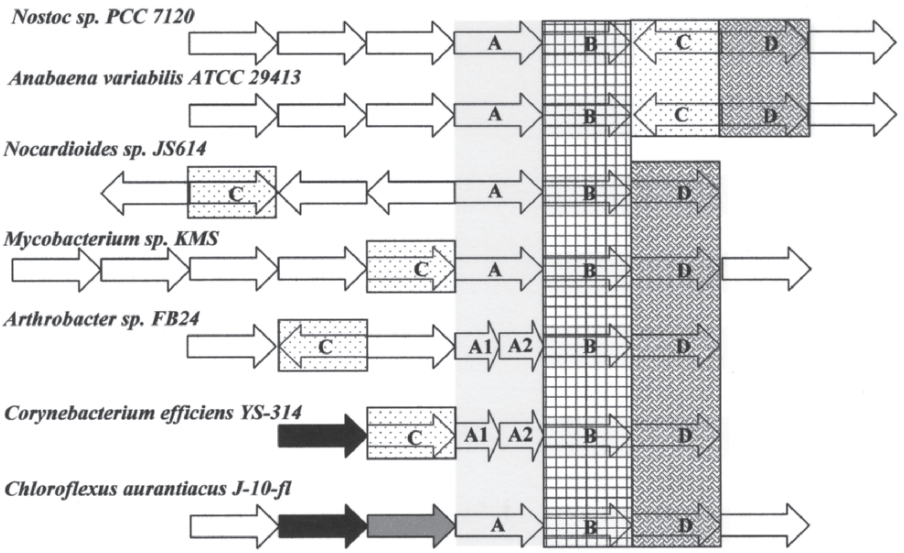

Figure 1-3. Group IV gene clusters shared by Nostocales, Actinobacteria, and Chloroflexales. **A** – Cellulose synthases or putative cellulose synthases, **B** – Antisigma factor antagonist, **C** – Sigma factor phosphatase, **D** – Antisigma factor regulation. Black arrows indicate putative diguanylate cyclases and gray arrow indicates bcsB homolog. The regions represented here are not drawn to scale

This regulatory system acts to confine gene transcription to the prespore during asymmetric cell division (Stragier and Losick 1996; Yudkin and Clarkson 2005). The presence of these regulatory components in close association with cellulose synthases may indicate controlled expression of cellulose synthase biosynthesis in differentiated cells during asymmetric cell division in the actinobacteria (spores) and nostocales (heterocysts and/or akinetes). With regard to this possibility in the heterocysts of the nostocales, it is interesting to note the existence of alternative sigma factors which are expressed only under nitrogen limiting conditions (Brahamsha and Haselkorn 1992).

The presence of syntenic genes in cyanobacteria and actinobacteria is consistent with phylogenetic trees demonstrating a close relationship of cyanobacteria and actinobacteria (Olsen et al. 1994; Yu et al. 2005). Interestingly, the organization of the gene cluster of *C. aurantiacus* is a chimera which contains elements of the Group IV gene cluster combined with a BcsB homolog and a diguanylate cyclase. Since the chloroflexales are generally considered to have branched prior to the divergence of cyanobacteria, gram positive bacteria, and proteobacteria (Olsen et al. 1994), this organization could represent the prototypical organization for Groups I, II, and IV. However, since *C. aurantiacus* exists primarily as a photoheterotroph living in close association with cyanobacteria, the possibility of lateral gene transfer from a cyanobacterium to members of the chloroflexales cannot be discounted.

The cellulose synthase sequences of *Arthrobacter* sp. FB24 and *Corynebacterium efficiens* YS-314 are divided into two open reading frames: the first containing domain A (U1 and U2) and the second containing domain B (U3 and U4). There is no report of cellulose biosynthesis in these bacteria and therefore, it is unknown whether this split enzyme is functional. However, if the products of these two ORFs can combine to create a functional cellulose synthase, they would be useful tools for experiments to determine substrate binding properties and catalytic function of the conserved domains.

6 CONCLUDING REMARKS

Current data suggest that cellulose biosynthesis is a bacterial invention and that eukaryotes acquired the process via multiple lateral gene transfers. Bacteria and eukaryota have independently evolved regulatory mechanisms and molecular structures to utilize the β-1,4-homopolymer synthesized by the catalytic activity of homologous cellulose synthase enzymes. The differences in accessory enzymes probably reflect not only convergent evolution to produce a cellulose I crystalline allomorph, but also inventions of alternative products such as cellulose II, noncrystalline cellulose, or nematic ordered cellulose.

As sequence databases continue to grow, it is certain that new cellulose synthase sequences and gene clusters will be identified. To be sure, increasing the library of available sequences is essential to the development of our understanding of the origin of cellulose biosynthesis and the evolutionary pathways utilized for its distribution. However, the primary challenges for researchers will be to elucidate the function of cellulose synthase associated enzymes and to characterize the cellulosic products synthesized by organisms with disparate enzymes and gene organizations. Without a firm grasp of the relationship of synthesizing components to the characteristics of the cellulosic product, we cannot hope to understand the genesis of the varied mechanisms and product morphologies we discover nor the evolutionary context from which they arose.

REFERENCES

Aloni Y., Delmer D.P., and Benziman M. 1982. Achievement of high rates of *in vitro* synthesis of 1, 4-beta-D-glucan: activation by cooperative interaction of the *Acetobacter xylinum* enzyme system with GTP, polyethylene glycol, and a protein factor. Proc Natl Acad Sci USA 79(21):6448–6452.

Amikam D. and Benziman M. 1989. Cyclic diguanylic acid and cellulose synthesis in *Agrobacterium tumefaciens*. J Bacteriol 171(12):6649–6655.

Amikam D. and Galperin M.Y. 2006. PilZ domain is part of the bacterial c-di-GMP binding protein. Bioinformatics 22(1):3–6.

Archibald J.M., Rogers M.B., Toop M., Ishida K., and Keeling P. 2003. Lateral gene transfer and the evolution of plastid targeted proteins in the secondary plastid-containing alga *Bigelowiella natans*. PNAS 100(13):7678–7683.

Ausmees N., Mayer R., Weinhouse H., Volman G., Amikam D., Benziman M., and Lindberg M. 2001. Genetic data indicate that proteins containing the GGDEF domain possess diguanylate cyclase activity. FEMS Microbiol Lett 204:163–167.

Benziman M., Haigler C.H., Brown, Jr. R.M., White A.R., and Cooper K.M. 1980. Cellulose biogenesis: polymerization and crystallization are coupled processes in *Acetobacter xylinum*. PNAS USA 77:6678–6682.

Blanton R.L., Fuller D., Iranfar N., Grimson M.J., and Loomis W.F. 2000. The cellulose synthase gene of *Dictyostelium*. Proc Natl Acad Sci USA 97:2391–2396.

Brahamsha B. and Haselkorn R. 1992. Identification of multiple RNA polymerase sigma factor homologs in the cyanobacterium *Anabaena* sp. strain PCC 7120: cloning, expression, and inactivation of the sigB and sigC genes. J Bacteriol 173(8):2442–50.

Brett C.T. 2000. Cellulose microfibrils in plants: biosynthesis, deposition, and integration into the cell wall. Int Rev Cytol 199:161–99.

Brown, Jr. R.M. 1985. Cellulose microfibril assembly and orientation: recent developments. J Cell Sci Suppl 2:13–32.

Brown, Jr. R.M., Franke W.W., Kleinig H., Falk H., and Sitte P. 1969. A cellulosic wall component produced by the golgi apparatus. Science 166:894–896.

Brown, Jr. R.M. 1996. The biosynthesis of cellulose. Pure Appl Chem 10:1345–1373.

Brown, Jr. R.M. and Montezinos D. 1976. Cellulose microfibrils: visualization of biosynthetic and orienting complexes in association with the plasma membrane. Proc Natl Acad Sci USA 73:143–147.

Brown, Jr. R.M., Willison J.H.M., and Richardson C.L. 1976. Cellulose biosynthesis in *Acetobacter xylinum*: 1. Visualization of the site of synthesis and direct measurement of the *in vivo* process. Proc Natl Acad Sci USA 73(12):4565–4569.

Dehal P., Satou Y., Campbell R.K., Chapman J., Degnan B., De Tomaso A., Davidson B., Di Gregorio A., Gelpke M., Goodstein D.M., Harafuji N., Hastings K.E., Ho I., Hotta K., Huang W., Kawashima T., Lemaire P., Martinez D., Meinertzhagen I.A., Necula S., Nonaka M., Putnam N., Rash S., Saiga H., Satake M., Terry A., Yamada L., Wang H.G., Awazu S., Azumi K., Boore J., Branno M., Chin-Bow S., DeSantis R., Doyle S., Francino P., Keys D.N., Haga S., Hayashi H., Hino K., Imai K.S., Inaba K., Kano S., Kobayashi K., Kobayashi M., Lee B.I., Makabe K.W., Manohar C., Matassi G., Medina M., Mochizuki Y., Mount S., Morishita T., Miura S., Nakayama A., Nishizaka S., Nomoto H., Ohta F., Oishi K., Rigoutsos I., Sano M., Sasaki A., Sasakura Y., Shoguchi E., Shin-i T., Spagnuolo A., Stainier D., Suzuki M.M., Tassy O., Takatori N., Tokuoka M., Yagi K., Yoshizaki F., Wada S., Zhang C., Hyatt P.D., Larimer F., Detter C., Doggett N., Glavina T., Hawkins T., Richardson P., Lucas S., Kohara Y., Levine M., Satoh N., and Rokhsar D.S. 2003. The draft genome of *Ciona intestinalis*: insights into chordate and vertebrate origins. Science 298:2157–2167.

Deinema M.H. and Zevenhuizen L.P. 1971. Formation of cellulose fibrils by gram-negative bacteria and their role in bacterial flocculation. Arch Mikrobiol 78(1):42–51.

Delmer D.P. 1999. Cellulose biosynthesis: exciting times for a difficult field of study. Annu Rev Plant Phys Plant Mol Biol 50:245–276.

Doolittle W. 1998. You are what you eat: a gene transfer ratchet could account for bacterial genes in eukaryotic nuclear genomes. Trends Genet 14:307–311.

García B., Latasa C., Solano C., García-del Portillo F., Gamazo C., and Lasa I. 2004. Role of the GGDEF protein family in *Salmonella* cellulose biosynthesis and biofilm formation. Mol Microbiol 54(1):264–277.

Giddings J.R. TH, Brower D.L., and Staehelin L.A. 1980. Visualization of particle complexes in the plasma membrane of *Micrasterias denticulata* associated with the formation of cellulose fibrils in primary and secondary cell walls. J Cell Biol 84 (2):327–339.

González V., Bustos P., Ramirez-Romero M.A., Medrano-Soto A., Salgado H., Hernandez-Gonzalez I., Hernandez-Celis J.C., Quintero V., Moreno-Hagelsieb G., Girard L., Rodriguez O., Flores M., Cevallos M.A., Collado-Vides J., Romero D., and Davila G. 2003. The mosaic structure of the symbiotic plasmid of *Rhizobium etli* CFN42 and its relation to other symbiotic genome compartments. Genome Biol 4(6):R36.

Grimson M.J., Haigler C.H., and Blanton R.L. 1996. Cellulose microfibrils, cell motility, and plasma membrane protein organization change in parallel during culmination in *Dictyostelium discoideum*. J Cell Sci 109 (Pt 13):3079–3087.

Guerrero G., Peralta H., Aguilar A., Diaz R., Villalobos M.A., Medrano-Soto A. and Mora J. 2005. Evolutionary, structural and functional relationships revealed by comparative analysis of syntenic genes in *Rhizobiales*. BMC Evol Biol 5:55.

Hotchkiss A.T. and Brown, Jr. R.M., 1988. Evolution of the cellulosic cell wall in the *Charophyceae*. In: Schuerch C. (ed.) Cellulose and Wood – Chemistry and Technology. . Wiley, New York, pp. 591–609.

Huang C.Y., Ayliffe M.A., and Timmis J.N. 2003. Direct measurement of the transfer rate of chloroplast DNA into the nucleus. Nature 422:72–76.

Kimura S., Chen H.P., Saxena I.M., Brown, Jr. R.M., and Itoh T. 2001a. Localization of c-di-GMP-binding protein with the linear terminal complexes of *Acetobacter xylinum*. J Bacteriol 183(19):5668–74.

Kimura S., Ohshima C., Hirose E., Nishikawa J., and Itoh T. 2001b. Cellulose in the house of the appendicularian *Oikopleura rufescens*. Protoplasma 216(1–2):71–74.

Korbel J.O., Jensen L.J., von Mering C., and Bork P. 2004. Analysis of genomic context: prediction of functional associations from conserved bidirectionally transcribed gene pairs. Nat Biotechnol 22(7):911–917.

Linder M., Winiecka-Krusnell J., and Linder E. 2002. Use of recombinant cellulose-binding domains of *Trichoderma reesei* cellulase as a selective immunocytochemical marker for cellulose in protozoa. Appl Environ Microbiol.

Marchler-Bauer A., Anderson J.B., Cherukuri P.F., DeWeese-Scott C., Geer L.Y., Gwadz M., He S., Hurwitz D.I., Jackson J.D., Ke Z., Lanczycki C.J., Liebert C.A., Liu C., Lu F., Marchler G.H., Mullokandov M., Shoemaker B.A., Simonyan V., Song J.S., Thiessen P.A., Yamashita R.A., Yin J.J., Zhang D., and Bryant S.H. 2005. CDD: a Conserved Domain Database for protein classification. Nucleic Acids Res 33:D192–D196.

Martin W., Rujan T., Richly E., Hansen A., Cornelsen S., Lins T., Leister D., Stoebe B., Hasegawa M., and Penny D. 2002. Evolutionary anaylsis of *Arabidopsis*, cyanobacterial, and chloroplast genomes reveals plastid phylogeny and thousands of cyanobacterial genes in the nucleus. PNAS 99(19):12246–12251.

Matthysse A.G., Deschet K., Williams M., Marry M., White A.R., and Smith W.C. 2004. A functional cellulose synthase from ascidian epidermis. Proc Natl Acad Sci USA 101(4):986–991.

Matthysse A.G., Marry M., Krall L., Kaye M., Ramey B.E., Fuqua C., and White A.R. 2005. The effect of cellulose overproduction on binding and biofilm formation on roots by *Agrobacterium tumefaciens*. Mol Plant Microbe Interact 18(9):1002–1010.

Matthysse A.G., Thomas D.L., and White A.R. 1995a. Mechanism of cellulose synthesis in *Agrobacterium tumefaciens*. J Bacteriol 177(4):1076–1081.

Matthysse A.G., White S., and Lightfoot R. 1995b. Genes required for cellulose synthesis in *Agrobacterium tumefaciens*. J Bacteriol 177(4):1069–1075.

Mayer R., Ross P., Weinhouse H., Amikam D., Volman G., Ohana P., Calhoon R.D., Wong H.C., Emerick A.W., and Benziman M. 1991. Polypeptide composition of bacterial cyclic diguanylic acid-dependent cellulose synthase and the occurrence of immunologically crossreacting proteins in higher plants. Proc Natl Acad Sci USA 88(12):5472–5476.

Mueller S.C. and Brown, Jr. R.M. 1980. Evidence for an intramembrane componentassociated with a cellulose microfibril synthesizing complex in higher plants. J Cell Biol 84:315–326.

Mühlethaler K. 1949. The structure of bacterial cellulose. Biochim Biophys Acta 3:527–535.

Nakashima K., Yamanda L., Satou Y., Azuma J., and Satoh N. 2004. The evolutionary origin of animal cellulose synthase. Dev Genes Evol 214(2):81–88.

Napoli C., Dazzo F., and Hubbell D. 1975. Production of cellulose microfibrils by *Rhizobium*. Appl Microbiol 30(1):123–31.

Nobles D.R., Jr. and Brown, Jr. R.M., Jr. 2004. The pivotal role of cyanobacteria in the evolution of cellulose synthases and cellulose synthase-like proteins. Cellulose 11:437–448.

Nobles D.R., Romanovicz D.K., and Brown, Jr. R.M., Jr. 2001. Cellulose in cyanobacteria. Origin of vascular plant cellulose synthase? Plant Physiol 127(2):529–542.

Okuda K.O., Sekida S., Yoshinaga S. and Suetomo Y. 2004. Cellulose synthesizing complexes in some chromophyte algae. Cellulose 11:365–376.

Olsen G.J., Woese C.R., and Overbeek R. 1994. The winds of (evolutionary) change: breathing new life into microbiology. J Bacteriol 176:1–6.

Preston R.D. 1974. Cellulose. In: The Physical Biology of Plant Cell Walls. Chapman & Hall, London, pp. 444–456.

Richmond T. 2000. Higher plant cellulose synthases. Genome Biology 1(4): reviews 3001.1–3001.6.

Roberts A.W. and Roberts E.M. 2004. Cellulose synthase (CesA) genes in algae and seedless plants. Cellulose 11:419–435.

Roberts E. 1991. Biosynthesis of cellulose II and related carbohydrates. PhD thesis. The Univeristy of Texas at Austin, Austin.

Roelofsen P.A. 1958. Cell wall structure as related to surface growth. Acta Botanica Neerlandica 7:77–89.

Römling U. (2002). Molecular biology of cellulose production in bacteria. Res Microbiol 153:205–212.

Ross P., Aloni Y., Weinhouse H., Michaeli D., Weinberger-Ohana P., Mayer R., and Benziman M. 1986. Control of cellulose synthesis in *Acetobacter xylinum*: a unique guanyl ologonucleotide is the immediate activator of the cellulose synthase. Carbohydrate Res 149:101–117.

Ross P., Mayer R., and Benziman M. 1991. Cellulose biosynthesis and function in bacteria. Microbiol Rev 55:35–58.

Saxena I.M. and Brown, Jr. R.M., 2005. Cellulose biosynthesis: current views and evolving concepts. Ann Bot (Lond) 96(1):9–21.

Saxena I.M., Brown, Jr. R.M., and Dandekar T. 2001. Structure-function characterization of cellulose synthase: relationship to other glycosyltransferases. Phytochemistry 57:1135–1148.

Saxena I.M., Brown, Jr. R.M., Fevre M., Geremia R., and Henrissat B. 1995. Multidomain architecture of beta-glycosyl transferases: implications for mechanism of action. J Bacteriol 177:1419–24.

Saxena I.M., Kudlicka K., Okuda K., and Brown, Jr. R.M. 1994. Characterization of genes in the cellulose synthesizing operon (acs operon) of *Acetobacter xylinum*: implications for cellulose crystallization. J Bacteriol 176:5735–5752.

Schüßler A., Hirn S. and Katsaros C. 2003. Cellulose synthesizing terminal complexes and morphogenesis in tip-growing of *Syringoderma phinneyi* (Phaeophyceae). Phycol Res 51:35–44.

Silver R.P., Prior K., Nsahlai C., and Wright L.F. 2001. ABC transporters and the export of capsular polysaccharides from gram-negative bacteria. Res Microbiol 152(3–4):357–364.

Spiers J., Kahn G., Bohannon J., Travisano M. and Rainey P.B. 2002. Adaptive divergence in experimental populations of *Pseudomonas fluorescens*. I. Genetic and phenotypic bases of wrinkly spreader fitness. Genetics 161:33–46.

Stragier P. and Losick R. 1996. Molecular genetics of sporulation in *Bacillus subtilis*. Annu Rev Genet 30:297–341.

Streit W.R., Schmitz R.A., Perret X., Staehelin C., Deakin W.J., Raasch C., Liesegang H., and Broughton W.J. 2004. An evolutionary hot spot: the pNGR234b replicon of *Rhizobium* sp. strain NGR234. J Bacteriol 186(2):535–542.

Tsekos I. 1999. The sites of cellulose synthesis in algae: diversity and evolution of cellulose-synthesizing enzyme complexes. J Phycol 35:625–655.

Yamada M. and Miyazaki T. 1976. Ultrastructure and chemical analysis of the cell wall of *Pythium debaryanum*. Jpn J Microbiol 20(2):83–91.

Yu Z.G., Zhou L.Q., Anh V.V., Chu K.H., Long S.C., and Deng J.Q. 2005. Phylogeny of prokaryotes and chloroplasts revealed by a simple composition approach on all protein sequences from complete genomes without sequence alignment. J Mol Evol 60(4):538–545.

Yudkin M.D. and Clarkson J. 2005. Differential gene expression in genetically identical sister cells: the initiation of sporulation in *Bacillus subtilis*. Mol Microbiol 56(3):578–589.

Zaar K. 1979. Visualization of pores (export sites) correlated with cellulose production in the envelope of the gram-negative bacterium *Acetobacter xylinum*.J Cell Biol 80(3):773–777.

Zogaj X., Bokranz W., Nimtz M., and Romling U. 2003. Production of cellulose and curli fimbrieae by members of the family *Enterobacteriaceae* isolated from the human gastrointestinal tract. Infect Immun 71(7):4151–4158.

Zogaj X., Nimtz M., Rohde M., Bokranz W., and Romling U. 2001. The multicellular morphotypes of *Salmonella typhimurium* and *Escherichia coli* produce cellulose as the second component of the extracellular matrix. Mol Microbiol 39:1452–1463.

CHAPTER 2

EVOLUTION OF THE CELLULOSE SYNTHASE (*CesA*) GENE FAMILY: INSIGHTS FROM GREEN ALGAE AND SEEDLESS PLANTS

ALISON W. ROBERTS[1]* AND ERIC ROBERTS[2]

[1]Department of Biological Sciences, University of Rhode Island; [2]Department of Biology, Rhode Island College, Providence, RI 02908-1991

Abstract

The structure of cellulose microfibrils has been correlated with the organization of the arrays of integral plasma membrane protein particles that synthesize them. These "terminal complexes" (TCs) are composed in part of cellulose synthase catalytic subunits (CesAs), which not only catalyze the polymerization of glucan chains, but also play a role in TC assembly. The catalytic domains of CesA proteins from prokaryotes and eukaryotes are conserved. However, differences in CesA structure between plants and bacteria presumably contribute to variation in TC and microfibril structure between these organisms. The genetic basis for this variation may be revealed by examining the *CesA* genes of green algae, a group of related organisms that nonetheless have different types of TCs. Vascular plants and their closest green algal relatives share rosette TCs and highly similar *CesA*s. This demonstrates a congruence of TC and CesA structure over deep time and provides a basis for analyzing the *CesA* genes of green algae with different types of TCs.

In seed plants, the members of large *CesA* gene families are differentially expressed during primary and secondary cell wall deposition, particularly in vascular tissue. Phylogenetic analysis of the *CesA* gene families from vascular plants and the nonvascular plant *Physcomitrella patens* is consistent with independent *CesA* diversification in the moss and vascular plant lineages. Characterization of *CesA* genes from *P. patens*, which is uniquely suited for targeted mutagenesis and analysis of TC structure by freeze-fracture electron microscopy, also provides a convenient model to manipulate and test the functions of domains potentially involved in TC assembly.

* Author for correspondence: Department of Biological Sciences, University of Rhode Island, Kingston, RI 02881; Tel: (401) 874-4098; Fax: (401) 874-5974; e-mail: aroberts@uri.edu

R.M. Brown, Jr. and I.M. Saxena (eds.), Cellulose: Molecular and Structural Biology, 17–34.

Keywords

algae, bryophytes, cellulose, cellulose synthase (CesA), cellulose-synthase like (Csl), moss, fern, *Mesotaenium caldariorum*, microfibril, *Physcomitrella patens*, terminal complex, vascular evolution.

Abbreviations

fluorescence resonance energy transfer (FRET), terminal complex (TC).

1 OVERVIEW

Cellulose microfibrils are remarkable in their structure, their mechanical properties, and their mechanism of synthesis. Composed of bundles of β-1,4-glucan chains, microfibrils range in diameter from about 3 nm in the primary cell walls of seed plants to 25 nm in some algae (Brown, Jr. 1985; Delmer 1987; Giddings and Staehelin 1991). Hydrogen bonding between the glucan chains that compose cellulose microfibrils results in a density-specific tensile strength exceeding that of many natural and manmade fibers (Niklas 1992). Cellulose is synthesized by integral plasma membrane protein complexes so labile that the most successful methods for producing cellulose *in vitro* yield only small quantities of short fibrils and this only when isolated plasma membrane vesicles remain intact (Lai-Kee-Him et al. 2002). Based on their distinctive hexagonal arrangement as visualized by freeze fracture electron microscopy, the complexes from land plants and some algae are known as "rosettes." However, the more general term for them is "terminal complex" (TC) reflecting their locations at the ends of microfibrils and the variety in their morphology among various cellulose-producing organisms (Figure 2-1).

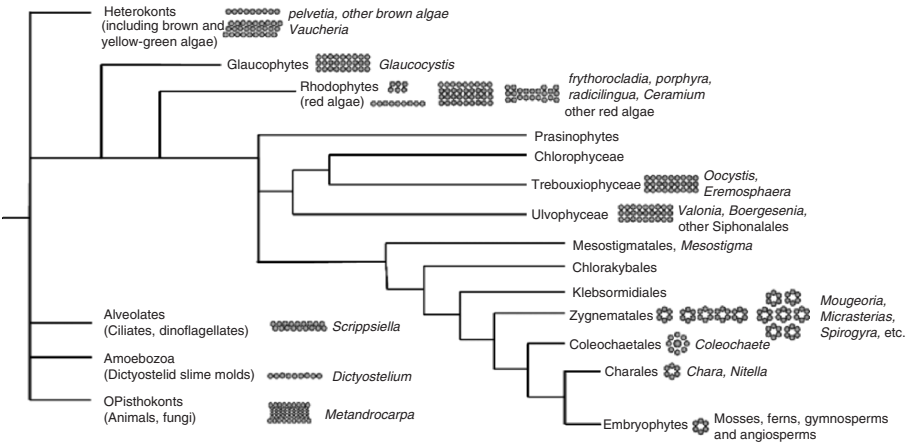

Figure 2-1. Phylogeny of plants and algae (based on the Tree of Life website; http://phylogeny.arizona.edu) showing representative terminal complex type (Tsekos 1999). Not all taxa or terminal complex types are shown. Branch lengths are arbitrary

Terminal complexes function as "nanospinnerets," moving in the plane of the plasma membrane as they extrude microfibrils across the cell surface (Montezinos 1982). Terminal complexes are thought to facilitate two distinct stages of cellulose synthesis: (1) polymerization of glucan chains and (2) assembly of those chains into microfibrils (Haigler et al. 1980; Haigler 1991; Saxena and Brown, Jr. 2005). The microfibrillar structure of commercial cellulose, nearly all of which is derived from a few species of seed plants, is relatively uniform (Delmer 1999). Other organisms, notably algae, produce cellulose in a variety of forms including thick microfibrils up to 25 nm in diameter (Sugiyama et al. 1985), flat ribbons of various dimensions (Tsekos 1999), and nonmicrofibrillar rodlets (Roberts 1991). Correlation between microfibril cross-sectional dimensions and TC morphology support the hypothesis that the structure of a microfibril is determined by the organization of the TC that synthesizes it (Giddings et al. 1980; Herth 1983; Itoh et al. 1984; Brown, Jr. 1985; Delmer 1987; Hotchkiss 1989; Tsekos 1999). For example, rosette TCs produce 3 nm microfibrils composed of 36 glucan chains (Herth 1983). In contrast, the larger TCs of the green alga *Valonia macrophysa* (Itoh and Brown, Jr. 1984; Itoh 1990) produce 25 nm microfibrils composed of up to 1,400 glucan chains (Sugiyama et al. 1985) and the long, narrow TCs of the cellulose-producing bacterium *Acetobacter xylinus* synthesize flat ribbons of cellulose up to 100 nm wide (Brown, Jr. et al. 1976). Furthermore, mutations and specific chemical agents that disrupt terminal complexes block microfibril assembly, leading to accumulation of amorphous glucan (Arioli et al. 1998; Peng et al. 2001; Lai-Kee-Him et al. 2002; Kiedaisch et al. 2003). Although TC morphology is an important determinant of microfibril properties (Tsekos 1999), the mechanisms underlying TC assembly and morphogenesis remain unknown.

Genes that encode the catalytic subunits of cellulose synthase (designated *CesA*, see Delmer 1999) carry the D,D,D,QXXRW signature motif, which is characteristic of processive β-glycosyl transferases (Saxena et al. 1995). First discovered in *A. xylinus* (Saxena et al. 1990; Wong et al. 1990), *CesA*s were later identified in cotton (Pear et al. 1996) and characterized functionally in *Arabidopsis* mutants (Arioli et al. 1998; Taylor et al. 1999; Taylor et al. 2000). The predicted products of plant and bacterial *CesA*s share a common structure (Figure 2-2) that includes N- and C-terminal transmembrane domains (TMD) and a cytoplasmic domain consisting of four conserved regions (U1 through U4) surrounding the D and QXXRW residues predicted to be involved in substrate binding and catalysis (Delmer 1999). These similarities have been interpreted as evidence that eukaryotic and prokaryotic CesAs are homologous, having arisen ultimately from a common ancestral processive β-glycosyl transferase (Nobles and Brown, Jr. 2004). However, orthology between specific eukaryotic CesAs and prokaryotic processive β-glycosyl transferases has not been proven.

CesA genes have been identified in hundreds of vascular plant species and extensively characterized in several including *Arabidopsis*, cotton, maize, rice, barley, and poplar (see http://cellwall.stanford.edu/). Seed plant *CesA*s differ from bacterial *CesA*s (Figure 2-2) by the presence of an N-terminal zinc-binding

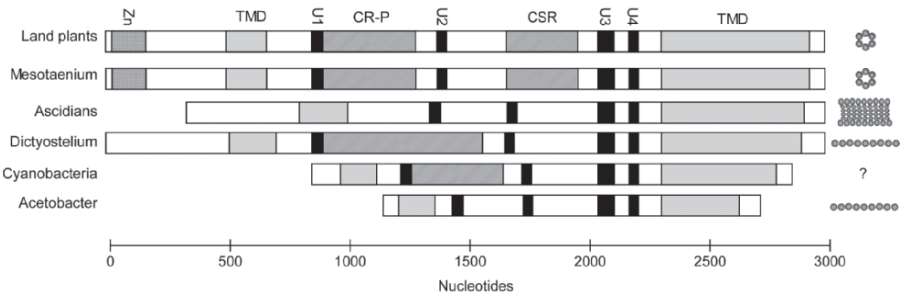

Figure 2-2. Comparison of *CesA* gene structure and TC organization in organisms in which both have been characterized. See text for abbreviations. Diagram based on data from Delmer 1999; Blanton et al. 2000; Nobles et al. 2001; Roberts et al. 2002; Matthysse et al. 2004; and Nakashima et al. 2004

domain (Zn), a conserved region (CR-P) between U1 and U2, and a more variable region (CSR) between U2 and U3 (Delmer 1999). Delmer (1999) proposed that plant *CesA*s evolved through the gradual acquisition of these domains. The CR-P appears to be the most ancient, having been identified in some cyanobacterial *CesA*s (Nobles et al. 2001). Seed plant *CesA* families are large. In *Arabidopsis*, analysis of mutant phenotypes and gene expression have revealed that some of the 10 members of the *CesA* gene family serve distinct functions in primary and secondary cell wall synthesis (Taylor et al. 1999; Fagard et al. 2000; Holland et al. 2000; Scheible et al. 2001). However, some *Arabidopsis CesA*s are coexpressed and genetic complementation and coprecipitation experiments have shown that cellulose synthesis in at least some *Arabidopsis* cell types involves the cooperative function of up to three distinct CesAs (Taylor et al. 2000; Scheible et al. 2001; Burn et al. 2002; Desprez et al. 2002; Taylor et al. 2003). It has also been proposed that the "D" class of *cellulose synthase-like* (*Csl*) genes encode cellulose synthases involved in tip growth (Doblin et al. 2001). Thus, the diversification of the *CesA* gene family in seed plants has been accompanied by divergence in function as well as spatial and temporal expression patterns.

Several lines of evidence support a role for *CesA* gene products in controlling TC assembly and thus, microfibril structure. First, immunolabeling of freeze-fracture replicas of TCs with antibodies raised against a *CesA* gene product demonstrated that CesA proteins reside within TCs (Kimura et al. 1999). Second, specific association between CesA subunits from both *Arabidopsis* and cotton have been demonstrated *in vitro* (Taylor et al. 2000; Kurek et al. 2002; Gardiner et al. 2003; Taylor et al. 2003). Third, the *Arabidopsis cesA1* (*rsw1*) mutation causes rosettes to disintegrate (Arioli et al. 1998). Fourth, deletion of any of the three *CesA*s required for secondary cell wall synthesis in *Arabidopsis* inhibits rosette assembly and secretion (Gardiner et al. 2003). Because the CesA proteins of *Acetobacter* (Figure 2-2), which form linear TCs, lack the zinc-binding domain, CR-P and CSR present in the CesA proteins of organisms with rosette

TCs (Delmer 1999; Roberts et al. 2002), these domains are obvious candidates for playing a role in particle association in rosettes. This hypothesis is supported by the results of *in vitro* assays that directly implicate the zinc-binding domain in rosette assembly (Kurek et al. 2002). Terminal complex dissociation in response to cellulose synthesis inhibitors (Mizuta and Brown, Jr. 1992; Peng et al. 2001; Kiedaisch et al. 2003) suggest that the particles that compose linear and rosette TCs are held together in different ways. One of these inhibitors (AE F150944) is effective in organisms with rosettes, but not linear TCs (Kiedaisch et al. 2003), whereas another (dichlorobenzonitrile) disrupts the linear TCs of *Vaucheria hamata* (Mizuta and Brown, Jr. 1992).

Much remains unknown about the evolution of *CesA* genes, including the identity of the prokaryotic ancestor(s) of eukaryotic *CesA*s, the relationship between CesA evolution and TC morphological variation, and the diversification and functional specialization of *CesA* genes within the angiosperm lineage. This review considers how characterization of the *CesA* genes and proteins of green algae and seedless plants can help address these fundamental questions.

2 THE PROKARYOTIC ANCESTRY OF EUKARYOTIC *CesAs*

Cellulose producing eukaryotes occur throughout the tree of life (Figure 2-1). In addition to plants, cellulose is produced by certain slime molds, oomycetes, ascidians, and diverse species of algae (Delmer 1999). The cellulose produced by these organisms is incorporated into a variety of cell coverings ranging from internal and external scales to thecae, sheaths, tunicas, and cell walls (Okuda 2002). Terminal complex organization varies among eukaryotes (Figure 2-1), but the particle arrangement is often conserved within evolutionary lineages (Brown, Jr. et al. 1983; Hotchkiss 1989; Tsekos 1999). Divergence in both TC organization and *CesA* domain structure among organisms in which both have been characterized (Figure 2-2) is consistent with the hypothesis that *CesA* genes determine TC organization and thus microfibril dimensions. However, these organisms, which include seed plants (Delmer 1999), a green alga (Hotchkiss et al. 1989; Roberts et al. 2002), a slime mold (Grimson et al. 1996; Blanton et al. 2000), and ascidians (Kimura and Itoh 1996, 2004; Matthysse et al. 2004; Nakashima et al. 2004), represent separate eukaryotic lineages thought to have arisen through independent acquisition of organelles by endosymbiosis (Bhattacharya et al. 2004). Thus, interpretation of the relationship between *CesA* and TC evolution is complicated by the possibility that widely divergent eukaryotic taxa may have acquired *CesA* genes independently through lateral gene transfer (Tsekos 1999; Nobles et al. 2001; Nakashima et al. 2004; Niklas 2004; Nobles and Brown, Jr. 2004).

Given a role for lateral gene transfer in the evolution of cellulose synthesis, four different scenarios could explain differences in TC structure in divergent eukaryotic lineages. First, mutation of the *CesA* ortholog within one of

the divergent lineages could lead to an alteration in interparticle association, followed by vertical transmission of the resulting change in TC structure within that lineage. Models based on this scenario have proposed that single synthases became associated first into particles (analogous to a single particle of a rosette, which would synthesize 4–15 glucan chains) and then into particle aggregates (terminal complexes) whose geometrical organization determines the cross-sectional dimensions of the microfibril (Brown, Jr. 1990; Tsekos 1999). Second, differences in TC organization could result from acquisition within divergent lineages of nonorthologous *CesA* subunits through lateral gene transfer from different prokaryotic donors. This is a likely explanation for the differences in TC organization in tunicates and land plants (Nakashima et al. 2004). Third, variation in the assembly of CesA subunits inherited from the same prokaryotic donor could arise from differences in cellular context between the eukaryotic hosts from divergent lineages. For example, linear and rosette TCs in green algae are assembled at different locations within the cell. Intact rosettes have been identified in Golgi vesicles, indicating that these TCs are secreted to the plasma membrane fully assembled (Giddings et al. 1980; Haigler and Brown, Jr. 1986). In contrast, at least some linear TCs assemble in the plasma membrane (Mizuta 1985; Mizuta and Brown, Jr. 1992; Tsekos 1999), perhaps a necessity due to their large size. Fourth, divergent lineages could functionally incorporate different *CesA* paralogs from a single prokaryotic donor. This has been proposed as an explanation for rosette versus linear TCs in the major green algal lineages (Nobles and Brown, Jr. 2004). Further characterization of genes encoding processive β-glycosyl transferases from both prokaryotes and eukaryotes will be required to test these hypotheses.

Cellulose synthesis has been demonstrated in a variety of prokaryotes including *A. xylinus*, *Agrobacterium tumefaciens*, *Rhizobium* species (Ross et al. 1991), the enteric bacteria *Escherichia coli* and *Salmonella typhimurium* (Zogaj et al. 2001), *Sarcina ventriculi* (Roberts et al. 1989) and several genera of cyanobacteria (Nobles et al. 2001). Similarity searches have identified genes encoding putative processive β-glycosyl transferases in a number of prokaryotes (Nobles and Brown, Jr. 2004). *A. xylinus* is the only prokaryote in which the site of cellulose synthesis at the plasma membrane been characterized by freeze fracture (Brown, Jr. et al. 1976). However, the linear TC and the unusual ability to produce a large extracellular ribbon of nearly pure cellulose are probably derived characters. Thus, it seems unlikely that the linear TCs of algae are homologous to those of *Acetobacter*. Evidence that the *CesA*s of green plants were acquired from cyanobacteria (Nobles et al. 2001) is provided by the observation that certain cyanobacterial *CesA*s contain an insertion (the CR-P region) that is also found in *CesA*s from seed plants and the charophycean green alga *Mesotaenium caldariorum* (Roberts et al. 2002), but not in bacterial *CesA*s. Conversely, the *CesA*s of ascidians (Matthysse et al. 2004; Nakashima et al. 2004), as well as *Csl*s from the A and C families of seed plant (Richmond and Somerville 2000), more closely resemble bacterial *CesA*s (Nobles and Brown, Jr. 2004). Phylogenetic

analyses have been based on the hypothesis that processive β-glycosyl transferases evolved ultimately from a single common ancestral protein, but that ancestor has not been identified.

3 GREEN ALGAL *CesAs* AND THE EVOLUTION OF TERMINAL COMPLEXES

The genetic basis for variation in TC morphology is more likely to be revealed through examination of the *CesA* genes descended from the same prokaryotic ancestor. The glaucophytes, red algae, green algae, and land plants are thought to be descended from a common ancestor derived from endosymbiotic acquisition of a plastid of cyanobacterial origin (Bhattacharya et al. 2004). This group includes organisms with many different types of TCs (Figure 2-1) and wide variation of microfibril structure (Tsekos 1996, 1999). *Erythrocladia*, representing the red algal subclass Bangiophycidae, has linear TCs with 4 rows of particles and produces ribbon-like microfibrils, whereas *Ceramium*, representing the red algal subclass Floridiophycidae, has linear TCs with single rows of particles and produces very small microfibrils (Tsekos 1999). The green algae and land plants form a monophyletic group with two major branches: (1) the streptophytes, which include the land plants and charophyte green algae (Charales, Coleochaetales, Zygnematales, Klebsormidiales, and Chlorokybales) and (2) the chlorophytes, which include the remaining green algae (McCourt 1995). The TCs of the chlorophyte green algae that have been examined are linear with three rows of particles. The only known except for *Halicystis*, which produces the cellulose II crystalline allomorph that does not occur as extended microfibrils (Roberts 1991). Membrane insertion of linear TCs in green algae also varies along taxonomic lines (Hotchkiss 1989). For example, the TCs of *Oocystis* (Trebouxiophyceae) appear to span only the outer leaflet of the plasma membrane, whereas the TCs of *Valonia* (Ulvophyceae) span the entire membrane. Rosette TCs have been found exclusively and almost universally in the streptophytes that have been examined (Brown, Jr. 1990; Tsekos 1999).

The *CesA* genes of *M. caldariorum*, a basal member of the charophycean green algae among which rosette TCs are thought to have arisen (Graham et al. 2000), are up to 59% identical at the amino acid level with conserved domain and intron-exon structure (Roberts et al. 2002; Roberts and Roberts 2004), demonstrating a congruence of CesA and TC structure. In an effort to identify CesA domains potentially involved in TC particle association, we have attempted to clone *CesA*s from the green algae *Oocystis apiculata* (Brown, Jr. and Montezinos 1976) and *Valonia ventricosa* (Itoh and Brown, Jr. 1984), which have linear TCs. Although degenerate primers based on conserved regions of the deduced amino acid sequences of plant and prokaryote *CesA* genes amplified *CesA* gene fragments from *M. caldariorum* (Roberts et al. 2002), this technique has not yet been successful with organisms that do not have rosette TCs, such as *Oocystis* and *Valonia*. The suggestion that the *CesA*s of chlorophyte green algae resemble the

B, E, and G families of *Csl*s (Nobles and Brown, Jr. 2004) may provide a basis for designing more effective degenerate primers.

The limited extent of *CesA* divergence since plants colonized the land (Roberts et al. 2002) also provides a basis for interpreting the relationship between *CesA* sequence and TC organization among the charophyte green algae. *Coleochaete scutata*, a charophyte green alga thought to be among the closest algal relatives of land plant, has a unique 8-particle TC (Okuda and Brown, Jr. 1992) that differs from the hexagonal rosettes that occur in both charophyte algae and land plants. Since the CesAs of *Coleochaete* would be expected to be generally similar to those of *M. caldariorum* because of their close phylogenetic relationship, any difference in CesA structure is likely to be related to TC structure. Members of the two earliest divergent charophyte orders, Klebsormidiales and Chlorokybales, have not been examined by freeze fracture or at a genetic level, but could provide valuable information on the origin of the rosette. If any members of these orders have nonrosette TCs, then differences in their CesA structure could also reveal domains involved in particle association. Another organism that will be useful to study is *Mesostigma viride*, a scaly unicellular flagellate that lacks a cell wall (Graham et al. 2000). Although its classification with the prasinophytes, which include the earliest divergent green algae, is supported by some analyses (Lemieux et al. 2000; Turmel et al. 2002), cytological characters along with extensive sequence comparisons place *M. viride* at the base of the charophyte lineage (Bhattacharya et al. 1998; Karol et al. 2001; Martin et al. 2002).

Rosettes that synthesize secondary cell wall microfibrils in *Arabidopsis* are composed of heterologous CesA triads (Taylor et al. 2000; Scheible et al. 2001; Gardiner et al. 2003; Taylor et al. 2003), and this may also be true for rosettes that synthesize primary cell wall microfibrils (Burn et al. 2002; Desprez et al. 2002; Doblin et al. 2002; Robert et al. 2004). Doblin et al. (2002) have proposed a modification of a previous model (Scheible et al. 2001) that explains the geometry of rosette TCs as a function of the inter- and intra-particle interaction between three distinct CesA subunits that associate with each other through distinct binding sites. Extending this model, a linear TC could assemble from one or perhaps two types of subunits. This is consistent with the observation that *CesA* genes occur singly and in pairs, respectively, in *Dictyostelium discoideum* (Blanton et al. 2000) and *A. xylinus* (Saxena and Brown, Jr. 1995; Umeda et al. 1999), both of which have linear TCs (Brown, Jr. et al. 1976; Grimson et al. 1996). However, consideration of the structure and mechanism of action of processive β-glycosyl transferases, has raised the possibility that two CesA subunits cooperate to synthesize a single glucan chain (Carpita and Vergara 1998; Saxena et al. 2001). Thus, distinct CesA subunits working in concert may be required so that each monomer added to the elongating glucan chain is rotated 180° compared to its neighbor (Perrin 2001; Vergara and Carpita 2001) or different subunits may be required to catalyze chain initiation and elongation (Peng et al. 2002; Read and Bacic 2002), in which case the rosette TC structure may be a byproduct of the cooperation of three different CesAs in the synthesis of a microfibril.

M. caldariorum may have just two *CesA* genes and to date it is unclear whether they interact within rosettes (Roberts and Roberts 2004). Further examination of *CesA* genes from *M. caldariorum* and nonvascular plants (see below) may clarify the relationship between *CesA* diversification and evolution and assembly of the rosette.

4 *CesA* DIVERSIFICATION AND THE EVOLUTION OF LAND PLANTS

4.1 Evolution of tracheary elements

The origin of tracheary elements with thick secondary cell walls was a key event in land plant evolution and a defining feature of the vascular plant lineage (Graham et al. 2000). However, much remains unknown about the evolution of tracheary elements and the process of secondary cell wall deposition. Although conducting cells known as hydroids occur in sporophytes and gametophytes of many species of mosses and liverworts, these tissues are structurally diverse and provide little insight into the origin of tracheary elements (Hebant 1977). For example, moss hydroids are elongated and empty at maturity, but their cell walls are thin and lack lignin (Hebant 1977). Some liverworts have water-conducting cells with patterned cell walls that are similar in appearance to those of tracheary elements. However, these patterns form by removal of wall material associated with plasmodesmata rather than by patterned secondary cell wall deposition (Ligrone et al. 2000). These observations, along with recent studies of cell wall composition in bryophytes, are consistent with multiple evolutionary origins of cells specialized for water conduction (Hebant 1977; Ligrone et al. 2000; Ligrone et al. 2002). In contrast, a recent report cites the role of auxin in the development of conducting tissues in moss sporophytes as support for homology with vascular tissue (Cooke et al. 2002).

Ultrastructural and developmental studies of tracheary elements from fossils and early divergent extant vascular plants have been undertaken in efforts to understand the evolution of secondary cell wall deposition. Whereas seed plant tracheary elements have homogeneous secondary cell walls, those of basal extant (Friedman and Cook 2000) and some fossil vascular plants (Kenrick and Crane 1991) have two distinct layers, an outer patterned electron-opaque "template layer" that becomes partially lignified and an inner, more heavily lignified, resistant layer that resembles the secondary cell wall of seed plant tracheary elements. Based on analysis of fossils, the tracheary elements of the earliest vascular plants had a single patterned secondary cell wall layer that is reminiscent of the template layer found in extant basal vascular plants (Kenrick and Crane 1991; Friedman and Cook 2000). This indicates that localized secondary cell wall deposition arose early in tracheary element evolution with the extent of lignification increasing over time (Friedman and Cook 2000). Tracheary element morphology varies greatly both within and among species of vascular plants,

but evolutionary trends are unclear. The origin of vessel elements, which are characterized by perforation plates formed by the digestion of the primary cell wall between adjacent cells, was once thought to coincide with the divergence of gymnosperms and angiosperms. However, vessel elements are now known to occur in most vascular plant lineages (Carlquist and Schneider 2001).

4.2 Functional specialization of CesA proteins

The observation that certain CesA proteins are expressed during primary cell wall synthesis, while others are expressed during secondary cell wall synthesis (Taylor et al. 1999; Fagard et al. 2000; Holland et al. 2000; Taylor et al. 2000; Burn et al. 2002; Taylor et al. 2003) suggests a relationship between *CesA* diversification and the evolution of tracheary elements. As reviewed previously, distinct triads of *CesA*s are thought to compose the rosettes responsible for secondary cell wall deposition in tracheary elements (*AtCesA4*,*7*,*8*) and in expanding tissues (*AtCesA1*,*3*,*6*) (Doblin et al. 2002). Primary and secondary cell walls differ in the orientation and spatial localization of cellulose microfibrils (Hepler 1981), apparent microfibril dimensions (Ha et al. 1998), and the amount of cellulose relative to other cell wall polymers (Ingold et al. 1988). These differences may arise from changes in the interaction of TC particles with each other and with the cytoskeleton. For example, rosettes are confined to developing secondary cell wall thickenings during tracheary element development (Herth 1985; Haigler and Brown, Jr. 1986; Schneider and Herth 1986), a pattern that is mirrored by the distribution of microtubules. In the zygnematalean alga *Micrasterias denticulata*, the secondary cell wall fibrils are composed of individual microfibrils assembled by rosettes aggregated into rows or large hexagonal arrays (Giddings et al. 1980). During secondary cell wall deposition in tracheary elements, rosettes associate in rows (Herth 1985). In some algae, the linear TCs become longer during secondary cell wall synthesis (Itoh 1990). Thus, an important property of CesAs specialized for secondary cell wall deposition may be their interactions within and between TCs or with the cellular structures that control TC localization or movement.

4.3 Tip growth and the function of *Cellulose synthase-like type D* (*CslD*) genes

The *CesA* gene superfamily also includes *CesA*-like (*Csl*) genes containing the D,D,D,QXXRW motif characteristic of processive glycosyl transferases (Richmond and Somerville 2001). The *Csl*s have been proposed to function in cell wall synthesis (Richmond and Somerville 2001), but only the *CslA* class has been characterized functionally (Dhugga et al. 2004; Liepman et al. 2005). The class of *Csl*s with highest sequence similarity to *CesA*s, the *CslD*s, are expressed in tip growing cells such as pollen tubes (Doblin et al. 2001) and root hairs (Favery et al. 2001; Wang et al. 2001). A mutation in one of the five *CslD*s in *Arabidopsis* (*AtCslD3*) causes root hairs to become distorted and rupture at the tips (Favery et al. 2001; Wang et al. 2001). Based on localization to the endomembrane system, it has been proposed that AtCslDs synthesize noncellulosic polysaccharides

(Favery et al. 2001). However, tobacco pollen tubes express *CslD*s but not *CesA*s during deposition of the cellulosic cell wall indicating that some CslDs may synthesize cellulose (Doblin et al. 2001; Doblin et al. 2003). Unlike the other classes of Csls, CslDs have a Zn-binding domain near the N-terminus (Doblin et al. 2001). Given that the Zn-binding domains of CesAs have been proposed to function in CesA-CesA binding (Kurek et al. 2002), it is an interesting question whether CslDs assemble as TCs. The *CslD* family is thought to have had an ancient origin (Doblin et al. 2001; Richmond and Somerville 2001), which is consistent with the occurrence of tip-growing cells in many algae, as well a fungi. Although *CslD*s were not identified in a screen *M. caldariorum CesA* genes, we have recently identified a *CslD* gene in the green alga *C. scutata* (Neill 2005). One salient difference between *C. scutata* and *M. caldariorum* is that *C. scutata* produces hairlike projections called chaetae, which can reasonably be expected to elongate by tip growth.

4.4 CesA and *CslD* genes of the moss *Physcomitrella patens*

Characterization of *CesA* gene superfamilies in nonvascular plants is one approach to revealing the relationship between CesA diversification and origin of vascular tissue. These studies are greatly facilitated by the development of genomic resources for model organisms (Pryer et al. 2002). The moss *P. patens* is a useful model for investigating plant gene function due to its unusually high rate of homologous recombination, which enables targeted mutagenesis (Schaefer 2002; Hohe et al. 2004; Schaefer and Zryd 2004; Cove 2005). *Physcomitrella patens* is also similar to vascular plants in having a large *CesA* gene superfamily. Through degenerate primer PCR and genomic library screening, we identified four *CesA* genes, one *CslD* gene and one *CesA* pseudogene from *P. patens* (Roberts and Roberts 2004). Searching of *P. patens* EST databases from the PEP project at Washington University/University of Leeds (http://genomeold.wustl.edu/est/index.php?moss=1), Physcobase at the National Institute for Basic Biology, Okazaki, Japan (http://moss.nibb.ac.jp/), and the University of Freiburg (http://www.cosmoss.org/) yielded a total of 65 cDNA clones representing 8 CesAs and 8 CslDs (Roberts et al. 2004).

Phylogenetic analysis of the *CesA* and *CslD* genes from *P. patens* supports the hypothesis that diversification within both gene families occurred independently in the moss and seed plants lineages. Initial phylogenetic analysis indicated that individual *Arabidopsis CesA*s and *CslD*s do not have orthologs in the *P. patens* genome (Roberts and Roberts 2004). This hypothesis was strengthened by recent analyses including additional full-length *P. patens CesA* and *CslD* genes (Roberts et al. 2004). The absence the orthologs of vascular plant *CesA*s and *CslD*s in *P. patens* has important implications for our understanding of the evolution of rosette TCs and tracheary elements. Phylogenetic analysis has provided strong evidence that the secondary cell wall *CesA* triad characterized in *Arabidopsis* (Gardiner et al. 2003) was present in the common ancestor of monocots and dicots (Tanaka et al. 2003; Appenzeller et al. 2004; Burton et al. 2004; Djerbi et al. 2004; Liang and Joshi 2004). This lead to speculation that all rosettes are

heterotrimers (Doblin et al. 2002). The apparent absence of orthologs of *AtCesA4, 7* and *8* in *P. patens* indicates that the evolution of the triad is more recent. A further implication is that secondary cell wall deposition in tracheary elements is a highly specialized process, involving functionally specialized *CesA* proteins. To date, it is not clear whether the diversification of the *CesA* gene family in land plants was a precondition for, or a consequence of, the evolution of tracheary elements with secondary cell walls. Analysis of *CesA* gene families in seedless vascular plants such as the fern *Ceratopteris richardii* may help answer this question.

Analysis of *P. patens* EST databases also indicates that *CslD* genes play a larger role in the development of moss gametophytes compared to seed plant sporophytes. In *P. patens*, 46% of all *CesA* superfamily ESTs are *CslD*s (Roberts et al. 2004). In contrast, *CesA*s are much more highly expressed than *CslD*s in *Arabidopsis* (Hamann et al. 2004). The question remains whether CslDs synthesize cellulose (Doblin et al. 2001; Doblin et al. 2003) or another cell wall polysaccharide (Favery et al. 2001). In the protonema of *Funaria hygrometrica*, a close relative of *P. patens*, rosette TCs are numerous in regions undergoing active tip growth (Reiss et al. 1984). This raises the possibility that CslDs, like CesAs, assemble into rosettes. Since tip-growing cells may be exceptions to the microtubule-microfibril paradigm for microfibril orientation (Emons et al. 1992), CslDs may differ from CesAs in their interactions with the cytoskeleton. It will be interesting to see if sequence analysis reveals a potential basis for such interactions.

5 ANALYSIS OF *CesA* FUNCTION BY TARGETED TRANFORMATION IN *P. patens*

The combined attributes of high rates of homologous recombination, haploid state of the protonema and leafy gametophyte, suitability for microscopic examination, a body complexity intermediate between that of algae and vascular plants, and the high similarity of many genes to those in higher plants make *P. patens* a useful and informative model for the investigation of cellulose synthesis. Homologous recombination in *P. patens* will make it possible to (1) knock out specific *CesA* and *Csl* genes, (2) replace *CesA*s with homologs lacking specific domains or chimeric genes assembled from domains present in the *CesA*s of different organisms, and (3) tag proteins to facilitate studies of gene expression, CesA turnover, intracellular dynamics, and interactions between CesAs and other proteins that compose TCs.

Acknowledgments

This work was supported by the National Research Initiative of the USDA Cooperative State Research, Education, and Extension Service, grant # 2003-35304-13233 to AWR, the National Science Foundation, grant #DBI 9872627 to

Deborah Delmer, and the University of Rhode Island Foundation. We gratefully acknowledge Deborah Delmer and the members of her lab, especially Monica Doblin, Pat Hogan and Yasushi Kawagoe for their helpful discussions.

REFERENCES

Appenzeller L., Doblin M., Barreiro R., Wang H., Niu X., Kollipara K., Carrigan L., Tomes D., Chapman M., and Dhugga K.S. 2004. Cellulose synthesis in maize: isolation and expression analysis of the cellulose synthase (*CesA*) gene family. Cellulose 11:287–299.

Arioli T., Peng L., Betzner A.S., Burn J., Wittke W., Herth W., Camilleri C., Höfte H., Plazinski J., Birch R., Cork A., Glover J., Redmond J., and Williamson R.E. 1998. Molecular analysis of cellulose biosynthesis in *Arabidopsis*. Science 279:717–720.

Bhattacharya D., Weber K., An S.S., and Berning-Koch W. 1998. Actin phylogeny identifies *Mesostigma viride* as a flagellate ancestor of the land plants. J Mol Evol 47:544–550.

Bhattacharya D., Yoon H.S., and Hackett J.D. 2004. Photosynthetic eukaryotes unite: endosymbiosis connects the dots. BioEssays 26:50–60.

Blanton R.L., Fuller D., Iranfar N., Grimson M.J., and Loomis W.F. 2000. The cellulose synthase gene of *Dictyostelium*. Proc Natl Acad Sci USA 97:2391–2396.

Brown, Jr. R.M., 1985. Cellulose microfibril assembly and orientation: Recent developments. J Cell Sci (Suppl.) 2:13–32.

Brown, Jr. R.M., 1990. Algae as tools in studying the biosynthesis of cellulose, nature's most abundant macromolecule. In: Wiessner W., Robinson D.G., and Starr R.C. (eds.) Experimental Phycology. Cell Walls and Surfaces, Reproduction, Photosynthesis. Springer-Verlag, Berlin Heidelberg New York London Paris Tokyo Hong Kong Barcelona, pp. 20–39.

Brown, Jr. R.M., Haigler C.H., Suttie J., White A.R., Roberts E., Smith C., Itoh T., and Cooper K. 1983. The biosynthesis and degradation of cellulose. J App Polymer Sci 37:33–78.

Brown, Jr. R.M., and Montezinos D. 1976. Cellulose microfibrils: Visualization of biosynthetic and orienting complexes in association with the plasma membrane. Proc Natl Acad Sci USA 73:143–147.

Brown, Jr. R.M., Willison J.H.M., and Richardson C.L. 1976. Cellulose biosynthesis in *Acetobacter xylinum*: Visualization of the site of synthesis and direct measurement of the *in vivo* process. Proc Natl Acad Sci USA 73:4565–4569.

Burn J.E., Hocart C.H., Birch R.J., Cork A.C., and Williamson R.E. 2002. Functional analysis of the cellulose synthase genes *CesA1*, *CesA2*, and *CesA3* in *Arabidopsis*. Plant Physiol 129:797–807.

Burton R.A., Shirley N.J., King B.J., Harvey A.J., and Fincher G.B. 2004. The *CesA* gene family of barley. Quantitative analysis of transcripts reveals two groups of co-expressed genes. Plant Physiol 134:224–236.

Carlquist S. and Schneider E.L. 2001. Vessels in ferns: structural, ecological, and evolutionary significance. Am J Bot 88:1–13.

Carpita N. and Vergara C. 1998. A recipe for cellulose. Science 279:672–673.

Cooke T.J., Poli D., Sztein A.E., and Cohen J.D. 2002. Evolutionary patterns in auxin action. Plant Mol Biol 49:319–338.

Cove D. 2005. The moss *Physcomitrella patens*. Annu Rev Genet 39:339–358.

Delmer D.P. 1987. Cellulose biosynthesis. Ann Rev Plant Physiol 38:259–290.

Delmer D.P. 1999. Cellulose biosynthesis: Exciting times for a difficult field of study. Annu Rev Plant Physiol Plant Mol Biol 50:245–276.

Desprez T., Vernhettes S., Fagard M., Refregier G., Desnos T., Aletti E., Py N., Pelletier S., and Höfte H. 2002. Resistance against herbicide isoxaben and cellulose deficiency caused by distinct mutations in same cellulose synthase isoform CESA6. Plant Physiol 128:482–490.

Dhugga K.S., Barreiro R., Whitten B., Stecca K., Hazebroek J., Randhawa G.S., Dolan M., Kinney A.J., Tomes D., Nichols S., and Anderson P. 2004. Guar seed β-mannan synthase is a member of the cellulose synthase super gene family. Science 303:363–366.

Djerbi S., Aspeborg H., Nilsson P., Sundberg B., Mellerowicz E., Blomqvist K., and Teeri T.T. 2004. Identification and expression analysis of genes encoding putative cellulose synthases (CesA) in the hybrid aspen, *Populus tremula* (L.) X *P. tremuloides* (Michx.). Cellulose 11:301–312.

Doblin M.S., De Melis L., Newbigin E., Bacic A., and Read S.M. 2001. Pollen tubes of *Nicotiana alata* express two genes from different β-glucan synthase families. Plant Physiol 125:2040–2052.

Doblin M.S., Kurek I., Jacob-Wilk D., and Delmer D.P. 2002. Cellulose biosynthesis in plants: from genes to rosettes. Plant Cell Physiol 43:1407–1420.

Doblin M.S., Vergara C.E., Read S., Newbigin E., and Bacic A. 2003. Plant cell wall biosynthesis: making the bricks. In: Rose J.K.C. (ed.) The Plant Cell Wall, Vol 8. Blackwell, Oxford, pp. 183–222.

Emons A.M.C., Derksen J., and Sassen M.M.A. 1992. Do microtubules orient plant cell wall microfibrils? Physiol Plant 84:486–493.

Fagard M., Desnos T., Desprez T., Goubet F., Refregier G., Mouille G., Mccann M., Rayon C., Vernhettes S., and Höfte H. 2000. *PROCUSTE1* encodes a cellulose synthase required for normal cell elongation specifically in roots and dark-grown hypocotyls of *Arabidopsis*. Plant Cell 12:2409–2423.

Favery B., Ryan E., Foreman J., Linstead P., Boudonck K., Steer M., Shaw P., and Dolan L. 2001. *KOJAK* encodes a cellulose synthase-like protein required for root hair cell morphogenesis in *Arabidopsis*. Genes Dev 15:79–89.

Friedman W.E. and Cook M.E. 2000. The origin and early evolution of tracheids in vascular plants: integration of palaeobotanical and neobotanical data. Phil Trans R Soc Lond B 355:857–868.

Gardiner J.C., Taylor N.G., and Turner S.R. 2003. Control of cellulose synthase complex localization in developing xylem. Plant Cell 15:1740–1748.

Giddings T.H., Jr., Brower D.L., and Staehelin L.A. 1980. Visualization of particle complexes in the plasma membrane of *Micrasterias denticulata* associated with the formation of cellulose fibrils in primary and secondary cell walls. J Cell Biol 84:327–339.

Giddings T.H., Jr. and Staehelin L.A. 1991. Microtubule-mediated control of microfibril deposition: a re-examination of the hypothesis. In: Lloyd C.W. (ed.) The Cytoskeletal Basis of Plant Growth and Form. Academic Press, New York, pp. 85–99.

Graham L.E., Cook M.E., and Busse J.S. 2000. The origin of plants: body plan changes contributing to a major evolutionary radiation. Proc Natl Acad Sci USA 97:4535–4540.

Grimson M.J., Haigler C.H., and Blanton R.L. 1996. Cellulose microfibrils, cell motility, and plasma membrane protein organization change in parallel during culmination in *Dictyostelium discoideum*. J Cell Sci 109:3079–3087.

Ha M.-A., Apperley D.C., Evans B.W., Huxham I.M., Jardine W.G., Vietor R.J., Reis D., Vian B., and Jarvis M.C. 1998. Fine structure in cellulose microfibrils: NMR evidence from onion and quince. Plant J 16:183–190.

Haigler C.H. 1991. Relationship between polymerization and crystallization in microfibril biogenesis. In: Haigler C.H. and Weimer P.J. (eds.) Biosynthesis and Biodegradation of Cellulose. Marcel Dekker, New York, pp. 99–124.

Haigler C.H. and Brown, Jr. R.M., 1986. Transport of rosettes from the Golgi apparatus to the plasma membrane in isolated mesophyll cells of *Zinnia elegans* during differentiation to tracheary elements in suspension culture. Protoplasma 134:111–120.

Haigler C.H., Brown, Jr. R.M., and Benziman M. 1980. Calcofluor white ST alters the *in vivo* assembly of cellulose microfibrils. Science 210:903–906.

Hamann T., Osborne E., Youngs H.L., Misson J., Nussaume L., and Somerville C. 2004. Global expression analysis of *CESA* and *CSL* genes in *Arabidopsis*. Cellulose 11:279–286.

Hebant C. 1977. The Conducting Tissues of Bryophytes. J. Cramer, Vaduz, p. 157.

Hepler P.K. 1981. Morphogenesis of tracheary elements and guard cells. In: Kiermayer O. (ed.) Cytomorphogenesis in Plants. Springer, Berlin, pp. 327–347.

Herth W. 1983. Arrays of plasma-membrane "rosettes" involved in cellulose microfibril formation of *Spirogyra*. Planta 159:347–356.

Herth W. 1985. Plasma-membrane rosettes involved in localized wall thickening during xylem vessel formation of *Lepidium sativum* L. Planta 164:12–21.

Hohe A., Egener T., Lucht J.M., Holtorf H., Reinhard C., Schween G., and Reski R. 2004. An improved and highly standardised transformation procedure allows efficient production of single and multiple targeted gene-knockouts in a moss, *Physcomitrella patens*. Curr Genet 44:339–347.

Holland N., Holland D., Helentjaris T., Dhugga K.S., Xoconostle-Cazares B., and Delmer D.P. 2000. A comparative analysis of the plant cellulose synthase (*CesA*) gene family. Plant Physiol 123:1313–1323.

Hotchkiss A.T., Jr. 1989. Cellulose biosynthesis: the terminal complex hypothesis and its relationship to other contemporary research topics. In: Lewis N.G. and Paice M.G. (eds.) Plant Cell Wall Polymers. Biogenesis and Biodegradation. American Chemical Society, Washington, DC, pp. 232–247.

Hotchkiss A.T., Jr., Gretz M.R., Hicks K.B., and Brown, Jr. R.M., 1989. The composition and phylogenetic significance of the *Mougeotia* (Charophyceae) cell wall. J Phycol 25:646–654.

Ingold E., Munetaka S., and Komamine A. 1988. Secondary cell wall formation: changes in cell wall constituents during the differentiation of isolated mesophyll cells of *Zinnia elegans* to tracheary elements. Plant Cell Physiol 29:295–303.

Itoh T. 1990. Cellulose synthesizing complexes in some giant marine algae. J Cell Sci 95:309–319.

Itoh T. and Brown, Jr. R.M., 1984. The assembly of cellulose microfibrils in *Valonia macrophysa* Kütz. Planta 160:372–381.

Itoh T., O'neil R.M., and Brown, Jr. R.M., 1984. Interference of cell wall regeneration of *Boergesenia forbesii* protoplasts by Tinopal LPW, a fluorescent brightening agent. Protoplasma 123:174–183.

Karol K.G., McCourt R.M., Cimino M.T., and Delwiche C.F. 2001. The closest living relatives of land plants. Science 294:2351–2353.

Kenrick P. and Crane P.R. 1991. Water-conducting cells in early fossil land plants: implications for the early evolution of tracheophytes. Bot Gaz 152:335–356.

Kiedaisch B.M., Blanton R.L., and Haigler C.H. 2003. Characterization of a novel cellulose synthesis inhibitor. Planta 217:922–930.

Kimura S. and Itoh T. 1996. New cellulose synthesizing complexes (terminal complexes) involved in animal cellulose biosynthesis in the tunicate *Metandrocarpa uedai*. Protoplasma 194:151–163.

Kimura S. and Itoh T. 2004. Cellulose synthesizing terminal complexes in the ascidians. Cellulose 11:377–383.

Kimura S., Laosinchai W., Itoh T., Cui X., Linder C.R., and Brown, Jr. R.M., 1999. Immunogold labeling of rosette terminal cellulose-synthesizing complexes in the vascular plant *Vigna angularis*. Plant Cell 11:2075–2085.

Kurek I., Kawagoe Y., Jacob-Wilk D., Doblin M., and Delmer D. 2002. Dimerization of cotton fiber cellulose synthase catalytic subunits occurs via oxidation of the zinc-binding domains. Proc Natl Acad Sci USA 99:11109–11114.

Lai-Kee-Him J., Chanzy H., Muller M., Putaux J.L., Imai T., and Bulone V. 2002. *In vitro* versus *in vivo* cellulose microfibrils from plant primary wall synthases: structural differences. J Biol Chem 277:36931–36939.

Lemieux C., Otis C., and Turmel M. 2000. Ancestral chloroplast genome in *Mesostigma viride* reveals an early branch of green plant evolution. Nature 403:649–652.

Liang X. and Joshi C.P. 2004. Molecular cloning of ten distinct hypervariable regions from the cellulose synthase gene superfamily in aspen trees. Tree Physiol 24:543–550.

Liepman A.H., Wilkerson C.G., and Keegstra K. 2005. Expression of cellulose synthase-like (*Csl*) genes in insect cells reveals that *CslA* family members encode mannan synthases. Proc Natl Acad Sci USA 102:2221–2226.

Ligrone R., Duckett J.G., and Renzaglia K.S. 2000. Conducting tissues and phyletic relationships of bryophytes. Phil Trans R Soc Lond B 355:795–813.

Ligrone R., Vaughn K.C., Renzaglia K.S., Knox J.P., and Duckett J.G. 2002. Diversity in the distribution of polysaccharide and glycoprotein epitopes in the cell walls of bryophytes: new evidence for the multiple evolution of water-conducting cells. New Phytol 156:491–508.

Martin W., Rujan T., Richly E., Hansen A., Cornelsen S., Lins T., Leister D., Stoebe B., Hasegawa M., and Penny D. 2002. Evolutionary analysis of *Arabidopsis*, cyanobacterial, and chloroplast

genomes reveals plastid phylogeny and thousands of cyanobacterial genes in the nucleus. Proc Natl Acad Sci USA 99:12246–12251.
Matthysse A.G., Deschet K., Williams M., Marry M., White A.R., and Smith W.C. 2004. A functional cellulose synthase from ascidian epidermis. Proc Natl Acad Sci USA 101:986–991.
McCourt R.M. 1995. Green algal phylogeny. Trends Ecol Evol 10:159–163.
Mizuta S. 1985. Evidence for the regulation of the shift in cellulose microfibril orientation in freeze-fractured plasma membrane of *Boergesenia forbesii*. Plant Cell Physiol 26:53–62.
Mizuta S. and Brown, Jr. R.M., 1992. Effects of 2,6-dichlorobenzonitrile and Tinopal LPW on the structure of the cellulose synthesizing complexes of *Vaucheria hamata*. Protoplasma 166:200–207.
Montezinos D. 1982. The role of the plasma membrane in cellulose microfibril assembly. In: Lloyd C.W. (ed.) The Cytoskeleton in Plant Growth and Development. Academic Press, London, pp. 147–162.
Nakashima K., Yamada L., Satou Y., Azuma J., and Satoh N. 2004. The evolutionary origin of animal cellulose synthase. Dev Genes Evol 214:81–88.
Neill A.A. 2005. A Cellulose synthase-like (*CslD*) gene from *Coleochaete scutata*. M.S. University of Rhode Island
Niklas K.J. 1992. Plant Biomechanics: An Engineeing Approach to Plant Form and Function. University of Chicago Press, Chicago, p. 622.
Niklas K.J. 2004. The cell walls that bind the tree of life. BioScience 54:831–841.
Nobles D.R., Jr. and Brown, Jr. R.M., 2004. The pivotal role of cyanobacteria in the evolution of cellulose synthases and cellulose synthase-like proteins. Cellulose 11:437–448.
Nobles D.R., Romanovicz D.K., and Brown, Jr. R.M., 2001. Cellulose in cyanobacteria. Origin of vascular plant cellulose synthase? Plant Physiol 127:529–542.
Okuda K. 2002. Structure and phylogeny of cell coverings. J Plant Res 115:283–288.
Okuda K. and Brown, Jr. R.M., 1992. A new putative cellulose-synthesizing complex of *Coleochaete scutata*. Protoplasma 168:51–63.
Pear J.R., Kawagoe Y., Schreckengost W.E., Delmer D.P., and Stalker D.M. 1996. Higher plants contain homologs of the bacterial *celA* genes encoding the catalytic subunit of cellulose synthase. Proc Natl Acad Sci USA 93:12637–12642.
Peng L., Kawagoe Y., Hogan P., and Delmer D. 2002. Sitosterol-β-glucoside as primer for cellulose synthesis in plants. Science 295:147–150.
Peng L., Xiang F., Roberts E., Kawagoe Y., Greve L.C., Kreuz K., and Delmer D.P. 2001. The experimental herbicide CGA 325 '615 inhibits synthesis of crystalline cellulose and causes accumulation of non-crystalline β-1,4-glucan associated with CesA protein. Plant Physiol 126:981–992.
Perrin R.M. 2001. Cellulose: how many cellulose synthases to make a plant? Curr Biol 11:R213–R216.
Pryer K.M., Schneider H., Zimmer E.A., and Banks J.A. 2002. Deciding among green plants for whole genome studies. Trends Plant Sci 7:550–554.
Read S.M. and Bacic T. 2002. Prime time for cellulose. Science 295:59–60.
Reiss H.D., Schnepf E., and Herth W. 1984. The plasma membrane of the *Funaria* caulonema tip cell: morphology and distribution of particle rosettes, and the kinetics of cellulose synthesis. Planta 160:428–435.
Richmond T.A. and Somerville C.R. 2000. The cellulose synthase superfamily. Plant Physiol 124:495–498.
Richmond T.A. and Somerville C.R. 2001. Integrative approaches to determining Csl function. Plant Mol Biol 47:131–143.
Robert S., Mouille G., and Hofte H. 2004. The mechanism and regulation of cellulose synthesis in primary walls: lessons from cellulose-deficient *Arabidopsis* mutants. Cellulose 11:351–364.
Roberts A.W., Bushoven J., Roberts E., and Goss C. 2004. Investigating the organization and function of the cellulose-synthesizing terminal complex using *Physcomitrella patens*. Plant Biology 2004 Abstract #624.
Roberts A.W. and Roberts E. 2004. Cellulose synthase (*CesA*) genes in algae and seedless plants. Cellulose 11:419–435.
Roberts A.W., Roberts E.M., and Delmer D.P. 2002. Cellulose synthase (*CesA*) genes in the green alga *Mesotaenium caldariorum*. Eukaryotic Cell 1:847–855.

Roberts E., Saxena I.M., and Brown, Jr. R.M., 1989. Biosynthesis of cellulose II. In: Schuerch C. (ed.) Cellulose and Wood: Chemistry and Technology. Wiley, New York, pp. 689–704.

Roberts E.M. 1991. Biosynthesis of cellulose II and related carbohydrates. PhD dissertation. University of Texas

Ross P., Mayer R., and Benziman M. 1991. Cellulose biosynthesis and function in bacteria. Microbiol Rev 55:35–58.

Saxena I.M. and Brown, Jr. R.M., 1995. Identification of a second cellulose synthase gene (*acsAII*) in *Acetobacter xylinum*. J Bacteriol 177:5276–5283.

Saxena I.M. and Brown, Jr. R.M., 2005. Cellulose biosynthesis: current views and evolving concepts. Ann Bot (Lond) 96:9–21.

Saxena I.M., Brown, Jr. R.M., and Dandekar T. 2001. Structure–function characterization of cellulose synthase: relationship to other glycosyltransferases. Phytochemistry 57:1135–1148.

Saxena I.M., Brown, Jr. R.M., Fevre M., Geremia R.A., and Henrissat B. 1995. Multidomain architecture of β-glycosyl transferases: implications for mechanism of action. J Bacteriol 177:1419–1424.

Saxena I.M., Lin F.C., and Brown, Jr. R.M., 1990. Cloning and sequencing of the cellulose synthase catalytic subunit gene of *Acetobacter xylinum*. Plant Mol Biol 15:673–683.

Schaefer D. and Zryd J.-P. 2004. Principles of targeted mutagenesis in the moss *Physcomitrella patens*. In: Wood A.J., Oliver M.J., and Cove D.J. (eds.) New Frontiers in Bryology: Physiology, Molecular Biology and Functional Genomics. Kluwer, Dordrecht, pp. 37–49.

Schaefer D.G. 2002. A new moss genetics: targeted mutagenesis in *Physcomitrella patens*. Annu Rev Plant Biol 53:477–501.

Scheible W.-R., Eshed R., Richmond T., Delmer D., and Somerville C. 2001. Modifications of cellulose synthase confer resistance to isoxaben and thiazolidinone herbicides in *Arabidopsis Ixr1* mutants. Proc Natl Acad Sci USA 98:10079–10084.

Schneider B. and Herth W. 1986. Distribution of plasma membrane rosettes and kinetics of cellulose formation in xylem development of higher plants. Protoplasma 131:142–152.

Sugiyama J., Harada H., Fujiyoshi Y., and Uyeda N. 1985. Lattice images from ultrathin sections of cellulose microfibrils in the cell wall of *Valonia macrophysa* Kütz. Planta 166:161–168.

Tanaka K., Murata K., Yamazaki M., Onosato K., Miyao A., and Hirochika H. 2003. Three distinct rice cellulose synthase catalytic subunit genes required for cellulose synthesis in the secondary wall. Plant Physiol 133:73–83.

Taylor N.G., Howells R.M., Huttly A.K., Vickers K., and Turner S.R. 2003. Interactions among three distinct CesA proteins essential for cellulose synthesis. Proc Natl Acad Sci USA 100:1450–1455.

Taylor N.G., Laurie S., and Turner S.R. 2000. Multiple cellulose synthase catalytic subunits are required for cellulose synthesis in *Arabidopsis*. Plant Cell 12:2529–2539.

Taylor N.G., Scheible W.-R., Cutler S., Somerville C.R., and Turner S.R. 1999. The *irregular xylem3* locus of *Arabidopsis* encodes a cellulose synthase required for secondary cell wall synthesis. Plant Cell 11:769–779.

Tsekos I. 1996. The supramolecular organization of red algal cell membranes and their participation in the biosynthesis and secretion of extracellular polysaccharides: a review. Protoplasma 193:10.

Tsekos I. 1999. The sites of cellulose synthesis in algae: Diversity and evolution of cellulose-synthesizing enzyme complexes. J Phycol 35:635–655.

Turmel M., Otis C., and Lemieux C. 2002. The complete mitochondrial DNA sequence of *Mesostigma viride* identifies this green alga as the earliest green plant divergence and predicts a highly compact mitochondrial genome in the ancestor of all green plants. Mol Biol Evol 19:24–38.

Umeda Y., Hirano A., Ishibashi M., Akiyama H., Onizuka T., Ikeuchi M., and Inoue Y. 1999. Cloning of cellulose synthase genes from *Acetobacter xylinum* JCM 7664: implication of a novel set of cellulose synthase genes. DNA Res 6:109–115.

Vergara C.E. and Carpita N.C. 2001. β-D-glycan synthases and the *CesA* gene family: lessons to be learned from the mixed-linkage (1->3),(1->4)β-D-glucan synthase. Plant Mol Biol 47:145–160.

Wang X., Cnops G., Vanderhaeghen R., De Block S., Van Montagu M., and Van Lijsebettens M. 2001. *AtCSLD3*, a cellulose synthase-like gene important for root hair growth in *Arabidopsis*. Plant Physiol 126:575–586.

Wong H.C., Fear A.L., Calhoon R.D., Eichinger G.H., Mayer R., Amikam D., Benziman M., Gelfand D.H., Meade J.H., Emerick A.W., Bruner R., Ben-Bassat A., and Tal R. 1990. Genetic organization of the cellulose synthase operon in *Acetobacter xylinum*. Proc Natl Acad Sci USA 87:8130–8134.

Zogaj X., Nimtz M., Rohde M., Bokranz W., and Romling U. 2001. The multicellular morphotypes of *Salmonella typhimurium* and *Escherichia coli* produce cellulose as the second component of the extracellular matrix. Mol Microbiol 39:1452–1463.

CHAPTER 3

THE CELLULOSE SYNTHASE SUPERFAMILY

HEATHER L. YOUNGS, THORSTEN HAMANN, ERIN OSBORNE, AND CHRIS SOMERVILLE*

Carnegie Institution, Department of Plant Biology, Stanford, CA 94305

Abstract

The completion of the *Arabidopsis thaliana* genome revealed ten cellulose synthase or *AtCESA* genes. Mutations in seven of the ten *AtCESA* genes have been studied. Studies indicate a requirement for three genes, *AtCESA1*, *AtCESA3*, and *AtCESA6*, in primary wall formation; whereas *AtCESA4*, *AtCESA7*, and *AtCESA8* may be involved in secondary cell wall formation. Genes with significant similarity to cellulose synthase-like (*CSL*) genes have been classified into eight distinct families. Thirty such genes have been identified in *Arabidopsis*. Members of the superfamily differ in their size, topology, and predicted physical properties.

Keywords

Arabidopsis, cellulose synthase (CESA), cellulose synthase-like (CSL), gene expression, predicted proteins.

Abbreviations

Arabidopsis thaliana (*At*), cellulose synthase (CES), constitutive expression of VSP1 (*cev*), cellulose synthase-like (CSL), ectopic lignin (*eli*), Fourier transform infrared (FTIR), *Gossypium hirsutum* (*Gh*), glycosyl transferase family II (GT-2), β-glucuronidase (GUS), kojak, a root hairless mutant (*kjk*), irregular xylem (*irx*), *Medicago trunculata* (*Mt*), *Nicotiana alata* (*Na*), isoelectric point (pI), procuste (*rc*), *Populus tremuloides* (*Pt*), resistance to *Agrobacterium tumefaciens* transformation (*rat*), radially swollen (*rsw*), the *Arabidopsis* information resource (TAIR), transmembrane domain (*T*MD), zinc binding domain (ZnBD).

1 INTRODUCTION

Cellulose is a simple polymer of unbranched β-1,4-linked glucan chains, which coalesce to form microfibrils. Extensive hydrogen bonding, between the glucan chains of the microfibrils and amongst the microfibrils themselves, yields a range of

* Author for correspondence: e-mail: crs@andrew2.stanford.edu

R.M. Brown, Jr. and I.M. Saxena (eds.), Cellulose: Molecular and Structural Biology, 35–48.

cellulose confomers that can form loose noncrystalline networks or robust crystalline structures. These provide a structural framework to the wall, which is crosslinked by hemicellulosic polymers and infiltrated with a dense pectic gel (Bacic et al. 1988; Carpita and McCann 2000). Noncellulosic polymers have relatively simple backbone structures that may be adorned with a varying complexity of carbohydrate branches (Table 3-1). It is likely that the polymers with β-linked homopolysaccharide backbones, such as that of xyloglucan, are synthesized by processive enzymes, whereas, the sugars comprising the branches are added to the backbone by nonprocessive enzymes, either following completion of the backbone chain or in concert with its biosynthesis (Henrissat et al. 2001; Perrin 2001). Polymers with α-1,4-linked backbone sugars, or heteropolysaccharide and mixed linkage backbones, such as the pectins (Table 3-3), are most likely synthesized by a different class of enzymes (Scheller et al. 1999).

Table 3-1. Basic structural composition of various cell wall polymers[a]

Polymer[a]	Backbone	Sidechains
Cellulose and Hemicelluloses		
Cellulose	β-1,4-glucan	None
Xylan	β-1,4-xylan	α-1,2-arabinose α-1,2-(4-O-methyl)-glucuronic acid
Xyloglucan	β-1,4-xylan	α-1,6-xylose α-1,2-fucosyl-β1,2-galactoysl-α1,6-xylose α-1,2-arabinosyl-α1,6-xylose
Mannan	β-1,4-mannan	α-1,6-galactose
Glucuronomannan	β-1,4-mannosyl-β-1,2-glucuronan	β-1,6-galactose α-1,3-arabinose
Glucomannan	β-1,4-glucosyl-(β-1,4-mannose)$_2$	α-1,6-galactose
Mixed-linked Glucan	β-1,3-glucosyl-(β-1,4-glucose)$_2$	None
Arabinogalactan II	β-1,3-galactan and β-1,6-galactan	β-1,3-arabinose
Pectins		
Galactan	β-1,4-galactan	None
Arabinogalactan I	β-1,4-galactan	(α-1,5-arabinosyl)$_2$-α-1,3-arabinose
Arabinan	α-1,5-arabinan	α-1,2-arabinose α-1,3-arabinose
Homogalacturonan	α-1,4-galacturonan	None
Xylogalacturonan	α-1,4-galacturonan	α-1,3-xylose
Rhamnogalacturonan I (RGI)	α-1,2-rhamnosyl-α-1,4-galacturonan	α-1,5-arabinan β-1,4-galactan arabinogalactan I
Rhamnogalacturonan II (RGII)	α-1,4-galacturonan	Various

[a]Brett and Waldron (1990); Carpita and McCann (2000).

2 IDENTIFICATION OF CELLULOSE SYNTHASE

Although cell-free synthesis of cellulose was claimed as early as 1964 (Karr 1976 and references therein), it was not possible to isolate the enzymes responsible for cellulose biosynthesis in plants by conventional biochemical techniques. A breakthrough in the identification of the enzymes came with the successful cloning of the cellulose synthesis operon of the bacterium *Acetobacter xylinum* (Saxena and Brown, Jr. 1990; Wong et al. 1990). Amino acid sequence analysis showed that cellulose synthase is a member of the glycosyl transferase family II (GT-2), which includes inverting processive nucleotide diphosphosugar glycosyl tranferases (Campbell et al. 1997; Saxena et al. 1995). Several conserved hydrophilic domains, including the proposed catalytic QXXRW motif (Table 3-2), were identified in the bacterial system. These conserved sequences were termed "U domains" to indicate "ubiquitous" presence in CESA proteins. Plant homologs of the bacterial cellulose synthase catalytic proteins were subsequently identified in an expressed sequence tag library from cotton (Pear et al. 1996).

The enzymes have several putative transmembrane domains (TMD). This is consistent with previous microscopic and biochemical data indicating that cellulose synthase is an integral membrane protein and that cellulose biosynthesis occurs at the plasma membrane (Mueller and Brown, Jr. 1980; Ross et al. 1991; Brown, Jr. et al. 1996; Delmer 1999). Visible by electron microscopy, the enzymes form large linear terminal complexes in the plasma membrane of bacteria and many algae whereas they form hexagonal rosette structures in higher plants and some algae (Mueller and Brown, Jr. 1980; Ross et al. 1991; Kimura et al. 1999). Delmer (1999) has speculated that the transmembrane domains may create a

Table 3-2. Protein model and conserved motifs for the rosette-forming eukaryotic cellulose synthase (*CESA*)

Protein Model[a]

Motif[b]	Amino Acid Sequence[c]
ZnBD	CQICGDDVGLAETGDVFVACNECAFPVCRPCYEYERKDGTQCCPQC
U1	DYPVDKVACYVSDDGSA
U2	TNGAYLLNVDCDHYFNNS
U3	SVTEDILTGFKMHARGWISIY
U4	RLNQVLRWALGSIEIL

[a]Model of the *Arabidopsis thaliana* CESA1 predicted protein. Black boxes represent putative transmembrane domains.

[b]Conserved 'U' motifs originally identified in bacterial cellulose synthases were used to identify the higher plant enzymes, which also contain a conserved zinc-binding domain (ZnBD) specific to the eukaryotic enzymes (Saxena et al. 1995).

[c]Sequences are for the *Arabidopsis* CESA1 protein. Proposed critical residues are underlined.

pore through which the glucan chain is extruded into the extracellular space. Each hexagonal plant cell rosette structure is thought to comprise six complexes of five or six enzymes, and synthesize microfibrils containing 30–36 glucan chains. In addition to the U domains, the plant enzymes contain a conserved N-terminal Zn-binding domain indicating a possible mechanism for association of the catalytic subunits (Table 3-1) (Kurek et al. 2001).

3 TOWARD A FUNCTIONAL ANALYSIS OF CELLULOSE SYNTHASE

Homology-based genomic identification of the *CESA* genes opened the door for meaningful genetic and biochemical studies and has been conclusively supported by both. *CESA* genes have been identified in numerous plant species. The completion of the *Arabidopsis thaliana* genome revealed ten cellulose synthase or *AtCESA* genes (Richmond 2000). Mutations in seven of the ten *AtCESA* genes have been studied (Table 3-3). The *rsw1-1* mutant, which was originally isolated on the basis of a temperature-sensitive root-swelling phenotype (Baskin et al. 1992), was found to carry an A549V mutation in the *AtCESA1* gene (Arioli et al. 1998). At the nonpermissive temperature, mutant plants produce less cellulose and more soluble β-1,4-glucan than wild-type plants. The mutation was proposed to interfere with assembly to the rosette synthase complex and aggregation of the β-1,4-glucan into microfibrils at the nonpermissive temperature (Arioli et al. 1988). Several additional alleles of *AtCESA1*, which have markedly reduced cellulose, have been reported (Williamson et al. 2001; Beeckman et al.

Table 3-3. The cellulose synthase (CESA)proteins of *Arabidopsis*

Protein	Gene Locus	Alleles[a]	Protein Length	Predicted pI[c]	Predicted TMD[b]	*Arabidopsis* ESTs[d]
CESA1	At4g32410	*rsw1*	1081	6.7	8	90
CESA2	At4g39350		1084	7.5	8	9
CESA3	At5g05170	*ixr1, eli1*, *cev1*	1065	7.6	8	49
CESA4	At5g44030	*irx5*	1049	8.0	8	10
CESA5	At5g09870		1069	7.3	8	10
CESA6	At5g64740	*prc1*, *ixr2*	1084	7.4	8	36
CESA7	At5g17420	*irx3*	1026	6.7	8	14
CESA8	At4g18780	*irx1*	985	7.1	8	12
CESA9	At2g21770		1088	6.9	8	1
CESA10	At2g25540		1065	6.5	8	8

[a]*rsw* = radially swollen (Arioli et al. 1998); *ixr* = isoxaben resistant (Scheible et al. 2001); *eli* = ectopic lignin (Cano-Delgado et al. 2000); *cev* = constitutive expression of VSP1 (Ellis et al. 2002); *irx* = irregular xylem (Turner and Somerville 1997); *prc* = procuste (Fagard et al. 2000).

[b]Based on intron/exon and transmembrane modeling (Richmond and Somerville 2000) using HmmTop v2.0 (Tusnády and Simon 2001).

[c]Isoelectric point predicted by ProtParam (http://us.expasy.org/tools/protparam.html).

[d]Expressed sequence tags reported by TAIR (http://www.*Arabidopsis*.org/).

2002; Gillmor et al. 2002). The embryos of nonconditional *AtCESA1* mutants are radially swollen in appearance, indicating decreased elongation even at early stages. Although the pattern of cell division appears relatively normal, incompletely formed cell walls are observed frequently (Beeckman et al. 2002). The epidermis of the mutants is markedly affected with an apparent complete loss of guard cells and pavement cell crenulation (Beeckman et al. 2002).

The radially swollen phenotype also occurs when wild-type plants are grown in the presence of the cellulose biosynthesis inhibitor, isoxaben. Mutations in *AtCESA3* and *AtCESA6* confer resistance to isoxaben (Scheible et al. 2001; Desprez et al. 2002). This is consistent with evidence that multiple AtCESA enzymes participate in the rosette structure (Taylor et al. 2003). Antisense studies also indicate a requirement for all three genes, *AtCESA1*, *AtCESA3* and *AtCESA6,* in primary wall formation (Burn et al. 2002). This finding is further supported by strong expression of *AtCESA1*, *AtCESA3* and *AtCESA6* in young expanding leaves (Hamann et al. 2004) and evidence from GUS:promoter fusion studies which indicates the genes are expressed in the same cells simultaneously (Scheible et al. 2001).

The different structures (e.g., degree of polymerization and crystallization) of cellulose in primary and secondary cell walls prompted the hypothesis that a separate complex of enzymes was specifically devoted to secondary wall biosynthesis (Karr 1976). This idea was supported by the isolation of the irregular xylem (*irx*) mutants with defects in the *AtCESA4*, *AtCESA7* and *AtCESA8* genes (Turner and Somerville 1997; Taylor et al. 1999, 2000, 2003). Stems of these mutants contained 30–50% less cellulose than wild-type plants (Turner and Somerville 1997; Taylor et al. 2003). Recent studies reveal that these three genes are coexpressed temporally and spatially in *Arabidopsis* stems and the proteins can be copurified (Hamann et al. 2004; Taylor et al. 2003). *AtCESA7* and *AtCESA9* gene expression apparently increase with leaf age (Hamann et al. 2004), providing additional evidence for the involvement of these genes in secondary wall formation. Together these data strongly support the involvement of three separate, coregulated, cellulose synthase proteins in secondary cellulose deposition.

Very little is known about the regulatory mechanisms underlying cell wall biogenesis. Preliminary evidence suggests that the *CESA* genes are regulated by circadian rhythm, hormones such as ethylene and cytokinin, salt stress and other factors (Hamann et al. 2004). There is also a proposed link between organization of the cortical microtubule cytoskeleton and cellulose deposition (Ledbetter and Porter 1963). Evidence from a variety of studies indicates that cortical microtubules are, in some way, involved in organizing cellulose deposition and microfibril orientation (Emons et al. 1992; Fowler and Quatrano 1997). Microscopic analysis of *rsw1* plants supports this proposed connection and suggests the relationship is bidirectional; decreased rates of cellulose synthesis apparently cause destabilization of cortical microtubule organization (Sugimoto et al. 2001). Interaction between cellulose biosynthesis and biotic stress-responsive pathways is indicated by analysis of a leaky *AtCESA3* mutant allele, *cev1* (Ellis et al. 2002). The *cev1* allele apparently

causes constitutive activation of both the jasmonate and ethylene signal pathways important in plant cell defense (Ellis and Turner 2001). *cev1* plants also apparently contain increased levels of pectin (Ellis and Turner 2001). Other instances of apparently compensatory increases in pectin have been documented in cellulose deficient mutant plants (Gillmor et al. 2002) and in cell cultures adapted to growth on an inhibitor of cellulose synthesis (Shedletzky et al. 1992). Another leaky *AtCESA3* allele, *eli1*, was isolated based on its production of ectopic lignin, presumably in response to cellulose deficiency (Cano-Delgado et al. 2000). These examples suggest the existence of complex regulatory processes that sense the functional properties of the cell wall and regulate complementary pathways to achieve cell walls with appropriate aggregate functionality.

There are now over 200 cellulose synthase sequences from at least 50 organisms in the public sequence databases. With the exception of the *CESA* genes of *Acetobacter* and those specifically expressed during fiber development in cotton (*GhCESA1*, *GhCESA2*) and during xylem development in poplar (*PtCESA2*, *PtCESA3*), few *CESA* genes from other organisms have been studied in detail (Holland et al. 2000). Not surprisingly, homologs of *CESA* genes are evident in the genomes of cyanobacteria and algae (Nobles et al. 2001; Roberts et al. 2002). The early divergence of *CESA* N-terminal sequences, the putative Zn-binding domain in particular, in the green algae appears to correlate with rosette versus linear terminal cellulose synthase complex formation (Roberts et al. 2002). The presence of several *CESA* sequences in the rosette forming green alga *Mesotaenium caldariorum* has interesting implications regarding temporal and/or spatial specificity of individual CESA proteins and may provide important clues to the composition of the early-evolving rosette complex.

4 IDENTIFICATION OF THE CELLULOSE SYNTHASE-LIKE GENES

In addition to the 10 *AtCESA* genes, 30 genes with significant similarity to cellulose synthase were identified in *Arabidopsis* (Table 3-4) (Richmond 2000). These cellulose synthase-like (*CSL*) genes have been classified into eight distinct families according to sequence divergence and intron/exon structures (Richmond 2000; Hazen et al. 2002). Together the *CESA* and *CSL* genes form the cellulose synthase superfamily. Interestingly, a *CSL* gene has also been identified in the cellulose-producing cyanobacterium, *Nostoc punctiforme* (Nobles et al. 2001), indicating an ancient lineage for these gene families.

The CSL proteins contain the GT-2 family signature as well as the conserved U domains containing catalytic aspartic acid residues and QXXRW motif (Table 3-2). Members of the superfamily differ in their size, topology, and predicted physical properties. A major difference between the proteins of the CSL and CESA families is the lack of the zinc-binding domain in most CSL family members (Richmond and Somerville 2000). This may indicate that CSL proteins do not participate in forming complexes to the same degree as the CESA proteins and supports a possible function of these enzymes in making single polymer chains rather than mul-

Table 3.4. The cellulose synthase-like (CSL) proteins of *Arabidopsis*

Name	Gene Locus	Predicted Protein Model[a,b]	Protein Length[a]	Predicted pI[c]	TMD[b]	ESTs[d]
CSLA1	At4g16590		554	9.2	7	9
CSLA2	At5g22740	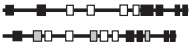	534	9.4	6 to 7	15
CSLA3	At1g23480	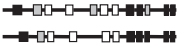	556	8.5	6 to 7	7
CSLA7[e]	At2g35650	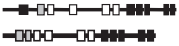	484	9	5 to 7	4
CSLA9 (*rat*4)[f]	At5g03760		533	9.2	6 to 7	9
CSLA10	At1g24070		585	8.8	7	2
CSLA11	At5g16190		504	9.3	6 to 7	3
CSLA14	At3g56000		535	6.5	5 to 6	2
CSLA15	At4g13410		500	8.8	4 to 6	0
CSLB1	At2g32610		757	7.3	8	5
CSLB2	At2g32620	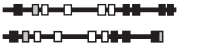	757	7.2	8	0
CSLB3	At2g32530		755	7.3	8	0
CSLB4	At2g32540		755	7.4	8	0
CSLB5	At4g15290		757	7.2	8	2
CSLB6	At4g15320		759	8.4	8	0
CSLC4	At3g28180		673	8.6	7	20
CSLC5	At4g31590		692	8.7	9	14
CSLC6	At3g07330		682	9.0	9	24
CSLC8	At2g24630		690	8.3	9	4
CSLC12	At4g07960	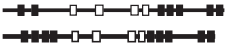	694	9.2	7 to 9	3
CSLD1	At2g33100		1036	7.9	8	1
CSLD2	At5g16910		1145	7.6	8	12
CSLD3 (*kjk*)[g]	At3g03050		1145	7.8	8	17
CSLD4	At4g3810		1111	6.6	8	2
CSLD5	At1g02730		1181	7.8	6 to 8	8
CSLD6	At1g32180		1181	7.8	8	0
CSLE	At1g55850		729	6.2	8	7
CSLG1	At4g24010		760	8.3	8	3
CSLG2	At4g24000		722	6.5	6 to 8	4
CSLG3	At4g23990		732	7.3	8	3

[a]Protein sequence based on intron/exon modeling performed by Todd Richmond (http://cellwall.stanford.edu/php/structure.php). Black boxes = putative transmembrane domains; White boxes = conserved 'U' domains; Grey boxes = hydrophobic regions manually.

[b]Transmembrane domains predicted with HmmTop v2.0 (Tusnády and Simon 2001).

[c]Isoelectric point predicted by ProtParam (http://us.expasy.org/tools/protparam.html).

[d]Expressed sequence tags reported by TAIR on July 1, 2003 (http://www.*Arabidopsis*.org/).

[e]An embryo lethal mutation (Goubet et al. 2003).

[f]*rat* refers to a mutant displaying resistance to *Agrobacterium tumefaciens*. (*Zhu* et al. 2003).

[g]*kjk* refers to *kojak*, a root-hairless mutant (Favery et al. 2001).

tichain fibrils. Biochemical evidence indicates that these polymers are mostly likely synthesized in the Golgi apparatus and exported into the extracellular space (Karr 1976; Carpita and McCann 2000). Thus, the localization of the CSL proteins to the Golgi has been proposed (Richmond and Somerville 2000).

Arabidopsis and rice appear to share only four of the gene families: *CSLA*, *CSLC*, *CSLD*, and *CSLE*. Rice appears to lack the *CSLG* and *CSLB* families and possess two additional families: *CSLF* and *CSLH*. Monocots and dicots do possess different cell wall architectures (Carpita and McCann 2000). Whether this classification of the *CSLs* truly represents a division between the monocots and dicots requires further study since biochemical functions have not yet been ascribed to the CSL proteins. Interestingly, the *CSL*s form two separate clades when compared with the *CESA* genes from plants and other organisms. The *CSLD*, *CSLG*, *CSLE* and *CSLB* families cluster with the plant *CESA* genes, whereas the *CSLA* family clusters with nonplant *CESA* genes (Richmond 2000). Although the *CSLC* family was not included in this analysis, its similarity to the *CSLC* family in *Arabidopsis* suggests that its members will also cluster with the nonplant *CESA* genes. This divergence at the gene level is further supported by analysis of the predicted protein structures. Analysis of the protein sequences (Table 3-4) supports the family assignments based on gene sequences and intron/exon structures.

Of all the *CSL* families, the *CSLD* family is most homologous to *CESA*, both at the gene and protein level (Richmond and Somerville 2000). At 1000 to 1200 amino acids, the CSLD proteins in *Arabidopsis* and rice are similar in size or larger than the CESA proteins and considerably larger than the other *CSL* gene products. The predicted isoelectric point (pI ~ 7) and relative positions of the eight transmembrane domains are similar to those of the CESAs (Tables 3-1 and 3-4). Members of the *CSLD* family in both *Arabidopsis* and rice contain very few introns. These factors all suggest the possibility that *CSLD* family members represent genetic ancestors of the *CESA* family and may also produce β-1,4-linked glucan (Richmond and Somerville 2000). Expression of the *CSLD* family members in *Arabidopsis* is quite varied. *AtCSLD2* is also expressed in older, expanded leaves, whereas *AtCSLD5* is expressed in flowers and young, expanding leaves (Hamann et al. 2004). *AtCSLD2* and *AtCSLD3* are strongly expressed in roots and negatively regulated by salt stress (Hamann et al. 2004). Additionally, *AtCSLD3* is negatively regulated by light and is apparently the only *CSL* negatively regulated by cytokinin (Hamann et al. 2004).

Expression of a tobacco *CSLD* (*NaCSLD1*) has been observed in growing pollen tubes (Doblin et al. 2001). *The enzyme* was proposed to function as a tip-growth specific cellulose synthase; however, root hairs, another tip-growing system, were not analyzed and no biochemical evidence for such a functional assignment was reported. *NaCSLD1*is an apparent ortholog of *AtCSLD4* (Doblin et al. 2001). Unfortunately, because of the incomplete information available for the tobacco genome, it is not currently possible to assess this assignment. The only mutant allele of a *CSLD* family member so far reported is *kojak*

(*kjk*), an allele of *AtCSLD3* exhibiting a defect in root hair formation (Favery et al. 2001). Northern and DNA chip analyses indicate that expression of the *Arabidopsis CSLD3* gene is not restricted to tip-growing cells (Favery et al. 2001; Hamann et al. 2004).

Of all the *CESA*/*CSL* superfamily members, the *CSLA* and *CSLC* genes are the most divergent from the *CESA* genes (Richmond and Somerville 2000). The predicted protein sequences of CSLA and CSLC family members in *Arabidopsis* exhibit some interesting features. Whereas, the CESA proteins and most other members of the other CSL families possess eight putative transmembrane domains, two in the N-terminus and six clustered in the C-terminus, most of the AtCSLA and AtCSLC proteins exhibit only four to five C-terminal transmembrane domains, respectively (Table 3-4). In addition, many of the AtCSLC predicted protein sequences contain hydrophobic regions around 50 amino acids C-terminal of the second putative transmembrane domain, which may represent two additional transmembrane domains. An additional hydrophobic region, located between the conserved U2 and U3 domains of the catalytic loop is apparent in the protein sequences of CSLA2 and CSLA9 (Table 3-4). The very interesting topologies of members of these two CSL families could have important functional consequences and merit further examination. For example, if the hydrophobic regions represent transmembrane domains which participate in forming a pore through which product is extruded, is the pore structure altered in these two families compared to the CESA and other CSL proteins and how does it affect catalysis, substrate specificity, product export, and regulation by binding partners? If these additional hydrophobic regions are not transmembrane domains, do they participate in protein–protein interactions thus specifying binding partners or are they simply involved in maintaining structural stability of the catalytic loops?

The CSLA and CSLC proteins exhibit basic pI values ranging from 8.3 to 9.2 for the CSLCs and 6.5 to 9.4 for the CSLAs (Table 3-4). There is a stretch rich in basic amino acids between the third and fourth C-terminal transmembrane domains. The other CSL family members contain a short acidic loop and putative transmembrane domain in this region. If the topology of the enzyme is such that the catalytic loop is in the cytosol (Delmer 1999), this basic loop is predicted to be extracellular. Its proximity to the proposed pore formed by the transmembrane domains is particularly intriguing. One possible role for this loop is in the formation of salt bridges with other protein partners, such as nonprocessive glycosyl transferases that may be involved in adding sugar branches. Alternatively, this loop may interact with the emerging carbohydrate chain, perhaps to facilitate chain extension. Hemicelluloses are mostly insoluble at neutral pH. A locally alkaline pH could conceivably facilitate production of these polymers.

Two mutations in the *Arabidopsis CSLA* family have been reported. A mutation of *CSLA9* (*rat4*) was isolated based on its ability to confer resistance to transformation by *Agrobacterium tumefaciens* (Zhu et al. 2003). A mutation

in the *AtCSLA7* gene results in an embryo lethal phenotype, severely affecting the pattern of cell division in the early globular stage and disrupting cellularization of the endosperm (Goubet et al. 2003). Pollen tube growth is also impaired in the mutant. *AtCSLA7* is expressed strongly in flowers, in accordance with a role in embryogenesis (Hamann et al. 2004). These results suggest that the *AtCSLA7* has a nonredundant, widespread function in *Arabidopsis* and may be particularly critical to establishing new wall placement and/or cell wall extension. Biochemical analysis of the walls of these mutants has not yet been reported.

Expression of the *AtCSLA* and *AtCSLC* genes also may indicate related functionality of the enzymes in these families (Hamann et al. 2004). Both *AtCSLA9* and *AtCSLC4* are expressed throughout the plant but show especially strong expression in stems (Hamann et al. 2004), consistent with a role for these enzymes in secondary wall formation. This, in turn, might suggest a role in hemicellulose production.

The *CSLG* family represents the only proposed dicot-specific family. There are three *CSLG* genes in the *Arabidopsis* genome arranged in tandem on chromosome four. The family may be larger in other dicots. For example, *Medicago truncatula* exhibits expressed sequence tags for six *CSLG* family members (Richmond and Somerville 2001). In *Arabidopsis* expression of the *CSLG* family members is relatively low, with *CSLG2* and *CSLG3* expressed in flowers and *CSLG1* and *CSLG3* expressed in leaves. Predicted protein sequences of the *AtCSLG* family members exhibit the closest similarity with those of the *CSLE* family member in *Arabidopsis* and rice. Like the *CESA* and *CSLD* proteins, members of the *CSLG* family from *Arabidopsis* and *Medicago* have eight putative transmembrane domains (Table 3-4). The *Arabidopsis* proteins in TAIR are annotated to contain a putative actinin-type actin binding motif (PROSITE PS00019 signature) in the C-terminal region of the protein between the fourth and fifth transmembrane domains. Although provocative, this assignment is dubious for two reasons. First, analysis of the *CSLG* family members of *Medicago* indicates some loss of this consensus sequence. Second, there is a second signature motif in the actinin-type proteins that appears to be essential for actin binding (PROSITE PS00020) which is absent in the *CSLG* predicted proteins.

In *Arabidopsis*, the *CSLB* family represents a tightly clustered group of six genes. The family is apparently absent from rice although the proposed cereal specific *CSLH* family appears related (Hazen et al. 2002). Predicted proteins of the CSLB family show structures very similar to the CSLD proteins, with eight putative transmembrane domains and neutral predicted pI values. There are few expressed sequence tags for this family in the *Arabidopsis* database, perhaps indicating a specialized function. The family exhibits very low levels of expression compared to the other *CSL* families (Hamann et al. 2004). *AtCSLB4* appears to be preferentially expressed in seedlings, whereas *AtCSLB5* is apparently preferentially expressed roots (Hamann et al. 2004). Several other family members, *AtCSLB1*, *AtCSLB2* and *AtCSLB6*, are negatively regulated by ethylene,

possibly indicating a role in cell expansion (Hamann et al. 2004). This is also supported by expression of *AtCSLB1*, *AtCSLB2* and *AtCSLB5* which appear to be preferentially expressed in young, expanding leaves compared to older leaves (Hamann et al. 2004).

There is only one *CSLE* gene in *Arabidopsis* (Richmond and Somerville 2000). The rice genome apparently encodes two *CSLE* genes. The OsCSLE2 predicted protein contains an altered *Q*XX*RW* domain with the sequence *Q*ILVLYK*RW* (Hazen et al. 2002). It will be interesting to see whether this protein is catalytically active. The sequences of the *CSLE* gene and encoded protein are sufficiently different from the other *CESA*/*CSL* superfamily members that the presence of only one copy of the gene in *Arabidopsis* is rather interesting. Expression of the *CSLE* gene is widespread with highest expression levels in seedlings, roots and older leaves (Hamann et al. 2004). The AtCSLE protein has the lowest predicted pI of the CSLs at 6.2. The overall topology is similar to that of the CSLB proteins except for a small hydrophobic region just N-terminal of the U1 domain.

Two apparent "cereal-specific" CSL families, *CSLF* and *CSLH* have been proposed. The rice *CSLF* family is highly related to both the *CESA*s and *CSLD*s (Hazen et al. 2002). Cereals produce a unique mixed-linkage glucan, which contains an alternating β-1,4-glucosyl-β-1,3-glucan backbone. It is therefore tempting to assign the CSLF proteins to production of this polymer, although this new family has not yet been the subject of biochemical analyses. The *CSLH* family is related to the *CSLB* family. Whether the *CSLF* and *CSLH* families are truly specific to monocots, cereals or the rice genome, or whether they are actually members of the *CSLD* and *CSLB* families will become evident as more full-length sequences in these families become available.

A role for the CESA enzymes in cellulose biosynthesis is well established. However, the biochemical function of the related CSL proteins is less certain. The phenotypes of the available mutations in *CSL* genes are consistent with the hypothesis that the *CSL* genes have roles in cell wall synthesis. Although mutations in many of the *CSL* genes show significant changes in the FTIR spectra of cell walls (Raab, Youngs, Milne and Somerville, unpublished), it has not yet been possible to identify reproducible differences in the amounts of cell wall polysaccharides. We believe that this reflects limitations in the analytical methods currently available for analysis of cell wall polysaccharide composition. In addition, we consider it possible that some changes in cell wall composition resulting from mutations in *CSL* genes may result in compensatory changes in other polysaccharides that tend to obscure the direct effects of the mutations.

Acknowledgments

This work was supported, in part, by grants from the US National Science Foundation and the US Department of Energy (DE-FG02-03ER20133). We thank Jennifer Milne and Michelle Facette for useful discussion of this manuscript.

REFERENCES

Arioli T., Peng L., Betzner A.S., Burn J., Wittke W., Herth W., Camilleri C., Hofte H., Plazinski J., Birch R., et al. 1998. Molecular analysis of cellulose biosynthesis in *Arabidopsis*. Science 279:717–720.

Bacic A., Harris P.J., and Stone B.A. 1988. Structure and function of plant cell walls. The Biochemistry of Plants 14:299–371.

Baskin T.I., Betzner A.S., Hoggart R., Cork A., and Williamson R.E. 1992. Root morphology mutants in *Arabidopsis thaliana*. Aust J Plant Physiol 19:427–437.

Beeckman T., Przemeck G.K.H., Stamatiou G., Lau R., Terryn N., De Rycke R., Inze D., and Berleth T. 2002. Genetic complexity of cellulose synthase A gene function in *Arabidopsis* embryogenesis. Plant Physiol 199:1883–1903.

Brett C. and Waldron K. 1990. *Physiology and Biochemistry of Plant Cell Walls*. Chapman & Hall, London.

Burn J.E., Hocart C.H., Birch R., Cork A., and Williamson R.E. 2002. Functional analysis of the cellulose synthase genes, CESA1, CESA2, and CESA3 in *Arabidopsis*. Plant Physiol 129:797–807.

Campbell J.A., Davies G.J., Bulone V., and Henrissat B. 1997. A classification of nucleotide-diphospho-sugar glycosyltransferases based on amino acid sequence similarities. Biochem J 326:929–939.

Cano-Delgado A.I., Metzlaff K., and Bevan M.V. 2000. The *eli1* mutation reveals a link between cell expansion and secondary cell wall formation in *Arabidopsis*. *Development* 127:3395–3405.

Carpita N. and McCann M. 2000. The cell wall. In Buchanan, B.B. Gruissem, W. Jones, R. (eds.) *Biochemistry and Molecular Biology of Plants*. American Society of Plant Physiologists, Maryland, pp. 52–108.

Delmer D.P. 1999. Cellulose biosynthesis: exciting times for a difficult field of study. Annu Rev Plant Physiol Plant Mol Biol 50:245–276.

Desprez T., Vernhettes S., Fagard M., Refregier G., Desnos T., Aletti E., Py N., Pelletier S., and Hofte H. 2002. Resistance against herbicide isoxaben and cellulose deficiency caused by distinct mutations in same cellulose synthase isoform CESA6. Plant Physiol 128:482–490.

Doblin Ms., DeMelis L., Newbigin E., Bacic A., and Read S.M. 2001. Pollen tubes of *Nicotiana alata* express two genes from different β-glucan synthase families. Plant Physiol 125:2040–2052.

Ellis C. and Turner J.G. 2001. The *Arabidopsis* mutant *cev1* has constitutively active jasmonate and ethylene signal pathways. Plant Cell 13:1025–1033.

Ellis C., Karafyllidis I., Wasternack C., and Turner J.G. 2002. The *Arabidopsis* mutant *cev1* links cell wall signaling to jasmonate and ethylene responses. Plant Cell 14:1557–1566.

Emons A.M.C., Derksen J., and Sassen M.M.A. 1992. Do microtubules orient plant cell wall microfibrils? Physiol Plantarum 84:486–493.

Fagard M., Desnos T., Desprez T., Goubet F., Refregier G., Mouille G., McCann M., Rayon C., Vernhettes S., and Hofte H. 2000. *PROCUSTE1* encodes a cellulose synthase required for normal cell elongation specifically in roots and dark-grown hypocotyls of *Arabidopsis*. Plant Cell 12:2409–2424.

Favery B., Ryan E., Foreman J., Linstead P., Boudonck K., Steer M., Shaw P., and Dolan L. 2001. *KOJAK* encodes a cellulose synthase-like protein required for root hair cell morphogenesis in *Arabidopsis*. Genes Dev 15:79–89.

Fowler J.E. and Quantrano R.S. 1997. Plant cell morphogenesis: plasma membrane interactions with the cytoskeleton and cell wall. Annu Rev Cell Dev Biol 13:697–743.

Gillmor C.S., Poindexter P., Loriaeu J., Palcic M.M., and Somerville C. 2002. α-Glucosidase I is required for cellulose biosynthesis and morphogenesis in *Arabidopsis*. J Cell Biol 156:100–1013.

Goubet F., Misrahi A., Park S.K., Zhang Z., Twell D., and Dupree P. 2003. AtCSLA7, a cellulose synthase-like putative glycosyltransferase, is important for pollen tube growth and embryogenesis in *Arabidopsis* Plant Physiol 131:547–557.

Hamann T., Osborne E., Youngs H.L., Misson J., Nussaume L., and Somerville C. 2004. Global expression analysis of *CesA* and *CSL* genes in *Arabidopsis*. Cellulose 11:279–286.

Hazen S.P., Scott-Craig J.S., and Walton J.D. 2002. Cellulose synthase-like genes of rice. *Plant Physiol* 128:336–340.

Henrissat B., Coutinho P.M., and Davies G.J. 2001. A census of carbohydrate-active enzymes in the genome of *Arabidopsis thaliana*. Plant Mol Biol 47:55–72.

Holland N., Holland D., Helentjaris T., Dhugga K., Xoconostle-Cazares B., and Delmer D.P. 2000. A comparative analysis of the plant cellulose synthase (*CESA*) gene family. Plant Physiol 123:1313–1323.

Karr A.L. 1976. Cell wall biogenesis. In: *Plant Biochemistry*, 3rd edn. Academic Press, New York, p. 405–426.

Kimura S., Laosinchai W., Itoh T., Cui X., Linder R., and Brown, Jr. R.M., 1999. Immunogold labeling of rosette terminal cellulose-synthesizing complexes in the vascular plant *Vigna angularis*. Plant Cell 11:2075–2085.

Kurek I., Kawagoe Y., Jacob-Wilk D., Doblin M., and Delmer D. 2002. Dimerization of cotton fiber cellulose synthase catalytic subunits occurs via oxidation of the zinc-binding domains. Proc Natl Acad Sci USA 99:11109–1114.

Mueller S.C. and Brown, Jr. R.M., 1980. Evidence for an intramembrane component associated with a cellulose microfibril-synthesizing complex in higher plants. J Cell Biol 84:315–326.

Nobles D.R., Romanovicz D.K., and Brown, Jr. R.M., 2001. Cellulose in cyanobacteria. Origin of vascular plant cellulose synthase? Plant Physiol 127:529–542.

Pear J., Kawagoe Y., Schreckengost W.E., Delmer D.P., and Stalker D.M. 1996. Higher plants contain homologs of the bacterial celA genes encoding the catalytic subunit of cellulose synthase. Proc Natl Acad Sci USA 93:12637–12642.

Perrin R., Wilkerson C., and Keegstra K. 2001. Golgi enzymes that synthesize plant cell wall polysaccharides: finding and evaluating candidates in the genomic era. Plant Mol Biol 47:115–130.

Richmond T.A. and Somerville C.R. 2000. The cellulose synthase superfamily. Plant Physiol 124:495–498.

Richmond T. 2000. Higher plant cellulose synthases. Genome Biol 1:reviews3001.1–3001.6.

Richmond T.A. and Somerville C.R. 2001. Integrative approaches to determining CSL function. Plant Physiol 47:131–143.

Roberts A.W., Roberts E., and Delmer D.P. 2002. Cellulose synthase (*CESA*) genes in the green alga *Mesotaenium caldarium*. Eukaryotic Cell 1:847–855.

Ross P., Mayer R., and Benziman M. 1991. Cellulose biosynthesis and function in bacteria. Microbial Rev 55:35–58.

Saxena I.M., Lin F.C., and Brown, Jr. R.M., 1990. Cloning and sequencing of the cellulose synthase catalytic subunit gene of *Acetobacter xylinum*. Plant Mol Biol 15:673–683.

Saxena I.M., Brown, Jr. R.M., Fevre M., Geremia R.A., and Henrissat B. 1995. Multidomain architecture of β-glycosyl transferases: implications for mechanism of action. J Bacteriol 177:1419–1424.

Shedletzky E., Shmuel M., Trainin T., Kalman S., and Delmer D. 1992. Cell-wall structure in cells adapted to growth on the cellulose-synthesis inhibitor 2,6-dichlorobenzonitrile - a comparison between 2 dicotyledonous plants and a gramineous monocot. Plant Physiol 100:120–130.

Scheible W.R., Eshed R., Richmond T., Delmer D., and Somerville C. 2001. Modifications of cellulose synthase confer resistance to isoxaben and thiazolidinone herbicides in the *Arabidopsis ixr1* mutants. Proc Natl Acad Sci USA 98:10079–10084.

Scheller H.V., Doong R.L., Rodley B.L., and Mohnen D. 1999. Pectin biosynthesis: a solubilized α-1,4-galctouronosyl transferase from tobacco catalyzes the transfer of galacturonic acid from UDP-galacturonic acid onto the reducing end of homogalacturonan. Planta 207:512–517.

Sugimoto K., Williamson R.E., and Wasteneys G.O. 2001. Wall architecture in the cellulose-deficient *rsw1* mutant of *Arabidopsis thaliana*: microfibrils but not microtubules lose their transverse alignment before microfibrils become unrecognizable in the mitotic and elongation zones of roots. Protoplasma 215:172–183.

Taylor N.G., Scheible W.R., Cutler S., Somerville C.R., and Turner S.R. 1999. The irregular xylem 3 locus of *Arabidopsis* encodes a cellulose synthase gene required for secondary cell wall synthesis. Plant Cell 11:769–780.

Taylor, N.G., Laurie S., and Turner S.R. 2000. Multiple cellulose synthase catalytic subunits are required for cellulose synthesis in *Arabidopsis*. Plant Cell 12:2529–2539.

Taylor N.G., Howells R.M., Huttly A.K., Vickers K., and Turner S.R. 2003. Interactions among three distinct CESA proteins essential for cellulose synthesis. Proc Natl Acad Sci USA 100:1450–1455.

Turner S.R. and Somerville C.R. 1997. Collapsed xylem phenotype of *Arabidopsis* identifies mutants deficient in cellulose deposition in the secondary cell wall. Plant Cell 9:689–701.

Tusnády G.E. and Simon I. 2001. The HMMTOP transmembrane topology prediction server. Bioinformatics 17:849–850.

Williamson R.E., Birch J.E., Baskin T.I., Arioli T., Betzner A.S., and Cork A. 2001. Morphology of *rsw1*, a cellulose-deficient mutant of *Arabidopsis thaliana*. Protoplasma 215:116–127.

Wong H., Fear A., Calhoon R., Eichinger G., Mayer R., Amikam D., Benziman M., Gelfand D., Meade J., Emerick A., Bruner R., Benbassat A., and Tal R. 1990. Genetic organization of the cellulose synthase operon in *Acetobacter xylinum*. Proc Natl Acad Sci USA 87:8130–8134.

Zhu Y., Nam J., Humara J.M., Mysore K.S., Lee L.-Y., Cao H., Valentine L., et al. 2003. Identification of *Arabidopsis rat* mutants. Plant Physiol 132:494–50

CHAPTER 4

CELLULOSE SYNTHESIS IN THE ARABIDOPSIS SECONDARY CELL WALL

NEIL G. TAYLOR[1] AND SIMON R. TURNER[2,*]

[1] *CNAP, Department of Biology, University of York, Heslington, York, YO10 5DD, UK;*
[2] *School of Biological Sciences, 3.614 Stopford Building, The University of Manchester, Oxford Road, Manchester, M13 9PT, UK*

Abstract

The identification of genes responsible for cellulose synthesis has led to a significant advance in our understanding of the production of this important polymer. The identification of these genes has been possible due to the isolation of cellulose deficient mutants. The *irregular xylem* (*irx*) mutants of *Arabidopsis* are caused by a severe reduction in cellulose synthesis in the secondary cell wall. Three *irx* mutants deficient in secondary cell wall cellulose are the result of mutations in three different members of the cellulose synthase catalytic subunit (*CesA*) gene family. The three proteins encoded by these genes all associate within the same membrane bound complex, and the presence of all three, but not their activity, is required for correct assembly and targeting of this complex to the plasma membrane. In wild-type plants CesA proteins colocalize with microtubules, however, microtubule assembly and stability appears to be independent of CesA protein localization. A GFP-tagged version of IRX3 has revealed a novel pattern of fluorescence suggesting that CesA protein localization may be a dynamic process in which it may be frequently removed and or/recycled from the plasma membrane. Another *irx* mutant was found to be the result of a mutation in the *KORRIGAN* gene, previously shown to be involved in primary cell wall cellulose synthesis. This protein does not appear to be an integral part of the cellulose synthase complex, and possibly acts late on in the process of cellulose synthesis.

Keywords

Arabidopsis, cell wall, cellulose, cellulose synthesis, irregular xylem, mutant.

* Author for correspondence: Tel: 44 (0) 161 2755751; Fax: 44 (0) 161 2753938; e-mail: Simon.turner@manchester.ac.uk

R.M. Brown, Jr. and I.M. Saxena (eds.), Cellulose: Molecular and Structural Biology, 49–61.

1 INTRODUCTION

Cellulose is an essential component of the plant primary cell wall, where it is considered a vital component of the load bearing network and an important determinant of the orientation of cell expansion. After a period of expansion some cell types lay down a thick secondary cell wall inside the primary wall. Cellulose is often the most abundant component of these plant secondary cell walls and can make up a large proportion of the dry weight of these walls.

Despite the importance and abundance of cellulose however, identification of the components of the cellulose synthesizing machinery has, until recently, been slow. Initial attempts to isolate components of the cellulose synthase complex (CSC) centered upon purifying cellulose synthase activity. However, this proved very difficult. This may be due to a number of factors such as the large size of the complex and/or the presence of labile cofactors. In addition, there are problems associated with assaying activity, which have resulted in only low levels of cellulose synthase activity in preparations that also contain very high levels of callose synthase activity (Kudlicka et al. 1995; Kudlicka and Brown, Jr. 1997). A recent study has reported high levels of cellulose synthesis *in vitro* from a solubilized microsome preparation from blackberry cell lines. While this method has been important in demonstrating cellulose synthase activity under relatively simple conditions, it is reported that these conditions are not suitable for assaying cellulose synthesis in *Arabidopsis* (Lai-Kee-Him et al. 2002) and does not involve purification of the complex.

Alternative approaches searching for genes demonstrating sequence similarity to genes involved in bacterial cellulose synthesis initially proved equally slow. It was not until 1996 that the first gene showing limited homology to these genes was identified from cotton (Pear et al. 1996).

Subsequent genetic approaches using the model plant *Arabidopsis thaliana* has led to the identification of several genes essential for cellulose synthesis.

2 *irx* MUTANT ISOLATION AND CHARACTERIZATION

A series of mutants were isolated from a screen involving the microscopic examination of cross sections of stems from a chemically mutagenized population. These mutations, termed *irregular xylem* (*irx1 to irx5*), caused a collapse of mature xylem cells in the inflorescence stems of *Arabidopsis* (Turner and Somerville 1997; Taylor et al. 2003) (Figure 4-1). This collapse of the xylem vessels is thought to be due to a weakness in the secondary cell wall of the xylem cells which results in them being unable to withstand the negative pressure generated during water transport up the stem. Consequently, such mutants should identify components that are essential for maintaining the physical properties of the xylem secondary cell wall. Although most frequently and conveniently studied in stems, the collapsed xylem phenotype was also seen in mature hypocotyls and in the primary root and petioles. In general the *irx* mutants otherwise appear little different to wild-type, though they may appear slightly smaller, darker green and with narrower leaves than the wild-type.

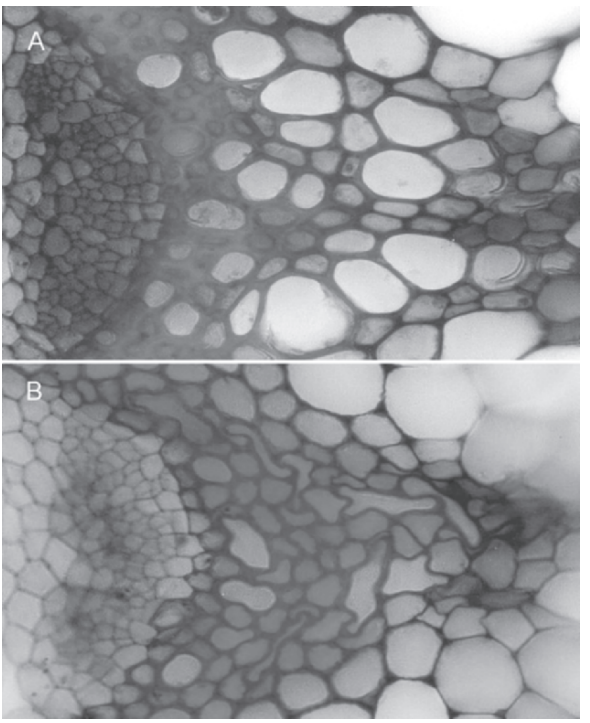

Figure 4-1. Irregular xylem phenotype. Toluidine blue stained sections of *Arabidopsis* vascular bundles from wild-type (**a**) and *irx1-1* (**b**)

One of the *irx* mutants (*irx4*) is attributed to a defect in the lignin biosynthesis gene cinnamoyl CoA reductase (Jones et al. 2001).

Analysis of the cell wall composition of the other 4 mutants (*irx1,2,3 and 5*) revealed that the only significant difference was a severe reduction in the amount of cellulose in the stems. Each mutant contains approximately a third the amount of cellulose of wild-type (Turner and Somerville 1997; Taylor et al. 2003). There are little if any changes in other components of the wall such as non-cellulose polysaccharides and phenolics (Turner and Somerville 1997). Furthermore, there was little, if any, change in cellulose content of the leaves. Together this data suggests that the mutants were caused by a specific reduction in cellulose synthesis in the secondary cell walls.

3 THREE CesAs ARE REQUIRED FOR SECONDARY CELL WALL CELLULOSE SYNTHESIS

Cloning the genes affected in *irx1*, *irx3* and *irx5* revealed all three mutations to be in different members of the cellulose synthase (CesA) gene family, showing high levels of homology to the previously identified cotton gene (Taylor et al. 1999;

Taylor et al. 2000; Taylor et al. 2003). There are 10 members of the CesA gene family in *Arabidopsis*. Using the now accepted nomenclature for these genes, *IRX1* corresponds to *AtCesA8*, *IRX3* corresponds to *AtCesA7* and *IRX5* corresponds to *AtCesA4*. It is clear from microscopic studies that the phenotype of the xylem vessels in these three mutants is indistinguishable (Turner and Somerville 1997; Taylor et al. 2000; Taylor et al. 2003). This, along with the fact that all three mutants have approximately a third of the cellulose of wild-type, indicates that these three genes are not redundant, and that they are active in the same cells. Tissue printing with antibodies specific to each of the three proteins revealed the presence of all three within the same cells (Turner and Somerville 1997; Taylor et al. 2003). Since all three proteins appeared to be required in the same cells, it was important to determine whether they interacted directly in the same protein complex. An epitope tag, consisting of the recognition sequence for a highly specific monoclonal antibody (RGSHHHH) and a hexahistidine sequence, was inserted at the amino terminus of the *IRX3* gene. This epitope tagged *IRX3* was then transformed into *irx3-1* plants, which lack IRX3 protein, and found to complement the mutation, confirming that the epitope tag had no effect on the function of the enzyme (Taylor et al. 2000).

In order to determine whether these three proteins were associated, detergent solubilized extracts from tagged IRX3 plants were bound to nickel resin to purify the tagged IRX3. A large proportion of the IRX3 bound to the resin, and was specifically eluted by increasing the imidazole concentration, consistent with the binding being due to the hexahistidine sequence. IRX1 and IRX5 were found to follow almost identical patterns of binding. Binding of these proteins was absolutely dependent on the presence of the histidine tagged IRX3, and other plasma membrane proteins did not bind to the resin demonstrating specific interactions between IRX3, IRX1 and IRX5 (Taylor et al. 2003).

4 FUNCTION OF MULTIPLE CesA PROTEINS DURING CELLULOSE SYNTHESIS

Three possibilities would explain the requirement for multiple CesA proteins: different CesA proteins assemble into separate complexes containing only a single type of CesA protein; different CesA proteins are randomly assembled dependent upon what subunits are available; or that the presence of three distinct CesA proteins is required for ordered assembly of the cellulose synthase complex. The first explanation does not fit the data described. Detailed analysis of *irx3-1* plants suggest that they have no cellulose in the secondary cell wall. If IRX1 and IRX5 were able to function independently from IRX3, they would still be able to synthesize at least some cellulose. Furthermore, the coprecipitation experiment described above suggest that IRX1, 3 and 5 all associate as part of the same complex which is clearly inconsistent with this idea. In order to distinguish the last two possibilities experiments were carried out using alleles in which one of the CesA proteins is missing. The idea is illustrated diagrammatically in

Figure 4-2a. In an *irx5-1* mutant the IRX5 protein is undetectable (Taylor et al. 2003). If the proteins randomly associate then IRX1 and IRX3 should still be able to form a complex (Figure 4-2a top). Immunoprecipitation using antibodies specific to each protein was used to investigate the interaction between these subunits in different mutant backgrounds. In wild-type, each of the antibodies is capable of precipitating all three proteins, consistent with them interacting in the same protein complex. In *irx5-1* plants, however, where there is no IRX5 protein, the IRX1 antibody no longer precipitated IRX3, and the IRX3 antibody no longer precipitated IRX1. This suggests that the presence of all three proteins

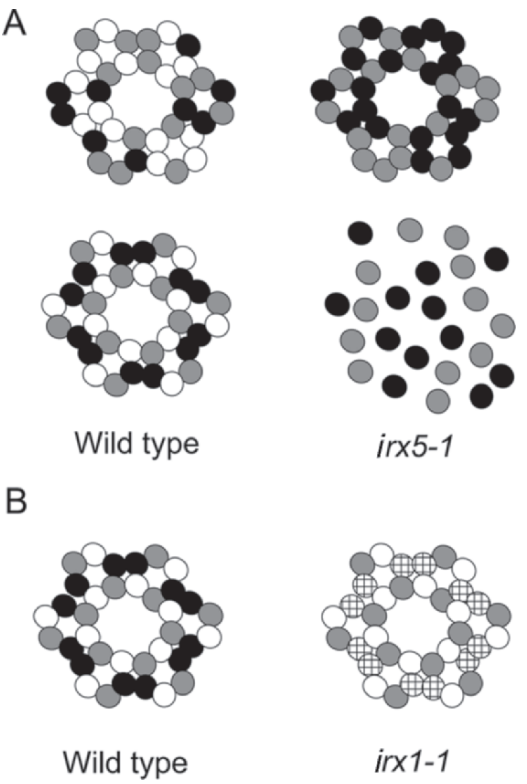

Figure 4-2. Organization of CesA proteins in the cellulose synthase complex. Diagram to illustrate the effect of different mutations on a model of the cellulose synthase complex. The wild-type complex is arbitrarily drawn as a hexameric structure with each lobe containing 6 CesA polypeptides, IRX1, IRX3 and IRX5 subunits are represented by black, grey, and white fill respectively. (**a**) The two possibilities represent IRX1, IRX3, and IRX5 assembled in either a random (top) or ordered (bottom) manner. If the assembly was random in an *irx5-1* mutant IRX1 and IRX3 would still associate into a functional complex (top) whereas the experimental data supports the ordered assembly (bottom), since in the absence of IRX5, IRX1, and IRX3 no longer associate. (**b**) In *irx1-1* mutants IRX1 subunits are represented by hashed shading to indicate the fact that the subunit is present, but considered not to function

is required for the correct assembly of the cellulose synthase complex. In the absence of any of the three CesA proteins the remaining subunits are no longer able to associate (Figure 4-2a bottom).

While the above experiments suggest that all three proteins are required for assembly of the complex they do not address whether the activity of all three proteins is required. The *irx1-1* allele is caused by a point mutation that alters a highly conserved aspartate residue believed to be absolutely essential to catalysis. The resulting protein is presumed to have no catalytic activity (Taylor et al. 2000), though there are comparable amounts of the mutant protein present compared to wild-type. Co-immunoprecipitation experiments from *irx1-1* extracts showed that antibodies specifically recognizing IRX3 and IRX5 are capable of precipitating IRX1 in a manner identical to that in wild-type (Taylor et al. 2003). Thus it appears that the presence, but not the activity, of all three proteins is essential for their correct assembly into a complex (Figure 4-2b).

Compared to *irx3-1* or *irx5-1, irx1-1* plants contain a smaller reduction in the amounts of cellulose in the secondary cell wall, despite the fact that IRX1 subunits are unlikely to be active. One possible explanation for this observation is that IRX3 and IRX5 are able to make some cellulose even in the absence of an active IRX1 subunit. If this idea is correct and IRX1, IRX3 and IRX5 all carry out a similar function within the cellulose synthase complex the prediction is that *irx1-1* plants will make abnormal cellulose with each cellulose synthase complex making fewer β(1-4)-glucose chains than in the wild-type.

5 LOCALIZATION OF CesA PROTEINS

In developing xylem vessels bands of microtubules mark the sites of secondary cell wall deposition. The *Arabidopsis* root is a convenient system for studying vessel development since protoxylem initiates in a predictable manner just behind the root apical meristem. In the youngest vessels in which IRX3 staining is detectable the protein appears dispersed within the cell and the microtubules exhibit no easily discernable pattern. As the vessels mature, microtubules become localized in bands at the plasma membrane, and some IRX3 staining becomes associated with these bands. At late stages of xylem development most of the IRX3 staining colocalizes with the microtubule bands and little is present in the cell (Figure 4-3). IRX1 and IRX5 also show this pattern of localization in developing xylem vessels (Gardiner et al. 2003).

In *irx3-1* or *irx5-1* plants that lack one of the CesA subunits the remaining two subunits do not localize to the plasma membrane. The remaining subunits appear to be retained within the cell, possibly within the endoplasmic reticulum. In plants containing an inactive form of one of the enzymes however (*irx1-1*), all three subunits are localized to the plasma membrane, indicating that the presence, but not the activity, of all three proteins is required for correct targeting to the plasma membrane (Gardiner et al. 2003) supporting the immunoprecipitation experiments outlined above.

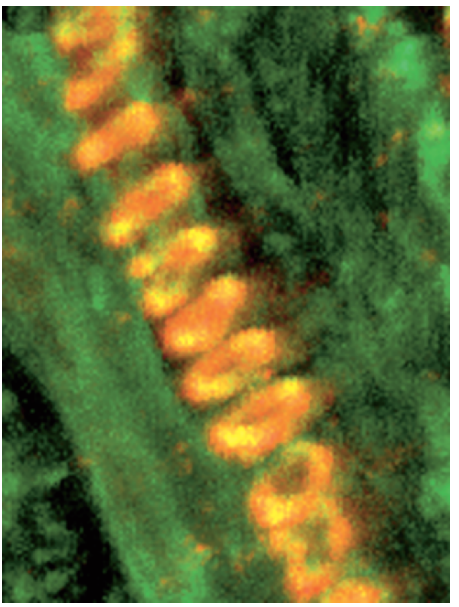

Figure 4-3. Colocalization of IRX3 with microtubules. Projection of a series of images obtained from confocal microscopy from immunolabeling on developing xylem. The orange colour represents the colocalization of IRX3 (red) with the cortical microtubules (green) (*See Color Plate of this figure beginning on page 355*)

These experiments demonstrate that in developing xylem microtubules and microfibrils appear to localize independently. For example, in *irx3-1* or *irx5-1* plants one of the subunits is missing and the two remaining subunits no longer localize to the plasma membrane. The pattern of microtubule banding, however, appears unaltered. This is in contrast to the result of (Fisher and Cyr 1998) who worked with cellulose synthesis inhibitors and suggested that cellulose synthesis was a requirement for normal microtubule organization.

Insertion of GFP close the amino terminus of IRX3 does not appear to alter the function of the protein since it is still able to complement the *irx3-1* mutation. Furthermore, localization of the IRX3:GFP as well as IRX1 and IRX5 all appears to be normal in these complemented plants (Gardiner et al. 2003). Analysis of GFP fluorescence with time revealed a very dynamic pattern of distribution. Generally, levels of GFP fluorescence are low and in a banded pattern, apart from localized regions of bright fluorescence. These region of bright fluorescence appear to correspond to a transient increase in fluorescence of the IRX3:GFP that is presumed to result from an alteration in the local environment of the fusion protein. One possible explanation is that the CesA proteins are constantly being removed and reinserted into the plasma membrane by a specialized organelle. Whether this proves to be the case awaits further analysis.

6 CONSERVATION OF *CesA* PROTEIN FUNCTION IN OTHER SPECIES

In order for information gained from studying *Arabidopsis* to be of use to industry it is important to establish that mechanisms of cellulose synthesis are conserved between *Arabidopsis* and commercially important species such as crop plants and trees. Studies on *CesA* genes in rice represent a powerful example of how well the mechanism of cellulose synthesis is conserved between diverse species. Three *brittle-culm* mutants of rice are the result of mutations in the rice orthologues of *AtCesA4*, *7* and *8* (Tanaka et al. 2003). This result suggests that in secondary cell walls a very similar mechanism of both cellulose synthesis and rosette organization is conserved between rice and *Arabidopsis*.

A series of studies on both poplar and pine suggest that multiple *CesA* proteins are required in the secondary cell wall during wood formation (Kalluri and Joshi 2003; Djerbi et al. 2004; Kalluri and Joshi 2004; Liang and Joshi 2004; Nairn and Haselkorn 2005). Further information on this topic may be found elsewhere in this issue.

7 OTHER *irx* GENES REQUIRED FOR SECONDARY CELL WALL FORMATION

The *kor* mutation was originally isolated on the basis of its elongation defect and subsequently was described as a cell-plate specific endoglucanase (Nicol et al. 1998; Zuo et al. 2000). The demonstration, however, that the cellulose deficient mutants *acw1* and *rsw2* are also alleles of *kor* suggest a role for this gene in cellulose biosynthesis. Map-based cloning of the mutation in *irx2* revealed that this too was an allele of *korrigan* (Szyjanowicz et al. 2004). In contrast to the *kor* alleles described above, however, both *irx2* alleles grow relatively normally. They do not appear to exhibit any of the elongation, radial swelling, or cell plate phenotype that have previously been described for other alleles of *kor*.

In addition to the fact that *irx2* alleles demonstrate no obvious visible primary cell wall phenotype, FTIR analysis also suggests that the primary cell walls of *irx2* plants contain normal amounts of cellulose. It is currently unclear why the two *irx2* alleles are specific to the secondary cell wall. Both mutations occur in highly conserved proline residues that are conserved in all 25 *Arabidopsis* endoglucanases as well as endoglucanases from a variety of fungi and bacteria. One possibility is that these mutations are very weak, and that the reduced activity of the mutated protein is sufficient to cope with the demands of primary cell wall cellulose synthesis, but is not sufficient for the rapid synthesis of cellulose in the secondary cell wall. An alternative explanation for why *irx2-1* and *irx2-2* only affects the secondary cell wall arises if KOR is part of a large protein complex. The single amino changes found in *kor* alleles such as *rsw2-1*, *rsw2-4* and *rsw2-2/acw1* are predicted to occur on the surface of the protein (Molhoj et al. 2002) and may well affect the ability of KOR to

form a complex. It is possible that plants may be more sensitive to mutations that affect the assembly of a protein complex than they are to mutations that reduce the catalytic activity of KOR. Whether this hypothesis is correct should be resolved once the protein complex containing KOR has been purified and characterized.

The function of KOR remains unclear. One suggestion is that it cleaves off glucose residues from a lipid-linked intermediate at the plasma membrane (Peng et al. 2002). Both coprecipitation experiments and localization studies suggest that KOR does not associate with the cellulose synthase complex at the plasma membrane. Using the histidine-tagged IRX3 described above and under conditions in which IRX1 is coprecipitated, KOR/IRX2 does not coprecipitate. Furthermore, in reciprocal experiments using a histidine tagged IRX2 no IRX3 is coprecipitated (Szyjanowicz et al. 2004). IRX2 localizes to the plasma membrane in developing xylem but the colocalization with microtubules is relatively poor compared to that of IRX3 (Szyjanowicz et al. 2004). The fact that KOR and IRX3 do not appear to associate, and the lack of colocalization between the two proteins, is hard to reconcile with the model proposed by (Peng et al. 2002) in which the cellulose synthase complex would incorporate the sugars released by KOR into the growing cellulose chains. In *irx2-1* plants the cells in the interfascicular region contain cell wall thickenings in the corners of the cells (Turner and Somerville 1997), the earliest sites of cell wall deposition (Altamura et al. 2001). This suggests that IRX2/KOR may be involved in a later stage of cellulose synthesis.

8 IDENTIFYING NOVEL GENES REQUIRED FOR SECONDARY CELL WALL FORMATION USING EXPRESSION PROFILING

Several excellent studies have demonstrated the power of using microarrays to study gene expression during secondary cell wall formation. Two recent studies have demonstrated the utility of exploiting the near genome wide *Arabidopsis* microarray that is currently available to identify genes expressed during secondary cell wall formation. Brown et al. (2005) used both custom and publicly available microarray data to identify genes co-expressed with *IRX3*, while Persson et al. (2005) used publicly available data to examine the expression of both the primary wall *CesA* genes (*CesA1,3* and *6*) and the secondary cell wall *CesA* genes (*IRX1,3* and *5*). While at least 7 novel *irx* mutations were identified only one appeared to result in a dramatic reduction in cellulose synthesis (Brown et al. 2005). This mutation was identified as a result of a mutation in the *COBRA-LIKE4* (*CBL4*) gene. Interestingly the orthologue of this gene had been previously identified in rice as being required for cellulose synthesis in the secondary cell wall (Tanaka et al. 2003). The function of the *COBRA* gene is the subject of an interesting debate. In the primary cell wall is suggested to be required for organization of cellulose microfibril orientation (Roudier et al. 2005). The argument is a classic "chicken and the egg": does an alteration in

cellulose microfibril orientation lead to a decrease in cellulose or do decreases in cellulose synthesis caused by *CBL* defects result in altered cellulose microfibril deposition. In the secondary cell wall, however, it is clear that defects in *CBL4* results in severe reductions in cellulose synthesis (Brown et al. 2005). Such a large defect is hard to explain by alterations in cellulose orientation alone.

9 ALTERNATIVE APPROACHES TO STUDYING CELLULOSE SYNTHESIS IN THE SECONDARY CELL WALL

Studies on mutants affecting cellulose synthesis in the primary cell wall have also led to the idea that three catalytic subunits are required for cellulose synthesis in these cell types. These genes are different from those required in the secondary cell wall (Arioli et al. 1998; Fagard et al. 2000; Scheible et al. 2001). Work on the *rsw1* mutant of *Arabidopsis* demonstrates that in addition to their catalytic function, CesA proteins are also essential for determining rosette structure. *rsw1-1* is caused by a comparatively small amino acid change (Ala to Val) in AtCesA1, yet at the restrictive temperature the hexameric rosettes are replaced by smaller structures (Arioli et al. 1998).

While it is clear that CesA proteins are integral parts of the CSC, the function of other genes isolated on the basis of their cellulose deficient phenotype is less clear. The cellulose deficient mutants *acw1*, *rsw2* and *irx2* are all alleles of *korrigan*. This mutant was originally isolated on the basis of its elongation defect, and is affected in the gene encoding a membrane bound endo-β(1-4)-glucanase. There is, however, no direct evidence that this protein is part of the cellulose synthase complex. Mutation of a gene encoding a novel plasma membrane protein of unknown function (Pagant et al. 2002), also causes a cellulose deficient phenotype, but its function remains unclear. The problems in identifying genes involved directly in cellulose synthesis are highlighted by work on *cyt1*, *rsw3* and *knf* mutants (Lukowitz et al. 2001; Burn et al. 2002; Gillmor et al. 2002). All mutants exhibit a severe phenotype consistent with a dramatic reduction in cellulose content. The defects are caused by mutations in genes exhibiting homology to mannose-1-phosphate guanyltransferase, glycosidase I and glycosidase II respectively. These enzymes are part of an essential pathway that processes carbohydrates during the assembly and folding of membrane proteins in the endoplasmic reticulum. So although a genetic approach has been successful in identifying candidates genes that may be involved in cellulose synthesis, it has become increasingly hard to distinguish those core components that are absolutely required for cellulose synthesis by the cellulose synthase complex from other components that are required for protein complex assembly or other general housekeeping functions within the cell. In order to distinguish those proteins directly involved in cellulose synthesis it will be necessary to purify the intact cellulose synthase complex.

Despite the problems associated with purifying the cellulose synthase complex and retaining high activity the isolation of several integral components of the complex has provided a number of tools to effect this purification. Epitope tagging is a method that is now widely used to facilitate the purification of protein complexes. The success of the is approach has been demonstrated by studies demonstrating the purification of several hundred protein complexes from yeast following the addition of FLAG (Ho et al. 2002) or TAP (Gavin et al. 2002) tag. Importantly, the method is applicable to both soluble and membrane bound complexes (Gavin et al. 2002). A functional epitope tagged version of IRX3 has been made and progress has been made in its use to purify the cellulose synthase complex (Taylor et al. 2004).

10 CONCLUSIONS

The isolation of mutants deficient in secondary cell wall cellulose synthesis has led to the identification of a number of genes essential for cellulose production. The identification of these genes and the discovery that three CesA proteins are involved in the same protein complex has answered some of the questions regarding the complexity of the cellulose synthase complex. That fact that all three proteins are required for the correct assembly and targeting of the complex to the plasma membrane will allow us to further dissect the roles of these and other proteins in cellulose synthesis. In addition, the identification of a protein that is involved in both primary and secondary cell wall cellulose synthesis may allow us to identify other common components between the primary and secondary cell wall cellulose synthesizing machinery.

REFERENCES

Altamura M.M., Possenti M., Matteucci A., Baima S., Ruberti I., and Morelli G. (2001). Development of the vascular system in the inflorescence stem of *Arabidopsis*. New Phytol. 151:381–389.

Arioli T., Peng L.C., Betzner A.S., Burn J., Wittke W., Herth W., Camilleri C., Hofte H., Plazinski J., Birch R., Cork A., Glover J., Redmond J., and Williamson R.E. (1998). Molecular analysis of cellulose biosynthesis in *Arabidopsis*. Science 279:717–720.

Brown D.M., Zeef L., Ellis J., Goodacre R., and Turner S.R. (2005). Identification of novel genes involved in secondary cell wall formation using expression profiling and reverse genetics. The Plant Cell 17:2281–2295.

Burn J.E., Hurley U.A., Birch R.J., Arioli T., Cork A., and Williamson R.E. (2002). The cellulose-deficient *Arabidopsis* mutant rsw3 is defective in a gene encoding a putative glucosidase II, an enzyme processing N-glycans during ER quality control. Plant J. 32:949–960.

Djerbi S., Aspeborg H., Nilsson P., Sundberg B., Mellerowicz E., Blomqvist K., and Teeri T.T. (2004). Identification and expression analysis of genes encoding putative cellulose synthases (*CesA*) in the hybrid aspen, Populus tremula (L.) x P-tremuloides (Michx.). Cellulose 11:301–312.

Fagard M., Desnos T., Desprez T., Goubet F., Refregier G., Mouille G., McCann M., Rayon C., Vernhettes S., and Hofte H. (2000). PROCUSTE1 encodes a cellulose synthase required for normal cell elongation specifically in roots and dark-grown hypocotyls of arabidopsis. Plant Cell 12:2409–2423.

Fisher D.D. and Cyr R.J. (1998). Extending the microtubule/microfibril paradigm - Cellulose synthesis is required for normal cortical microtubule alignment in elongating cells. Plant Physiol. 116:1043–1051.

Gardiner J.C., Taylor N.G., and Turner S.R. (2003). Control of cellulose synthase complex localization in developing xylem. Plant Cell 15:1740–1748.

Gavin A.C., Bosche M., Krause R., Grandi P., Marzioch M., Bauer A., Schultz J., Rick J.M., Michon A.M., Cruciat C.M., Remor M., Hofert C., Schelder M., Brajenovic M., Ruffner H., Merino A., Klein K., Hudak M., Dickson D., Rudi T., Gnau V., Bauch A., Bastuck S., Huhse B., Leutwein C., Heurtier M.A., Copley R.R., Edelmann A., Querfurth E., Rybin V., Drewes G., Raida M., Bouwmeester T., Bork P., Seraphin B., Kuster B., Neubauer G., and Superti-Furga G. (2002). Functional organization of the yeast proteome by systematic analysis of protein complexes. Nature 415:141–147.

Gillmor C.S., Poindexter P., Lorieau J., Palcic M.M., and Somerville C. (2002). alpha-glucosidase I is required for cellulose biosynthesis and morphogenesis in *Arabidopsis*. J. Cell Biol. 156:1003–1013.

Ho Y., Gruhler A., Heilbut A., Bader G.D., Moore L., Adams S.L., Millar A., Taylor P., Bennett K., Boutilier K., Yang L.Y., Wolting C., Donaldson I., Schandorff S., Shewnarane J., Vo M., Taggart J., Goudreault M., Muskat B., Alfarano C., Dewar D., Lin Z., Michalickova K., Willems A.R., Sassi H., Nielsen P.A., Rasmussen K.J., Andersen J.R., Johansen L.E., Hansen L.H., Jespersen H., Podtelejnikov A., Nielsen E., Crawford J., Poulsen V., Sorensen B.D., Matthiesen J., Hendrickson R.C., Gleeson F., Pawson T., Moran M.F., Durocher D., Mann M., Hogue C.W.V., Figeys D., and Tyers M. (2002). Systematic identification of protein complexes in Saccharomyces cerevisiae by mass spectrometry. Nature 415:180–183.

Jones L., Ennos A.R., and Turner S.R. (2001). Cloning and characterization of irregular xylem4 (irx4): a severely lignin-deficient mutant of *Arabidopsis*. Plant J. 26:205–216.

Kalluri U.C. and Joshi C.P. (2003). Isolation and characterization of a new, full-length cellulose synthase cDNA, *PtrCesA5* from developing xylem of aspen trees. J. Exp. Bot. 54:2187–2188.

Kalluri U.C. and Joshi C.P. (2004). Differential expression patterns of two cellulose synthase genes are associated with primary and secondary cell wall development in aspen trees. Planta 220:47–55.

Kudlicka K., Brown, Jr. R.M., Li L.K., Lee J.H., Shin H., and Kuga S. (1995). Beta-glucan synthesis in the cotton fiber.4. In vitro assembly of the cellulose I Allomorph. Plant Physiol. 107:111–123.

Kudlicka K. and Brown, Jr. R.M. (1997). Cellulose and callose biosynthesis in higher plants.1. Solubilization and separation of (1->3)- and (1->4)-beta-glucan synthase activities from mung bean. Plant Physiol. 115:643–656.

Lai-Kee-Him J., Chanzy H., Muller M., Putaux J.L., Imai T., and Bulone V. (2002). In vitro versus in vivo cellulose microfibrils from plant primary wall synthases: Structural differences. J. Biol. Chem. 277:36931–36939.

Liang X. and Joshi C.P. (2004). Molecular cloning of ten distinct hypervariable regions from the cellulose synthase gene superfamily in aspen trees. Tree Physiol. 24:543–550.

Lukowitz W., Nickle T.C., Meinke D.W., Last R.L., Conklin P.L., and Somerville C.R. (2001). *Arabidopsis* cyt1 mutants are deficient in a mannose-1-phosphate guanylyltransferase and point to a requirement of N-linked glycosylation for cellulose biosynthesis. Proc. Natl. Acad. Sci. USA 98:2262–2267.

Molhoj M., Pagant S.R., and Hofte H. (2002). Towards understanding the role of membrane-bound endo-beta-1,4- glucanases in cellulose biosynthesis. Plant Cell Physiol. 43:1399–1406.

Nairn C.J. and Haselkorn T. (2005). Three loblolly pine *CesA* genes expressed in developing xylem are orthologous to secondary cell wall *CesA* genes of angiosperms. New Phytol. 166:907–915.

Nicol F., His I., Jauneau A., Vernhettes S., Canut H., and Hofte H. (1998). A plasma membrane-bound putative endo-1,4-beta-D-glucanase is required for normal wall assembly and cell elongation in *Arabidopsis*. EMBO J. 17:5563–5576.

Pagant S., Bichet A., Sugimoto K., Lerouxel O., Desprez T., McCan M., Lerouge P., Vernhetles S., and Hofte H. (2002). KOBITO1 encodes a novel plasma membrane protein necessary for normal synthesis of cellulose during cell expansion in *Arabidopsis*. Plant Cell 14:2001–2013.

Pear J.R., Kawagoe Y., Schreckengost W.E., Delmer D.P., and Stalker D.M. (1996). Higher plants contain homologs of the bacterial *celA* genes encoding the catalytic subunit of cellulose synthase. Proc. Natl. Acad. Sci. USA 93:12637–12642.

Peng L.C., Kawagoe Y., Hogan P., and Delmer D. (2002). Sitosterol-beta-glucoside as primer for cellulose synthesis in plants. Science 295:147–150.

Persson S., Wei H., Milne J., Page G.D., P. and Somerville C. (2005). Identification of genes required for cellulose synthesis by regression analysis of public microarray data sets. Proc. Natl. Acad. Sci. USA 102:8633–8638.

Roudier F., Fernandez A., Fujita M., Himmelspach R., Borner G., Schindelman G., Song S., Baskin T., Dupree P., Wasteneys G., and Benfey P. (2005). COBRA, an *Arabidopsis* extracellular GPI-anchored protein, specifically controls highly anisotropic expansion through its involvement in cellulose microfibril orientation. The Plant Cell 17:1749–1763.

Scheible W.R., Eshed R., Richmond T., Delmer D., and Somerville C.R. (2001). Modifications of cellulose synthase confer resistance to isoxaben and thiazolidinone herbicides in *Arabidopsis* Ixr1 mutants. Proc. Natl. Acad. Sci. USA 98:10079–10084.

Szyjanowicz P.M.J., McKinnon I., Taylor N.G., Gardiner J., Jarvis M.C., and Turner S.R. (2004). The irregular xylem 2 mutant is an allele of korrigan that affects the secondary cell wall of *Arabidopsis* thaliana. Plant J. 37:730–740.

Tanaka K., Murata K., Yamazaki M., Onosato K., Miyao A., and Hirochika H. (2003). Three distinct rice cellulose synthase catalytic subunit genes required for cellulose synthesis in the secondary wall. Plant Physiol. 133:73–83.

Taylor N.G., Scheible W.R., Cutler S., Somerville C.R., and Turner S.R. (1999). The irregular xylem3 locus of arabidopsis encodes a cellulose synthase required for secondary cell wall synthesis. Plant Cell 11:769–779.

Taylor N.G., Laurie S., and Turner S.R. (2000). Multiple cellulose synthase catalytic subunits are required for cellulose synthesis in *Arabidopsis*. Plant Cell 12:2529–2539.

Taylor N.G., Howells R.M., Huttly A.K., Vickers K., and Turner S.R. (2003). Interactions among three distinct CesA proteins essential for cellulose synthesis. Proc. Natl. Acad. Sci. USA 100: 1450–1455.

Taylor N.G., Gardiner J.C., Whiteman R., and Turner S.R. (2004). Cellulose synthesis in the *Arabidopsis* secondary cell wall. Cellulose 11:329–338.

Turner S.R. and Somerville C.R. (1997). Collapsed xylem phenotype of *Arabidopsis* identifies mutants deficient in cellulose deposition in the secondary cell wall. Plant Cell 9:689–701.

Zuo J.R., Niu Q.W., Nishizawa N., Wu Y., Kost B., and Chua N.H. (2000). KORRIGAN, an *Arabidopsis* endo-1,4-beta-glucanase, localizes to the cell plate by polarized targeting and is essential for cytokinesis. Plant Cell 12:1137–1152.

CHAPTER 5

FROM CELLULOSE TO MECHANICAL STRENGTH: CARBON FLUX AND RELATIONSHIP OF THE CELLULOSE SYNTHASE GENES TO DRY MATTER ACCUMULATION IN MAIZE

ROBERTO BARREIRO AND KANWARPAL S. DHUGGA*

Crop Genetics Research and Development
Pioneer Hi-Bred International, Inc., a DuPont Company, 7300 NW 62nd Avenue, P.O. Box 1004, Johnston, IA 50131

Abstract

Stalk strength in maize is primarily determined by the amount of cellulose in a unit length of the internode. An increase in cellulose concentration of the cell wall, aside from allowing simultaneous improvements in stalk strength and harvest index, will increase the value of stover as a feedstock for ethanol production. Sucrose synthase makes UDP-glucose, substrate for cellulose formation, from uridine diphosphate (UDP) and sucrose whereby it conserves the energy of the glycosidic bond. The alternative route of UDP-glucose formation through UDP-glucose pyrophosphorylase, in contrast, consumes two equivalents of uridine triphosphate (UTP), making it an energy-intensive process. *In vivo*, the reaction catalyzed by sucrose synthase operates in the direction of UDP-glucose formation because of deviation of the relationship between mass action ratio (*in vivo* ratio of products to substrates) and *Keq* from unity. A reduction in the amount of enzyme could be compensated by this mechanism without affecting the magnitude of net flux. Since cellulose is crystallized into microfibrils immediately after synthesis, the reaction of cellulose synthase is considered to be far from equilibrium. Cellulose synthase may thus exert considerable control on carbon flux into cellulose. We isolated 12 members of the *CesA* gene family from maize. Upon phylogenetic analysis, three of the maize *CesA* genes, *ZmCesA10-12*, clustered with the *Arabidopsis CesA* sequences that had previously been shown to be involved in secondary wall formation. These three genes were coordinately expressed across multiple tissues, suggesting that they might interact with each other to form a functional cellulose synthase complex. Isolation of the expressed *CesA* genes from maize and their association with primary or

* Author for correspondence: Tel: 515-270-3951; Fax: 515-334-4788; e-mail: Kanwarpal.Dhugga@Pioneer.com

R.M. Brown, Jr. and I.M. Saxena (eds.), Cellulose: Molecular and Structural Biology, 63–83.

secondary wall formation has made it possible to test their respective roles in cellulose synthesis in different cell types through association genetics, mutational genetics, or a transgenic approach. This information would be useful in improving stalk strength in cereals.

Keywords

cellulose synthase, cell wall, CesA, flexural strength, flux control analysis, gene expression profiling, MPSS, phylogeny, secondary wall, stalk lodging, vascular bundles.

Abbreviations

cellulose synthase (*CesA*), expressed sequence tag (EST), irregular xylem(*Irx*), massively parallel signature sequencing (MPSS), weight (wt.).

1 INTRODUCTION

Cellulose is the major wall constituent in the supporting tissues of mature plant cells. The paracrystalline structure of cellulose, that results from energy minimization by the formation of inter- and intrachain hydrogen bonds, makes it mechanically the strongest known organic molecule on density basis (Niklas 1992). It is natural then that cellulose is the primary determinant of strength in structural tissues.

Stalk lodging, which results from mechanical failure of the stalk tissue anywhere below the ear node before harvest, results in significant yield losses in maize (Duvick and Cassman 1999). Lodging, also a problem in other cereal crops, is influenced by morphological traits as well as environmental conditions. An indicator of dry matter partitioning efficiency is harvest index, the ratio of the grain to the total aboveground biomass. Introduction of dwarfing genes into small grain cereals allowed for substantial increases in their harvest indices (Sinclair 1998). Dwarfing also made them less likely to lodge mainly by reducing torque on the top-heavy straw. This architectural alteration allowed for higher fertilizer inputs, resulting in increased biomass and thus grain production. In contrast, harvest index in maize has remained essentially unchanged at ~50% in the modern hybrids when compared with the older varieties (Russell 1985; Tollenaar and Wu 1999). Yield improvements in maize have thus been realized primarily from the increases in total biomass per unit land area. Most of the biomass increase has resulted from increased planting density although some can also be attributed to an increase in plant height. With increasing planting density, maize stalks become mechanically weaker and thus susceptible to lodging because of the resulting reduction in individual plant mass.

Identification of chemical constituents that contribute to mechanical strength and the corresponding molecular mechanisms responsible for their formation are prerequisite steps toward using the tools of genetic engineering to reduce the incidence of lodging in cereal crops. The biochemical approach was only partially successful in the isolation of polysaccharide synthases (Dhugga and Ray 1994, Dhugga 2005). In comparison, genomic technologies made it easier to isolate the gene families that affect cell wall formation and to associate their expression patterns with different tissues in the plant (Delmer 1999; Holland et al. 2000; Dhugga 2001; Richmond and Somerville 2001). This review will cover

the role of cellulose in stalk strength, flux of carbon into cellulose through cellulose synthases (*CesA*), alteration of cellulose formation in plants, and the roles different members of the *CesA* gene family from maize play in cellulose synthesis in different cell types as inferred from expression profiling.

2 ROLE OF CELLULOSE IN STALK STRENGTH

Dry matter in a unit length of the maize stalk explained approximately half of the variation in mechanical strength (Appenzeller et al. 2004). Structural dry matter, which was derived by removing the soluble contents from the total dry matter, accounted for approximately 80% of the mechanical strength and was thus a superior indicator of strength than total dry matter. A still greater proportion of the internodal flexural strength (85%) was explained when only cellulose content in a unit length of the stalk was considered. This finding is consistent with cellulose being the most abundant and strongest constituent of the cell wall, making up ~50% of the total dry matter in a mature corn stalk.

These results suggest that one of the avenues to improve mechanical strength of the maize stalk is to increase cellulose concentration in existing dry matter. Conversion of other polysaccharides and free sugars into cellulose is bioenergetically neutral so is not expected to adversely affect plant performance (Sinclair and de Wit 1975). *CesA* genes offer a suitable target for a biotechnological approach to accomplish this objective.

3 CARBON FLUX THROUGH CELLULOSE SYNTHASE

Kinetic information on cellulose synthesis is scarce in the literature. The in vitro studies reported are limited almost exclusively to experimental systems, such as bacteria and elongating cotton and flax fibers (Aloni et al. 1982; Delmer et al. 1993; Li et al. 1993). Li et al. (1993), analyzing cellulose synthase activity in cotton fibers, reported the K_m and V_{max} for UDP-glucose to be respectively 0.4 mM and 2.8 nmol•min^{-1}•mg protein^{-1}. If cellulose synthase exhibits similar properties *in vivo* then it must operate under substrate-saturated conditions since the concentration of UDP-glucose in the cytosol is 1–3 mM (Dancer et al. 1990; Krause and Stitt 1992; Winter et al. 1993, 1994).

True estimates of V_{max} for cellulose synthase, however, are still problematic. Delmer (1993, personal communications), for example, has noted that the rates for cellulose synthesis in vitro reported by Li et al. (1993) were no more than 5% of those occurring *in vivo* during primary wall synthesis.

An estimate of the carbon flux into cellulose could also be drawn based on an average value of net primary productivity (NPP) for crops, which can also be expressed on a leaf area basis. According to Leopold and Kriedemann (1975), a reasonable growth rate for sunflower leaves could be ~85 g dry wt•m^{-2}•week^{-1}. For maize, an average NPP value calculated from results published by Uhart and Andrade (1995) resulted in ~56 g dry wt•m^{-2}•week^{-1}. Averaging these two

figures and converting the units, the rate of dry matter deposition would amount to approximately 698 ng dry wt•cm^{-2}•min^{-1}. Considering that cellulose constitutes one third of the primary cell wall, approximately 30% of the increase in dry weight during growth would result from carbon allocation into the cellulose fraction of cell walls. This increase in dry mass can be expressed on a fresh weight basis by using an average value for specific leaf weight for maize of 0.009 g fresh wt•cm^{-2} (Barreiro 1999). Therefore, the rate of cellulose deposition in maize leaves expressed on a fresh weight basis would be approximately 160 nmoles of glucosyl units•g fresh wt^{-1}•min^{-1}. Flux through cellulose synthase measured *in vivo* in our lab using maize coleoptiles fed with radiolabeled sucrose at 30°C was 118 ± 37 nmoles of glucose•g^{-1} fresh wt•min^{-1} (N = 21) (Barreiro, unpublished). These results should be interpreted with caution since the accuracy of fluxes measured *in vivo* using radiolabeled substrates is limited by the estimation of the specific radioactivity within the enzyme microenvironment. However, these rates, estimated from NPP values or measured *in vivo*, were also consistent with fluxes ranging from 51 to 213 nmoles of glucose equivalents incorporated•g^{-1} fresh wt•min^{-1} obtained with simulations using a formal model incorporating complex kinetic equations and metabolic parameters determined experimentally (Barreiro 1999).

Sensitivity analyses run with a mathematical model in which simulated carbon fluxes through cellulose synthase are contrasted to changes in V*f* (limiting velocity in the direction of cellulose synthesis), indicate that fluxes are linear with respect to V*f* as expected for a condition in which the median substrate concentration is saturating (Barreiro 1999). According to these simulations, increases in the expression of cellulose synthases should correlate linearly with increases in cellulose production, providing that the substrate pool remains saturating at the steady state. Moreover, in reactions where the mass action ratio is far from the ratio of products to substrates in equilibrium, i.e., when the change in actual free energy of the reaction is different from zero, the flux is affected primarily by the enzymatic rate and not by the concentration of metabolites. Cellulose synthase is a multi-protein complex, however, and simultaneous up-regulation of genes encoding non-CesA complex members may be required for improved flux of carbon into cellulose.

4 ALTERATION OF CELLULOSE FORMATION IN PLANTS

In addition to its role as the primary determinant of tissue strength, a trait that is of significant interest in agriculture, cellulose constitutes the most abundant renewable energy resource on Earth. More than 200 million metric tons of stover is produced just from maize in the USA every year. About one-third of this could potentially be utilized for ethanol production (Kadam and McMillan 2003). The worldwide production of lignocellulosic wastes from cereal stover and straw is estimated to be ~3 billion tons per year (Kuhad

and Singh 1993). An increase in cellulose and reduction in lignin contents in the stover material is considered to be beneficial for ethanol production in biorefineries. Lignin is also a target for reduction because it is an undesirable constituent for silage digestibility and the paper industry (Hu et al. 1999; Li et al. 2003a).

Availability of the first plant *CesA* gene, which was isolated by sequencing only a few hundreds of the expressed sequence tags (EST) from developing cotton fibers at a stage when secondary wall was being deposited at a rapid rate (Pear et al. 1996), facilitated the isolation of similar sequences from other species based on homology, including a weakly related set of genes that was termed cellulose synthase-like (*Csl*) (Holland et al. 2000; Richmond and Somerville 2000; Wu et al. 2000; Hazen et al. 2002). Multiple copies of *CesA* have been identified in every plant species investigated. The *CesA* genes are believed to encode the catalytic subunits of the rosette, also referred to as terminal complex that is located in the plasma membrane (Kimura et al. 1999).

Characterization of several cellulose-deficient mutants of *Arabidopsis* allowed the isolation of a number of genes that affect cellulose synthesis. Some of these genes turned out to be members of the *CesA* gene family (Turner and Somerville 1997; Arioli et al. 1998; Taylor et al. 1999, 2000; Fagard et al. 2000; Desprez et al. 2002; Ellis et al. 2002; Cano-Delgado et al. 2003). Others encoded proteins for *N*-glycan synthesis and processing (Boisson et al. 2001; Lukowitz et al. 2001; Burn et al. 2002; Gillmor et al. 2002), a membrane-anchored β-1,4-endoglucanase, Korrigan (Nicol et al. 1998), a membrane-anchored protein of unknown function that might be a part of the cellulose synthase complex, Kobito (Pagant et al. 2002), and Cobra, a putative GPI-anchored protein, which upon being inactivated, dramatically reduced culm strength in rice (Li et al. 2003b). These genes encode proteins with diverse functions that influence cellulose synthesis either directly or indirectly. Precise functions of these proteins remain unknown, however.

Mutations in some of the *CesA* genes involved in primary wall formation caused severely altered phenotypes, which was expected given the role of primary walls in cell expansion starting early in development (Arioli et al. 1998; Fagard et al. 2000; Beeckman et al. 2002; Ellis et al. 2002). The mutant *CesA* genes involved in secondary wall formation affected the visual phenotype only slightly but caused a reduction in cellulose concentration in xylem cells, which was reflected in the diminished mechanical strength of the stem tissue (Turner and Somerville 1997; Taylor et al. 1999, 2000, 2003; Tanaka et al. 2003; Zhong et al. 2003).

Korrigan was originally identified as an extremely dwarf mutant with a lesion in a plasma membrane-associated β-1,4-endoglucanase (Nicol et al. 1998). The Korrigan protein is believed to be involved in the cellulose synthase complex that functions during primary or secondary wall formation (Nicol et al. 1998; Molhoj et al. 2002; Szyjanowicz et al. 2004). Its exact function remains to be determined although given its relationship to the cellulase type of hydrolases, it has been

postulated to play a role in terminating or editing the glucan chains emerging from the cellulose synthase complex before their crystallization into a cellulose microfibril (Matthysse et al. 1995; Nicol et al. 1998; Delmer 1999). Alternatively, it could cleave sterol from the sterol-glucoside primer that has been reported to initiate glucan chain formation for subsequent extension by the plant CesA complex (Molhoj et al. 2002; Peng et al. 2002). However, recent evidence does not support this role (Scheible and Pauly 2004).

Alteration of cellulose production in economically important plants using a transgenic approach has been the subject of only a few studies (Hu et al. 1999; Tang and Sturm 1999; Levy et al. 2002; Li et al. 2003a). An antisense approach used to reduce lignin content was reported to increase the proportion of cellulose in aspen stem wood (Hu et al. 1999; Li et al. 2003a). Aside from the fact that some of the apparent increase in cellulose level could be explained by the compensatory effects of nonlignin wall constituents, the estimate for cellulose concentration was derived from sugar composition and not from direct measurements of its crystalline form, making it difficult to discern the compounding effect of glucose present in other forms, such as free sugars. An interaction between cellulose and lignin deposition has also been recognized in *Arabidopsis* and rice. The *eli1-1 and eli1-2* mutants, defective in the *AtCesA3* gene, had reduced levels of cellulose and showed aberrant deposition of lignin in cells that do not normally become lignified (Cano-Delgado et al. 2000, 2003). Ectopic lignification was also observed in other mutants such as the *AtCesA1* mutant *rsw1-1* and *lion's-tail* (Hauser et al. 1995), or defective in *Korrigan* (Cano-Delgado et al. 2000).

5 MASS ACTION AND METABOLIC CONTROL

Sucrose synthase (SuSy) provides another potential pathway for controlling cellulose production. SuSy cleaves sucrose in the presence of uridine diphosphate (UDP) into UDP-glucose and fructose, thereby conserving the energy of the glycosidic bond:

$$\text{UDP-glucose} + \text{Fructose} \underset{v-1}{\overset{v+1}{\rightleftarrows}} \text{Sucrose} + \text{UDP}$$

Considering the free energy of hydrolysis of sucrose as -6.6 Kcal•mol^{-1} and the energy of the α-D-glycosyl phosphate bond in UDP-glucose as -7.6 Kcal•mol^{-1}, the estimated change in free energy for the reaction in vitro results in -1 Kcal•mol^{-1} in favor of sucrose synthesis (Cardini et al. 1955). The apparent equilibrium constant (*Keq*) can be calculated from its relationship to the standard free energy (ΔG^0) by the following equation:

$$\Delta G^0 = -2.303\ RT \log_{10} Keq$$

Where R equals 1.987×10^{-3} Kcal•mol^{-1}•°K^{-1} and T equals 25°C (298°K), then

$$Keq = 10^{\frac{-1\ \text{Kcal/mol}}{-1.36\ \text{Kcal/mol}}} = 5.44$$

This parameter falls within the range of values from 1.4 to 8 determined experimentally based on substrate concentrations at equilibrium (Cardini et al. 1955; Neufeld and Hassid 1963; Avigad 1964; Kruger 1997). Since this reaction is thermodynamically close to equilibrium, the net flux ($v = v^{+1} - v^{-1}$) will represent only a fraction of the unidirectional flux the enzyme could catalyze in the absence of products. *In vivo*, the net carbon flux through this enzyme will be a function of the relative size of substrate and product pools at the steady state according to the mass action ratio (Hess 1963; Bücher and Russman 1964). For the reaction catalyzed by SuSy:

$$\Gamma = \frac{[\text{Sucrose}][\text{UDP}]}{[\text{UDP} - \text{glucose}][\text{Fructose}]}$$

The net flux *in vivo* through SuSy can be altered by a relatively small shift in the mass action ratio away from its equilibrium position (*Keq*). To obtain net flux in favor of UDP-glucose formation, the reaction must be displaced from equilibrium such that Γ is higher than *Keq*. The disequilibrium $\left(\frac{\Gamma}{Keq}\right)$ ratio can be related to the change in free energy using the following equation (Rolleston 1972; Stitt 1989):

$$\Delta G = 2.303\ RT \log_{10}\left(\frac{\Gamma}{Keq}\right)$$

Thus, an increase in the divergence of mass action ratio *in vivo* will increase the change in free energy through the reaction. This disequilibrium ratio can also be linked to flux by the ratio of the forward and reverse reaction velocities according to the equation derived by Hess and Brand (1965) from a rate equation based on Michaelis-Menten kinetics:

$$\frac{v^{-1}}{v^{+1}} = \frac{\Gamma}{Keq}$$

Figure 5-1 shows the sensitivity analysis for changes in sucrose concentration and the ratio of reverse and forward reaction velocities. The parameters for Figure 5-1 were calculated using the ranges of substrate and product concentrations found in the literature. UDP-glucose was reported to vary between 1.4 to 3.2 mM (Dancer et al. 1990; Krause and Stitt 1992; Barreiro 1999). Reported fructose levels range from 0.1 to 1.5 mM (Winter et al. 1994; Krapp and Stitt 1995), however, the concentration of cytoplasmic fructose assumed in the calculations could be higher than the concentration found *in vivo* because of the existence of high fructokinase activity in the cytoplasm (Gardner et al. 1992; Renz and Stitt 1993; Renz et al. 1993). Cytosolic UDP concentrations vary from 0.35 to 1.3 mM (Isherwood and Selvendran 1970; Stitt 1989; Dancer et al. 1990; Barreiro 1999) and those for sucrose from 13 to 103 mM (Winter et al. 1993, 1994; Pilon-Smits 1995; Krapp and Stitt 1995; Barreiro 1999).

The cytoplasmic concentrations chosen for each metabolite are not only associated with the range found in the literature but also close to the ranges of apparent

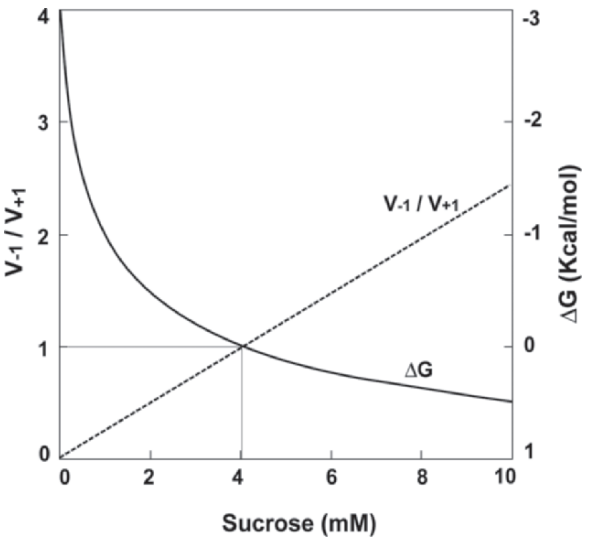

Figure 5-1. Sensitivity analysis of v − 1/v + 1 and change in free energy as a function of sucrose concentration. Negative values for the change in free energy indicate that the net flux of the reaction proceeds in the direction of sucrose synthesis

Km values for SuSy cited therein (Stitt and Steup 1985; Buczynski et al. 1993; Quick and Schaffer 1996; Barreiro 1999). We followed this approach since the optimal physiological concentration for substrates of a reaction displaced from equilibrium is at its *Km* (Rolleston 1972). For the sensitivity analysis the concentration of sucrose was varied, while the rest of the metabolites were clamped at the following concentrations: UDP-glucose 3 mM, fructose 0.1 mM, and UDP 0.4 mM.

The concentration gradient between metabolic pools on each side of the reaction could overcome the chemical bond energetic gradient, in favor of the mass action gradient, favoring sucrose hydrolysis in sink tissues. The threshold of sucrose concentration beyond which the net flux reverses is difficult to assess in a system with a dynamic equilibrium.

Under physiological conditions (assuming that the metabolite concentrations chosen for the calculations are similar at the steady state *in planta*), sucrose concentrations higher than ~4 mM could reverse the net flux of carbon through SuSy in favor of UDP-glucose synthesis due to mass action (Figure 5-1). If we assume that the physiological sucrose concentration within the cytoplasm remains near 50 mM (Barreiro 1999; Rohwer and Botha 2001) then the net flux of carbon through SuSy in sink tissues operates in the direction of UDP-glucose formation. This is consistent with experimental results using radioactive tracers (DeFekete and Cardini 1964; Milner and Avigad 1964; DeFekete 1969; Pavlinova 1971; Huber et al. 1996; Viola 1996; Geigenberger et al. 1997) and with simulations from a mathematical model built with a framework to simulate general pathways (Mendes 1993) and fitted with parameters determined experimentally

(Barreiro 1999). However, the reaction becomes readily reversible when the concentrations of sucrose within the enzyme microenvironment drop to values lower than ~4 mM (Figure 5-1).

Because of its proximity to equilibrium, the forward and reverse reactions catalyzed by SuSy will be affected in the same magnitude whenever the enzyme concentration is changed. As a consequence, the net direction of carbon flux through the enzyme will not be affected; therefore, increasing the expression of this enzyme per se may not increase the flux of carbon into the cellulose pool. On the other hand, decreasing the expression of SuSy, could cause a reduction of the UDP-glucose pool to the extent of limiting the cellulose synthetic rate. When this occurs *in vivo*, the UDP-glucose pool needs to be maintained by an alternative metabolic route that requires more energy to operate (Dhugga et al. 2002). Under stressful conditions, where SuSy expression may be severely attenuated, overexpression of the enzyme may help augment against yield losses.

An alternative metabolic route for UDP-glucose synthesis could be catalyzed by UDP-glucose pyrophosphorylase (UGPase). Both SuSy and UGPase are cytosolic enzymes and thus could contribute to the UDP-glucose pool in this compartment (Entwistle and ApRees 1988).

The metabolic path for UDP-glucose synthesis through UGPase, when considering sucrose as a precursor, has more intermediate steps than the route through SuSy. Whereas the formation of UDP-glucose through SuSy has only one step against a thermodynamic gradient, the route through UGPase has two: the phosphorylation of glucose, with a change in free energy of ~4.7 Kcal•mol^{-1}, and the conversion of glucose 6-P through glucose-1-P into UDP-glucose with a change in free energy of ~2.9 Kcal•mol^{-1}.

The available evidence, although scarce, suggests that the alternative route for the cytoplasmic UDP-glucose pool plays a relatively smaller role in comparison to SuSy. Carrot plants with an antisense version of the main form of SuSy had reduced SuSy activity in roots. Aside from having lower levels of UDP-glucose, these transgenic plants also had reduced levels of cellulose, starch, and total dry matter (Tang and Sturm 1999). Similarly, antisense downregulation of SuSy in potato tubers led to a reduction in cellulose formation (Haigler et al. 2001).

Figure 5-1 shows that the disequilibrium ratio (i.e., $v - 1/v + 1$) for the reaction catalyzed by SuSy can be influenced by a relative small shift in free energy away from equilibrium. Under normal growing conditions, manipulation of SuSy substrate levels to influence the magnitude of the net flux may therefore be a more effective way of controlling the quantity of cellulose deposited in the cell walls rather than altering its expression level.

6 THE CELLULOSE SYNTHASE GENE FAMILY

The *CesA* and *Csl* genes are generally expressed at a low level as judged from their occurrence in EST databases and from gene expression studies (Dhugga 2001). Yet, their transcripts can occur at higher frequencies in specific tissues,

for example, *GhCesA1* and *2* were identified amongst late-stage cotton fiber ESTs (Pear et al. 1996) and the mannan synthase gene was isolated from guar endosperm (Dhugga et al. 2004). In each case, the tissue where the ultimate product of the gene was being actively deposited was utilized to construct an EST database.

Genes involved in secondary wall formation are usually underrepresented in EST databases because many of the source cDNA libraries are derived from immature tissues. From a cDNA library from the transition zone of an elongating maize internode, a region in the stalk where the rate of secondary wall formation is higher than in the elongation zone, three additional full-length *CesA* genes *ZmCesA10*, *ZmCesA11*, and *ZmCesA12* were isolated (Appenzeller et al. 2004). These genes mapped to chromosomes 1, 3 and 7, respectively. Another gene, *ZmCesA7*, which was not previously assigned to any chromosome, mapped to chromosome 7 (Holland et al. 2000).

The deduced amino acid sequences of the three additional maize *CesA* genes were phylogenetically closer to the sequences from *Arabidopsis* that had previously been shown to be involved in secondary wall formation (Appenzeller et al. 2004). ZmCesA10, ZmCesA11, and ZmCesA12 grouped with AtCesA4 (Irx5), AtCesA8 (Irx1), and AtCesA7 (IrxX3), respectively, and are the probable orthologs of these genes (Figure 5-2). Likewise, OsCesA7, OsCesA4, and OsCesA9 are the orthologous sequences in rice (Tanaka et al. 2003), as are respectively the barley HvCesA4, HvCesA5/7 and HvCesA8 sequences (Burton et al. 2003). This suggests that the different subclasses of the CesA genes were formed early in higher plant evolution, before the divergence of monocots and dicots (Holland et al. 2000). Phylogenetic clustering of ZmCesA10-12 with the Irx sequences from *Arabidopsis* and their highest expression in the transition zone of the internode suggest that these genes are involved in secondary wall formation. Gene expression profiling studies described in the following section lend further support to this suggestion.

In comparison to ZmCesA10-12, the nine other maize sequences clustered in three groups: ZmCesA1, 2 and 3 form one group, ZmCesA4, 5 and 9 form another, and ZmCesA6, 7 and 8 form the third group (Figure 5-2). The first set of sequences lie in the same clade as AtCesA1 and 10, the second set clusters with AtCesA3 and the third set cluster with AtCesA2, 5, 6 and 9. Mutational analyses of *AtCesA1* (Arioli et al. 1998), *AtCesA3* (Scheible et al. 2001; Ellis et al. 2002; Cano-Delgado et al. 2003) and *AtCesA6* (Fagard et al. 2000; Desprez et al. 2002) have shown that these genes play a role in primary wall cellulose synthesis. Based on phylogenetic relationship, the maize CesA1-9 sequences may therefore be involved in primary cell wall formation; however, they are more divergent from their *Arabidopsis* relatives compared to ZmCesA10-12 (Appenzeller et al. 2004). Further, the maize sequences that cluster with AtCesA1, 3 and 10 appear to have duplicated at a higher rate than those that cluster with the other *Arabidopsis* sequences.

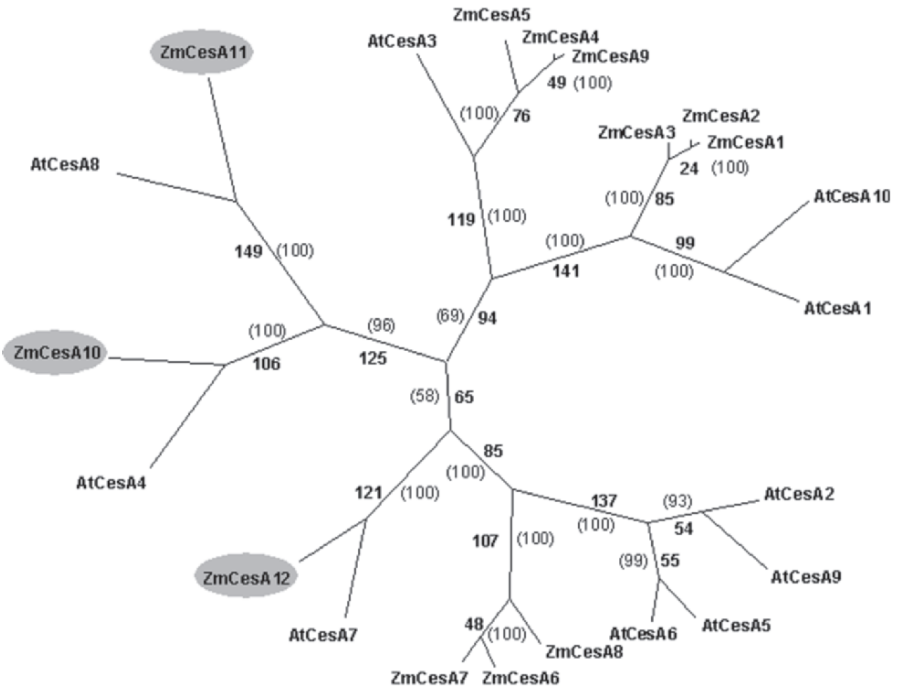

Figure 5-2. Unrooted single most parsimonious tree of the *CesA* proteins from maize and *Arabidopsis* determined by the Branch and Bound algorithm of PAUP (Swofford 1998). Branch lengths are proportional to the inferred number of amino acid substitutions, which are shown in bold font. Bootstrap values from 500 replicates (Felsenstein 1985) are represented as a percentage and are shown in parentheses. Reproduced with kind permission of Springer Science and Business Media from Appenzeller et al., 2004, Cellulose 11: 287–299, Fig. 2. © 2004 Kluwer Academic Publishers.

7 EXPRESSION ANALYSIS OF THE *ZmCesA* GENE FAMILY

Expression profiling of multiple tissues from a maize inbred line, B73, was carried out using massively parallel signature sequencing (MPSS) technology (Brenner et al. 2000; Brenner et al. 2000; Hoth et al. 2002; Meyers et al. 2002; Appenzeller et al. 2004). This technique entails cloning cDNAs onto synthetic beads such that each bead contains multiple copies of only one species of cDNA. Sequence tags 17–20 nucleotides long are then obtained from more than a million beads in parallel. Theoretically, the whole expressed genome is analyzed by the MPSS technology each time a library is screened for unique tags (Brenner et al. 2000a,b). Quantitative measures of the expression levels of different gene tags in the MPSS, as opposed to the ratios across paired tissues or treatments in the microarray-based platforms, combined with the depth of signature sequencing for each of the libraries make it possible to compare gene expression patterns across multiple, independent experiments. The technique is designed to select the 3′-most tag

from the cDNA. The abundance of each tag is a measure of the expression level of an individual *CesA* mRNA in the tissue the library is derived from.

ZmCesA1-8, with the exception of *ZmCesA2*, were expressed at different levels in the majority of the tissues (Appenzeller et al. 2004). In contrast, *ZmCesA10, 11* and *12* were selectively expressed in the stalk, a tissue rich in secondary wall. All three genes were the most highly expressed of the *CesA* genes in the stalk tissue. Secondary wall-rich cells account for ~80% of the dry matter in the maize stalk (K.S. Dhugga, unpublished). The expression pattern of *ZmCesA10-12* was therefore consistent with these genes being involved in cellulose synthesis for secondary wall formation. The observation that there are two groups of *CesA* sequences expressed mainly in primary or secondary wall forming cells has also been reported in barley (Burton et al. 2003) as well as *Arabidopsis* (reviewed in Doblin et al. 2002) and is likely to be a general phenomenon among plant species.

None of the *CesA* genes was detected in mature pollen grains (Dhugga 2001; Appenzeller et al. 2004). Doblin et al. (2001) also did not detect the expression of the *CesA* genes in *Nicotiana alata* pollen tubes. A *Csl* gene, *NaCslD1*, was the most highly expressed *Csl* gene in pollen tubes of *N. alata* and was specifically expressed in this tissue (Doblin et al. 2001). Based on this, it was suggested that, in addition to the *CesA* genes, *CslD* genes were possible candidates for making cellulose.

The pattern of expression of *ZmCesA10*, *11* and *12* was very similar across all the libraries studied. The expression pattern of all three genes paralleled the cellulose content in the three different tissues from an elongating internode, i.e., elongation zone, transition zone, and isolated vascular bundles (Appenzeller et al. 2004). Gene expression was lowest in the elongation zone, the tissue with the least amount of cellulose, followed by the transition zone with increased expression and cellulose content, with the vascular bundles having the highest expression and cellulose levels. *ZmCesA1* and *6–8* may be mainly responsible for making cellulose in the nonvascular, ground tissue cells in the maize stalk. These genes were also expressed in the vascular bundles where they may be involved in the formation of the walls of phloem elements as well as of fiber cells before the onset of secondary wall deposition (Appenzeller et al. 2004). Whereas *ZmCesA1, 7,* and *8* were expressed at a higher level in the elongation zone, *ZmCesA3, 5*, and *6* were expressed at a higher level in the transition zone.

ZmCesA6 showed maximal expression in leaves and was the most highly expressed *CesA* gene in this tissue (Appenzeller et al. 2004). Unopened leaves derived from a young plant at 4-leaf stage were dissected from the base and delineated as follows: cell division zone, elongation zone, and transition zone. Again, the expression of *ZmCesA6* was the highest of all the *CesA* genes in the leaf (Appenzeller et al. 2004). The expression of *ZmCesA6* was lowest in the cell division zone, increased in the expansion zone, and increased dramatically in the transition zone. *ZmCesA1*, *4*, *6–8,* and *10–12* had a similar type of expression pattern, with the levels of highest expression seen in the transition zone of the leaf. It is likely that *ZmCesA1* and *6–8* were responsible for making cellulose in leaf cells where primary wall synthesis was taking place such as mesophyll cells,

phloem elements, and fiber cells in vascular bundles before the onset of secondary wall formation. *ZmCesA10-12* seemed responsible for making cellulose in cells undergoing secondary wall synthesis in the vascular bundles. In contrast, *ZmCesA3* and *5*, the two other *CesA* genes expressed in the leaf, were expressed at their highest level in the cell division zone and were the most abundantly expressed of the *CesA* genes in this region of the leaf. Transcript levels declined in the expansion zone and were at their lowest level in the transition zone. This type of expression profile was suggestive of these genes participating in the synthesis of cellulose at the phragmoplast and possibly in the early stages of primary wall synthesis in elongating cells.

ZmCesA5 is also the highest expressed *CesA* gene in the developing endosperm (Appenzeller et al. 2004). It was previously proposed to be involved in mixed-linked glucan (MLG) formation in corn endosperm, where it is most highly expressed (Dhugga 2001). Unlike its role in cell elongation where MLG transiently accumulates in the wall, this polysaccharide is terminally deposited in the endosperm walls in cereal grains to varying degrees (Carpita 1996). This could be a remnant of MLG being the main source of carbohydrate storage in ancestral species before starch assumed this role (Dhugga et al. 2004). The expression of only six of the twelve *CesA* genes was detected in the endosperm, as observed in the earlier analysis. *ZmCesA5* was the most highly expressed of the *CesA* genes throughout the first 45 days of endosperm development, peaking at 12–20 days after pollination (Appenzeller et al. 2004). The pattern of *ZmCesA5* expression further supports a role for this gene in mixed-linked glucan synthesis. However, additional evidence is needed to substantiate this role. In addition, its role in cellulose formation cannot be ruled out.

Only three of the twelve maize *CesA* genes, *ZmCesA10, 11*, and *12*, appeared to be truly coordinately expressed. The expression of the remaining genes, where it occurred, was more overlapping in nature than coordinate (Appenzeller et al. 2004). The level of overlapped varied, however. The expression of *ZmCesA1, ZmCesA7* and *ZmCesA8* overlapped quite significantly. In contrast, the expression of *ZmCesA2* and *ZmCesA6* was independent of any of the other *CesA* genes. Whereas *ZmCesA2* was expressed in only 3 of the 76 libraries at a level exceeding 10 ppm, *ZmCesA6* was expressed in nearly all the libraries. *ZmCesA3* and *ZmCesA5* had similar expression patterns only with respect to one another and no other *CesA* gene. A lack of correlation of *ZmCesA2* and *ZmCesA6* with any of the *CesA* genes and moderate correlation among the other genes discussed above suggests that the relatively high correlation coefficients observed among some of the gene pairs may have biological relevance. Except *ZmCesA10-12* genes, which are expressed in the secondary wall forming cells, all the remaining genes appear to be largely expressed in the primary wall forming cells. Whether the clustering of the putatively primary wall forming genes based on their overlapping expression patterns into different groups has any functional relevance remains to be determined.

Dimerization of the CesA proteins has been proposed for the formation of a functional cellulose synthase complex (Scheible et al. 2001; Kurek et al. 2002).

All three of the *Arabidopsis* secondary wall forming CesA sequences (AtCesA8/Irx1, AtCesA7/Irx3 and AtCesA4/Irx5) have been reported to be involved in the formation of a functional cellulose synthase complex (Gardiner et al. 2003; Taylor et al. 2003). We propose that ZmCesA11, ZmCesA12 and ZmCesA10 have similar functional roles to these *Arabidopsis* proteins, respectively. Theoretically, only two subunits are necessary to provide juxtaposed catalytic sites for the formation of a β-glycosidic bond without having to rotate the chain after each bond is formed (Dhugga 2001). This could be accomplished either by a homo- or a heterodimer. That the combinations of CesA proteins in rosettes may be different between cell types of the same tissue and also amongst cells of the same type has also been proposed (Doblin et al. 2002). The significance of the presence of more than two CesA polypeptides in the same rosette still remains unclear.

8 RATIONALE FOR FUTURE TRANSGENIC WORK

According to the summation theorem of Metabolic Control Analysis (MCA) (Kacser and Burns 1973; Heinrich and Rapoport 1974; Kell and Westerhoff 1986; Cornish-Bowden et al. 1995; Fell 1996; Heinrich and Schuster 1996), changes in the concentrations of individual enzymes within a metabolic pathway tend to have little effect on metabolic fluxes and on the phenotype under most conditions (Thatcher et al. 1998). However, changes in individual enzyme concentrations could affect the size of metabolite pools even when the alterations in flux are minimal. Because of mass action effects, the change in a metabolic pool could lead to a shift of other coupled metabolites and change the flux at the nonequilibrium reactions in the pathway.

Metabolic simulations using a kinetic model suggest that the magnitude and net direction of carbon fluxes in the far-from-equilibrium reactions are influenced by changes in mass action relationships and total activity rather than by alteration in substrate affinity (Barreiro 1999). Since cellulose synthase is at the end of a metabolic route, and there is no other known branching path to bypass the synthesis of cellulose through this enzyme, it is likely to have a high flux control coefficient (the scaled partial derivative of a system variable such as flux) with respect to enzyme activities. If this is true *in vivo*, an increase in abundance of this enzyme should correlate with an increase in cellulose production, providing that the overexpressed enzyme is targeted in the proper amount to the appropriate subcellular location.

Overexpression of a cellulose-binding domain (CBD) has been reported to result in increased cellulose production in poplar (Levy et al. 2002). It was proposed that the CBD increased the rate of cellulose production by slowing down the rate of crystallization of the glucan chains into microfibrils, which is believed to limit the rate of cellulose synthesis in intact cells. This idea is based on the earlier finding that calcofluor white, a fluorescent dye commonly used to detect cellulose, interfered with the crystallization of the glucan chains into microfibrils (Haigler et al. 1980).

Atkinson (1977) pointed out that a limiting factor in cell structure is its solvation capacity. This limitation does not allow for each metabolite to fill the water volume of a cell to reach its operating concentration. According to Srere (1987), about 80% of the metabolic intermediates have just one use in the cell and this is possibly an evolutionary strategy to overcome the solvation capacity of the cell. An important consequence of this strategy is the metabolic organization through the formation of sequential multienzyme complexes with the concomitant channeling capabilities (Srere 1987). This view of cellular metabolism conceptualizes that, in order to be effective in metabolic control, an enzyme has to be expressed in the proper amount and that does not always correlate with the amount of transcript present (Siedow and Stitt 1998). Moreover, to participate in metabolic control, the participating enzymes need to be positioned in the adequate location to support the channel structure.

Since the control capacity at a particular steady state is distributed among the intervening enzymes, any attempt to engineer a change in the flux towards cellulose will need a careful study of the system and will probably involve the manipulation of more than one parameter (enzymes amount, kinetic constants, and metabolite pools). According to kinetic simulations, near-equilibrium reactions are more easily affected by mass action effects while enzymes catalyzing reactions that are far from equilibrium can alter the flux through modifications in their V*f* (Barreiro 1999). However, there are no fixed rules to alter metabolic systems at will but it is possible to engineer them by understanding the control coefficients involved and the local properties of the reactions involved. This will most likely involve altering the metabolic mass action ratios, modifying the activities of key enzymes, and stimulating the synthesis of end-products such as cellulose, to drive fluxes out of the intermediary metabolism.

9 SUMMARY

Cellulose in a unit length of the stalk below the ear node in maize is the main determinant of mechanical strength, a trait of considerable importance in agriculture. The majority of cellulose in the stalk is in the vascular bundles, which occur throughout the cross-section of the stalk but are densely packed among the peripheral sclerenchymatous cell layers collectively referred to as rind. Three of the twelve maize *CesA* genes, *ZmCesA10-12,* appear to be involved in secondary wall formation and the remaining nine in primary wall formation. The putatively primary wall forming genes can be grouped into different clusters based on their expression patterns, however, the functional significance of these groupings is not clear at this point. Availability of the secondary wall forming *CesA* genes has made it possible to isolate their promoter elements. These promoters will allow the expression of the *CesA* and other genes in specific cell types where cellulose could be increased at the expense of hemicellulose, soluble sugars and potentially lignin with the goal of improving stalk strength. Another opportunity would be to increase cellulose formation in the parenchymatous cells. In either

case, the harvest index must not be adversely impacted in order to maintain or increase grain yield while altering the composition of the existing biomass.

REFERENCES

Aloni Y., Delmer D.P., and Benziman M. 1982. Achievement of high rates of *in vitro* synthesis of 1,4-β-D-glucan: activation by cooperative interaction of the *Acetobacter xylinum* enzyme system with GTP, polyethylene glycol and protein factor. Proc Natl Acad Sci USA 79:6448–6452.

Appenzeller L., Doblin M., Barreiro R., Wang H., Niu X., Kollipara K., Carrigan L., Tomes D., Chapman M., and Dhugga K.S. 2004. Cellulose synthesis in maize: isolation and expression analysis of the cellulose synthase (*CesA*) gene family. Cellulose 11:287–299.

Arioli T., Peng L., Betzner Andreas S., Burn J., Wittke W., Herth W., Camilleri C., Hofte H., Plazinski J., Birch R., Cork A., Glover J., Redmond J., and Williamson R.E. 1998. Molecular analysis of cellulose biosynthesis in *Arabidopsis*. Science 279:717–720.

Atkinson D.E. 1977. Cellular energy metabolism and its regulation. Academic Press, London.

Avigad G. 1964. Sucrose-uridine diphosphate glucosyltransferase from jerusalem artichoke tubers. J Biol Chem 239:3613–3618.

Barreiro R. 1999. Metabolic control analysis of carbon pathways. PhD thesis. UMI Dissertation Services. UMI database number 9944792: p. 376.

Beeckman T., Przemeck G.K.H., Stamatiou G., Lau R., Terryn N., De Rycke R., Inze D., and Berleth T. 2002. Genetic complexity of cellulose synthase: a gene function in *Arabidopsis* embryogenesis. Plant Physiol 130:1883–1893.

Boisson M., Gomord V., Audran C., Berger N., Dubreucq B., Granier F., Lerouge P., Faye L., Caboche M., and Lepiniec L. 2001. *Arabidopsis* glucosidase I mutants reveal a critical role of N-glycan trimming in seed development. EMBO J 20:1010–1019.

Brenner S., Johnson M., Bridgham J., Golda G., Lloyd D.H., Johnson D., Luo S., McCurdy S., Foy M., Ewan M., Roth R., George D., Eletr S., Albrecht G., Vermaas E., Williams S.R., Moon K., Burcham T., Pallas M., DuBridge R.B., Kirchner J., Fearon K., Mao J.I., and Corcoran K. 2000a. Gene expression analysis by massively parallel signature sequencing (MPSS) on microbead arrays. Nature Biotechnol 18:630–634.

Brenner S., Williams S.R., Vermaas E.H., Storck T., Moon K., McCollum C., Mao J.I., Luo S., Kirchner J.J., Eletr S., DuBridge R.B., Burcham T., and Albrecht G. 2000b. In vitro cloning of complex mixtures of DNA on microbeads: physical separation of differentially expressed cDNAs. Proc Natl Acad Sci USA 97:1665–1670.

Bücher T. and Russmann W. 1964. Angew Chem Ed. Engl 3:426.

Buczynski S.R., Thom M., Chourey P., and Maretzki A. 1993. Tissue distribution and characterization of sucrose synthase isozymes in sugarcane. J Plant Physiol 142:641–646.

Burn J.E., Hurley U.A., Birch R.J., Arioli T., Cork A., and Williamson R.E. 2002. The cellulose-deficient *Arabidopsis* mutant rsw3 is defective in a gene encoding a putative glucosidase II: an enzyme processing N-glycans during ER quality control. Plant J 32:949–960.

Burton R.A., Shirley N.J., King B.J., Harvey A.J., and Fincher G.B. 2003. The CesA gene family of barley: quantitative analysis of transcripts reveals two groups of co-expressed genes. Plant Physiol 134:224–236.

Cano-Delgado A.I., Metzlaff K., and Bevan M.W. 2000. The eli1 mutation reveals a link between cell expansion and secondary cell wall formation in *Arabidopsis thaliana*. Development 127: 3395–3405.

Cano-Delgado A., Penfield S., Smith C., Catley M., and Bevan M. 2003. Reduced cellulose synthesis invokes lignification and defense responses in *Arabidopsis* thaliana. Plant J 34:351–362.

Cardini C.E., Leloir L.F., and Chiriboga J. 1955. The biosynthesis of sucrose. J Biol Chem 214:149–155.

Carpita N.C. 1996. Structure and biogenesis of the cell walls of grasses. Ann Rev Plant Physiol Plant Mol Biol 47:445–476.

Cornish-Bowden A., Hofmeyr J.-H.S., and Cárdenas M.L. 1995. Strategies for manipulating metabolic fluxes in biotechnology. Bioorg Chem 23:439–449

Dancer J., Ekkehard-Neuhaus H., and Stitt M. 1990. Subcellular compartmentation of uridine nucleotides and nucleoside-5′-diphosphate kinase in leaves. Plant Physiol 92:637–641.

DeFekete M.A.R. and Cardini C.E. 1964. Mechanism of glucose transfer from sucrose into the starch granule of sweet corn. Arch Biochem Biophys 104:173.

DeFekete M.A.R. 1969. Zum stoffwechsel der starke. Planta 87:311.

Delmer D. 1999. Cellulose biosynthesis: exciting times for a difficult field of study. Annu Rev Plant Physiol Plant Mol Biol 50:245–276.

Delmer D.P., Ohana P., Gonen L., and Benziman M. 1993. *In vitro* synthesis of cellulose in plants – still a long way to go! Plant Physiol 103:307–308.

Desprez T., Vernhettes S., Fagard M., Refregier G., Desnos T., Aletti E., Py N., Pelletier S., and Hofte H. 2002. Resistance against herbicide isoxaben and cellulose deficiency caused by distinct mutations in same cellulose synthase isoform CESA6. Plant Physiol 128:482–490.

Dhugga K.S. 2001. Building the wall: genes and enzyme complexes for polysaccahride synthases. Curr Opin Plant Biol 4:488–493.

Dhugga K.S. 2005. Plant Golgi cell wall synthesis: From genes to enzyme activities. Proc Natl Acad Sci USA 102:1815–1816.

Dhugga K.S. and Ray P.M. 1994. Purification of 1,3-beta-glucan synthase activity from pea tissue: two polypeptides of 55 kDa and 70 kDa copurify with enzyme activity. Eur J Biochem 220: 943–953.

Dhugga K.S., Helentjaris T., and Niu X. 2002. Manipulation of sucrose synthase genes to improve stalk and grain quality. World Patent WO2002067662 A1.

Dhugga K.S., Barreiro R., Whitten B., Stecca K., Hazebroek J., Randhawa G.S., Dolan M., Kinney A.J., Tomes D., Nichols S., and Anderson P. 2004. Guar seed beta-mannan synthase is a member of the cellulose synthase super gene family. Science 303:363–366.

Doblin M.S., De M.L., Newbigin E., Bacic A., and Read S.M. 2001. Pollen tubes of Nicotiana alata express two genes from different beta-glucan synthase families. Plant Physiol 125:2040–2052.

Doblin M.S., Kurek I., Jacob W.D., and Delmer D.P. 2002. Cellulose biosynthesis in plants: from genes to rosettes. Plant and Cell Physiol 43:1407–1420.

Duvick D.N. and Cassman K.G. 1999. Post-green revolution trends in yield potential of temperate maize in the north-central United States. Crop Sci 39:1622–1630.

Ellis C., Karafyllidis I., Wasternack C., and Turner J.G. 2002. The *Arabidopsis* mutant cev1 links cell wall signaling to jasmonate and ethylene responses. Plant Cell 14:1557–1566.

Entwistle G. and ApRees T. 1988. Enzymic capacities of amyloplasts from wheat (*Triticum aestivum*) endosperm. Biochem J 255:391–396.

Fagard M., Desnos T., Desprez T., Goubet F., Refregier G., Mouille G., McCann M., Rayon C., Vernhettes S., and Hofte H. 2000. PROCUSTE1 encodes a cellulose synthase required for normal cell elongation specifically in roots and dark-grown hypocotyls of *Arabidopsis*. Plant Cell 12:2409–2423.

Fell D.A. 1996. Understanding Metabolic Control. Portland Press, London.

Felsenstein J. 1985. Confidence limits on phylogenies: an approach using the bootstrap. Evolution 39:783–791.

Gardiner J.C., Taylor N.G., and Turner S.R. 2003. Control of cellulose synthase complex localization in developing xylem. Plant Cell 15:1740–1748.

Gardner A., Davies H.V., and Burch L.R. 1992. Purification and properties of fructokinase from developing tubers of potato (*Solanum tuberosum* L.). Plant Physiol 100:178–183.

Geigenberger P., Reimholz R., Geiger M., Merlo L., Canale V., and Stitt M. 1997. Regulation of sucrose and starch metabolism in potato tubers in response to short-term water deficit. Planta 201:502–518.

Gillmor C.S., Poindexter P., Lorieau J., Palcic M.M., and Somerville C. 2002. Alpha-glucosidase I is required for cellulose biosynthesis and morphogenesis in *Arabidopsis*. J Cell Biol 156:1003–1013.

Haigler C.H., Brown, Jr. R.M., and Benziman M. 1980. Calcofluor white ST alters the *in vivo* assembly of cellulose microfibrils. Science 210:903–906.

Haigler C.H., Ivanova D.M., Hogan P.S., Salnikov V.V., Hwang S., Martin K., and Delmer D.P. 2001. Carbon partitioning to cellulose synthesis. Plant Mol Biol 47:29–51.

Hauser M.T., Morikami A., and Benfey P.N. 1995. Conditional root expansion mutants of *Arabidopsis*. Development 121:1237–1252.

Hazen S.P., Scott C.J.S., and Walton J.D. 2002. Cellulose synthase-like genes of rice. Plant Physiol 128:336–340.

Heinrich R. and Rapoport T.A. 1974. A linear steady-state treatment of enzymatic chains: general properties, control and effector strength. Eur J Biochem 42:89–95.

Heinrich R. and Schuster S. 1996. The Regulation of Cellular Systems. Chapman & Hall, New York.

Hess B. 1963. In: Wright B. (ed.) Control Mechanisms in Respiration and Fermentation. Ronald Press, New York, p. 333.

Hess B. and Brand K. 1965. In: Chance B., Estabrook, R.W., and Williamson, J.R. (eds.) Control of Energy Metabolism. Academic Press, New York, p. 111.

Holland N., Holland D., Helentjaris T., Dhugga K.S., Xoconostle-Czares B., and Delmer D.P. 2000. A comparative analysis of the plant cellulose synthase (*CesA*) gene family. Plant Physiol 123:1313–1323.

Hoth S., Morgante M., Sanchez J.P., Hanafey M.K., Tingey S.V., and Chua N.H. 2002. Genome-wide gene expression profiling in *Arabidopsis* thaliana reveals new targets of abscisic acid and largely impaired gene regulation in the abi1-1 mutant. J Cell Sci 115:4891–4900.

Huber S.C., Huber J.L., Liao P.C., Gage D.A., Michael R.W., Chourey P.S., Hannah L.C., and Koch K. 1996. Phosphorylation of serine-15 of maize leaf sucrose synthase. Occurrence *in vivo* and possible regulatory significance. Plant Physiol 112:793–802.

Hu W.J., Harding S.A., Lung J., Popko J.L., Ralph J., Stokke D.D., Tsai C.J., and Chiang V.L. 1999. Repression of lignin biosynthesis promotes cellulose accumulation and growth in transgenic trees. Nat Biotechnol 17:808–812.

Isherwood F.A. and Selvendran R.R. 1970. A note on the occurrence of nucleotides in strawberry leaves. Phytochemistry 9:2265–2269.

Kacser H. and Burns J.A. 1973. The control of flux. Symp Soc Exp Biol 27:65–107.

Kacser H. and Burns J.A. 1987. Control of metabolism: what do we have to measure? Trends Biochem Sci 7:1149–1161.

Kadam K.L. and McMillan J.D. 2003. Availability of corn stover as a sustainable feedstock for bio-ethanol production. Bioresour Technol 88:17–25.

Kell D.B. and Westerhoff H.V. 1986. Towards a rational approach to the optimization of flux in microbial biotransformations. Trends in Biotechnol 4:137–142.

Kimura S., Laosinchai W., Itoh T., Cui X., Linder C.R., and Brown, Jr. R.M., 1999. Immunogold labeling of rosette terminal cellulose-synthesizing complexes in the vascular plant *Vigna angularis*. Plant Cell 11:2075–2085.

Krapp A. and Stitt M. 1995. An evaluation of direct and indirect mechanisms for the "sink regulation" of photosynthesis in spinach: change in gas exchange, carbohydrates, metabolites, enzyme activities and steady-state transcript levels after cold-girdling source leaves. Planta 195:313–323.

Krause K.P. and Stitt M. 1992. Sucrose-6-phosphate levels in spinach leaves and their effects on sucrose-phosphate synthase. Phytochemistry 31:1143–1146.

Kruger N.J. 1997. Carbohydrate synthesis and degradation. In: Dennis D.T., Turpin D.H., Lefebvre D.D., and Layzell D.B. (eds.) Plant Metabolism Longman, Essex, UK, pp. 83–104.

Kuhad R.C. and Singh A. 1993. Lignocellulose biotechnology: current and future prospects. Critic Rev Biotechnol 13:151–172.

Kurek I., Kawagoe Y., Jacob W.D., Doblin M., and Delmer D. 2002. Dimerization of cotton fiber cellulose synthase catalytic subunits occurs via oxidation of the zinc-binding domains. Proc Natl Acad Sci USA 99:11109–11114.

Leopold A.C. and Kriedemann P.E. 1975. Plant growth and development. McGraw-Hill, New York.

Levy I., Shani Z., and Shoseyov O. 2002. Modification of polysaccharides and plant cell wall by endo-1,4-beta-glucanase and cellulose-binding domains. Biomol Eng 19:17–30.

Li L.K., Drake R.R., Clement S., and Brown, Jr. R.M. 1993. β-Glucan synthesis in the cotton fiber. II. Regulation and kinetic properties of β-glucan synthases. Plant Physiol 101:1143–1148.

Li L., Zhou Y., Cheng X., Sun J., Marita J.M., Ralph J., and Chiang V.L. 2003a. Combinatorial modification of multiple lignin traits in trees through multigene cotransformation. Proc Natl Acad Sci USA 100:4939–4944.

Li Y.H., Qian O., Zhou Y.H., Yan M.X., Sun L., Zhang M., Fu Z.M., Wang Y.H., Han B., Pang X.M., Chen M.S., and Li J.Y. 2003b. BRITTLE CULM1, which encodes a COBRA-like protein, affects the mechanical properties of rice plants. Plant Cell 15:2020–2031.

Lukowitz W., Nickle T.C., Meinke D.W., Last R.L., Conklin P.L., and Somerville C.R. 2001. *Arabidopsis* cyt1 mutants are deficient in a mannose-1-phosphate guanylyltransferase and point to a requirement of N-linked glycosylation for cellulose biosynthesis. Proc Natl Acad Sci USA 98:2262–2267.

Matthysse A.G., White S., and Lightfoot R. 1995. Genes required for cellulose synthesis in *Agrobacterium tumefaciens*. J Bacteriol 177:1069–1075.

Mendes P. 1993. GEPASI: a software package for modeling the dynamics, steady states and control of biochemical and other systems. Comput Appl Biosci 9:563–571.

Meyers B.C., Morgante M., and Michelmore R.W. 2002. TIR-X and TIR-NBS proteins: Two new families related to disease resistance TIR-NBS-LRR proteins encoded in *Arabidopsis* and other plant genomes. Plant J 32:77–92.

Milner Y. and Avigad G. 1964. The UDP-glucose: D-fructose glucosyltransferase system from sugar beet roots. XXXIV Meeting Israel Chem Soc 2:316.

Molhoj M., Pagant S., and Hofte H. 2002. Towards understanding the role of membrane-bound endo-beta-1,4-glucanases in cellulose biosynthesis. Plant Cell Physiol 43:1399–1406.

Neufeld E.F. and Hassid W.Z. 1963. Biosynthesis of saccharides from glycopyranosyl esters of nucleotides ("sugar nucleotides"). Advan Carbohyd Chem 18:309.

Nicol F., His I., Jauneau A., Vernhettes S., Canut H., and Hoefte H. 1998. A plasma membrane-bound putative endo-1,4-beta-D-glucanase is required for normal wall assembly and cell elongation in *Arabidopsis*. EMBO J 17:5562–5576.

Niklas K.J. 1992. Plant Biomechanics: an engineering approach to plant form and function. The University of Chicago Press, Chicago, p. 607.

Pagant S., Bichet A., Sugimoto K., Lerouxel O., Desprez T., McCann M., Lerouge P., Vernhettes S., and Hofte H. 2002. Kobito1 encodes a novel plasma membrane protein necessary for normal synthesis of cellulose during cell expansion in *Arabidopsis*. Plant Cell 14:2001–2013.

Pavlinova O.A. 1971. Sucrose metabolism in the sugar beet root. Sov Plant Physiol 18:611–619.

Pear J.R., Kawagoe Y., Schreckengost W.E., Delmer D.P., and Stalker D.M. 1996. Higher plants contain homologs of the bacterial celA genes encoding the catalytic subunit of cellulose synthase. Proc Natl Acad Sci USA 93:12637–12642.

Peng L., Kawagoe Y., Hogan P., and Delmer D. 2002. Sitosterol-beta-glucoside as primer for cellulose synthesis in plants. Science 295:147–148.

Quick W.P. and Schaffer A.A. 1996. Sucrose metabolism in sources and sinks. In: Zamski E. and Schaffer A.A. (eds.) Photoassimilate Distribution in Plants and Crops: Source-Sink Relationships pp. 115–156. Marcel Dekker, New York.

Renz A. and Stitt M. 1993. Substrate specificity and product inhibition of different forms of fructokinases and hexokinases in developing potato tubers. Planta 190:166–175.

Renz A., Merlo L., and Stitt M. 1993. Partial purification from potato tubers of three fructokinases and three hexokinases which show differing organ and developmental specificity. Planta 190:156–165.

Richmond T.A. and Somerville C.R. 2000. The cellulose synthase superfamily. Plant Physiol 124:495–498.

Richmond T.A. and Somerville C.R. 2001. Integrative approaches to determining Csl function. Plant Mol Biol 47:131–143.

Rohwer J.M. and Botha F.C. 2001. Analysis of sucrose accumulation in the sugar cane culm on the basis of *in vitro* kinetic data. Biochem J 358:437–445.

Rolleston F.S. 1972. A theoretical background to the use of measured intermediates in the study of the control of intermediary metabolism. Curr Top Cell Reg 5:47–75.

Russell W.A. 1985. Evaluation of plant, ear, and grain traits of maize cultivars representing seven eras of breeding. Maydica 30:85–90.

Scheible W.R. and Pauly M. 2004. Glycosyltransferases and cell wall biosynthesis: novel players and insights. Curr Opin Plant Biol 7:285–295.

Scheible W.R., Eshed R., Richmond T., Delmer D., and Somerville C. 2001. Modifications of cellulose synthase confer resistance to isoxaben and thiazolidinone herbicides in *Arabidopsis* Ixr1 mutants. Proc Natl Acad Sci USA 98:10079–10084.

Siedow J.N. and Stitt M. 1998. Plant Metabolism: where are all those pathways leading us? Curr Opin Plant Biol 1:197–200.

Sinclair T.R. 1998. Historical changes in harvest index and crop nitrogen accumulation. Crop Sci 38:638–643.

Sinclair T.R. and de Wit C.T. 1975. Photosynthate and nitrogen requirement for seed production by various crops. Science 189:565–567.

Srere P.A. 1987. Complexes of sequential metabolic enzymes. Ann Rev Biochem 56:21–56.

Stitt M. 1989. Control of sucrose synthesis: estimation of free energy charges, investigation of the contribution of equilibrium and non-equilibrium reactions and estimation of elasticities and flux control coefficients. In: Barber, J. (ed.) Techniques and new Developments in Photosynthetic Research. Plenum Press, London, pp. 365–392.

Stitt M. and Steup M. 1985. Starch and sucrose degradation. In: Douce R. and Day D.A. (eds.) Higher Plant Cell Respiration. Springer, Heidelberg, pp. 347–390.

Swofford D.L. 1998. PAUP*: Phylogenetic Analysis Using Parsimony (and other Methods), Version 4. Sinauer Associates, Inc. Publishers, Sunderland, Massachusetts.

Szyjanowicz P.M.J., McKinnon I., Taylor N.G., Gardiner J., Jarvis M.C., and Turner S.R. 2004. The irregular xylem 2 mutant is an allele of korrigan that affects the secondary cell wall of *Arabidopsis thaliana*. Plant J 37:730–740.

Tanaka K., Murata K., Yamazaki M., Onosato K., Miyao A., and Hirochika H. 2003. Three distinct rice cellulose synthase catalytic subunit genes required for cellulose synthesis in the secondary wall. Plant Physiol 133:73–83.

Tang G.Q. and Sturm A. 1999. Antisense repression of sucrose synthase in carrot (*Daucus carota* L.) affects growth rather than sucrose partitioning. Plant Mol Biol 41:465–479.

Taylor N.G., Scheible W.R., Cutler S., Somerville C.R., and Turner S.R. 1999. The irregular xylem3 locus of *Arabidopsis* encodes a cellulose synthase required for secondary cell wall synthesis. Plant Cell 11:769–779.

Taylor N.G., Laurie S., and Turner S.R. 2000. Multiple cellulose synthase catalytic subunits are required for cellulose synthesis in *Arabidopsis*. Plant Cell 12:2529–2539.

Taylor N.G., Howells R.M., Huttly A.K., Vickers K., and Turner S.R. 2003. Interactions among three distinct CesA proteins essential for cellulose synthesis. Proc Natl Acad Sci USA 100: 1450–1455.

Thatcher J.W., Shaw J.M., and Dickinson W.J. 1998. Marginal fitness contributions of nonessential genes in yeast. Proc Natl Acad Sci USA 95:253–257.

Tollenaar M. and Wu J. 1999. Yield improvement in temperate maize is attributable to greater stress tolerance. Crop Sci 39:1597–1604.

Turner S.R. and Somerville C.R. 1997. Collapsed xylem phenotype of *Arabidopsis* identifies mutants deficient in cellulose deposition in the secondary cell wall. Plant Cell 9:689–701.

Uhart S.A. and Andrade F.H. 1995. Nitrogen deficiency in maize. I. Effects on crop growth, development, dry matter partitioning, and kernel set. Crop Sci 35:1376–1383.

Viola R. 1996. Hexose metabolism in discs excised from developing potato (*Solanum tuberosum* L.) tubers. II. Estimations of fluxes *in vivo* and evidence that fructokinase catalyses a near rate-limiting reaction. Planta 198:186–196.

Winter H., Robinson D.G., and Heldt H.W. 1993. Subcellular volumes and metabolite concentrations in barley leaves. Planta 191:180–190.

Winter H., Robinson D.G., and Heldt H.W. 1994. Subcellular volumes and metabolite concentrations in spinach leaves. Planta 193:530–535.

Wu L., Joshi C.P., and Chiang V.L. 2000. A xylem-specific cellulose synthase gene from aspen (*Populus tremuloides*) is responsive to mechanical stress. Plant J. 22:495–502.

Zhong R.Q., Morrison W.H., Freshour G.D., Hahn M.G., and Ye Z.H. 2003. Expression of a mutant form of cellulose synthase AtCesA7 causes dominant negative effect on cellulose biosynthesis. Plant Physiol 132:786–795.

CHAPTER 6

CELLULOSE BIOSYNTHESIS IN FOREST TREES

KRISTINA BLOMQVIST*, SORAYA DJERBI, HENRIK ASPEBORG, AND TUULA T. TEERI

AlbaNova University Center, Royal Institute of Technology, School of Biotechnology, SE-10691 Stockholm, Sweden

Abstract

Wood formation is a fundamental biological process of significant economic and commercial interest. During wood formation, most glucose from the carbohydrate metabolism is channeled to cellulose in the secondary cell walls. The cellulose microfibrils associate with hemicellulose, proteins, and lignin to form the strong and flexible biocomposite known as wood. As the main wood component, cellulose is essential for the survival of trees and for their exploitation by man.

In spite of this, the molecular details of cellulose biosynthesis have remained obscure in all plants. In particular, the toughness of wood cells makes it hard to isolate active enzymes and study cellulose synthesis in trees. Functional genomics provides powerful new tools to study complex metabolic processes. In this way, 18 *CesA* genes have been recently identified in the genome sequence of *Populus trichocarpa*.

Expression profiling during wood formation has shown that four of these genes are specifically upregulated during xylogenesis and/or tension wood formation. Other genes that follow the same expression pattern as the wood-related *CesA* genes encode the putative Korrigan ortholog PttCel9A and a novel microtubule associated protein PttMAP20. Cell suspension cultures of hybrid aspen with elevated expression of the secondary cell wall specific *PttCesA* genes have been used for efficient *in vitro* synthesis of cellulose, which will facilitate future studies of this challenging process in trees.

Keywords

cellulose synthesis, CesA, hybrid aspen, expression profiling, plant cell wall, wood formation.

* Author for correspondence: Kristina Blomqvist; Ullsaxvägen 12, 75648 Uppsala, Tel: +46-18-301771. email: kristina.bl@telia.com

R.M. Brown, Jr. and I.M. Saxena (eds.), Cellulose: Molecular and Structural Biology, 85–106.

1 THE PROPERTIES OF WOOD

Trees are nature's largest and longest living organisms and, like all plants, cannot escape any environmental challenges. They have therefore evolved a survival strategy based on metabolic flexibility, sturdy cells and efficient transportation of metabolites between roots and leaves, which can be over 100 meters apart. The canopy of a tree carries the leaves, which are its carbohydrate factory, while the long trunk serves to hold the leaves above other plants to win the competition for light for efficient photosynthesis. In order to produce such a gigantic and long-lasting stem, trees synthesize wood. Wood is resistant to most environmental challenges, including microbial attack, which leads to its extreme durability. Wood is also cheap to maintain since most of the cells in a tree trunk are dead: as little as 1% of a tree consists of living cells (Mirov and Hasbrouck 1976). Two major classes of trees have evolved independently, the gymnosperms (i.e., conifers such as pine, spruce and fir) and the angiosperms (i.e., broad-leaf trees). The angiosperms are further subdivided into monocotyledons (palm trees, bamboo, etc.) and dicotyledons (birch, oak, maple, etc.).

1.1 Formation of wood cells

Wood has a structure that ideally combines strength with flexibility. This is achieved by the production of complex multilayered cell walls composed of cellulose microfibrils embedded in a matrix of hemicellulose and lignin. In a tree, over 90% of the wood cells are arranged along the axis of the trunk or branches to transport water from the roots to the leaves. All the different cell types in a tree originate from a single layer of multipotent dividing cells termed the vascular cambium. There are two types of cambial cells – the long narrow fusiform initial cells, which develop into the axial cells; and the ray initials, which form the radial cells. Some of these cells continue to divide whereas others differentiate either inwards into the xylem cells, or outwards into the phloem cells. The xylem has two main functions. One is to transport water, nutrients, and hormones whereas the other is to provide mechanical support to the plant. The phloem provides paths for the distribution of the photosynthetic product, sucrose, involved in plant growth and development. Gymnosperms produce soft wood, which has a relatively simple structure consisting of three axial and three radial cell types (Figure 6-1). In contrast, the hard wood produced by the angiosperms is usually built of 5–6 different axial and 4 different radial cell types with more advanced cell morphology (Fujita and Harada 2001). The gymnosperms and angiosperms also differ in the type of reaction wood (compression wood *versus* tension wood) and leaf structure (needles versus leaves) that they produce.

The rigidity of the plant cell wall serves as a protection against weather and microorganisms, but it also limits the growth of the plant and complicates the transportation of metabolites. To circumvent the negative effects of such a rigid structure, the plant cell wall is built in multiple layers containing different

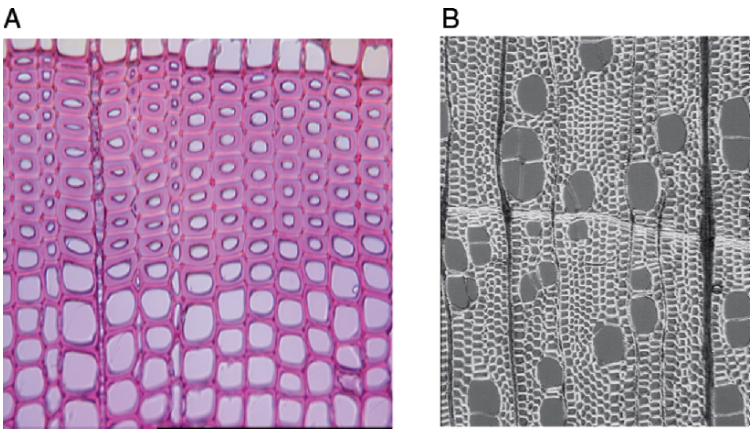

Figure 6-1. Transverse sections of woody tissues in softwood (pine, **A**) and hardwood (birch, **B**). The majority of softwood tracheids occur in organized rows (**A**) while hardwood contains rows of fibers interrupted by large vessels (**B**). Seasonal variation of the cell wall thickness in the softwood tracheids is clearly visible in (**A**). Courtesy of Geoff Daniel, Swedish University of Agriculture Sciences. With permission (*See Color Plate of this figure beginning on page 355*)

constituents, which allows for greater flexibility during cell development (Fujita and Harada 2001; Mellerowicz et al. 2001). During xylogenesis (wood formation), three different cell wall layers are produced, the middle lamella, the primary cell wall and the secondary cell wall (Figure 6-2).

The middle lamella consists mainly of pectin and some lignin. The primary cell wall is elastic and contains a mesh of cellulose microfibrils associated with hemicellulose, pectin and proteins. Proteins in the primary wall can perturb the interactions between the cellulose microfibrils and hemicellulose, allowing the

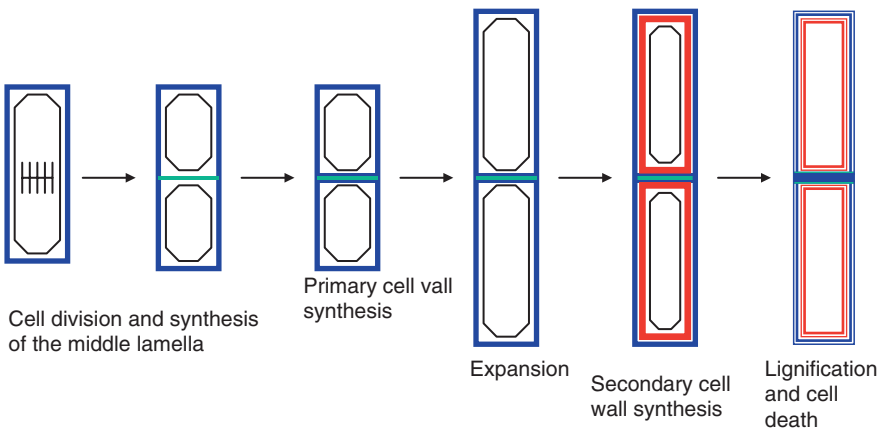

Figure 6-2. A schematic representation of cell wall synthesis during plant cell development (*See Color Plate of this figure beginning on page 355*)

cell to grow and expand into its characteristic shape (Cosgrove 1999; Kohorn 2001). It is only after the cells have reached their final size that the synthesis of the thick secondary cell walls begins. In secondary walls, cellulose microfibrils are laid down in highly ordered, parallel arrangements in three different layers (S1, S2, S3). The angle of the deposition of cellulose microfibrils differs between the different S-layers, and it is this that confers the strong and durable characteristic to wood (Chaffey et al. 1999; Funada 2000; Plomion et al. 2001). The microfibril angle also varies depending on the age and type of wood. For instance, increased microfibril angle in juvenile and compression wood results in a higher degree of flexibility (Emons and Mulder 2000; Plomion et al. 2001). The molecular mechanisms responsible for the patterned orientation of microfibrils have not been fully resolved, although it is obvious that the cortical microtubules are somehow involved in this process. Ledbetter and Porter (1963) reported that cortical microtubules lie in parallel with the microfibrils. Later, it was shown that cells treated with colchicine to disrupt microtubules, suffer from disturbed patterns of secondary thickenings (Torrey et al. 1971; Baskin 2001). Following these early findings, many different investigations have addressed the role of microtubules in controlling the microfibril orientation, but a mechanistic explanation has not yet been achieved (recently reviewed by Oda and Hasezawa 2006).

Secondary cell wall formation is finalized by lignification and followed by programmed cell death, during which the plasma membrane collapses and the cell dies. Lignification proceeds from the middle lamella through the primary cell wall and inwards over the secondary cell wall. In the final stages of xylogenesis, the deposition of chemical components known as extractives, result in the formation of heartwood, which is the least permeable and most durable form of wood (Plomion et al. 2001).

1.2 Reaction wood

Wood structure within a given tree species is not uniform but varies depending on the conditions under which the tree is growing. For example, trees compensate for exposure to wind or other types of bending pressure by the production of reaction wood. In softwood, the formation of reaction wood is induced on the compressed side of a bending trunk (compression wood), whereas in hardwood, reaction wood is formed on the elongated side of the trunk (tension wood). Reaction wood cells are morphologically similar to normal wood cells but differ in their cell wall structure and chemical composition.

Compression wood has high lignin content while tension wood cells produce an extra cell wall layer, the gelatinous layer (G-layer) (Figure 6-3). The G-layer is composed of almost pure crystalline cellulose and it is deficient in lignin and hemicelluloses. Owing to the high cellulose content of tension wood, gene expression profiling followed by functional studies can be used as a valuable tool for identifying genes and proteins specifically involved in cellulose biosynthesis (Andersson-Gunneras et al. 2006).

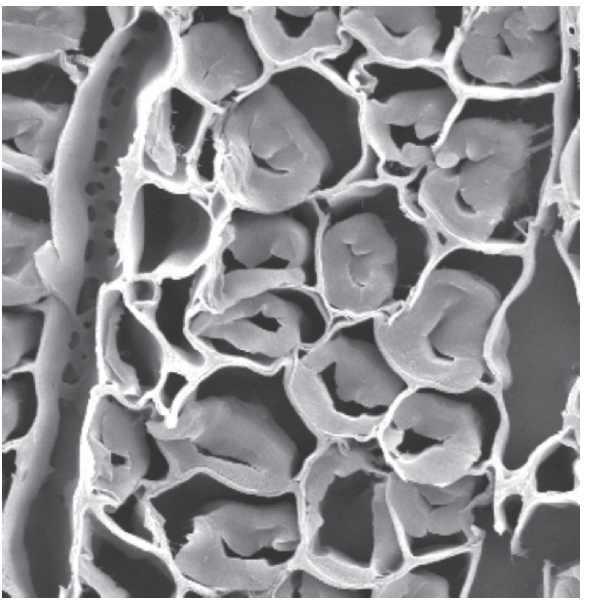

Figure 6-3. A gelatinous layer (G-layer) is formed on the inside of the S2 layer in tension wood fibers from *Populus tremuloides*. Courtesy of Geoff Daniel, Swedish University of Agriculture Sciences. With permission

2 CELLULOSE SYNTHESIS

Cellulose is the most abundant polysaccharide in nature with approximately 180 billion tons produced and broken down every year (Engelhardt 1995). Cellulose, which occurs as microfibrils, is the component responsible for the excellent load bearing properties of plant cell walls (for a summary for the cellulose content of the different cell wall layers, see Table 6-1). The cellulose microfibrils in wood fibers are important raw material for the pulp and paper industries, and those in cotton and hemp for the textile industries. Moreover, the renewable plant fibers have substantial potential to replace man-made fibers in fiber-reinforced thermosets and thermoplastics to produce environmentally friendly materials (Mohanty et al.

Table 6-1. The amount of cellulose (%) compared to the total amount of polysaccharides within the different cell layers of wood

Wood species	ML + P	S1	S2 (outer)	S2 (inner) + S3
Pine	33.4	55.2	64.3	63.6
Spruce	35.5	61.5	66.5	47.5
Birch	41.4	49.8	48.0	60.0

(After Meier 1964 and Daniel 2003). ML, middle lamella; P, primary cell wall; S1, S2, S3, different layers of the secondary cell walls.

2001; Klemm et al. 2005). However, despite the potential for broad commercial use, the detailed structure of plant fibers and the underlying mechanisms of cellulose biosynthesis remain poorly understood.

2.1 Rosettes: the machinery of cellulose synthesis

Cellulose is a linear polymer of glucose residues connected by (1→4)-β-linkages to a high degree of polymerization (DP). In some species of algae, cellulose chains of up to 20,000 glucose units have been observed, while somewhat lower DP is observed in cellulose chains produced by higher plants, including trees. Cellulose is synthesized by large protein complexes associated with the plasma membrane (reviewed by Doblin et al. 2002). The first cellulose-synthesizing complex was identified by electron microscopy of freeze-fractured plasma membranes in the algae *Oocystis apiculata* (Brown, Jr. and Montezinos 1976). The complexes appeared at the tip of the cellulose microfibrils and were therefore named terminal complexes (TC). The TC of *O. apiculata* are organized in transverse rows but early experiments with vascular plants revealed hexagonal structures termed rosettes (Mueller and Brown, Jr. 1980; Brown, Jr. 1996). Even though the rosettes seem to be highly conserved in vascular plants, none have so far been identified in woody plants. In part, this is certainly a result of the experimental difficulties of studying the hard woody tissues. However, it is also possible that the synthesis and assembly of the thick, multilayered secondary cell walls of wood require unusual arrangements of the cellulose synthesizing complexes.

2.2 *CesA* and *Csl*

Cellulose synthesis, i.e., the polymerization of glucose from the substrate UDP-glucose, is catalyzed by the enzyme cellulose synthase (UDP-glucose-(1,4)-β-glucan glucosyl transferase, EC 2.4.1.12). Genes encoding cellulose synthases (*CesA*) were first identified in the cellulose-synthesizing bacterium *Acetobacter xylinum* (Saxena et al. 1990; Wong et al. 1990), followed by the identification of two putative *CesA* genes in cotton (Pear et al. 1996). Immunolocalization studies of plant plasma membranes indicate that the CesA proteins are indeed part of the rosette complex (Kimura et al. 1999). Today, a large number of *CesA,* as well as *CesA*-like (*Csl*) genes, forming a large super family, have been identified and sequenced from many plants (see Burton et al. 2005), including trees such as poplar (Sterky et al. 1998; Wu et al. 2000; Samuga and Joshi 2002; Joshi 2003; Kalluri and Joshi 2003; Djerbi et al. 2004; Samuga and Joshi 2004; Djerbi et al. 2005), pine (Allona et al. 1998; Nairn and Haselkorn 2005) and Eucalyptus (Ranik and Myburg 2006).

Sequence analyses revealed that the proteins encoded by the *CesA* genes belong to family 2 glycosyl transferases, which characteristically display a two-domain structure (Saxena et al. 1995; Saxena and Brown, Jr. 1997; Henrissat et al. 2001). The N-terminal A-domain contains the D…D(x)D motif common to all family 2 members. The C-terminal B-domain carries the QxxRW motif characteristic

of polymerizing transferases, which include chitin synthases and hyaluronan synthases (Saxena et al. 1995; Saxena and Brown, Jr. 1997; Campbell et al. 1998; Coutinho et al. 2003). Structural evidence of family 2 and other glycosyl transferases suggests that the A-domain binds the nucleotide sugar, and the B-domain the acceptor substrate, which together form the functional active site (Charnock and Davies 1999; Charnock et al. 2001).

The role of the CesA proteins on cellulose biosynthesis has so far been mainly addressed at the genetic level by studying cell wall mutants of *Arabidopsis thaliana* (reviewed by Williamson et al. 2002). At least 10 different *CesA* genes have been identified in the *Arabidopsis* genome, indicating a functional redundancy or tissue-specific function of this class of proteins. Through analysis of mutant phenotypes, several of the *CesA* genes have been linked to cellulose synthesis either in primary or secondary cell walls. At least five genes, *AtCesA1*, *2, 3, 5* and *6*, are expressed during primary cell wall synthesis (Arioli et al. 1998; Fagard et al. 2000; Scheible et al. 2001; Burn et al. 2002; Desprez et al. 2002; Doblin et al. 2002). Further, it has been proposed that the AtCesA3 and AtCesA6 proteins together form an active protein complex, in which the involvement of even AtCesA1 may be required (Desprez et al. 2002). Mutations affecting the *AtCesA4* (*irx5*), *AtCesA7* (*irx3*) and *AtCesA8* (*irx1*) genes lead to cellulose deficient phenotypes with collapsed xylem suggesting that the corresponding three CesA isoenzymes are needed for the secondary cell wall synthesis (Turner and Somerville 1997; Taylor et al. 1999; Holland et al. 2000; Taylor et al. 2000; Taylor et al. 2003). On the other hand, a missense mutation in one of these, AtCesA7, seems to disturb cellulose biosynthesis during both primary and secondary cell wall formation (Zhong et al. 2003).

Owing to the long generation times and the tough structure of wood, it is much more difficult to study cellulose biosynthesis in trees than in annual plants such as *Arabidopsis*. Nevertheless, the use of tree models is necessary due to the existence of many unique features of wood-forming trees, such as secondary xylem formation, juvenile to mature wood transition and heartwood formation. Species of *Populus* are excellent models of forest trees (Mellerowicz et al. 2001). The advantages of using poplars as models are the relatively small genome size (550 Mbp compared to approx. 15,500 Mbp in average for gymnosperms), their fast growth characteristics and easy transformation capabilities. In addition, an extensive Expressed Sequence Tag (EST) database (Sterky et al. 2004; http://www.populus.db.umu.se/) and the recently completed genome sequence (http://genome.jgi-psf.org/Poptr1/Poptr1.home.html) have paved the way for functional genomics in poplars. They are also genetically close to *Arabidopsis*, which facilitates comparative functional studies between the two model systems (Bradshaw et al. 2000; Bhalerao et al. 2003).

Similar to *Arabidopsis*, 10 different *CesA* genes were first identified (Djerbi et al. 2004) by analyzing EST sequences in a collection of tissue specific cDNA libraries of poplars (Sterky et al. 2004). These *CesA* genes were named *PttCesA* (for *Populus tremula* × *tremuloides*, *Ptt*) followed by a number (1–9) reflecting

their order of discovery as proposed by Delmer (1999). A multiple alignment of the 10 PttCesA protein sequences revealed the presence of the conserved D…D(x)D and QxxRW sequence motifs as well as the transmembrane domain structure shared by the CesA proteins so far identified (Saxena et al. 1995; Saxena and Brown, Jr. 1997; Campbell et al. 1998; Delmer 1999). All of the hybrid aspen CesA proteins also contained the two N-terminal zinc finger domains proposed to have an important role in the dimerization of the CesA catalytic subunits and thus in the rosette assembly (Kurek et al. 2002). Since the zinc finger domain is the main feature distinguishing the CesA proteins from CesA-like proteins (Richmond 2000), it is likely that the genes do indeed code for enzymes involved in cellulose biosynthesis.

Interestingly, screening of the recently completed genome sequence of *Populus trichocarpa* revealed at least 18 *CesA* gene models (Djerbi et al. 2005; Geisler-Lee et al. 2006). The identified genes were grouped in seven gene pairs, one group of three sequences and one single gene. No sequences corresponding to the gene pair, CesA6-1 and CesA6-2 were found in *Arabidopsis* or hybrid aspen, while one homologous gene has been identified in the rice genome and an active transcript in *Populus tremuloides* (Djerbi et al. 2005). A phylogenetic analysis suggests that the CesA genes previously associated with secondary cell wall synthesis originate from a single ancestor gene and group in three distinct subgroups. The large number of *CesA* genes in trees compared to other plants suggests that their large size and intensive periods of cellulose synthesis during wood formation may require additional copies of cellulose synthases.

Comparison of the number of EST-clones corresponding to each of the *PttCesA* genes in the different hybrid aspen EST libraries revealed that, similar to *Arabidopsis*, different sets of *CesA* genes seem to characterize primary and secondary cell wall synthesis (Figure 6-4) (Djerbi et al. 2004).

Further expression analyses by real-time PCR (Figure 6-5A,B) and cDNA microarrays (Figure 6-6) revealed that genes encoding the putative *CesA* isoenzymes, PttCesA1, PttCesA3-1, PttCesA3-2 and PttCesA9 were clearly

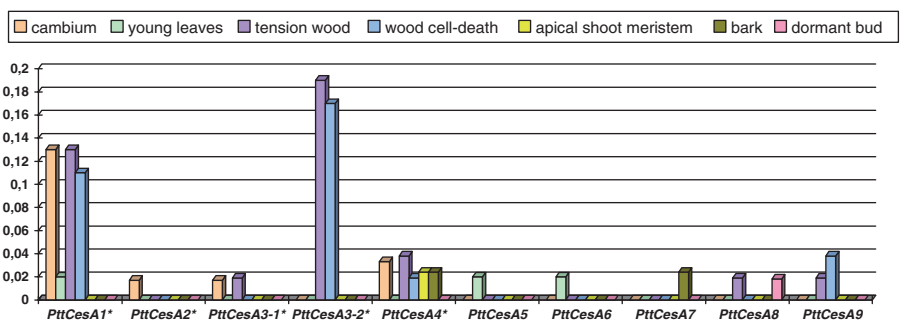

Figure 6-4. Relative abundance of the ten different PttCesA clones in the different tissue specific EST libraries from *Populus tremula* (L.) × *tremuloides* (Michx.). Data from Djerbi et al. 2003 (*See Color Plate of this figure beginning on page 355*)

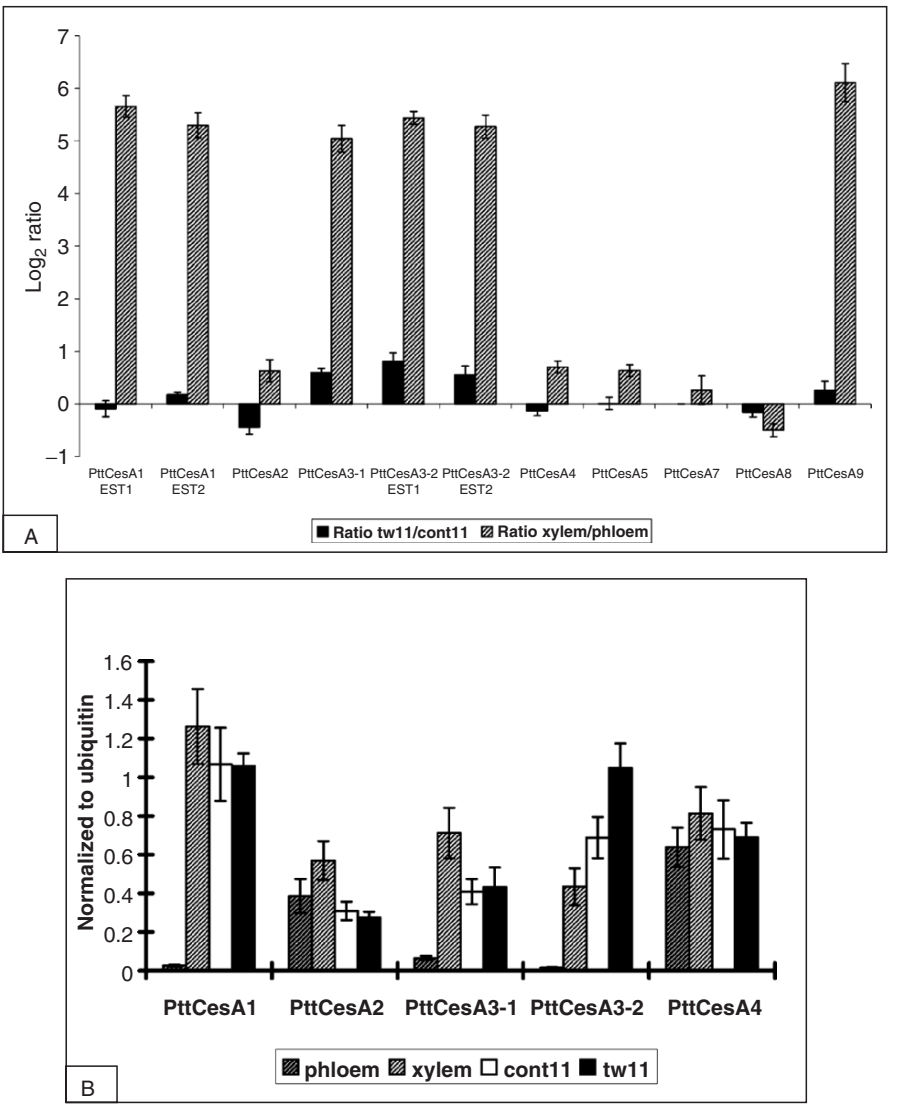

Figure 6-5. (**A**) Microarray expression ratios of the different CesA genes from *Populus tremula* (L.) × *tremuloides* (Michx.) in xylem versus phloem and in tension wood versus xylem (tw11/cont11) (data from Djerbi et al. 2003). (**B**) Relative expression levels of PttCesA's from *Populus tremula* (L.) × *tremuloides* (Michx.) normalized to the putative ubiquitin protein ligase-1 (ubiquitin) in phloem, xylem, tension wood (bent 11 days, tw11) and xylem (unbent control, cont11). Data from Djerbi et al. 2003

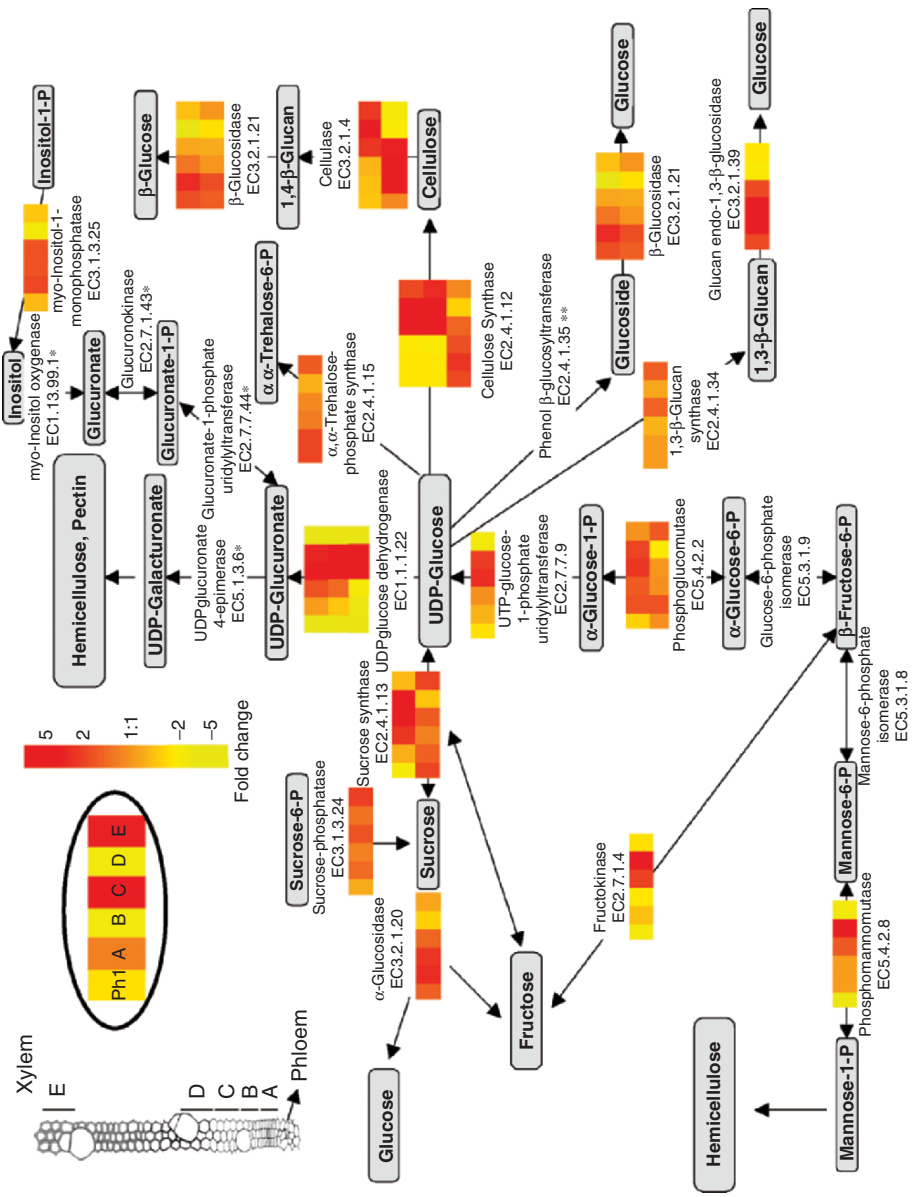
Xylem
Phloem
E
D
C
B
A
Ph1 A B C D E
Fold change
5
2
1:1
–2
–5
Hemicellulose, Pectin
Inositol
myo-Inositol oxygenase EC1.13.99.1*
Inositol-1-P
myo-Inositol-1-monophosphatase EC3.1.3.25
Glucuronate
Glucuronokinase EC2.7.1.43*
Glucuronate-1-P
UDP-Galacturonate
UDPglucuronate 4-epimerase EC5.1.3.6*
Glucuronate-1-phosphate uridylyltransferase EC2.7.7.44*
UDP-Glucuronate
α,α-Trehalose-phosphate synthase EC2.4.1.15
α,α-Trehalose-6-P
β-Glucose
β-Glucosidase EC3.2.1.21
1,4-β-Glucan
Cellulase EC3.2.1.4
Cellulose
Cellulose Synthase EC2.4.1.12
UDP-Glucose
UDPglucose dehydrogenase EC1.1.1.22
UTP-glucose-1-phosphate uridylyltransferase EC2.7.7.9
Phenol β-glucosyltransferase EC2.4.1.35 **
Glucoside
β-Glucosidase EC3.2.1.21
Glucose
1,3-β-Glucan synthase EC2.4.1.34
1,3-β-Glucan
Glucan endo-1,3-β-glucosidase EC3.2.1.39
Glucose
α-Glucose-1-P
Phosphoglucomutase EC5.4.2.2
α-Glucose-6-P
Glucose-6-phosphate isomerase EC5.3.1.9
β-Fructose-6-P
Mannose-6-phosphate isomerase EC5.3.1.8
Mannose-6-P
Phosphomannomutase EC5.4.2.8
Mannose-1-P
Hemicellulose
Sucrose synthase EC2.4.1.13
Sucrose
Sucrose-6-P
Sucrose-phosphatase EC3.1.3.24
α-Glucosidase EC3.2.1.20
Glucose
Fructose
Fructokinase EC2.7.1.4

upregulated in xylem (Figure 6-5A, Figure 6-6) (Djerbi et al. 2004). Owing to their high amino acid sequence similarity and xylem-specific expression, PttCesA3-1 and PttCesA3-2 could represent functionally redundant copies. However, *PttCesA3-2* seems to be expressed to a somewhat higher level in the tension wood forming tissues, and also occurs in numerous EST clones in the tension wood specific cDNA library. This gene is also induced in undifferentiated, granular hybrid aspen cell cultures directly after subcultivation involving mechanical damage, which suggests that the promoter responds to mechanical stress or wounding (Ohlsson et al. 2006).

In this, it resembles the promoter of the xylem-specific *PtrCesA1* gene from *Populus tremuloides*, which is very similar to *PttCesA3-1* and *PttCesA3-2*, and which was shown to be activated by tension stress in transgenic tobacco expressing the promoter-β-glucuronidase (GUS) fusions (Wu et al. 2000).

One of the *CesA* genes, *PttCesA2*, which was constitutively expressed during xylogenesis and tension wood formation (Djerbi et al. 2004) as well as over the entire growth curve of undifferentiated hybrid aspen cell suspension cultures (Ohlsson et al. 2006) seems to be activated on the opposite side of a tension wood induced stem (Andersson-Gunneras et al. 2006). The rest of the hybrid aspen *CesA* genes are relatively evenly expressed over the hybrid aspen tissues studied by Djerbi et al. (2004). However, owing to the limited dataset so far analyzed, it is possible that further tissues specific patterns of *CesA* gene expression will be revealed in tissues not yet investigated. Interestingly, the *PttCesA2* and *PttCesA4* genes were not downregulated upon induction of the secondary wall specific *CesA* genes in the hybrid aspen cell cultures (Ohlsson et al. 2006). Even in other plants, there is no conclusive evidence to indicate that the CesA enzymes participate exclusively in the formation of one or another type of cell wall (Williams et al. 2002). In fact, the proposed primary wall specific genes, *AtCesA1*, *3* and *6* continue their expression in developing vascular tissues of *Arabidopsis* (Doblin et al. 2002), and the proposed xylem-specific *PtrCesA1* gene of *Populus tremula* is also clearly expressed in leaves (Samuga and Joshi 2002). It is therefore logical to assume that tissue-specific activation of selected sets of tree *CesA* genes simply serves to increase the number of functional rosettes

Figure 6-6. Expression profiles of selected genes encoding enzymes influencing cellulose synthesis in *Populus tremula* (L.) × *tremuloides* (Michx.) (data from Hertzberg et al. 2001). The tissues sampled were: Ph, phloem; A, cambium; B, early expansion; C, late expansion, early secondary wall synthesis; D, secondary wall synthesis; and E, programmed cell death. In each zone, the expression level of selected genes is given relative to the average expression in the combined zones (A–E). The color code indicates expression levels ranging from fivefold downregulation (*yellow*) to fivefold upregulation (*deep orange*). The metabolites of each pathway are shown in the *gray boxes*. The enzymatic reactions are indicated by *arrows* accompanied by the name and the EC number of the relevant enzyme. If more than one gene has been identified for a given enzyme, the expression level of each gene is shown separately. *No genes have been cloned coding for a protein involved in this reaction. **No plant genes have been found representing a protein involved in this reaction (*See Color Plate of this figure beginning on page 355*)

during periods of intensive cellulose synthesis, rather than to replace pre-existing rosettes composed of functionally different triplets of the CesA isoenzymes.

2.3 Other enzymes and proteins involved in cellulose synthesis

Biochemical analyses suggest that, in addition to cellulose synthases, many other enzymes and proteins contribute to cellulose synthesis, either by direct or by indirect involvement in the rosettes. So far, 12 polypeptides that appear to be associated with cellulose synthase activity have been tentatively identified, but none have yet been thoroughly characterized (Kudlicka and Brown, Jr. 1997). In addition to the *CesA* proteins, the involvement of cortical microtubules (recently reviewed by Wasteneys 2004; Wasteneys and Yang 2004; Oda and Hasezawa 2006) and actin microfilaments (Seagull et al. 1987) has been proposed to facilitate the alignment of the cellulose microfibrils as they are deposited in the cell wall. Studies of cell wall mutants in *Arabidopsis* have revealed genes that encode proteins that may be involved in this process. In the *Arabidopsis fra2* mutant, an altered cortical microtubule orientation coincides with aberrant deposition of microfibrils in the primary walls of elongating cells and in the secondary walls of fiber cells (Burk et al. 2001; Burk and Ye 2002). Another interesting *Arabidopsis* mutant, *fra1*, shows no defect in cortical microtubule organization, cell wall composition or secondary wall thickening, but suffers from altered microfibril deposition which results in reduced mechanical strength of the fibers (Zhong et al. 2002). The corresponding *FRA1* gene codes for a kinesin-like protein, which may thus be one of the components controlling microfibril alignment. Furthermore, evidence obtained by studying developing xylem vessels in *Arabidopsis* roots suggests that intact microtubules may be necessary for correct positioning of the three secondary cell wall associated CESA proteins in the plasma membrane (Gardiner et al. 2003). Finally, elegant recent experiments relying on functional yellow fluorescent protein fusion proteins with cellulose synthase in transgenic *Arabidopsis* plants suggest a relatively direct mechanism for guidance of cellulose deposition by the cytoskeleton (Paredez et al. 2006). In agreement with these observations, expression profiling over the developing xylem in hybrid aspen revealed that out of the 14 different tubulin genes in the dataset, 10 were strongly upregulated during late expansion and early xylogenesis (Hertzberg et al. 2001). Interestingly, recent data shows that the gene with the highest relative level of expression during early secondary cell wall synthesis in hybrid aspen encodes a novel microtubule associated protein designated *Ptt*MAP20 (Rajangam et al. 2006). This protein was found to share a conserved TPX2 domain with a kinesin-like protein, $Xklp_2$, binding to microtubules in *Xenopus* (Wittmann et al. 2000). Distant similarity was also detected to stathmins, small phosphoproteins contributing to microtubulin dynamics in vertebrates (Rubin and Atweh 2004). Both native and recombinant *Ptt*MAP20 were shown to bind to *in vitro* assembled, taxol stabilized mammalian and hybrid aspen microtubules, and immunolocalization studies revealed that *Ptt*MAP20 colocalize

with cortical microtubules in xylem tissues (Rajangam et al. 2006). It is thus possible that PttMAP20 is one of the putative microtubule associated proteins that mediate the proposed communication between cortical microtubules and cellulose microfibrils.

Another protein apparently involved in cellulose biosynthesis is the membrane-associated endo-(1,4)-β-glucanase (EC3.2.1.4), also called Korrigan (KOR) (Nicol et al. 1998; Lane et al. 2001; Sato et al. 2001). The KOR protein seems to copurify with plasma membrane markers (Brummell et al. 1997; Nicol et al. 1998) while localization studies using fusion proteins with different marker proteins suggest that KOR resides in the intracellular organelles or at least undergoes regulated intracellular cycling (Zuo et al. 2000; Robert et al. 2005). Mutations in the *KOR* gene cause severely cellulose deficient phenotypes in *Arabidopsis* (Mølhøj et al. 2002 and references therein). KOR appears to be needed during periods of intensive cellulose synthesis as massive accumulation of KOR is observed during secondary wall deposition in cotton (Peng et al. 2002). The gene for the corresponding enzyme in hybrid aspen, *PttCel9A*, is clearly upregulated in the xylem (Hertzberg et al. 2001) (Figure 6-6), and in tension wood (Andersson-Gunneras et al. 2006). Coexpression during tension wood development of a putative ortholog of KOR with the three secondary cell wall associated *CesA* genes has also been noted in *Populus tremuloides* (Bhandari et al. 2006).

KOR belongs to Family 9 glycoside hydrolases, which use an inverting reaction mechanism, and this means that transglycosylation can be ruled out. Rather, it is speculated that KOR might contribute by removing the proposed sitosterol primer of cellulose synthesis, or by facilitating the association of the cellulose chains in an organized microfibril (Peng et al. 2001; Mølhøj et al. 2002). Characterization of a recombinant KOR expressed in *Pichia pastoris* exhibited activity on lowly substituted CMC (carboxymethyl cellulose) and amorphous cellulose, but not on xylan, xyloglucan or crystalline cellulose (Mølhøj et al. 2001; Master et al. 2004). Further, molecular modeling of the *Ptt*Cel9A sequence onto the crystal structure of a homologous bacterial enzyme revealed interesting differences in the active site structures of the bacterial and plant enzymes (Master et al. 2004). The absence of several key determinants of substrate binding suggested either very low activity on β-(1,4)-glucans or activity on a different substrate. So far, extremely low catalytic activity of a putative poplar ortholog of KOR has been demonstrated (Master et al. 2004), but in spite of both biochemical and physiological data, the mechanism by which KOR activity contributes to cellulose biosynthesis remains obscure.

Some of the cell wall mutants, such as the *mur* mutants in *Arabidopsis*, affect downstream enzymes, which supply substrates for the glycosyl transferases involved in cell wall synthesis (Williamson et al. 2002). These types of mutations usually lead to a significant overall reduction in the rate of cellulose synthesis. Sucrose synthase (SuSy) (EC2.4.1.13) catalyzes the reversible conversion of sucrose and UDP to UDP-glucose and fructose thereby channeling sucrose into numerous pathways, including cell wall and starch biosynthesis.

Downregulation of SuSy generally results in brittle cell walls and reduced size of starch grains (Chourey et al. 1998). In maize, three different isoforms, SH1 (Shrunken 1), SUS1 (Sucrose synthase 1), and SUS3 have been shown to provide substrate for different pathways (Chourey et al. 1998; Carlson et al. 2002). One sucrose synthase (SuSy) situated on the plasma membrane of cotton has been proposed to channel UDP-glucose to the cellulose synthase, CesA (Amor et al. 1995; Haigler et al. 2001; Salnikov et al. 2001). Aspects of sugar metabolism related to cellulose synthesis in forest trees have been studied by expression analysis in hybrid aspen (Hertzberg et al. 2001). Among the 2995 unique cambial EST-clones of hybrid aspen, 42 coded for proteins with sequence similarity to 22 different enzymes involved in sugar metabolism (Hertzberg et al. 2001). Subsequent expression profiling in the different stages of xylogenesis (Figure 6-6) revealed that the expression of one of the two isoenzymes of SuSy followed that of the xylem specific genes, *PttCesA1* and *PttCesA3-1* (Hertzberg et al. 2001). In contrast, the second SuSy isoenzyme was more evenly expressed in all tissues with a slight downregulation during secondary wall synthesis (zone D, Figure 6-6), which suggests involvement in starch synthesis or general sugar metabolism.

Another enzyme influencing the metabolic flux to cellulose synthesis is fructokinase (EC2.7.1.4). This enzyme converts fructose, a potent inhibitor of SuSy, into fructose-6-P, which can be converted further to UDP-glucose using an alternative metabolic route (Kanayama et al. 1998; Delmer and Haigler 2002). Three enzymes, which participate in the alternative route, fructokinase, phosphoglucomutase (PGM) (EC 5.4.22), and UDP-glucose pyrophosphorylase (UTP-glucose-1-phosphate uridyltransferase) (EC2.7.7.9), were upregulated during xylogenesis in hybrid aspen (zones C and D, Figure 6-6). The gene encoding for the fourth enzyme, Glucose-6-phosphate isomerase, was not included in the dataset. Nevertheless, the expression patterns of the three studied genes strongly suggest that the alternative route contributes to cellulose synthesis during xylogenesis by increasing the pool of available UDP-glucose.

2.4 Other metabolic processes involved in cell wall biosynthesis

Interestingly, in *Pinus pinaster*, fructokinase is also abundantly present in compression wood (Plomion et al. 2000), i.e., in a tissue with high content of lignin. In this case the fructokinase probably functions to provide substrate for glycolysis and deeper into the TCA-cycle in order to accumulate energy or to produce metabolites for other processes. An antisense inhibition of 4-coumarate: coenzyme A ligase decreased lignin biosynthesis by 45% in *Populus tremuloides* (Michx.), which was compensated for by a 15% increase in the cellulose content (Hu et al. 1999). Further, a mutation in the *AtCesA* gene activated lignin synthesis in *Arabidopsis* (Cano-Delgado et al. 2003). These are good examples of the metabolic flexibility of plants, which allows for a dynamic connection between lignin and cellulose synthesis.

Other polysaccharides, such as hemicelluloses and pectins, are also needed to produce a functional plant cell wall. Pectins consist of D-galacturonate, L-rhamnose, L-arabinose and D-galactose and are abundant in young cell walls, where they influence cell wall extensibility (McCann et al. 1993; Goldberg et al. 1986). Hemicelluloses consist of a large group of heteropolysaccharides containing D-xylose, L-arabinose, L-rhamnose, L-fucose, D-mannose, D-galactose, or D-glucose in different combinations. They often associate with cellulose microfibrils providing structural strength to the cell wall, or serve as an interface between cellulose and lignin. While cellulose synthesis occurs at the plasma membrane, hemicelluloses and pectins are synthesized in the Golgi apparatus, followed by transportation to the cell wall. When cultured tobacco and tomato plants are grown in the presence of an inhibitor of cellulose synthesis, 2,6-dichlorobenzonitrile, the resulting cell walls contain almost no cellulose, but are enriched in uronic-acid-rich pectins, and an excess of xyloglucan is found in the medium (Shedletzky et al. 1992). Similarly, accumulation of uronic-acid-rich polymers was observed in *Arabidopsis* mutants with impaired cellulose synthesis or reduced expression of the *CesA* genes (Burton et al. 2000; Sato et al. 2001). Cellulose deficiency resulting from the *kor-1* mutation also led to differences in pectin content and composition (His et al. 2001). It thus seems that the noncellulosic polysaccharides can sometimes compensate for loss or reduction of cellulose in the cell walls.

Similarly to cellulose, hemicellulose and pectins are synthesized through sugar nucleotide precursors by a large number of glycosyl transferases (Scheible and Pauly 2004). Many of the UDP-sugars can be derived from UDP-glucuronic acid (Zablackis et al. 1995), which is an important intermediate in cell wall biosynthesis (Amino et al. 1985; Robertson et al. 1995). UDP-glucuronic acid is synthesized by oxidation of UDP-glucose or – indirectly – through oxidation of inositol, and the route chosen seems to vary during plant development (Dalessandro and Northcote 1977; Seitz et al. 2000). An expression analysis of the inositol pathway was not possible on the hybrid aspen microarrays as none of the relevant genes have been identified. However, the xylem specific upregulation of the gene encoding UDP-glucose dehydrogenase (EC1.1.1.22), which produces UDP-glucuronate from UDP-glucose, suggests that this pathway plays an important role during the secondary wall formation (Hertzberg et al. 2001). Even the gene encoding phosphomannomutase (EC5.4.2.8) was specifically upregulated in zone D and could therefore be responsible for providing mannose for glucomannan formation.

3 IN VITRO CELLULOSE SYNTHESIS

Attempts to synthesize cellulose *in vitro* by using detergent solubilized enzymes frequently lead to the accumulation of callose, a linear (1→3)-β-D-glucan (Delmer 1987; Okuda et al. 1993). Even in the few cases where successful *in vitro* cellulose synthesis has been demonstrated, i.e., in blackberry (Lai Kee Him et al. 2002), cotton and mung bean (Kudlicka et al. 1995; Kudlicka et al. 1996; Kudlicka and

Brown, Jr. 1997), callose appears as a major product. Nonetheless, it has been observed that higher ratios of cellulose to callose are obtained *in vitro* when the calcium concentration in the reaction mixtures is decreased (Okuda et al. 1993). Also, cellulose synthesis is lower *in vivo* when elicitors are used to induce callose synthesis (Delmer and Amor 1995). From such observations, it has been proposed that callose and cellulose synthase activities are coregulated by cations, and that (1→3) and (1→4)β-D-glucans may be synthesized by the same enzyme (Delmer 1999). However, as pointed out by Bulone (2003), experimental verification of such hypotheses is still awaiting successful isolation of homogeneous preparations of active enzymes. Recently cell suspension cultures of hybrid aspen have been developed as a rapid and convenient model system to study plant cell wall biosynthesis (Ohlsson et al. 2006). mRNA expression analysis indicated activation of the xylem specific cellulose synthase genes, *PttCesA1* and *PttCesA3-1* in the later stages of growth of these cultures. Interestingly, when *in vitro* cellulose synthesis was carried out using detergent extracts from the aging cell cultures, a higher ratio of cellulose versus callose was observed (Colombani et al. 2003). The hybrid aspen cell suspension cultures may thus provide a convenient model system for future studies of the mechanisms of both cellulose and callose biosynthesis.

Acknowledgments

Professor Vincent Bulone and Dr. Johan Edqvist are acknowledged for valuable input and critical reading of the manuscript. This work was supported by the European Commission grant QLK5-CT2001-00443.

REFERENCES

Allona I., Quinn M., Shoop E., Swope K., St Cyr S., Carlis J., Riedl J., Retzel E., Campbell M.M., Sederoff R., and Whetten R.W. 1998. Analysis of xylem formation in pine by cDNA sequencing. Proc Natl Acad Sci USA 95(16):9693–9698.

Andersson-Gunneras S., Mellerowicz E.J., Love J., Segerman B., Ohmiya Y., Coutinho P.M., Nilsson P., Henrissat B., Moritz T., and Sundberg B. 2006. Biosynthesis of cellulose-enriched tension wood in Populus: global analysis of transcripts and metabolites identifies biochemical and developmental regulators in secondary wall biosynthesis. Plant J 45:144–165.

Amino S., Takeuchi Y., and Komamine A. 1985. Changes in the enzyme activities involved in formation and interconversion of UDP-sugars during cell cycle in a synchronous culture of *Catharanthus roseus*. Physiol Plant 64:111–117.

Amor Y., Haigler C.H., Johnson S., Weinscott M., and Delmer D. 1995. A membrane-associated form of sucrose synthase and its potential role in synthesis of cellulose and callose in plants. Proc Natl Acad Sci USA 92:9353–9357.

Arioli T., Peng L., Betzner A.S., Burn J., Wittke W., Herth W., Camilleri Höfte H., Plazinski J., Birch R., Cork A., Glover Redmond J., and Williamson R.E. 1998. Molecular analysis of cellulose biosynthesis in *Arabidopsis*. Science 279:717–720.

Baskin T.I. 2001. On the alignment of cellulose microfibrils by cortical microtubules: a review and a model. Protoplasma 215:150–171. Review.

Bhandari S., Fujino T., Thammanagowda S., Zhang D., Xu F., and Joshi C.P. 2006. Xylem-specific and tension stress-responsive coexpression of KORRIGAN endoglucanase and three secondary

wall associated cellulose synthase genes in aspen trees. Planta 222(4):828–837. Mar 3 [Epub ahead of print].

Bhalerao R., Nilsson O., and Sandberg G. 2003. Out of the woods: forest biotechnology enters the genomic era. Curr Opin Biotech 14:206–213.

Bradshaw H.D.J., Ceulemans R., Davis J., and Stettler R.F. 2000. Emerging model systems in plant biology: poplar (*Populus*) as a model forest tree. J Plant Growth Regulation 19:306–313.

Brown, Jr. R.M. and Montezinos D. 1976. Cellulose microfibrils: visualization of biosynthetic and orienting complexes in association with the plasma membrane. Proc Natl Acad Sci USA 73:143–147.

Brown, Jr. R.M., 1996. The biosynthesis of cellulose. Pure Appl Chem 10:1345–1373.

Brummell D.A., Catala C., Lashbrook C.C., and Bennett A.B. 1997. A membrane-anchored E-type endo-1,4-beta-glucanase is localized on Golgi and plasma membranes of higher plants. Proc Natl Acad Sci USA 94:4794–4799.

Bulone V. 2003. *In vitro* synthesis and analysis of plant (1→3)-β-D-glucans and cellulose: a key step towards the characterization of glucan synthases.

Burk D.H. and Ye Z.-H. 2002. Alteration of oriented deposition of cellulose microfibrils by mutation of a katanin-like microtubule severing protein. Plant Cell 14:2145–2160.

Burk D.H., Liu B., Zhong R., Morrison, W.H., and Ye Z.-H. 2001. A katanin-like protein regulates normal cell wall biosynthesis and cell elongation. Plant Cell 13:807–827.

Burn J.E., Hocart C.H., Birch R.J., Cork A.C., and Williamson R.E. 2002. Functional analysis of the cellulose synthase genes *CesA1*, *CesA2*, and *CesA3* in *Arabidopsis*. Plant Physiol 129:797–807.

Burton R.A., Gibeaut D.M., Bacic A., Findlay K., Roberts K., Hamilton A., Baulcombe D.C., and Fincher G.B. 2000. Virus-induced silencing of a plant cellulose synthase gene. Plant Cell 12:691–706.

Burton R.A., Farrokhi N., Bacic A., and Fincher G.B. 2005. Plant cell wall polysaccharide biosynthesis: real progress in the identification of participating genes. Planta 221(3):309–312.

Campbell J.A., Davies G.J., Bulone V.V., and Henrissat B. 1998. A classification of nucleotide-diphospho-sugar glycosyltransferases based on amino acid sequence similarities. Biochem J 329:719.

Cano-Delgado A., Penfield S., Smith C., Catley M., and Bevan M. 2003. Reduced cellulose synthesis invokes lignification and defense responses in *Arabidopsis thaliana*. Plant J 34:351–362.

Carlson S.J., Chourey P.S., Helentjaris T., and Datta R. 2002. Gene expression studies on developing kernels of maize sucrose synthase (SuSy) mutants show evidence for a third SuSy gene. Plant Mol Biol 49:15–29.

Chaffey N., Barnett J., and Barlow P. 1999. A cytoskeletal basis for wood formation in angiosperm trees: the involvement of cortical microtubules. Planta 208:19–30.

Charnock S.J. and Davies G.J. 1999. Structure of the nucleotide-diphospho-sugar transferase, SpsA from *Bacillus subtilis*, in native and nucleotide-complexed forms. Biochemistry 38:6380–6385.

Charnock S.J., Henrissat B., and Davies G.J. 2001. Three-dimensional structures of UDP-sugar glycosyltransferases illuminate the biosynthesis of plant polysaccharides. Plant Physiol 125:527–531.

Chourey P.S., Taliercio E.W., Carlson S.J., and Ruan Y.L. 1998. Genetic evidence that the two isozymes of sucrose synthase present in developing maize endosperm are critical, one for cell wall integrity and the other for starch biosynthesis. Mol Gen Genet 259:88–96.

Cosgrove D.J. 1999. Enzymes and other agents that enhance cell wall extensibility. Annu Rev Plant Physiol Plant Mol Biol 50:391–417.

Colombani A., Djerbi S., Bessueille L., Blomqvist K., Ohlsson A., Berglund T., Teeri T., and Bulone V. 2003. *In vitro* synthesis of (1→3)-β-D-glucan (callose) and cellulose by detergent extracts of membranes from cell suspension cultures of hybrid aspen. Submitted for publication in Cellulose.

Coutinho P.M., Deleury E., Davies G.J., and Henrissat B. 2003. An evolving hierchical family classification for glycosyltransferases. J Mol Biol 328:307–317.

Dalessandro G. and Northcote D.H. 1977. Changes in enzymatic activities of nucleoside diphosphate sugar interconversions during differentiation of cambium to xylem in sycamore and poplar. Biochem J 162:267–279.

Delmer D.P. 1987. Cellulose biosynthesis. Ann Rev Plant Physiol 38:259–290.

Delmer D.P. 1999. Cellulose biosynthesis: exiting times for a difficult field of study. Annu Rev Plant Physiol Plant Mol Biol 50:245–276.

Delmer D.P. and Amor Y. 1995. Cellulose biosynthesis. Plant Cell 7:987–1000.

Delmer D.P. and Haigler C.H. 2002. The regulation of metabolic flux to cellulose, a major sink for carbon in plants. Metab Engin 4:22–28.

Desprez T., Vernhettes S., Fagard M., Refregier G., Desnos T., Aletti E., Py N., Pelletier S., and Höfte H. 2002. Resistance against herbicide isoxaben and cellulose deficiency caused by distinct mutations in same cellulose synthase isoform *CESA6*. Plant Physiol 128:482–490.

Djerbi S., Aspeborg H., Nilsson P., Sundberg B., Mellerowicz E., Blomqvist K., and Teeri T.T. 2004. Identification and expression analysis of genes encoding putative cellulose synthases (*CesA*) in the hybrid aspen, *Populus tremula* (L.) x *P. tremuloides* (Michx.). Cellulose 11:301–312.

Djerbi S., Lindskog M., Arvestad L., Sterky F., and Teeri T.T. 2005. The genome sequence of black cottonwood (Populus trichocarpa) reveals 18 conserved cellulose synthase (*CesA*) genes. Planta 221:739–746.

Doblin M.S., Kurek I., Jacob-Wilk D., and Delmer D.P. 2002. Cellulose biosynthesis in plants: from genes to rosettes. Plant Cell Physiol 43:1407–1420.

Emons A.-M.C., and Mulder B.M. 2000. How the deposition of cellulose microfibrils builds cell wall architecture. Trends Plant Sci 5:35–40.

Engelhardt J. 1995. Sources, industrial derivatives, and commercial applications of cellulose. Carbohydr Eur 12:5–14.

Fagard M., Desnos T., Desprez T., Goubet F., Refregier G., Mouille G., McCann M., Rayon C., Vernhettes S., and Höfte H. 2000. PROCUSTE1 encodes a cellulose synthase required for normal cell elongation specifically in roots and dark-grown hypocotyls of *Arabidopsis*. Plant Cell 12:2409–2424.

Fujita M. and Harada H. 2001. Ultrastructure and formation of wood cell wall. In Hon D.N.-S. and Shirashi N. (eds.) Wood and Cellulosic Chemistry, 2nd edn. Marcel Dekker, New York, pp. 1–49.

Funada R. 2000. Control of wood structure. In Nick P. (ed.) Plant Microtubules. Springer, Berlin, pp. 51–82.

Gardiner J.C., Taylor N.G., and Turner S.R. 2003. Control of cellulose synthase complex localization in developing xylem. Plant Cell 15:1740–1748.

Geisler-Lee J., Geisler M., Coutinho P.M., Segerman B., Nishikubo N., Takahashi J., Aspenborg H., Djerbi S., Master E., Andersson-Gunneråas S., Sundberg B., Karpinski S., Teeri T.T., Kleczkowski L.A., Henrissat B., and Mellerowicz E.J. 2006. Poplar Carbohydrate Active Enzymes (CAZymes). Gene identification and expression analyses. Plant Physiol 140:946–962.

Goldberg R., Morvan C., and Roland J.C. 1986. Composition, properties and localization of pectins in young and mature cells of the mung bean hypocotyl. Plant Cell Physiol 27:417–429.

Haigler C.H., Ivanova-Datcheva M., Hogan P.S., Salnikov V.V., Hwang S., Martin K., and Delmer D.P. 2001. Carbon partitioning to cellulose synthesis. Plant Mol Biol 47:29–51.

Henrissat B., Coutinho P.M., and Davies G.J. 2001. A census of carbohydrate-active enzymes in the genome of *Arabidopsis thaliana*. Plant Mol Biol 47:55–72.

Hertzberg M., Aspeborg H., Schrader J., Andersson A., Erlandsson R., Blomqvist K., Bhalerao R., Uhlen M., Teeri T.T., Lundeberg J., Sundberg B., Nilsson P., and Sandberg G. 2001. A transcriptional roadmap to wood formation. Proc Natl Acad Sci USA 98:14732–14737.

His I., Driouich A., Nicol F., Jauneau A., and Höfte H. 2001. Altered pectin composition in primary cell walls of korrigan, a dwarf mutant of *Arabidopsis* deficient in a membrane-bound endo-1, 4-beta-glucanase. Planta 212(3):348–358.

Holland N., Holland D., Helentjaris T., Dhugga K.S., Xoconostle-Cazares B., and Delmer D.P. 2000. A comparative analysis of the plant cellulose synthase (CesA) gene family. Plant Physiol 123(4):1313–1324.

Hu W.-J., Harding S.A., Lung J., Popko J.L., Ralph J., Stokke D.D., Tsai C.-J., and Chiang V.L. 1999. Repression of lignin biosynthesis promotes cellulose accumulation and growth in transgenic trees. Nature Biotech 17:808–812.

Joshi C. 2003. Xylem-specific and tension stress-responsive expression of cellulose synthase genes from aspen trees. Appl Biochem Biotechnol 105:17–26.

Kalluri U.C. and Joshi C.P. 2003. Isolation and characterization of a new, full-length cellulose synthase cDNA, PtrCesA5 from developing xylem of aspen trees. J Exp Bot 54(390): 2187–2188.

Kanayama Y., Granot D., Dai N., Petreikov M., Schaffer A., Powell A., and Bennett A.B. 1998. Tomato fructokinases exhibit differential expression and substrate regulation. Plant Physiol 117:85–90.

Kohorn B.D. 2001. WAKs; cell wall associated kinases. Curr Opin Cell Biol 13:529–533.

Kimura S., Laosinchai W., Itoh T., Cui X., Linder C.R., and Brown, Jr. R.M., 1999. Immunogold labeling of rosette terminal cellulose-synthesizing complexes in the vascular plant *Vigna angularis*. Plant Cell 11:2075–2086.

Klemm D., Heublein B., Fink H.P., and Bohn A. 2005. Cellulose: fascinating biopolymer and sustainable raw material. Angewandte Chemie – Internat Ed 44:3358–3393.

Kudlicka K. and Brown, Jr. R.M., 1997. Cellulose and callose biosynthesis in higher plants. I. Solubilization and separation of (1->3)- and (1->4)-[beta]-glucan synthase activities from mung bean. Plant Physiol 115:643–656.

Kudlicka K., Brown, Jr. R.M. Li L., Lee J.H., Shin H., and Kuga S. 1995. β-Glucan synthesis in the cotton fiber. IV. *In vitro* assembly of the cellulose I allomorph. Plant Physiol 107:111–123.

Kudlicka K., Lee J.H., and Brown, Jr. R.M., 1996. A comparative analysis of *in vitro* cellulose synthesis from cell-free extracts of mung bean (*Vigna radiata*, Fabaceae) and cotton (*Gossypium hirsutum*, Malvaceae). Am J Bot 83:274–284.

Kurek I., Kawagoe Y., Jacob-Wilk D., Doblin M., and Delmer D. 2002. Dimerization of cotton fiber cellulose synthase catalytic subunits occurs via oxidation of the zinc-binding domains. Proc Natl Acad Sci USA 99:11109–11114.

Lai Kee Him J., Chanzy H., Müller M., Putaux J.L., Imai T., and Bulone V. 2002. *In vitro versus in vivo* cellulose microfibrils from plant primary wall synthases: structural differences. J Biol Chem 277:36931–36939.

Lane D.R., Wiedemeier A., Peng L., Höfte H., Vernhettes S., Desprez T., Hocart C.H., Birch R.J., Baskin T.I., Burn J.E., Arioli T., Betzner A.S., and Williamson R.E. 2001. Temperature-sensitive alleles of RSW1 link the KORRIGAN endo-1,4-β-glucanase to cellulose synthesis and cytokinesis in *Arabidopsis*. Plant Physiol 126:278–288.

Ledbetter M.C. and Porter K.R. 1963. A "microtubule" in plant cell fine structure. J Cell Biol 19:239–250.

Master E., Rudsander U., Zhou W., Henriksson H., Divne C., Denman S., Wilson D., and Teeri T.T. 2004. Recombinant expression and enzymatic characterization of PttCel9A, a KOR homologue from *Populus tremula* × *tremuloides*. Biochemistry 43:10080–10089.

McCann M.C., Stacey N.J., Wilson R., and Roberts K. 1993. Orientation of macromolecules in the cell walls of elongating carrot cells. J Cell Sci 106:1347–1356.

Meier H. 1964. General chemistry of cell walls and distribution of the chemical constituents across the wall. In: Zimmermann M.H. (ed.) The Formation of Wood in Forest Trees. Academic Press, New York, pp. 137–151.

Mellerowicz E.J., Baucher M., Sundberg B., and Boerjan W. 2001. Unravelling cell wall formation in the woody dicot stem. Plant Mol Biol 47:239–274.

Mirov N.T. and Hasbrouck J. 1976. The Story of Pines. Indiana University Press, Bloomington, IN, p. 16.

Mohanty A.K., Misra M., and Drzal L.T. 2001. Surface modification of natural fibers and erformance of the resulting biocomposites. Composite Interfaces 8:313–343.

Mølhøj M., Ulvskog P., and Dal Degan F. 2001. Characterization of a functional soluble form of a *Brassica napus* membrane-anchored endo-1,4-beta-glucanase heterologously expressed in Pichia pastoris. Plant Physiol 127:674–684.

Mølhøj M., Pagant S., and Höfte H. 2002. Towards understanding of the role of membrane-bound endo-β-1,4-gölucanases in cellulose biosynthesis. Plant Cell Physiol 43:1399–1406.

Mueller S.C. and Brown, Jr. R.M., 1980. Evidence for an intramembrane component associated with a cellulose microfibril-synthesizing complex in higher plants. J Cell Biol 84(2):315–326.

Nairn C.J. and Haselkorn T. 2005. Three loblolly pine CesA genes expressed in developing xylem are orthologous to secondary cell wall CesA genes of angiosperms. New Phytologist 166(3): 907–915.

Nicol F., His I., Jauneau A., Vernhettes S., Canut H., and Höfte H. 1998. A plasma membrane-bound putative endo-1,4-β-D-glucanase is required for normal wall assembly and cell elongation in *Arabidopsis*. EMBO J 19:5563–5576.

Oda Y. and Hasezawa S. 2006. Cytoskeletal organization during xylem cell differentiation. J Plant Res, 119(3):167–177. Mar 29; [Epub ahead of print]

Ohlsson A.B., Djerbi S., Winzell A., Bessueille L., Ståldal L., Li X.G., Blomqvist K., Bulone V., Teeri T.T., and Berglund T. 2006. Cell suspension cultures of *Populus tremula* x *tremuloides* exhibit a high level of cellulose synthase gene expression that coincides with increased *in vitro* cellulose synthase activity. Protoplasma, 228(4):221–229. in press.

Okuda K., Li L., Kudlicka K., Kuga S., and Brown, Jr. R.M., 1993. [beta]-Glucan synthesis in the cotton fiber. I. Identification of [beta]-1,4- and [beta]-1,3-glucans synthesized *in vitro*. Plant Physiol 101(4):1131–1142.

Paredez A.R., Somerville C.R., and Ehrhardt D.W. 2006. Visualization of cellulose synthase demonstrates functional association with microtubules. Science, 312(5779):1491–1495. Apr 20 [Epub ahead of print].

Pear J.R., Kawagoe Y., Schreckengost W.E., Delmer D.P., and Stalker D.M. 1996. Higher plants contain homologs of the bacterial *celA* genes encoding the catalytic subunit of cellulose synthase. Proc Natl Acad Sci USA 93:12637–12642.

Peng L., Kawagoe Y., Hogan P., and Delmer D. 2002. Sitosterol-beta-glucoside as primer for cellulose synthesis in plants. Science 295:147–150.

Plomion C., Pionneau C., Brach J., Costa P., and Baillères H. 2000. Compression wood-responsive proteins in developing xylem of maritime pine (*Pinus pinaster* Ait.). Plant Physiol 123:959–969.

Plomion C., Leprovost G., and Stokes A. 2001. Wood formation in trees. Plant Physiol 127:1513–1523.

Rajangam A.S., Aspeborg H., Arvestad L., Pansri P., Tan T.-C., Hober S., Blomqvist K., Divne C., Bulone V., Sundberg B., Mellerowicz E., and Teeri T.T. 2006. *Ptt*MAP20, a novel microtubule-associated protein in the secondary cell wall forming tissues of *Populus tremula* x *tremuloides*. Submitted for publication.

Ranik M. and Myburg A.A. 2006. Six new cellulose synthase genes from *Eucalyptus* are associated with primary and secondary cell wall biosynthesis. Tree Physiology 26:545–556.

Richmond T. 2000. Higher plant cellulose synthases. Genome Biol 1: REVIEWS3001.

Robertson D., Beech I., and Bolwell G.P. 1995. Regulation of the enzymes of UDP-sugar metabolism during differentiation of french bean. Phytochem 39:21–28.

Robert S., Bichet A., Grandjean O., Kierzkowski D., Satiat-Jeunemaitre B., Pelletier S., Hauser M.T., Hofte H., and Vernhettes S. 2005. An *Arabidopsis* endo-1,4-beta-D-glucanase involved in cellulose synthesis undergoes regulated intracellular cycling. Plant Cell 17(12):3378–3389.

Rubin C.I. and Atweh G.F. 2004. The role of stathmin in the regulation of the cell cycle. J Cell Biochem 93:242–250.

Salnikov V.V., Grimson M.J., Delmer D.P., and Haigler C.H. 2001. Sucrose synthase localizes to cellulose synthesis sites in tracheary elements. Phytochem 57:823–833.

Samuga A. and Joshi C. 2002. A new cellulose synthase gene (PtrCesA2) from aspen xylem is orthologous to Arabidopsis AtCesA7 (irx3) gene associated with secondary cell wall synthesis. Gene 296:237.

Samuga A. and Joshi C.P. 2004. Cloning and characterization of cellulose synthase-like gene, PtrCSLD2 from developing xylem of aspen trees. Physiol Plant 120(4):631–641.

Sato S., Kato T., Kakegawa K., Ishii T., Liu Y.-G., Awano T., Takabe K., Nishiyama Y., Kuga T., Sato S., Nakamura Y., Tabata T., and Shibata D. 2001. Role of the putative membrane-bound endo-1,4-β-glucanase KORRIGAN in cell wall elongation and cellulose synthesis in *Arabidopsis thaliana*. Plant Cell Physiol 42:251–263.

Saxena I.M., Lin F.C., and Brown, Jr. R.M., 1990. Cloning and sequencing of the cellulose synthase catalytic subunit gene of *Acetobacter xylinum*. Plant Mol Biol 15:673–683.

Saxena I.M., Brown, Jr. R.M., Fevre M., Geremia R.A., and Henrissat B. 1995. Multidomain architecture of beta-glycosyl transferases: implications for mechanism of action. J Bacteriol 177:1419–1424.

Saxena I.M., and Brown, Jr. R.M., 1997. Identification of cellulose synthase(s) in higher plants:sequence analysis of processive β-glycosyltransferases with the common motif ′D,D,D35Q(R,Q)XRW′. Cellulose 4:33–49.

Scheible W.R., Eshed R., Richmond T., Delmer D., and Somerville C. 2001. Modifications of cellulose synthase confer resistance to isoxaben and thiazolidinone herbicides in *Arabidopsis Ixr1* mutants. Proc Natl Acad Sci USA 98:10079–10084.

Scheible W.R. and Pauly M. 2004. Glycosyltransferases and cell wall biosynthesis: novel players and insights. Curr Opin Plant Biol 7:285–95. Review.

Seagull R.W., Falconer M.M., and Weerdenburg C.A. 1987. Microfilaments: dynamic arrays in higher plant cells. J Cell Biol 104:995–1004.

Seitz B., Klos C., Wurm M., and Tenhaken R. 2000. Matrix polysaccharide precursors in *Arabidopsis* cell walls are synthesized by alternate pathways with organ-specific expression patterns. Plant J 21:537–546.

Shedletzky E., Shmuel M., Trainin T., Kalman S., and Delmer D.P. 1992. Cell wall structure in cells adapted to growth on the cellulose-synthesis inhibitor 2,6-dichloro-benzonitrile (DCB): a comparison between two dicotyledonous plants and a graminaceous monocot. Plant Physiol 100:120–130.

Sterky F., Regan S., Karlsson J., Hertzberg M., Rohde A., Holmberg A., Amini B., Bhalerao R., Larsson M., Villarroel R., Van Montagu M., Sandberg G., Olsson O., Teeri T.T., Boerjan W., Gustafsson P., Uhlen M.-, Sundberg B., and Lundeberg J. 1998. Gene discovery in the wood-forming tissues of poplar: analysis of 5, 692 expressed sequence tags. Proc Natl Acad Sci USA 95:13330–13335.

Sterky F., Bhalerao R.R., Unneberg P., Segerman B., Nilsson P., Brunner A.M., Campaa L., Jonsson Lindvall J., Tandre K., Strauss S.H., Sundberg B., Gustafsson P., Uhlen M., Bhalerao R.P., Nilsson O., Sandberg G., Karlsson J., Lundeberg J., and Jansson S. 2004. A populus EST resource for plant functional genomics. Proc Natl Acad Sci USA 2004 Sep 21;101(38):13951–13956

Taylor N.G., Scheible W.R., Cutler S., Somerville C.R., and Turner S.R. 1999. The *irregular xylem3* locus of *Arabidopsis* encodes a cellulose synthase required for secondary cell wall synthesis. Plant Cell 11:769–780.

Taylor N.G., Laurie S., and Turner S.R. 2000. Multiple cellulose synthase catalytic subunits are required for cellulose synthesis in *Arabidopsis*. Plant Cell 12:2529–2540.

Taylor N.G., Howells R.M., Huttly A.K., Vickers K., and Turner S.R. 2003. Interactions among three distinct CesA proteins essential for cellulose synthesis. Proc Natl Acad Sci USA 100:1450–1455.

Torrey J.G., Fosket D.E., and Hepler P.K. 1971. Xylem formation: a paradigm of cytodifferentiation in higher plants. Am Scient 59:338–352.

Turner S.R. and Somerville C.R. 1997. Collapsed xylem phenotype of *Arabidopsis* identifies mutants deficient in cellulose deposition in the secondary cell wall. Plant Cell 9:689–701.

Wasteneys G.O. 2004. Progress in understanding the role of microtubules in plant cells. Curr Opin Plant Biol 7:651–660.

Wasteneys G.O. and Yang Z. 2004. New views on the plant cytoskeleton. Plant Physiol 136:3884–3891.

Williamson R.E., Burn J.E., and Hocart C.H. 2002. Cellulose synthesis: mutational analysis and genomic perspectives using *Arabidopsis thaliana*. CMLS, Cell Mol Life Sci 58:1475–1490.

Wittmann T., Wilm M., Karsenti E., and Vernos I. 2000. TPX2, A novel xenopus MAP involved in spindle pole organization. J Cell Biol 149:1405–1418.

Wong H.C., Fear A.L., Calhoon R.D., Eichinger G.H., Mayer R., Amikam D., Benziman M., Gelfand D.H., Meade J.H., Emerick A.W., et al. 1990. Genetic organization of the cellulose synthase operon in *Acetobacter xylinum*. Proc Natl Acad Sci USA 87:8130–8134.

Wu L., Joshi C.P., and Chiang V.L. 2000. A xylem-specific cellulose synthase gene from aspen (*Populus tremuloides*) is responsive to mechanical stress. Plant J 22:495–502.

Zablackis E., Huang J.J., Muller B., Darvill A.G., and Albersheim P. 1995. Characterization of the cell-wall polysaccharides of *Arabidopsis thaliana* leaves. Plant Physiol 107:1129–1138.

Zhong R., Burk D.H., Morrison III, W.H., and Ye Z.-H. 2002. A kinesin-like protein essential for oriented deposition of cellulose microfibrils and cell wall strength. Plant Cell 14:3101–3117.

Zhong R., Morisson III, H., Freshour G.D., Hahn M.G., and Ye Z.-H. 2003. Expression of a mutant form of cellulose synthase AtCesA7 causes dominant negative effect on cellulose biosynthesis. Plant Physiol 132:786–795.

Zuo J., Niu Q.W., Nishizawa N., Wu Y., Kost B., and Chua N.H. 2000. KORRIGAN, an Arabidopsis endo-1,4-beta-glucanase, localizes to the cell plate by polarized targeting and is essential for cytokinesis. Plant Cell 12(7):1137–1152.

CHAPTER 7

CELLULOSE BIOSYNTHESIS IN ENTEROBACTERIACEAE

UTE RÖMLING*

Department of Microbiology, Tumor and Cell Biology (MTC), Box 280, Karolinska Institutet, SE-17177 Stockholm, Sweden

Abstract

Distinct bacterial species belonging to the family of Enterobacteriaceae harbor a characteristic cellulose biosynthesis operon (*bcs*). A regulatory network for cellulose biosynthesis has been identified in ***Salmonella typhimurium***. Transcription of the bcs operon is constitutive, while cellulose biosynthesis is activated on the post-transcriptional level by AdrA, a GGDEF domain containing protein. AdrA is under the tight positive control of the transcriptional regulator CsgD, which itself is regulated by a wide variety of environmental stimuli and global regulatory proteins. However, regulation of cellulose biosynthesis varies widely among species and even within a species. In ***S. typhimurium*** in cellulose is commonly coexpressed with curli fimbriae, a proteinaceous component whereby the two extracellular matrix components interact with each other fulfilling distinct roles in cell-cell interactions and biofilm formation.

Keywords

Curli fimbriae, electron microscopy, environmental conditions, *Escherichia coli*, GGDEF domain, *ompR*, regulation, *rpoS*, *Salmonella typhimurium*, thin aggregative fimbriae.

Abbrevations

bp, base pair; ORF, open reading frame.

1 INTRODUCTION

Recently, enzymatic and chemical analysis in combination with genetic studies revealed that *Salmonella enterica* serotype Typhimurium (*S. typhimurium*) is capable to produce cellulose as an exopolysaccharide (Zogaj et al. 2001). The

* For correspondence: Tel: +46-8-524-87319; Fax: +46-8-330744; e-mail: ute.romling@mtc.ki.se

R.M. Brown, Jr. and I.M. Saxena (eds.), Cellulose: Molecular and Structural Biology, 107–122.

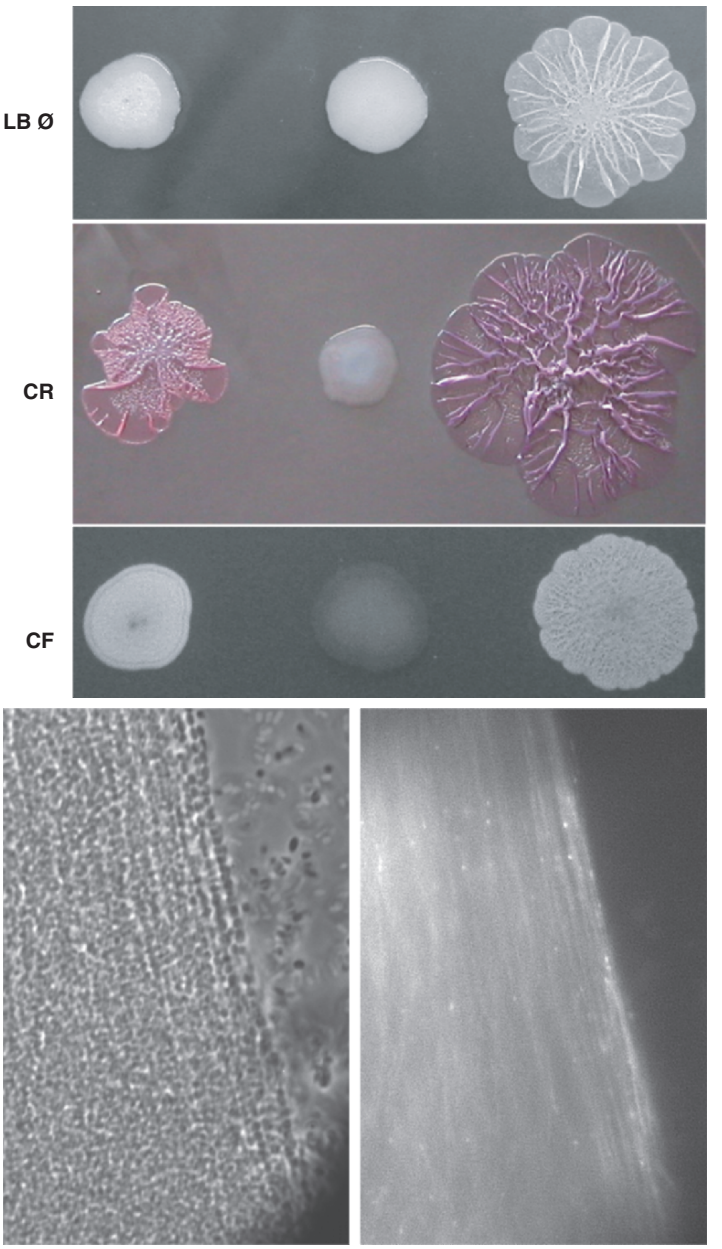

Figure 7-1. Salmonella typhimurium expressing cellulose. (**a**) *S. typhimurium* colonies grown for 48 h on a regular Luria Bertani agar plate without salt (LBØ), a Congo Red plate (CR) and a Calcofluor plate (CF). *Left*: strain that expresses cellulose; *middle*: strain that does not express cellulose. *Right*: strain that expresses cellulose and curli fimbriae. (**b**) Microscopy of cellulose expressing *S. typhimurium* after treatment with Calcofluor. *Left*: Phase contrast; *right*: fluorescence microscopy. Magnification ×600 (*See Color Plate of this figure beginning on page 355*)

bacteria that express cellulose display a characteristic colony morphology when grown on an agar plate and show fibrous cellulose fibers by fluorescence microscopy (Figure 7-1).

Cellulose production confers bacterial cell–cell interactions, adhesion to abiotic surfaces (biofilm formation) and chlorine resistance to the organism (Römling et al. 2000; Zogaj et al. 2001; Solano et al. 2002). Beginning studies shed some light on the molecular mechanisms of cellulose biosynthesis and regulation in *S. typhimurium* and the epidemiology of cellulose biosynthesis in Enterobacteriaceae.

2 THE CELLULOSE BIOSYNTHESIS OPERON IN *Salmonella typhimurium* AND *Escherichia coli*

In *S. typhimurium* and *Salmonella enteritidis*, the two divergently transcribed operons, *yhjRQbcsABZC-bcsEFG* are required for cellulose biosynthesis (Zogaj et al. 2001, Figure 7-2; Solano et al. 2002). The two operons had been identified by random transposon mutagenesis while selecting for mutants with altered capacities to bind the dyes Congo Red and/or Calcofluor when grown on agar plates.

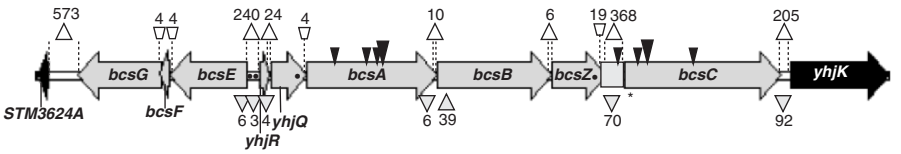

Gene	Position in LT2 genome	ORF (bp)	size of protein (kDa)	Shine–Dalgarno sequence	TAAGGAGGT
bcsG	3806420 - 3808099	1680	62. 2	3806400 – 3806408	A**AAG**TCAAG
bcsF	3806232 - 3806423	192	7. 2	3806217 - 3806225	CGC**GGAG**CG
bcsE	3804664 - 3806235	1572	59. 3	3804644 – 3804652	**TAA**AC**AGTT**
yhjR	3804216 - 3804419	204	7. 6	3804426 – 3804434	A**AAG**G**AG**CA
yhjQ	3803463 - 3804191	729	26. 7	3804208 – 3804216	A**ATGGCGAT**
bcsA	3800842 - 3803466	2625	100. 4	3803480 – 3803488	A**AA**C**G**TCCG
bcsB	3798531 - 3800831	2301	84. 3	3800839 – 3800847	C**AATGATG**A
bcsZ	3797418 - 3798527	1107	41. 6	3798535 – 3798543	TG**A**CC**ATG**A
*bcsC**	3793894 - 3797055	3162	115.9	3797067 – 3797076	**TA**TCA**A**TC**T**
bcsC	3793894 - 3797436	3543	129.8	3797446 – 3797455	**TA**CCTGAC**T**

Figure 7-2. Structure of the cellulose biosynthesis operon *bcs* in *Salmonella typhimurium* and *Escherichia coli*. *Arrowheads* represent the open reading frames (ORFs). Symbols above the ORFs show overlap of (▽) or distance between (Δ) ORFs in bps. Symbols below the ORFs show insertions (▲) or deletions (▼), which occur in *S. typhimurium* LT2 as compared to *Escherichia coli* K-12. *Closed arrows* just above the ORFs indicate transposon insertions in *bcsA* and *bcsC*. The *larger arrow* indicates the position of the transposon used to study transcriptional regulation of the respective gene. The table summarizes the features of *bcs* genes using the positioning in the genome of the sequenced LT2 strain. The start codon proposed for bcsC in E. Coli K-12 leads to a shorter ORF (bcsC*).

Highly homologous operons are present in *E. coli*, and deletion of *bcsA*, the catalytic subunit of cellulose synthase in a recently isolated fecal strain, has proven that it also encodes for cellulose biosynthesis in this species ((Zogaj et al. 2001, our unpublished data). Besides minor changes, annotation of open reading frames in *S. typhimurium* LT2 and *E. coli* K-12 is virtually identical with the exception of *bcsC*. The proposed start codon for *bcsC* in *E. coli* has no equivalent in *S. typhimurium*. Alternative start codons common to both species are found up- and downstream of this site. The proposed upstream start codon leads to an ORF which overlaps with *bcsZ* by 19 bp. Strikingly, the use of this sites would lead to an preterminated out-of-frame product in the laboratory strain *E. coli* K-12, but not in all other up to now sequenced natural *E. coli* strains, which include two enterohemorrhagic, one uropathogenic, one enteroaggregative and one enteropathogenic strain. This fact would explain why *E. coli* K-12 does not produce cellulose.

When compared to the classical type 1 cellulose biosynthesis operon of *Gluconacetobacter xylinus* that produces the cellulose I allomorph under laboratory conditions the cellulose biosynthesis operons of *Salmonella* spp. and *E. coli* have both, homologous and unique components (Figure 7-3). As in *G. xylinus bcsA,* which encodes for the catalytic subunit of the cellulose synthase, and *bcsB,* which

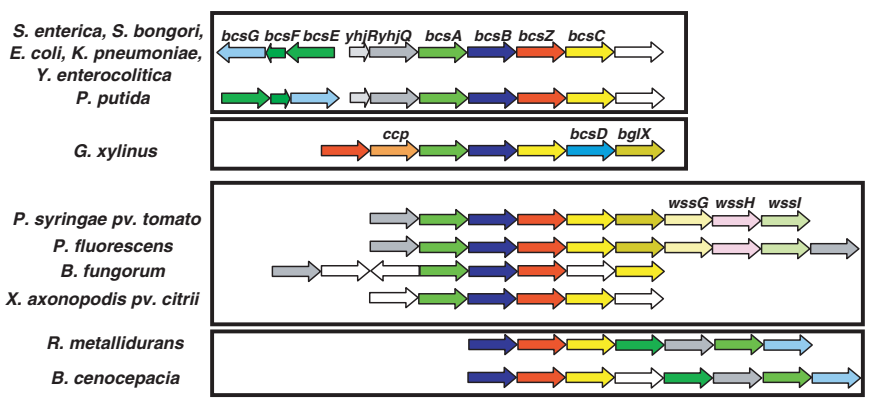

Figure 7-3. Comparison of the cellulose biosynthesis operons *bcs* of Enterobacteriaceae with organisatorically closely related *bcs* operons. ORFs that encode homologous genes involved in cellulose biosynthesis have the same color. *White arrows* indicate genes with no apparent association with cellulose production. Sequences: *Salmonella typhimurium* (AJ315148); *Escherichia coli* (NC 000913); *Pseudomonas putida* KT2440 (NC 002947); *Gluconacetobacter xylinus* (AB015802); *Pseudomonas fluorescens* SJW25 (AY074776); *Xanthomonas axonopodis* pv. *citrii* (NC_003919). Preliminary sequence data for *Pseudomonas syringae* pv. *tomato* were obtained from The Institute for Genomic Research at http://www.tigr.org, for *Burkholderia fungorum* LB400 and *Ralstonia metallidurans* CH34 from the DOE Joint Genome Institute at http://www.jgi.doe.gov/JGI_microbial/html/index.html, for *Burkholderia cenocepacia* J2315, *Salmonella bongori* and *Yersinia enterocolitica* 0:8 from the Sanger center at http://www.sanger.ac.uk/Projects/Microbes/ and for *Klebsiella pneumoniae* from the University of Washington at http://genome.wustl.edu/projects/bacterial/ (*See Color Plate of this figure beginning on page 355*)

encodes a c-di-GMP binding protein, are subsequently arranged in the operon. A cellulase family D member, *bcsZ*, is located within the cellulose biosynthesis operon in *Salmonella* spp. and *E. coli* downstream of *bcsAB*. Although the laboratory strain *E. coli* K-12 is not capable of producing cellulose, a functional cellulase gene could be cloned from the *bcs* operon (Park and Yun 1999). *BcsZ* is required for cellulose biosynthesis in *G. xylinus* (Koo et al. 1998), but in this species the cellulose biosynthesis operon does not contain the gene. However, it is frequently found in close vincinity upstream of the operon.

BcsC, which is required for cellulose biosynthesis *in vivo*, is part of the cellulose biosynthesis operon in Enterobacteriaceae and *G. xylinus*. *BcsC* contains a N-terminal membrane domain and several tetratrico peptide repeats (TRPs) motifs, indicating that it might participate in protein–protein interactions.

Other genes are unique to *G. xylinus* and the Enterobacteriaceae. There is no evidence that Enterobacteriaceae have a homologue of *bcsD*, the last gene in the *bcs* operon in *G. xylinus*, on their chromosome. Also the ccp gene (alternatively called ORF2), located just upstream of *bcsA* is unique to *G. xylinus*. These two genes have been shown to be required for optimal cellulose production and are involved in the control of crystallization by assembling the glucan chains into cellulose I allomorphs (Saxena et al. 1994; Nakai et al. 2002). The lack of those genes in Enterobacteriaceae suggests that the crystallization structure of the glucan chains might be different in those bacteria.

There are also several genes that seem to be unique for cellulose biosynthesis in Enterobacteriaceae. The *yhjQ* gene located upstream of *bcsA* might actually be part of the *bcs* operon as its open reading frame overlaps with the one of *bcsA* by 4 bps (Figure 7-2). Sequence homology search identified *yhjQ* to encode a homologue belonging to the Soj-family, chromosomally encoded ATPases involved in chromosome partitioning and cell division. Consistent with this *in silico* analysis, insertional inactivation of *yhjQ* in *E. coli* K-12 caused abnormal cell division which resulted in incomplete partitioning of the chromosome and filamentous cells at 42°C (Kim et al. 2002). How a *yhjQ* mutation affects cellulose biosynthesis was not studied, since *E. coli* K-12 does not produce cellulose. However, one can envisage that *yhjQ* coordinates cellulose biosynthesis with DNA replication and cell division as the Soj protein coordinates basic cellular processes in *Bacillus subtilis* (Sullivan and Maddock 2000). Why there is a tight coupling of cellulose biosynthesis, and a possible precise positioning of the cellulose synthase complex in the membrane in Enterobacteriaceae, but not in *G. xylinus* remains to be elucidated. Little is known about the role of the divergently transcribed *bcsEFG* operon in cellulose biosynthesis. *BcsE* is predicted to encode for a cytoplasmatically located protease, while *bcsG* encodes for an inner membrane protein of unknown function. Whether *yhjR* (ORF that encodes for a 67 aa long polypeptide) and *yhjT* (63 aa) encode for functional polypeptides involved in cellulose biosynthesis, remains to be shown. Both genes are conserved, since they are also found in the *Pseudomonas putida* cellulose biosynthesis operon (Figure 7-3), although not annotated in the original sequence information.

3 REGULATION OF THE EXPRESSION OF THE *bcsABZC* OPERON

The organization of the *yhjRQbcsABZC-bcsEFG* operons is depicted in Figure 7-2. The two groups of convergently transcribed ORFs are either separated by only a few bps or overlap. Computional analysis in *E. coli* predicts four transcriptional units with one sigma 70-like promoter each*; yhjRQ*, *bcsABZ*, *bcsC* and *bcsEFG*. However, the transcriptional regulatory pattern must be more complex, since, for example, complementation of polar mutations in *bcsZ* does not readily restore cellulose biosynthesis (our unpublished results).

In *S. typhimurium* the transcriptional regulation of the *bcsABZC* operon by environmental conditions was studied with *lacZ*-fusions located in *bcsA* and *bcsC* (Zogaj et al. 2001). Transcription of both genes is growth phase dependent with approximately threefold higher expression in the stationary than logarithmic growth phase. Expression of both genes was highest under aerobic conditions in liquid culture (Luria Broth (LB) without the salt component) and decreased more than twofold under all other conditions such as microaerophilic or anaerobic growth conditions, plate-growth, iron depletion, on minimal medium, under high salt and in rich medium supplemented with glucose as carbon source. However, under all growth conditions substantial transcriptional activity has been found, so that transcription of the *bcsABZC* operon can be considered constitutive. Most surprisingly, transcription of neither *bcsA* nor *bcsC* was dependent on positive regulators of cellulose biosynthesis (see below), *rpoS*, the starvation sigma factor in stationary phase, and *csgD*, a transcriptional response regulator, suggesting that the activation of cellulose biosynthesis takes place at a post-transcriptional level. Those data indicate a situation similar as in *G. xylinus* where membrane fractions showed cellulose biosynthesis activity despite no obvious cellulose production of corresponding whole cells (Saxena and Brown, Jr. 1995) suggesting that synthesis of the cellulose synthase and its activation are separated events. Constitutive expression of the structural genes, but a missing factor for post-transcriptional activation of cellulose biosynthesis could be an explanation for this phenomenon.

4 REGULATION OF CELLULOSE BIOSYNTHESIS

A regulatory cascade leading to the activation of cellulose biosynthesis has been established in *S. typhimurium* (Figure 7-4a). In plate-grown cells, which harbor an intact cellulose biosynthesis operon, expression of AdrA from a low copy number plasmid is sufficient to initiate temperature independent cellulose biosynthesis (Zogaj et al. 2001).

In the natural situation, the chromosomally encoded *adrA* itself is tightly regulated by CsgD (formerly called AgfD), a response regulator of the UhpA (FixJ) family on the transcriptional level (Römling et al. 2000). Under all environmental conditions examined, throughout the bacterial growth phase in liquid culture, plate-growth at 28°C and 37°C, on minimal medium, under iron

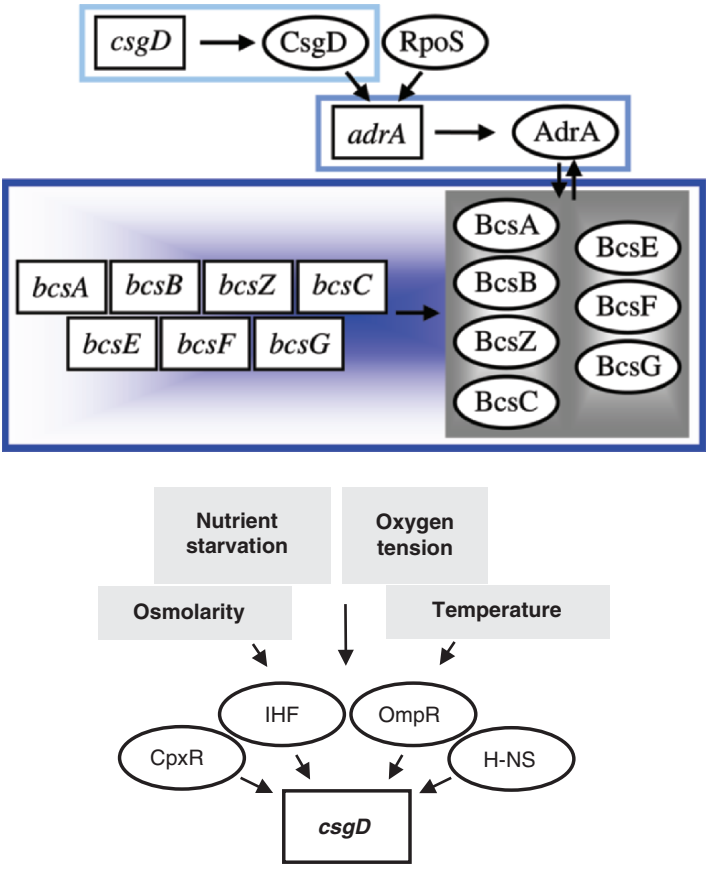

Figure 7-4. (**a**) The cellulose biosynthesis module with regulatory units. Cellulose biosynthesis is activated by the direct or indirect interaction of the AdrA protein with gene products from the *bcs* operons. Transcription of *adrA* is conducted by CsgD together with the second principal sigma factor in stationary phase, RpoS. (**b**) Environmental conditions and global regulatory proteins that influence expression of *csgD* (*See Color Plate of this figure beginning on page 355*)

depletion, under anaerobic conditions and under aerobic conditions in liquid medium, stationary-phase expression of *adrA* was strictly dependent on *csgD* expression. At high salt concentrations, *csgD* is not expressed and hence, *adrA* expression does not take place. However, CsgD is only required for transcription of *adrA*, but not for further steps downstream in the regulatory cascade leading to cellulose biosynthesis (Zogaj et al. 2001).

Another gene, which is required for cellulose biosynthesis is *rpoS* (Römling et al. 1998b, 2000). *RpoS* encodes for the second principal sigma factor in stationary phase, conferring survival properties to various stresses (Hengge-Aronis 1999). As in the case of *csgD*, *rpoS* is solely required for the transcriptional activation of *adrA*,

but not for further steps downstream in the regulatory cascade leading to cellulose biosynthesis. Consequently, the transcription of *bcsA* and *bcsC* was not dependent on *rpoS* (Zogaj et al. 2001).

However, activation of cellulose biosynthesis via the *csgD-adrA* regulatory pathway is not absolute. We have described one *S. enteritidis* strain, where cellulose biosynthesis is at least partially independent of *csgD*, *adrA* and *rpoS* (Römling et al. 2003). In *S. enteritidis*, specific environmental conditions have been reported where cellulose biosynthesis is at least independent of *csgD* and *rpoS* (Solano et al. 2002). In adherence test medium (ATM), which contains sufficient amount of carbon source, but does not support the growth of bacteria, since it is lacking phosphate and the divalent cation magnesium, cellulose was produced after less than 40 min of incubation. Addition of inorganic sources of phosphate, nitrogen, and sulfur or iron, magnesium, or calcium ions abolished cellulose production (Solano et al. 1998). Again, those circumstances resemble activation of cellulose biosynthesis in *G. xylinus* where cellulose biosynthesis was observed in resting cells (Hestrin 1954).

5 REGULATION OF *csgD* EXPRESSION

Under most environmental conditions, cellulose biosynthesis is activated through the transcriptional regulator *csgD*. CsgD itself is regulated on the transcriptional and presumably also post-transcriptional level by a wide variety of environmental stimuli (Gerstel and Römling 2001; Römling et al. 1998b). Nutrient depletion, oxygen tension, osmolarity, and temperature are major factors that influence the expression of *csgD* (Figure 7-4b). *CsgD* is expressed when the bacterial cells reach a certain density in the culture, approximately 3×10^8 cells/ml. Under those conditions, starvation by various nutrients like phosphorus and nitrogen is the trigger to increase expression of *csgD*. Oxygen tension regulates *csgD* expression in a complex interplay with the nutrient source. Reduced oxygen tension (microaerophilic conditions) provided an optimum of *csgD* expression in rich medium, while aerobic conditions are optimal for *csgD* expression in a medium limited for nutrients (minimal medium). High osmolarity abolishes the expression of *csgD*. Cellulose biosynthesis seems to follow this expression pattern via *adrA* expression as judged from the phenotype on plates, since at the moment, no quantitative assay for cellulose production in *S. typhimurium* is available.

Another level of regulation of *csgD* expression is mutations on the chromosome. As the well studied isolates *S. typhimurium* ATCC14028 and SR-11, virtually all *S. typhimurium* and *S. enteritidis* strains isolated from human infections, animal and food express the *csgD* gene in a temperature regulated way, whereby transcription is observed at temperatures below 30°C, but not at 37°C (Römling et al. 1998a, 2003). However, independently isolated mutants of ATCC14028 and SR-11 showed a temperature deregulated expression of *csgD*. The two mutants had individual point mutations in the *csgD* promoter region, which conferred the derepressed expression (Römling et al. 1998b). Consequently, cellulose

biosynthesis was temperature independent in the mutants, but expressed only at temperatures below 30°C in the wild type.

On the molecular level, several globally acting DNA-binding protein bind to the *csgD* promoter region and build up a three-dimensional nucleoprotein complex to ensure tight regulation of expression (Prigent-Combaret et al. 2001; Gerstel et al. 2003). As a key regulator, the transcriptional regulator *ompR* is absolutely required, yet not sufficient to confer *csgD* expression. The alternative sigma factor *rpoS* is also required, but only in strains that express *csgD* temperature regulated.

6 FUNCTION OF AdrA

The function of CsgD in cellulose biosynthesis is solely the activation of *adrA*. But what are the specific mechanisms with which AdrA regulates cellulose biosynthesis? *AdrA,* in a monocistronic operon, encodes for a 371 aa long protein. It contains a highly hydrophobic N-terminal integral membrane domain, named MASE2 (membrane associated sensor; (Nikolskaya et al. 2003)), and a C-terminal GGDEF domain, also called DUF1 (domain of unknown function). The GGDEF domain is considered to be the effector domain. Also in other bacteria, *Rhizobiium leguminosarum* bv. *trifolii* and *Pseudomonas fluorescens*, GGDEF domain containing proteins activate cellulose biosynthesis (Ausmees et al. 1999, 2001; Spiers et al. 2002). In *G. xylinus*, two highly homologous proteins with the domain structure <sensory domain-GGDEF-EAL> confer either cyclization of two GTP molecules or cleavage of c-di-GMP (Tal et al. 1998).

By sequence similarity in combination with molecular modeling, the GGDEF domain has been suggested to confer nucleotide cyclization activity (Pei and Grishin 2001), but this function has to be experimentally proven. However, it is not very far fetched to speculate that the GGDEF domain might synthesize the cyclic nucleotide c-di-GMP, which has been identified as the allosteric activator for cellulose biosynthesis in *G. xylinus* (Ross et al. 1991).

The GGDEF/DUF1 domain is highly abundant, over 750 proteins of the presently sequenced 256 microbial genomes contain this domain, although a phenotype or function has been reported for only a handful of those genes mainly in the context of studies concerning bacterial development (Hecht and Newton 1995; Jones et al. 1999; Gronewold and Kaiser 2001; Boles and McCarter 2002). If the function of the GGDEF domain is in fact the production of c-di-GMP, those data mean that c-di-GMP is an important, yet unidentified global second messenger in bacteria. However, GGDEF domain proteins are not equally distributed among the microorganisms (Galperin et al. 2001). GGDEF domain containing proteins are highly abundant in Gram-negative free-living bacteria, which also can have pathogenic potential. In Gram-positive bacteria this domain occurs in much lower numbers, if at all; obligate parasites have only one or no copy of the GGDEF domain; and archaea miss this domain at all.

S. typhimurium has 12 copies of this domain. That all 12 proteins with this domain are involved in the regulation of cellulose biosynthesis, but under different

environmental conditions, seems unlikely, but cannot be completely excluded. Alternatively, other cellular processes might be regulated by GGDEF domain containing proteins.

7 OCCURRENCE OF THE CELLULOSE BIOSYNTHESIS OPERON AMONG ENTEROBACTERIAL SPECIES

The cellulose biosynthesis operon is not present in all species within the family of Enterobacteriaceae, nor is cellulose constitutively expressed by those species that harbor the genetic information. Whole genome sequence analysis revealed that the cellulose biosynthesis operon is present in *S. enterica* serovars and *S. bongori*, in *E. coli, Shigella* spp., which are actually subspecies of *E. coli*, *Klebsiella pneumoniae*, *Erwinia chrysantemii* strain 3937, *Erwinia carotovora* subsp. *atroseptica* SCRI 1043.06 and *Yersinia enterocolitica* type O:8. In addition, work in our group has detected *bcsA*, the catalytic subunit of cellulose synthase, in *Citrobacter* spp., *Citrobacter freundii*, *Citrobacter koserilfarmeri*, *Enterobacter aerogenes*, *Enterobacter cloacae, Enterobacter sakazakii*, *Klebsiella oxytoca*, and *Raoultella ornithinolytica* (Zogaj et al. 2003).

But where had *S. typhimurium* or, more accurate, an enterobacterial common ancestor acquired this operon? The G+C content of the *yhjRQbcsABZC* operon in *S. typhimurium* is 58%, whereby the average G+C content of the *S. typhimurium* genome is 53%. This fact suggested that the cellulose biosynthesis operon comes from a bacterial species with higher G+C content. Actually, highly homologous sequences, not only on the protein, but also on the nucleotide level are found in the unrelated saprophytic soil bacterium *Pseudomonas putida* KT2440 (Figure 7-3). However, already in *P. putida* only the core genes *yhjRQbcsABZC* are in the same order as in Enterobacteriaceae. The sequence of the *bcsEFG* operon is rearranged through reversion. In the plant pathogen *Pseudomonas syringae* pv. *tomato* and the rhizosphere isolate *P. fluorescens* SWB25, there are additional variants of the cellulose biosynthesis operon (Spiers et al. 2002). Downstream of the respective *bcsC* homologue there is a gene cluster called *wssGHI*, which is paralogous to a gene cluster carrying out acetylation of another exopolysaccharide, namely alginate, in *P. aeruginosa*. It has been suggested that the *wssGHI* gene cluster confers acetylation of the glucan chain, whereby a second copy of the Soj-homologue *yhjQ*, *wssJ*, located downstream of the *wssGHI* genes in *P. fluorescens*, positions the enzyme complex nearby the cellulose synthase.

Also other soil bacteria like species from the medically, agriculturally and environmentally important Burkholderia complex, *Burkholderia fungorum* LB400 and *Burkholderia cenocepacia* J2315 (previously called *Burkholderia* (*Pseudomonas*) *cepacia*) and the heavy metal resistant *Ralstonia metallidurans* CH34 (previously called *Ralstonia eutropha* and *Alcaligenes eutrophus*) and the plant pathogen *Xanthomonas axonopodis* pv. *citrii* (da Silva et al. 2002) harbor variations of the cellulose biosynthesis operon. The similarities in organization of the *bcs* operon are reflected by the distances of the respective catalytic subunits of the cellulose synthase BcsA in the phylogram (compare Figure 7-2 and Figure 7-5).

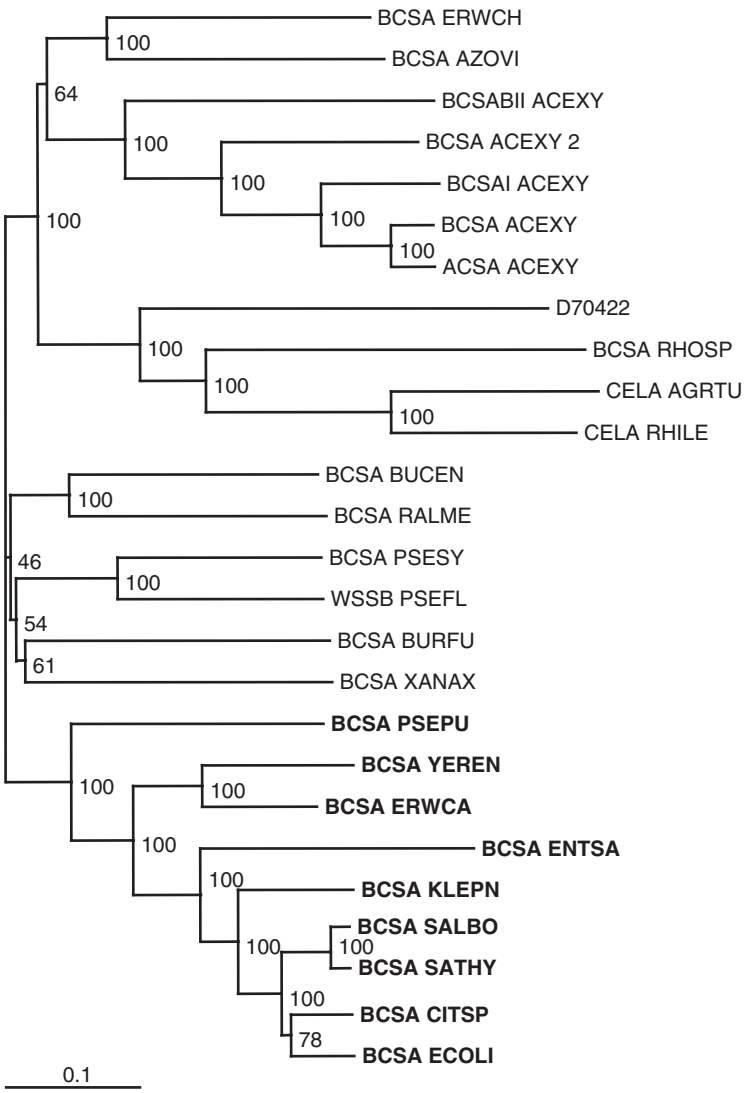

Figure 7-5. Phylogram of relationships of bacterial cellulose synthase BcsA. All enterobacterial BcsA proteins besides *Erwinia chrysantemii* cluster with BcsA from *Pseudomonas putida* KT2440. Sequences were aligned in Clustalx using the default mode and processed manually afterwards. The tree was constructed using the neighborhood joining (NJ) method of Saitou and Nei and subjected to 10,000 bootstrap trials. Numbers on nodes indicate percentages of bootstrap values. The tree was drawn with TreeView. The scale indicates amino acid substitutions per site. Protein sequences used in Figure 7-5: D70422 (*Aquifex aeolicus* BcsA); BCSA_ACEXY (BAA31463.1); ACSA_ACEXY (P19449); BCSAI_ACEXY (BAA77585.1); BCSA_ACEXY_2 (P21877); BCSABII_ACEXY (BAA77593.1); CELA_AGRTU (NP_357298.1); CELA_RHILE (AAC41436.1); BCSA_PSEFL (AAL71842); BCSA_PSEPU (NP_744780); BCSABCSA_SATHY (CAC44015.1); BCSA_ECOLI (P37653); BCSA_ENTSA (CAD56669); BCSA_CITSP (CAD56668); BCSA_XANAX (AAM38358). BCSA_PSESY and BCSA_ERWCH were from The Institute for Genomic Research at http://www.tigr.org, BCSA_AZOVI, BCSA_BURFU, BCSA_RALME and BCSA_RHOSP from the DOE Joint Genome Institute at http://www.jgi.doe.gov/JGI_microbial/html/index.html and BCSA_YEREN, BCSA_ERWCA, BCSA_SALBO and BCSA_BUCEN from the Sanger center at http://www.sanger.ac.uk/Projects/Microbes/ and BCSA_KLEPN from the University of Washington at http://genome.wustl.edu/projects/bacterial/

8 DIFFERENTIAL EXPRESSION OF CELLULOSE AMONG *Enterobacteriaceae*

Study on the expression of cellulose in over 800 *S. enterica* isolates from human infections, food and animals revealed serovar specific expression patterns, which could be correlated with disease severity in the respective hosts (Römling et al. 2003). *S. typhimurium* and *S. enteritidis* isolates consistently expressed cellulose at 28°C on agar plates, while isolates of the serovars *Salmonella typhi*, *Salmonella choleraesuis* and of the variant *S. typhimurium* var. Copenhagen did not express cellulose. However, when expressed by strains of serovars Typhimurium and Enteritidis, we observed that cellulose is always coexpressed with proteinaceous appendaces, the curli fimbriae (see below).

Cellulose expression showed a more variable pattern in *E. coli*, an important inhabitant of the human gastrointestinal tract as well as a pathogen. A substantial proportion of commensal isolates of *E. coli* expressed cellulose at 28°C and/or 37°C, although always together with curli fimbriae (our unpublished data). In uropathogenic isolates, however, cellulose expression could occur without concomitant curli expression (our unpublished data). Otherwise, no systematic investigations about the expression of cellulose have been carried out in *E. coli* strains. Bacterial species isolated from the gastrointestinal tract showed a variable, genus specific expression of cellulose (Zogaj et al. 2003). While *Citrobacter* isolates showed temperature dependent expression of cellulose, *Enterobacter* isolates displayed temperature independent or preferential expression at 37°C. *Klebsiella* isolates did not express cellulose when plate-grown. However, we recently discovered few cellulose-positive colonies derived from *K. pneumoniae* strain DSM12082, which was isolated from a pond (Zogaj et al. 2001).

9 COEXPRESSION OF CELLULOSE WITH CURLI FIMBRIAE

In *S. typhimurium* and *S. enteritidis* serovars and in commensal *E. coli* strains cellulose is usually coexpressed with curli fimbriae, a proteinaceous component. As cellulose biosynthesis, expression of curli fimbriae is regulated by CsgD on the transcriptional level. In fact, the *csgD* gene is part of the *csgDEFG-csgBA(C)* biosynthesis operon and presumably directly activates the *csgBA(C)* operon (Römling et al. 1998a).

The major characteristic of curli fimbriae is their binding capacity to diverse substrates, ranging from proteins present in the human host to hydrophilic and hydrophobic abiotic surfaces such as glass and polystyrene (Ben Nasr et al. 1996; Olsen et al. 1989; Austin et al. 1998; Herwald et al. 1998; Olsen et al. 1998; Römling et al. 1998b). Not unexpectedly, curli fimbriae also interact with the glucan chains of cellulose coexpressed with curli fimbriae on the bacterial surface (Zogaj et al. 2001; White et al. 2003). The interaction is evident in that the otherwise free-floating glucan bundles of cellulose are tightly wrapped around

the bacterial cells when curli fimbriae were coexpressed. Through those, presumable noncovalent, interactions the properties of the bacterial colonies were change dramatically (Figure 7-1a). The bacteria are firmly interconnected in a rigid network and their surface is highly hydrophobic. Actually, cellulose from those bacteria was not digestible with cellulase even after extended hours using high concentrations of enzyme, although the digestion of cellulose alone was no problem (Zogaj et al. 2001).

The interaction and distinct roles of cellulose and curli fimbriae can be seen in various assays. Electron microscopy studies revealed that fine cellulose fibers were produced peritrichously by *S. typhimurium* (Römling and Lunsdorf 2003). On the other hand, curli fimbriae appear as 2–3 nm wide, curled appendages. When expressed together, the material appears diffuse (White et al. 2003). Distinct biofilms are formed by cellulose and curli fimbriae (Römling et al. 2001). Cellulose mainly provided loose adherence at the air–liquid interface, while curli fimbriae mediated tight interactions below the surface of the liquid. The two extracellular matrix components also fullfill different roles in bacterial cell–cell interaction. Cellulose fibers provide elastic, long-range interconnections, while curli fimbriae mediate rigid, but easily breakable connections between individual cells. It can be concluded that cellulose fibers have a structural function, while curli fimbriae provide stabilization. Because of the functional similarities of cellulose and accessory components to the plant system, we have referred to the phenotype of the microbial colonies as "bacterial wood" (Zogaj et al. 2001).

10 CONCLUSIONS

Recently, the molecular basis of cellulose biosynthesis has been detected in *S. typhimurium* and other Enterobacteriaceae. With this discovery, however, new questions did arise concerning various aspects such as the mode of cellulose biosynthesis, its regulation, function, epidemiology, structure and interaction of cellulose with other components. At present, answers are only partially available, if at all. The availability of well characterized and fully sequenced strains together with efficient tools for genetic manipulation, however, gives hope that fairly soon light will be shed at least to some aspects of cellulose biosynthesis in Enterobacteriaceae.

Acknowledgments

Research of U.R. is supported by the Karolinska Institutet ("Elitforskartjänst"), and Vetenskapsradet grants B5107-20005701/2000 and K2002-06X-14232-01A. I thank Xhavit Zogaj for experimental support and preparation of Figure 7.1b and 7-2. Release of sequence data prior to publication from the DOE Joint Genome Institute, the Sanger Center, TIGR and University of Washington is gratefully acknowledged.

REFERENCES

Ausmees N., Jonsson H., Hoglund S., Ljunggren H., and Lindberg M. 1999. Structural and putative regulatory genes involved in cellulose synthesis in *Rhizobium leguminosarum* bv. trifolii. Microbiology 145:1253–1262.

Ausmees N., Mayer R., Weinhouse H., Volman G., Amikam D., Benziman M., and Lindberg M. 2001. Genetic data indicate that proteins containing the GGDEF domain possess diguanylate cyclase activity. FEMS Microbiol Lett 204:163–167.

Austin J.W., Sanders G., Kay W.W., and Collinson S.K. 1998. Thin aggregative fimbriae enhance *Salmonella enteritidis* biofilm formation. FEMS Microbiol Lett 162:295–301.

Ben Nasr A., Olsen A., Sjobring U., Muller-Esterl W., and Bjorck L. 1996. Assembly of human contact phase proteins and release of bradykinin at the surface of curli-expressing *Escherichia coli*. Mol Microbiol 20:927–935.

Boles B.R. and McCarter L.L. 2002. *Vibrio parahaemolyticus* ***scrABC***, a novel operon affecting swarming and capsular polysaccharide regulation. J Bacteriol 184:5946–5954.

da Silva A.C., Ferro J.A., Reinach F.C., Farah C.S., Furlan L.R., Quaggio R.B., Monteiro-Vitorello C.B., Van Sluys M.A., Almeida N.F., Alves L.M., do Amaral A.M., Bertolini M.C., Camargo L.E., Camarotte G., Cannavan F., Cardozo J., Chambergo F., Ciapina L.P., Cicarelli R.M., Coutinho L.L., Cursino-Santos J.R., El-Dorry H., Faria J.B., Ferreira A.J., Ferreira R.C., Ferro M.I., Formighieri E.F., Franco M.C., Greggio C.C., Gruber A., Katsuyama A.M., Kishi L.T., Leite R.P., Lemos E.G., Lemos M.V., Locali E.C., Machado M.A., Madeira A.M., Martinez-Rossi N.M., Martins E.C., Meidanis J., Menck C.F., Miyaki C.Y., Moon D.H., Moreira L.M., Novo M.T., Okura V.K., Oliveira M.C., Oliveira V.R., Pereira H.A., Rossi A., Sena J.A., Silva C., de Souza R.F., Spinola L.A., Takita M.A., Tamura R.E., Teixeira E.C., Tezza R.I., Trindade dos Santos M., Truffi D., Tsai S.M., White F.F., Setubal J.C., and Kitajima J.P. 2002. Comparison of the genomes of two ***Xanthomonas*** pathogens with differing host specificities. Nature 417:459–463.

Galperin M.Y., Nikolskaya A.N., and Koonin E.V. 2001. Novel domains of the prokaryotic two-component signal transduction systems. FEMS Microbiol Lett 203:11–21.

Gerstel U. and Römling U. 2001. Oxygen tension and nutrient starvation are major signals that regulate ***agfD*** promoter activity and expression of the multicellular morphotype in *Salmonella typhimurium*. Environ Microbiol 3:638–648.

Gerstel U., Park C., and Romling U. 2003. Complex regulation of ***csgD*** promoter activity by global regulatory proteins. Mol Microbiol 49:639–654.

Gronewold T.M. and Kaiser D. 2001. The ***act*** operon controls the level and time of C-signal production for *Myxococcus xanthus* development. Mol Microbiol 40: 744–756.

Hecht G.B. and Newton A. 1995. Identification of a novel response regulator required for the swarmer-to-stalked-cell transition in *Caulobacter crescentus*. J Bacteriol 177:6223–6229.

Hengge-Aronis R. 1999. Interplay of global regulators and cell physiology in the general stress response of *Escherichia coli*. Curr Opin Microbiol 2:148–152.

Herwald H., Morgelin M., Olsen A., Rhen M., Dahlback B., Muller-Esterl W., and Bjorck L. 1998. Activation of the contact-phase system on bacterial surfaces–a clue to serious complications in infectious diseases. Nat Med 4:298–302.

Hestrin S. and Schramm, M. 1954. Synthesis of cellulose by *Acetobacter xylinum*. Biochem J 58:345–352.

Jones H.A., Lillard J.W., Jr., and Perry R.D. 1999. HmsT, a protein essential for expression of the haemin storage (Hms+) phenotype of *Yersinia pestis*. Microbiology 145 (Pt 8):2117–2128.

Kim M.K., Park S.R., Cho S.J., Lim W.J., Ryu S.K., An C.L., Hong S.Y., Park Y.W., Kahng G.G., Kim J.H., Kim H., and Yun H.D. 2002. The effect of a disrupted ***yhjQ*** gene on cellular morphology and cell growth in *Escherichia coli*. Appl Microbiol Biotechnol 60:134–138.

Koo H.M., Song S.H., Pyun Y.R., and Kim Y.S. 1998. Evidence that a beta-1,4-endoglucanase secreted by *Acetobacter xylinum* plays an essential role for the formation of cellulose fiber. Biosci Biotechnol Biochem 62:2257–2259.

Nakai T., Nishiyama Y., Kuga S., Sugano Y., and Shoda M. 2002. ORF2 gene involves in the construction of high-order structure of bacterial cellulose. Biochem Biophys Res Commun 295:458–462.

Nikolskaya A.N., Mulkidjanian A.Y., Beech I.B., and Galperin M.Y. 2003. MASE1 and MASE2: two novel integral membrane sensory domains. J Mol Microbiol Biotechnol 5:11–16.

Olsen A., Jonsson A., and Normark S. 1989. Fibronectin binding mediated by a novel class of surface organelles on *Escherichia coli*. Nature 338:652–655.

Olsen A., Wick M.J., Morgelin M., and Bjorck L. 1998. Curli, fibrous surface proteins of *Escherichia coli*, interact with major histocompatibility complex class I molecules. Infect Immun 66:944–949.

Park Y.W. and Yun H.D. 1999. Cloning of the *Escherichia coli* endo-1,4-D-glucanase gene and identification of its product. Mol Gen Genet 261:236–241.

Pei J. and Grishin N.V. 2001. GGDEF domain is homologous to adenylyl cyclase. Proteins 42:210–216.

Prigent-Combaret C., Brombacher E., Vidal O., Ambert A., Lejeune P., Landini P., and Dorel C. 2001. Complex regulatory network controls initial adhesion and biofilm formation in *Escherichia coli* via regulation of the ***csgD*** gene. J Bacteriol 183:7213–7223.

Ross P., Mayer R., and Benziman M. 1991. Cellulose biosynthesis and function in bacteria. Microbiol Rev 55:35–58.

Römling U. and Lunsdorf H. 2003. Cellulose biosynthesis in *Enterobacteriaceae*. Cellulose 11:413–418.

Römling U., Bian Z., Hammar M., Sierralta W.D., and Normark S. 1998a. Curli fibers are highly conserved between *Salmonella typhimurium* and *Escherichia coli* with respect to operon structure and regulation. J Bacteriol 180:722–731.

Römling U., Sierralta W.D., Eriksson K., and Normark S. 1998b. Multicellular and aggregative behaviour of *Salmonella typhimurium* strains is controlled by mutations in the ***agfD*** promoter. Mol Microbiol 28:249–264.

Römling U., Rohde M., Olsen A., Normark S., and Reinköster J. 2000. AgfD, the checkpoint of multicellular and aggregative behaviour in *Salmonella typhimurium* regulates at least two independent pathways. Mol Microbiol 36:10–23.

Römling U., Bokranz W., Rabsch W., Zogaj X., Nimtz M., and Tschäpe, H. 2003. Occurrence and regulation of the multicellular morphotype in *Salmonella serovars* important in human disease. Int J Med Microbiol 293:273–285.

Römling U., Rohde M., Olsen A., Normark S., and Reinkoster J. The multicellular morphotypes of *Salmonella typhimurium* and *Escherichia coli* produce cellulose as the second component of the extracellular matrix. Mol Microbiol 39:1452–1463.

Saxena I.M., Kudlicka K., Okuda K., and Brown, Jr. R.M., 1994. Characterization of genes in the cellulose-synthesizing operon (***acs*** operon) of *Acetobacter xylinum*: implications for cellulose crystallization. J Bacteriol 176:5735–5752.

Saxena I.M. and Brown, Jr. R.M., 1995. Identification of a second cellulose synthase gene (*acsAII*) in *Acetobacter xylinum*. J Bacteriol 177:5276–5283.

Solano C., Sesma B., Alvarez M., Humphrey T.J., Thorns C.J., and Gamazo C. 1998. Discrimination of strains of *Salmonella enteritidis* with differing levels of virulence by an *in vitro* glass adherence test. J Clin Microbiol 36:674–678.

Solano C., Garcia B., Valle J., Berasain C., Ghigo J.M., Gamazo C., and Lasa I. 2002. Genetic analysis of *Salmonella enteritidis* biofilm formation: critical role of cellulose. Mol Microbiol 43:793–808.

Spiers A.J., Kahn S.G., Bohannon J., Travisano M., and Rainey P.B. 2002. Adaptive divergence in experimental populations of *Pseudomonas fluorescens*. I. Genetic and phenotypic bases of wrinkly spreader fitness. Genetics 161:33–46.

Sullivan S.M. and Maddock J.R. 2000. Bacterial sporulation: pole-to-pole protein oscillation. Curr Biol 10: R159–161.

Tal R., Wong H.C., Calhoon R., Gelfand D., Fear A.L., Volman G., Mayer R., Ross P., Amikam D., Weinhouse H., Cohen A., Sapir S., Ohana P., and Benziman M. 1998. Three ***cdg*** operons control cellular turnover of cyclic di-GMP in *Acetobacter xylinum*: genetic organization and occurrence of conserved domains in isoenzymes. J Bacteriol 180:4416–4425.

White A.P., Gibson D.L., Collinson S.K., Banser P.A., and Kay W.W. 2003. Extracellular polysaccharides associated with thin aggregative fimbriae of *Salmonella enterica* and *Serovar enteritidis*. J Bacteriol 185:5398–5407.

Zogaj X., Nimtz M., Rohde M., Bokranz W., and Römling U. 2001. The multicellular morphotypes of *Salmonella typhimurium* and *Escherichia coli* produce cellulose as the second component of the extracellular matrix. Mol Microbiol 39:1452–1463.

Zogaj X., Bokranz W., Nimtz M., and Römling U. 2003. Production of cellulose and curli fimbriae by members of the family *Enterobacteriaceae* isolated from the human gastrointestinal tract. Infect Immun 71:4151–4158.

CHAPTER 8

IN VITRO SYNTHESIS AND ANALYSIS OF PLANT (1→3)-β-D-GLUCANS AND CELLULOSE: A KEY STEP TOWARDS THE CHARACTERIZATION OF GLUCAN SYNTHASES

VINCENT BULONE*

Royal Institute of Technology (KTH), School of Biotechnology, AlbaNova University Center, SE-106 91 Stockholm, Sweden.

Abstract

The isolation and characterization of plant mutants affected in cellulose biogenesis have allowed the identification of a family of genes involved in this fundamental process. A specific attention has been given in the last years to genetic and molecular biology approaches, mainly because of the difficulty to assay and purify to homogeneity cellulose synthase complexes. At this stage, it is necessary to reconsider the importance of biochemical approaches, not only to firmly demonstrate *in vitro* that the proteins coded by the isolated genes are indeed able to catalyze cellulose synthesis, but also to isolate and identify directly the different components of the synthesizing machinery. The recent progress made in the field of *in vitro* synthesis of cellulose is promising and it will certainly allow the purification and biochemical characterization of plant cellulose synthases in the near future. In this review, a particular attention is given to the description and critical analysis of the *in vitro* approaches that have been developed for the study of plant cellulose synthases and the related enzymes callose synthases. An important problem raised by these biochemical investigations is the analysis of the *in vitro* polysaccharides. This aspect is integrated in the discussion, with a presentation of strategies and methods for high-throughput assays of β-glucan synthases and detailed structural characterization of *in vitro* products.

Keywords

biochemical approaches for the study of glucan synthases, (1→3)-β-D-glucan (callose) and cellulose synthases, *in vitro* synthesis of callose and cellulose, structural and morphological characterization of *in vitro* polysaccharides.

* For correspondence: Tel: (+46) 8 5537 8841; Fax: (+46) 8 5537 8468; e-mail: vincent.bulone@biotech.kth.se

R.M. Brown, Jr. and I.M. Saxena (eds.), Cellulose: Molecular and Structural Biology, 123–145.

Abbreviations

3-[(3-cholamidopropyl)dimethylammonio]-1-propane sulfonate (CHAPS), dimethylsulfoxide (DMSO), ethylene glycol-bis(β-aminoethyl ether)-*N*,*N*,*N*′,*N*′-tetraacetic acid (EGTA), 3-[*N*-morpholino]propanesulfonic acid (Mops), nuclear magnetic resonance (NMR), transmission electron microscopy (TEM).

1 INTRODUCTION

The biosynthesis of cellulose, which is one of the major plant cell wall polysaccharides, is still far from being completely understood despite the efforts made in the past few decades to identify the enzymes involved in this important process. The main difficulty has been to isolate in an active form the enzyme cellulose synthase which is involved in cellulose polymerization, and to characterize it directly using biochemical approaches. Cellulose synthase is a membrane-bound complex that has been observed in membranes of several organisms by electron microscopy, using freeze fracture techniques (Brown, Jr. 1996; Kimura et al. 1999). The plant enzymes are organized as hexagonal supramolecular structures designated as rosettes, with a sixfold symmetry (Brown, Jr. 1996). They are highly unstable and extractions from plasma membranes using detergents usually yield enzyme preparations that synthesize *in vitro* no or very little cellulose from the substrate UDP-glucose. Instead, the major product obtained *in vitro* from detergent extracts is callose, i.e. a linear (1→3)-β-D-glucan (Delmer 1987; Okuda et al. 1993). Interestingly, it has been shown that when callose synthase is induced *in vivo* using elicitors cellulose synthesis decreases proportionally (Delmer and Amor 1995). In addition, the first *in vitro* experiments that led to some cellulose synthesis showed that the production of (1→4)-β-D-glucans is favored over the synthesis of callose when calcium is chelated by EGTA (Okuda et al. 1993). From these results, it has been proposed that the synthesis of callose and cellulose is performed by the same enzyme that polymerizes either polysaccharides, depending on its conformation and on regulation processes that may involve divalent cations or changes in the phosphorylation state (Delmer 1999). Demonstration of such hypotheses requires the isolation of pure enzymes in an active form, an objective that has still to be achieved. Altogether, these observations clearly show that it is difficult to analyze and discuss the mechanisms of cellulose synthesis without considering the synthesis of callose. However, this does not mean that (1→3)-β-D-glucan synthesis in plants is a phenomenon of secondary importance. Actually, callose synthesis is essential in normal plant development and plays a central role in the plant defense response to various stresses (Stone and Clarke 1992). For instance, (1→3)-β-D-glucans are deposited transiently at the cell plate during cell division and are found as components of specialized cell walls such as those of pollen mother cells (Stone and Clarke 1992). They are also associated with sieve plates and plasmodesmatal canals at various stages of plant growth and development (Stone and Clarke 1992). Callose deposition is known to occur when plant tissues are stressed, e.g., after microbial infection or wounding (Stone and Clarke 1992).

As a consequence of the difficulty to apply biochemical approaches to the study of callose and cellulose biosynthesis, many groups have focused their efforts on the identification of genes that are required for the synthesis of these polysaccharides. This has allowed important progress since a number of genes that are likely to be directly responsible for callose and cellulose synthesis have been described (Delmer 1999; Doblin et al. 2002). In the case of cellulose synthase, the first genes were identified in the cotton fiber by Pear et al. (1996). Since then, numerous functional homologues designated as *CesA* have been isolated from other organisms such as *Arabidopsis thaliana* (Arioli et al. 1998; Taylor et al. 1999; Fagard et al. 2000; Taylor et al. 2000; Scheible et al. 2001), *Zea mays* (Holland et al. 2000), *Nicotiana alata* (Doblin et al. 2001), *Hordeum vulgare* (Burton et al. 2004), and *Populus tremula* × *tremuloides* (Djerbi et al. 2004). Interestingly, all the protein sequences deduced from these genes bear the consensus D,D,D,QXXRW motif common to all members of glycosyltransferase family 2, which comprises other polysaccharide synthases, like chitin and hyaluronan synthases (Saxena et al. 1995; Campbell et al. 1997; see also the Carbohydrate-Active Enzymes server http://afmb.cnrs-mrs.fr/CAZY/index.html (Coutinho and Henrissat 1999)). However, none of the *CesA* genes show any significant similarity with plant genes (Cui et al. 2001; Doblin et al. 2001; Hong et al. 2001; Li et al. 2003) homologous to *fks1* from *Saccharomyces cerevisiae* (Douglas et al. 1994), a gene proposed to encode the catalytic subunit of the yeast (1→3)-β-D-glucan synthase. The plant Fks proteins, designated GSL ("Glucan Synthase-Like"), do not have the D, D, D, QXXRW signature. They are grouped in glycosyltransferase family 48 and constitute a family of their own (Coutinho and Henrissat 1999). The most convincing biochemical data linking callose biosynthesis to a GSL protein have been obtained in barley (Li et al. 2003). In this work, the authors have shown for the first time that amino acid sequences from a highly enriched 250-kDa protein present in a fraction exhibiting (1→3)-β-D-glucan synthase activity correspond to amino acid sequences deduced from a barley *fks 1*-like gene designated *HvGSL1*. Interestingly, at least six independent *GSL* genes were identified in barley (Li et al. 2003). These genes showed sequence identity ranging from 40 to 60%. They may code for isoforms of HvGSL1 or for proteins with another yet unknown function. It is possible that some GSL proteins do not actually catalyze the polymerization of (1→3)-β-D-glucans but are involved in other processes. It is noteworthy that the function of the yeast Fks proteins is also being debated. It has been proposed that these proteins may not be involved in the catalysis of (1→3)-β-D-glucan synthesis, but in other mechanisms such as, for instance, the transport of β-glucans (Eng et al. 1994; Garrett-Engele et al. 1995; Cabib et al. 2001; Dijkgraaf et al. 2002). This idea is further supported by the observation that, unlike the plant GSL and yeast Fks proteins, the catalytic subunit of the (1→3)-β-D-glucan synthase from an *Agrobacterium* species shares similarities with other processive glycosyltransferases (Stasinopoulos et al. 1999) and is classified in glycosyltransferase family 2 together with the *CesA* proteins (Coutinho and Henrissat 1999). Despite the progress brought by the identification of the plant

GSL genes and the biochemical characterization of the barley HvGSL1 protein, the glycosyltransferase activity of most GSL proteins and of the corresponding Fks proteins from yeast remains to be demonstrated *in vitro*. Likewise, the catalytic activity of the products of the *CesA* genes has not been proved *in vitro*. From these observations, it appears important to reconsider biochemical approaches as important tools towards the characterization of cellulose and callose synthases. Undoubtedly, *in vitro* experiments represent a key step to achieve this objective.

Even though it is still not possible to assay cellulose synthases routinely, the results obtained on the blackberry (Lai Kee Him et al. 2002) and on the cotton and mung bean enzymes (Kudlicka et al. 1995; Kudlicka et al. 1996; Kudlicka and Brown, Jr. 1997) are promising for the direct characterization of cellulose synthases using biochemical approaches. In particular, globular structures which likely correspond to the synthesizing enzyme complexes have been found associated to *in vitro* cellulose microfibrils (Figure 8-1) (Kudlicka and Brown, Jr. 1997; Lai Kee Him et al. 2002).

In the best case, up to 1 mg of cellulose could be synthesized (Lai Kee Him et al. 2002). These experiments have allowed a complete characterization of the *in vitro* cellulose using physical and chemical techniques, but callose was still the major product in the reaction mixture (Lai Kee Him et al. 2002). Thus, it remains now to improve the *in vitro* procedure to isolate higher amounts of complexes composed of cellulose and synthesizing enzymes in order to be able to identify the different proteins required for cellulose polymerization. Promising models for such improvement are the recently established cell suspension cultures of hybrid aspen (*Populus tremula* × *tremuloides*) (Ohlsson et al. 2006). The first

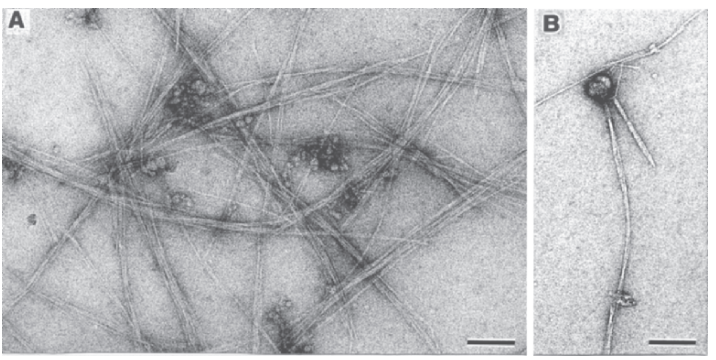

Figure 8-1. TEM images of the cellulose synthesized *in vitro* by the blackberry cellulose synthase extracted with taurocholate. The reaction mixture was as described in Table 8-1. Examinations were made after negative staining with 2% uranyl acetate. (**a**) Purified *in vitro* cellulose treated with the Updegraff (1969) reagent. (**b**) A typical example of an *in vitro* microfibril associated with a globular structure that may correspond to the synthesizing complex. This sample was not treated with the Updegraff reagent to preserve the globular structures. Bars = 100 nm. Reproduced from Lai Kee Him et al. 2002 with permission.

in vitro experiments performed on this system indicate that up to 50% of cellulose can be synthesized when the membrane-bound enzymes are extracted from cells harvested in the stationary growth phase (Colombani et al. 2004). However, even if such biochemical approaches appear to be a crucial step for the characterization of glucan synthases, it is now clear that substantial progress can be achieved only with a multidisciplinary strategy that integrates *in vitro* experiments coupled to product characterization, proteomics, immunochemical methods, molecular biology and expression analysis of the key genes.

The next sections of this review are focused on the description of *in vitro* approaches for the study of callose and cellulose synthases. Particular attention is given to the characterization of *in vitro* products. This is an important problem since non-rigorous analyses of glucan structures based for instance on the solubility in various solvents or on the resistance of the *in vitro* products towards chemical treatments may be misleading. Also, the strategy and the techniques to be used will differ depending on the objective of the characterization. The aim is generally to demonstrate that the reaction mixtures recovered after multiple *in vitro* assays contain the expected products. In addition to the demonstration that the synthesis occurred *de novo*, it is also important to determine accurately the type of linkage present in the products, which means for β-glucan synthases to be able to distinguish between (1→3)-β- and (1→4)-β-linked glucosyl units. In other situations, more detailed structural information can help understand biosynthetic processes. This usually requires the optimization of the composition of the synthetic reaction mixtures in order to obtain sufficient amounts of product for characterization using complementary physical and chemical techniques. Some of these techniques destroy the sample or lead to a loss of the three-dimensional organization of the polymers, whereas others allow the recovery of the *in vitro* polysaccharides in their original state. Therefore, the strategy used for a detailed structural characterization should take into account not only the amount of product available, but also the effect that the techniques successively used on a given sample may have on its structure and organization.

2 *IN VITRO* APPROACHES FOR THE STUDY OF β-GLUCAN SYNTHESIS

2.1 Optimization of the conditions for callose and cellulose synthesis

Protocols used for *in vitro* approaches have been described using several plant models such as, for instance, the cotton fiber (Okuda et al. 1993; Kudlicka et al. 1995; Kudlicka et al. 1996), *Lolium multiflorum* (Bulone et al. 1995), *A. thaliana* (Lai Kee Him et al. 2001), blackberry (Lai Kee Him et al. 2002) and recently the hybrid aspen (Colombani et al. 2004). The optimization of the conditions for *in vitro* synthesis of callose and cellulose has been discussed in more details in the report of Colombani et al. (2004), where the results obtained with the enzymes

from cell suspension cultures of the hybrid aspen are compared with those available in the literature. The assay conditions for glucan synthases have also been reviewed by Stone and Clarke (1992). Typically, these enzymes are assayed by measuring the incorporation of radioactive glucose from UDP-D-[^{14}C]glucose or UDP-D-[^{3}H]glucose into ethanol-insoluble polysaccharides. The mixture used to assay these processive glycosyltransferases usually contains 5 μM to 5 mM UDP-glucose, a membrane preparation or a detergent extract as a source of enzyme, one or several bivalent cations, and a disaccharide such as cellobiose, which activates enzymes. The pH is maintained in the range 7–8 and the temperature between 20°C and 30°C. The membrane fractions are prepared by differential centrifugation after the cells have been homogenized, usually using a mortar and pestle when the enzymes are to be isolated from plant tissues (see for instance Okuda et al. 1993 and Kudlicka and Brown, Jr. 1997), or a French press (Bulone et al. 1995; Lai Kee Him et al. 2001; Lai Kee Him et al. 2002) or a cell disrupting bomb (Colombani et al. 2004) when the starting biological material is a suspension of cells grown *in vitro*. Detergent extractions can then be performed to isolate the membrane-bound enzymes in an active form.

For the study of callose synthesis, the detergents that are commonly used are CHAPS (Sloan et al. 1987; Dhugga and Ray 1991; Wu et al. 1991; Bulone et al. 1995; Lai Kee Him et al. 2001; Li et al. 2003; Colombani et al. 2004), digitonin (Okuda et al. 1993; Kudlicka and Brown, Jr. 1997) and octylglucoside (Lai Kee Him et al. 2001). These detergents generally allow the preparation of relatively stable enzyme fractions that have a high callose synthase activity. It has been shown that detergents that belong to other families, like for instance the sulfobetain zwittergent 3–12, decanoyl-*N*-methylglucamide and glycodeoxycholate can also be efficient (Lai Kee Him et al. 2001). It seems however that these last detergents cannot be used to extract the enzyme from all plant species. For instance, we have observed that glycodeoxycholate allows the solubilization of the callose synthase from *A. thaliana*, but that it does not yield active preparations when microsomal fractions from blackberry are used as a source of enzyme (unpublished observations). Conversely, detergents that are efficient to extract the enzyme from blackberry in an active form, e.g., Brij 58, were not able to preserve the activity from *A. thaliana* cells. Also, one must be aware that some detergents may activate enzymes upon extraction and that the levels of activity recovered can be the result of both an efficient extraction and a stimulation of activity. This has been observed for instance with the detergent octylglucoside (Lai Kee Him et al. 2001). Other detergents like CHAPS, zwittergent 3–16 and lysophosphatidylcholine have been reported to activate glucan synthases from pollen tubes of *N. alata*, but in this case the activation was shown on particulate enzyme preparations and not after solubilization of the callose synthase from microsomal fractions (Li et al. 1997). These observations indicate that the level of activity recovered in detergent extracts can be dramatically affected by the nature of the detergent used for enzyme extraction. Several reports also show that the morphology and size of (1→3)-β-D-glucans synthesized *in vitro* by

fractions obtained with different detergents are affected by the nature of the detergent tested (Lai Kee Him et al. 2001; Lai Kee Him et al. 2003; Colombani et al. 2004). It was suggested that the detergents may have an effect on the general organization of the glucan synthase complexes, on the levels of activity and, indirectly, on the morphology and size of the *in vitro* products (Lai Kee Him et al. 2001). However, the mode of action of the detergents used and its consequence on enzyme activity remain to be determined at the molecular level.

The general assay mixture described above can be modified to test the effect of various components on the level of activity. When starting a study on a new plant species, it is important to test various conditions of assay for optimization. β-Glucosides, disaccharides such as cellobiose, laminaribiose or gentiobiose, and cellodextrins have been described as activators of plant callose synthases (Morrow and Lucas 1986; Hayashi et al. 1987; Li and Brown, Jr. 1993; Ng et al. 1996). In some instances, like for the enzymes from *A. thaliana* (Lai Kee Him et al. 2001) and the hybrid aspen (Colombani et al. 2004), the activation is rather low and does not exceed 10–15%. It has been proposed that β-glucosides and disaccharides act as allosteric activators of the enzymes (Morrow and Lucas 1986; Hayashi et al. 1987), although this has not been experimentally demonstrated. It has also been suggested that cellobiose may mimic an endogenous primer that would initiate polymerization of glucosyl units (MacLachlan 1982). However, the use of radioactive cellobiose showed that the activator is not incorporated in the final product during *in vitro* synthesis experiments (Hayashi et al. 1987). The mode of action of cellobiose on callose synthase activity remains to be determined, and the requirement of a primer for (1→3)-β-D-glucan synthase is still not demonstrated. Despite the fact that the effect of cellobiose is not understood at the molecular level, it is almost systematically added in *in vitro* assay mixtures.

Calcium and magnesium seem to play an important role in the regulation of callose and cellulose synthases. When doing *in vitro* experiments, it is important to test the effect of these cations on callose and cellulose synthase activities since it is possible to favor the synthesis of either polysaccharides, depending on the respective concentrations of calcium and magnesium in the medium. Calcium is required for (1→3)-β-D-glucan synthase activity from most plant species (Kauss et al. 1983; Delmer et al. 1984; Morrow and Lucas 1986; Hayashi et al. 1987; MacCormack et al. 1997; Lai Kee Him et al. 2001; Colombani et al. 2004), except for the developmentally expressed callose synthase from *N. alata* pollen tubes (Schlüpmann et al. 1993). Interestingly, in the case of enzyme preparations from cotton fiber, the addition of magnesium in the assay mixture combined with a decrease in calcium concentration favored the *in vitro* synthesis of cellulose (Okuda et al. 1993). Similar results were obtained recently using cell suspension cultures of hybrid aspen as a source of enzyme (Colombani et al. 2004). However, these results contrast with those obtained with the enzyme from blackberry (Lai Kee Him et al. 2002). In this case, the highest yields of *in vitro* cellulose were observed in the absence of cations when taurocholate was used

to extract the membrane-bound proteins, whereas the addition of magnesium (8 mM) was necessary to obtain detectable amounts of cellulose with Brij 58 extracts (Lai Kee Him et al. 2002). It seems that the presence of cations is not always a requirement for *in vitro* synthesis of cellulose by the blackberry enzyme (Lai Kee Him et al. 2002), as opposed to the situation in the cotton fiber (Okuda et al. 1993; Kudlicka et al. 1995; Kudlicka et al. 1996; Peng et al. 2002). It is possible that, in the case of blackberry, several isoforms of cellulose synthase with different cation requirements were extracted by the two detergents taurocholate and Brij 58. These results also indicate that the choice of the detergent to extract cellulose synthases in an active form is critical. Indeed, digitonin seems to be the best detergent for *in vitro* synthesis of cellulose with the enzymes from cotton fiber (Okuda et al. 1993; Kudlicka et al. 1995; Kudlicka et al. 1996) and the hybrid aspen (Colombani et al. 2004), while it is only with Brij 58 and taurocholate extracts that cellulose synthesis was possible in the case of the blackberry enzyme (Lai Kee Him et al. 2002). Furthermore, no cellulose was synthesized when taurocholate and Brij 58 extracts from *A. thaliana* were used in the conditions described for the blackberry enzyme (Lai Kee Him et al. 2002). It is likely that the cellulose synthases from various plant species have a different lipid environment and, consequently, that the extraction of active enzyme complexes from a given species depends on the structure of the detergent used. This would explain why the choice of the detergent is very critical for a successful *in vitro* synthesis of cellulose.

It seems that it is only when the rosettes are kept intact that the synthesis of cellulose I is possible *in vivo* (Arioli et al. 1998). The organization of the catalytic subunits in rosette-like structures has also been proposed as a requirement for *in vitro* synthesis of cellulose (Lai Kee Him et al. 2002). This hypothesis is supported by the occurrence at the tips of *in vitro* cellulose microfibrils of globular particles that may correspond to rosette-like structures (Figure 8-1) (Kudlicka and Brown, Jr. 1997; Lai Kee Him et al. 2002). *In vivo*, it is possible that such structures are located within membrane microdomains that have a specific lipid composition. In this hypothesis, the detergents that preserve the cellulose synthases active would extract the enzymes as intact complexes, together with structural lipids required for the cohesion of the multimeric synthases. To keep following this idea, the use of relatively strong detergents that would lead to a true solubilization of the proteins composing the enzyme complexes would also provoke the disruption of the whole machinery and, consequently, a loss or a dramatic decrease in cellulose synthesis. Interestingly, the production of lipids belonging to the sterol family has recently been shown to be crucial for cellulose synthesis as well as for cell elongation and cell wall expansion (Schrick et al. 2004). It is possible that sterols are directly involved in the stabilization of the cellulose synthase machinery, both in plasma membranes and after protein extraction with the relatively mild detergents that preserve cellulose synthase activity.

In all experiments performed by Brown, Jr. and coworkers on the cotton fiber enzyme (Okuda et al. 1993; Kudlicka et al. 1995; Kudlicka et al. 1996), as well as in our *in vitro* experiments on blackberry (Lai Kee Him et al. 2002) and hybrid

aspen (Colombani et al. 2004), no primer was added in the reaction mixture to achieve *in vitro* synthesis of cellulose. It is only recently that a sitosterol-β-glucoside has been identified as a putative primer for *in vitro* synthesis of cellulose in the cotton fiber (Peng et al. 2002). It is likely that any preparation obtained from plant membranes after detergent extraction contains such a primer. However, it is also possible that the *in vitro* synthesis of cellulose does not always start *de novo*, but that the polymerization of the chains occurs from preexisting (1→4)-β-D-glucan chains. It will be interesting in future experiments to see whether the addition of sitosterol-β-glucoside in reaction mixtures can lead to the synthesis of higher amounts of cellulose during *in vitro* experiments. In the next step, it will be important to demonstrate whether sitosterol-β-glucoside or any other kind of primer is really required for initiation of cellulose polymerization *in vivo*.

Altogether, these data indicate that the conditions for *in vitro* synthesis of cellulose must be optimized for each plant species and that there is no general recipe that can be applied regardless of the source of enzyme and conditions of extraction from the plasma membrane. So far, the only factor that is common to the protocols that have led to the highest *in vitro* synthesis of cellulose is the use of Mops buffer. In particular, in studies on the blackberry (Lai Kee Him et al. 2002), cotton fiber (Kudlicka et al. 1996; Peng et al. 2002) and mung bean enzymes (Kudlicka et al. 1996), as well as in our recent work on hybrid aspen (Colombani et al. 2004), Mops has been described as the buffer of choice over the previously used Tris to improve the yields of *in vitro* cellulose. The conditions that have led to successful *in vitro* syntheses of cellulose are summarized in Table 8-1.

Table 8-1. Optimal conditions for *in vitro* synthesis of cellulose. The conditions that gave the highest cellulose synthase activity with enzyme preparations from blackberry (Lai Kee Him et al. 2002), hybrid aspen (Colombani et al. 2004), cotton fiber and mung bean (Kudlicka et al. 1995 and 1996) are compared. 50 mM Mops buffer was used at a pH of 6.8 for the blackberry cellulose synthase, as opposed to 100 mM and pH 7.0 for the enzyme from hybrid aspen. For the cotton fiber and mung bean cellulose synthases, 50 mM Mops buffer was used at pH 7.5. The concentrations of detergents used to extract the enzymes in an active form are given in parentheses. Adapted from Colombani et al. 2004.

	Blackberry		Hybrid aspen	Cotton fiber, mung bean
	Brij 58 extract	*Taurocholate extract*	*Digitonin extract*	
	(0.05%)	(0.3%)	(1%)	(0.05%)
Mops buffer	+	+	+	+
Cellobiose (20 mM)	+	+	+	+
Mg^{2+} (8 mM)	+	–	+	+
Ca^{2+} (1 mM)	–	–	+	+
UDP-glucose (1 mM)	+	+	+	+
Cyclic 3′,5′-GMP (100 μM)	–	–	–	+
NaN_3 (3 mM)	–	–	–	+
Digitonin (0.05%)	–	–	–	+

2.2 Structural characterization of *in vitro* products

2.2.1 Methods adapted to high-throughput assays

The optimization of *in vitro* conditions for the synthesis of β-glucans must be validated by careful structural characterization of the products recovered in the reaction mixtures. When multiple conditions are tested, it is important to have a rapid and accurate method that will enable the distinction between (1→3) and (1→4) linked β-glucosyl residues. The use of methods that rely on differences of solubility of the *in vitro* products should be avoided or at least combined with more specific techniques. Even though (1→3)-β-D-glucans are usually described to be soluble in NaOH solutions as opposed to cellulose, their solubility in alkali is not always complete. This is particularly true for *in vitro* (1→3)-β-D-glucans of a high degree of polymerization such as those recently characterized by Pelosi et al. (2003). We have actually noticed that some (1→3)-β-D-glucans remain partially insoluble when NaOH concentrations as high as 3 M are used (unpublished observation). Also, the addition of divalent cations like magnesium in the assay mixture has been reported to lead to the synthesis of (1→3)-β-D-glucans of a lower solubility in alkali (Hayashi et al. 1987). Therefore, the isolation of a glucan synthase product that is insoluble in aqueous NaOH solutions does not prove beyond doubt that it corresponds to cellulose, especially if divalent cations have been used during *in vitro* synthesis. Crystalline cellulose is known to be resistant to the Updegraff treatment which consists of heating the polymer for 30 min at 100°C in a mixture of concentrated acetic and nitric acids (Updegraff 1969). (1→3)-β-D-Glucans are usually hydrolyzed in the Updegraff reagent and the resistance of a β-glucan to this treatment is often used to demonstrate the presence of cellulose in a given sample. Even though this method combined with incubations in NaOH solutions is very useful for isolating cellulose from a complex mixture (Lai Kee Him et al. 2002), it does not always hydrolyze completely (1→3)-β-D-glucans. Consequently, the Updegraff reagent must always be used together with more specific methods to prove that cellulose synthesis occurred. Conversely, the Updegraff reagent is so drastic that poorly crystalline (1→4)-β-D-glucans such as those synthesized by Peng et al. (2002) are usually sensitive to the treatment. Even cellulose microfibrils isolated from primary walls are partially hydrolyzed by the acid mixture (Figure 8-2) (Lai Kee Him et al. 2002). Therefore, the sensitivity of a sample towards this reagent can only demonstrate that the initial preparation does not contain crystalline cellulose, which does not mean that no (1→4)-β-D-glucans were originally present.

To date, it appears that the most rapid and reliable methods for high-throughput assays of glucan synthases rely on the use of radioactive substrate. When UDP-[^{14}C]glucose or UDP-[^{3}H]glucose are added in the reaction mixture during synthesis, hydrolysis of the *in vitro* products in the presence of specific glycoside hydrolases is usually sufficient to demonstrate the synthesis of callose and/or cellulose. This method does not only prove that the expected products were synthesized, but it also shows that the synthesis of β-glucans occurred *de novo* and that the polymers analyzed are not contaminations from the microsomal

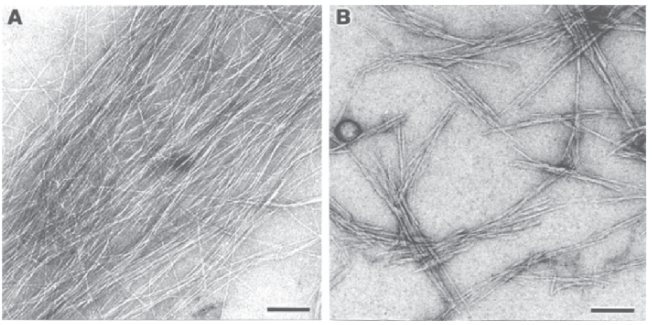

Figure 8-2. TEM images of the cellulose extracted from primary walls of blackberry cells. The samples were negatively stained with 2% uranyl acetate before observation. The cellulose microfibrils were observed before (**a**) and after (**b**) Updegraff treatment. The microfibrils treated with the Updegraff reagent were cut into fragments of 200–300 nm, indicating a low crystallinity. Bars = 100 nm. Reproduced from Lai Kee Him et al. 2002 with permission.

fraction or the cell wall. It can be completed by the analysis of oligosaccharides released upon enzymatic hydrolysis, for instance by thin layer chromatography (Okuda et al. 1993; Bulone et al. 1995). The use of glycoside hydrolases is reasonably rapid and reliable for high-throughput assays of glucan synthases. However, one should be aware that some commercial preparations of (1→3)-β-D-glucanases are contaminated with cellulases, and vice versa. Therefore, before applying this method to the identification of *in vitro* products, it is recommended to test the specificity of the hydrolase preparations on well-characterized polysaccharides.

An interesting alternative to the radioactive UDP-glucose substrates to assay callose synthases is the use of the fluorochrome from aniline blue which specifically interacts with linear (1→3)-β-D-glucans (Evans et al. 1984). A microtiter-based fluorescence assay was developed on the principle of this interaction (Shedletzky et al. 1997). Briefly, the method consists of stopping the glucan synthase reaction by adding a highly concentrated NaOH solution to the reaction mixture. The *in vitro* (1→3)-β-D-glucans are then solubilized at 80°C in the alkaline solution and incubated in the presence of the aniline blue fluorochrome. The fluorescence measured can be linked to the amount of glucose incorporated into (1→3)-β-D-glucan chains, after calibration of the assay with standard curves obtained with radioactive substrate. The major problem with this method is that it relies on the solubility of (1→3)-β-D-glucans in NaOH. Actually, the levels of callose synthase activity are underestimated when the solubility of the *in vitro* products decreases (Shedletzky et al. 1997). This is particularly true when the *in vitro* synthesis is performed in the presence of magnesium (Hayashi et al. 1987; Shedletzky et al. 1997). Therefore, the application of the method is limited to the study of *in vitro* synthesis reactions that yield (1→3)-β-D-glucans that are perfectly soluble in NaOH at 80°C. As discussed above, this is not always the case, and the solubility of the newly synthesized products depends on their degrees of polymerization and crystallinity, which

seem to vary with the conditions of assay, enzyme source and detergent used for extraction (Lai Kee Him et al. 2001; Pelosi et al. 2003). Also, even though the fluorochrome is specific for (1→3)-β-D-glucans (Evans et al. 1984), the assay does not allow the quantification of the cellulose that may be present in the sample. For these reasons, the use of radioactive UDP-glucose combined with hydrolysis experiments of *in vitro* products with specific enzymes, is by far the most commonly used method for a rapid and reliable identification of *in vitro* β-glucans.

2.2.2 Detailed structural characterization of in vitro products

The physical and chemical techniques listed in Table 8-2 provide detailed structural information that can help understand some aspects related to the polymerization and crystallization of polysaccharides. They are complementary and it is actually not possible to have a complete structural characterization of a given polymer by using only one of these techniques. Other methods based on transmission electron microscopy examinations and involving cellulases coupled

Table 8-2. Methods for the characterization of *in vitro* products synthesized by (1→3)-β-D-glucan synthases. The information that can be obtained with each method and the expected results for linear *in vitro* (1→3)-β-D-glucans such as callose are presented (after Bulone et al. 1995; Lai Kee Him et al., 2001; Pelosi et al. 2003). The average amount of product required for the different techniques as well as the possibility to recover the sample after each type of analysis are also indicated. Adapted from Colombani et al. 2004.

Method and information obtained	Expected results for *in vitro* (1→3)-β-D-glucans	Amount of product required/ possibility of sample recovery
Solubility (distinction between (1→3)-β-D-glucan and cellulose; however, this method is not completely reliable)	Insoluble in water Usually soluble in DMSO Usually soluble in 1 M NaOH	~1 mg When soluble, the sample can be recovered by dialysis against distilled water
Infrared spectroscopy (identification of linkage type/structure)	Absorption band at 889.5 cm^{-1}	~1 mg Sample recovery possible
Methylation (gas chromatography coupled to mass spectrometry) (identification of linkage type and estimation of the degree of polymerization if <100)	~100% (1→3)-linked glucose (if the degree of polymerization is higher than 100)	>100 µg Sample is hydrolyzed and cannot be recovered
^{13}C-NMR spectroscopy in DMSO (or NaOH) solution (structure)	Resonance signals at 60.9, 68.5, 72.9, 76.4, 86.2 and 103.1 ppm assigned to carbons-6, -4, -2, -5, -3 and -1 of (1→3)-β-glucan	~10 mg Sample can be recovered after dialysis against distilled water, with a loss of the native conformation

(*Continued*)

Table 8–2. (*Continued*)

Method and information obtained	Expected results for in vitro (1→3)-β-D-glucans	Amount of product required/ possibility of sample recovery
Solid state ^{13}C-NMR spectroscopy (cross-polarization/magic angle spinning NMR spectroscopy) (structure, organization of the chains, indication of degree of crystallinity)	Resonance signals at 61.1, 68.1, 74.2, 77.4, 86.8 and 103.6 ppm assigned to carbons -6, -4, -2, -5, -3 and -1 of (1→3)-β-glucan. The intensity of an additional signal at 76.0 ppm (attributed to C5) seems to be higher for (1→3)-β-D-glucans with a low molecular weight and a loose packing (Pelosi et al. 2003).	>10 mg Recovery of the sample in native state
X-ray diffraction (crystal structure and degree of crystallinity)	Organized as triple helices Usually low degree of crystallinity	~1 mg when using a conventional diffractometer Recovery of the sample in native state
Static light scattering in DMSO solutions (estimation of the degree of polymerization)	High degree of polymerization (depending on the conditions of synthesis) (Pelosi et al. 2003)	mg amounts (variable depending on the number of measurements at different concentrations and on the concentrations required to be under dilute regime conditions) Sample can be recovered after dialysis against distilled water, with a loss of the native conformation
Reaction with the aniline blue fluorochrome	Strong UV fluorescence induced (Evans et al. 1984)	<1 mg Fluorochrome difficult to remove completely
TEM (negative staining, cryo-TEM) (morphology)	Microfibrillar morphology	µg amounts Sample cannot be recovered

to gold particles have been used to distinguish microfibrils of callose and cellulose synthesized *in vitro* (Okuda et al. 1993; Kudlicka et al. 1995; Kudlicka et al. 1996; Kudlicka and Brown, Jr. 1997).

However, the latter methods do not provide any structural detail and it is important to couple them with physical and chemical analyses. The techniques presented in Table 8-2 have all been successfully applied to the characterization of *in vitro* (1→3)-β-D-glucans synthesized by enzymes from plants (*L. multiflorum*,

Bulone et al. 1995; *A. thaliana*, Lai Kee Him et al. 2001; *R. fruticosus*, Lai Kee Him et al. 2003 and Pelosi et al. 2003) and from the Oomycete *Saprolegnia monoica* (Pelosi et al. 2003). Some of them require relatively large amounts of *in vitro* product. It is therefore necessary to scale up the synthetic reactions to be able to use these methods to perform a detailed structural characterization. Also, some techniques like methylation analysis destroy the sample, while others like liquid NMR spectroscopy lead to a loss of the native conformation of the polysaccharide chains (Table 8-2). However, in this last case, the sample that is dissolved in dimethylsulfoxide or NaOH for the purpose of the analysis can be recovered by precipitation after extensive dialysis against distilled water. An example of a typical ^{13}C-NMR spectrum corresponding to a linear (1→3)-β-D-glucan synthesized *in vitro* by a plant enzyme is shown in Figure 8-3.

The method becomes much more sensitive when the substrate used during *in vitro* synthesis contains a sugar moiety that is enriched in ^{13}C. Recently, we have shown, with the example of a callose synthase from blackberry, that only 100 µg of (1→3)-β-D-glucan synthesized *in vitro* is sufficient for ^{13}C-NMR analysis when the synthesis reaction is performed using UDP-[U-^{13}C]glucose, i.e. a UDP-glucose molecule in which the glucosyl residue is uniformly enriched in ^{13}C (Fairweather et al. 2004). In our experiments, the UDP-[U-^{13}C]glucose was synthesized using

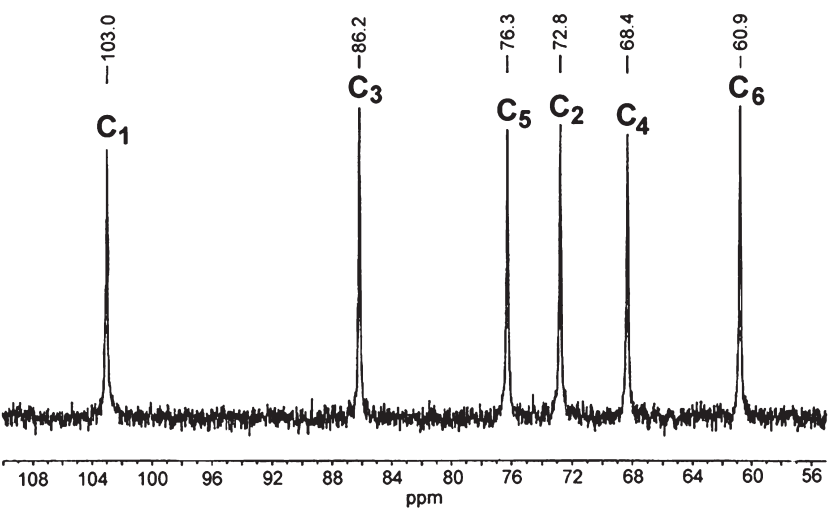

Figure 8-3. ^{13}C-NMR spectrum of the (1→3)-β-D-glucan synthesized *in vitro* by the callose synthase from blackberry. The chemical shifts at 60.9, 68.4, 72.8, 76.3, 86.2, and 103.0 ppm were measured at 75 MHz in $(CD_3)_2SO$ at 295 K, by reference to the central peak of the $(CD_3)_2SO$ multiplet (39.5 ppm). The spectrum is characteristic of a strictly linear (1→3)-β-D-glucan (Saito et al. 1977; Bulone et al. 1995; Lai Kee Him et al. 2001). Reproduced from Lai Kee Him et al. 2002 with permission.

a chemical approach, but the synthesis can also be achieved using commercially available enzymes (Ma and Stöckigt 2001). The method based on the use of ^{13}C-enriched sugar donors is so sensitive that even solid-state NMR spectroscopy can be applied to the structural characterization of *in vitro* products (Fairweather et al. 2004). It has several advantages over other analytical methods:

1. It is very sensitive and requires low amounts of *in vitro* products (~100 times less polysaccharide is required compared with the same analysis performed on a non-enriched polymer).
2. It provides a direct structural characterization of the *in vitro* product, as opposed to biochemical techniques that rely on the use of radioactive substrate and a subsequent hydrolysis of the polysaccharides with specific hydrolases. In the case of β-glucans, liquid ^{13}C-NMR analysis allows distinction between (1→3) and (1→4) linkages for products that are soluble in DMSO. For high molecular weight polymers that are insoluble in solvents commonly used for liquid ^{13}C-NMR analysis, such as cellulose, solid-state NMR spectroscopy can be used for structural characterization. In addition, solid-state NMR spectroscopy provides information on the conformation of the glucan chains in a given preparation as well as structural details that cannot be obtained with liquid NMR spectroscopy and methylation analysis. For instance, in the case of cellulose, solid-state NMR spectroscopy allows the determination of the proportions of the I_α and I_β allomorphs in the sample (Atalla and VanderHart 1984).
3. The method proves directly that the product analyzed was newly synthesized since the molecule is enriched in ^{13}C.
4. It can be applied to the study of any glycosyltransferase after synthesis of the corresponding ^{13}C-enriched sugar donor.

An alternative to NMR spectroscopy is methylation analysis. Even though this method involves an acid hydrolysis of the sample, it remains the most sensitive chemical technique for determination of linkage type when ^{13}C-enriched substrates are not available for NMR analysis of *in vitro* products. Compared with NMR spectroscopy performed on polysaccharides that are not enriched in ^{13}C, only hundreds of μg of sample (i.e. 20–30 times less sample) are required for methylation analysis. Moreover, when methylation analysis is applied to radioactively labeled polymers, it also proves that the polysaccharides analyzed were newly synthesized. The method involves several chemical modifications of the polysaccharide to be analyzed, i.e. methylation in the presence of methyl iodide, acid hydrolysis, reduction and acetylation (see for example Harris et al. 1984). Separation by gas chromatography of the resulting alditol acetates is usually sufficient to distinguish between (1→3) and (1→4) linkages, on the basis of the retention times of the derivatives on the column and by comparison with well-characterized standards. However, it is preferable to couple gas chromatography to mass spectrometry (GC/MS) to firmly identify the derivatives characteristic of (1→3) and (1→4) linkages (Figure 8-4). In some instances, the method can also allow an estimation of the degree of polymerization of a polysaccharide, especially if the starting individual chains consist of less than 100 sugar residues (100 is the lowest detection limit of

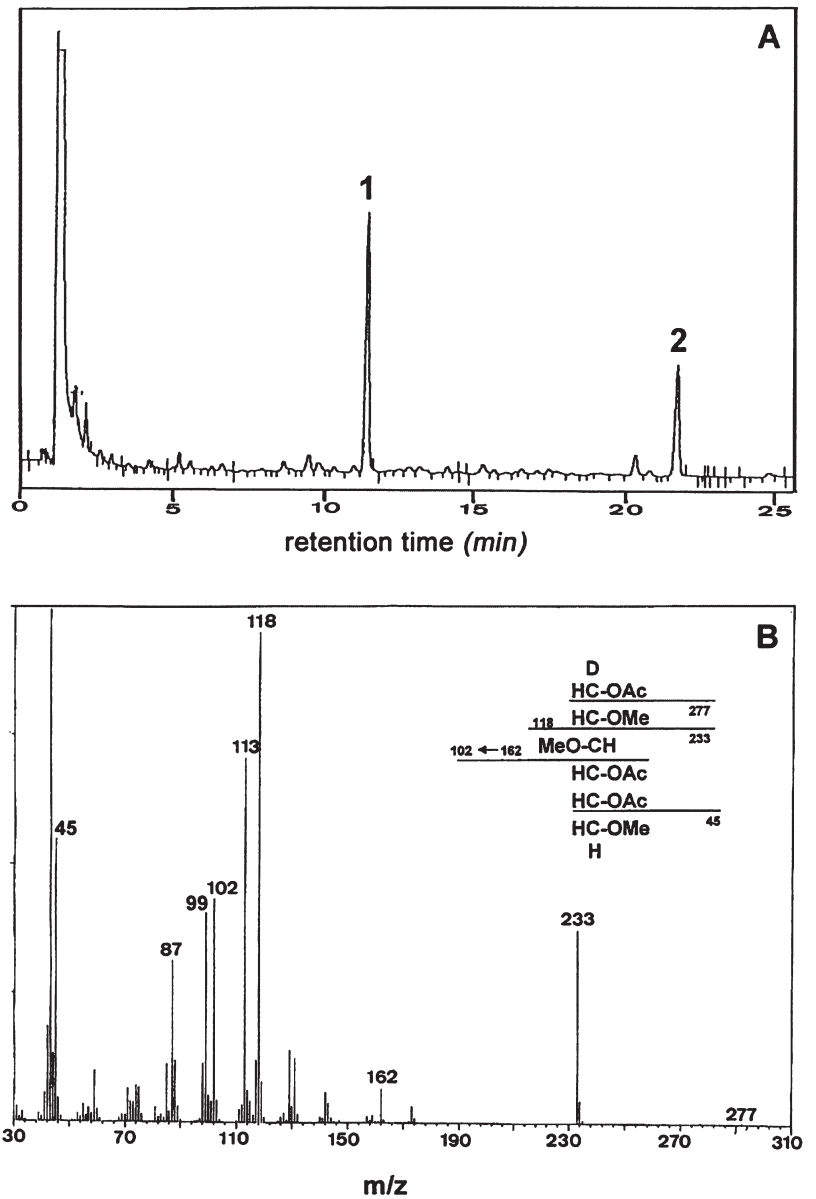

Figure 8-4. Methylation analysis of *in vitro* β-D-glucans. (**a**) Gas chromatography of the permethylated alditol acetate obtained from methylation analysis of the cellulose synthesized *in vitro* by the enzyme from blackberry. Peak 1, derivative characteristic of (1→4) linked glucosyl units. Peak 2, internal standard (*myo*-inositol). The derivative characteristic of (1→3) linked glucosyl units usually elutes 1 min before the major derivative visible in the chromatogram (not shown; see Bulone et al. 1995). (**b**) Structural characterization by electron impact mass spectrometry of the 1,4,5-tri-*O*-acetyl-2,3,6-tri-*O*-methyl-D-glucitol derivative corresponding to peak 1 in A and characteristic of (1→4) linked glucosyl units.

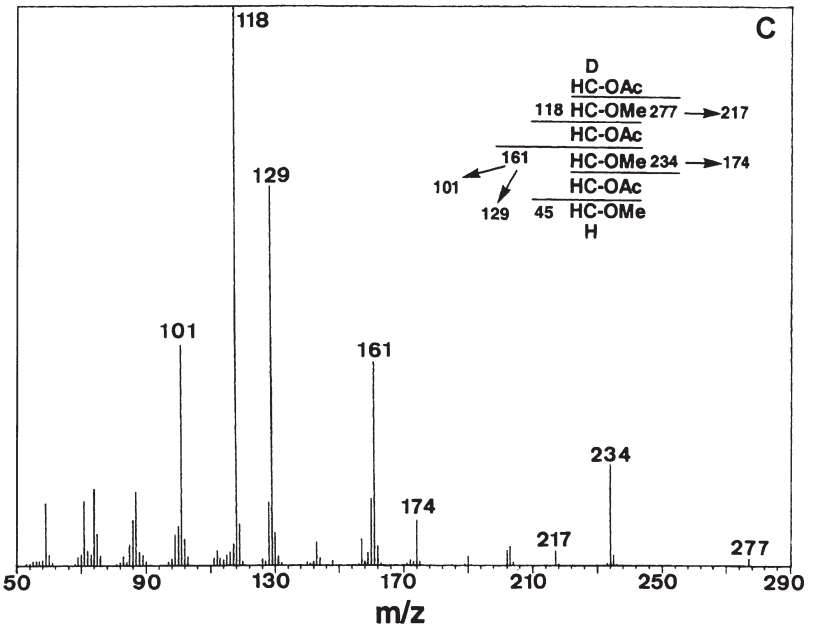

Figure 8-4. (*Continued*) (**c**) As in (**b**) but for 1,3,5-tri-*O*-acetyl-2,4,6-tri-*O*-methyl-D-glucitol which is characteristic of (1→3) linked glucosyl units. (**a**) and (**b**) are from Lai Kee Him et al. 2002, whereas (**c**) is from Lai Kee Him et al. 2001 (reproduced with permission).

the method). The disadvantage of the methylation technique is that it does not indicate if different linkages are originally present in the same or different molecules. Also, unlike NMR spectroscopy, it does not allow the distinction between α and β linkages. In order to avoid the repetition of time-consuming large-scale *in vitro* synthesis experiments, it is preferable to perform the different analyses presented in Table 8-2 on the same sample. Thus, it is recommended, when using successively these techniques on a given preparation, to start the structural characterization with the non-destructive methods such as x-ray diffraction and solid state NMR.

The importance to achieve detailed structural characterization of *in vitro* products is illustrated by the application of the methods listed in Table 8-2 to the analysis of *in vitro* (1→3)-β-D-glucans synthesized under various conditions. For instance, it has been shown that for a given plant species the morphology and the stucture of the *in vitro* products are affected by the nature of the detergent used to extract the membrane-bound synthases (Lai Kee Him et al. 2001). Also, for a given detergent, enzymes from different plant species do not necessarily synthesize products that have the same morphology and structure (Lai Kee Him et al. 2001; Colombani et al. 2004). From these observations, it seems important

to study the lipid environment of the callose synthases from various origins. This should help understand why and how detergents affect the morphology and the structure of the *in vitro* (1→3)-β-D-glucans. In a previous study on *A. thaliana*, it was suggested that detergents may have an effect on the general organization and structure of the enzyme complex during extraction from the plasma membrane and, indirectly, on the morphology and structure of the *in vitro* (1→3)-β-D-glucans (Lai Kee Him et al. 2001). However, this hypothesis remains to be demonstrated. Interestingly, in another example where enzymes from *S. monoica* were used for the synthesis of (1→3)-β-D-glucans, it was shown that other parameters like the pH of the *in vitro* reaction mixture can influence the morphology, the degree of polymerization, the crystallinity and the structure of *in vitro* products (Pelosi et al. 2003). Even though many questions related to the mechanisms of polymerization and crystallization of polysaccharides are still unsolved, it seems that it will be possible in the near future to synthesize polysaccharides with specific properties by controlling *in vitro* reactions that involve glucan synthases from various organisms.

Some of the techniques presented in Table 8-2 have also been used to characterize the cellulose synthesized *in vitro* by cell-free extracts from blackberry (Lai Kee Him et al. 2002) and cotton fiber (Okuda et al. 1993; Kudlicka et al. 1995; Kudlicka et al. 1996). In these cases, it was possible to demonstrate that the purified *in vitro* products consisted exclusively of (1→4) β-linked glucosyl moieties, that they had a high molecular weight and that they corresponded to crystalline microfibrils that diffracted as cellulose. It is however only for the cellulose synthase studies on blackberry that multiple analyses could be performed on the same sample (Lai Kee Him et al. 2002). This was possible because one milligram of pure cellulose could be synthesized *in vitro* for the first time. Nonetheless, this amount was not sufficient to allow an accurate determination of the degree of polymerization of the β-glucan chains and to estimate, for instance by solid-state NMR spectroscopy (Atalla and VanderHart 1984), the proportions of the I_α and I_β allomorphs. It remains therefore to further improve the yields of *in vitro* cellulose to be able to obtain a more detailed structural analysis than the one described by Lai Kee Him et al. (2002). Such an achievement would also facilitate the assay of cellulose synthases and their direct characterization using biochemical approaches. A promising model for this type of biochemical studies is the suspension cultures of hybrid aspen (Ohlsson et al. 2006) from which it was possible to isolate cellulose synthase preparations that could synthesize *in vitro* up to 50% of cellulose (Colombani et al. 2004).

2.3 Purification of callose and cellulose synthases

When a reliable assay method is available for glucan synthases, and once it has been demonstrated that the *in vitro* products were synthesized *de novo* and that they correspond to the expected polysaccharides, biochemical approaches can be used to obtain enriched enzyme preparations. The reports

available in the literature on the purification of plant glucan synthases are so far almost exclusively related to callose synthases. It is only in the case of mung bean that a preliminary separation of callose and cellulose synthases has been achieved using native polyacrylamide gel electrophoresis (Kudlicka and Brown, Jr. 1997). However, none of the 12 proteins that appeared to be specifically associated with cellulose synthase activity have been characterized so far. The lack of biochemical information on plant cellulose synthases is mainly due to the difficulty of assaying these enzymes routinely. Proteins of molecular weights of 30–35 and 50–67 kDa have been described to be potentially involved in callose synthase activity. The main techniques used for these investigations were product entrapment and/or gradient centrifugation, immunochemical techniques or photoaffinity labeling with substrate analogues. For instance, proteins of 26–37 kDa were enriched in callose synthase preparations from *Beta vulgaris* (Wu et al. 1991; Wu and Wasserman 1993), *Brassica oleracea* (Fredrikson et al. 1991), *Gossypium hirsutum* (Delmer et al. 1991), *Oryza sativa* (Kuribayashi et al. 1992), *Lolium multiflorum* (Bulone et al. 1995) and hybrid aspen (Colombani et al. 2004). Monoclonal antibodies that immunoprecipitate the callose synthase from *Glycine max* were also able to recognize by Western blot a 31-kDa protein (Fink et al. 1990). Other proteins in the range of 30 kDa or 50–67 kDa have also been identified by photoaffinity labeling (Wu et al. 1991; Delmer et al. 1991; Dhugga and Ray 1991; Li and Brown, Jr. 1993; Dhugga and Ray 1994). Despite the numerous results available, there is no report that describes the sequencing of these proteins. In addition, the molecular weights of the proteins identified using the biochemical approaches described above markedly differ from the molecular weights of the proteins that were identified in *Daucus carota* (Lawson et al. 1989) and *N. alata* (Turner et al. 1998). For instance, in the latter case, a 190-kDa protein was found to copurify with enzyme activity. Also, the plant GSL proteins, which have been proposed to correspond to catalytic subunits of callose synthases, have a molecular weight in the range 220–250 kDa (Cui et al. 2001; Doblin et al. 2001; Hong et al. 2001; Li et al. 2003). It is likely that several proteins of a lower molecular weight, such as those cited above, are part of a multimeric complex and required for callose synthesis. It remains however that despite the substantial progress made with the identification of the *GSL* genes, the precise protein composition of plant callose synthase complexes and the function of each of the different subunits potentially involved in (1→3)-β-D-glucan synthesis are not known.

The development of highly sensitive proteomic methods for the characterization of membrane-bound proteins should facilitate the systematic sequencing of all the proteins that are present in fractions with high callose synthase activity. Also, the progress made on *in vitro* synthesis of cellulose is promising and proteomic analysis may also be used on fractions enriched in cellulose synthases in the near future. This approach combined with detailed structural characterization of *in vitro* products, immunochemical methods, molecular biology and gene

expression analyses should provide important information on the composition of the glucan synthase complexes, and consequently on the mechanisms of biosynthesis of callose and cellulose.

REFERENCES

Arioli T., Peng L., Betzner A.S., Burn J., Wittke W., Herth W., Camilleri C., Höfte H., Plazinski J., Birch R., Cork A., Glover J., Redmond J., and Williamson R.E. 1998. Molecular analysis of cellulose biosynthesis in *Arabidopsis*. Science 279:717–720.

Atalla R.H. and VanderHart D.L. 1984. Native cellulose: a composite of two distinct crystalline forms. Science 223:283–285.

Brown, Jr. R.M., 1996. The biosynthesis of cellulose. J Macromol Sci Pure Appl Chem 10:1345–1373.

Bulone V., Fincher G.B., and Stone B.A. 1995. *In vitro* synthesis of a microfibrillar (1→3)-β-glucan by a ryegrass (*Lolium multiflorum*) endosperm (1→3)-β-glucan synthase enriched by product entrapment. Plant J 8:213–225.

Burton R.A., Shirley N.J., King B.J., Harvey A.J., and Fincher G.B. 2004. The *CesA* gene family of barley. Quantitative analysis of transcripts reveals two groups of co-expressed genes. Plant Physiol 134:224–236.

Cabib E., Roh D.H., Schmidt M., Crotti L.B., and Varma A. 2001. The yeast cell wall and septum as paradigms of cell growth and morphogenesis. J Biol Chem 276:19679–19682.

Campbell J.A., Davies G.J., Bulone V., and Henrissat B. 1997. A classification of nucleotide-diphospho-sugar glycosyltransferases based on amino acid sequence similarities. Biochem J 326:929–939.

Colombani A., Djerbi S., Bessueille L., Blomqvist K., Ohlsson A., Berglund T., Teeri T.T., and Bulone V. 2004. *In vitro* synthesis of (1→3)-β-D-glucan (callose) and cellulose by detergent extracts of membranes from cell suspension cultures of hybrid aspen. Cellulose 11:313–327.

Coutinho P.M. and Henrissat B. 1999. Carbohydrate-active enzymes server. Available at: http://afmb.cnrs-mrs.fr/CAZY/index.html

Cui X., Shin H., Song C., Laosinchai W., Amano Y., and Brown, Jr. R.M., 2001. A putative plant homolog of the yeast (1→3)-β-glucan synthase subunit FKS1 from cotton (*Gossypium hirsutum* L.) fibers. Planta 213:223–230.

Delmer D.P. 1987. Cellulose biosynthesis. Ann Rev Plant Physiol 38:259–290.

Delmer D.P. 1999. Cellulose biosynthesis: exciting times for a difficult field of study. Annu Rev Plant Physiol Plant Mol Biol 50:245–276.

Delmer D.P. and Amor Y. 1995. Cellulose biosynthesis. Plant Cell 7:987–1000.

Delmer D.P., Solomon M., and Read S.M. 1991. Direct photolabeling with [^{32}P]UDP-glucose for identification of a subunit of cotton fiber callose synthase. Plant Physiol 95:556–563.

Delmer D.P., Thelen M., and Marsden M.P.F. 1984. Regulatory mechanisms for the synthesis of β-glucans in plants. In: Dugger W.M. and Bartnicki-Garcia S. (eds.) Structure, Function, and Biosynthesis of Plant Cell Walls. American Society of Plant Physiologists, Rockville, MD, pp. 133–149.

Dhugga K.S. and Ray P.M. 1991. A 55-kDa plasma membrane-associated polypeptide is involved in (1→3)-β-glucan synthase activity in pea tissue. FEBS Lett 278:283–286.

Dhugga K.S. and Ray P.M. 1994. Purification of (1→3)-β-glucan synthase activity from pea tissue. Two polypeptides of 55 kDa and 70 kDa copurify with enzyme activity. Eur J Biochem 220:943–953.

Dijkgraaf G.J., Abe M., Ohya Y., and Bussey M. 2002. Mutations in Fks1p affect the cell wall content of (1→3)-β- and (1→6)-β-glucan in *Saccharomyces cerevisiae*. Yeast 19:671–690.

Djerbi S., Aspeborg H., Nilsson P., Mellerowicz E., Sundberg B., Blomqvist K., and Teeri T.T. 2004. Identification and expression analysis of genes encoding putative cellulose synthases (*CesA*) in the hybrid aspen, *Populus tremula* (L.) × *P. tremuloides* (Michx.). Cellulose 11:301–312.

Doblin M.S., De Melis L., Newbigin E., Bacic A., and Read S.M. 2001. Pollen tubes of *Nicotiana alata* express two genes from different β-glucan synthase families. Plant Physiol 125:2040–2052.

Doblin M.S., Kurek I., Jacob-Wilk D., and Delmer D.P. 2002. Cellulose biosynthesis in plants: from genes to rosettes. Plant Cell Physiol 43:1407–1420.

Douglas C.M., Foor F., Marrinan J.A., Morin N., Nielsen J.B., Dahl A.M., Mazur P., Baginsky W., Li W., El-Sherbeini M., Clemas J.A., Mandala S.M., Frommer B.R., and Kurtz M.B. 1994. The *Saccharomyces cerevisiae FKS1* (*ETG1*) gene encodes an integral membrane protein which is a subunit of (1→3)-β-glucan synthase. Proc Natl Acad Sci USA 91:12907–12911.

Eng W.-K., Faucette L., McLaughlin M.M., Cafferkey R., Koltin Y., Morris R.A., Young P.R., Johnson R.K., and Livi G.P. 1994. The yeast *FKS1* gene encodes a novel membrane protein, mutations in which confer FK506 and cyclosporin A hypersensitivity and calcineurin-dependent growth. Gene 151:61–71.

Evans N.A., Hoyne P.A., and Stone B.A. 1984. Characteristics and specificity of the interaction of a fluorochrome from aniline blue (Sirofluor) with polysaccharides. Carbohydr Polym 4:215–230.

Fagard M., Desnos T., Desprez T., Goubet F., Refregier G., Mouille G., McCann M., Rayon C., Vernhettes S., and Höfte H. 2000. *PROCUSTE1* encodes a cellulose synthase required for normal cell elongation specifically in roots and dark-grown hypocotyls of *Arabidopsis*. Plant Cell 12:2409–2423.

Fairweather J.K., Lai Kee Him J., Heux L., Driguez H., and Bulone V. 2004 Structural characterization by ^{13}C-NMR spectroscopy of products synthesized *in vitro* by polysaccharide synthases using ^{13}C-enriched glycosyl donors: application to a UDP-glucose:(1→3)-β-D-glucan synthase from blackberry (*Rubus fruticosus*). Glycobiology 14:775–781.

Fink J., Jeblick W. and Kauss H. 1990. Partial purification and immunological characterization of (1→3)-β-glucan synthase from suspension cells of *Glycine max*. Planta 181:343–348.

Fredrikson K., Kjellbom P., and Larsson C. 1991. Isolation and polypeptide composition of (1→3)-β-glucan synthase from plasma membranes of *Brassica oleracea*. Physiol Plant 81:289–294.

Garrett-Engele P., Moilanen B., and Cyert M.S. 1995. Calcineurin, the Ca^{2+}/calmodulin-dependent protein phosphatase is essential in yeast mutants with cell integrity defects and in mutants that lack a functional vacuolar H^+-ATPase. Mol Cell Biol 15:4103–4114.

Harris P.J., Henry R.J., Blakeney A.E., and Stone B.A. 1984. An improved procedure for the methylation analysis of oligosaccharides and polysaccharides. Carbohydr Res 127:59–73.

Hayashi T., Read S.M., Bussell J., Thelen M., Lin F.C., Brown, Jr. R.M., and Delmer D.P. 1987. UDP-glucose: (1→3)-β-glucan synthases from mung bean and cotton. Differential effects of calcium and magnesium on enzyme properties and on macromolecular structure of the glucan product. Plant Physiol 83:1054–1062.

Holland N., Holland D., Helentjaris T., Dhugga K.S., Xoconostle-Cazares B., and Delmer D.P. 2000. A comparative analysis of the plant cellulose synthase (*CesA*) gene family. Plant Physiol 123:1313–1323.

Hong Z., Delauney A.J., and Verma D.P.S. 2001. A cell plate-specific callose synthase and its interaction with phragmoplastin. Plant Cell 13:755–768.

Kauss H., Koehle H., and Jeblick W. 1983. Proteolytic activation and stimulation by calcium of glucan synthase from soybean cells. FEBS Lett 158:84–88.

Kimura S., Laosinchai W., Itoh T., Cui X., Linder C.R., and Brown, Jr. R.M., 1999. Immunogold labeling of rosette terminal cellulose-synthesizing complexes in the vascular plant *Vigna angularis*. Plant Cell 11:2075–2086.

Kudlicka K. and Brown, Jr. R.M., 1997. Cellulose and callose biosynthesis in higher plants I. Solubilization and separation of (1→3)- and (1→4)-β-glucan synthase activities from mung bean. Plant Physiol 115:643–656.

Kudlicka K., Brown, Jr. R.M., Li L., Lee J.H., Shin H., and Kuga S. 1995. β-Glucan synthesis in the cotton fiber. IV. *In vitro* assembly of the cellulose I allomorph. Plant Physiol 107:111–123.

Kudlicka K., Lee J.H., and Brown, Jr. R.M., 1996. A comparative analysis of *in vitro* cellulose synthesis from cell-free extracts of mung bean (*Vigna radiata*, Fabaceae) and cotton (*Gossypium hirsutum*, Malvaceae). Am J Bot 83:274–284.

Kuribayashi I., Kimura S., Morita T. and Igaue I. 1992. Characterization and solubilization of β-glucan synthases from cultured rice cells. Biosci Biotechnol Biochem 56:388–393.

Lai Kee Him J., Chanzy H., Müller M., Putaux J.L., Imai T., and Bulone V. 2002. *In vitro versus in vivo* cellulose microfibrils from plant primary wall synthases: structural differences. J Biol Chem 277:36931–36939.

Lai Kee Him J., Chanzy H., Pelosi L., Putaux J.L., and Bulone V. 2003. Recent developments in the field of *in vitro* biosynthesis of plant β-glucans. In: Gross R.A. and Cheng H.N. (eds.) Biocatalysis in Polymer Science. ACS Symposium Series N°840, American Chemical Society, Washington DC, pp. 65–77.

Lai Kee Him J., Pelosi L., Chanzy H., Putaux J.-L., and Bulone V. 2001. Biosynthesis of (1→3)-β-glucan (callose) by detergent extracts of a microsomal fraction from *Arabidopsis thaliana*. Eur J Biochem 268:4628–4638.

Lawson S.G., Mason T.L., Sabin R.D., Sloan M.E., Drake R.R., Haley B.E., and Wasserman B.P. 1989. UDP-glucose: (1→3)-β-glucan synthase from *Daucus carota* L. Characterization, photoaffinity labeling, and solubilization. Plant Physiol 90:101–108.

Li H., Bacic A. and Read S.M. 1997. Activation of pollen tube callose synthase by detergents. Plant Physiol 114:1255–1265.

Li L. and Brown, Jr. R.M., 1993. β-Glucan synthesis in the cotton fiber. II. Regulation and kinetic properties of β-glucan synthases. Plant Physiol 101:1143–1148.

Li J., Burton R.A., Harvey A.J., Hrmova M., Wardak A.Z., Stone B.A., and Fincher G.B. 2003. Biochemical evidence linking a putative callose synthase gene with (1→3)-β-D-glucan biosynthesis in barley. Plant Mol Biol 53:213–225.

Ma X. and Stöckigt J. 2001. High yielding one-pot enzyme-catalyzed synthesis of UDP-glucose in gram scales. Carbohydr Res 333:159–163.

MacCormack B.A., Gregory A.C., Kerry M.E., Smith C., and Bolwell G.P. 1997. Purification of an elicitor-induced glucan synthase (callose synthase) from suspension cultures of French bean (*Phaseolus vulgaris* L.): purification and immunolocation of a probable M(r)-65,000 subunit of the enzyme. Planta 203:196–203.

MacLachlan G.A. 1982. Does cellulose synthesis require a primer? In: Brown, Jr. R.M., (ed.) Cellulose and Other Natural Polymer Systems. Plenum Press, New York, pp. 327–339.

Morrow D.L. and Lucas W.J. 1986. (1→3)-β-Glucan synthase from sugar beet. I. Isolation and solubilization. Plant Physiol 81:171–176.

Ng K., Johnson E., and Stone B.A. 1996. Specificity of binding of β-glucoside activators of ryegrass (1→3)-β-glucan synthase and the synthesis of some potential photoaffinity activators. Plant Physiol 111:12227–12231.

Ohlsson A.B., Djerbi S., Winzell A., Bessueille L., Staldal V., Li X., Blomqvist K., Bulone V., Teeri T.T., and Berglund T. 2006. Cell suspension cultures of *Populus tremula* × *tremuloides* exhibit a high level of cellulose synthase gene expression that coincides with increased *in vitro* cellulose synthase activity. Protoplasma 228:221–229.

Okuda K., Li L., Kudlicka K., Kuga S., and Brown, Jr. R.M., 1993. β-Glucan synthesis in the cotton fiber. I. Identification of (1→4)-β- and (1→3)-β-glucans synthesized *in vitro*. Plant Physiol 101:1131–1142.

Pear J.R., Kawagoe Y., Schreckengost W.E., Delmer D.P., and Stalker D.M. 1996. Higher plants contain homologs of the bacterial *celA* genes encoding the catalytic subunit of cellulose synthase. Proc Natl Acad Sci USA 93: 12637–12642.

Pelosi L., Imai T., Chanzy H., Heux L., Buhler E., and Bulone V. 2003. Structural and morphological diversity of (1→3)-β-D-glucans synthesized *in vitro* by enzymes from *Saprolegnia monoïca*. Comparison with a corresponding *in vitro* product from blackberry (*Rubus fruticosus*). Biochemistry 42:6264–6274.

Peng L., Kawagoe Y., Hogan P., and Delmer D. 2002. Sitosterol-β-glucoside as primer for cellulose synthesis in plants. Science 295:147–150.

Saito H., Ohki T., and Sasaki T. 1977. A ^{13}C nuclear magnetic resonance study of gel forming (1→3)-β-D-glucans. Evidence of the presence of single-helical conformation in a resilient gel of a curdlan-type polysaccharide 13140 from *Alcaligenes faecalis* var. *myxogenes* IFD 13140. Biochemistry 16:908–914.

Saxena I.M., Brown, Jr. R.M., Fèvre M., Geremia R.A., and Henrissat B. 1995. Multidomain architecture of β-glycosyl transferases: implications for mechanism of action. J Bacteriol 177:1419–1424.

Scheible W.R., Eshed R., Richmond T., Delmer D., and Somerville C. 2001. Modifications of cellulose synthase confer resistance to isoxaben and thiazolidinone herbicides in *Arabidopsis Ixr1* mutants. Proc Natl Acad Sci USA 98:10079–10084.

Schlüpmann H., Bacic A., and Read S.M. 1993. A novel callose synthase from pollen tubes of *Nicotiana*. Planta 191:470–481.

Schrick K., Fujioka S., Takatsuto S., Stierhof Y.-D., Stransky H., Yoshida S., and Jürgens G. 2004. A link between sterol biosynthesis, the cell wall, and cellulose in *Arabidopsis*. Plant J 38:227–243.

Shedletzky E., Unger C., and Delmer D.P. 1997. A microtiter-based fluorescence assay for (1,3)-β-glucan synthase assay. Anal Biochem 249:88–93.

Sloan M.E., Rodis P., and Wasserman B.P. 1987. Chaps solubilization and functional reconstitution of β-glucan synthase from red beet (*Beta vulgaris* L.) storage tissue. Plant Physiol 85:516–522.

Stasinopoulos S.J., Fisher P.R., Stone B.A., and Stanisich V.A. 1999. Detection of two loci involved in (1,3)-β-glucan (curdlan) biosynthesis by *Agrobacterium* sp. ATCC31749, and comparative sequence analysis of the putative curdlan synthase gene. Glycobiology 9:31–41.

Stone B.A. and Clarke A.E. 1992. Chemistry and Biology of (1→3)-β-Glucans. La Trobe University Press, Melbourne, Australia.

Taylor N.G., Laurie S., and Turner S.R. 2000. Multiple cellulose synthase catalytic subunits are required for cellulose synthesis in *Arabidopsis*. Plant Cell 12:2529–2540.

Taylor N.G., Scheible W.R., Cutler S., Somerville C.R., and Turner S.R. 1999. The irregular *xylem3* locus of *Arabidopsis* encodes a cellulose synthase required for secondary cell wall synthesis. Plant Cell 11:769–780.

Turner A., Bacic A., Harris P.J., and Read S.M. 1998. Membrane fractionation and enrichment of callose synthase from pollen tube of *Nicotiana alata* Link et Otto. Planta 205:380–388.

Updegraff D.M. 1969. Semi-micro determination of cellulose in biological materials. Anal Biochem 32:420–424.

Wu A. and Wasserman B.P. 1993. Limited proteolysis of (1→3)-β-glucan (callose) synthase from *Beta vulgaris* L: topology of protease-sensitive sites and polypeptide identification using Pronase E. Plant J 4:683–695.

Wu A., Harriman R.W., Frost D.J., Read S.M., and Wasserman B.P. 1991. Rapid enrichment of CHAPS-solubilized UDP-glucose: (1→3)-β-glucan (callose) synthase from *Beta vulgaris* L. by product entrapment. Entrapment mechanisms and polypeptide characterization. Plant Physiol 97:684–692.

CHAPTER 9

SUBSTRATE SUPPLY FOR CELLULOSE SYNTHESIS AND ITS STRESS SENSITIVITY IN THE COTTON FIBER

CANDACE H. HAIGLER*

North Carolina State University, Department of Crop Science and Department of Plant Biology, Box 7620, 4401 Williams Hall, Raleigh, NC 27695-7620

Abstract

Research on cotton fiber has figured prominently in the first steps toward understanding the metabolic control of cellulose biogenesis under normal and stressed conditions for at least two reasons. First, fiber secondary walls are composed of almost 100% cellulose that is deposited over a period of at least 20 days. Second, these extraordinary seed epidermal trichomes can be readily isolated in bulk as a pure cell type or cultured *in vitro* as part of an easily manipulated ovule/fiber system. This chapter summarizes changes in the amount and physical characteristics of cellulose throughout cotton fiber development. Mechanisms of cellulose biogenesis are reviewed, including the role of plasma membrane "rosette" protein complexes containing cellulose synthases and the relationship of cellulose microfibril orientation to microtubules. Biochemical mechanisms participating in β-1,4-glucan chain polymerization are discussed, including a possible lipid-linked primer, cycling of carbon between hexose phosphates and triose phosphates, and sucrose degradation and resynthesis within fibers. Particular emphasis is given to recently emerging evidence that a particulate form of sucrose synthase degrades sucrose to channel UDP-glucose to secondary wall cellulose synthases in both cotton fibers and tracheary elements. The recycling of the concurrently released fructose, after its phosphorylation by fructokinase, for synthesis of additional intrafiber sucrose is discussed. A role for sucrose phosphate synthase in mediating intrafiber sucrose synthesis is proposed. Finally, the adverse effects of cool temperature on the rate of fiber cellulose synthesis and fiber quality, as demonstrated in the field and *in vitro*, are described, along with data demonstrating that intrafiber flux to sucrose from exogenous glucose is particularly sensitive to cool temperature stress.

* For correspondence: Professor of Crop Science and Plant Biology, North Carolina State University, Department of Crop Science, Box 7620, 4401 Williams Hall, Raleigh NC 27695-7620, Tel: 919-515-5645; Fax: 919-515-5315; e-mail: candace_haigler@ncsu.edu

R.M. Brown, Jr. and I.M. Saxena (eds.), Cellulose: Molecular and Structural Biology, 147–168.

Keywords

abiotic stress, actin, callose synthesis, carbohydrate metabolism, carbon flux, cellulose microfibrils, cellulose synthesis, cool temperature, cotton fiber, fiber maturity, Gossypium species, *in vitro* ovule culture, microtubules, rosette microfibril terminal complexes, secondary cell wall, sucrose cycling, sucrose synthase, sucrose phosphate synthase, tracheary element, triose phosphates.

Abbreviations

gene/protein with a critical role in cellulose synthesis (CesA), days post anthesis (DPA), fructose (Fru), glucose (Glu), sucrose phosphate synthase (SPS), sucrose (Suc), sucrose synthase (SuSy), particulate SuSy (P-SuSy), soluble SuSy (S-SuSy).

1 INTRODUCTION

Cellulose synthesis has the potential to be regulated at several levels including: (1) amount and modulation of enzymes immediately involved in the processes of glucan chain polymerization and microfibril biogenesis; and (2) supply of carbon. Because cellulose represents a large carbon sink and is deposited essentially irreversibly in plants, its synthesis can be expected to be under tight control. This is likely to be especially true for cellulose synthesis during deposition of secondary walls that contain abundant cellulose. In cellulose-rich cotton fibers, secondary wall deposition is ~100-fold stronger carbon sink than primary wall deposition, which corresponds directly to the increased rate of cellulose synthesis (Benedict et al. 1980). Furthermore, short-term plant survival does not require cellulose synthesis, which supports formation of new tissues and organs during growth. Therefore, downregulation of cellulose synthesis during stress so that carbon can be directed toward basic metabolism and specific stress responses may be part of the mechanisms promoting plant evolutionary success.

Research to place cellulose synthesis within its general metabolic context and investigation of the stress sensitivity of cellulose synthesis has only recently begun. Current knowledge is based mainly on investigation of cotton fibers and xylem tracheary elements, both of which deposit secondary walls of economic importance. Because their secondary walls contain abundant cellulose, evidence about metabolic patterns related to cellulose synthesis can be expected to be more apparent in these cell types. It is also of interest to compare and contrast their regulatory systems: secondary walls in cotton fibers are composed of almost pure cellulose and have been the target of domestication and product-related selection as a textile fiber for over 5,000 years. Many of the textile properties of cotton fibers (e.g., fiber wall thickness or maturity, strength, dyeability, and extensibility) are directly dependent on the amount and properties (e.g., degree of polymerization, crystallite size, and microfibril orientation) of cellulose (Ramey 1986; Triplett 1993; Hsieh 1999). The yield of fiber, assuming adequate fiber number and length, is determined by the weight of secondary wall cellulose. In contrast, the cellulose content and properties within tree xylem have been under less selection through domestication and breeding.

This chapter will summarize current knowledge about cellulose synthesis in cotton fiber with particular emphasis on substrate supply and its stress sensitivity.

Evidence from other cell types will be mentioned in order to assess the generality of mechanisms operating in cotton fiber. Results from research on *Gossypium hirsutum*, *G. arboreum,* and *G. barbadense* are sometimes intermixed. *G. hirsutum*, the most common commercial species of upland cotton, is an allotetraploid of diploid A and D genomes that was formed 1–2 million years ago (Liu et al. 2001). *G. barbadense*, also grown commercially in compatible environments for production of high quality fiber, represents species divergence after the same original polyploidization event (Wendel et al. 1999). *G. arboreum* represents the A-genome; cultivated in Asia, it also has thick fiber secondary walls (Applequist et al. 2001). The basic mechanisms regulating cellulose synthesis in the different species are expected to be similar, although variation in synthetic efficiency and/or developmental timing of cellulose synthesis may help determine fiber quality differences.

Experimental results obtained from fibers grown *in vivo* and *in vitro* are included in the discussion; these systems have very similar developmental programs differing mainly by accelerated fiber development (at constant warm temperature) but a lesser magnitude of secondary wall deposition *in vitro* (Meinert and Delmer 1977). Even though cultured ovules require glucose (Glc) rather than sucrose (Suc) as an exogenous substrate, there are indications that intrafiber metabolism is similar to plants that have sucrose as the transport sugar. For example, the relative amounts of Glc, fructose (Fru), and Suc in fibers from cultured ovules (Martin and Haigler 2004) are similar to those reported in fibers grown *in vivo* (Jaquet et al. 1982; Basra et al. 1990; Ruan et al. 1997).

Basic principles of cotton fiber development have been reviewed elsewhere (Basra and Malik 1984; Ryser 1985; Ryser 1999), and one other review has focused on fiber cellulose synthesis (Delmer 1999). Basic principles of cellulose synthesis are reviewed in other chapters in this volume. In some cases, this chapter cites reviews or research articles that contain primary references for older results.

2 OVERVIEW OF COTTON FIBER CELLULOSE BIOGENESIS

2.1 The role of cellulose biogenesis in cotton fiber development

Cotton fibers are greatly elongated (>2.25 cm) seed epidermal hairs (trichomes) that cover the ~30 cotton seeds within one cotton boll. The cotton fiber is valuable as a model system for research on cellulose biogenesis because primary and secondary wall deposition occur as prolonged, separable, developmental stages in a cell that is able to be isolated completely from other cell types. Timing of developmental events in cotton fiber is referenced as days post anthesis (DPA). The developmental transitions are not temporally regulated, but instead occur after particular increments of fiber differentiation. This implies that references to events occurring on particular DPA are only approximations of the timing that might occur under another growing condition. For example, the onset of

fiber wall thickening is delayed if development proceeds more slowly under cool temperatures (Haigler et al. 1991). Secondary wall deposition can persist until 60 DPA in a cool, but prolonged, growing season (Thaker et al. 1989).

In *G. hirsutum*, typical primary walls ~0.5 μM thick and containing 20–25% cellulose along with pectin, xyloglucan, and protein (Meinert and Delmer 1977) are synthesized during fiber elongation. Primary wall deposition proceeds alone until 14–17 DPA, then a transition phase with concurrent primary and secondary wall deposition occurs between 15–24 DPA (representing deposition of the "winding layer"), followed by predominantly secondary wall synthesis until at least 40 DPA. The first period of wall thickening (12–16 DPA in one experiment) is accomplished by continued synthesis in the same proportions of primary wall components (Meinert and Delmer 1977), an observation that is consistent with increasing wall birefringence while the cellulose microfibrils remain transversely oriented (Seagull 1986). The secondary wall finally attains a thickness of 3–6 μM around the whole circumference of the fiber, becoming thinner only at the fiber tip.

In *G. barbadense*, it is clear that the overlap between primary and secondary wall deposition occurs within each fiber rather than in the fiber population because the overlapping period is greatly prolonged, and 90% of secondary wall deposition is complete before elongation ceases (DeLanghe 1986). It is thought that elongation continues exclusively at the fiber tip as secondary wall is deposited over most of the cell surface. At maturity, an autolytic process may occur, although no direct evidence on the mechanism of fiber death is available. The final extent of secondary wall deposition under optimal environmental conditions is genetically determined for a given cultivar, which is manifested both *in vivo* and *in vitro* (Ramey et al. 1986; Thaker et al. 1989; Haigler et al. 1991). The sensing mechanisms that lead to termination of fiber development are unknown, but may relate to fiber mass (Schubert et al. 1976; Basra and Malik 1984) as supported by the failure of experiments to determine fiber expansion mechanisms by attaching small beads to the surface because the fiber stopped growing (Seagull 1995). Finally, boll opening followed by fiber drying and twisting occur. The drying causes fiber collapse into an ellipsoidal form (if its cell wall is not overly thick), changes in physical properties of the cellulose, and twisting to form convolutions (4–7/mm) that aid spinning (DeLanghe 1986; Hsieh 1999).

Presumably, signal transduction pathways and expression of particular transcription factors regulate the developmental transitions via initiation of gene expression cascades. Genes expressed in a stage-specific manner have been identified in cotton fiber (Kim and Triplett 2001), although there is also evidence that some mRNA transcripts are synthesized and some cell biological processes occur during primary wall deposition that are important for later high-rate deposition of secondary wall cellulose (Davidonis 1993; Triplett 1998). The requirement for particular proteins to facilitate cellulose deposition at each stage is illustrated by the immature cotton fiber mutant (*imim*), which has a recessive, single-locus genetic lesion that prevents the last phase of high-rate cellulose synthesis. Final dry weight and crystalline cellulose content of *imim* fibers were 66.7% and 22.5%,

respectively, of the values for the *G. hirsutum* cv. TM-1 parent (Kohel et al. 1993; Benedict et al. 1994). Downstream cellular effects of genetic regulation are illustrated by the increase in H_2O_2 concentration that occurs at the onset of cotton fiber secondary wall deposition (Potikha et al. 1999). There is evidence that oxidative conditions may promote the dimerization of CesA proteins via their N-terminal Zn-finger domains (Kurek et al. 2002), which may aid formation of the multimeric protein aggregates (rosettes) that are characteristic of cellulose synthesis.

2.2 Changes in cellulose characteristics throughout cotton fiber development

Several features of cellulose biogenesis change with the developmental transitions. There is a shift between low (20–25%) and high (>95%) cellulose content at the primary wall and secondary wall stages, respectively (Carpita and Delmer 1981). The dilution effect of secondary wall accumulation on primary wall properties indicates that the secondary wall must be almost pure cellulose. (The dilution effect is revealed by sequential x-ray fluorescence microscopy analysis of Ca^{++} concentration, which is extensively cross-linked in the primary wall; Wartelle et al. 1995). At the transition phase, the rate of cellulose synthesis increases ~100-fold (Meinert and Delmer 1977). There is a shift in the angle of the microfibrils relative to the longitudinal fiber axis, with angles of ~70°–90°, 45°–55°, and 20° during the primary wall, transition, and secondary wall stages, respectively (Arthur 1990; Rebenfield 1990). There is an increase in the degree of polymerization of the glucan chains from an average of ~4,000 DP in primary walls (in a polydisperse population) to ~10,000 DP (in a monodisperse population) in secondary walls (Timpa and Triplett 1993). There is an increase in the degree of microfibril bundling (Willison and Brown, Jr. 1977) and crystallinity, which likely relates to the depletion of cellulose-binding matrix molecules during secondary wall deposition. In primary walls, the microfibrils exhibit cellulose IV crystallinity due to poor order in the lateral dimension, which is indicative of small microfibril diameter (Chanzy et al. 1978). Cellulose I microfibrils with higher crystallite size (3.5–5.5 nm) are typical of the secondary wall stage (Hu and Hsieh 1996; Ryser 1999). As is typical for higher plants, 60–80% of cotton cellulose is in a crystallographic sub-class of cellulose I called cellulose Iβ (Atalla and VanderHart 1984; O'Sullivan 1997). It has been reported that rosettes that contain cellulose synthase (CesA) enzymes are more abundant during primary wall deposition compared to secondary wall deposition (Willison 1983), which appears to be illogically correlated with the lower primary wall cellulose content. However, the lability of rosettes in the context of specimen handling for freeze fracture (Herth 1989) warrants cautious interpretation of this result. Secondary wall stage cotton fibers optimally fixed by cryogenic methods contain active Golgi bodies (Salnikov et al. 2003), which have been shown to deliver rosettes to the plasma membrane during secondary wall synthesis in tracheary elements (Haigler and Brown, Jr. 1986).

2.3 The role of the microtubules in cotton fiber cellulose synthesis

Morphological evidence and altered microfibril orientation in the presence of microtubule antagonists implicate cortical microtubules as participants in regulating microfibril angle in cotton fibers (Seagull 1993), which has been supported by genetic evidence in xylem fibers expressing a mutant gene for a microtubule accessory protein (Burk and Ye 2002). However, the mechanism linking microtubule and microfibril orientation is unknown, although microtubule-based establishment of special plasma membrane domains to channel rosette movement may be involved (reviewed in Baskin 2001). Putative proteins that cross-link microtubules with the fiber plasma membrane can be seen in electron micrographs (Ryser 1999; Haigler and coworkers, unpublished), and they may be part of such a mechanism. The increases in tubulin amount and microtubule number and length that occur at the onset of secondary wall deposition further support a specific relationship of microtubules with high-rate cellulose synthesis (Kloth 1989; Seagull 1992). The appearance of unique β-tubulin isotypes at the onset of secondary wall deposition suggests unique functions of a stage-specific microtubule array (Dixon et al. 1994). During secondary wall deposition "reversals" are formed in the cell wall as the sign of the microfibril helix reverses, a change that is predicted by the same reversal in the orientation of cortical microtubules. The reversals occur at variable intervals of ~0.3–1 mm so that ~100 may occur over the length of the fiber (Rebenfield 1990; Hsieh 1999).

2.4 Molecular biology of cotton fiber cellulose biogenesis

A breakthrough in our understanding of vascular plant cellulose biogenesis came with the identification of two putative *CesA* genes–*GhCesA1* and *GhCesA2* – which were expressed preferentially during secondary wall deposition in cotton fibers (Pear et al. 1996). Based on preliminary data, *GhCesA-3* is expressed at both the primary (14 DPA) and secondary wall (24 DPA) stages of fiber development (Laosinchai et al. 2000). A role for this class of proteins in cellulose biogenesis has now been confirmed multiple times by analysis of *Arabidopsis* mutants (Williamson et al. 2001; Doblin et al. 2002). Freeze fracture immunolabeling has shown that the plasma membrane bound protein aggregates (rosettes) associated with cellulose synthesis contain a CesA-type protein with immunological similarity to GhCesA1 (Kimura et al. 1999).

Following the identification of *CesA* genes in multiple species, phylogenetic analysis of translated amino acid sequences revealed a group of genes, including *GhCesA1* and *GhCesA2*, that is expressed preferentially in secondary-walled cells. In comparison with *Arabidopsis*, corn, and rice, it can be expected that cotton contains a family of at least 10 *CesA* genes. In analogy with *Arabidopsis*, at least three unique CesA proteins may be required and have nonredundant roles in both cotton fiber primary and secondary wall synthesis (Williamson et al. 2001; Doblin et al. 2002). The polyploid nature of *G. hirsutum* (Applequist

et al. 2001) suggests that redundancy of the gene family is also likely to exist, which may explain *GhCesA4* (AF413210) having 96% nucleotide identify and similar expression to *GhCesA1* (Kim and Triplett 2001). In contrast to some other species, experimental polyploid cotton appears to retain multiple homologous coding sequences in the genome followed by independent evolution of the homologs (Liu et al. 2001). Atypically for ten different genes studied, *GhCesA1* (called CelA2 in this study) from two species of extant A-genome diploid cotton and from allotetraploid *G. hirsutum* showed evidence of pseudogenization occurring prior to polyploidization. *GhCesA-2* (called CelA1 in this study) also occurs in genomes of A and D diploids and showed no evidence of pseudogenization (Cronn et al. 1999). A possible *GhCesA-1* pseudogene allows the possibility that A-genome diploid cotton may require fewer functional *CesA* genes to support secondary wall synthesis, but this nonfunctional gene could also be compensated through functional homologs.

2.5 Biochemistry of cotton fiber cellulose biogenesis

The biochemical pathway of glucan chain polymerization in vascular plants remains to be defined, and different CesA proteins may have different roles in a multistep biosynthetic process. A recombinant fragment of GhCesA1 bound UDP-Glc *in vitro*, as was expected for a cellulose synthase, and the binding activity was abolished by mutagenesis of aspartate residues within the catalytic site (Pear et al. 1996). However, GhCesA1 expressed in yeast catalyzed only the synthesis of sterylcellotriose from supplied sterylglucoside and UDP-Glc (Doblin et al. 2002), which could be explained by abnormal arrest of the protein in the endoplasmic reticulum as determined by freeze fracture immunolabeling of an epitope-tagged protein (Haigler, Grimson, Hogan, and Delmer, unpublished) or a different catalytic role for the native protein than final glucan chain polymerization. The latter possibility correlates with a lipid intermediate in cellulose synthesis by prokaryotic *Agrobacterium tumefaciens* (Matthysse et al. 1995b) and the accumulation of a soluble glucan bound to sitosterol-β-glucoside in cotton fibers treated with the cellulose-synthesis-inhibiting herbicide, CGA 325′615 (Peng et al. 2001b). Soluble glucan made in the *rsw1 Arabidopsis* mutant in *AtCesA1* is also lipid-linked (Williamson et al. 2001). In cotton fiber extracts, another cellulose synthesis inhibitor, 2,6-dichlorobenzonitrile (DCB), blocks the synthesis of the sitosterol-β-glucoside, and the inhibition is partly reversed by sterylglucoside addition (Peng et al. 2001b).

A role for other types of proteins in glucan chain polymerization and crystallization is just now emerging through analysis of *Arabidopsis* mutants with abnormal phenotypes including depleted cellulose (Williamson et al. 2001; Doblin et al. 2002). These include: (1) a membrane associated cellulase; (2) a katinin-like protein that alters the assembly of the cortical microtubule array, cellulose microfibril orientation, and cellulose quantity; (3) three enzymes catalyzing protein *N*-glycosylation; and (4) a membrane-anchored protein, KOBITO1,

with unknown function. A current unifying hypothesis without proof is that Korrigan cleaves a cellodextrin from the glucolipid, a catalytic activity that is inhibited by improper glycosylation. However, alternative mechanisms are suggested by a cellulase that may act as a transglycosylase in cellulose synthesis by *Agrobacterium tumefaciens* (Matthyse et al. 1995a). Unpublished results have also suggested the existence of a UDP Glc:protein transglucosylase that covalently glucosylates two 38 kDa cytosolic proteins that are part of a large (>1000 kDa) complex from *in vitro* cotton fibers (Buchala 1999). A requirement for other proteins is further supported by the synthesis of cellulose *in vitro* in association with large, detergent-solubilized, complexes (Hayashi et al. 1987; Kudlicka and Brown, Jr. 1997; Lai-Kee-Him et al. 2002).

3 SUBSTRATE SUPPLY FOR COTTON FIBER CELLULOSE BIOGENESIS

3.1 A role for sucrose synthase

Substantial evidence implicates UDP-Glc as the immediate substrate for cellulose polymerization in vascular plants including cotton fiber (Franz 1969; Carpita and Delmer 1981). UDP-Glc was the most abundant nucleotide in the fiber and its concentration increased in parallel with stage-specific increases in the cellulose synthesis rate: 0.2, 1.2, and 2.1 µmol/boll at 13, 17, and 21 DPA, respectively. The UDP-Glc for cellulose synthesis could be supplied by: (1) sucrose synthase (SuSy; E.C. 2.4.1.13; Suc + UDP ←→ UDP-Glc + Fru); or (2) by UDP-Glc pyrophosphorylase (Glc-1-P + UTP ←→ UDP-Glc + PPi) (Figure 9-1). Addressing first the possible participation of UDP-Glc pyrophosphorylase, this enzyme activity increases 1.8× along with the increased rate of cellulose synthesis at the onset of cotton fiber secondary wall deposition (Wafler and Meier 1994). Pulse-chase experiments with ^{14}C-Glc fed to cultured cotton ovules/fibers were consistent with carbon flow through Glc-6-phosphate and glucose-1-phosphate to UDP-Glc and cellulose (Carpita and Delmer 1981). In cultured carrot cells fed Suc or Glc, the Suc was hydrolyzed extracellularly, Glc was taken up by the cells, and carbon moved through the hexose phosphates toward cell wall glucan synthesis (Kanabus et al. 1986). UDP-Glc pyrophosphorylase may sometimes provide UDP-Glc for cellulose synthesis, but the data can also be reconciled with a primary role for sucrose synthase (Delmer 1999).

Sucrose synthase commonly acts in the direction of UDP-Glc synthesis in heterotrophic tissues, and its possible role in glucan synthesis was proposed long ago (Rollit and Maclachlan 1974 and other references in Haigler et al. 2001). Until recently, SuSy had been studied as only a soluble enzyme (S-SuSy), and this enzyme activity was 20, 770, and 1300 nmol/min/g fresh weight fiber at 10, 15, and 25 DPA, respectively (Basra et al. 1990). Despite minimization of real increases by the increasing weight of secondary wall cellulose, this pattern suggests a strong relationship of SuSy (some of which may have been solubilized during cell fractionation, see below) to high rate, secondary wall, cellulose

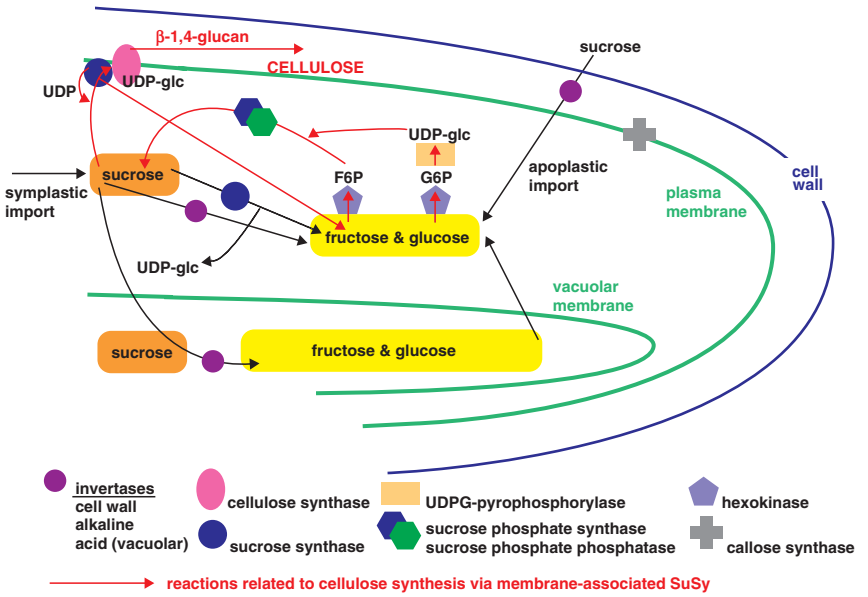

Figure 9-1. Diagram of key enzymes, metabolites, and pathways associated with cellulose synthesis in secondary wall stage cotton fibers. (Figure 10 from: Haigler et al. 2001. Carbon partitioning to cellulose synthesis. Plant Mol Biol 47:29–51. Reproduced with kind permission from Springer Science and Business Media). (*See Color Plate of this figure beginning on page 355*)

synthesis. Supporting this possibility, permeabilized, secondary wall stage cotton fibers showed a 140-fold preference for Suc vs. UDP-Glc as the substrate for cellulose synthesis (Pillonel 1980), a finding that has been supported by later experiments (Amor et al. 1995).

Recent evidence strongly implicates the involvement in cellulose synthesis of a membrane-associated (or particulate) form of sucrose synthase (called P-SuSy, in contrast to soluble S-SuSy) that may channel UDP-Glc to the cellulose synthase (Amor et al. 1995). This implies that UDP-Glc for cellulose synthesis does not form a large pool, and the free pool of UDP-Glc may have only an indirect role in cellulose synthesis (see below on sucrose phosphate synthase). In secondary wall stage cotton fibers, over 50% of the SuSy activity was in the form of P-SuSy, and 15–25% P-SuSy existed in pea embryos and sunflower hypocotyls (Barratt et al. 2001; Kutschera and Heiderich 2002). Upon Suc hydrolysis by SuSy, the energy of the glycosidic bond is directly used to form UDP-Glc so that half as much energy is required compared to synthetic activity of UDP-Glc pyrophosphorylase (Wagner and Backer 1992). No energy input is required when Glc is transferred from UDP-Glc to the growing glucan chain, and an energy-conserving mechanism based on SuSy may facilitate the synthesis of large quantities of cellulose. In addition, UDP is recycled to SuSy without accumulating in the cytoplasm, thereby avoiding inhibitory effects on glucan synthases (Delmer 1999).

Although direct channeling between SuSy and CesA has not been proven, several kinds of evidence support a role for SuSy in cellulose synthesis. This subject has recently been reviewed in detail (Haigler et al. 2001) and will be briefly summarized here. SuSy was detected as a UDP-Glc-binding protein during cotton fiber secondary wall deposition, and semi-permeabilized cotton fibers synthesized β-1,4-glucan more efficiently from exogenous Suc than from Glc or UDP-Glc. There was a correlation between increasing cellulose synthesis rate and increasing P-SuSy during cotton fiber development (Amor et al. 1995) and in sunflower hypocotyls stimulated with increased nutrients to thicken via new cell wall synthesis (here S-SuSy also increased; Kutschera and Heiderich 2002). Both the expression of *Sus* genes (encoding sucrose synthase; nomenclature according to Hannah et al. 1994) and SuSy activity increase during wood formation (Hauch and Magel 1998; Hertzberg et al. 2001; Schrader and Sauter 2002). In some transgenic plants or mutants, decreased SuSy activity was associated with decreased cellulose content, although the relationship was not linear possibly because of multiple *Sus* genes/SuSy isoforms or a low level of metabolic control at this step. For example, in pea embryos, 95% downregulation of one of three SuSy isoforms was associated with 30% decrease in starch but no change in cellulose content, suggesting that a particular SuSy isoform does participate in cellulose synthesis (Barratt et al. 2001). The same argument was made based on analysis of two corn mutants (Chourey et al. 1998). At least one *Sus* gene was expressed uniformly throughout cotton fiber development (Shimizu et al. 1997), and it remains to be determined whether special functions of SuSy during cotton fiber secondary wall deposition are achieved through expression of another *Sus* gene or through differential regulation of one SuSy isoform.

Electron microscopic immunolocalization using cryogenic methods that preserved native ultrastructure and should have prevented protein movement placed SuSy between the cortical microtubules and the plasma membrane in tracheary elements and cotton fibers (Salnikov et al. 2001, 2003). In tracheary elements, patterned SuSy distribution corresponded to patterned sites of secondary wall cellulose synthesis where rosettes containing CesA (Kimura et al. 1999) occur in the plasma membrane (Haigler and Brown, Jr. 1986). P-SuSy is predicted to be a tightly-associated peripheral membrane protein; high salt or mild detergent did dissociate it from cotton microsomes (Amor et al. 1995). In tracheary elements (Salnikov et al. 2001), but not cotton fibers (Salnikov et al. 2003), actin was able to be localized between SuSy and the microtubules, which is consistent with biochemical evidence that SuSy is an actin-binding protein (Winter et al. 1998). SuSy coprecipitated from cotton fiber extracts with actin and tubulin (Haigler et al. 2001). Based on results from tracheary elements where microtubules are patterned but actin is distributed over the whole cell surface, it is more likely that a microtubule-related mechanism determines the patterned localization of SuSy. Other linking proteins between the plasma membrane, integral membrane proteins, SuSy, and the cortical cytoskeleton are likely to exist. Changes in phosphorylation and/or intracellular calcium concentration may also relate to the

shifts between S-SuSy and P-SuSy. It has been hypothesized that S-SuSy may supply UDP-Glc for general metabolic needs, whereas the proportion of P-SuSy has a major regulatory role in partitioning of carbon to cellulose (Delmer 1999). A model has been suggested whereby stress conditions in cellulose-synthesizing cells could cause reversion of P-SuSy to S-SuSy and concurrent downregulation of high-rate cellulose synthesis (Haigler et al. 2001).

In cotton fibers where the antibody used for immunolocalization was homologous, SuSy was extremely abundant near the plasma membrane during secondary wall deposition (Salnikov et al. 2003). In contrast, it could be only sparsely localized near the plasma membrane during primary wall deposition (Haigler et al. 2001). In differentiating tracheary elements of *Zinnia elegans* for which the antibody was heterologous, SuSy was readily detected near the plasma membrane underneath patterned secondary wall thickenings, but it could not be detected underneath the intervening primary walls or in cells induced to expand via primary wall synthesis (Salnikov et al. 2001). Such results can be rationalized in terms of the lower percentage and amount of cellulose in primary cell walls or in terms of a lesser role for P-SuSy in primary wall cellulose synthesis. The extent of P-SuSy immunolabeling at sites of *Zinnia* tracheary element secondary wall synthesis was much lower than in cotton fiber, which could reflect reality in xylem cells synthesizing only 40% cellulose or the use of a heterologous antibody. Substantial P-SuSy was sometimes (Amor et al. 1995), but not always (Ruan et al. 2003), detected biochemically during cotton fiber primary wall deposition, and the variability may reflect conversion of P-SuSy to S-SuSy during cell fractionation. Analysis of mutant or transformed plants with reduced SuSy activity support a role for SuSy in primary wall cellulose synthesis (reviewed in Haigler et al. 2001; Ruan et al. 2003), but it is possible that S-SuSy can provide the lesser amount of UDP-Glc for cellulose synthesis through the general cytosolic pool during that stage.

In light of a possible multistep mechanism for cellulose synthesis in which synthesis of a cellodextrin primer may be a first step (Peng et al. 2001a), it is possible that both free UDP-Glc and UDP-Glc channeled from SuSy participate in cellulose synthesis. Perhaps free UDP-Glc provides the substrate for primer synthesis, whereas UDP-Glc channeled via P-SuSy provides the substrate for polymerization of high molecular weight secondary wall cellulose *in vivo*. This division would allow the bulk of the carbon to be provided through the most energy efficient mechanism, while a requirement for a primer may provide one means of regulating cellulose biosynthesis. It is also possible that the two pathways, one based on free UDP-Glc and one based on sucrose as a source of channeled UDP-Glc, are used alternatively or in different ratios at different stages of development or under different environmental conditions. It should be noted that crystalline cellulose microfibrils can be made *in vitro* from detergent extracts of membranes of cotton fibers (at 20 DPA) and other plants that are supplied with UDP-Glc (Kudlicka et al. 1995; Lai-Kee-Him et al. 2002), implying that channeling of substrate from SuSy is not obligatory. However, *in vitro* cellulose

synthesis is not efficient, and the polymerizing enzymes may be dissociated from proteins that support their function *in vivo*.

Curiously, in the cryogenically fixed and embedded cotton fibers where native molecular distribution was expected to be preserved, SuSy was also immunolocalized in an exoplasmic zone about 0.3 µM deep outside the plasma membrane (Salnikov et al. 2003). The validity of this observation was confirmed using two polyclonal antibodies to cotton and bean SuSy, affinity purified antibody to cotton SuSy, and the preimmune sera and irrelevant polyclonal antibodies as controls. Immunolabeling at 24 and 30 DPA showed that this zone also contained the ß-1,3 glucan, callose (Salnikov et al. 2003), which has long been known by fluorochromatic staining to persist in this general area throughout secondary wall deposition (Waterkeyn 1981). The exoplasmic SuSy may be discarded there after its cellular role is finished or it could have a role in the synthesis of callose. Callose may be required in cotton fiber secondary walls to provide a space for the crystallization and final orientation of cellulose microfibrils in the exoplasmic zone in the absence of typical matrix molecules (DeLanghe 1986). In addition to work with cotton fibers, other data implicate SuSy as a participant in callose synthesis, at least under some conditions (reviewed in Haigler et al. 2001; Subbaiah and Sachs 2001). Callose is also readily synthesized from exogenous UDP-Glc *in vitro* in many systems including semi-permeabilized cotton fibers (Pillonel et al. 1980; Amor et al. 1985). There may be a distinction between the biochemical pathways related to developmentally controlled (dependent on SuSy?) vs. wound-induced callose synthesis (using free UDP-Glc?), or other cellular differences may correlate with use of UDP-Glc provided by one or the other mechanism.

4 INTRAFIBER SUCROSE SYNTHESIS AS A SOURCE OF CARBON FOR SECONDARY WALL CELLULOSE SYNTHESIS

Although there is evidence that fibers import translocated Suc symplastically through plasmodesmata at the fiber foot (Ryser 1992; Ruan et al 1997), Glc and Fru may also provide carbon for secondary wall cellulose synthesis after conversion to Suc within the fiber. Large and approximately equally sized pools of Glc and Fru exist in the fibers, where they are mostly stored in the vacuole (Carpita and Delmer 1981; Jaquet et al. 1982; Buchala 1987; Basra et al. 1990; Hendrix 1990; Waffler and Meier 1994; Ruan et al. 1997). These hexoses are abundantly produced through degradation of translocated Suc by S-SuSy and stored to generate turgor pressure (Ruan et al. 2003), among other possible uses. In addition, P-SuSy involved in cellulose synthesis generates one Fru with each cycle, and invertases can release both Glc and Fru. Cotton fibers have high levels of wall-bound and cytoplasmic invertases during both primary and secondary wall deposition, although there is a peak in activity at the transition between the two stages (Basra et al. 1990). In the presence of multiple degradative enzymes, the fiber Suc pool is sixfold to tenfold smaller than the Glc and Fru pools both

in vivo and *in vitro* (Carpita and Delmer 1981; Jaquet et al. 1982; Basra et al. 1990; Martin and Haigler 2004). The size of the fiber Suc pool did not change with exposure to 15°C (which hinders cellulose synthesis, Haigler et al. 1991), but the flux from Glc to Suc was greatly suppressed at 15°C compared to 34°C (Martin and Haigler 2004). These results show that absolute pool sizes are not as revealing of metabolism related to cellulose synthesis as fluxes through the pools.

During secondary wall deposition in cotton fiber, a large percentage of the Fru released by the activity of P-SuSy must be recycled into cellulose biosynthesis through resynthesis of Suc in order to account for ~80% of the total carbon being directed toward cellulose synthesis both *in vivo* and *in vitro* (Mutsaers 1976; Roberts et al. 1992). The use of one UTP or ATP to phosphorylate Fru via fructokinase is a minor energetic cost compared to inefficient use of the Fru released by SuSy, and each Fru shunted toward glycolysis can replace this energy in a 36:1 ratio. Cotton fibers do synthesize Suc; much of the ^{14}C-Glc supplied to cultured ovules/fibers is converted to Suc within the fiber (Carpita and Delmer 1981; Martin and Haigler 2004). The concurrent accumulation of a small amount of ^{14}C-Fru (Martin and Haigler 2004) suggests that glucokinase and phosphoglucoisomerase were active in fiber so that ^{14}C-Glc-6-P was isomerized to ^{14}C-Fru-6-P. This can be used along with UDP-Glc by sucrose phosphate synthase/sucrose phosphate phosphatase to synthesize Suc containing ^{14}C-Fru, which would be released as SuSy channels UDP-Glc to the cellulose synthase. Little change in the amount of ^{14}C-Fru during 2 h pulse labeling (Martin and Haigler 2004) would be consistent with the rapid phosphorylation of a metabolically active pool of ^{14}C-Fru so that this carbon could be used to synthesize additional sucrose to support cellulose synthesis. Such a scenario in cotton fiber is supported by studies of woody tissue; after feeding poplar leaves with asymmetrically radiolabeled sucrose followed by analysis of stem tissue, cellulose was made equally from carbon originally in the glucose and fructose moieties (T. Hayashi, personal communication). The importance of fructokinase for cycling carbon toward cellulose synthesis is consistent with data showing that downregulation of one, but not another, isoform of fructokinase in tomato plants caused reduced stem and root growth, which could result from hindered cellulose synthesis. However, cellulose content in the tomato plants was not determined (Odanaka et al. 2002).

Other data also support the passage of carbon through diverse metabolic pools before its use for cellulose synthesis. Isotopic fractionation data demonstrate a substantial contribution to cellulose of carbon that has been cycled between the hexose phosphates and the triose phosphates in *Lemna* growing heterotrophically on Suc, photoheterotrophically with Suc and light, and autotrophically. Interestingly, the percentage exchange was greater when photosynthesis was occurring: 80%, 70%, and 40% under autotrophic, photoheterotrophic, and heterotrophic conditions, respectively. Starch and cellulose were synthesized from a common pool of triose phosphates (Yakir and DiNiro 1990). Similar results were obtained for potato tubers sprouting in the dark or light (with greening) (DiNiro and Cooper 1989) and for wood cellulose synthesized from exogenous

Glc (Hill et al. 1995). Cycling between hexoses and the triose phosphates is catalyzed by pyrophosphate:Fru-6-phosphate 1-phosphotransferase [PFK(PPi)], and this is the most active phosphofructokinase in secondary wall stage cotton fibers (Waffler and Meier 1994). The activity of PFK(PPi) would also consume PPi released by UDP-Glc pyrophosphorylase acting in the synthetic direction (Delmer 1999) to generate the UDP-Glc required by sucrose phosphate synthase (SPS; see below).

5 A ROLE FOR SUCROSE PHOSPHATE SYNTHASE IN INTRAFIBER CELLULOSE SYNTHESIS

Data suggest that synthesis of sucrose from hexoses within the fiber involves SPS acting coordinately with sucrose phosphate phosphatase. SPS catalyzes the irreversible reaction, Fru-6-P + UDP-Glc $\rightarrow$ Suc-P + UDP, which is the first committed step of the Suc synthesis pathway. SPS exerts a high level of control over this process in leaves (Lunn and MacRae 2003), which is facilitated by extensive regulatory mechanisms (G6P activation, Pi inhibition, phophorylation at multiple sites, and interaction with 14-3-3 proteins) that allow fine control of flux through Suc (Huber and Huber 1996; Winter and Huber 2000). It has recently been shown that SPS is active during high rate cellulose synthesis for secondary wall deposition in heterotrophic cotton fibers and tracheary elements. The *in vitro* tracheary element differentiation system was particularly useful in showing a strong correlation between increasing SPS activity and episodic high-rate secondary wall cellulose synthesis even though the exogenous carbon source was sucrose (Babb and Haigler 2001). Based on analogy with other systems (Schrader and Sauter 2002), it might be proposed that SPS activity increases to facilitate Suc synthesis as starch is degraded, but no starch grains were visible in hundreds of secondary wall stage cotton fibers examined by electron microscopy (Salnikov et al. 2003). In addition, it was experimentally determined that the increase in SPS activity in differentiating tracheary elements did not depend on the availability of starch for degradation (Babb and Haigler 2001).

In summary, increased SPS activity in secondary wall stage cotton fibers and tracheary elements is likely to be related to cellulose synthesis. In addition to facilitating efficient carbon use, SPS activity would also result in depletion of cytoplasmic Fru, which is an end-product inhibitor of SuSy (Doehlert 1987). The Suc degradation by P-SuSy and Suc synthesis by SPS in cellulose-synthesizing cells describes a "futile cycle" that exists in many heterotrophic cell types (reviewed in Huber and Huber 1996). A need for both of these enzymes in efficient cellulose synthesis shows that the cycle can be useful (Haigler et al. 2001). It is likely that the cycle has regulatory value through ability to affect the intracellular flux to sucrose similar to that conferred by several sucrose cycles in tomato fruit (Nguyen-Quoc and Foyer 2001). Genomic sequencing has revealed four and five SPS genes in *Arabidopsis* and rice, respectively, and knowledge is lacking of how the cellular activities of the encoded enzymes may differ (Lunn and MacRae

2003). It will be of interest to determine if a particular SPS isozyme is related to cellulose synthesis.

6 STRESS SENSITIVITY OF CELLULOSE SYNTHESIS

Although the fiber is somewhat shielded from effects on the whole plant due to being part of a reproductive structure with physiological priority, several agronomic stresses that minimize plant vigor and/or photosynthate production alter fiber properties in ways that suggest less cellulose deposition within secondary walls. (Often lower fiber maturity was not directly determined, but rather inferred from reductions in micronaire or bundle strength.) Such stresses include both excess and limited water, low light due to clouds, fungal disease, and premature defoliation (Ramey 1986; Pettigrew 1994).

Of more interest are stresses that have direct effects on the cellulose biosynthetic process. For example, both dryland production conditions and cool temperatures adversely affect the degree of polymerization of cotton fiber cellulose by unknown mechanisms (Timpa and Wanjura 1989; Timpa 1992). More mechanistic information is available about the adverse effects of cool temperatures on cellulose deposition in *G. hirsutum*. In this case, cellulose synthesis is more sensitive than respiration (a representative of general metabolic processes) and synthesis of callose. As determined from feeding ^{14}C-Glc to cultured ovules/fibers, cellulose synthesis is optimal between 28–37°C and severely hindered below 22°C. The apparent Q_{10} values between 18–28°C equaled 3.13 and 4.28 for respiration and cellulose synthesis, respectively (Roberts et al. 1992). (For comparison, many plant enzymatic processes such as respiration in other plants and the dark reactions of photosynthesis have Q_{10} = 2–3 in the physiological temperature range.) Similarly, in *G. arboreum*, cellulose synthesis in the fiber had an apparent Q_{10} = 6 between 15–25°C, whereas callose synthesis had an apparent Q_{10} = 2.3 (Pillonel and Meier 1985). Lowering the temperature *in vitro* from 30°C to 10°C increased the ratio of newly synthesized callose/cellulose in cotton fibers more than four times (Buchala and Meier 1985). Interestingly, cellulose synthesis in 21 DPA secondary-wall-stage cotton fibers was more sensitive to 22°C and 15°C than cellulose synthesis in the ovules to which they were attached, which may have had a mixture of primary wall synthesis (for embryo growth and seed expansion) and secondary wall synthesis (for wall thickening in seed coat cells) (Roberts et al. 1992). This observation could relate to different pathways for cellulose synthesis at different developmental stages (one dependent on P-SuSy and one using free UDP-Glc) or to other factors such as a stress-induced bias toward partitioning carbon toward the seed itself rather than to the fibers that originally aided seed dispersal in nature.

Hindered cellulose synthesis at moderate temperatures < 22°C correlates with the subtropical origins of perennial *Gossypium* species and the short period of only ~300 years during which they were adapted as annual crops in temperate regions (Ramey 1986). Within a short growing season, the cool temperature sensi-

tivity has adverse effects on yield and fiber quality, particularly fiber secondary wall thickness (maturity) that correlates with low individual fiber strength (Gipson 1986). The frequent occurrence of cool nights in temperate cotton growing regions results in "rings" within the fiber wall that are revealed by swelling of cross-sections in cuprammonium solution. These rings are not discontinuities in the wall, although they are weak zones in the swollen cross-sections so that splitting under pressure occurs there preferentially (Haigler et al. 1991). The layer of cellulose synthesized at night is more porous and less crystalline, which probably explains its differential swelling to reveal the ring (DeLanghe 1986; Gipson 1986).

Fibers growing on ovules cultured *in vitro* under cycling warm/cool temperatures, but in the presence of a constant supply of Glc, also contain rings. Therefore, a large part of the cool temperature sensitivity of cellulose synthesis exists within the ovule/fiber tissues without dependence on whole-plant phenomena such as sugar translocation (Haigler et al. 1991). This fact was first suggested by the accumulation of simple sugars in the cotton boll during secondary wall deposition under cool nights (DeLanghe 1986; Ramey 1986). There is variability between cultivars in the severity of the cool night hindrance of net cellulose accumulation (Gipson 1986), but no commercial cultivar analyzed *in vitro* retained greater than 24% of its maximum rate of cellulose synthesis at 15° compared to 34°C (Haigler et al. 1994; Martin and Haigler 2004). The similarity of *in vitro* results (Glc as exogenous substrate) (Haigler et al. 1991; Roberts et al. 1992) with field results (Suc as the transport sugar) (Gipson 1986; Thaker et al. 1989) also suggests that the major cool temperature hindrance is not related to this difference.

In transgenic plants with glucosidase II downregulated, less cellulose accumulates in the field even though no phenotype is observed in the greenhouse. This was suggested to be due to stress in the field (Taylor et al. 2000), but it might also occur because high light in the field can support more cellulose synthesis such that a lower level of glucosidase II becomes rate limiting. Because of the high carbon demand of cellulose synthesis, plants are likely to downregulate this process during environmental stress to favor metabolism that supports short-term survival rather than growth. Although potentially helpful for natural survival, such downregulation may not be necessary in agricultural crops. If it could be prevented, crops might be harvested earlier or with higher cellulose content.

Sucrose phosphate synthase (SPS) has been implicated in the temperature stress sensitivity of cellulose synthesis. In cotton fibers, exposure to 15°C nights suppresses SPS activity (even during the next warm day; Tummala 1996), and 15°C reduces flux from Glc to Suc (Martin and Haigler 2004). In cellulose-sink cells, SPS could support cellulose synthesis by synthesizing Suc *de novo* and/or by recycling Fru released from sucrose by SuSy back to Suc. Transgenic cotton constitutively overexpressing SPS produces fibers with increased cellulose content under cool night temperatures in a growth chamber (Haigler et al. 2000). Given the economic importance of cellulose and its special role

in plant biochemistry as a large carbon sink composed of structural fibrils, we can expect much future research directed toward understanding how cellulose synthesis is integrated into general cellular metabolism. These data coupled with further understanding of mechanisms of glucan chain polymerization and microfibril biogenesis will provide clues to biotechnological strategies for modification of cellulose content and/or properties (Delmer and Haigler 2002).

Acknowledgments

Related research in the author's laboratory was partially supported by NSF grant DBI 9872627 and by grants from Cotton Inc., Cary, North Carolina and the Texas Advanced Research and Technology Programs.

REFERENCES

Amor Y., Haigler C.H., Wainscott M., Johnson S., and Delmer D.P. 1995. A membrane-associated form of sucrose synthase and its potential role synthesis of cellulose and callose in plants. Proc Natl Acad Sci USA 92:9353–9357.

Applequist W.L., Cronn R., and Wendel J.F. 2001. Comparative development of fiber in wild and cultivated cotton. Evol Dev 3:3–17.

Arthur J.C. 1990. Cotton. In: Kroschwitz J.I. (ed.) Polymers: fibers and textiles, a compendium. Wiley, New York, pp. 118–141.

Atalla R.H. and VanderHart D.L. 1984. Native cellulose: a composite of two distinct crystalline forms. Science 223:283–285.

Babb V.M. and Haigler C.H. 2001. Sucrose phosphate synthase activity rises in correlation with high-rate cellulose synthesis in three heterotrophic systems. Plant Physiol 127:1234–1242.

Baskin T.I. 2001. On the alignment of cellulose microfibrils by cortical microtubules: a review and a model. Protoplasma 215:150–171.

Barratt D.H.P., Barber L., Kruger N.J., Smith A.M., Wang T.L., and Martin C. 2001. Multiple, distinct isoforms of sucrose synthase in pea. Plant Physiol 127:655–664.

Basra A.S. and Malik C.P. 1984. Development of the cotton fiber. Int Rev Cytol 89:65–113.

Basra A.S., Sarlach R.S., Nayyar H., and Malik C.P. 1990. Sucrose hydrolysis in relation to development of cotton (*Gossypium* spp.) fibres. Indian J Expt Biol 28:985–988.

Benedict C.R., Schubert A.M., and Kohel R.J. 1980. Carbon metabolism in developing cotton seed: sink demand and the distribution of assimilates. Proc. Beltwide Cotton Prod. Res. Conf. National Cotton Council, Memphis, pp. 346–351.

Benedict C.R., Kohel R.J., and Jividen. G.M. 1994. Crystalline cellulose and cotton fiber strength. Crop Sci 34:147–151.

Buchala A.J. and Meier, H. 1985. Biosynthesis of ß-glucans in growing cotton (*Gossypium arboreum* L. and *Gossypium hirsutum* L.) fibers. In: Brett C.T. and Hillman J.R. (eds.) Biochemistry of plant cell walls. Cambridge University Press, Cambridge, pp. 220–241.

Buchala A.J. 1987. Acid β-fructofuranoside fructohydrolase (invertase) in developing cotton (*Gossypium arboreum* L.) fibres and its relationship to β-glucan synthesis from sucrose fed to the fibre apoplast. J Plant Physiol 127:219–230.

Buchala A.J. 1999. Noncellulosic carbohydrates in cotton fibers. In: Basra A.S. (ed.) Cotton Fibers: Developmental Biology, Quality Improvement, and Textile Processing, The Haworth Press, New York, pp. 113–136.

Burk D.H. and Ye Z.-H. 2002. Alteration of oriented deposition of cellulose microfibrils by mutation of a katanin-like microtubule severing protein. Plant Cell 14:2145–2160.

Carpita N.C. and Delmer D.P. 1981. Concentration and metabolic turnover of UDP-Glucose in developing cotton fibers. J Biol Chem 256:308–315.

Chanzy H., Imada K., and Vuong R. 1978. Electron diffraction from the primary wall of cotton fibers. Protoplasma 94:299–306.

Chourey P.S., Taliercio E.W., Carlson S.J., and Ruan Y.L. 1998. Genetic evidence that the two isozymes of sucrose synthase present in developing maize endosperm are critical, one for cell wall integrity and the other for starch biosynthesis. Mol Gen Genet 259:88–96.

Cronn R.C., Small R.L., and Wendel J.F. 1999. Duplicated genes evolve independently after polyploid formation in cotton. Proc Natl Acad Sci USA 96:14406–14411.

Davidonis G. 1993. Cotton fiber growth and development *in vitro*: effects of tunicamycin and monensin. Plant Sci 88:229–236.

DeLanghe E.A.L. 1986. Lint development. In: Mauney J.R. and Stewart J. McD. (eds.) Cotton Physiology. The Cotton Foundation, Memphis, TN, pp. 325–350.

Delmer D.P. 1999. Cellulose biosynthesis in developing cotton fibers. In: Basra A.S. (ed.) Cotton Fibers: Developmental Biology, Quality Improvement, and Textile Processing. The Haworth Press, New York, pp. 85–112.

Delmer D.P. and Haigler C.H. 2002. The regulation of metabolic flux to cellulose, a major sink for carbon in plants. Metabolic Eng 4:22–28.

DiNiro M.J. and Cooper L.W. 1989. Post-photosynthetic modification of oxygen isotope ratios of carbohydrates in the potato: implications for paleoclimatic reconstruction based upon isotopic analysis of wood cellulose. Geochimica et Cosmochimica Acta 53:2573–2580.

Dixon D.C., Seagull R.W., and Triplett B.A. 1994. Changes in the accumulation of a- and ß-tubulin isotypes during cotton fiber development. Plant Physiol 105:1347–1353.

Doblin M.S., Kurek K., Jacob-Wilk D., and Delmer D.P. 2002. Cellulose biosynthesis in plants: from genes to rosettes. Plant Cell Physiol 43:1407–1420.

Doehlert D.C. 1987. Substrate inhibition of maize endosperm sucrose synthase by fructose and its interaction with glucose inhibition. Plant Sci 52:153–157.

Franz G. 1969. Soluble nucleotides in growing cotton hair. Phytochem 8:737–741.

Gipson J.R. 1986. Temperature effects on growth, development, and fiber properties. In: Mauney J.R. and Stewart J. McD. (eds.) Cotton Physiology. The Cotton Foundation, Memphis, TN, pp. 47–56.

Haigler C.H. and Brown, Jr. R.M., 1986. Transport of rosettes from the Golgi apparatus to the plasma membrane in isolated mesophyll cells of *Zinnia elegans* during differentiation to tracheary elements in suspension culture. Protoplasma 134:111–120.

Haigler C.H., Rao N.R., Roberts E.M., Huang J.Y., Upchurch D.P., and Trolinder N.L. 1991. Cultured cotton ovules as models for cotton fiber development under low temperatures. Plant Physiol 95:88–96.

Haigler C.H., Taylor J.G., and Martin L.K. 1994. Temperature dependence of fiber cellulose biosynthesis: Impact on fiber maturity and strength. In: Proceedings of the Biochemistry of Cotton Workshop, Galveston, TX, September 28–30. Cotton Inc., Raleigh, NC, pp. 95–100.

Haigler C.H., Cai W., Martin L.K., Tummala J., Anconetani R., Gannaway J.G., Jividen G.J., and Holaday A.S. 2000. Mechanisms by which fiber quality and fiber and seed weight can be improved in transgenic cotton growing under cool night temperatures. Proc Beltwide Cotton Conference, National Cotton Council, Memphis, p. 483.

Haigler C.H., Ivanova-Datcheva M., Hogan P.S., Salnikov V.V., Hwang S., Martin L.K., and Delmer D.P. 2001. Carbon partitioning to cellulose synthesis. Plant Mol Biol 47:29–51.

Hannah L.C., Frommer W., Su J.-C., Chourey P., and Park W. 1994. Sucrose synthases. Plant Mol Biol Rep 12:S72.

Hauch S. and Magel E. 1998. Extractable activities and protein content of sucrose-phosphate synthase, sucrose synthase, and neutral invertase in trunk tissue of *Robinia pseudoacacia* L. are related to cambial wood production and heartwood formation. Planta 207:266–274.

Hayashi T., Read S.M., Bussell J., Thelen M., Lin F.-C., Brown, Jr. R.M., and Delmer D.P. 1987. UDP-glucose: (1→3)-ß-glucan synthase from mung bean and cotton. Plant Physiol 83:1054–1062.

Hendrix D.L. 1990. Carbohydrates and carbohydrate enzymes in developing cotton ovules. Physiol Plant 78:85–92.

Herth W. 1989. Inhibitor effects on putative cellulose synthetase complexes of vascular plants. In: Schuerch C. (ed.) Cellulose and Wood: Chemistry and Technology. Wiley, New York, pp. 795–810.

Hertzberg M., Aspeborg H., Schrader J., Andersson A., Erlandsson R., Blomqvist K., Bhalerao R., Uhlen M. Teeri T.T., Lundeberg J., Sundberg B., and Nilsson P. 2001. A transcriptional road map to wood formation. Proc Natl Acad Sci 98:14732–14737.

Hill S.A., Waterhouse J.S., Field E.M., Switsur V.R., and Rees A.P.T. 1995. Rapid recycling of triose phosphates in oak stem tissue. Plant Cell Environment 18:931–936.

Hsieh Y.L. 1999. Structural development of cotton fibers and linkages in fiber quality, In: Basra A.S. (ed.) Cotton Fibers: Developmental Biology, Quality Improvement, and Textile Processing. The Haworth Press, New York, pp. 137–166.

Hu X.P. and Hsieh Y.L. 1996. Crystalline structure of developing cotton fibers. J Polym Sci: Part B: Polymer Physics 34:1451–1459.

Huber S.C. and Huber J.L. 1996. Role and regulation of sucrose-phosphate synthase in higher plants. Annu Rev Plant Physiol Plant Mol Biol 47:431–444.

Jaquet J.P., Buchala A.J., and Meier H. 1982. Changes in the non-structural carbohydrate content of cotton (*Gossypium* spp.) fibres at different stages of development. Planta 156:481–486.

Kanabus J., Bressan R.A., and Carpita N.C. 1986. Carbon assimilation in carrot cells in liquid culture. Plant Physiol 82:363–368.

Kim H.J. and Triplett B.A. 2001. Cotton fiber growth in planta and *in vitro*. Models for plant cell elongation and cell wall biogenesis. Plant Physiol 127:1361–1366.

Kimura S., Laosinchai W., Itoh T., Cui X., Linder R., and Brown, Jr., R.M., 1999. Immunogold labeling of rosette terminal cellulose-synthesizing complexes in the vascular plant *Vigna angularis*. Plant Cell 11:2075–2085.

Kloth R.H. 1989. Changes in the level of tubulin subunits during development of cotton (*Gossypium hirsutum*) fiber. Physiol Plant 76:37–41.

Kohel R.J., Benedict C.R., and Jividen G.M. 1993. Incorporation of ^{14}C-glucose into crystalline cellulose in aberrant fibers of mutant cotton. Crop Sci 33:1036–1040.

Kudlicka K. and Brown, Jr. R.M., 1997. Cellulose and callose biosynthesis in higher plants. I. Solubilization and separation of (1→3)- and (1→4)-β-glucan synthase activities from mung bean. Plant Physiol 115:643–656.

Kudlicka K., Brown, Jr. R.M., Li L., Lee J.H., Shin H., and Kuga S. 1995. β-glucan synthesis in the cotton fiber. IV. *In vitro* assembly of the cellulose I allomorph. Plant Physiol 107:111–123.

Kurek I., Kawagoe Y., Jacob-Wilk D., Doblin M., and Delmer D. 2002. Dimerization of cotton fiber cellulose synthase catalytic subunits occurs via oxidation of the zinc binding domains. Proc Natl Acad Sci 99:11109–11104.

Kutschera U. and Heiderich A. 2002. Sucrose metabolism and cellulose biosynthesis in sunflower hypocotyls. Phys Plant 114:372–379.

Lai-Kee-Him J., Chanzy H., Müller M., Putaux J.L., Imai T., and Bulone V. 2002. *In vitro* versus *in vivo* cellulose microfibrils from plant primary wall synthases: structural differences. J Biol Chem 277:36931–36939.

Laosinchai W., Cui X., and Brown, Jr. R.M., 2000. A full-length cDNA of cotton cellulose synthase has high homology with the *Arabidopsis* RSW1 gene and the cotton CelA1 gene (PGR 00-002). Plant Physiol 122:291.

Liu B., Brubaker C.L., Mergeai G., Cronn R.C., and Wendel J.F. 2001. Polyploid formation in cotton is not accompanied by rapid genomic changes. Genome 44:321–330.

Lunn J.E. and MacRae E. 2003. New complexities in the synthesis of sucrose. Curr Op Plant Biol 6:208–214.

Martin L.K. and Haigler C.H. 2004. Cool temperature hinders flux from glucose to sucrose during secondary wall synthesis in secondary wall stage cotton fibers. Cellulose 11:339–349.

Matthysse A.G., White S., and Lightfoot R. 1995a. Genes required for cellulose synthesis in *Agrobacterium tumefaciens*. J Bacteriol 177:1069–1075.

Matthysse A.G., Thomas D.O.L., and White A.R. 1995b. Mechanism of cellulose synthesis in *Agrobacterium tumefaciens*. J Bacteriol 177:1076–1081.

Meinert M.C. and Delmer D.P. 1977. Changes in biochemical composition of the cell wall of the cotton fiber during development. Plant Physiol 59:1088–1097.

Mutsaers H.J.W. 1976. Growth and assimilate conversion of cotton bolls (*Gossypium hirsutum* L.) 1. Growth of fruits and substrate demand. Ann Bot 40:301–315.

Nguyen-Quoc B. and Foyer C.H. 2001. A role for futile cycles involving invertase and sucrose synthase in sucrose metabolism of tomato fruit. J Expt Bot 52:881–889.

Odanaka S., Bennett A.B., and Kanayama Y. 2002. Distinct physiological roles of fructokinase isozymes revealed by gene-specific suppression of Frk1 and Frk2 expression in tomato. Plant Phys 129:1119–1126.

O'Sullivan A.C. 1997. Cellulose: the structure slowly unravels. Cellulose 4:173–207.

Pear J., Kawagoe Y., Schreckengost W., Delmer D.P., and Stalker D. 1996. Higher plants contain homologs of the CelA genes that encode the catalytic subunit of the bacterial cellulose synthases. Proc Natl Acad Sci USA 93:12637–12642.

Peng L., Kawagoe Y., Hogan P., and Delmer D. 2001a. Sitosterol-ß-glucoside as primer for cellulose synthesis in plants. Science 295:147–150.

Peng L., Xian F., Roberts E., Kawagoe Y., Greve L.C., Kreuz K., and Delmer D.P. 2001b. The experimental herbicide CGA 325′615 inhibits synthesis of crystalline cellulose and causes accumulation of non-crystalline β-1,4-glucan associated with CesA protein. Plant Physiol 126:981–992.

Pettigrew W.T. 1994. Source-to-sink manipulation effects on cotton fiber quality. Agron J 87:947–952.

Pillonel C. and Meier H. 1985. Influence of external factors on callose and cellulose synthesis during incubation *in vitro* of intact cotton fibers with [^{14}C]sucrose. Planta 165:76–84.

Pillonel C., Buchala A.J., and Meier H. 1980. Glucan synthesis by intact cotton fibres fed with different precursors at the stages of primary and secondary wall formation. Planta 149:306–312.

Potikha T.S., Collins C.C., Johnson D.I., Delmer D.P., and Levine A. 1999. The involvement of hydrogen peroxide in the differentiation of secondary walls in cotton fibers. Plant Physiol 119:849–858.

Ramey H.H., Jr. 1986. Stress influences on fiber development. In: Mauney J.R. and Stewart J. McD. (eds.) Cotton Physiology. The Cotton Foundation, Memphis, TN, pp. 351–360.

Rebenfield L. 1990. Fibers. In: Kroschwitz J.I. (ed.) Polymers: Fibers and Textiles: A Compendium. Wiley, New York, pp. 219–305.

Roberts E.M., Nunna R.R., Huang J.Y., Trolinder N.L., and Haigler C.H. 1992. Effects of cycling temperatures on fiber metabolism in cultured cotton ovules. Plant Physiol 100:979–986.

Rollit J. and Maclachlan G.A. 1974. Synthesis of wall glucan from sucrose by enzyme preparations from *Pisum sativum*. Phytochem 13:367–374.

Ruan Y.-L., Chourey P.S., Delmer D.P., and Perez-Grau L. 1997. The differential expression of sucrose synthase in relation to diverse patterns of carbon partitioning in developing cotton seed. Plant Physiol 115:375–385.

Ruan Y.-L., Llewellyn D.J., and Furbank R.T. 2003. Suppression of sucrose synthase gene expression represses cotton fiber cell initiation, elongation, and seed development. The Plant Cell 15:952–964.

Ryser U. 1985. Cell wall biosynthesis in differentiating cotton fibres. Eur J Cell Biol 39:236–256.

Ryser U. 1992. Ultrastructure of the epidermis of developing cotton (*Gossypium*) seeds: Suberin, pits, plasmodesmata, and their implications for assimilate transport into cotton fibers. Amer J Bot 79:14–22.

Ryser U. 1999. Cotton fiber initiation and histodifferentiation. In: Basra A.S. (ed.) Cotton Fibers: Developmental Biology, Quality Improvement, and Textile Processing, The Haworth Press, New York, pp. 1–46.

Salnikov V.V., Grimson M.J., Delmer D.P., and Haigler C.H. 2001. Sucrose synthase localizes to cellulose synthesis sites in tracheary elements. Phytochem 57:823–833.

Salnikov V., Grimson M.J., Seagull R.W., and Haigler C.H. 2003. Localization of sucrose synthase and callose in freeze substituted, secondary wall stage, cotton fibers. Protoplasma 221:175–184.

Shimizu Y., Aotsuka S., Hasegawa O., Kawada T., Sakuno T., Sakai F., and Hayashi T. 1997. Changes in levels of mRNA for cell wall-related enzymes in growing fiber cells. Plant Cell Physiol 38:375–378.

Schrader S. and Sauter J.J. 2002. Seasonal changes of sucrose-phosphate synthase and sucrose synthase activities in poplar wood (*Populus x Canadensis* Moench robusta) and their possible role in carbohydrate metabolism. J Plant Physiol 159:833–843.

Schubert A.M., Benedict C.R., Gates C.E., and Kohel R.J. 1976. Growth and development of the lint fibers of Pima S-4 cotton. Crop Sci 16:539–543.

Seagull R.W. 1986. Changes in microtubule organization and wall microfibril orientation during *in vitro* cotton fiber development: an immunofluorescent study. Can J Bot 64:1373–1381.

Seagull R.W. 1992. A quantitative electron microscopic study of changes in microtubule arrays and wall microfibril orientation during *in vitro* cotton fiber development. J Cell Sci 101:561–577.

Seagull R.W. 1993. Cytoskeletal involvement in cotton fiber growth and development. Micron 24:643–660.

Seagull R.W. 1995. Cotton fiber growth and development: evidence for tip synthesis and intercalary growth in young fibers. Plant Physiol (Life Sci Adv) 14:27–38.

Subbaiah C.C. and Sachs M.M. 2001. Altered patterns of sucrose synthase phophorylation and localization precede callose induction and root tip death in anoxic maize seedlings. Plant Physiol 125:585–594.

Taylor M.A., Ross H.A., McRae D., Stewart D., Roberts I., Duncan G., Wright F., Millam S., and Davies H.V. 2000. A potato α-glucosidase gene encodes a glycoprotein-processing α-glucosidase II-like activity. Demonstration of enzyme activity and effects of down-regulation in transgenic plants, Plant J 24:305–316.

Thaker V.S., Saroop S., Vaishnav P.P., and Singh Y.D. 1989. Genotypic variations and influence of diurnal temperature on cotton fiber development. Field Crops 22:1–13.

Timpa J.D. 1992. Molecular chain length distributions of cotton fiber: developmental, varietal, and environmental influences. In: Benedict C.R. (ed.) Proceedings of cotton fiber cellulose: structure, function, and utilization conference. National Cotton Council, Memphis, TN, pp. 199–210.

Timpa J.D. and Wanjura D.F. 1989. Environmental stress responses in molecular parameters of cotton cellulose. In Schuerch C. (ed.) Cellulose and Wood—Chemistry and Technology. Wiley, New York, pp. 1145–1156.

Timpa J.D. and Triplett B.A. 1993. Analysis of cell-wall polymers during cotton fiber development. Planta 189:101–108.

Triplett B.A. 1993. Using biotechnology to improve cotton fiber quality: progress and perspectives, In: Cellulosics: Pulp, Fibre, and Environmental Aspects. Ellis Horwood, Chichester, UK, pp. 135–140.

Triplett B.A. 1998. Stage-specific inhibition of cotton fiber development by adding a-amanitin to ovule cultures. *In vitro* cell dev biol-plant 34:27–33.

Tummala J. 1996. Response of sucrose phosphate synthase activity to cool temperatures in cotton. M.S. thesis, Texas Tech University, Lubbock, TX.

Waffler U. and Meier H. 1994. Enzyme activities in developing cotton fibres. Plant Physiol Biochem 32:697–702.

Wagner K.G. and Backer A.I. 1992. Dynamics of nucleotides in plants studied on a cellular basis. In: Jeon K.W. and Friedlander M. (eds.) International Review of Cytology: A Survey of Cell Biology. Academic Press, San Diego, CA, pp. 1–84.

Wartelle L.H., Bradow J.M., Hinojasa O., Pepperman A.B., Sassenrath-Cole G.F., and Dastoor P. 1995. Quantitative cotton fiber maturity measurements by x-ray fluorescence spectroscopy and AFIS. J Agric Food Chem 43:1219–1223.

Waterkeyn L. 1981. Cytochemical localization and function of the 3-linked glucan callose in the developing cotton fibre cell wall. Protoplasma 106:49–60.

Wendel J.F., Small R.L., Cronn R.C., and Brubaker C.L. 1999. Genes, jeans, and genomes: reconstructing the history of cotton. In: van Raamsdonk L.W.D. and denNijs J.C.M. (eds.) Plant Evolution in Man-Made Habitats: Proceedings of the VIIth Symposium, IOPB. Hugo de Vries Laboratory, Amsterdam, pp. 133–159.

Williamson R.E., Burn J.E., and Hocart C.H. 2001. Cellulose synthesis: mutational analysis and genomic perspectives using *Arabidopsis thaliana*. Cell Mol Life Sci 58:1–16.

Willison J.H.M. 1983. The morphology of supposed cellulose-synthesizing structures in higher plants. J Appl Polym Sci: Appl Polym Symp 37:91–105.

Willison J.H.M. and Brown, Jr. R.M. 1977. An examination of the developing cotton fiber: wall and plasmalemma. Protoplasma 92:21–41.

Winter H. and Huber S.C. 2000. Regulation of sucrose metabolism in higher plants: Localization and regulation of activity of key enzymes. Crit Rev Plant Sci 19:31–67.

Winter H., Huber J.L., and Huber S.C. 1998. Identification of sucrose synthase as an actin-binding protein. FEBS Lett 430:205–208.

Yakir D. and DiNiro M.J. 1990. Oxygen and hydrogen isotope fractionation during cellulose metabolism in *Lemna gibba* L. Plant Physiol 93:325–352.

CHAPTER 10

A PERSPECTIVE ON THE ASSEMBLY OF CELLULOSE-SYNTHESIZING COMPLEXES: POSSIBLE ROLE OF KORRIGAN AND MICROTUBULES IN CELLULOSE SYNTHESIS IN PLANTS

INDER M. SAXENA AND R. MALCOLM BROWN, JR.*

Section of Molecular Genetics and Microbiology, School of Biological Sciences, The University of Texas at Austin, Austin, TX 78712

Abstract

Cellulose is synthesized on the plasma membrane by protein complexes referred to as terminal complexes (TCs). In plants, the TCs are visualized by freeze-fracture electron microscopy as rosettes with a sixfold symmetry. Each rosette synthesizes a cellulose microfibril containing approximately 36 glucan chains. So far, only the cellulose synthase catalytic subunit (CesA) is shown to be localized to the rosette complex, and it is suggested that at least 36 CesA molecules are present in each rosette. Moreover, from analysis of the *CesA* genes, it is predicted that at least three different CesAs are required for assembly of the rosette and the cellulose microfibril. How the different CesA subunits assemble into a rosette structure is not clearly understood. In our view, the assembly of the rosette proceeds in stages, beginning from the rough endoplasmic reticulum (ER) to the plasma membrane, with the final assembly of the rosette structure taking place on the plasma membrane. The membrane-localized endo-1,4-β-D-glucanase, KORRIGAN is probably involved in digesting the noncrystalline cellulose product formed from an assembly of six CesA subunits that compose a rosette particle and is transported to the plasma membrane via vesicles. These rosette particles then assemble into a complete rosette TC in the plasma membrane when the glucan chains synthesized from closely placed particles associate to form crystalline cellulose I microfibrils. The role of microtubules in aligning cellulose microfibrils has been widely debated, and we believe that microtubules probably are involved in aligning the cellulose microfibrils in an indirect manner by "channelizing" the direction of microfibril assembly.

* Author for correspondence: Section of Molecular Genetics and Microbiology, School of Biological Sciences, The University of Texas at Austin, Austin, TX 78712, Tel: 512-471-3364; Fax: 512-471-3573; e-mail: rmbrown@mail.utexas.edu

R.M. Brown, Jr. and I.M. Saxena (eds.), Cellulose: Molecular and Structural Biology, 169–181.

Keywords

cellulose, cellulose biosynthesis, cellulose-synthesizing complex, cellulose synthase, KORRIGAN, microtubules.

1 INTRODUCTION

Cellulose may not be a universal biomacromolecule, yet the capability to synthesize cellulose is a much more universal property than previously understood. The realization that the capability to synthesize cellulose may be more widespread has occurred essentially from sequencing of genomes of a large number of organisms, mostly microorganisms. From these studies, genes encoding the cellulose synthase and a few other proteins have been identified in many bacterial species (Römling 2002). Although the genes for cellulose synthesis are present in these organisms, it is not known if all these organisms do in fact synthesize cellulose. Cellulose synthesis has been known for some time in bacterial species such as *Acetobacter xylinum* and *Agrobacterium tumefaciens* (Ross et al. 1991), but recently it has been demonstrated in bacteria such as *Escherichia coli*, *Salmonella typhimurium*, *Pseudomonas fluorescens* and others, and in many of these cases the cellulose is found associated with biofilms (Zogaj et al. 2001; Spiers and Rainey 2005). Unlike bacterial cells, cellulose produced by plant cells is a structural component of the cell wall and the direction of cellulose synthesis helps determine cell growth and elongation.

In general, organisms that synthesize cellulose microfibrils do so from organized cellulose-synthesizing sites on the membrane that are often referred to as terminal complexes (TCs). The crystalline nature of cellulose implies an ordered arrangement of glucan chains in cellulose microfibrils and hence the suggestion that the cellulose-synthesizing sites in the cell are organized such that the glucan chains are able to interact with each other and form a crystalline structure while they are being synthesized (coupled polymerization-crystallization). The first organized site of cellulose synthesis was observed as a linear arrangement of particles in three rows in the green alga *Oocystis apiculata* (Brown, Jr. and Montezinos 1976). Two major arrangements of cellulose-synthesizing sites (linear and rosette) have since been identified in most cellulose-synthesizing organisms, and the cellulose synthase has been localized to the rosette complex in plants (Kimura et al. 1999). While it is obvious that an ordered array of cellulose synthases is required for synthesis of cellulose microfibrils, it is not very clear as to how these enzyme molecules are organized in TCs in the different cellulose producing organisms. Considering what is known about the role of different genes and proteins during cellulose synthesis, we wish to present a renewed perspective on the assembly of TCs in cellulose-synthesizing organisms, and more specifically the assembly of the rosette TC and the role that KORRIGAN (KOR) and the microtubules may have in influencing this and cellulose microfibril assembly in plants.

2 STRUCTURE AND COMPOSITION OF CELLULOSE-SYNTHESIZING COMPLEXES

Cellulose-synthesizing TCs were first observed by freeze-fracture electron microscopy. In general, they are visualized as intramembranous particles that are organized either as a linear row or as a rosette-like structure on the P-fracture face of the plasma membrane (Brown, Jr. 1996). Lately it has also been possible to visualize the cytosolic side of the rosette TCs in membrane sheets prepared from plants (http://www.botany.utexas.edu/facstaff/facpages/mbrown/bowling/default2.html). While bacteria, such as *A. xylinum,* have a single row of particles organized as a linear TC and all land plants have a hexameric rosette TC, great diversity in TC architecture is observed in the algae (Tsekos 1999). Both linear and rosette TCs are found in the algae, with the linear TCs and rosettes in turn being organized in rows in certain algae.

In spite of the fact that TCs are relatively large membrane-embedded structures, biochemical approaches to isolate and identify the protein composition of the TCs has been challenging. However, a protein aggregate suggestive of the TC has been found attached to cellulose microfibrils synthesized *in vitro* using membrane extracts from plants (Lai-Kee-Him J 2002; Laosinchai 2002) and cellulose synthase was localized to this protein aggregate (Laosinchai 2002).

Much of our understanding of the TCs has, in fact, been obtained from genetic and microscopic analyses. Interestingly, genetic analysis of cellulose-deficient mutants in plants led to the proposal that the rosette TC contains three different nonredundant cellulose synthases, and mutation in any one of these results in a defect in the assembly of cellulose microfibrils (Taylor et al. 2003). In addition, the cellulose synthases identified for cellulose synthesis in the primary cell wall are different from the cellulose synthases required for cellulose synthesis in the secondary cell wall (Robert et al. 2004). In spite of the failure to localize any other protein except the cellulose synthase to the rosette TC, other proteins have been predicted by mutant analysis to be associated with the complex and these may have a direct or indirect role in cellulose synthesis.

One of the intriguing proteins that is suggested to have a role in cellulose synthesis is KOR, a membrane-bound endo-1,4-β-D-glucanase. Mutations in the *KOR* gene lead to an altered phenotype and a reduction in the amount of cellulose (Nicol et al. 1998). Based on the features of the mutants, the KOR protein has been suggested to be involved in cellulose biosynthesis (Mølhøj et al. 2002). However, the mechanism of KOR function during cellulose synthesis is not clearly understood. Recent experiments using GFP-labeled KOR demonstrate that this protein is present in intracellular compartments and probably undergoes cycling between these compartments and the plasma membrane (Robert et al. 2005). In a later section, we will suggest a possible role of KOR in cellulose biosynthesis.

The intramembrane particles in a linear TC or in a rosette have been observed quite well by freeze-fracture, but not much is known with respect to the cytoplasmic face of these particles. From sequence analysis of cellulose synthases, a

large globular region of this protein is predicted to be present in the cytosol and as such the TC is predicted to be much larger on the cytosolic side than what is observed on the cell surface following freeze-fracture (Saxena and Brown, Jr. 2005). Since the globular region contains the putative active site of the cellulose synthase and possibly other site(s) for protein–protein interaction, knowledge of the cytosolic region of TCs is crucial for understanding not only the mechanism of cellulose synthesis but also as to how the TC is assembled and regulated. In the absence of isolated TCs, electron microscopic observations provide some very interesting clues to the nature of the cytosolic side of these complexes. Early evidence with respect to the dimensions of the cytosolic region of TCs was obtained from thin sections of the linear TCs in the alga *Boergesenia forbesii* (Kudlicka et al. 1987). Recently, using membrane fragments it was possible to visualize the cytoplasmic face of the rosette complex in plants and the dimensions observed in these studies suggest that a much larger region of the complex extends into the cytoplasm (Bowling 2005). In addition, cortical microtubules and clathrin-coated vesicles are clearly observed on the cytosolic side of the membrane fragments (Bowling 2005). Even though no other proteins have been identified in association with the cytosolic region of the TCs, it is possible that this region may interact with a variety of proteins, including the cytoskeleton, either directly or indirectly through other proteins.

3 STAGES IN THE ASSEMBLY OF THE ROSETTE TERMINAL COMPLEX IN PLANTS

It is assumed that each rosette TC in plants contains 36 cellulose synthase molecules, each of which is presumably involved in the synthesis of a single glucan chain. Each rosette is composed of six particles and each particle is therefore considered to be an assemblage of six cellulose synthase molecules. The current view holds that the rosette TCs in plants are assembled in the Golgi apparatus, where they exist in an inactive state (Haigler and Brown, Jr. 1986). The rosette TCs are subsequently transported via cytoplasmic vesicles from the Golgi apparatus to the plasma membrane where they are activated for cellulose synthesis. While rosette TCs also have been observed in vesicles in the alga *Micrasterias denticulata* (Giddings et al. 1980), a linear row of particles representing TC precursors have been observed in large, dense cytoplasmic vesicles, quite different from the Golgi vesicles, in the alga *Botrydiopsis intercedens* (Okuda et al. 2004).

The observation of TCs in vesicles suggests that the TCs are assembled prior to their insertion in the plasma membrane and are transported from the Golgi apparatus via an exocytic pathway. However, at this point it is not completely certain if the vesicles containing the TCs are part of an exocytic or an endocytic pathway. Clathrin-coated endocytic vesicles are known to form at the plasma membrane, and in certain cases recycling of components have been reported to occur from the plasma membrane to the Golgi apparatus (Neumann et al. 2003). Moreover, it is not very clear as to how the cellulose synthases stay inactive until they are present in

the plasma membrane, although suggestions have been made that the activation of cellulose synthases is regulated by their phosphorylation state (Somerville 2006).

In our view, being membrane proteins, the cellulose synthase polypeptide chains are synthesized on the rough endoplasmic reticulum (ER), where they undergo folding and probably assemble into a higher order structure. Although assembly of the cellulose synthases into a rosette can proceed completely in the ER or in the Golgi apparatus or the plasma membrane or can take place in stages, it is more likely that at least some assembly occurs in the ER. The ER ensures proper folding and assembly of proteins through a rather strict quality control mechanism in which unfolded or misassembled proteins are transported to the cytosol where they are targeted for destruction in the proteasome (Lord et al. 2000). ER-associated protein degradation (ERAD) is well documented in yeast and mammalian cells, and is now shown in plants as well (Di Cola et al. 2005; Müller et al. 2005). That the cellulose synthases or some component(s) of the cellulose-synthesizing machinery undergoes modification in the ER is evident from analysis of cellulose-deficient mutants such as *cyt1*, *knf* and *rsw3* that have defects in genes encoding mannose-1-phosphate guanylyltransferase (Lukowitz et al. 2001), α-glucosidase I (Gillmor et al. 2002) and glucosidase II (Burn et al. 2002) respectively. All these enzymes are required for the processing of *N*-linked glycans on ER-synthesized proteins, and this processing is essential for the proper folding and assembly of these proteins.

If a significant role is assigned to the quality control mechanism for proper folding and assembly of cellulose synthases in the ER, and some role is assigned to the influence of glucan chain crystallization on the rosette structure, then the assembly of the fully functional rosette TC can be visualized to take place in two stages. In the first stage, two copies each of three different cellulose synthases assemble to form a complex (rosette particle) containing six cellulose synthase molecules in the ER. The cellulose synthases in a single rosette particle assemble by protein–protein interaction using either the RING finger motif or another motif present in the cellulose synthases (Doblin et al. 2002). Requirement for three different cellulose synthases is based upon genetic and biochemical analyses that suggest interaction of specific cellulose synthases in the ER before they are transported (Taylor et al. 2003). The complex, assembled in the ER is then transported to the Golgi apparatus either by COPII vesicles or by direct ER-Golgi connections, and from the Golgi to the plasma membrane by Golgi-derived vesicles (Neumann et al. 2003). In any case, the rosette particle composed of six cellulose synthase molecules does not assemble into a higher-order structure (the rosette) in the intracellular compartments in the absence of crystalline cellulose formation. The single rosette particles cannot be differentiated from other intramembranous particles, and with freeze fracture, only the fully assembled rosette TC with six particles can be definitively shown to be associated with cellulose microfibrils (Mueller and Brown, Jr. 1980). The topology of the assembled complex of cellulose synthases in the ER, Golgi and the vesicles is such that the globular region containing their active site faces the cytosol. In the presence of UDP-glucose in the cytosol, cellulose synthase

molecules may be able to synthesize and secrete glucan chains into the lumen of these intracellular compartments, or they may stay in an inactive state. If glucan chain synthesis is initiated in the ER, the individual cellulose synthases would still be able to assemble into a single rosette particle, but not into the complete rosette TC. In this case, the glucan chains attached to cellulose synthases would only form glucan chain aggregates with six glucan chains and this would not be a crystalline product. Alternatively, if no glucan chains are synthesized in the intracellular compartments, no cellulose will be formed and as a result the rosette particles would not assemble into a rosette TC. Interestingly, intracellular synthesis of cellulose has been observed during scale formation in the Golgi apparatus in *Pleurochrysis* where crystalline cellulose forms a complex with other components in a spatial and temporal manner (Brown, Jr. and Romanovicz 1976; Romanovicz and Brown, Jr. 1976). Although scales are not found in plants, limited synthesis of noncrystalline cellulose may certainly take place in intracellular compartments in plants. In any case, the Golgi-derived vesicles containing the rosette particles fuse with the plasma membrane and the rosette particles can now assemble into the rosette TC in the plasma membrane. In the plasma membrane, the rosette particles may still be attached to the glucan chains, if synthesis occurred in the intracellular compartments. Alternatively, synthesis may initiate in the plasma membrane if the cellulose synthases are activated in the plasma membrane.

See Figure 10-1 for an illustration of two-step assembly of the rosette TC.

4 POSSIBLE ROLE OF KORRIGAN IN THE DIGESTION OF GLUCAN CHAINS AND IN THE SECOND STAGE OF THE ASSEMBLY OF THE TERMINAL COMPLEX

Most workers in the field agree that KOR probably has an indirect role in cellulose biosynthesis *in vivo*, but so far it has not been possible to assign a specific role to this protein in this process. In simple terms, it is believed that KOR hydrolyzes

Figure 10-1. Two-step assembly of the rosette terminal complex (TC) in plants. In the first stage, a cellulose synthase particle complex containing six cellulose synthase molecules is assembled in the ER by protein–protein interactions. Single rosette particles synthesize glucan chains that will stay attached as noncrystalline cellulose in the ER and other intracellular compartments. KOR is also synthesized in the ER and it may be transported from the Golgi apparatus in vesicles with or without the rosette particles. The vesicles carrying the rosette particles and/or KOR may be directed to sites of cellulose synthesis by the microtubules. Once the vesicles carrying the cellulose synthases and KOR fuse with the plasma membrane and the rosette particles are present in the plasma membrane, KOR is able to digest the noncrystalline cellulose. In the second stage, the assembly of the individual rosette particles into a hexameric rosette TC structure is favored by the assembly of glucan chains into a crystalline cellulose product. KOR can also digest the noncrystalline cellulose while in the Golgi apparatus, and under these circumstances assembly of the rosette can take place in the Golgi apparatus itself. KOR does not digest crystalline cellulose. The assembled rosette TC continues to synthesize cellulose microfibril and the movement of the cellulose synthase in the plasma membrane is governed by the rate of cellulose synthesis. The rosette particles, KOR, and in some cases even the rosette TC may be recycled from the plasma membrane (*See Color Plate of this figure beginning on page 355*)

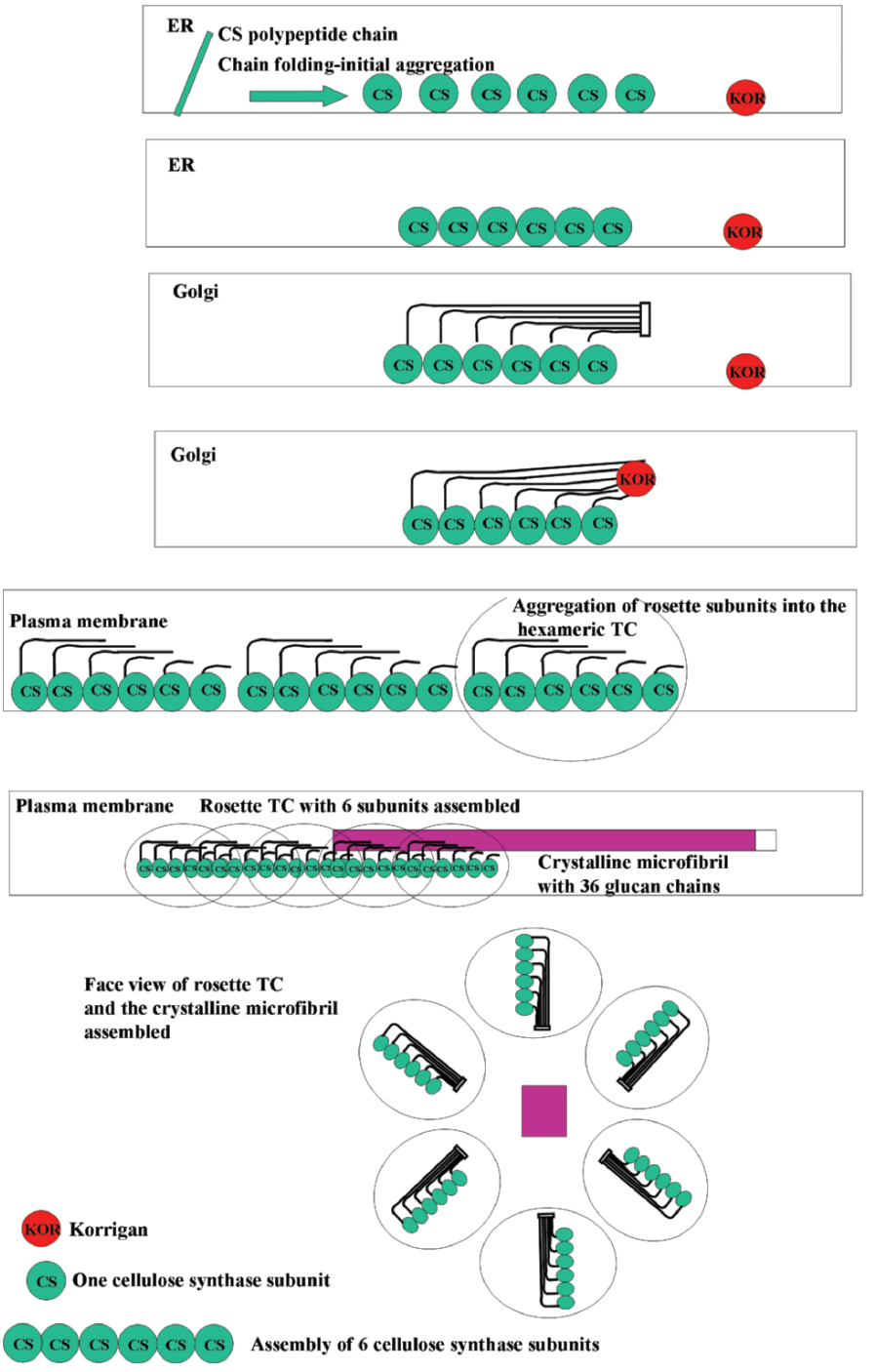
ER
CS polypeptide chain
Chain folding-initial aggregation
CS
KOR
ER
Golgi
Golgi
Plasma membrane
Aggregation of rosette subunits into the hexameric TC
Plasma membrane
Rosette TC with 6 subunits assembled
Crystalline microfibril with 36 glucan chains
Face view of rosette TC and the crystalline microfibril assembled
KOR Korrigan
CS One cellulose synthase subunit
Assembly of 6 cellulose synthase subunits

glucan chains in noncrystalline cellulose, and may possibly relieve stress generated during assembly of glucan chains in cellulose microfibrils (Mølhøj et al. 2002). Enzymatic analysis of a recombinantly-obtained soluble form of a KOR homolog from *Brassica napus* showed that this protein has substrate specificity for low substituted carboxymethyl cellulose and amorphous cellulose, but does not hydrolyze crystalline cellulose or the oligosaccharides cellotriose, cellotetraose and cellopentaose (Mølhøj et al. 2001). Similar properties also have been observed in a soluble form of the KOR homolog obtained from *Populus* (Master et al. 2004).

We believe that the KOR protein present in the plasma membrane is indirectly involved in the assembly of the rosette TC in plants by digesting the noncrystalline cellulose product attached to the rosette particles. It is known that polymerization and crystallization are coupled steps, and that crystallization influences the rate of polymerization during cellulose synthesis (Benziman et al. 1980). In the absence of crystallization, the polymerization reaction probably lasts only for a short period of time even though the enzyme may be fully active. Removal of the noncrystalline product attached to the cellulose synthase allows polymerization to continue, but in a more directed and controlled sense. Here we have a type of "editing mechanism" whereby the KOR protein removes disordered glucan chains that are not yet crystallized but that were critical in keeping the rosette particles in close proximity for final assembly which can take place once a fully crystalline ordered cellulose I microfibril begins to emerge from the TC. Once the noncrystalline cellulose is removed from the rosette particles, and where sufficient numbers of rosette particles are present to simultaneously produce the glucan chain aggregates, the glucan chain aggregates (we suggest a glucan chain aggregate consisting of six glucan chains bound by hydrophobic interactions) (Cousins and Brown, Jr. 1995) from each particle are able to associate with glucan chain aggregates from the other particles. This now becomes the second stage of crystallization, namely a hydrogen bonding interaction between the glucan chain aggregates to result in the crystallization of a cellulose I microfibril (Cousins and Brown, Jr. 1997a, b) and consequently, the polymerization-crystallization-induced assembly of a complete rosette TC. Therefore the cellulose–cellulose glucan chain association could ultimately lead to the final assembly of the hexameric rosette TC.

Obviously, crystallization of glucan chains is not the only mechanism required for assembly of the rosette TC. Most likely, certain features of the cellulose synthase protein influences either the assembly or the stability of the rosette TC, as is very clearly demonstrated in the disassembly of the rosette TCs in the *rsw1* mutant of *Arabidopsis* at restrictive temperature (Arioli et al. 1998). An even more interesting observation is the increase in the amount of noncrystalline cellulose, probably produced by the rosette particles in this mutant at the restrictive temperature (Arioli et al. 1998). In wild-type cells, a significant amount of the noncrystalline cellulose is digested by KOR on the plasma membrane. Recycling of the KOR from the plasma membrane occurs much more frequently and although most of the KOR is shown by microscopy to be localized in intracellular vesicles (Robert et al. 2005), its presence has been shown in isolated membrane fractions

as well (Nicol et al. 1998). It is expected that in the absence of KOR activity, many more particles with attached glucan chains will be present in the plasma membrane, and this will result in increase in the production of noncrystalline cellulose. Although a defect in KOR would affect the assembly of the particles into the rosette structure, reduced assembly of rosette TCs and cellulose microfibrils would proceed as long as some rosette particles are brought sufficiently close together before the synthesis of the glucan chains takes place. To a lesser extent, other proteins with an endoglucanase activity may be able to remove the noncrystalline cellulose and allow assembly of the rosette TC. Interestingly, *Arabidopsis* root-swelling mutants defective in KOR (*rsw2*) are cellulose-deficient but produce increased amounts of noncrystalline cellulose in comparison to wild-type cells (Lane et al. 2001), suggesting a role for KOR in the assembly of cellulose microfibrils possibly via assembly of the rosette TC.

5 ROLE OF MICROTUBULES IN CELLULOSE BIOSYNTHESIS

Understanding the relationship between cellulose microfibrils and cortical microtubules in plant cells has been an area of great interest and debate (Baskin 2001; Wasteneys 2004). While almost everyone agrees that the anisotropic growth of plant cells is dependent on the synthesis of cellulose microfibrils in a direction perpendicular to the elongating axis, what is not clear is the mechanism that determines the direction of cellulose biosynthesis or in other words, the ordering of the cellulose-synthesizing complexes on the plasma membrane. Evidence supporting the view that microtubules influence the direction of cellulose synthesis has come mostly from studies using inhibitors of microtubule formation. Although no direct interaction has been observed between microtubules and the cellulose-synthesizing complexes, two different versions of how microtubules may guide the cellulose-synthesizing complexes in the plasma membrane are prevalent in the literature (Baskin 2001). In one case, it is believed that during cellulose synthesis, the cellulose-synthesizing complexes move in the plasma membrane within tracks created by cortical microtubules associating with the plasma membrane. The result is that the cellulose microfibrils co-align with the underlying microtubules.In this case, the interaction between the microtubules and the cellulose-synthesizing complexes is indirect. Alternatively, the cellulose-synthesizing complexes are thought to be attached to the microtubules directly or indirectly through other protein(s) and the movement of the cellulose-synthesizing complexes during cellulose synthesis is guided by these microtubules (Paredez et al. 2006). However, in this case, the rate of movement of the rosette TCs in plants would be governed by the rate of synthesis of the cellulose microfibrils, and this movement would be affected if the TCs are attached to the microtubules. In fact, we know that the rate-limiting step in cellulose polymerization is directly controlled by the crystallization process (Benziman et al. 1980). In this work, it was demonstrated that the rate of polymerization increases up to four times the control rate when crystallization is inhibited by Calcofluor. From such observations, it is obvious

that the rate-limiting step in cellulose biosynthesis is the crystallization step. If the rosette TCs were directly associated with microtubules, the rate of cellulose synthesis would be greatly reduced or even terminated; however, this does not appear to be the case. Thus, it appears highly unlikely that any direct association of rosette TCs takes place with microtubules but rather, these act indirectly by "channelizing" the direction of microfibril assembly. One interesting indirect consequence of such "channelization" would be that aggregates of rosette TCs, each with their parallel cellulose microfibrils, could indirectly control the overall rate of cellulose synthesis. If clusters of cellulose microfibrils held together by hydrogen bonds occurs, then the overall synthesis of cellulose in this case would be rate-limiting.

While these two models suggest that it is the microtubules that guide the cellulose-synthesizing complexes and determine the orientation of the cellulose microfibrils in the plant cell wall, other models suggest that the cellulose microfibrils that are attached to the cellulose synthases determine the direction of movement of the cellulose-synthesizing complexes in the plasma membrane and as such the microtubules have no direct role in determining the direction of cellulose microfibril synthesis (Emons and Mulder 1998). This model is based on geometrical constraints and it states that the microfibrils are "deposited along paths determined by the geometry of the cell alone" and a function for microtubules is not clearly understood. In our view, favoring the indirect model that cellulose microfibrils do align with the microtubules, it is more likely that the microtubules have additional indirect functions in cellulose biosynthesis, especially in exocytosis by directing transport of vesicles containing the cellulose synthases and the KOR proteins to sites of cellulose synthesis in the plasma membrane (Robert et al. 2005).

6 SUMMARY

Since the discovery of TCs as cellulose-synthesizing sites almost three decades ago, we are now beginning to get a better understanding of their composition and how they may be assembled. The localization of the cellulose synthase (Kimura et al. 1999) and the analyses suggesting the presence of three nonredundant cellulose synthases (Taylor et al. 2003) in the rosette TC in plants were major milestones, but it is only now that we have begun to get a look at the cytosolic side of these large multimeric complexes (Bowling 2005). From the dimensions of the cytosolic region of the rosette TCs, it is apparent that they may not be attached to any cytoskeletal structure. In fact, the rosettes extend so deeply into the cytoplasm that they would actually displace the parallel array of cortical microtubules. That plasma membrane recycling occurs much more frequently is validated by the occurrence of a large number of clathrin-coated pits and vesicles observed in membrane sheets (Bowling 2005). Although more information is beginning to be obtained about the cellular localization and dynamic properties of cellulose synthase complexes (Paredez et al. 2006), it is not entirely clear as to how these complexes are assembled. We believe that the glucan chains attached to the cellulose synthases play a

major role in the final assembly of these complexes and propose that the initiation of cellulose synthesis via glucan chain polymerization and limited aggregation could lead to the hierarchical assembly of the sixfold complete rosette TC in plants. KOR may be involved in an editing function by removal of noncrystalline cellulose attached to single rosette particles and allowing the particles to assemble into a rosette when crystalline cellulose is formed.

Acknowledgments

The authors would like to acknowledge support from the Division of Energy Biosciences, Department of Energy (Grant DE-FG03-94ER20145) and the Welch Foundation (Grant F-1217).

REFERENCES

Arioli T., Peng L., Betzner A.S., Burn J., Wittke W., Herth W., Camilleri C., Höfte H., Plazinski J., Birch R., Cork A., Glover J., Redmond J., and Williamson R.E. 1998. Molecular analysis of cellulose biosynthesis in *Arabidopsis*. Science 279:717–720.

Baskin T.I. 2001. On the alignment of cellulose microfibrils by cortical microtubules: a review and a model. Protoplasma 215:150–171.

Benziman M., Haigler C.H., Brown, Jr. R.M., White A.R., and Cooper K.M. 1980. Cellulose biogenesis: Polymerization and crystallization are coupled processes in *Acetobacter xylinum*. Proc Natl Acad Sci USA 77:6678–6682.

Bowling A.J. 2005. Imaging the cytoplasmic domain of the rosette cellulose-synthesizing terminal complex. Ph.D. dissertation, The University of Texas, Austin.

Brown, Jr. R.M., 1996. The biosynthesis of cellulose. J Macromol Sci Pure Appl Chem A33:1345–1373.

Brown, Jr. R.M., and Montezinos D. 1976. Cellulose microfibrils: Visualization of biosynthetic and orienting complexes in association with the plasma membrane. Proc Natl Acad Sci USA 73:143–147.

Brown, Jr. R.M., and Romanovicz D.K. 1976. Biogenesis and structure of Golgi-derived cellulosic scales in *Pleurochrysis*. I. Role of the endomembrane system in scale assembly and exocytosis. Applied Polymer Symposium No. 28:537–585.

Burn J.E., Hurley U.A, Birch R.J., Arioli T., Cork A. and Williamson R.E. 2002. The cellulose-deficient *Arabidopsis* mutant *rsw3* is defective in a gene encoding a putative glucosidase II, an enzyme processing N-glycans during ER quality control. Plant J 32:949–960.

Cousins S.K. and Brown, Jr. R.M., 1995. Cellulose I microfibril assembly: computational molecular mechanics energy analysis favours bonding by van der Waals forces as the initial step in crystallization. Polymer 36:3885–3888.

Cousins S.K. and Brown, Jr. R.M., 1997a. X-ray diffraction and ultrastructural analyses of dye-altered celluloses support van der Waals forces as the initial step in cellulose crystallization. Polymer 38:897–902.

Cousins S.K. and Brown, Jr. R.M., 1997b. Photoisomerization of a dye-altered β-1, 4 glucan sheet induces the crystallization of a cellulose-composite. Polymer 38:903–912.

Di Cola A., Frigerio L., Lord J.M., Roberts L.M., and Ceriotti A. 2005. Endoplasmic reticulum-associated degradation of ricin A chain has unique and plant-specific features. Pl Physiol 137: 287–296.

Doblin M.S., Kurek I., Jacob-Wilk D., and Delmer D.P. 2002. Cellulose biosynthesis in plants: from genes to rosettes. Plant Cell Physiology 43:1407–1420.

Emons A.M.C. and Mulder B.M. 1998. The making of the architecture of the plant cell wall: How cells exploit geometry. Proc Natl Acad Sci USA 95:7215–7219.

Giddings T.H., Jr., Brower D.L., and Staehelin L.A. 1980. Visualization of particle complexes in the plasma membrane of *Micrasterias denticulata* associated with the formation of cellulose fibrils in primary and secondary cell walls. Journal of Cell Biology 84:327–339.

Gillmor C.S., Poindexter P., Lorieau J., Palcic M.M. and Somerville C. 2002. α-glucosidase I is required for cellulose biosynthesis and morphogenesis in *Arabidopsis*. J Cell Biol 156:1003–1013.

Haigler C.H. and Brown, Jr. R.M., 1986. Transport of rosettes from the Golgi apparatus to the plasma membrane in isolated mesophyll cells of *Zinnia elegans* during differentiation to tracheary elements in suspension culture. Protoplasma 134:111–120.

Kimura S., Laosinchai W., Itoh T., Cui X., Linder C.R., and Brown, Jr. R.M., 1999. Immunogold labeling of rosette terminal cellulose-synthesizing complexes in the vascular plant *Vigna angularis*. Plant Cell 11:2075–2085.

Kudlicka K., Wardrop A., Itoh T., and Brown, Jr. R.M., 1987. Further evidence from sectioned material in support of the existence of a linear terminal complex in cellulose synthesis. Protoplasma 136:96–103.

Lai-Kee-Him J., Chanzy H., Müller M., Putaux J.-L., Imai T., and Bulone V. 2002. *In vitro* versus *in vivo* cellulose microfibrils from plant primary wall synthases: structural differences. J Biol Chem 277:36931–36939.

Lane D.R., Wiedemeier A., Peng L., Höfte H., Vernhettes S., Desprez T., Hocart C.H., Birch R.J., Baskin T.I., Burn J.E., Arioli T., Betzner A.S., and Williamson R.E. 2001. Temperature-sensitive alleles of *RSW2* link the KORRIGAN endo-1,4-β-glucanase to cellulose synthesis and cytokinesis in *Arabidopsis*. Pl Physiol 126:278–288.

Laosinchai W. 2002. Molecular and biochemical studies of cellulose and callose synthase. Ph.D. dissertation, The University of Texas, Austin.

Lukowitz W., Nickle T.C., Meinke D.W., Last R.L., Conklin P.L., and Somerville C.R. 2001. *Arabidopsis cyt1* mutants are deficient in a mannose-1-phosphate guanylyltransferase and point to a requirement of N-linked glycosylation for cellulose biosynthesis. Proc Natl Acad Sci USA 98:2262–2267.

Lord J.M., Davey J., Frigerio L., and Roberts L.M. 2000. Endoplasmic reticulum-associated protein degradation. Seminars in Cell and Dev Biol 11:159–164.

Master E.R., Rudsander U.J., Zhou W., Henriksson H., Divne C., Denman S., Wilson D.B., and Teeri T.T. 2004. Recombinant expression and enzymatic characterization of PttCel9A, a KOR homologue from *Populus tremula x tremuloides*. Biochemistry 43:10080–10089.

Mølhøj M., Ulvskov P., and Degan F.D. 2001. Characterization of a functional soluble form of a *Brassica napus* membrane-anchored endo-1,4-β-glucanase heterologously expressed in *Pichia pastoris*. Pl Physiol 127:674–684.

Mølhøj M., Pagant S., and Höfte H. 2002. Towards understanding the role of membrane-bound endo-beta-1,4-glucanases in cellulose biosynthesis. Plant Cell Physiol 43:1399–1406.

Mueller S.C. and Brown, Jr. RM., 1980. Evidence for an intramembrane component associated with a cellulose microfibril synthesizing complex in higher plants. Journal of Cell Biology 84:315–326.

Müller J., Piffanelli P., Devoto A., Miklis M., Elliott C., Ortmann B., Schulze-Lefert P., and Panstruga. 2005. Conserved ERAD-like quality control of a plant polytopic membrane protein. Plant Cell 17:149–163.

Neumann U., Brandizzi F., and Hawes C. 2003. Protein transport in plant cells: In and out of the Golgi. Ann Bot 92:167–180.

Nicol F., His I., Jauneau A, Vernhettes S., Canut H., and Höfte H. 1998. A plasma membrane-bound putative endo-1,4-beta-D-glucanase is required for normal wall assembly and cell elongation in *Arabidopsis*. EMBO J 17:5563–5576.

Okuda K., Sekida S., Yoshinaga S., and Suetomo Y. 2004. Cellulose-synthesizing complexes in some chromophyte algae. Cellulose 11:365–376.

Paredez A.R., Somerville C.R., and Ehrhardt D.W. 2006. Visualization of cellulose synthase demonstrates functional association with microtubules. Science 312:1491–1495.

Robert S., Mouille G., and Höfte H. 2004. The mechanism and regulation of cellulose synthesis in primary walls: lessons from cellulose-deficient *Arabidopsis* mutants. Cellulose 11:351–364.

Robert S., Bichet A., Grandjean O., Kierzkowski D., Satiat-Jeunemaître B., Pelletier S., Hauser M.-T., Höfte H., and Vernhettes S. 2005. An *Arabidopsis* endo-1,4-beta-D-glucanase involved in cellulose synthesis undergoes regulated intracellular cycling. Plant Cell 17:3378–3389.

Romanovicz D.K. and Brown, Jr. R.M., 1976. Biogenesis and structure of Golgi-derived cellulosic scales in *Pleurochrysis*. I. Scale composition and supramolecular structure. Applied Polymer Symposium No. 28:587–610.

Römling U. 2002. Molecular biology of cellulose production in bacteria. Res Microbiol 153:205–212.

Ross P., Mayer R., and Benziman M. 1991. Cellulose biosynthesis and function in bacteria. Microbiol Rev 55:35–58.

Saxena I.M. and Brown, Jr. R.M., 2005. Cellulose biosynthesis: current views and evolving concepts. Ann Bot 96:9–21.

Somerville C. 2006. Cellulose synthesis in higher plants. Annu Rev Cell Dev Biol 22:53–78.

Spiers A.J. and Rainey P.B. 2005. The *Pseudomonas fluorescens* SBW25 wrinkly spreader biofilm requires attachment factor, cellulose fibre and LPS interactions to maintain strength and integrity. Microbiology 151:2829–2839.

Taylor N.G., Howells R.M., Huttly A.K., Vickers K., and Turner S.R. 2003. Interactions between three distinct CesA proteins essential for cellulose synthesis. Proc Natl Acad Sci USA 100:1450–1455.

Tsekos I. 1999. The sites of cellulose synthesis in algae: diversity and evolution of cellulose-synthesizing enzyme complexes. J Phycol 35:635–655.

Wasteneys G.O. 2004. Progress in understanding the role of microtubules in plant cells. Curr Opin Plant Biol 7:651–660.

Zogaj X., Nimtz M., Rohde M., Bokranz W., and Römling U. 2001. The multicellular morphotypes of *Salmonella typhimurium* and *Escherichia coli* produce cellulose as the second component of the extracellular matrix. Mol Microbiol 39:1452–1463.

CHAPTER 11

HOW CELLULOSE SYNTHASE DENSITY IN THE PLASMA MEMBRANE MAY DICTATE CELL WALL TEXTURE

ANNE MIE EMONS[1]*, MIRIAM AKKERMAN[1], MICHEL EBSKAMP[1,3], JAN SCHEL[1], AND BELA MULDER[1,2]

[1]*Laboratory of Plant Cell Biology, Department of Plant Sciences, Wageningen University, Arboretumlaan 4, 6703 BD Wageningen, The Netherlands;*
[2] *FOM Institute for Atomic and Molecular Physics (AMOLF), Kruislaan 407,1098 SJ Amsterdam, The Netherlands;*
[3] *Genetwister Technologies, P.O. Box 193, 6700 AD Wageningen, The Netherlands*

Abstract

Cellulose microfibrils are deposited by cellulose synthases into the cell wall in often strikingly regular patterns. Here we discuss several mechanisms that have been put forward to explain the alignment of cellulose microfibrils that gives rise to ordered cell wall textures: the hypothesis that *cortical microtubules align cellulose microfibrils* during their deposition, the *liquid crystal hypothesis* in which cellulose microfibrils self-assemble into textures after their deposition, the *templated incorporation hypothesis*, and *the geometrical theory* in which the density of active cellulose synthase complexes inside the plasma membrane may dictate the architecture of the cell wall.

Keywords

cell wall architecture, cellulose microfibrils, cellulose synthase, cortical microtubules, geometrical model.

Abbreviations

cellulose microfibril (CMF), cellulose synthase activation domain (CSAD).

1 TEXTURES OF CELLULOSE MICROFIBRILS

The cell wall texture is a composite of cellulose microfibrils (CMFs) arranged in one CMF thick lamellae. The orientation of the CMFs within a lamella is constant, but may vary from lamella to lamella. The most striking texture is the helicoidal wall, which consists of subsequent lamellae in which the orientation of the CMFs

* For correspondence: Tel: 31 317 484329; Fax: 31 317 485005; e-mail: annemie.emons@wur.nl

R.M. Brown, Jr. and I.M. Saxena (eds.), Cellulose: Molecular and Structural Biology, 183–197.

changes by a constant angle. Other wall textures are the axial, helical, crossed-polylamellate, transverse and the random wall textures, and combinations of these. Since wall texture is cell type and developmental stage specific, it must be highly regulated by the cell it embraces. Irrespective of the type of wall texture (review Emons 1991), cellulose microfibrils are produced by plasma membrane embedded cellulose synthase complexes (Kimura et al. 1999) which in freeze fracture images are observed as particle rosettes (first observation: Mueller and Brown, Jr. 1980).

Being crystalline and outside the plasma membrane, CMFs of plant cell walls were among the first structures that were reliably visualized with electron microscopy (Frey-Wyssling et al. 1948; Preston et al. 1948; reviewed by Preston, 1974). Roelofsen and Houwink (1953) showed that CMFs are deposited transverse to the cell elongation direction of elongating plant cells, but that CMFs in outer lamellae have an oblique to longitudinal alignment. They suggested that in previously deposited, older wall layers the originally transverse CMFs rotate to a longitudinal orientation during cell elongation. This is known as the "multi net growth" hypothesis (Roelofsen 1959). For epidermal cells from the style of *Petunia,* Wolters-Arts and Sassen (1991) have shown that this realignment indeed takes place. In a recent publication Refrégier et al. (2004) also suggest realignment of CMFs in older wall layers of elongating hypocotyl cells of dark-grown *Arabidopsis* seedlings after transverse deposition of CMFs in the innermost wall layer.

An alternative to the "multi net growth" hypothesis was the "ordered subunit" hypothesis of Roland and coworkers (review 1977), in which CMFs are laid down during deposition in subsequently different directions. Deposition in subsequently different orientations should surely take place in nonexpanding cells or cell parts having walls with various CMF orientations. The important question of the regulation of the deposition orientation of CMFs is still subject of lively scientific debate.

We have formulated a geometrical, mathematical theory for CMF ordering during their deposition, which allows production of axial, helical, crossed, helicoidal, and random wall textures (Emons 1994; Emons and Kieft 1994; Emons and Mulder 1997; 1998; 2000; 2001; 2001; Emons et al. 2002; Mulder et al. 2004). Before reviewing our theory, we first discuss the most important alternate CMF ordering hypotheses that have been proposed: (1) microtubule-directed CMF orientation, (2) self-assembly like liquid crystals, (3) templated incorporation hypothesis. In addition, we will respond to criticism that has been put forward against the geometrical theory and discuss those predictions from the theory that can be tested experimentally and, therefore, potentially, verify or falsify the theory.

2 HYPOTHESES ABOUT CELLULOSE MICROFIBRIL ORDERING MECHANISMS

2.1 Microtubule-directed microfibril orientation

In 1962, Green stated that "…the control of the cylindrical cell form in plants appears to reside in the orientation of the reinforcing CMFs in the side walls…" and that "…control of new synthesis of oriented wall texture is shown to be in

turn related to the orientation of cytoplasmic elements in the cell periphery…" (Green 1962). The first statement may be logical, and is often taken for granted, but has not been proven in a direct way. In the second statement Green foretells the existence of intracellular polymers (i.e., cortical microtubules), but also predicts that "…long elements in the cytoplasm adjacent to the wall can become aligned into the direction of maximum strain…" (i.e., the direction of cell elongation), which is perpendicular to the CMFs being deposited. This orientation of the long cytoplasmic structures in the direction of maximum strain is a logical prediction from a physical point of view. However, when cortical microtubules were indeed observed one year later (Ledbetter and Porter 1963), they appeared, in contrast to Green's prediction, to run in the same orientation as the CMFs. This led to the hypothesis that not their presence but their orientation determines nascent CMF direction. This evoked the still unanswered question of what orders the microtubules; apparently, this is not the direction of maximum strain of a growing cell.

The textbook dogma about the ordering mechanism of nascent CMFs, since 1963 (Ledbetter and Porter), is the "alignment hypothesis" (term given in review of Baskin 2001). This hypothesis was derived from the observation that CMFs run perpendicular to the axis of cell elongation, like the microtubules, and the experimental results that showed altered CMF ordering after microtubule depolymerization in such cells. Later, the theory has been worked out, hypothesizing an ordering mechanism in which the microtubules direct the cellulose synthases (Heath 1974), or channel them through the plane of the plasma membrane (Herth 1980; Giddings and Staehelin 1988). This hypothesis, that cortical microtubules exert control over nascent CMFs, is not supported by the work on nonelongating parts of Equisetum *hyemale* root hairs and other work on nonelongating cells (reviewed in Emons et al. 1992).

Strong evidence against the alignment hypothesis further comes from the recent work of Wasteneys and coworkers. By using drugs and temperature sensitive mutants they showed that CMFs align properly in the absence of normal cortical microtubules (Sugimoto et al. 2003; Himmelsbach et al. 2003). Interestingly, an orientation of both of them perpendicular to the growth axis appears to be a precondition for cell elongation in the right direction. (review: Wasteneys and Galway 2003). Another example of cells with nonparallel cortical microtubules and CMFs is found in the maturation zone of water-stressed *Zea mays* roots, where cortical microtubule arrays turn right handedly, but CMFs left-handedly (Baskin et al. 1999). Baskin and coworkers (2004) have recently demonstrated quantitatively that local CMF alignment does not require cortical microtubules. The growth pattern in cells mildly treated with microtubules drugs shifted from anisotropic in the direction of the root to more isotropic. At the same time, the net alignment of cortical microtubules acquired a less strictly transverse orientation. Polarized light microscopy of CMFs, which gives overall CMF direction of whole cell walls, showed unaltered net CMF orientation, but with deviations from the transverse orientation in the oryzalin-treated cells larger than in the controls. Field emission scanning electron microscopy of innermost wall layers showed local deviations from the transverse orientation in the drug treated cells.

These authors conclude that cortical microtubules are dispensable for CMF alignment locally, but not globally.

It is important to realize that, in most instances, the elongation direction changes after microtubule depolymerization as well (Baskin 2001) and this was not checked in studies relating cortical microtubule orientation to the orientation of nascent CMFs. Thus, microtubule depolymerization has apparently two effects that may or may not be related: change of CMF orientation and change of cell elongation direction, i.e., cell form acquisition. One cannot infer from the results whether cortical microtubule depolymerization has an effect on both parameters independently, or on CMF orientation and, therefore, cell elongation direction, or rather cell elongation direction and, therefore, CMF orientation. This problem is not merely the problem of correlation that we often come upon in cell biology, like the suggestion that if cortical microtubules align with nascent CMFs their orientations should have a causal relationship, or even that the one orients the other. In the drug experiments in which one actor, the cortical microtubule presence, changes two items, orientation of nascent CMFs and cell elongation direction, this goes a step further. In logical reasoning, if A influences B and C, one cannot conclude that B influences C, or C influences B, or that the two are independent. Therefore, elongating cells are not the ideal cells to study the "microtubule – microfibril syndrome" with microtubule drug application. Full-grown cells do not have this problem and are the cells of choice to solve this question. For such an investigation, not the local banded secondary wall deposition in xylem cells, in which the deposition is so dense that individual cortical microtubules and CMFs cannot be discerned, should be used, but the smooth and constant secondary cell wall deposition in most full-grown plant cells.

2.2 The liquid crystalline self-assembly hypothesis

Under suitable thermodynamical conditions, many substances composed of or containing highly elongated chiral molecules form a state of matter known as the cholesteric liquid crystalline phase. In this otherwise liquid phase the molecules spontaneously align, with the direction of alignment rotating in a manner akin to a helical staircase with a pitch (= repeat distance) typically in the order of 500 nm. The apparent structural similarity between the ubiquitous helicoidal texture of fibrous extracellular matrices in nature and the cholesteric liquid crystalline phase first led Bouligand (1976) to propose the hypothesis that cell wall texture could arise from a liquid crystalline self-organization principle. Although in essence an idea based solely on analogy, it nevertheless captured the imagination of many researchers. Especially intriguing was the observation by Abeysekera and Willison (1987) of apparently spontaneous helicoidal order in the pre-release mucilage of quince. Later, several groups established that suspensions or melts, containing cellulose or cellulose derivatives, can form cholesteric liquid crystalline phases (Vian et al. 1994).

In our view, however, liquid crystalline self-organization is a highly unlikely mechanism for cell wall texture formation. In order to obtain a thermodynamically self-organized state, of which a liquid crystal is just one example, a number of requirements need to be met. First of all, a sufficient number of molecules must simultaneously interact. Secondly, the thermodynamical equilibrium state must be reached, requiring the molecules to exhibit both sufficient mobility and changes of conformation to equilibrate all pertinent degrees of freedom. It is not clear that any of these conditions hold at any given stage of cell wall deposition. The CMFs are deposited sequentially from membrane-bound cellulose synthases. They are co-deposited with matrix material into the limited space between the plasma membrane and the already extant cell wall. Under these circumstances their mobility is extremely reduced, if not nonexistent. The same holds a fortiori for the conformational changes. A CMF whose length can safely be assumed to be many microns is essentially a macroscopic object. Even when such an object is in good thermal contact with its environment (e.g., in a low molecular weight solvent) the relaxation times, corresponding to slow long-wavelength modes, become exceedingly large. Moreover, liquid crystalline arrangements are highly sensitive to boundary conditions and equilibrium configurations are readily suppressed by unfavourable pinning of particle orientations at interfaces. The conditions of extreme confinement under which CMF deposition takes places are extremely unlikely to be conducive to the formation of bulk equilibrium phases. Finally, the hypothesis appears limited to addressing the formation of helicoidal textures, and thus begs the question of how other common textures, such as helical and crossed-polylamellate, that can even occur side-by-side with the helicoidal texture within the same cell wall, could be explained by the same mechanism.

2.3 Templated incorporation hypothesis

In his review Baskin (2001), outlines his ideas for a unifying model of CMF alignment. In this, he proposes a "templated incorporation" mechanism, in which templating molecules guide the orientation of nascent microfibrils. These templating molecules attach either to previously deposited CMFs or to plasma membrane proteins that bind cortical microtubules. In this way, both the case in which microtubules apparently do not play a role in the CMF orientation and the case where it is believed they do, can be dealt with in a single conceptual framework. Although at present there is no evidence for the existence of the templating molecules, the hypothesis is an intriguing one. However, an explanation for the sustained orientational order over distances of micrometers, as observed in cell wall lamellae, would require in our view an unrealistic degree of correlated alignment between the templating molecules. To transmit orientational information from one CMF to another CMF or from a microtubule to a CMF in a reliable fashion would require that the templating molecules always bind in fixed orientation to the fibers involved. It is not clear that the relatively disordered surface of a CMF or the inevitable molecular flexibility of the hypothesized

membrane-microtubule associated proteins allow this requirement to be met. Furthermore, the "guiding" fibers (microtubules or microfibrils) are themselves not perfectly aligned to begin with, which causes nearby templating molecules to have a distribution of orientations. We believe that these effects will accumulate so that the inherent molecular disorder will be amplified to destroy any original imposed ordering after the deposition of just a few lamellae. Himmelspach et al. (2003) reported that CMFs recovered in transverse patterns, without a well-ordered preexisting microfibril template in *Arabidopsis mor1–1* with disrupted cortical microtubules. These authors conclude that cellulose microfibril orientation is largely generated by mechanisms that do not rely on any templates.

3 THE GEOMETRICAL MODEL FOR CELLULOSE MICROFIBRIL ORIENTATION

In his review Baskin (2001) has also assessed the generality of the hypothesis that microtubules align CMFs. In that paper he states that "alignment of CMFs can occur independently of microtubules", showing that an alternative to the alignment hypothesis must exist. We have proposed that the default mechanism, which determines the orientation of CMFs as they are deposited in the absence of other influences, is geometrical in origin. Based on the observation that CMFs always appear approximately evenly spaced in close-packed lamellae and that their average distance apart does not depend on their orientation with respect to the cell axis, the geometrical close packing rule was formulated (Emons 1994):

$$\sin \alpha = \frac{Nd}{2\pi R}$$

This formula relates the CMF winding angle α to the number of CMFs being deposited (N), the distance d between them and the radius R of the cell. This explicit mathematical rule is the corner stone of a dynamic developmental model, which rests on the assumption that new active cellulose synthases insert into the plasma membrane through exocytosis of Golgi vesicles, or else, are activated within moving localized regions along the cell, the cellulose synthase activation domains (CSAD) (Figure 11-1). The rate at which new synthases become active is under cellular control and regulated, and the microtubules may well play a yet unknown role in this process, as discussed before (Emons and Mulder 1998, 2001). Once activated in the plasma membrane, the cellulose synthases move forward propelled by the forces generated in the CMF deposition and/or crystallization process. In the course of time, their angle of motion with respect to the cell axis is continuously adapted to the changing number of other cellulose synthases in their neighborhood in order to satisfy the geometrical close packing constraint. The CMFs deposited follow the tracks of the cellulose synthases and as such constitute a "recording" of their motion. The final ingredient of the model is that cellulose synthases have a finite active lifetime.

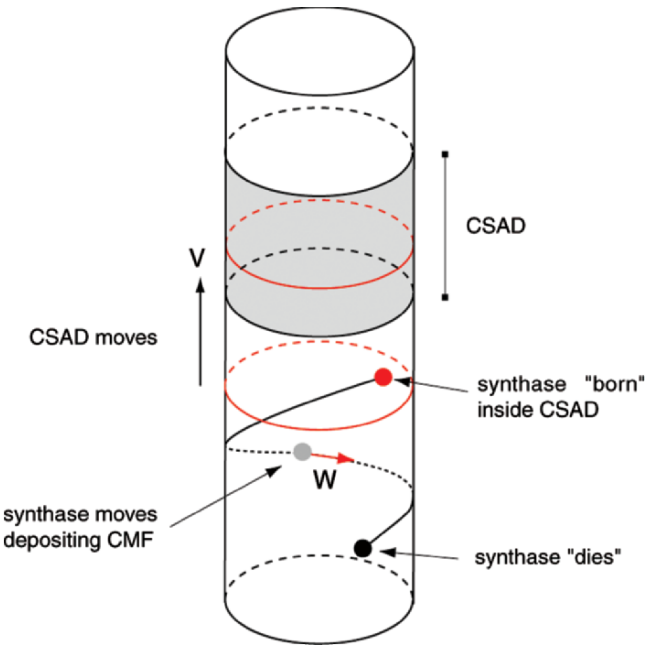

Figure 11-1. The cellulose synthase life cycle. After being inserted into the plasma membrane within a cellulose synthase activation domain (CSAD: located between the red circles at the time of deposition) the synthase moves with an average speed w within the plasma membrane, leaving a cellulose microfibril in its wake. The direction of motion and hence the angle the deposited CMF makes with the cell axis is determined by the local density of other synthases. The CMF synthase becomes inactive after a characteristic lifetime $t^{\dagger}$, which determines the length of the microfibrils. The CSAD itself, here shown in grey, moves with a speed v in the direction opposite to that of the CMF synthases (*See Color Plate of this figure beginning on page 355*)

The elements outlined above are cast into the form of a partial differential equation describing the evolution, both in space and in time, of the density of active cellulose synthases present in the plasma membrane. This equation takes the following form on a cylindrical cell of radius R

$$\frac{\partial N(z,t)}{\partial t} - \frac{wd}{2\pi R} N(z,t) \frac{\partial N(z,t)}{\partial z} = \varphi(N,z,t) - \varphi^{\dagger}(N,z,t)$$

where w is the speed with which the synthase moves and d the effective width of a CMF plus adherent matrix material, i.e., the distance between neighboring CMFs. φ is the local rate of synthase production for which we choose the following form

$$\varphi(N,z,t) = \frac{N_*}{t_*(1-\gamma)}\left(1-\frac{N(z,t)}{N_{\max}}\right)^{\gamma} = \text{if } N(z,t) < N_* \text{ and z is located inside a CSAD}$$

In all other cases $\varphi = 0$. The parameter γ controls the shape of the synthase production curve and ranges between zero and one. Synthase production stops when the maximum density

$$N_{\max} = \frac{2\pi R}{d}$$

is reached, which for stationary CSAD would happen after time t_*. The insertion domains are assumed to have a length l and travel at a speed v. Finally, the local rate of rosette de-activation $\varphi^\dagger$ needs to be determined. This rate depends on the full evolution of the density in a time interval of length $t^\dagger$ (= the synthase lifetime). Fortunately, the resultant equations are of a type that can be readily solved with entirely classical techniques. The solutions of these equations can be reinterpreted in terms of the tracks of the cellulose synthases, and hence the orientations of the deposited CMFs, thus leading directly to the cell wall texture. Because of its geometrical origin, the model has only a small number (4) of relevant parameters (Table 11-1). We have shown that by varying these parameters several known cell wall textures can be reproduced by this fully predictive mathematical model: the axial, helical, helicoidal, and crossed wall texture (Figure 11-2). Recently arguments were put forward to relate it also to the random texture. In this view the random cell wall in fact is a helicoidal wall, however with such large spacings between the microfibrils that the texture looks to be random (Mulder et al. 2004).

The geometrical model provides a conceptual framework for the alignment mechanism of CMFs, which unites examples where cortical microtubules are and are not parallel to nascent cellulose microfibrils, and in which they do not directly move or channel the synthases but may be involved in their activation inside the plasma membrane. The basic line is as follows: by *default* CMFs go straight unless obstructed and their alignment depends mainly on the number of cellulose synthases simultaneously active at any position in the plasma membrane. The geometrical model does not rule out that cortical microtubules bind to the plasma membrane so tightly that synthase movement is obstructed, which could be the case in elongating cells in which both polymers are always in line with each other and transverse to the cell elongation direction, (Emons and Mulder 1998; Emons et al. 2002).

Table 11-1. Relevant parameters of the geometrical model

Length of the CSAD	$\lambda = \frac{l}{wt_*}$
Speed of the CSAD	$\beta = \frac{v}{w}$
Synthase lifetime	$\tau^\dagger = \frac{t^\dagger}{t_*}$
Synthase production curve shape	γ

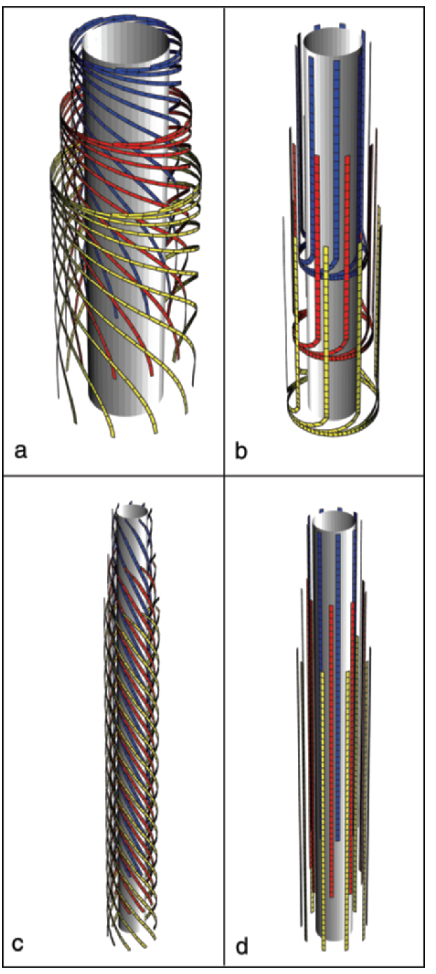

Figure 11-2. Different cell wall textures as predicted by the geometrical model. The ribbons shown represent the tracks of CMFs, obtained from the explicit solutions to the CMF evolution equation. (**a**) The helicoidal texture in which the angle of orientation between subsequent lamellae changes by a constant amount. (**b**) A crossed polylamellate texture with alternate lamellae with transverse and axial oriented CMFs. (**c**) A purely axial texture. (**d**) A helical texture in which the CMFs have an almost constant winding angle (*See Color Plate of this figure beginning on page 355*)

4 A ROLE FOR CORTICAL MICROTUBULES IN LOCALIZING CELL WALL DEPOSITION

Green came to the idea of transverse CMFs determining cell elongation direction because he viewed plant cell growth primarily as "…the yielding of cell wall to the turgor pressure of the cell vacuole …" (Green 1962). However, apart from wall yielding to turgor pressure, a second, equally important process is involved in cell elongation, which is the wall deposition itself. For anisotropically longitudinally elongating cells, we not only have to look for a mechanism that allows wall yielding in the right direction, but also for one that channels new wall material to the right cell faces. In an anisotropically longitudinally elongating cell, these should be the sidewalls. Transversely aligned microtubules are in a very

good arrangement to be part of this positioning mechanism. A putative glycosylphosphatidylinositol (GPI)-anchored protein COBRA, which is mainly localized at the longitudinal sides of elongating root cells (Schindelman et al. 2001) and a kinesin-like protein (Zhong et al. 2002) may be involved in this process. Since wall material enters the cell wall as the content of Golgi vesicles, the microtubules, looping around the cell's sidewalls, and not the transverse walls, could be part of a system that locates the Golgi bodies or the Golgi vesicles to those cell faces. Evidence for microtubules, possibly acting in such a way, is the localization under the bands of cellulose in xylem cells, reviewed by Baskin (2001), and in *Arabidopsis* mutants shown by Gardiner et al. (2003). One should realize, however, that determining exocytosis or activation sites, by a yet unknown mechanism, is a completely different function for cortical microtubules than orienting cellulose synthases during CMF deposition, either by directing the synthases or channeling them through the plasma membrane. Recent work by a consortium of plant researchers (Roudier et al. 2005) shows COBRA to be required for the oriented deposition of cellulose microfibrils and to be aligned in narrow bands perpendicular to the long axis of diffuse anisotropically elongating cells in a pattern different from, but depending on, cortical microtubule organization.

The geometrical model also does not rule out, even favors the idea, that cortical microtubules are (part of) the mechanism that regulates the sites and or amounts of cellulose synthase insertion, i. e., exocytosis or activation areas in the plasma membrane. Inferring from our knowledge of tip growing cells this would require modulation of the actin cytoskeleton (Miller et al. 1999; de Ruijter et al. 1999; Ketelaar et al. 2002, 2003), as well as of calcium ion gradients at those sites (de Ruijter et al. 1998). However, we cannot rule out that exocytosis goes on everywhere and that synthases are activated, or even assembled, locally inside the plasma membrane. The crucial factor in the geometrical model is that density of active cellulose synthases in the plasma membrane is the default determining factor for CMF direction control. Intuitively and scientifically, this factor is directly linked to CMF ordering since the CMF synthase complexes are the nanomachines that spin out the fibrils themselves. This self-ordering mechanism is tightly controlled by the cell, which controls cellulose synthase activation in the plasma membrane.

5 CRITICISM ON THE GEOMETRICAL MODEL

In his review, Baskin (2001) presents a criticical discussion of the geometrical model. On page 157, he states: "…several of the model's assumptions appear to contradict observations". The points he specifically mentions are:

(1) The geometry of the root hair changes with colchicine treatment but the helicoid does not (Emons et al. 1990). (2) and the density of neither the CMFs (Emons 1989) (3) nor the rosettes (Emons 1985) changes with the distance from the apex according to the model's assumptions." Here we take the opportunity to comment on the issues he raises.

Ad (1). As shown in Emons et al. 1990, the geometry of the new part of the hair is wider after colchicine treatment than before colchicine treatment. In this article, we state that the type of texture has not changed; it has remained helicoidal. Of course, not every change in morphology is enough to change the *type* of texture. Furthermore, a detailed analysis of this wall after colchicine treatment, nor measurements of angles between CMFs in subsequent lamellae and with the long axis of the hair, nor a mathematical working out of these measurements have been carried out. Of much more interest is the fact that the cell wall texture in old *Equisetum hyemale* root hairs, in which the cell dimension has changed drastically because the lumen of the cell has almost completely been filled with cell wall, has become axial (Emons and Wolters-Arts 1983). This is like the geometrical model would predict (Emons 1994; Emons and Mulder 1998) and this change is gradual with a helical transition phase in between the helicoidal and axial textures, (Emons and Wolters-Arts 1983), apparently depending on the cell width.

Ad (2). In fact, the areal density of CMFs (= total length of CMF per unit area, measured on a scale sufficiently large with respect to the mean distance between the CMFs) within a lamella does not increase at all, not in reality and neither in the model. One of the striking observations made on the helicoidal cell wall of *Equisetum hyemale* root hairs was that the distance between the cellulose microfibrils within lamellae does not depend on the CMF orientation in those lamellae. Moreover, the length of an area with a certain orientation as measured along the plasma membrane also does not depend on the CMF orientation (Emons 1989). Therefore, although the resulting cell wall locally seems to consist of lamellae with microfibrils having regularly rotating CMF angle, the deposition mechanism could never be that of helices with a constant pitch being wound around the plasma membrane at consecutively different angles. This would namely give rise to short areas having transverse microfibrils and long areas with longitudinal microfibrils. The cornerstone of the geometrical model (Emons 1994; Mulder and Emons 2001) is the change in the *number of active synthases* at a given location. These changes arise from the interplay between the motion of synthases, the creation of new synthases inside the CSADs and the inevitable deactivation of synthases. In our view a CSAD encompasses the whole circumference of a cell. When a CSAD passes any location in the cell, the number of cellulose synthases locally increases. An increased number of synthases implies an increase in the winding angle. In this way, lamellae with different angles are being formed in the model.

Ad (3). The density of rosettes in freeze fracture images cannot be measured in areas of the plasma membrane that are sufficiently large. We hope to have a GFP-cellulose synthase fusion construct soon. The only observations that could be made in the freeze fracture study are densities of rosettes in areas with good platinum shadowing, which in a bent surface can never be optimal for the whole surface. Areas with and areas without rosettes were observed; and when there were rosettes present their density was up to 15 per μm^2 (Emons 1985).

Another problem one could have with the geometrical model is that it would not be able to account for local differences in texture in different faces of the same cell, as are seen in epidermal cells of leaves. However there is no reason to suppose that a cell would not be able to regulate the cellulose to matrix ratio and, therefore, its wall texture in different wall facets.

6 OUTLOOK ON THE VERIFICATION/FALSIFICATION OF THE GEOMETRICAL THEORY

The geometrical theory predicts definite effects on the CMF angle and hence on the resultant wall texture following changes in the amount of active synthases (N), the cellulose to matrix ratio (d) and cell geometry (D). The amount of active synthases, moreover, is determined in a definite fashion by the intrinsic parameters of the model shown in Table 11-1: the length of the CSAD, the speed of movement of CSAD, the cellulose synthase lifetime and synthase production curve shape. To verify, falsify, or improve the model we should measure these parameters and relate them to the types of textures formed.

Based on the theoretical results, a next round of experiments has been defined and is being carried out in our laboratory: (1) wall texture of root hairs of wild type and *rsw1* mutant of *Arabidopsis* is analyzed, (2) insertion or activation sites of cellulose synthases in the plasma membrane of diffuse growing cells are being determined, (3) measurements of physical parameters of CMFs *in vitro* are being performed, and (4) the theory is further being worked out. The geometrical model for cell wall texture formation is gaining importance now that, from work on *Arabidopsis* mutants, the microtubule or microfibril paradigm does not seem to be as straightforward as once thought and cannot explain CMF orientation regulation in general.

A kinesin-like protein (FRA1) influences cell wall strength and the oriented deposition of CMFs, at least in fiber cells, without effecting cortical microtubule alignment (Zhong et al. 2002). Fibers are fragile, stems are stronger than in the wild type and the plants are shorter caused by short cells, although wall composition is unchanged. Still, an ordered, helicoidal-like (Zhong et al. 2002, Figure 4), cell wall is being produced. Our conclusion from the FRA1 phenotype is not necessarily in favor of cortical microtubules functioning in the regulation of CMF orientation. The interesting results of this work rather show that (1) CMF orientation determines mechanical cell and tissue properties, (2) transverse CMF orientation correlates with the degree of cell elongation, (3) cortical microtubule orientation by itself cannot determine CMF orientation, nor degree of cell elongation, but can be involved in determining elongation direction, (4) a kinesin-like protein that binds tubulin is needed for CMF patterning transverse to the elongation direction and may well be involved in determining the location of the CSADs inside the plasma membrane. A change in patterning of cellulose synthases in the plasma membrane in our model would give rise to a different wall texture. How the geometrical model behaves in elongating cells is a task we still have to undertake.

Plant cell walls have tremendous commercial value. Understanding and manipulation of their properties will greatly enhance their application. We are not close to understanding the complete process. However, the future is bright. Now that we have mutants, GFP-constructs, and advanced microscopes, we have the tools to verify or falsify existing hypotheses and build up the basis of a consistent theory.

After writing this chapter new information about the movement of the cellulose synthase complexes came from the laboratory of Somerville in Stanford (Paredez et al. 2006). The work of Paredez et al. proves that the synthase complex indeed moves inside the plasma membrane, steered by the propulsive force of cellulose microfibril generation, its own product, and that in the cells examined, the microtubules are guide tracks. The work also shows that it is highly improbable that a direct attachment exists between the cellulose synthase complex and the cortical microtubule, since the complexes move along microtubules bidirectionally. The microtubules could be fences for the complexes and once the complexes bump into them have to follow them, which brings us to the starting point of our hypothesis: "rosettes go straight unless obstructed."

Indeed, in this recent work, it is shown in addition that when the cortical microtubules are completely depolymerized, cellulose synthase complexes move in highly ordered patterns!

REFERENCES

Abeysekera R.M. and Willison J.H.M. 1987. A spiral helicoid in a plant cell wall. Cell Biol Int Rep 11:75–79.

Baskin T.I., Meekes H.T.H.M., Liang B.M., and Sharp R.E. 1999. Regulation of growth anisotropy in well-watered and water-stressed maize roots. II. Role of cortical microtubules and cellulose microfibrils. Plant Physiol 119:681–692.

Baskin T.I. 2001. On the alignment of cellulose microfibrils by cortical microtubules: A review and a model. Protoplasma 215:150–171.

Baskin T.I., Beemster G.T.S., Judy-March J.E., and Marga F. 2004. Disorganization of cortical microtubules stimulates tangential expansion and reduces the uniformity of cellulose microfibril alignment among cells in the root of *Arabidopsis*. Plant Physiol 135:2279–2290.

Bouligand Y. 1976. Biological analogs to liquid crystals.la Recherche 7:474–476.

Emons A.M.C. and Wolter-Arts A.M.C. 1983. Cortical microtubules and microfibril deposition in the cell wall of root hairs of *Equisetum hyemale*. Protoplasma 117:68–81.

Emons A.M.C. 1985. Plasma-membrane rosettes in root hairs of *Equisetum hyemale*. Planta 163:350–359.

Emons A.M.C. 1989. Helicoidal microfibril deposition in a tip growing cell and micro-tubuli alignment during tip morphogenesis: a dry-cleaving and freeze substitution study. Can J Bot 67:2401–2408.

Emons A.M.C., Wolters-Arts A.M.C., Traas J.A. and Derksen J. 1990. The effect of colchicine on microtubules and microfibrils in root hairs. Acta Bot Neerl 39:19–27.

Emons, A.M.C. 1991. Role of particle rosettes and terminal globules in cellulose synthesis. In: Haigler C.H. and Weimer P.J. (eds.) Biosynthesis and biodegradation of cellulose. Marcel Dekker, New York, pp. 71–98.

Emons A.M.C., Derksen J., and Sassen M.M.A. 1992. Do microtubules orient plant cell wall microfibrils? Physiol Plant 84:486–493.

Emons A.M.C. 1994. Winding threads around plant cells: a geometrical model for microfibril deposition. Plant Cell Environment 17:3–14.

Emons A.M.C. and Kieft H. 1994. Winding threads around plant cells: applications of the geometrical model for microfibril deposition. Protoplasma 180:59–69.

Emons A.M.C. and Mulder B.M. 1997. Plant cell wall architecture. Comments Theor Biol 4:115–131.
Emons A.M.C. and Mulder B.M. 1998. The making of the architecture of the plant cell wall: How cells exploit geometry. Proc Natl Acad Sci USA 95:7215–7219.
Emons A.M.C. and Mulder B.M. 2000. How the deposition of cellulose microfibrils build cell wall architecture. Trends in Plant Science 35–40.
Emons A.M.C. and Mulder B.M. 2001. Microfibrils build architecture: A geometrical model. In: Molecular Breeding of Woody Plants. Elsevier Science, Amsterdam, pp. 111–119.
Emons A.M.C., Schel J.H.N., and Mulder B.M. 2002. The geometrical model for microfibril deposition and the influence of the cell wall matrix. Plant Biol 4:22–26.
Frey-Wyssling A., Mühletaler K., and Wyckoff R.W.G. 1948. Mikrofibrillenbau der Pflanzlichen Zellwände. Experientia 4:475.
Gardiner J.C., Taylor N.G., and Turner S.R. 2003. Control of cellulose synthase complex localization in developing xylem. The Plant Cell 15:1740–1748.
Giddings T.H. and Staehelin L.A. 1988. Spatial relationship between microtubules and plasma-membrane rosettes during the deposition of primary wall microfibrils in *Closterium* sp. Planta 173:22–30.
Green P.B. 1962. Mechanism for plant cellular morphogenesis. Science 138:1404–1405.
Heath I.B. 1974. A unified hypothesis for the role of membrane bound enzyme complexes and microtubules in plant cell wall synthesis. J Theor Biol 48:445–449.
Herth W. 1980. Calcofluor white and Congo red inhibit chitin microfibril assembly of *Poterioochromonas*: Evidence for a gap between polymerization and microfibril formation. J Cell Biol 87:442–450.
Himmelspach R., Williamson R.E., and Wasteneys G.O. 2003. Cellulose microfibril alignment recovers from DCB-induced disruption despite microtubule disorganization. Plant J 36:565–575.
Ketelaar T., Faivre-Moskalenko C., Esseling J.J., de Ruijter N.C.A., Grierson C.S., Dogterom M., and Emons A.M.C. 2002. Positioning of nuclei in *Arabidopsis* root hairs: an actin-regulated process of tip growth. The Plant Cell 14:2941–2955.
Ketelaar T., de Ruijter N.C.A. and Emons A.M.C. 2003. Unstable f-actin specifies the area and microtubule direction of cell expansion in *Arabidopsis* root hairs. The Plant Cell 15:285–292.
Kimura S., Laosinchai W., Itoh T., Cui X.J., Linder C.R., and Brown, Jr. R.M. 1999. Immunogold labeling of rosette terminal cellulose-synthesizing complexes in the vascular plant *Vigna angularis*. The Plant Cell 11:2075–2085.
Ledbetter M.C. and Porter K.R. 1963. A 'microtubule' in plant cell fine structure. J Cell Biol 19:239–250.
Miller D.D., de Ruijter N.C.A., Bisseling T., and Emons A.M.C. 1999. The role of actin in root hair morphogenesis: studies with lipochito-oligosaccharide as a growth stimulator and cytochalasin as an actin perturbing drug. Plant J 17:141–154.
Mueller S.C. and Brown, Jr. R.M. 1980. Evidence for an intramembrane component associated with a cellulose microfibril-synthesizing complex in higher plants. J Cell Biol 84:315–326.
Mulder B.M. and Emons A.M.C. 2001. A dynamical model for plant cell wall architecture formation. J Math Biol 42:261–289.
Mulder B.M., Schel J.H.N., and Emons A.M.C. 2004. How the geometrical model for plant cell wall formation enables the production of a random texture. Cellulose 11:395–401.
Paredez A.R., Somerville C.R., and Ehrhardt D.W. 2006. Visualization of cellulose synthase demonstrates functional association with microtubules. Science 312: 1491–1495.
Preston R.D., Nicolai E., Reed R., and Millard A. 1948. An electron microscope study of cellulose in the wall of *Valonia ventricosa*. Nature 162:665–667.
Preston R.D. 1974. The Physical Biology of Plant Cell Walls. Chapman & Hall, London.
Refrégier G., Pelletier S., Jaillard D., and Höfte H. 2004. Interaction between wall deposition and cell elongation in dark-grown hypocotyl cells in *Arabidopsis*. Plant Physiol 135:1–10.
Roelofsen P.A. and Houwink A.L. 1953. Architecture and growth of the primary cell wall in some plant hairs and in the Phycomyces sporangiophore. Acta Bot Neerl 2:218.
Roelofsen P.A. 1959. The Plant Cell Wall. Bornträger, Berlin.
Roland, J.C. and Vian, B. 1977. The wall of the growing pant cell: its three-dimensional organization. Int Rev Cytol 61:129–165.

Roudier, F., Fernandes, A.G., Fujita, M., Himmelspach, R., Bomer, G.H.H., Schindelman, G., Song, S., Baskin, T.I., Dupree, P., Wasteneys, G.O., and Benfey, P.N. 2005. COBRA, an *Arabidopsis* extracellular glycosyl-phosphatidyl inositol-anchored protein, specifically controls highly anisotropic expansion through its involvement in cellulose microfibril orientation. The Plant Cell 17:1749–1783.

de Ruijter N.C.A., Rook M.B., Bisseling T., and Emons A.M.C. 1998. Lipochito-oligosaccharides re-initiate root hair tip growth in *Vicia sativa* with high calcium and spectrin-like antigen at the tip. Plant J 13:341–350.

de Ruijter N.C.A., Bisseling T., and Emons A.M.C. 1999. *Rhizobium* Nod factors induce an increase in sub-apical fine bundles of actin filaments in *Vicia sativa* root hairs within minutes. Mol Plant Microbe Int 12:829–832.

Schindelman G., Morikami A., Jung J., Baskin T.I., Carpita N.C., Derbyshire P., McCann M.C., and Benfey P.N. 2001. COBRA encodes a putative GPI-anchored protein, which is polarly localized and necessary for oriented cell expansion in *Arabidopsis*. Genes and Development 15:1115–1127.

Sugimoto K., Himmelspach R., Williamson R.E., and Wasteneys G.O. 2003. Mutation or drug-dependent microtubule disruption causes radial swelling without altering parallel cellulose microfibril deposition in *Arabidopsis* root cells. The Plant Cell 15:1414–1429.

Vian B., Reis D., Darzens D., and Roland J.C. 1994. Cholesteric-like crystal analogs in glucuronoxylan-rich cell-wall composites. Experimental approach of a cellular reassembly from native cellulosic suspension. Protoplasma 180:70–81.

Wolters-Arts A.M.C. and Sassen M.M.A. 1991. Deposition and reorientation of cellulose microfibrils in elongating cells of *Petunia* stylar tissue. Planta 185:179–189.

Wasteneys G.O. and Galway M. 2003. Remodeling the cytoskeleton for growth and form: An overview with some new views. Annu Rev Plant Biolo 54:691–722.

Zhong R.Q., Burk D.H., Morrison W.H., and Ye Z.H. 2002. A kinesin-like protein is essential for oriented deposition of cellulose microfibrils and cell wall strength. The Plant Cell 14:3101–3117.

CHAPTER 12

CELLULOSE-SYNTHESIZING COMPLEXES OF A DINOFLAGELLATE AND OTHER UNIQUE ALGAE

KAZUO OKUDA* AND SATOKO SEKIDA

Graduate School of Kuroshio Science, Kochi University, Kochi 780-8520, Japan

Abstract

Cellulose-synthesizing terminal complexes (TCs) are observed as particle arrays on the fractured faces of membranes by freeze-fracture electron microscopy and assumed to be enzyme complexes that synthesize cellulose microfibrils. Several distinct TCs have been reported in various organisms from prokaryotes to animals. Among them, the dinoflagellate *Scrippsiella hexapraecingula* is only one species that has been known to have a TC so far in the protistian supergroup Alveolates. In *S. hexapraecingula* thecal plates in motile cells and a pellicle in nonmotile cells contain cellulose microfibrils. TC appears on the plasma membrane of the nonmotile cells and consists of two rows of particles. Microfibrils synthesized by these TCs are bundles composed of fine fibrils about 2 nm in diameter. The heterokontophytes are thought to be one of algal lineages that have been established through secondary endosymbioses. In the heterokontophytes, three distinctive TCs synthesize thin, ribbon-like cellulose microfibrils in common, which include a single linear row type TC in the Eustigmatophyceae and the Phaeophyceae, a diagonal row TC type in the Xanthophyceae, and a 2–3 row TC type in the Phaeothamniophyceae. The diversity and evolution of TCs are discussed.

Keywords

Cellulose microfibril, cellulose-synthesizing terminal complex, dinophyte, heterokontophyte, evolution, freeze fracture.

1 INTRODUCTION

Cellulose microfibrils are synthesized generally by plasma membrane-bound enzymes (Brown, Jr. 1985, 1996). Freeze-fracture investigations first demonstrated particle arrays in association with the tip of microfibril impression in the fractured plasma membrane (Brown, Jr. and Montezinos 1976). The particle arrays have

* For correspondence: Tel: +81 88 844 8314; Fax: +81 88 844 8314; e-mail: okuda@cc.kochi-u.ac.jp

R.M. Brown, Jr. and I.M. Saxena (eds.), Cellulose: Molecular and Structural Biology, 199–215.

been called terminal complexes (TCs), which are assumed to function as cellulose-synthesizing enzyme complexes. There is evidence now that a TC is the site of cellulose synthesis (Kimura et al. 1999). Several distinct TCs have been found in various organisms (Brown, Jr. and Montezinos 1976; Peng and Jaffe 1976; Willison and Brown, Jr. 1978; Zaar 1979; Mueller and Brown, Jr. 1980; Giddings et al. 1980; Mizuta et al. 1989; Itoh 1990; Tsekos and Reiss 1992; Tsekos et al.1996; Grimson et al. 1996; Sekida et al. 2004; Okuda et al. 2004), and species belonging to the same phylogenetic group are considered to have the same type of TC (Brown, Jr. 1985; Okuda 2002). TCs are categorized into two main types, rosette and linear. Rosette TCs are found in charophycean green algae and land plants. Linear TCs occur in three types: as a single row in prokaryotes, brown algae and some red algae. They occur as multiple rows in glaucophycean algae, some red algae, chlorophycean and ulvophycean green algae, phaeothamniophycean algae, dinoflagellates, slime molds, and invertebrates such as tunicates (Kimura and Itoh 1996). They also occur as diagonally arranged rows in xanthophycean algae. It has been pointed out that distinct TCs synthesize microfibrils with characteristic morphologies (Kuga and Brown, Jr. 1989). This suggests a relationship between the organization of TCs and microfibril assembly (Brown, Jr. 1996).

Dinoflagellates with ciliates and apicomplexans comprise the Alveolates that is one of the most biologically diverse supergroups of eukaryotic microorganisms (Cavalier-Smith 1993). Recently, a new TC was found in a species of dinoflagellates first in the Alveolates (Sekida et al. 2004). The heterokontophytes include photosynthetic members belonging to another supergroup the Stramenopiles. Some distinct TCs have been known to occur in the monophyletic heterokontophycean algae (Okuda et al. 2004). In this chapter, we focus on the structures of cellulose microfibrils and TCs in the two algal groups, dinoflagellates and heterokontophytes and discuss the evolution of TCs. Several elegant reviews related to cellulose microfibril assembly and TCs have been already published (Brown, Jr. et al. 1983; Brown, Jr. 1985, 1996; Emons 1991; Quader 1991; Tsekos 1999).

2 ASSEMBLY OF CELLULOSE MICROFIBRILS IN DINOFLAGELLATES

Structures of cell coverings in dinoflagellate cells are unique. Motile dinoflagellate cells possess a cell covering variously termed the theca, amphiesma or cortex (Dodge and Crawford 1970; Dodge 1971; Netzel and Dürr 1984). The plasma membrane enclosing the cell is the outermost component. Beneath the plasma membrane lies a single layer of flattened vesicles termed amphiesmal vesicles, which in armored dinoflagellates enclose the thecal plates. Some gonyaulacoid and peridinioid species undergo ecdysis prior to cell division, shedding the theca and flagella (Taylor 1987). After ecdysis, the motile cells transform into nonmotile cells or cysts and form thick cell coverings termed the pellicle or cyst wall (Swift and Remsen 1970; Morrill 1984; Bricheux et al. 1992; Höhfeld and Melkonian 1992).

Thecal plates contain microfibrils (Dodge and Crawford 1970) that may be cellulosic (Morrill and Loeblich 1983), and are made of materials supplied from

cytoplasmic vesicles (Wetherbee 1975). The results of several histochemical treatments suggest the presence of cellulose in thecal plates (Loeblich 1970). However, Nevo and Sharon (1969) reported that the major component of thecal plates in *Peridinium* consists of a mixed β-1,3- and β-1,4-glucan which differed from cellulose in its x-ray diffraction pattern. In nonmotile cells, the pellicle contains a sporopollenin-like substance and/or cellulosic components in some species (Morrill and Loeblich 1981, 1983), but the cyst walls of *Pyrocystis* spp. consist of cellulose microfibrils (Swift and Remsen 1970). Sekida et al. (1999, 2004) confirmed the presence of cellulose in both thecal plates and pellicles in *Scrippsiella hexapraecingula* by electron diffraction analyses.

S. hexapraecingula is an armored, peridinioid species and possesses a simple, asexual life cycle, in which the motile cells alternate with the nonmotile cells diurnally in culture (Figure 12-1). This species forms two distinct cell coverings,

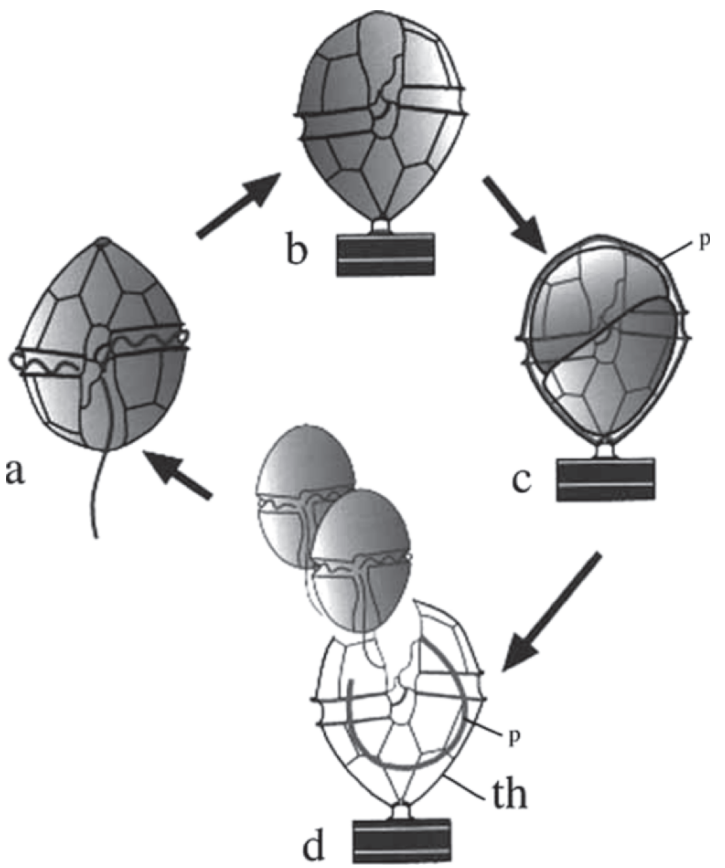

Figure 12-1. Schematic drawing of life cycle stages of a marine dinoflagellate *Scrippsiella hexapraecingula*. (**a**) Motile cells during light period. (**b**) Transformation from motile to nonmotile stage, ecdysis occurring. (**c**) Cell division and formation of daughter cells. (**d**) New motile cells released from the parental cell coverings. p, pellicle; th, thecal plate

amphiesmal vesicles containing thecal plates in the motile cells and pellicles in the nonmotile cells (Sekida et al. 2001a). According to Sekida et al. (2004), soon after the motile cells escaped from the pellicles of the nonmotile cells and began to swim, they start to produce incipient thecal plates in amphiesmal vesicles, which form as depositions of groups of granular materials stained with Calcofluor White M2R (Figure 12-2). The number of granules increased, so that thin sheet-like thecal plates developed (Figures 12-3 and 12-4). No microfibril is present in plate materials during these early stages of thecal plate development (Figures 12-2–12-4). Individual thecal plates become close to each other with a shape specific to this species more than 30 min after the motile cells began to swim (Figure 12-5). Microfibrils then begin to be deposited in the thecal plates first (Figure 12-6). Most of microfibrils isolated from the thecal consist of several fine fibrils 3–4 nm in diameter (Figure 12-7), whereas some other microfibrils are flat, ribbon-like structures with a thickness of about 3 nm and a width of 10–20 nm (Sekida et al. 1999).

The microfibrils show a strong positive reaction to cellobiohydrolase I-conjugated colloidal gold (CBH-I gold) labeling, suggesting that they are cellulose in nature. This is further confirmed by electron diffraction analysis (Figures 12-13 and 12-14).

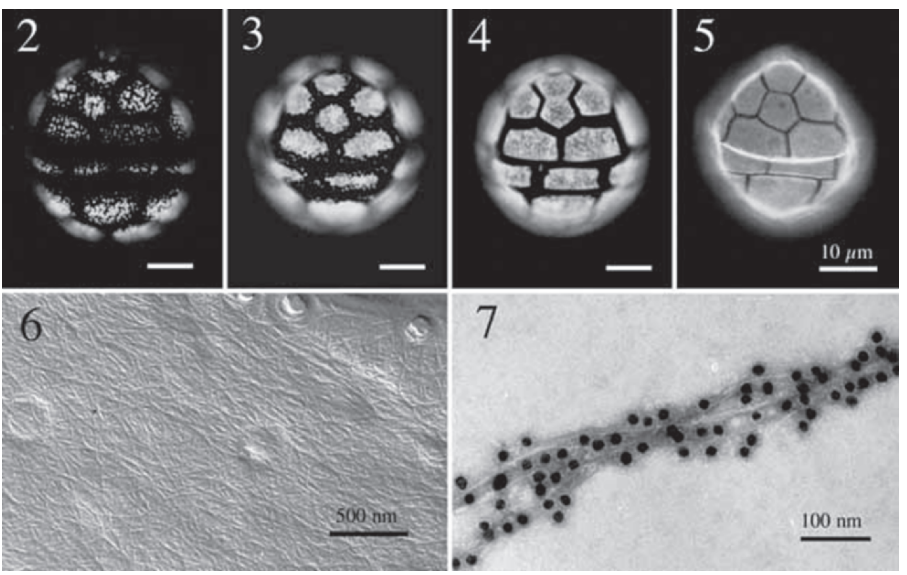

Figures 12-2 to 12-7. Thecal plate formation in motile cells of *Scrippsiella hexapraecingula* in images **2**–**5**. Fluorescence images of thecal plates stained with calcofluor white M2R. Dorsal views of motile cells 5 min (**2**), 10 min (**3**), 15 min (**4**), and 30 min (**5**) after motile cells began to swim out of pellicles. A bar in **2**–**5** indicates 10 μm. Image **6**: Replica of a mature thecal plate, showing the surface structure of the thecal plate exposed by extraction of amorphous materials. Note microfibrils deposited in the thecal plate with random orientations. Image **7**: Microfibrils labeled with CBH-I gold particles, which were isolated from thecal plates.

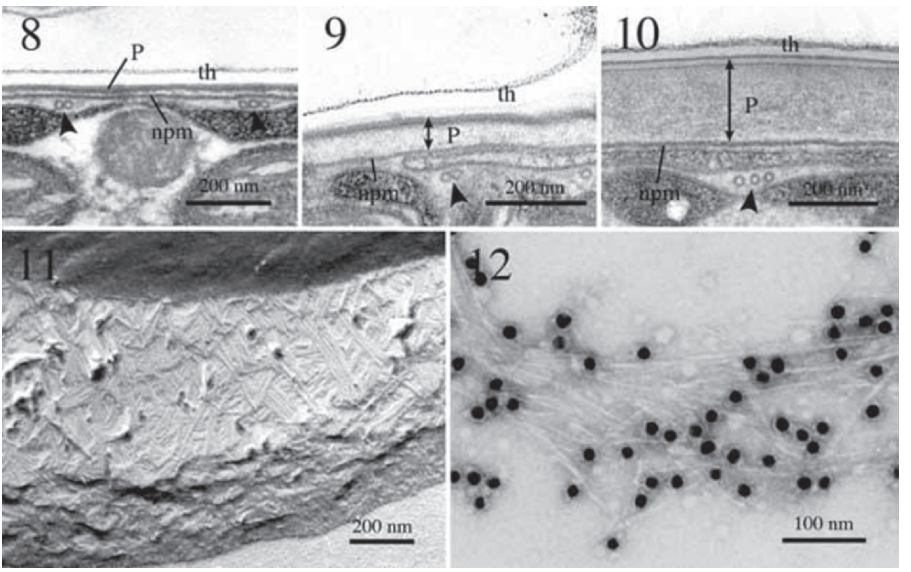

Figures 12-8 to 12-12. Pellicle formation in nonmotile cells of *Scrippsiella hexapraecingula*. Images **8**–**10**: Cross sections of nonmotile cells. Image **8**: Thin pellicle (P) on the plasma membrane (npm) of a nonmotile cell just after ecdysis. Image **9**: Pellicle (P) thickening in a nonmotile cell 15 min after ecdysis. Image **10**: Thick pellicle (P) in a nonmotile cell 2 h after ecdysis. Image **11**: Electron micrograph of freeze-fractured pellicle in a nonmotile cell 5–6 h after ecdysis. Note lateral association of some microfibrils. Image **12**: Microfibrils labeled with CBH-I gold particles, which were isolated from thecal plates. Arrowheads show microtubules th, thecal plate.

In *S. hexapraecingula*, the pellicle develops at the outside of the plasma membrane of nonmotile cells after ecdysis (Sekida et al. 2001a). Just after ecdysis, the cell produces an electron-dense, thin layer (Figure 12-8). Thirty minutes after ecdysis, an electron-transparent layer is deposited on the electron-dense, thin layer (Figure 12-9) and develops as the pellicle thickens to about 300 nm until 2 h after ecdysis (Figure 12-10). The electron-transparent layer appears homogeneous in thin sections (Figure 12-10), but it actually contains closely packed microfibrils (Figure 12-11). Microfibrils isolated from the pellicle have diameters of 2–14 nm and consist of very fine fibrils (about 2 nm in diameter) (Figure 12-12), which are more slender than those in the thecal plates. The microfibrils are identified as cellulose by labeling with CBH-I gold (Figure 12-12) as well as by their electron diffraction pattern (Figures 12-13 and 12-15).

In *S. hexapraecingula*, amphiesmal vesicle membranes in the motile cells and the plasma membrane in the nonmotile cells were examined by freeze-fracture electron microscopy to determine whether they contained cellulose-synthesizing TCs (Sekida et al. 2004). According to Sekida et al. (2004), no microfibril impression was found in the protoplasmic face (PF) and the extracellular face (EF) of either the inner or outer amphiesmal vesicle membranes in the motile cells. No particle

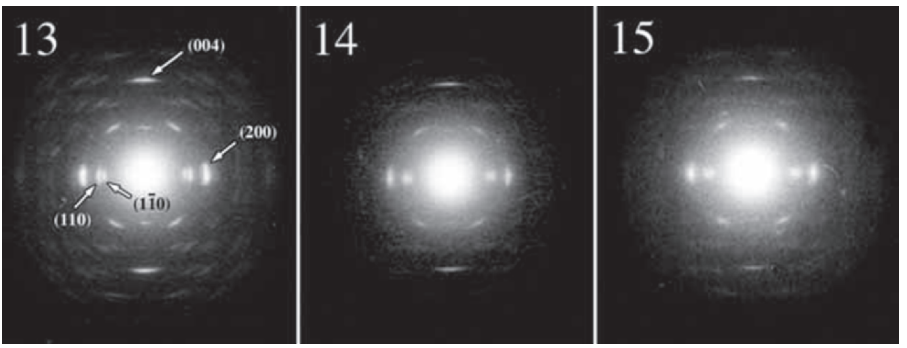

Figures 12-13 to 12-15. Electron diffraction patterns of cellulose microfibrils isolated from the tunicate *Halocynthia* as a standard cellulose sample (**13**), microfibrils isolated from thecal plates (**14**), and pellicles (**15**) of *Scrippsiella hexapraecingula*. Note the typical equatorial (110, 1$\bar{1}$0, 200) and meridional (004) reflections of cellulose I.

aggregates that could be TCs were observed on the fracture faces in any of 200 specimens examined. However, Sekida et al. (2004) found that TCs are present in the nonmotile cells 0.5–3 h after ecdysis but they are not observed more than 4 h after ecdysis. In the nonmotile cells of *S.hexapraecingula*, microfibrils of the pellicle and their impressions on the EF of the plasma membrane are arranged with random orientations (Figure 12-17). Some microfibrils are associated laterally with each other to form a band that is often curved. Particle arrays are found only in the PF of the plasma membrane (Figure 12-16). Since these particle arrays are associated with the ends of individual microfibril impressions, they are regarded as TCs (Sekida et al. 2004). This was the first to report the presence of TCs in dinoflagellates. The TCs consist of two rows of particles (Figures 12-16, 12-18 to 12-21). The particles have diameters of 5–15 nm (an average of 9.1 nm) and are not necessarily arranged at regular intervals. The number of particles ranges from 5 to 40 and averages 19. The TCs have a length of 62.5–290 nm (139.4 nm average) and a width of 15–31 nm (21.5 nm average). The TCs of *S. hexapraecingula* form two rows, and thus are of the linear multiple row type. However, the multiple rows of TCs of *S. hexapraecingula* differ from those of other species in two ways. *S. hexapraecingula* has two rows of TCs, while glaucophycean, chlorophycean, and ulvophycean green algae have three rows (Willison and Brown, Jr. 1978; Brown, Jr. and Montezinos 1976; Itoh 1990). The TCs of *S. hexapraecingula* are also irregularly spaced, while in some red algae, which have from 2 to 4 rows of TCs (Tsekos 1999), the TCs are almost regularly spaced. Thus, *S. hexapraecingula* has a new linear type of TC that has not been found in other organisms examined so far. In *S. hexapraecingula*, several TCs up to 7 are often associated laterally with each other and formed a cluster (Figures 12-16, 12-18–12-21). These clusters may synthesize a band of microfibrils and consolidate to function as a single TC, because they were followed by parallel impressions of microfibrils (below broken lines in Figure 12-16). This is consistent with

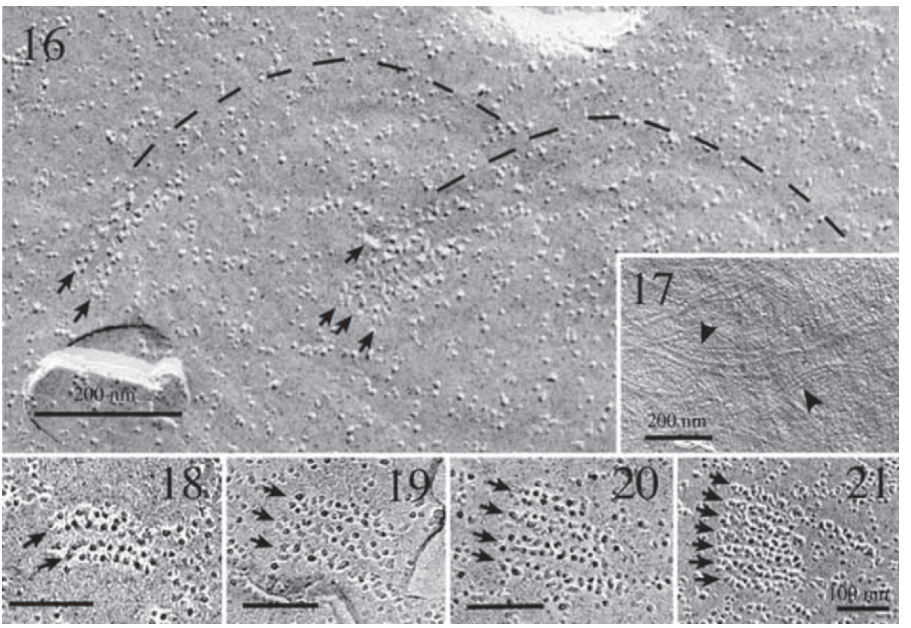

Figures 12-16 to 12-21. Electron micrographs of freeze-fractured plasma membranes of nonmotile cells in *Scrippsiella hexapraecingula*. (**16**) TCs (arrows) in the PF of the plasma membrane. Parallel microfibril impressions seen below broken lines. (**17**) Microfibril impressions in the EF of the plasma membrane. Note lateral association of some microfibrils (arrowheads). (**18–21**) Consolidation of TCs. Two (**18**), three (**19**), four (**20**) or seven (**21**) TCs consolidating as a cluster. A bar in **18**–**21** indicates 100 nm.

the case where individual rosette TCs form hexagonal arrays during secondary wall formation in zygnematalean green algae belonging to the Charophyceae (Giddings et al. 1980), and with the formation of multiple linear TCs in a slime mold (Grimson et al. 1996). The consolidation of TCs might be the result of parallel evolution in distinct phylogenetic groups.

3 OCCURRENCE OF DISTINCT TCs IN THE HETEROKONTOPHYTA

Heterokontophytes are a large phylogenetic group including at least eleven taxonomic classes (Kawachi et al. 2002) and exhibit a great diversity in thallus organizations, growth patterns, habitats and life histories, which may be equivalent to that in chlorophytes. Although a relatively small number of investigations on cellulose and TCs in heterokontophytes have been carried out, at least three distinct TCs have been reported so far in the four classes, the Phaeophyceae, the Xanthophyceae, the Phaeothamniophyceae, and the Eustigmatophyceae. The presence of cellulose was shown in several species of the Phaeophyceae (Cronshaw et al. 1958) and the Xanthophyceae (Parker et al. 1963) by x-ray diffraction and chemical analyses. In the zygote of the phaeophycean alga *Pelvetia*, Peng and Jaffe (1976) found

single linear particle rows associated with the tip of microfibril imprints in the freeze-fractured plasma membrane first. Peng and Jaffe (1976) regarded the linear particle rows as elements for orienting microfibrils. Later, in other eight species of the Phaeophyceae, similar linear particle rows have been confirmed to occur at the ends of microfibril imprints in the PF of the plasma membrane and then assumed to be TCs (Katsaros et al. 1996; Reiss et al. 1996; Tamura et al. 1996; Schüßler et al. 2003). Each of TCs in these phaeophycean algae consists of a single liner row of particles 6–7 nm in diameter (Figure 12-22) and synthesizes a thin, ribbon-like cellulose microfibril with a uniform thickness (Figure 12-23). Individual particles constituting TCs may be composed of two closely packed subunits (Reiss et al. 1996). The number of TC particles varies between 10–100, concomitant with microfibrils with a variable width in the range of 2.6–30 nm in *Sphacelaria* (Tamura et al. 1996). A higher density of TCs has been shown in the apical area of tip growing cells in *Syringoderma* (Schüßler et al. 2003). The occurrence of short linear particle rows in Golgi vesicles suggests that TC precursors may be transported to the plasma membrane via these vesicles (Reiss et al. 1996).

Mizuta et al. (1989) found a TC on the PF of the plasma membrane in the xanthophycean alga *Vaucheria hamata* first, which is quite distinctive from TCs in phaeophycean algae. After Mizuta et al. (1989), TCs have been found in other two xanthophycean species *Botrydium stoloniferum* (Sekida et al. 2001b) and *Botrydiopsis intercedens* (Okuda et al. 2004). These xanthophycean algae have TCs composed of diagonal rows of particles (Figure 12-24) and assemble a thin, ribbon-like microfibril (Figure 12-25). The number of particles in an individual diagonal row and the number of diagonal rows constituting a TC vary (Table 12-1). As shown in Table 12-1, there are slight differences in TC and microfibril structures among the xanthophycean species so far examined. The length of TCs in *B. intercedens* and *V. hamata* is longer than that in *B. stoloniferum*. However, TCs in *B. intercedens* consist of a smaller number of diagonal rows than those in *V. hamata*, since spacings between neighboring diagonal rows in *B. intercedens* are larger than those in *V. hamata*. In the TC of *B. stoloniferum*, the number of particles in diagonal rows at the both ends of the TC is about half as much as that in the other diagonal rows, whereas the length of diagonal rows among a TC is almost the same in *B. intercedens* and *V. hamata*. Furthermore, cellulose microfibrils synthesized by TCs in *B. intercedens* and *B. stoloniferum* are thicker than those in *V. hamata*. According to Mizuta et al. (1989) and Mizuta and Brown, Jr. (1992a), *Vaucheria* TCs are separated into two types: TCs associated with microfibril impressions that are presumably active in microfibril formation; TCs unassociated with microfibril impressions that are presumably inactive in microfibril formation. The average number of diagonal rows in the former TCs is about 14, while in the latter TCs it is about 8. Such two types of TC also have been found in *B. intercedens*, but TCs unassociated with microfibril impressions usually appear in group (Okuda et al. 2004). In *Vaucheria*, TC assembly occurs directly on the plasma membrane from particulate precursors (globules) that are supplied by Golgi vesicles to the plasma membrane (Mizuta and Brown, Jr. 1992a)

and may be inhibited by Tinopal LPW (Mizuta and Brown, Jr. 1992b). Unlike in *Vaucheria*, in *B. intercedens* diagonal rows of particles also appear in the PF of cytoplasmic vesicles different from Golgi vesicles (Okuda et al. 2004). The diagonal rows of particles are assumed to be TC precursors that may be loaded into the plasma membrane through the fusion of the cytoplasmic vesicles (Okuda et al. 2004).

Bailey et al. (1998) established the class Phaeothamniophyceae in heterokontophytes. Recently, a new type of TC was found on the PF of the plasma membrane in three species belonging to the Phaeothamniophyceae (Okuda et al. 2004). The TC generally consists of three linear rows of particles in these species (Figure 12-26). However, *Phaeothamnion confervicola* and *Stichogloea doederleinii* have also TCs composed of two linear rows of particles. In *P. confervicola*, asymmetric TCs sometimes occurred, where one row was shorter than the other two. Microfibrils in these three species are characteristic of a thin, ribbon-like structure (Figure 12-27). TCs consisting of 3 linear rows of particles also occur in glaucophycean (Willison and Brown, Jr. 1978), chlorophycean (Brown, Jr. and Montezinos 1976) and ulvophycean (Itoh 1990) green algae. However, the TCs of the phaeothamniophycean species differ from those of these other species in three ways. The TCs of the phaeothamniophycean species are observed only on the PF of the plasma membrane, while TCs are found only on the EF in *Glaucocystis* (Willison and Brown, Jr. 1978) and *Oocystis* (Brown, Jr. and Montezinos 1976) and on both the PF and the EF in ulvophycean algae (Itoh 1990). The TCs of the phaeothamniophycean species synthesize thin, ribbon-like microfibrils with 1–4 nm in thickness and 2–20 nm in width (Okuda et al. 2004), but in the ulvophycean algae much larger microfibrils are synthesized, for example, *Valonia* microfibrils being 20 nm wide and 17 nm thick in average (Kuga and Brown, Jr. 1989). Finally, the length of the TCs of phaeothamniophycean species is relatively short, ranging from 25–100 nm (Okuda et al. 2004). The TCs of *Oocystis* are about 500 nm long (Brown, Jr. and Montezinos 1976), and in *Valonia* the length of the TCs ranges 150–600 nm (350 nm average) during the primary wall formation and 255–799 nm (558 nm average) during the secondary wall formation (Itoh 1990). The dinoflagellate species *Scrippsiella hexapraecingula* has a TC only composed of two linear rows of particles (Sekida et al. 2004).

Okuda et al. (2004) reported the presence of TCs in the Eustigmatophyceae first. The TC of the eustigmatophycean alga *Pseudocharaciopsis minuta* consists of a single linear row of particles on the PF of the plasma membrane (Figure 12-28). Microfibrils isolated from the cells of *P. minuta* may be flat, ribbon-like structures, but most of microfibrils are observed to consist of several fine fibrils 2–4 nm in diameter (Figure 12-29). This type of TC found in *P. minuta* corresponds to that in phaeophycean algae in particle arrangement and formation of thin, ribbon-like microfibrils. Linear rows constituting TCs are occasionally missing particles or consist of some shorter rows with a gap in both eustigmatophycean (Okuda et al. 2004) and phaeophycean (Reiss et al. 1996) algae.

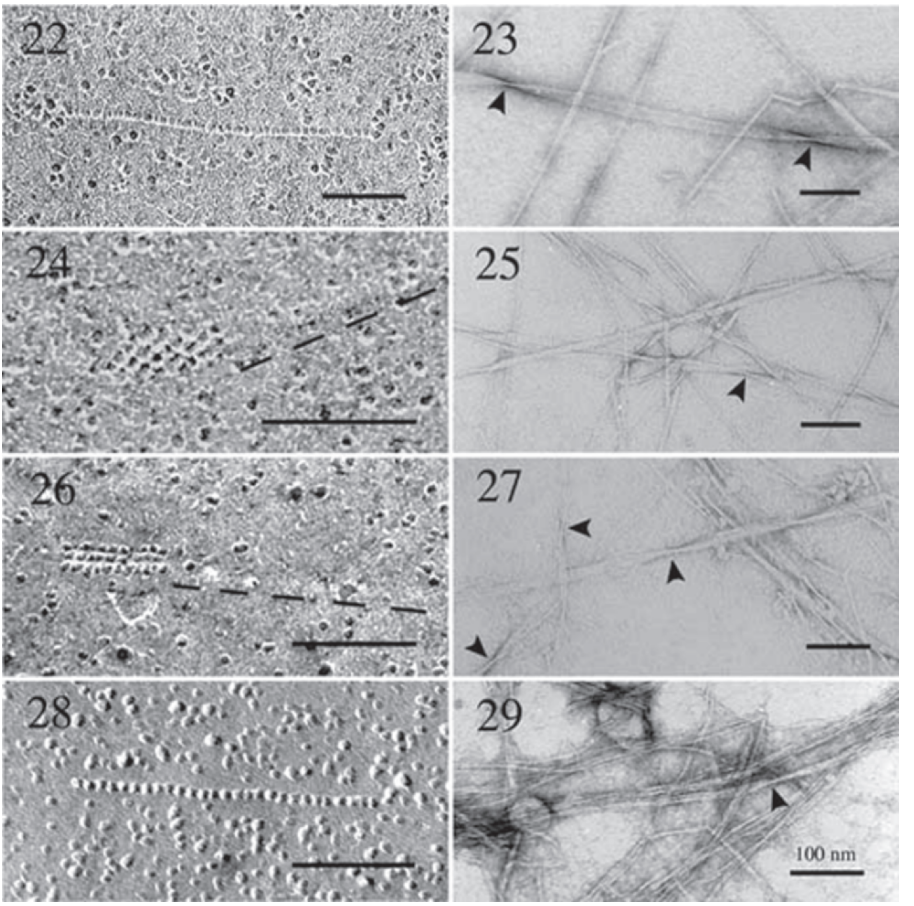

Figures 12-22 to 12-29. Structures of TCs and cellulose microfibrils in heterokontophycean algae. TC (**22**) and microfibrils (**23**) in the phaeophycean alga *Sphacelaria rigidula*. TC (**24**) associated with a microfibril impression (**25**) at the upper side of a broken line in the xanthophycean alga *Botrydium stoloniferum*. TC (**26**) associated with a microfibril impression (**27**) at the upper side of a broken line in the phaeothamniophycean alga *Phaeothamnion confervicola*. TC (**28**) and microfibrils (**29**) in eustigmatophycean alga *Pseudocharaciopsis minuta*. Arrowheads showing thin microfibrils twisted. Each bar indicates 100 nm.

The fact that all heterokontophycean species so far examined synthesize thin, ribbon-like cellulose microfibrils is consistent with the postulation that heterokontophytes constitute a monophyletic algal lineage evolved by the secondary endosymbiosis between a heterokontic protozoan and a chlorophyll *c*-containing eukaryotic alga (Kowallik 1993; McFadden 2001). This contrasts with the case of the Chlorophyta, because in the Chlorophyta chlorophycean and ulvophycean algae synthesize much larger cellulose microfibrils than those synthesized by charophycean algae (see below). In heterokontophytes, each of

Table 12-1. Structural characteristics of TCs and cellulose microfibrils in xanthophycean algae *Botrydiopsis interceden, Botrydium stolonifelum* and *Vaucheria hamata*

Characters	*Botrydiopsis intercedens*	*Botrydium stolonifelum**1	*Vaucheria hamata**2
TC structure	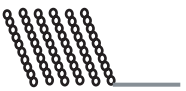		
TC length (nm)	137-[198]-333	30-[80]-130	100-[192]-360
TC width (nm)	53-[60]-71	23-[45]-68	50-[62]-80
Number of diagonal rows	3-[6.2]-8	3-[5.7]-9	6-[14]-25
Number of particles in each diagonal row	6-[10.5]-14	2-[5.7]-10	2-[6.7]-10
Spacing between neighboring diagonal rows (nm)	2.7-[6.3]-8.3	2.5-[3.9]-6.7	1.6-[2.5]-3.2
Particle diameter (nm)	4.4-[6.3]-9.3	7.8×5.8	7×3.5
Microfibril structure		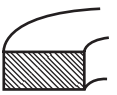	
Microfibril width (nm)	3-[7.7]-17.5	3-[12.6]-35	2-[20.8]-45
Microfibril thickness (nm)	3.8-[4.4]-5	2.5-[4.9]-8.3	0.8-[1.6]-2.2

Parentheses showing means values.
*[1]Data adopted from Sekida et al. (2001b).
*[2]Data adopted from Mizuta et al. (1989) and Mizuta and Brown, Jr. (1992a).

three distinct TCs known at present assembles thin, ribbon-like microfibrils. Therefore, a whole of heterokontophytes may be a good example to give evidence for that extant TCs had modified or evolved from a common original TC phylogenetically. The heterokontophyte algae consist of eleven major taxonomic groups: eustigmatophytes, dictyochophytes, pelagophytes, bacillariophytes, synurophytes, chrysophytes, raphidophytes, pinguiophytes, xanthophytes, phaeophytes, phaeothamniophytes (Kawachi et al. 2002). Among them, phaeophytes, xanthophytes and phaeothamniophytes include multicellular forms with cell walls, and phaeophytes are thought to be the most evolved group in the Heterokontophyta (Clayton 1989). According to recent gene sequence analyses on *rbc*L genes, the Eustigmatophyceae form the basal clade in the *rbc*L tree, and the Phaeophyceae, the Xanthophyceae and the Phaeothamniophyceae are included in the same clade (Bailey et al. 1998; Kawachi et al. 2002). Further the Phaeothamniophyceae are sister taxa to the Phaeophyceae and Xanthophyceae clades according to Kawachi et al. (2002). Based on the *rbc*L tree, the Eustigmatophyceae diverged earliest from the origin of chromophytes. This suggests that the origin had the same TC type of a single linear row as extant eustigmatophycean

algae. If this would be true, the Phaeophyceae would have inherited the basic organization of original TCs since extant phaeophycean algae have the TC type of a single linear row. The Phaeothamniophyceae have distinct TCs from the TCs of the Phaeophyceae and the Xanthophyceae. This suggests that the following events happened: When the Phaeophyceae, the Xanthophyceae and the Phaeothamniophyceae diverged from their common origin, the diagonal row TC type of the Xanthophyceae would have evolved independently from that of a single linear row. In the Phaeothamniophyceae, the 2–3 linear row TC type would have been acquired from a single linear row TC type.

4 DIVERSIFICATION IN CELLULOSE MICROFIBRIL ASSEMBLY

Cellulose is found widely in different phylogenetic groups such as prokaryotes, slime molds, glaucophytes, chlorophytes including land plants, rhodophytes, haptophytes, chromophytes, fungi and invertebrates (Richmond 1991). Diverse TCs have evolved, although all the TCs have the same function in cellulose microfibril assembly. TC organization may be related to microfibril structure, i.e., the mode of crystallizing cellulose molecules into a microfibril (Okuda et al. 1994). Microfibril features assembled by distinct TCs may fall into five groups (Figure 12-30). A dinophycean species has a TC of random or two rows of particles, which produces a bundle composed of 2-nm microfibrils. A thin, ribbon-like microfibril is synthesized by a TC consisting of a single linear row of particles in the Phaeophyceae and in the gram-negative bacterium *Acetobacter xylinum* (Zaar 1979), by a TC of several diagonal rows of particles in the Xanthophyceae, by a TC of 2–3 linear rows of particles in the Phaeothamniophyceae or by a TC of several transverse rows of particles in the Rhodophyceae (Tsekos and Reiss 1992). Large microfibrils are synthesized by TCs consisting of multiple linear rows of particles in some members of the Chlorophyceae (Brown, Jr. and Montezinos 1976) and the Ulvophyceae (Itoh 1990) and in a species in the Glaucophyta (Willison and Brown, Jr. 1978). A TC called a rosette in charophycean green algae and land plants synthesizes a microfibril with a diameter of 3.5 nm (Brown, Jr. 1996). Finally, large microfibrils in the tunicate *Metandrocarpa uedai* are synthesized by quite unique TCs and consist of almost pure cellulose Iβ cellulose crystalline (Kimura and Itoh 1996).

The presently known variations in TC organization and microfibril structure reflect a divergent evolution for cellulose synthases and their regulation. This suggests that some distinct origins that had acquired and evolved the organized enzyme structure essential for cellulose microfibril assembly occurred independently in different evolutionary lines. According to the endosymbiont hypothesis based on gene sequences of *rbc*L, the divisions Rhodophyta, Glaucophyta and Chlorophyta arose through the endosymbiosis of a photoautotrophic bacterium (a cyanobacterium) with a heterotrophic flagellate (McFadden et al. 1995). Members belonging to these divisions might have acquired the ability to synthesize cellulose from cyanobacteria (Figure 12-31),

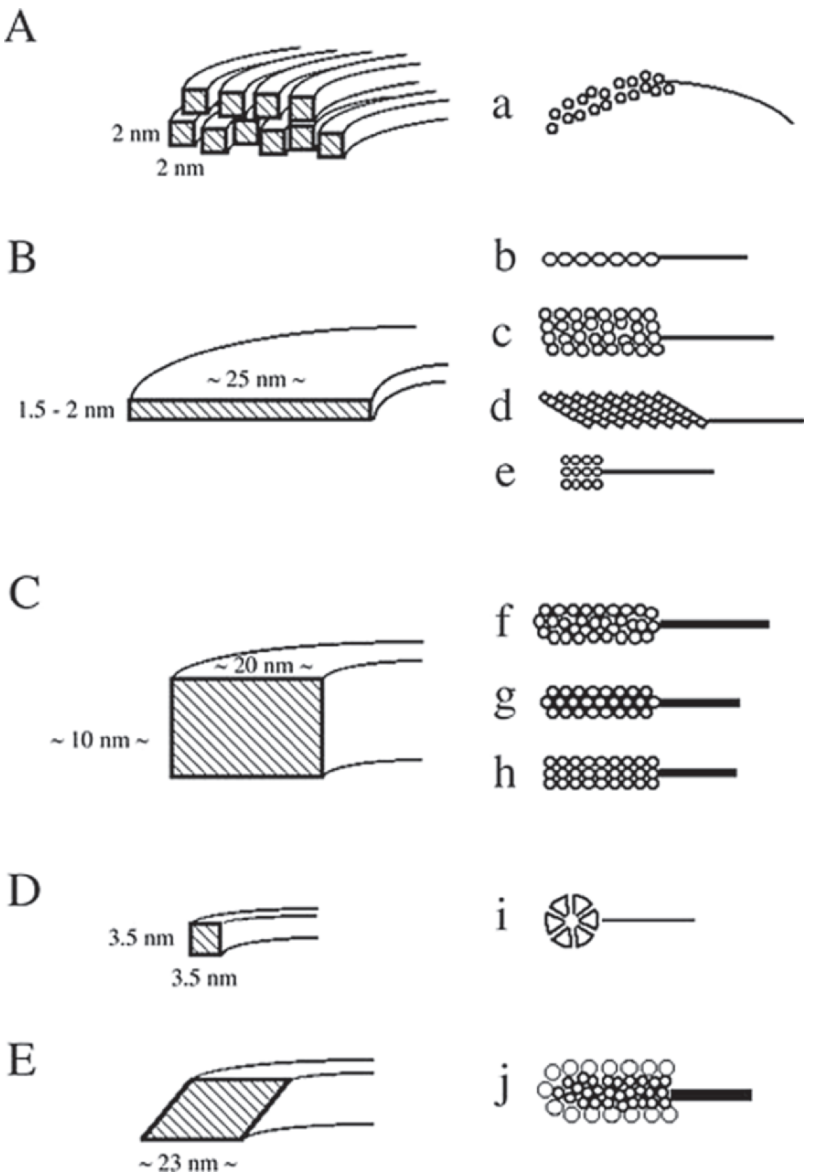

Figure 12-30. Structures of cellulose microfibrils synthesized by distinct TCs. Note cross sectional views of cellulose microfibrils (oblique lines) and particle arrangement of TCs on the fractured face of the plasma membrane. (**A**) A bundle consisting of 2-nm fine fibrils, which is synthesized by a dinoflagellate TC (**a**). (**B**) A thin, ribbon-like microfibril synthesized by each of phaeophycean and eustigmatophycean TCs (**b**), and rhodophycean (**c**), xanthophycean (**d**), and phaeothamniophycean TCs (**e**). (**C**) A large microfibril synthesized by each of ulvophycean (**f**), chlorophycean (**g**), and glaucophycean TCs (**h**). (**D**) A 3.5-nm microfibril synthesized by a rosette TC (**i**). (**E**) A microfibril with a parallelogrammic section synthesized by a tunicate TC (**j**).

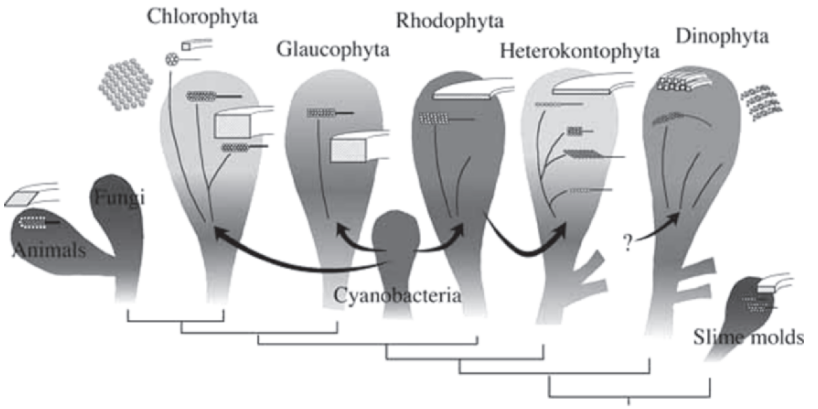

Figure 12-31. TC organization and microfibril structure in an evolutionary aspect, based on a phylogenetic tree. Modified after McFadden et al. (1994).

since certain cyanobacteria produce cellulose (De Winder et al. 1990). Further, the phylogenetic tree based on gene sequences of 18S rRNA suggests that the other algal divisions arose form different heterotrophic flagellate ancestors, through the incorporation of a primaeval photosynthetic, eukaryotic alga (McFadden et al. 1994).

The Heterokontophyta are suggested to have evolved when primaeval heterokonts incorporated rhodophyte-like algae as chloroplasts into the cells. The ability to synthesize cellulose in the Heterokontophyta might have brought from such rhodophyte-like algae, since the TCs of the Rhodophyta and the Heterokontophyta assemble similar thin, ribbon-like microfibrils (Figure 12-31). The TCs of the dinoflagellate *Scrippsiella* seem to be primitive, because the microfibrils synthesized are aggregates or bundles consisting of fine 2-nm-fibrils. The Dinophyta consist of diverse species containing chloroplasts that originated from distinct photosynthetic eukaryotes such as rhodophyte-, heterokontophyte- and haptophyte-like algae (Yoon et al. 2002). However, the way of acquiring the ability to synthesize cellulose through endosymbiosis with photosynthetic cells cannot be applied to cases in cellulose-producing animal, fungi and slime molds. In the ancestors of these organisms, genes involved in cellulose synthesis might have been transduced from other cellulose-producing organisms with mediated by viruses independently (Brown, Jr. 1990).

REFERENCES

Bailey J.C., Bidigare R.R., Christensen S.J., and Andersen R.A. 1998. Phaeothamniophyceae *classis nova*: a new lineage of chromophytes based upon photosynthetic pigments, *rbc*L sequence analysis and ultrastructure. Protist 149:245–263.

Bricheux G., Mahoney D.G., and Gibbs S.P. 1992. Development of the pellicle and thecal plates following ecdysis in the dinoflagellate *Glenodinium foliaceum*. Protoplasma 168:159–171.

Brown, Jr. R.M. 1985. Cellulose microfibril assembly and orientation: recent developments. J Cell Sci (Suppl.) 2:13–32.

Brown, Jr. R.M. 1990. Algae as tools in studying the biosynthesis of cellulose, nature's most abundant macromolecule. In: Wiessner W., Robinson D.G. and Starr R.C. (eds.) Experimental Phycology, vol. 1, Cell walls and surfaces, reproduction, photosynthesis. Springer, Berlin, pp. 20–39.

Brown, Jr. R.M. 1996. The biosynthesis of cellulose. J Macromol Sci- Pure Appl Chem A33:1345–1373.

Brown, Jr. R.M., and Montezinos D. 1976. Cellulose microfibrils: visualization of biosynthetic and orienting complexes in association with the plasma membrane. Proc Natl Acad Sci USA 73:143–147.

Brown, Jr. R.M., Haigler C.H., Suttie J., White A.R., Roberts E., Smith C., Itoh T., and Cooper K. 1983. The biosynthesis and degradation of cellulose. J Appl Poly Sci Appl Poly Symp 37:33–78.

Cavalier-Smith T. 1993. Kingdom protozoa and its 18 phyla. Microbiol Rev 57:953–994.

Clayton M.N. 1989. Brown algae and chromophyte phylogeny. In: Green J.C., Leadbeater B.S.C. and Diver W.L. (eds.) The Chromophyte Algae: Problems and Perspectives—Systematics Association Special, vol. 38. Clarendon Press, Oxford, pp. 229–253.

Cronshaw J., Myers A., and Preston R.D. 1958. A chemical and physical investigation of the cell walls of some marine algae. Biochim Biophys Acta 27:89–103.

De Winder B., Stal L.J., and Mur L.R. 1990. *Crinalium epipsammum* sp. now: a filamentous cyanobacterium with trichomes composed of elliptical cells and containing poly-β-(1,4)-glucan (cellulose). J General Microbiol 136:1645–1653.

Dodge J.D. 1971. Fine structure of the Pyrrophyta. Bot Rev 37:481–508.

Dodge J.D. and Crawford R.M. 1970. A survey of thecal fine structure in the Dinophyceae. Bot J Linn Soc 63:53–67.

Emons, A.M.C. 1991. Role of particle rosettes and terminal globules in cellulose sythesis. In: Haigler C.H. and Weimer P.J. (eds.) Biosynthesis and Biodegradation of Cellulose. Marcel Dekker, New York, pp. 71–98.

Giddings T.H. Jr., Brower D.L., and Staehelin L.A. 1980. Visualization of particle complexes in the plasma membrane of *Micrasterias denticulata* associated with the formation of cellulose fibrils in primary and secondary cell walls. J Cell Biol 84:327–339.

Grimson M.J., Haigler C.H., and Blanton R.L. 1996. Cellulose microfibrils, cell motility, and plasma membrane protein organization change in parallel during culmination in *Dictyostelium discoideum*. J Cell Sci 109:3079–3087.

Höhfeld I. and Melkonian M. 1992. Amphiesmal ultrastructure of dinoflagellates: a reevaluation of pellicle formation. J Phycol 28:82–89.

Itoh T. 1990. Cellulose synthesizing complexes in some giant marine algae. J Cell Sci 95:309–319.

Katsaros C., Reiss H.-D., and Schnepf E. 1996. Freeze-fracture studies in brown algae: putative cellulose-synthesizing complexes on the plasma membrane. Eur J Phycol 31:41–48.

Kawachi M., Inouye I., Honda D., O'Kelly C.J., Bailey J.C., Bidigare R.R., and Andersen R.A. 2002. The Pinguiophyceae *classis nova*, a new class of photosynthetic stramenopiles whose members produce large amounts of omega-3 fatty acids. Phycol Res 50:31–47.

Kimura S. and Itoh T. 1996. New cellulose synthesizing complexes (terminal complexes) involved in animal cellulose biosynthesis in the tunicate *Metandrocarpa uedai*. Protoplasma 194:151–163.

Kimura S., Laosinchai W., Itoh T., Cui X., Linder C.R., and Brown, Jr. R.M. 1999. Immunogold labeling of rosette terminal cellulose-synthesizing complexes in the vascular plant *Vigna angularis*. Plant Cell 11:2075–2085.

Kowallik K.V. 1993. Origin and evolution of plastids from chlorophyll a+c containing algae, suggested ancestral relationships to red and green algal plastids. In: Lesin R.A. (ed.) Origins of plastids—symbiogenesis, prochlorophytes and the origins of chloroplasts. Chapman and Hall, New York, pp. 223–263.

Kuga S. and Brown, Jr. R.M. 1989. Correlation between structure and the biogenic mechanisms of cellulose: new insights based on recent electron microscopic findings. In: Schuerch C. (ed.) Cellulose and wood-chemistry and technology. Wiley, New York, pp. 677–688.

Loeblich A.R. III. 1970. The amphiesma or dinoflagellate cell covering. In: Yochelson E.L. (ed.) Proceedings of the North American Paleontology Convention Chicago, Illinois. Allen Press, Lawrence, KS, pp. 867–929.

McFadden G.I. 2001. Primary and secondary endosymbiosis and the origin of plastids. J Phycol 37:951–959.

McFadden G.I., Gilson P.R., and Hill D.R.A. 1994. *Goniomonas*: rRNA sequences indicate that this phagotrophic flagellate is a close relative of the host component. Eur J Phycol 29:29–32.

McFadden G.I., Gilson P.R., and Waller R. 1995. Molecular phylogeny of chlorarachniophytes based on plastid rRNA and *rbc*L sequences. Arch Protistenkd 145:231–239.

Mizuta S. and Brown, Jr. R.M. 1992a. High resolution analysis of the formation of cellulose synthesizing complexes in *Vaucheria hamata*. Protoplasma 166:187–199.

Mizuta S. and Brown, Jr. R.M. 1992b. Effects of 2,6-dichlorobenzonitrile and Tinopal LPW on the structure of the cellulose synthesizing complexes of *Vaucheria hamata*. Protoplasma 166:200–207.

Mizuta S., Roberts E.M., and Brown, Jr. R.M. 1989. A new cellulose synthesizing complex in *Vaucheria hamata* and its relation to microfibril assembly. In: Schuerch C. (ed.) Cellulose and Wood-Chemistry and Technology. Wiley, New York, pp. 656–676.

Morrill L.C. 1984. Ecdysis and the location of the plasma membrane in the dinoflagellate *Heterocapsa niei*. Protoplasma 119:8–20.

Morrill L.C. and Loeblich A.R. III. 1981. The dinoflagellate pellicular wall layer and its occurrence in the division Pyrrhophyta. J Phycol 17:315–323.

Morrill LC. and Loeblich, A.R. III. 1983. Ultrastructure of the dinoflagellate amphiesma. Int Rev Cytol 82:151–180.

Mueller S.C. and Brown, Jr. R.M. 1980. Evidence for an intramembrane component associated with a cellulose microfibril synthesizing complex in higher plants. J Cell Biol 84:315–326.

Netzel H. and Dürr G. 1984. Dinoflagellate cell cortex. In: Spector D. (ed.) Dinoflagellates. Academic Press, Orlando, FL, pp. 43–105.

Nevo Z. and Sharon N. 1969. The cell wall of *Peridinium westii*, a noncellulosic glucan. Biochim Biophys Acta 173:161–175.

Okuda K. 2002. Structure and phylogeny of cell coverings. J Plant Res 115:283–288.

Okuda K., Sekida S., Yoshinaga S., and Suetomo Y. 2004. Cellulose-synthesizing complexes in some chromophyte algae. Cellulose 11:365–376.

Okuda K., Tsekos I., and Brown, Jr. R.M. 1994. Cellulose microfibril assembly in *Erythrocladia subintegra* Rosenv.: an ideal system for understanding the relationship between synthesizing complexes (TCs) and microfibril crystallization. Protoplasma 180:49–58.

Peng H.B. and Jaffe L.F. 1976. Cell wall formation in *Pelvetia* embryos: a freeze-fracture study. Planta 133:57–61.

Parker C.W., Preston R.D., and Fogg E.G. 1963. Studies of the structure and chemical composition of the cell walls of *Vaucheria* and Saprolegniaceae. Proc Roy Soc B 158:435–445.

Quader H. 1991. Role of linear terminal complexes in cellulose synthesis. In: Haigler C.H. and Weimer P.J. (eds.) Biosynthesis and biodegradation of cellulose. Marcel Dekker, New York, pp. 51–69.

Reiss H.-D., Katsaros C., and Galatis B. 1996. Freeze-fracture studies in the brown alga *Asteronema rhodochortonoides*. Protoplasma 193:46–57.

Richmond P.A. 1991. Occurrence and function of native cellulose. In: Haigler C.H. and Weimer P.J. (eds.) Biosynthesis and biodegradation of cellulose. Marcel Dekker, New York, pp. 5–23.

Schüßler A., Hirn S., and Katsaros C. 2003. Cellulose synthesizing terminal complexes and morphogenesis in tip-growing cells of *Syringoderma phinneyi* (Phaeophyceae). Phycol Res 51:35–44.

Sekida S., Horiguchi T., and Okuda K. 1999. Direct evidence for cellulose microfibrils present in thecal plates of the dinoflagellate *Scrippsiella hexapraecingula*. Hikobia 13:65–69.

Sekida S., Horiguchi T., and Okuda K. 2001a. Development of the cell covering in the dinoflagellate *Scrippsiella hexapraecingula* (Peridiniales, Dinophyceae). Phycol Res 49:163–176.

Sekida S., Shibagaki R., and Okuda K. 2001b. A putative cellulose-synthesizing terminal complex in *Botrydium stoloniferum* (Xanthophyceae). Hikobia 13:457–462.

Sekida S., Horiguchi T., and Okuda K. 2004. Development of thecal plates and pellicle in the dinoflagellate *Scrippsiella hexapraecingula* (Peridiniales, Dinophyceae) elucidated by changes in stainability of the associated membranes. Eur J Phycol 39:105–114.

Swift E. and Remsen C.C. 1970. The cell wall of *Pyrocystis* spp. (Dinococcales). J Phycol 6:79–86.

Tamura H., Mine I., and Okuda K. 1996. Cellulose-synthesizing terminal complexes and microfibril structure in the brown alga *Sphacelaria rigidula* (Sphacelariales, Phaeophyceae). Phycol Res 44:63–68.

Taylor F.J.R. 1987. Dinoflagellate morphology. In: Taylor F.J.R. (ed.) The biology of dinoflagellates. Blackwell Scientific, Oxford, pp. 24–91.

Tsekos I. 1999. The sites of cellulose synthesis in algae: diversity and evolution of cellulose-synthesizing enzyme complexes. J Phycol 35:635–655.

Tsekos I. and Reiss H.-D. 1992. Occurrence of the putative microfibril-synthesizing complexes (linear terminal complexes) in the plasma membrane of the epiphytic marine red alga *Erythrocladia subintegra* Rosenv. Protoplasma 169:57–67.

Tsekos I., Okuda K., and Brown, Jr. R.M. 1996. The formation and development of cellulose-synthesizing linear terminal complexes (TCs) in the plasma membrane of the marine red alga *Erythrocladia subintegra* Rosenv. Protoplasma 193:33–45.

Wetherbee R. 1975. The fine structure of *Ceratium tripos*, a marine armored dinoflagellate. III. Thecal plate formation. J Ultrastr Res 50:77–87.

Willison J.H.M. and Brown, Jr. R.M. 1978. Cell wall structure and deposition in *Glaucocystis*. J Cell Biol 77:103–119.

Yoon H.S., Hackett J.D., and Bhattacharya D. 2002. A single origin of the peridinin- and fucoxanthin-containing plastids in dinoflagellates through tertiary endosymbiosis. Proc Natl Acad Sci USA 99:11724–11729.

Zaar K. 1979. Visualization of pores (export sites) correlated with cellulose production in the envelope of the gram-negative bacterium *Acetobacter xylinum*. J Cell Biol 80:773–777.

CHAPTER 13

BIOGENESIS AND FUNCTION OF CELLULOSE IN THE TUNICATES

SATOSHI KIMURA*[1] AND TAKAO ITOH[2]

[1]*The University of Tokyo, Graduate School of Agriculture and Life Science, Department of Biomaterials Sciences, 1–1–1 Yayoi, Bunkyo-ku, Tokyo 113–8657, Japan*
[2]*Research Institute for Sustainable Humanosphere, Kyoto University, UJi, Kyoto 611–0011, Japan*

Abstract

Tunicates are well known as the only animals to produce cellulose. The cellulose microfibrils of the tunicates are generally large in width and are highly crystalline. They are composed of almost pure monoclinic cellulose I (the Iβ allomorph). Electron microscopic approaches were performed to clarify the site for cellulose biogenesis and the distribution and function of cellulose in the tunicates. A freeze-fracture investigation revealed a new type of cellulose-synthesizing enzyme complex (TC) on the plasma membrane of epidermal cells in several species of ascidians. The finding of TCs in a member of the animal kingdom indicates that cellulose assembly by TCs is a phenomenon common to all three major groups of organisms. The biogenesis of cellulose was also found in the vacuole of a unique cell, glomerulocyte that accumulates bundled cellulose microfibrils in the cell by tapering off its vacuole. Cellulose microfibrils were found in several regions in the body of tunicates. A network form of cellulose microfibrils derived from the glomerulocyte is distributed in the hemocoel. Another unique cellulosic structure, the tunic cord, is located in the siphons. These cellulosic structures act for mechanical support of the body. The most primitive tunicates, the appendicularians, also produces highly crystalline cellulose. They make a highly ordered mesh structure with cellulose microfibrils and utilize the cellulose mesh as a feeding filter. In this chapter, we describe a variety of cellulosic structures as well as cellulose biosynthesis in tunicates.

Keywords

tunicates, cellulose, terminal complexes, ascidians, cellulose biosynthesis, glomerulocyte

* For correspondence: Tel: +81 3 5841 5241; Fax: +81 3 5684 0299; e-mail: kimura@sbp.fp.a.u-tokyo.ac.jp

R.M. Brown, Jr. and I.M. Saxena (eds.), Cellulose: Molecular and Structural Biology, 217–236.

1 INTRODUCTION

Various approaches utilized for studying cellulose biosynthesis have suggested that the synthesis and structure of cellulose is characterized by diverse features among the cellulose-synthesizing organisms. To obtain a unified view of cellulose biosynthesis, it is important to review the biosynthesis of cellulose in the various cellulose-synthesizing organisms. Considerable progress has been made in the study of cellulose biosynthesis in plants and bacteria, and although it is known that a group of animals, the tunicates, makes cellulose, an understanding of the site and the mechanism of cellulose biosynthesis in this group of organisms has not been very clear. Therefore, we have investigated the biogenesis and functions of cellulose in the tunicates.

Tunicata (commonly called urochordates, tunicates, sea squirts) is the subphylum of filter feeders with input and output siphons. Like other chordates, tunicates possess a notochord during their early stages of development. The name "Tunicata" is derived from the unique integumentary tissue, the tunic, which entirely covers the epidermis. Tunicates are well known as the only animals to produce cellulose (Richmond 1991). Cellulose formed as crystalline microfibrils, is a major component of the tunic, and the cellulose microfibrils are deposited in a multilayered texture with a bundled structure parallel to the epidermis. The subphylum Tunicata includes three classes; all species possess tunic in the classes Ascidiacea and Thaliacea. Animals in the third class of the Tunicata, the Appendicularia, do not possess the tunic. However, appendicularians secrete a balloon-like gelatinous structure called the house that acts as a feeding apparatus, and the house is constituted of cellulose microfibrils, (Kimura et al. 2001).

Ascidians are the major group of organisms in the Tunicata, and are found mostly on hard surfaces such as rocks, jetty pilings and coral rubble (Goodbody 1974). They also grow on sea grasses and other vegetation in the sea grass lagoon. An ascidian is a complex animal; it usually has a circulatory system, a digestive system, a heart and other organs. It generates a one-way current through its body and part of the gut is modified to filter out planktons from this water flow. The entire animal is encased in a little bag which is the tunic. In fact, Ascidiacea means "a little bag" (Figure 13-1a, b). The biology and biochemistry of the tunic has been studied mainly in the ascidians, because they are the sessile forms of tunicates and are easy to culture. The other groups are pelagic tunicates. To date, it has been found that the tunic of ascidians and thaliaceans, and the house of appendicularians contain cellulose microfibrils of high crystallinity that act as skeletal structures in these tissues (Hirose et al. 1999; Kimura et al. 2001). Thus, cellulose production is a characteristic feature common to all tunicates. Furthermore, many interesting functions of cellulose have been shown in the tunicates. Here, we describe biogenesis and function of cellulose in the tunicates using electron microscopy and provide information on (1) the site of cellulose biosynthesis, (2) cellulose biosynthesis in the glomerulocyte, (3) new cellulosic structure in the tunicates, and (4) structure and function of cellulose in the appendicularian which is the most primitive tunicate.

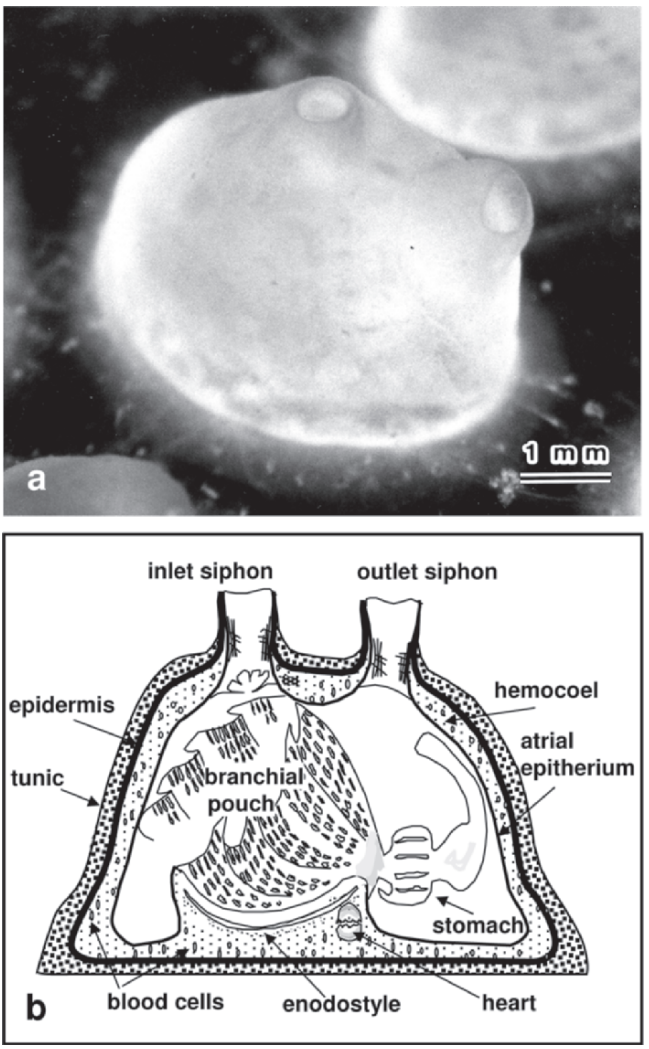

Figure 13-1. Light microscopic image of an ascidian (**a**) and a schematic representation of the structural plan of its body (**b**). An adult zooid of *Metandrocarpa uedai* (**a**) is approximately 5 mm in length and 3 mm in width. Ascidians of this small size are suitable for study using microscopic approaches. Cellulose is a major component of the outer protective tissue (tunic) of ascidians (**b**). Cellulose is also found in the basal region of the siphons and hemocoel in selected ascidians

2 TEXTURE OF THE TUNIC IN THE ASCIDIANS

Early descriptions of the occurrence of cellulose in the tunicates were provided by Berrill (1950) and Endean (1955a, b, 1961). Berrill (1950) described that the tunic contains approximately 60% cellulose, 27% nitrogen-containing components and, in the fresh condition, approximately 90% water. The development of the tunic

varies greatly in different groups of the tunicates. In colonial forms it may be thin and translucent, or highly colored, whereas in the *Pyuridae* it reaches its greatest development and contains numerous tunic cells originating in the epidermis or blood cells released from the blood vessels which ramify in the tunic.

The crystallographic identification of tunicin with cellulose I of plants was established by Rånby (1952). It was shown by electron microscopic studies that the cellulose in the tunic is aggregated in the form of microfibrils similar to those of plant cellulose. Rånby (1952) also estimated the width of the cellulose microfibrils to be approximately 12 nm. Other investigations of the tunic were directed to the study of the manner of aggregation of the cellulose microfibrils and their orientation in relation to the shape of the animal. Endean reported the presence of a network of fibers in the tunic of *Pyura* (Endean 1955a, b) and of *Phallusia* (Endean 1961). Deck et al. (1966) noted some similarities between the texture of cellulose in the tunic of *Perophora* and that of plant cell walls. Detailed information of the tunicate cellulose including its crystalline features (Belton et al. 1989; Yamamoto et al. 1989) and the ultrastructure of the microfibrils (Daele et al. 1992; Kimura and Itoh 1996, 1997; Helbert et al. 1998a, b) is now available. Summarizing these results, the appearance of the ascidian tunic is shown in Figure 13-2. Normally, the cellulose microfibril of tunicates is composed of the almost-pure cellulose I_β allomorph with high crystallinity (inset in Figure 13-2b) and having a rectangular cross-sectional shape with 10–20 nm width (inset in Figure 13-2c). Hundreds of cellulose microfibrils are bundled in the tunic and the shape and dimension of the microfibril bundle varies depending on the ascidian species (Figures 13-2a–c). The microfibril bundles are deposited in a multilayered texture parallel to the outer face of the epidermis with random (Figures 13-2a, b) or cholesteric-like (helicoidal) orientation in the case of *Halocynthia aurantium* (Figure 13-2d).

The site of formation of cellulose has generally been accepted as being in the epidermal cells (Berrill 1950; Deck et al 1966). On the other hand, some researchers have identified blood cells in the tunic vessels with the amoeboid cells of the tunic and concluded that these amoebocyte cells (ferrocytes) may be involved in the formation of cellulose microfibrils.

3 CELLULOSE-SYNTHESIZING TERMINAL COMPLEXES IN THE ASCIDIANS

Studies on the biogenesis of cellulose microfibrils in the tunicates have focused mainly on the tunic of ascidians. Results from studies with various species of ascidians have suggested that the epidermal cell is the most probable site for synthesis of tunic cellulose in the majority of ascidians (Millar 1951; Deck et al. 1966; Dilly 1969; Cloney and Grimm 1970; Smith 1970; Terakado 1970; Wardrop 1970; Stievenart 1971; Katow and Watanabe 1978; Torrence and Cloney 1981; Cloney and Cavey 1982; Robinson et al. 1983). However, these early studies did not show the details of the mechanism and the exact site of synthesis of cellulose in the epidermal cell of ascidians.

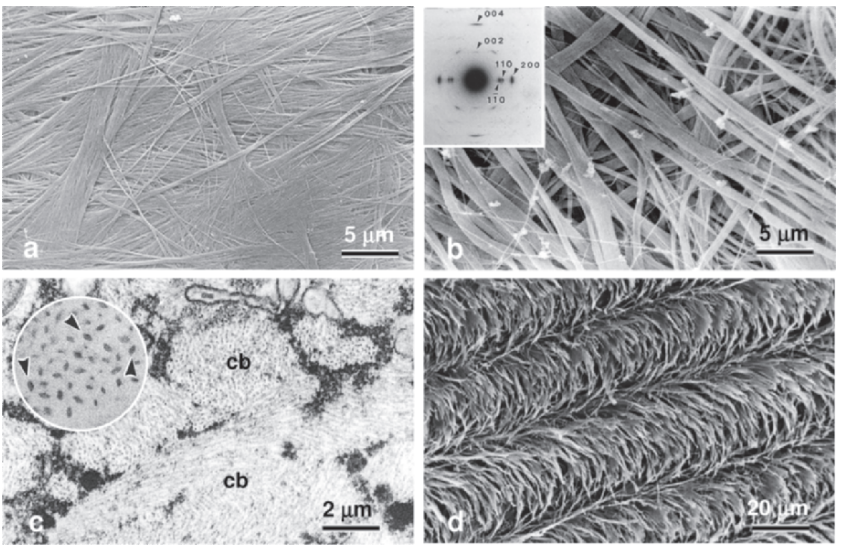

Figure 13-2. Electron micrographs showing texture of cellulose microfibril in the ascidian tunic. Usually, the cellulose microfibrils are bundled by forming polylamellate arrangements in the tunic of ascidians. The dimensions of the microfibril bundles and their orientation are extremely different among species of the ascidians. (**a**) Scanning electron microscope (SEM) image of the innermost layer of tunic in *Metandrocarpa uedai* after treatment with Updegraff reagent. (Figure 1, from Kimura S. and Itoh T. 1996. New cellulose-synthesizing complexes (terminal complexes) involved in animal cellulose biosynthesis in the tunicate *Metandrocarpa uedai*. Protoplasma 194:151–163. Reproduced with kind permission of Springer Science and Business Media.) (**b**) SEM image of the innermost layer of tunic in *Polyandrocarpa misakiensis* after treatment with Updegraff reagent. An inset image in (**b**) shows selected area electron diffraction pattern of cellulose microfibrils obtained from the tunic. Typical reflections of cellulose I_β with high crystallinity are detected in the diffraction pattern. (**c**) Cross-sectioned image of tunic of *M. uedai*. Bundled cellulose microfibrils (cb) are deposited with polylamellate arrangements in the tunic. A diffraction contrast image of the cross-sectioned cellulose microfibril in *M. uedai* shows a typical parallelogram shape (inset of **c**). (**d**) In the case of *Halocynthia aurantium*, cholesteric-like (helicoidal) deposition of cellulose bundles is observed with SEM in an oblique section of the tunic

In general, organisms that produce cellulose such as plants, bacteria, algae and slime molds, are known to synthesize and assemble cellulose microfibrils at multimeric enzyme complexes (terminal complexes = TCs) that are embedded in the plasma membrane of the cell (Brown, Jr. 1996; Grimson et al. 1996). The number and arrangement of particles in the TCs, observed by freeze-fracture electron microscopy, varies among different organisms. It is suggested that the difference in structure of TCs results in the diversity of dimension and crystallinity of cellulose microfibrils. We have focused on the visualization and characterization of the TCs in the epidermal cells of selected ascidians using freeze-fracture techniques. Compared with higher plant tissues, the visualization of TCs in the epidermal cells is rather difficult. This, because of the low probability of obtaining a fracture face

of the epidermal cell membrane facing the tunic. Another difficulty is that the epidermis consists of only a single cell layer in the entire body of an ascidian.

The first successful observation of TCs in tunicates was achieved using a small colonial ascidian, *Metandrocarpa uedai* (Kimura and Itoh 1996). We found a new type of TC in the ascidians (Kimura and Itoh 1996; Kimura and Itoh 2004) and it was clear from our studies that cellulose microfibrils in the tunicates also are synthesized at TCs. Furthermore, this evidence confirmed the role of TCs in cellulose synthesis in all groups of organisms. The TCs of *M. uedai,* categorized as linear TCs, were found only in the plasma membrane side of epidermal cells facing the tunic and never in the side that contained the tight junctions. Thus, the secretion of cellulose microfibrils occurs only into the tunic. Moreover, the TCs in *M. uedai* have a unique feature that is not found in conventional linear TCs. The TCs of *M. uedai* have a concave structure on the protoplasmic fracture face (PF face) of epidermal cell membrane (Figures 13-3a, b). The concave region of the TC is packed with a number of membrane particles that are approximately 7 nm in diameter (Figure 13-3b).

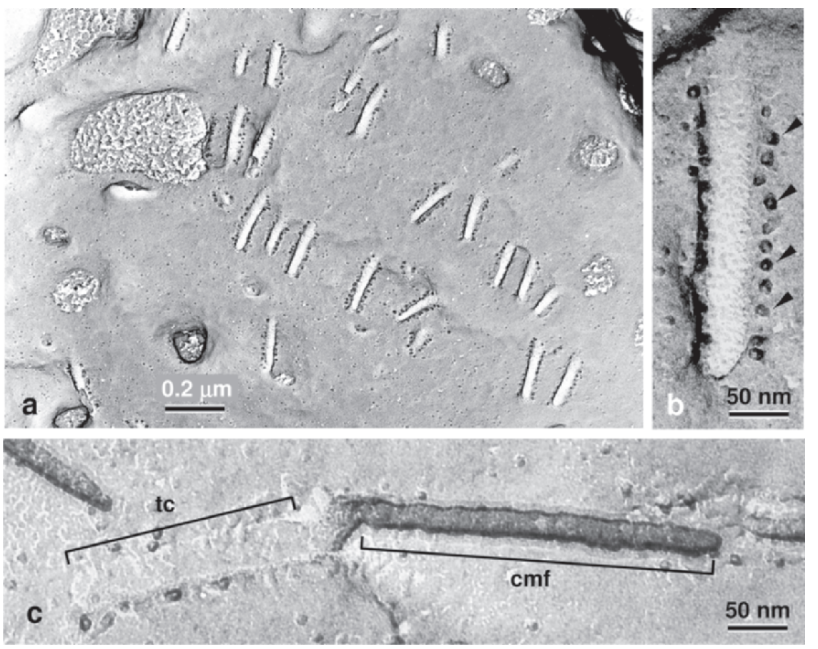

Figure 13-3. Freeze-fracture images showing cellulose-synthesizing terminal complexes (TCs) of *Metandrocarpa uedai*. (**a**) Linear shaped TCs consist of two kinds of membrane particles, and they are located on the P-fracture face of the epidermal cell membrane facing the tunic. In the case of *M. uedai*, TCs are grouped in almost the same direction on the epidermal cell membrane. (Figure 3a from: Kimura, S. and Itoh, T. 2004. Cellulose-synthesizing terminal complexes in the ascidians. Cellulose 11:377–383. Reproduced with kind permission of Springer Science and Business Media). (**b**) Almost all of the TCs of *M. uedai* have fairly deep membrane depressions filled with small membrane particles, and surrounded by large membrane particles in a single row (*arrowheads*). (**c**) Cellulose microfibril (cmf) of pseudo replica connecting with the terminus of a TC

Furthermore, the concave region is surrounded by a single row of distinct membrane particles that are approximately 14 nm in diameter (arrowheads in Figure 13-3b). Thus, the TCs in ascidians consist of two types of membrane particles. Convex structures, complementary to TCs on the PF-face, are also observed on the exoplasmic fracture face (EF-face) of epidermal cell membrane where no particles surround the TCs. Interestingly, it was often observed that some TCs are directly connected with termini of microfibrils. It appears that the concave region of TCs is filled with an amorphous-like material which may assemble into cellulose microfibrils (Figure 13-3c). The amorphous-like material may contain glucan chains before crystallization into cellulose. Similar linear-shaped TCs (Figure 13-4) are observed in different species of ascidians (Kimura and Itoh 2005). These observations indicate that the unique structure of ascidian TCs is an inherited characteristic common to the ascidians. We also investigated the detailed structure of TCs among individual species of ascidians with special attention to the large membrane particles that are found only in the ascidian TCs. As for the TCs of *Metandrocarpa* (Figure 13-3b) and *Polyzoa* (Figure 13-4b), the large membrane particles are clearly observed at the edge of the TC depression, and the orientation of the particles show a distinct single row. On the other hand, TCs of both *Halocynthia* (Figure 13-4a) and *Perophora* (Figure 13-4c) have only a few large particles with an indistinct row. These observations suggest that the large membrane particles of ascidian TCs may not participate directly in the biosynthesis and crystallization of cellulose microfibrils. However, the small membrane particles may play a direct role in the biosynthesis and crystallization of cellulose microfibril in the ascidians.

In general, cellulose microfibrils are often bundled by forming a polylamellate arrangement in the tunic of ascidians. The dimensions of the microfibril bundles and their orientation are extremely different among species of ascidians (Kimura and Itoh 2004). These microfibril bundles are observed not only in the middle and outer region but also in the inner region of the tunic. This suggests that the cellulose microfibrils are bundled immediately after synthesis at the TCs. Thus, grouping of TCs on the epidermal cell may be involved in the formation of microfibril bundles and support for this hypothesis is provided in Figures 13-2a and 13-3a. The grouping of TCs on epidermal cells coincides with the presence of cellulose microfibrils in the innermost layer of the tunic (Figure 13-2a) and the formation of microfibril bundles is most probably regulated by the arrangement of TCs on the plasma membrane. It is assumed that some anchor-like structure that determines the orientation of TCs is present in the cytoplasm of epidermal cells. At present, we have no definite information as to how the TCs are localized and arranged on the plasma membrane.

The pelagic tunicates consist of four groups; Pyrosomata, Doliolidae, Salpidae and Appendicularіata. It has been known that pyrosomas, doliolids and salps have a tunic surrounding the body of the zooid. The existence of cellulose in selected pelagic tunicates has been also investigated (Belton et al. 1989; Hirose et al. 1999). Cellulose I microfibrils with high crystallinity and large width (up to 20 nm) are found in the tunic of three groups: Pyrosomas, doliolids and salps.

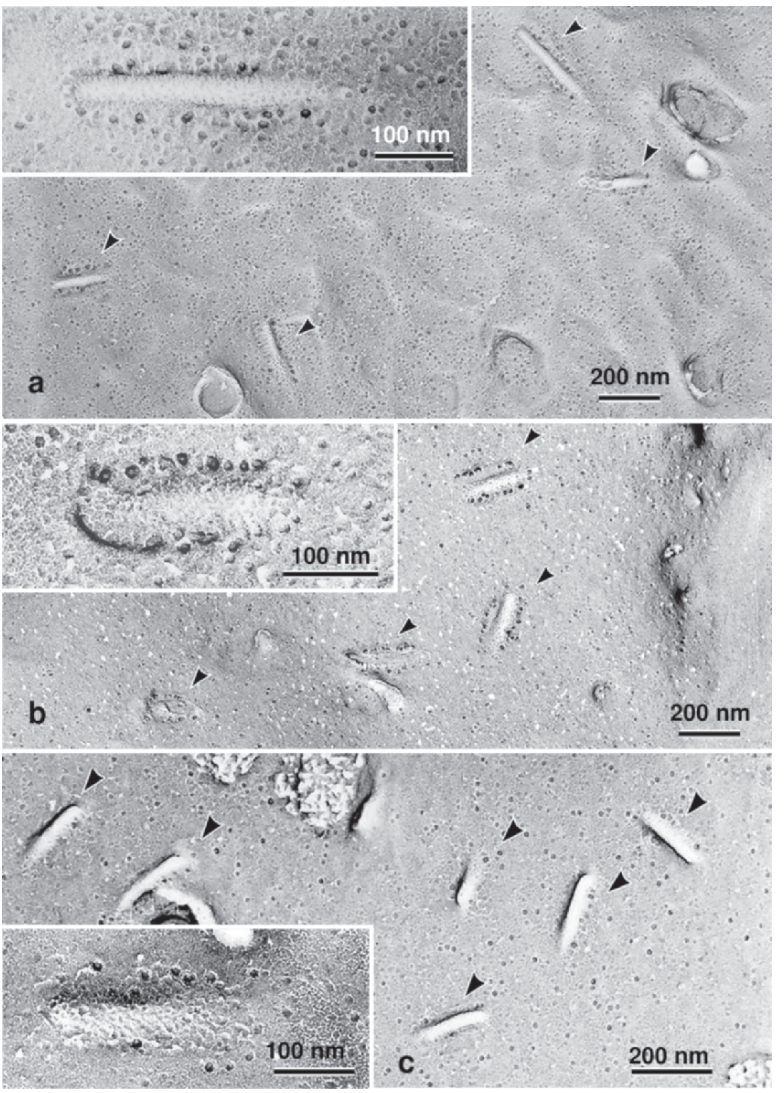

Figure 13-4. Freeze-fracture images of TCs in the epidermal cell membrane of *Halocynthia roretzi* (**a**), *Polyzoa vesiculiphora* (**b**), and *Perophora japonica* (**c**). (Figure 2 from: Kimura, S. and Itoh T. 2004. Cellulose-synthesizing terminal complexes in the ascidians. Cellulose 11:377–383. Reproduced with kind permission of Springer Science and Business Media). The occurrence of TCs (*arrowheads* in each figure) is similar to that found in *M. uedai* and other ascidians. The TCs in these ascidians were found only on the plasma membrane of the epidermal cells, and they contained the deep membrane depression filled with small membrane particles and surrounded by large particles (*inset* in each figure)

The structural features of cellulose microfibrils in these pelagic tunicates are quite similar to that of ascidians. This evidence indicates that the cellulose-synthesizing ability is an inherited character common to ascidians and thaliaceans. It is also reported that the basic structures of the tunic and the epidermis of ascidians and thaliaceans are almost the same (Hirose et al. 1999). The tunic cellulose in the thaliaceans may be synthesized by TCs on the plasma membrane of epidermal cells similar to the ascidians.

4 A NOVEL CELLULOSE-SYNTHESIZING SITE IN THE TUNICATES

The glomerulocyte was first described by George (1939) as a blood cell in the budding styelid ascidian, *Polyandrocarpa tincta*. The glomerulocyte is a large discoidal cell with the central perinuclear cytoplasm surrounded by a concentrically-arranged fiber structure. Mukai et al. (1990) studied the glomerulocyte of *Polyandrocarpa misakiensis* using electron microscopy and histochemistry, and showed that the fiber structure of glomerulocyte resembles the tunic fibers. These authors also reported that immature glomerulocytes are scattered with the epidermal cells of the zooids. Later, Hirose and Mukai (1992) demonstrated that the glomerulocytes are derived from epidermal cells. In 1995, the bundles of microfibrils in the glomerulocyte as well as the tunic were identified as cellulose I microfibrils using selected area electron diffraction analysis (Kimura and Itoh 1995). Furthermore, using ultrathin-sectioning techniques, it was found that individual cellulose microfibrils are primarily assembled in structures, tentatively identified as vacuole-like structures, and subsequently bundled at a tapering region within the vacuole-like structure in the glomerulocyte.

The glomerulocyte, usually scattered in epidermal tissue, and the disk plane is parallel to the outer surface of the tunic. Figures 13-5a and b show mature glomerulocytes in *M.uedai*. Most of the mature glomerulocytes of *M. uedai* contain thick bundles of microfibrils with 15 or more layers just under the cell membrane of the glomerulocytes (Figures 13-5a and b). The bundles of cellulose microfibrils are surrounded by a unit membrane structure, as observed with an electron microscope. The diameter of glomerulocytes of *M. uedai* is approximately 12 μm in the long axis and 4 μm in the short axis. The size of glomerulocytes is similar among *P. misakiensis* (Mukai et al. 1990; Hirose and Mukai 1992) and *P. tincta* (George 1939). In contrast, extremely large glomerulocytes are found in *Polyzoa vesiculiphora* (Kimura and Itoh 1997). The cellulose skeleton in the glomerulocyte is easily visualized after treatment with the Updegraff reagent (Updegraff 1969) or KOH solution to remove noncellulosic substances (Figure 13-5c). The size of glomerulocytes in *Polyzoa* is 50 μm in mean diameter, and their cellulose bundles are 1 μm in mean diameter. Cellulose microfibrils, 12 × 16 nm in mean width are packed at high density in each cellulose bundle, as observed following ultrathin sectioning.

In order to examine the process of development of cellulose bundles in the glomerulocyte, we investigated a series of developing glomerulocytes using ultrathin sectioning electron microscopy. An early stage of glomerulocyte development

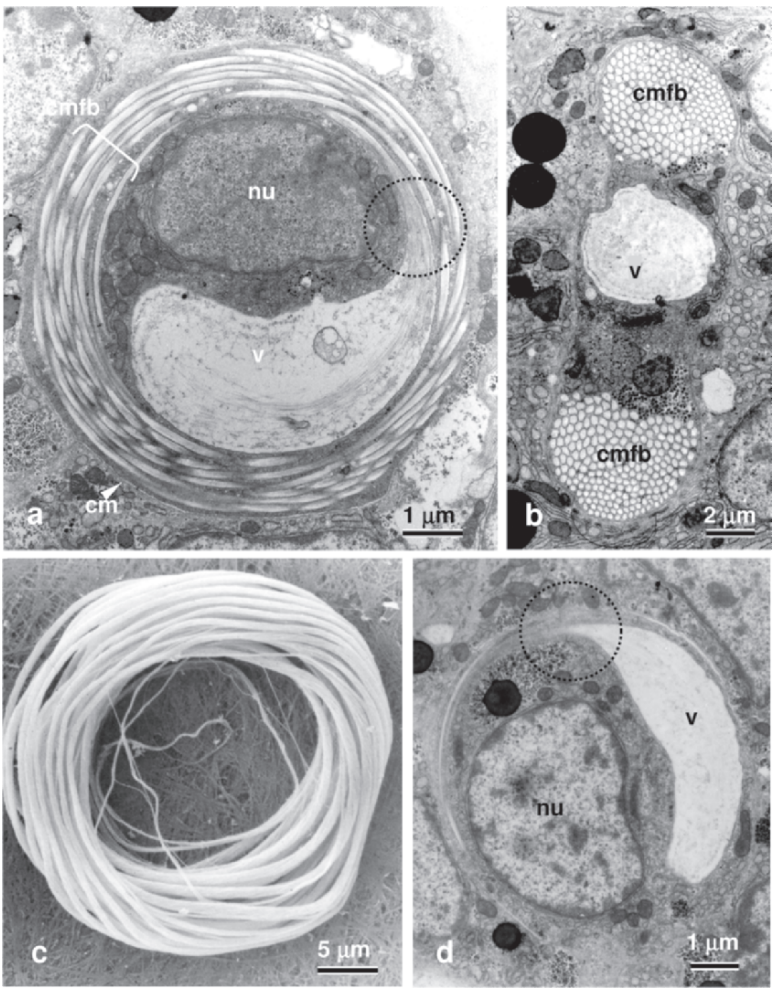

Figure 13-5. Electron micrographs showing glomerulocytes in *M. uedai*. The glomerulocyte has a flat disc shape. Therefore, it appears circular in tangential section in (**a**) and elliptical in cross section in (**b**). (Figures 5b and 3b from: Kimura, S. and Itoh, T. 1995 Evidence for the role of the glomerulocyte in cellulose synthesis in the tunicate, *Metandrocarpa uedai*. Protoplasma 186:24–33. Reproduced with kind permission of Springer Science and Business Media). The outer zone of the cell, just under the cell membrane (cm) is occupied by many tube-like structures filled with cellulose microfibril bundles (mfb). The central zone of the glomerulocytes is occupied by a nucleus (nu) and a large vacuole (v). The assembly of cellulose microfibrils gradually proceeds by tapering off of the glomerulocyte (*circled line* in **a**). (**c**) SEM image of cellulose bundles obtained from the glomerulocyte of *Polyzoa vesiculiphora*. The cellulose skeletons of glomerulocytes are clearly visible after treatment with Updegraff reagent that removes noncellulosic substances. (Figure 13 from: Kimura, S. and Itoh, T. 1997. Cellulose network of hemocoel in selected compound styelid ascidians J Electron Microsc 46:327–335. Reproduced with kind permission of Oxford University Press). (**d**) An early developmental stage of the glomerulocyte in *M. uedai*. A large vacuole (v) with its tapering end is observed (*circled line*), and the cell has only initiated the bundling of microfibrils. (Figure 5a from: Kimura, S. and Itoh, T. 1995. Evidence for the role of the glomerulocyte in cellulose synthesis in the tunicate, *Metandrocarpa uedai*. Protoplasma 186:24–33. Reproduced with kind permission of Springer Science and Business Media).

is shown in Figure 13-5d. A large vacuole with its tapering end is observed in the glomerulocyte and in this stage, only the initiation of microfibril bundling is observed. The tapering end of the bundle is observed at the periphery of the cytoplasm along the cell membrane of the glomerulocyte. In the inflated region of the vacuole, numerous cellulose microfibrils are observed, and these are dispersed as single microfibrils within the inflated region of the vacuole. Furthermore, it is found that the single microfibrils are gradually bundled at the tapering region of the vacuole. These observations indicate that the unit membrane surrounding the cellulose bundles is derived from the vacuole membrane, and the bundling of microfibrils occurs by tapering of the vacuole. The microfibril is first synthesized as a single fibril in the vacuole and bundled later by the unidirectional tapering process of the vacuole. Further observations revealed the presence of microtubules in the tapering region of the vacuole. The microtubules surround the vacuole membrane and are oriented parallel to the direction of the tapering vacuole. Overall, the glomerulocyte provides the first account of the involvement of a vacuole-like membrane in cellulose synthesis among living organisms. The only known exception regarding the site of cellulose synthesis is in the haptophycean alga, *Pleurochrysis*, which synthesizes cellulose microfibrils in the Golgi apparatus (Brown, Jr. 1969; Romanovicz 1982). The vacuole in the glomerulocyte is therefore considered to be the second exception to the plasma membrane-localized cellulose-synthesizing site common to most organisms.

5 OCCURRENCE OF A CELLULOSE NETWORK IN THE HEMOCOEL OF ASCIDIANS

Some ascidians possess two more cellulosic structures other than the tunic. These cellulosic structures have been observed by scanning electron microscopy after treatment with the Updegraff reagent (Updegraff 1969) that removes non-cellulosic substances. One of these cellulosic structures is a cellulose network that is distributed in the hemocoel (the tissue equivalent to a blood vessel of vertebrates) (Kimura and Itoh 1997), and the other is a coiled cord-like structure called the tunic cord (Kimura and Itoh 1998).

The cellulose network is an entangled bundle of cellulose microfibrils in the hemocoel. The diameter of each bundle is approximately 0.16 μm in *M. uedai* and *P. misakiensis*. However, the bundle is fairly large and approximately 1 μm in diameter in *P. vesiculiphora*. The pore size of the cellulose network is not constant and Figure 13-6 shows scanning electron microscope images of the cellulose network from *Polyandrocarpa*. The cellulose network has been found in only a limited group of ascidians that possess the glomerulocyte as a common character. In electron microscopic observations, a number of cellulose skeletons derived from glomerulocytes are observed in the cellulose networks (Figures 13-6b and c). Most of them show a distorted appearance due to the loosening of cellulose microfibrils to make the network (Figure 13-6c). The glomerulocytes are involved in the synthesis of cellulose microfibrils in their vacuole-like structures and the cellulose microfibrils are bundled by tapering-off of the vacuole-like structures.

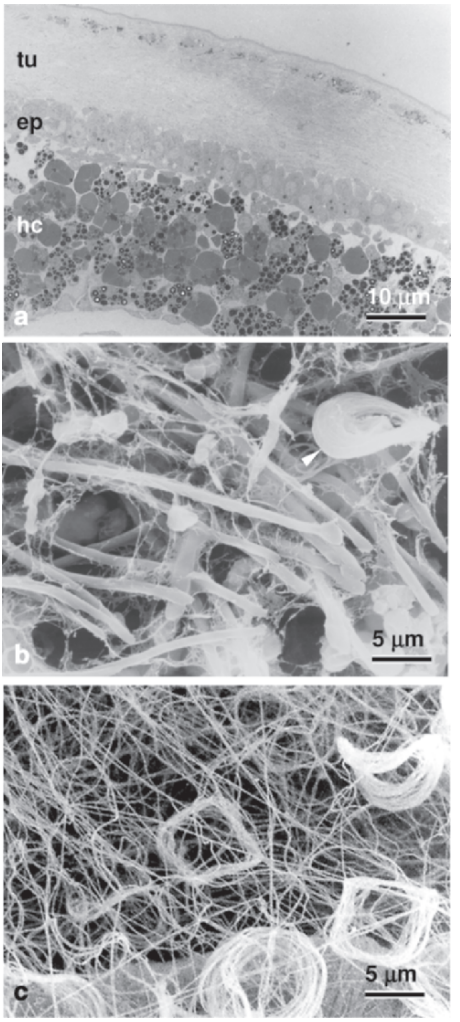

Figure 13-6. Occurrence of cellulose network in the hemocoel. (**a**) An electron micrograph showing a cross section of *Polyandrocarpa misakiensis* from the dorsal side of its body. A thin tunic (tu) and epidermis (ep) with single cell layer covers the body. The hemocoel (hc) is filled with blood cells. (Figure 2a from: Kimura, S. and Itoh, T. 1995. Evidence for the role of the glomerulocyte in cellulose synthesis in the tunicate, *Metandrocarpa uedai*. Protoplasma 186:24–33. Reproduced with kind permission of Springer Science and Business Media). (**b**) SEM image of the hemocoel of *P. misakiensis*. The cellulose networks (fine network structure) and cellulose skeleton of glomerulocyte (*arrowhead*) are barely observed before treatment with Updegraff reagent. (**c**) After removal of the noncellulosic material by Updegraff reagent, numerous fibrous structures (cellulose networks) and cellulose skeletons of glomerulocytes become visible

The tapering-off of the vacuole-like structure occurs continuously, so that only a single and long cellulose bundle is packed in the inner periphery of glomerulocytes (Kimura and Itoh 1995). Therefore, it is considered that the glomerulocytes accumulate cellulose microfibrils like a winding thread of reel in the cell. It appears that this particular assemblage of cellulose is convenient for the formation of a cellulose network in the hemocoel. After producing thick bundles of cellulose microfibrils, the glomerulocytes are transferred into the hemocoel where they release ring bundles of cellulose or cellulose skeleton after their death. The bundles of cellulose are untied in the hemocoel for making the cellulose network (Figure 13-7). Thus, these ascidians which have glomerulocytes, utilize cellulose not only for the

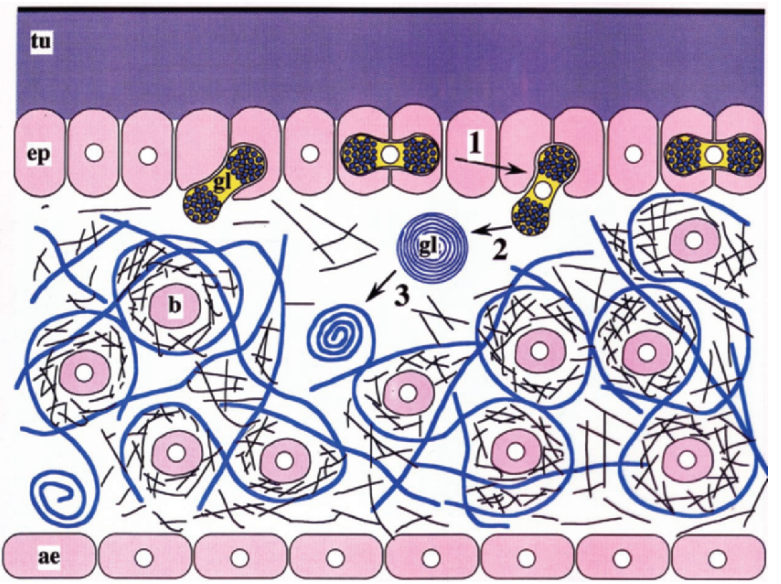

Figure 13-7. A schematic illustration showing the step-wise involvement of glomerulocytes in the formation of a cellulose network in the hemocoel: (**1**) glomerulocytes are transferred into hemocoel; (**2**) bundles of cellulose skeleton are released in the hemocoel; (**3**) cellulose microfibrils of the skeleton are untied to make cellulose network. Tu = tunic, ep = epidermis, gl = glomerulocyte, ae =atrial epitherium, b = blood cell (*See Color Plate of this figure beginning on page 355*)

protective tissue of the tunic but also for the network structure in the hemocoel. These observations provide further information for understanding the role of cellulose microfibrils in the cellulosic organisms including plants.

However, the role of the cellulose network in these ascidians is enigmatic. A possible explanation is that the cellulose network forms a skeletal structure for other extracellular matrix components in the hemocoel. Observations made by scanning electron microscopy suggest that the cellulose network and noncellulosic fine meshwork structure form a cross-linked meshwork structure (Kimura and Itoh 1997). These observations are similar to those indicating a relationship between collagen fibers and other matrix materials in the connective tissues of animals. The distribution of the cellulose network is almost uniform in the hemocoel. It is possible that the cellulose fibers are immediately connected to other matrix components once they are released from the cellulose skeleton of the glomerulocyte. Apart from all this, a few interesting questions still remain to be addressed, such as why do only these ascidians contain cellulose in the hemocoel? To understand in detail the role of cellulose in the hemocoel, it will be necessary to first characterize the noncellulosic fibrous materials in the hemocoel. Moreover, a comparative study of the composition of the extracellular matrix components in these and other ascidians that have no cellulose in their hemocoel will also be required.

6 STRUCTURE AND FUNCTION OF THE TUNIC CORD IN THE ASCIDIANS

The tunic cord is a distinctive structure in *P.misakiensis*, first described by Mukai et al. (1990). The tunic cord was studied using light microscopy coupled with histochemical techniques, and it was shown that the stainability of tunic cords was very similar to the tunic. These observations led to the suggestion that the tunic cords probably act as connectors between the tunic and the mantle (Mukai et al. 1990). In 1998, the ultrastructure and chemical nature of tunic cords was investigated using electron microscopic techniques (Kimura and Itoh 1998).

The tunic cords which are mainly composed of cellulose, are easily observed by scanning electron microscopy after treatment with the Updegraff reagent. The tunic cord is a new cellulosic structure that follows the tunic and the cellulose network in the hemocoel of *P. misakiensis*. It is a cord-like coiled structure that is 5–30 μm in diameter and 0.1–5.0 mm in length, as observed in both the light microscope and the scanning electron microscope (Figure 13-8). The tunic cords originate and elongate from the dorsal tunic, and their terminal ends have a swollen and ornamented structure (Figure 13-8d). Scanning and transmission electron microscopy coupled with electron diffraction analysis show that the tunic cords are composed of bundled microfibrils of cellulose I_β of high crystallinity. Cellulose microfibril bundles are packed in the entire region of the tunic cord at high density. The cellulose microfibril features are very similar between the tunic cord and the tunic, except that the tunic cord contains no tunic cells at all. The tunic cord is surrounded by a single layer of epidermal cells, and these could be involved in producing cellulose microfibrils. We believe that the basal region of tunic cords is an active elongation region. The tunic cords are often connected to internal tunic of siphons. The connections are similar to eyelet structures (Figures 13-8a and 8b). Moreover, the tunic cords are highly coiled in shape, like a spring (Figure 13-8c). These features of tunic cords suggest some role for the opening and closing of the siphon of the ascidian. However, tunic cords show the same coiled shape in all stages, even during the siphon opening.

Short tunic cords are often observed in the internal tunic with tight connections and no coiled structure (Figure 13-8b). One possible function of the tunic cords may be to provide physical support by connecting the dorsal and internal tunic of the siphon through the hemocoel. The rim of the internal tunic continues to the atrial epithelium with a single cell layer (Figure 13-1b). This region is considered to be weak in terms of mechanical strength that is required for opening and closing of the siphon. Since the short tunic cords are seen in the eyelet structures, both the dorsal and the internal tunic could be tightly connected by tunic cords during expansion and shrinkage of the zooid by eyelet structures. However, it is still unclear as to why only *P. misakiensis* have tunic cords among the ascidians. Further examination and structural comparisons including the siphons and hemocoel of *P. misakiensis* and other ascidians will be required to answer this question.

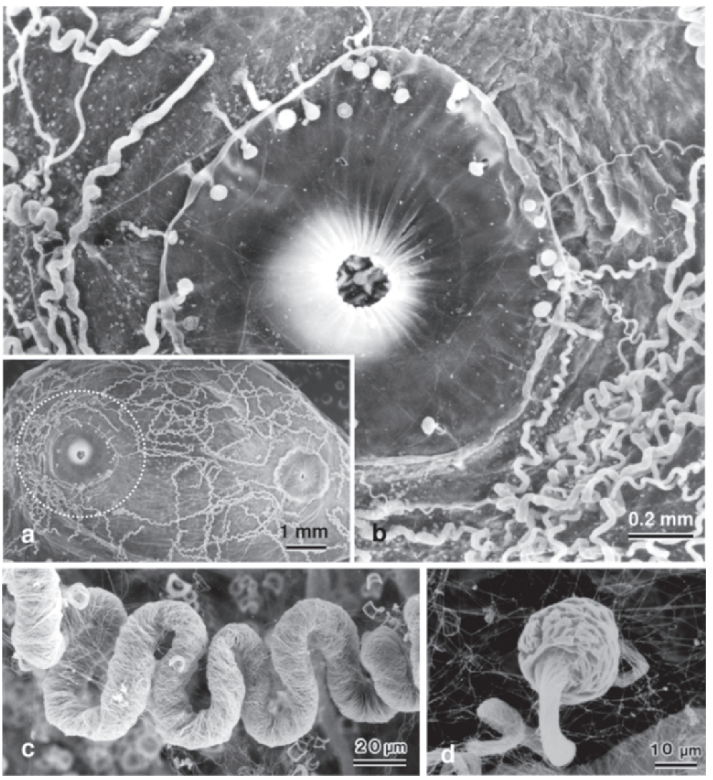

Figure 13-8. SEM images of the tunic cords in *P. misakiensis* after treatment with Updegraff reagent. (**a**) Numerous tunic cords in random arrays are located on the inner surface of dorsal tunic. (**b**) A magnified image of a siphon, highlighted by a circle in (**a**). Tunic cords are often connected to the rim of the internal tunic just like an eyelet structure. Most of the tunic cords are coiled (**c**) and the apical end is observed as a swollen and ornamented structure (**d**). (Figures 11, 5, and 7 from: Kimura, S. and Itoh, T. 1998. A new cellulosic structure, the tunic cord in the ascidian *Polyandrocarpa misakiensis*. Protoplasma 204:94–102. Reproduced with kind permission of Springer Science and Business Media).

7 OCCURRENCE OF HIGHLY CRYSTALLINE CELLULOSE IN THE MOST PRIMITIVE TUNICATE, THE APPENDICULARIANS

The appendicularians (also called larvaceans), another group in the Tunicata, are unusually delicate and difficult to see or capture, and most are only a couple of millimeters in size. They are a pelagic, tadpole-like class of zooplankton (Figure 13-9a). Molecular phylogeny based on 18S rDNA sequences suggests that the appendicularians share an ancestor with other groups of tunicates (Wada and Satoh 1994; Wada 1998). However, the appendicularians do not possess the tunic; they secrete a balloon-like gelatinous structure called a “house” that acts as a feeding apparatus (Figure 13-9b) (Flood and Dibel 1998). It is possible

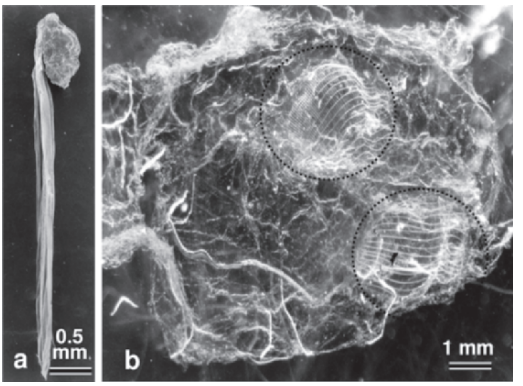

Figure 13-9. SEM image of the zooid of an appendicularian, *Oikopleura rufescens* (**a**) and macrophotograph of its house (**b**). The zooid of *O. rufescens* is tadpole-shaped. It has a small trunk that is 0.8 mm in length and a long tail that is 5 mm in length. The house of *O. rufescens* is a typical oikopleurid house which is a spherical, gelatinous structure that possess two inlet filters (*circled line* in **b**)

that the house corresponds to a kind of tunic in the appendicularians and we have investigated whether the house contains cellulose (Kimura et al. 2001). The house of an appendicularian, *Oikopleura rufescens,* is a typical oikopleurid house, which is a spherical, gelatinous structure that possesses two inlet filters as a filter feeding mesh structure (Figure 13-9b). Electron diffraction analysis shows the presence of highly crystalline cellulose I_β similar to the tunic cellulose of ascidians, in purified house (Figure 13-10c). The presence of cellulose in the

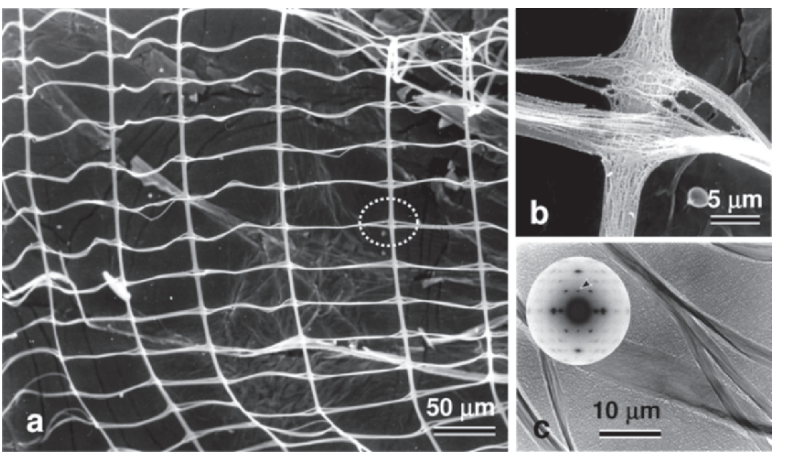

Figure 13-10. Ultrastructure of the inlet filter in the house of *O. rufescens*. (**a**) SEM image of the inlet filter shows a highly ordered meshwork structure like an elaborately woven textile. A stitch of the meshwork (*circled line* in **a**) is composed of orthogonally arranged bundles of cellulose microfibrils. (**b**) Cellulose microfibrils in the house are bundled, and (**c**) consist of highly crystalline cellulose I_β similar to that of ascidians (*inset* in **c**). (Figure 2 from: Kimura, S., Ohshima, C., Hirose, E., Nishikawa, J., and Itoh, T. 2001. Cellulose in the house of the appendicularian *Oikopleura rufescens*. Protoplasma 216:71–74. Reproduced with kind permission of Springer Science and Business Media).

house indicates that the cellulose-synthesizing ability is a characteristic common to all tunicates, i.e., ascidians, thaliaceans, and appendicularians. The crystalline features and dimensions of cellulose microfibrils in appendicularians are similar to those observed in the ascidians and thaliaceans (Belton et al. 1989; Daele et al. 1992; Okamoto et al. 1996; Hirose et al. 1999).

The inlet filter of the house of *O.rufescens* builds up a highly ordered meshwork structure like an elaborately woven textile (Figures 13-10a and b). The meshwork is extremely precise, with errors in the interval between woof threads of the inlet filter of less than 1.7μm. To make the house, the *Oikopleurid* appendicularians synthesize house rudiment in the trunk region, and expand a new house after escaping from the old one (Flood and Deibel 1998). It is of interest that the mechanism responsible for constructing such a highly ordered meshwork of house rudiment is a simple process of expansion. However it remains to be seen as to how the cellulose bundles in the house rudiment are formed and packed.

8 ORIGIN OF CELLULOSE SYNTHASE IN THE TUNICATES

Molecular phylogeny based on the 18S rDNA sequences suggested that tunicates are a monophyletic group and that the appendicularians diverged early from the tunicates (Wada and Satoh 1994; Wada 1998). The occurrence of cellulose in appendicularians indicates that the common ancestor of all tunicates already possessed the ability to produce highly crystalline cellulose I. From these observations, it would appear that other animals close to the tunicates, such as cephalochordates, vertebrates and hemichordates, might also produce cellulose or possess the cellulose-synthesizing genes. However, many questions remain to be addressed regarding the evolutionary significance of cellulose synthesis in the animal kingdom. The sequencing of the genome of an ascidian, *Ciona intestinalis* in 2002 was a grand achievement and it provided information for understanding cellulose biosynthesis in the tunicates (Dehal et al. 2002). Phylogenetic analysis of the cellulose synthase from *C.intestinalis* (Ci-CesA) and cellulose synthases from other sources suggested that the *Ci-CesA* gene was probably acquired by horizontal transfer from bacteria (Matthysse et al. 2003; Nakashima et al. 2004). Recently, Sasakura et al. (2005) analyzed a recessive mutant of *Ci-CesA* in *C.intestinalis* and showed that *Ci-CesA* has three functions: cellulose biosynthesis, proper formation of the tunic, and a role in metamorphosis. These functions suggest that cellulose acts not only as a structural polymer for mechanical support of the body, but it may also have some physiological functions in the tunicates.

9 SUMMARY

Electron microscopic analyses revealed the structure, assembly, bundling and functions of cellulose in the tunicates. For the first time, cellulose-synthesizing enzyme complexes (TCs) of new type and shape were found on epidermal cells, just under the tunic, in several species of ascidians. Current evidence supports

the view that assembly of cellulose microfibril by TCs is a universal phenomenon in the biological kingdom. Investigations of ascidian TCs also revealed a direct connection of TCs with the termini of microfibrils and these were successfully visualized for the first time among cellulose-producing organisms. The glomerulocyte is another cell that synthesizes cellulose in ascidians. Cellulose biosynthesis in the glomerulocyte occurs in the vacuole, and cellulose microfibrils are bundled by tapering of the vacuole. This process occurs continuously and as a result, several layered cellulose bundles are deposited in the cell. The glomerulocyte also provides the first account of the involvement of vacuole in the synthesis of cellulose among cellulose-producing organisms. The bundles of cellulose microfibrils, synthesized in the glomerulocyte, are released into the hemocoel where they form a cellulose network. This network may act as a skeletal structure in the hemocoel. The cellulose network is the second cellulosic structure of tunicates, apart from the tunic. The third cellulosic structure, the tunic cord, was found in the ascidian, *Polyandrocarpa* for the first time. The tunic cords have a specialized structure that is coiled cord-like in shape with swollen and ornamented terminal ends. The terminal ends of tunic cords are often connected to the internal tunic of the siphons with eyelet structures. The function of the tunic cord may be to provide mechanical support between the tunic and the mantle. Highly crystalline cellulose was found for the first time in the most primitive tunicate, the appendicularian, where it is a major component of the appendicularian house which is a feeding apparatus of the organism. In the house, cellulose microfibrils form a highly ordered meshwork structure like a woven textile. The finding of cellulose in the appendicularian indicates that cellulose-synthesizing ability is a characteristic common to all tunicates.

REFERENCES

Belton P.S., Tanner S.F., Cartier N., and Chanzy H. 1989. High-resolution solid-state ^{13}C nuclear magnetic resonance spectroscopy of tunicin, animal cellulose. Macromolecules 22:1615–1617.

Berrill N.J. 1950. The Tunicata. The Ray Society, London.

Brown, Jr. R.M. 1969. Observations on the relationship of the Golgi apparatus to wall formation in the marine Chrysophycean alga, *Pleurochrysis scherfferii* Pringsheim. J Cell Biol 41:109–123.

Brown, Jr. R.M. 1996. The biosynthesis of cellulose. Pure Appl Chem 10:1345–1373.

Cloney R.A. and Cavey M.J. 1982. Ascidian larval tunic: extra-embryonic structures influence morphogenesis. Cell Tissue Res 222:547–562.

Cloney R.A. and Grimm L. 1970. Transcellular emigration of blood cells during ascidian metamophosis. Z Zellforsch 107:157–173.

Daele V.Y., Revol J.-F., Gaill F., and Gofinet G. 1992. Characterization and supermolecular architecture of the cellulose-protein fibrils in the tunic of the sea peach (*Halocynthia papollosa*, Ascidiacea, Urochordata). Biol Cel 76:87–96.

Deck J.D., Hey E.D., and Revol J.-P. 1966. Fine structure and origin of the tunic of *Perophora viridis*. J Morphol 120:267–280.

Dehal P., Satou Y., Campbell R.K., Chapman J., Degnan B., DeTomaso A., Davidson B., DiGregorio A., Gelpke M., and Goodstein D.M., et al. 2002. The draft genome of *Ciona intestinalis*: insights into chordate and vertebrate origins. *Science* 298:2157–2167.

Dilly P.N. 1969. The ultrastructure of the tadpole larva of *Ciona intestinalis*. Z Zellforsch 95:331–346.

Endean R. 1955a. Studies of the blood and test of some Australian ascidians. II The test of *Pyura stlonifera* (Heller). Aust J Mar Freshw Res 6:139–156.
Endean R. 1955b. Studies of the blood and test of some Australian ascidians. III The formation of the test of *Pyura stlonifera*. Aust J Mar Freshw Res 6:157–164.
Endean R. 1961. The test of the ascidian, *Phalusia mammillata*. Q J Microsc Sci 102:107–117.
Flood P.R. and Deibel D. 1998. The appendicularian house. In: Bone Q. (ed.), The Biology of Pelagic Tunicates. Oxford University Press, Oxford, pp 105–124.
George W.C. 1939. A comparative study of the blood of the tunicates. Q J Microsc Sci 81:391–428.
Goodbody I. 1974. The physiology of ascidian. Adv Mar Biol 12:1–149.
Grimson M.J., Haigler C.H., and Blanton R.L. 1996. Cellulose microfibrils, cell motility, and plasma membrane protein organization change in parallel during culmination in *Dictyostelium discoideum*. J Cell Sci 109:3079–3087.
Helbert W., Sugiyama J., Kimura S., and Itoh T. 1998a. High-resolution electron microscopy on ultrathin sections of cellulose microfibrils generated by glomerulocytes in *Polyzoa vesicuriphora*. Protoplasma 203:84–90.
Helbert W., Nishiyama Y., Okano T., and Sugiyama J. 1998b. Molecular imaging of *Halocynthia papillosa* cellulose. J Strct Biol 124:42–50.
Hirose E., Kimura S., Itoh T., and Nishikawa J. 1999. Tunic of pyrosomas, doliolids and salps (Thaliacea, Urochordata): morphology and cellulosic components. Biol Bull 196:113–120.
Hirose E. and Mukai H. 1992. An ultrastructural study on the origin of glomerulocytes, a type of blood cell in a styelid ascidian, *Polyandrocarpa misakiensis*. J Morphol 211:269–273.
Katow H. and Watanabe H. 1978. Fine structure and possible role of ampullae on tunic supply and attachment in compound ascidian, *Botryllus primigenus* OKA. J Ultrastruct Res 64:23–34.
Kimura, S. and Itoh, T. 1995. Evidence for the role of glomerulocyte in cellulose synthesis in the tunicate, *Metandrocarpa uedai*. Protoplasma 186:24–33.
Kimura S. and Itoh T. 1996. New cellulose synthesizing complexes (terminal complexes) involved in animal cellulose biosynthesis in the tunicate *Metandrocarpa uedai*. Protoplasma 194:151–163.
Kimura S. and Itoh T. 1997. Cellulose network of hemocoel in selected compound styelid ascidians. J Electron Microsc 46:327–335.
Kimura S. and Itoh T. 1998. A new cellulosic structure, the tunic cord in the ascidian *Polyandrocarpa misakiensis*. Protoplasma 204:94–102.
Kimura S. and Itoh T. 2005. Cellulose synthesizing terminal complexes in the ascidians. Cellulose 11:377–383.
Kimura S., Ohshima C., Hirose E., Nishikawa J., and Itoh T. 2001. Cellulose in the house of the appendicularian *Oikopleura rufescens*. Protoplasma 216:71–74.
Matthysse A.G., Deschet K., Williams M., Marry M., White A.R., and Smith W.C. 2003. Proc Natl Acad Sci USA 101:986–991.
Millar R.H. 1951. The stolonic vessels of the Didemnidae. Q J Microsc Sci 92:249–254.
Mukai H., Hashimoto K., and Watanabe H. 1990. Tunic cords, glomerulocytes, and eosinophilic bodies in a styelid ascidian, *Polyandrocarpa misakiensis*. J Morphol 206:197–210.
Nakashima K., Yamada L., Satou Y., Azuma J., and Satoh N. 2004. The evolutionary origin of animal cellulose synthase. Dev Genes Evol 214:81–88.
Okamoto T., Sugiyama J., and Itoh T. 1996. Structural diversity of ascidian cellulose. Wood Res 83:27–29.
Rånby B.G. 1952. Physico-chemical investigations on animal cellulose (Tunicin). Arkiv Kemi 4: 241–248.
Richmond P.A. 1991. Occurrence and functions of native cellulose. In: Haigler C.H. and Weimer P.J. (eds.), Biosynthesis and Biodegradation of Cellulose. Marcel Dekker, New York, pp. 5–23.
Robinson W.E., Kustin K., and Mcleod G.C. 1983. Incorporation of [^{14}C] glucose into the tunic of the ascidian, *Ciona intestinalis* (Linnaeus). J Expl Zool 225:187–195.
Romanovicz D.K. 1982. The role of Golgi apparatus in the biosynthesis of natural polymer systems with particular reference to cellulose. In: Brown, Jr. R.M. (ed.), Cellulose and other Natural Polymer Systems. Plenum Press, New York, pp. 127–148.

Sasakura Y., Nakashima K., Awazu S., Matsuoka T., Nakayama A., Azuma J., and Satoh N. 2005. Transposon-mediated insertional mutagenesis revealed the functions of animal cellulose synthase in the ascidian *Ciona intestinalis*. Proc Natl Acad Sci USA 102:15134–15139.

Smith M.J. 1970. The blood cells and tunic of the ascidian *Halocynthia aurantium* (Pallas). I. Hematology, tunic morphology, and partition of cells between blood and tunic. Biol Bull 138:354–378.

Stievenart J. 1971. Recherches sur la morphologie et etude histochimique de la tunique d' *Halocynthia papillosa* Gun. Annales de la Societe Royale Zoologique de Belgique 101:25–56.

Terakado K. 1970. Tunic formation in the larva of an ascidian, *Perophora orientalis*. Sci Rep Saitama Univ 5B:183–191.

Torrence S.A. and Cloney R.A. 1981. Rhythmic contraction of the ampullar epidermis during metamorphosis of the ascidian *Molgura occidentalis*. Cell Tissue Res 216:293–312.

Updegraff. D.M. 1969. Semimicro determination of cellulose in biological materials. Anal Biochem 32:420–424.

Wada H. 1998. Evolutionary history of free-swimming and sessile lifestyles in urochordates as deduced from 18S rDNA molecular phylogeny. Mol Biol Evol 15:1189–1194.

Wada H. and Satoh N. 1994. Details of the evolutionary history from invertebrates to vertebrates, as deduced from the sequences of 18SrDNA. Proc Natl Acad Sci USA 91:1801–1804.

Wardrop A.B. 1970. The structure and formation of test of *Pyura stolonifera* (Tunicate). Protoplasma 70:73–86.

Yamamoto H., Horii F., and Hirai A. 1989. Structural changes of native cellulose crystals induced by annealing in aqueous alkaline and acid solutions at high temperatures. Macromolecules 22:4130–4132.

CHAPTER 14

IMMUNOGOLD LABELING OF CELLULOSE-SYNTHESIZING TERMINAL COMPLEXES

TAKAO ITOH[1], SATOSHI KIMURA*[2], AND R. MALCOLM BROWN, JR.[3]

[1]Research Institute for Sustainable Humanosphere, Kyoto University, Uji, Kyoto 611–0011, Japan; [2]The University of Tokyo, Graduate School of Agriculture and Life Science, Department of Biomaterials Sciences, 1–1–1 Yayoi, Bunkyo-ku, Tokyo 113–8657, Japan; [3]Section of Molecular Genetics and Microbiology, School of Biological Sciences, The University of Texas at Austin, Austin, TX 78712, USA

Abstract

Rosette TCs that are visualized exclusively by freeze-fracture electron microscopy have long been thought of as "putative" cellulose-synthesizing terminal complexes (TCs). We succeeded in directly demonstrating that the TCs contain cellulose synthases by the application of novel techniques combined with both freeze-fracture and immunogold labeling. Since the purification of cellulose synthases has not succeeded in higher plant cells, we cloned *GhCesA* using cotton cDNA libraries and prepared polyclonal antibodies against the GhCesA protein. We were successful in applying SDS-FRL techniques to plant cells for the first time by using mixtures of cellulases and pectolyases to digest cell walls after freeze replication and immunogold labeling. Using SDS-FRL, the antibodies of cellulose synthases specifically labeled the rosette TCs in the plasma membrane of higher plant cells. This provided direct evidence that the rosettes contain the catalytic subunit of the cellulose synthase. In this chapter, we have analyzed the mechanism of labeling compared with actual dimensions of rosettes, gold particles, and antibodies.

Keywords

cellulose biosynthesis, fracture labeling, Gh*CesA*, rosette, terminal complexes, *Vigna angularis*.

* For correspondence: Tel: +81 3 5841 5241; Fax: +81 3 5684 0299; e-mail: kimura@sbp.fp.a.u-tokyo.ac.jp

R.M. Brown, Jr. and I.M. Saxena (eds.), Cellulose: Molecular and Structural Biology, 237–255.

1 INTRODUCTION

It is well known that the rosette and linear terminal complexes (TCs) can be observed by the freeze-fracture replication technique. The structures revealed by this technique are known as "putative" cellulose-synthesizing TCs. Kimura et al. (1999) demonstrated that TCs in vascular plants contain cellulose synthases using a novel technique of sodium dodecyl sulfate (SDS)-solubilized freeze fracture replica labeling (SDS-FRL). The localization of the cellulose synthase to the TC was accomplished almost 40 years after the hypothesis of Roelofsen (1958) in which he stated that enzyme complexes could be involved in cellulose biosynthesis. It has been more than 30 years since the discovery of the first TC by Brown, Jr. and Montezinos (1976) and in particular, 26 years after the discovery of rosette TCs in plants by Mueller and Brown, Jr. (1980).

Until recently the only way to visualize linear and rosette TCs depended on the application of the freeze-fracture replication technique. We have now succeeded in visualizing the components of TCs by applying freeze replica labeling techniques coupled with the solubilization of plant materials with SDS. In contrast, it has not been possible yet to prepare and purify cellulose synthases from plant cells. Success with the SDS-FRL technique in localizing cellulose synthases to the rosette TCs in plants was based on the ability to clone and express a region of the cotton cellulose synthase (GhCesA) and to obtain polyclonal antibodies against this region of the cellulose synthase. These antibodies allowed specific labeling of the cellulose synthases in the rosette TCs on the plasma membrane of Azuki beans (*Vigna angularis*) (Kimura et al. 1999). Similarly, polyclonal antibodies raised against a 93-kd protein, obtained during purification of cellulose synthase activity from the bacterium *Acetobacter xylinum,* was found to be useful in labeling the linear TCs in this bacterium by the SDS-FRL technique (Kimura et al. 2001). Based on these experiments we now have direct proof that the rosette TCs contain cellulose synthase subunits that catalyze cellulose biosynthesis, and linear TCs in *A. xylinum* contain subunits of cyclic-di-guanylic acid (c-di-GMP) binding proteins that activate cellulose biosynthesis.

In the present article we will discuss the difficulties associated with understanding the composition of the TCs and the application of the SDS-FRL technique in unraveling the contents of the TCs.

2 THE CELLULOSE-SYNTHESIZING MACHINERY (TERMINAL COMPLEXES)

Roelofsen (1958) first suggested that native cellulose might be assembled, polymerized and crystallized by the action of a large enzyme complex located at the growing tip of the microfibril. Interestingly, Dobberstein and Kiermayer (1972) visualized ordered particle complexes within "f-vesicles" of the Golgi apparatus in the green alga *Micrasterias denticulata,* and these particles were implicated in the biosynthesis of cellulose. This work is significant historically, because what

was later to be beautifully imaged by freeze fracture was first observed in sectioned material. Preston (1964) presented the ordered granule hypothesis based on the his observations of freeze-dried replicas of the innermost cell wall layer after plasmolysis in the marine algae *Valonia* and *Chaetomorpha*. Three-layered and rectangular enzyme particle-complexes were thought to be involved in cellulose biosynthesis, and according to this model, cellulose microfibrils were thought to be synthesized in three different directions. It is well known now that microfibrils are synthesized unidirectionally with parallel or antiparallel directions (Brown, Jr. 1978; Itoh and Brown, Jr. 1984).

More than 10 years after the presentation of Preston's hypothesis, Brown, Jr. and Montezinos (1976) first discovered a plasma membrane particle complex associated with the ends of cellulose microfibrils in the alga, *Oocystis apiculata*. This complex was a linear multimeric structure, termed as a linear terminal complex (TC), and it consisted of three rows of subunit particles. The complex was found to be intimately associated with microfibrils, as clearly evidenced by impressions of microfibrils leading from and associated with the complex. In the same year, Brown, Jr. et al. (1976) also observed a single row of particles in the outer membrane of *A. xylinum* and showed that this type of particle row is the cellulose-synthesizing machinery that is involved in cellulose biosynthesis. In 1980, Mueller and Brown, Jr. found a different arrangement of particles, a cluster or rosette of six particles, associated with the terminus of cellulose microfibril impressions on the P-fracture face of the plasma membrane in root tip cells of maize that were actively involved in cellulose synthesis. In the same year, Giddings et al. (1980) found octagonal arrays of rosettes in the plasma membrane of *M. denticulata*, and these arrays are involved in the synthesis of banded cellulose microfibrils in this alga. Since then, numerous studies have implicated rosette TCs (frequently called rosettes) in cellulose microfibril assembly (Emons 1991, 1994; Herth 1984, 1985a, b; 1987, 1989; Herth and Weber 1984; Hotchkiss and Brown, Jr. 1987, 1988; Hotchkiss et al. 1989; Itoh 1990; Itoh and Brown, Jr. 1984; Mizuta et al. 1989; Mueller and Brown, Jr. 1982; Rudolph et al. 1989; Tsekos 1999; Tsekos and Reiss 1992; Okuda et al. 1994; Brown, Jr. 1996). As shown in Figure 14-1, different types of TCs have been identified in cellulose-producing organisms; however, TCs are categorized into two types, linear and rosette. Almost all species of land plants that include vascular plants, Pterophyta and Bryophyta have solitary rosette TCs. On the contrary, a variety of linear and rosette types of TCs are found in Protista. Different arrangements of linear rows of subunit particles form linear TCs and different groupings of rosette TCs from single to more than ten rosettes organized in regular arrays are observed in this group of organisms (Tsekos 1999; Grimson et al. 1996).

A. xylinum is the only organism in Monera that shows TCs with a single row of particles. To date, genes for cellulose synthesis have been identified in many bacterial species including *A. xylinum*, *Agrobacterium tumefaciens*, *Rhizobium* spp. (Ross et al. 1991); *Escherichia coli*, *Klebsiella pneumoniae*, *Salmonella typhimurium* (Zogaj et al. 2001); and cyanobacteria (Nobles et al. 2001). In particular, *Acetobacter*

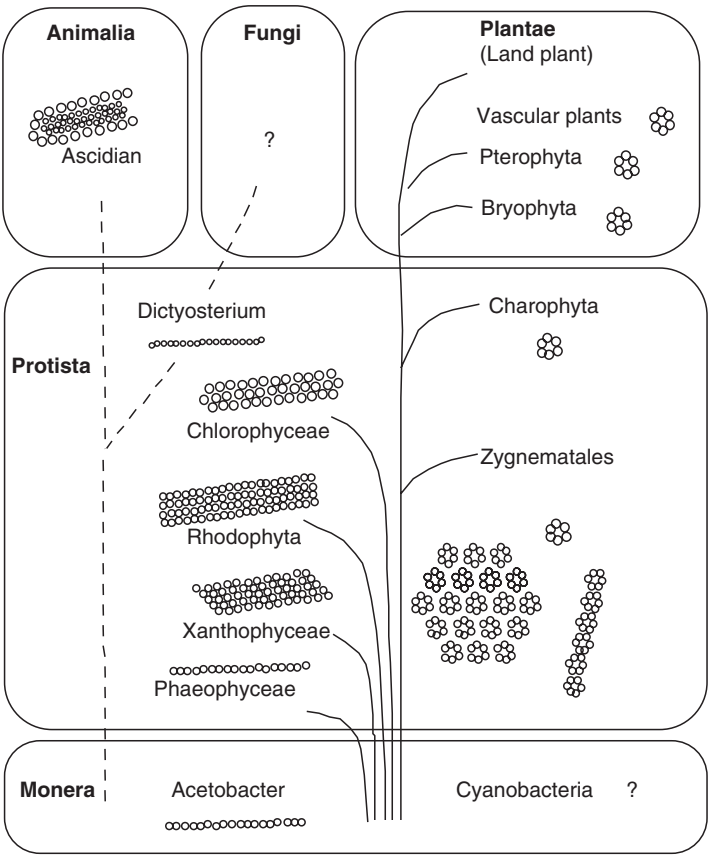

Figure 14-1. Different morphological forms of cellulose-synthesizing terminal complexes in five different biological kingdoms. (Figure 1 from: Itoh, T. 2002. Immunogold labeling of terminal cellulose-synthesizing complexes-demonstration coupled by freeze fracture and immunogold labeling techniques. Regulation of Plant Growth and Development (in Japanese) 37:44–50. Reproduced with kind permission of The Japanese Society for Chemical Regulation of Plants.)

and *Agrobacterium* have been used as model organisms for studying cellulose biosynthesis from a molecular biological and biochemical perspective. However, in spite of great progress in understanding cellulose biosynthesis in *Agrobacterium*, the TCs in this bacterium have not been well characterized. The inability to visualize TCs in *Agrobacterium* may be due to the difference between the actual fractured membrane and the location of TCs particles. The occurrence of cellulosic microfibrils has also been reported in cyanobacteria, but the presence of TCs is not confirmed in this group of organisms. Cyanobacteria would be a key group to understand the structure and function of TCs in relation to evolution because the origin of green plants is traced back to these organisms.

Furthermore, we have found specific types of linear TCs in ascidians that are members of the animal kingdom and that are phylogenetically apart from plants (Kimura and Itoh 1996). In short, almost all cellulosic organisms have shown the presence of TCs. However, TCs have not been observed in any kind of cellulosic fungi. It has long been thought that Oomycetes are a cellulose-synthesizing fungus; however, recent advances in molecular phylogeny show that Oomycetes cluster with the stramenophiles group in protista together with Heterokonta, based on the morphology of zoospore and analysis of the 18S rRNA sequence (Peer and Wacher 1997; Saunders 1997). This means that fungi are the only group of organisms that do not show the occurrence of TCs as well as cellulose biosynthesis.

Before 1999 only indirect evidence was available for the involvement of TCs in cellulose biosynthesis. Firstly, TCs could be observed at the terminus of cellulose microfibril impressions. Secondly, the linear TCs in *Oocystis apiculata* could be observed as a pair in different developmental stages of TC growth, suggesting that individual TCs in a pair may move in opposite directions by producing cellulose microfibrils (Brown, Jr. 1978). Thirdly, the length of linear TCs was shown to increase during the transition from primary wall to secondary wall formation in *Valonia* and *Boergesenia* (Itoh and Brown, Jr. 1988). There was no direct evidence to prove that cellulose synthases are localized in TCs on the plasma membrane until 1999 when Kimura et al. demonstrated that rosette TCs are labeled by CesA antibodies using freeze replica labeling techniques.

3 ADVANCES IN THE UNDERSTANDING OF CELLULOSE SYNTHASES

Research on cellulose biosynthesis has greatly advanced with the use of the bacterium *A. xylinum* as an experimental material. This bacterium produces a ribbon-like cellulose product at the surface of the cell. In 1987, c-di-GMP was shown to accelerate cellulose biosynthesis (Ross et al. 1987) and it is now possible to demonstrate *in vitro* cellulose-synthesizing activity in membrane and purified fractions obtained from this bacterium. Cellulose synthases are supposed to be attached to the terminus of cellulose microfibrils and based on the heavy weight of the cellulose, product entrapment was used to purify cellulose synthases from the other proteins in a manner similar to that applied for purification of chitin synthases (Kang et al. 1984). Two proteins that are required for cellulose synthesis were isolated and purified from *A. xylinum* by two groups in 1990 and 1991. One of these proteins was identified as the catalytic subunit of cellulose synthase (Lin et al. 1990), and the other protein was shown to bind c-di-GMP and activate the catalytic subunit (Mayer 1991). The gene encoding the cellulose synthase catalytic subunit of *A. xylinum* was identified by determining the partial amino acid sequence of the cellulose synthase catalytic subunit and by analysis of mutants defective in cellulose production. At present, a number of proteins are suggested to be involved in cellulose biosynthesis in *A. xylinum*. Genes encoding these proteins are organized in an operon. The cellulose-synthesizing operon contains four

structural genes *bcsA*, *bcsB*, *bcsC*, and *bcsD*. In addition, other genes such as those that encode for an endoglucanase and a protein of an unknown function are also required for cellulose biosynthesis. The *bcsA* gene encodes for the cellulose synthase catalytic subunit and the *bcs B* gene encodes for the c-di-GMP-binding protein that activates the cellulose synthase. (Wong et al. 1990). The *bcsC* and *bcsD* genes are thought to be involved in the secretion of cellulose microfibrils by controlling either crystallization or polymerization.

The identification of genes that encode cellulose synthases in *A. xylinum* made possible the molecular biological approach for identification of cellulose-synthase genes in plants. The screening for cellulose-synthase genes in plants was actively pursued using antibodies and nucleic acid probes derived from *A. xylinum*. However, it was not found possible to isolate the cellulose synthase genes from plants using the *A. xylinum* gene as a probe (Delmer and Amor 1995). In parallel with these experiments, amino acid sequence analysis was performed to identify conserved regions in enzymes that catalyze formation of β-1,4 linkages including cellulose synthase, hyaluronan synthase and chitin synthase (Delmer and Amor 1995; Saxena et al., 1995). In 1996, Pear et al. performed random sequencing of cDNA libraries made from cotton fibers during secondary wall formation and isolated cDNA clones that encoded amino acid sequences that contained the conserved regions identified in the *A. xylinum* cellulose synthase.

The cotton cellulose-synthase (Gh*CesA*) genes isolated by Pear et al. (1996) were found to be homologous to the *CesA* genes identified in *Arabidopsis* by analysis of mutants affected in cellulose biosynthesis. (Arioli et al. 1998; Taylor et al. 1999). Recently, it was confirmed that the GhCesA proteins show cellulose-synthesizing activity and it is suggested that although cellulose is directly synthesized from the precursor UDP-glucose, a lipid intermediate sitosterol-β-glucoside works as a primer for cellulose synthesis (Peng et al., 2002; Read and Basic, 2002).

4 HOW TO PROVE IF THE ROSETTE OR LINEAR TC IS THE CELLULOSE-SYNTHESIZING MACHINERY?

So far the evidences to suggest that TCs contain cellulose synthases were all indirect. In many cases, rosette TCs can not be visualized easily by freeze fracture replication technique even during stages of active cellulose biosynthesis in some plant cells. Therefore, we had to await for advances in immunocytochemical techniques coupled with freeze-fracture electron microscopy to demonstrate directly that rosette TCs contain the catalytic subunit of cellulose synthase and the linear TCs in *A. xylinum* contain the c-di-GMP-binding protein that activates cellulose synthesis.

However, we had to overcome two major difficulties before applying the freeze-fracture technique coupled with immunogold labeling. First, it has been believed that conventional freeze-fracture technique does not allow for immunogold labeling. This is because the replica membrane made of platinum and carbon does not show any reaction with the antibody. This difficulty was overcome by utilizing

the SDS-solubilized freeze-fracture replica labeling technique first developed by Fujimoto (1995). The most important point about the immunochemical reaction as applicable to replica membrane is that the inner half of the cell membrane that is physically fixed by platinum-shadowing during freeze fracture will not dissolve with SDS. According to Fujimoto et al. (1996), artificial membranes produced by a mixture of α-phosphatidylcholine and L-α-phosphatidyl-L-serine and 100% L-α-phosphatidyl-L-serine did not dissolve after they were strengthened by a platinum-carbon replica membrane.

Second, it has not been possible to isolate and purify cellulose synthases from higher plants and so it has been difficult to prepare antibodies against this protein. This problem was overcome by expressing a fragment of the cotton CesA cDNA that encoded the catalytic region of a cotton cellulose synthase in *E. coli* and using the recombinant protein for obtaining polyclonal antibodies.

5 LABELING OF FREEZE FRACTURE REPLICAS

The authors applied the fracture labeling technique termed SDS-FRL to plant cells for the first time (Kimura et al. 1999). This technique was initially developed for animal cells by Fujimoto (1995) to bridge the gap between biochemistry and the unique morphology that is revealed by splitting the bimolecular leaflet of membranes. However, the application of this technique to plant cells has been difficult because the cell wall remains after the SDS treatment and obscures evaluation of the replicas of the fractured face of the membrane. The harsh acid treatments customarily used for conventional freeze-fracture techniques will dissolve completely not only the cell wall materials but also the bulk of the antigens present in the cytosol and the plasma membrane that may be recognized by specific antibodies.

The authors overcame this difficulty by treating the tissue attached to the replicas with a cellulase mixture commonly used for obtaining plant protoplasts. Figure 14-2 shows the comparison between conventional freeze-fracture and SDS-FRL techniques. The procedures of freeze-fracturing (a) followed by shadowing (b) are the same in both techniques. In the conventional freeze-fracture technique, plant tissues attached to the replica membrane are dissolved completely after chromic acid (Figure shows sulfuric acid and does not show the labeling of steps) treatment (c), including cell wall and cytoplasmic materials. In contrast, replica membrane attached to plant tissue are treated by a mixture of cellulase, pectolyase and proteinase inhibitor (c') in SDS-FRL technique. The replica membrane is further treated with SDS after dissolving the cell wall. After washing, the replica membrane is labeled with the CesA antibody or preimmune serum (d). Following labeling, the replica membrane is washed and treated with a secondary antibody conjugated to colloidal gold (10nm). The replica membrane is washed with PBS after this step, fixed with 0.5% glutaraldehyde, washed with distilled water twice, and placed on Formvar-coated grids for observing under transmission electron microscope. Using this protocol,the rosette TC was

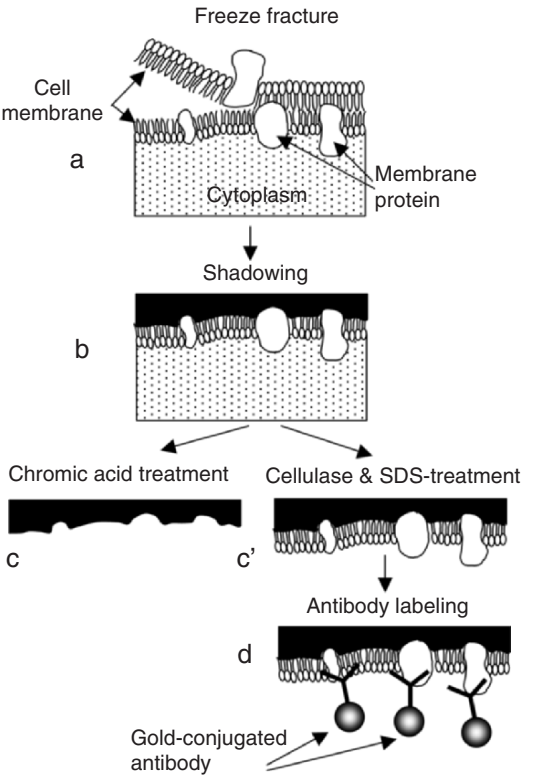

Figure 14-2. Comparison of SDS-FRL and conventional freeze-fracture techniques (**a**) freeze fracturing, (**b**) shadowing, (**c**) chromic acid treatment, (**c′**) Cellulase and SDS treatment, (**d**) antibody labeling. (Figure 2 from: Itoh, T. and Kimura S. 2001. Cellulose synthases are localized in terminal complexes. Journal of Plant Research: 114:483–489. Reproduced with kind permission of Springer Science and Business Media and the Botanical Society of Japan).

labeled with CesA antibodies on the P-fracture face of cells in the elongating hypocotyls of Azuki bean (Figure 14-3).

It was observed that 74% of gold particles were attached to rosettes or within 20 nm from the edges of rosette particles. Individual rosette was labeled with 1–4 gold particles, but usually with 1–2 gold particles (inset of Figure 14-3).

Labeling of the linear TCs of *A. xylinum* was performed using an antibody raised against the 93-kd protein that is suggested to be the c-di-GMP-binding protein. Procedures for labeling of the linear TCs of *A. xylinum* are similar to that utilized for labeling of the rosette TCs of plants except for the added steps for digestion of the peptidoglycan. The digestion of the peptidoglycan by lysozyme prior to SDS solubilization was found to be a prerequisite for freeze-fracture labeling of membrane proteins in *A. xylinum*. Lysozyme digests the

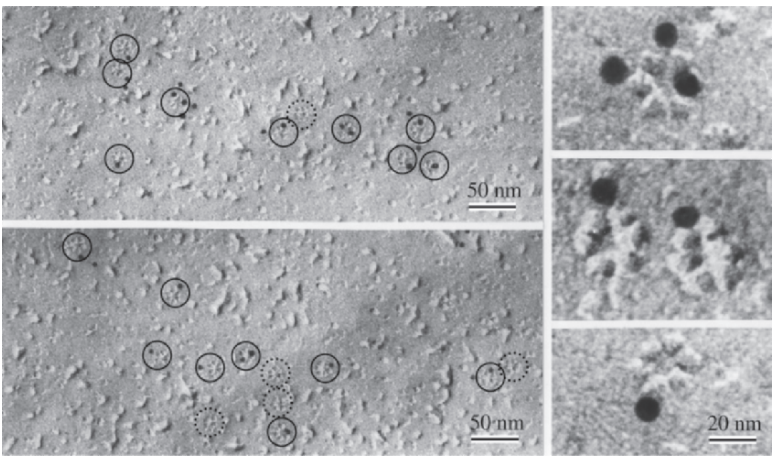

Figure 14-3. Numerous rosette TCs were labeled. Only one (*dotted circle*) of ten clearly visible rosette TCs is not labeled (*upper left*). Four (*dotted circle*) of twelve clearly visible rosette TCs are not labeled (*lower left*). A higher magnification of a rosette TC labeled with three gold particles is shown in upper right of the figure. A higher magnification of two rosette TCs each labeled with single gold particle is shown in middle right of the figure. A higher magnification of a rosette TC labeled with single gold particle is shown in *lower right* of the figure. (Itoh, T., Kimura, S., and Brown, Jr. R.M. 2004. Theoretical considerations of immunogold labeling of cellulose-synthesizing terminal complexes. Cellulose 11:385–394. Reproduced with kind permission of Springer Science and Business Media).

peptidoglycan and therefore allows the cell debris to be removed, which is done by harsh acid treatments in conventional freeze-fracture. The replicas obtained by freeze replica labeling appear similar to those obtained by conventional freeze-fracture techniques. The linear TCs of *A. xylinum* exhibit ordered particle arrays within single or double rows. The bacterial cell in Figure 14-4a shows the PF-face of its outer membrane (OM) and a single row of TC subunits with a cellulose ribbon attached at its terminus (arrow). Upon closer examination, the gold particles are observed to be attached along a single row of TCs. In the case of *A. xylinum*, almost all of the fractured planes occur through the outer membrane. In other words, the fractured cytoplasmic membrane is rarely observed in *A. xylinum* although it is more commonly observed in other Gram negative bacteria (Beveridge, 1999). The frequency of cytoplasmic membrane fractures is less than 5% based on the observation of more than one hundred cells. Even in the case where we successfully visualized the fractured plane of the cytoplasmic membrane, only part of this membrane was exposed. Furthermore, TC structures were never observed on the cytoplasmic membrane (CM) of *A. xylinum*. Figure 14-4b and 14-4c show a fractured plane occurring in the OM. Antibody labeling of TCs was not observed in a typical row of particles (Figure 14-4b). However, TCs showing a line of depressions or pits with an indistinct particle arrays were positively labeled (arrows, Figure 14-4c).

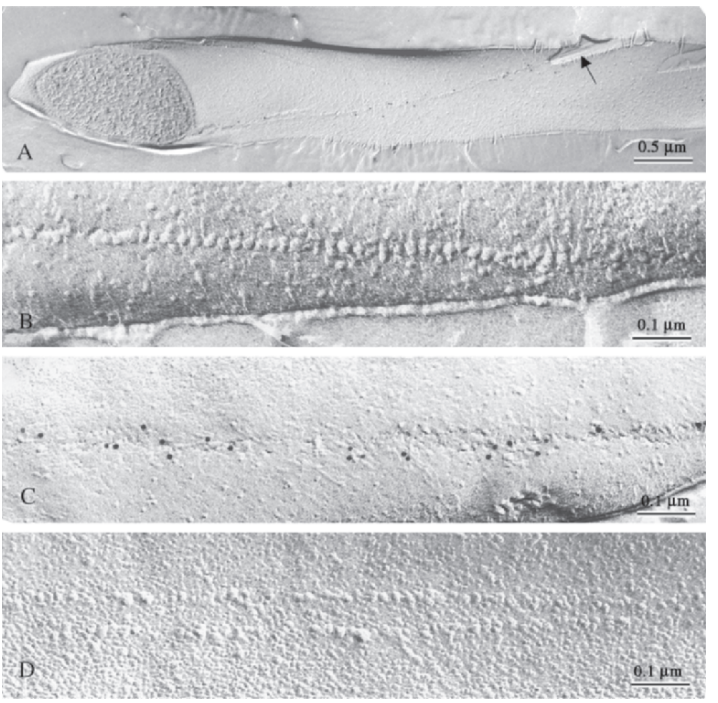

Figure 14-4. Fracture-labeled images (PF face, panels A to C; EF-face, panel D) showing reaction with the c-di-GMP-binding protein (93-kDa protein) antibody. Panel A and C show a typical fracture-labeled image of *A. xylinum*. The TC appears to be a single row along the longitudinal axis of the bacterial cell. A ribbon (arrow) of cellulose microfibrils is attached to the end of the TC row (Panel A). The 93-kDa protein antibody is distributed along the TC row on the PF face of the OM. The labeled TCs are visible as a row of slight depressions (or pits) with indistinct particles and small holes that may be due to particle displacement (Panel C). The TCs showing a distinct particle row on the PF face of the OM are not labeled with antibodies (Panel B). Panel D shows TCs with double rows on the EF face of the OM. The TCs on the EF face of the OM are never labeled by the antibodies (Figure 2a from: Kimura, S., Chen, H P., Saxena, I.M., Brown, Jr. R.M., and Itoh.T. 2001. Localization of c-di-GMP-binding protein with the linear terminal complexes of Acetobacter xylinum. J Bacteriol 183:5668–5674. Reproduced with kind permission of the American Society for Microbiology).

Evidence for understanding the topology of the bacterial membranes is furthermore obtained from a very rare case of freeze fracture which shows a distinct row of TC particles and pits in a single line at the same time on the PF-face of OM (Figure 14-5). The TCs in this region of the pits were exclusively labeled with antibodies. Two different features associated with the linear rows on the PF- face of OM are noted: (i) a pit or depressed region with indistinct particles (Figure 14-5b); and, (ii) a distinct, single row of particles (Figure 14-5c). The gold particles are localized only in the former, but not in the latter. In addition, these same TC particles can be found associated with the outer leaflet of the OM in all cases; however, TCs on the E-fracture face are never labeled in any case

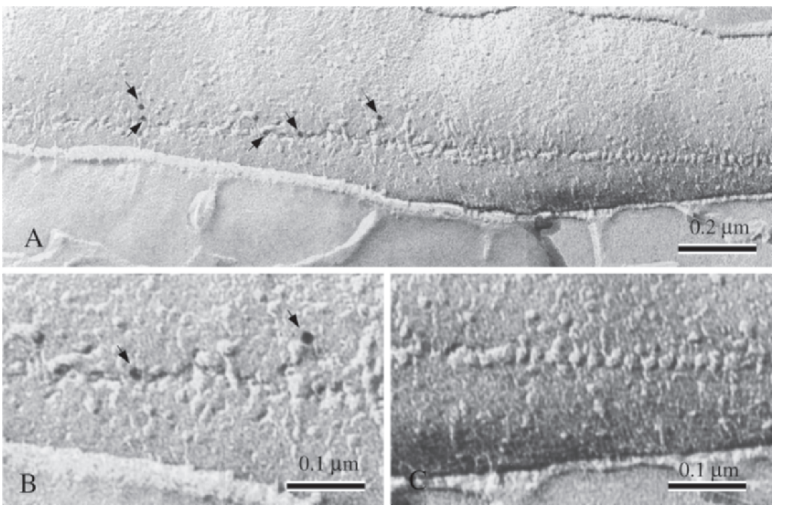

Figure 14-5. Fracture labeled image showing two types of TCs structure revealed on the PF-face of the OM. The distinct TC particles (*right half* of Figure 14-5**a**, Figure 14–5**c**) and depressions (or pits) with particles (left half of Figure 14-5**a**, Figure 14-5**b**) are visualized in a single row on the same PF-face of the OM. Moreover, the labeling of gold particles can be seen only in the region with depressions (*arrows* in Figure 14-5**a** and 14-5**b**). (Figure 5a is Figure 3 from: Kimura, S., Chen, H P., Saxena, I.M., Brown, Jr. R.M., and Itoh,T. 2001. Localization of c-di-GMP-binding protein with the linear terminal complexes of Acetobacter xylinum. J Bacteriol 183:5668–5674. Reproduced with kind permission of the American Society for Microbiology).

(Figure 14-4d). These membrane particles often appear complementary with the pit-like structures or depressions in the PF-face of OM.

6 SPECIFIC LABELING OF ROSETTE TCS

According to preliminary western blot analysis, the antibody to the recombinant cellulose synthase recognized an antigen of 130kd from three vascular plants - cotton, *Arabidopsis* and *Vigna radiata*. These results suggest that the catalytic subunit is conserved among a number of vascular plants. The antibody also recognized proteins obtained from cotton fibers during primary and secondary wall development. The specific labeling of rosette TCs on the P-fracture face of plasma membrane by the CesA antibody therefore provides direct proof that the rosette TC contains the catalytic subunit of cellulose synthases.

Labeling of the rosettes with gold-conjugated secondary antibody showed that the gold particles were present not only on the rosette TCs but also within 20 nm from the edge of the rosettes. The distance of 20 nm from the edge of the rosettes is within the range of the sum of the lengths of the primary plus secondary antibodies that has been determined to be 27 nm (Sarma et al. 1971). In fact, the actual distance from the antigens, cellulose synthases, may extend to more than

27 nm as the proteins within the rosette particles are denatured by SDS treatment. However, the authors have been conservative and used the distance of 20 nm between the gold particle and the rosette for quantitative analysis. When preimmune serum was used as the primary antibody, less than 2% of the rosette TCs were labeled with gold particles, which supports the specificity of the CesA antibodies. When the preimmune data is compared with data where the CesA antibodies were used the results are even more distinct. When we measured the distance from the center of the gold particle to the edge of the nearest rosette TC, it was found that 84% of the gold particles were closer than 20 nm (Figure 14-6). These results demonstrate that the antibodies to cellulose synthase specifically label a morphological structure that has been independently identified as associated with the end of cellulose microfibrils and suggested to be the site of the enzyme complex (Mueller and Brown, Jr., 1980).

It is also important to note that there is no specificity of antibody labeling on the E-fracture face of plasma membrane in *V. radiata*. This reinforces the concept that the catalytic region of the cellulose synthase lies truly on the cytoplasmic side of the plasma membrane, an observation that is congruent with the site of the catalytic domain predicted from sequencing data (Pear et al. 1996).

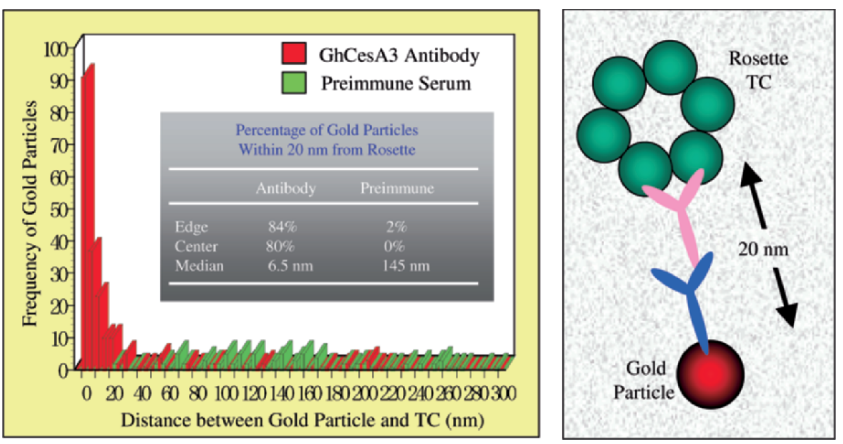

Figure 14-6. Frequency distributions of the number of gold particles associated with the immune serum containing antibodies to cellulose synthase and the preimmune control serum as a function of the measured distance to the center and the edge of the nearest rosette TC (*left*). Schematic diagram for the measurement of the distance between gold particles and rosette TC (*right*) is also shown (green:rosette, pink:primary antibody to cellulose synthase, blue:secondary antibody, red: gold particle the 93 kDa antibody-labeled particles. (**a**) Schematic diagram for the measurement of the distance between gold particles and linear TCs. The distance (double arrowheads) between the edge of gold particles and the linear TCs is indicated by the dotted line. (**b**) Frequency distribution of the number of gold particles associated with the 93 kDa protein antibody is shown as a function of the measured distance (nanometers) to the linear TC. Total number of gold particles measured was 277, taken from 30 different cells (*See Color Plate of this figure beginning on page 355*)

7 SPECIFIC LABELING OF LINEAR TCs

The distribution of gold particles associated with linear TCs in *A. xylinum* is shown in Figure 14-7. The distance between the TCs and gold particles was calculated by measuring the vertical distance between the edge of gold particles and a linear row of TC particles (Figure 14-7a, double arrowheads). For frequency analysis, 277 gold particles were randomly sampled from 30 different cells that had a single row of TCs. We neglected the measurement of this distance where the bacterium had double rows of TCs. Seventy five percent of the 277 gold particles were found within 20 nm of the linear row (shown as a dotted line in Figure 14-7a) of TCs. Most gold particles were found within 10–14 nm, with a median distance of 9.3 nm from the linear row (Figure 14-7b).

8 THE MECHANISM OF LABELING OF CELLULOSE SYNTHASES

The key point of antibody labeling in SDS-FRL is to label the cytoplasmic region of cellulose synthases using the modified freeze-fracture technique combined with cell wall digestion and SDS treatment. Transmembrane proteins

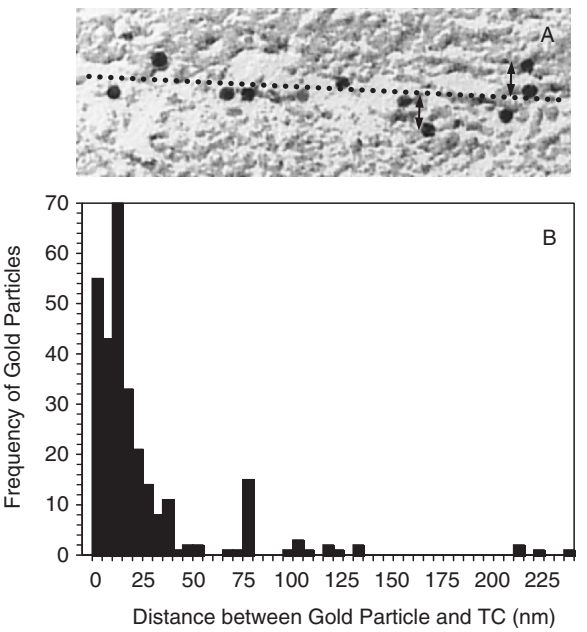

Figure 14-7. The distribution of gold particles associated with linear TCs in *A. xylinum*. (Figure 4 from: Kimura, S., Chen, H.P., Saxena, I.M., Brown, Jr. R.M., and Itoh, T. 2001. Localization of c-di-GMP-binding protein with the linear terminal complexes of *Acetobacter xylinum*. J Bacteriol 183:5668–5674. Reproduced with kind permission of the American Society for Microbiology).

present in the rosette TC and that have large regions exposed to the cytoplasmic side were labeled by this method. SDS treatment is a prerequisite for this method to work and it is also important that the rosette TC proteins stay attached to the replica membrane. It is extremely important to note that Fujimoto et al (1996) demonstrated by analysis of membrane proteins and lipids that these components are not removed by SDS treatment from the inner half of the fractured plasma membrane. This suggests that the semimembrane lipoprotein complex may be enzymatically active. The suitability of this idea can be demonstrated if the inner half of fractured plasma membrane synthesizes *in vitro* cellulose upon addition of UDP-glucose and we are in the process of testing this idea.

Another point in understanding the mechanism of CesA antibody labeling is to determine the number of gold particles that can be associated with a single TC. The diameter of both the gold particles and antibodies is 10 nm. Therefore, the diameter of the complex of gold particle and antibodies is approximately 30 nm (lower left, Figure 14-8). The diameter of a rosette TC is 25 nm. The actual image of a rosette labeled with these gold particles is shown in upper right of Figure 14-8. When we drew a Figure using the above mentioned dimensions, the illustration as shown in the middle right of Figure 14-8 was obtained. The lower right of Figure 14-8 shows the side view. It is surprising to see such a close match between the actual image (upper right of Figure 14-8) and its illustration (or modified) (middle right of Figure 14-8).

9 FUTURE PERSPECTIVES ON SDS-FRL AND RESEARCH IN CELLULOSE BIOSYNTHESIS

Immuno-gold electron microscopy applied to SDS-FRL is a superb technique to demonstrate the localization of membrane-associated proteins not only in plant cells but also in bacterial cells. Now that it has been confirmed that the rosette TCs of higher plants contain the catalytic subunit of cellulose synthases, the question is how many *CesA* genes are involved in cellulose biosynthesis in individual plant species. About ten *CesA* genes have been identified in *Arabidopsis* (Richmond 2000; Holland et al. 2000) and interactions among three different CesA proteins is shown to be required for cellulose synthesis in *Arabidopsis* (Taylor et al., 2003) and *rice* (Tanaka et al. 2003). These findings suggest that three different CesA genes have a role in cellulose synthesis at the same time. However, it is not known whether the three different CesA proteins are present in the same TC or not. In order to prove these possibilities, we need to prepare antibodies against several different CesA proteins that can be labeled with different sizes of gold particles allowing for double- or triple-labeling in this application of SDS-FRL.

The specific labeling of c-di-GMP-binding protein to a single row of cellulose-synthesizing TCs in the outer fractured membrane of *A. xylinum* should allow localization of other proteins in these complexes (Kimura et al., 2001). In the near future, it will be possible to localize crystallization proteins and pore

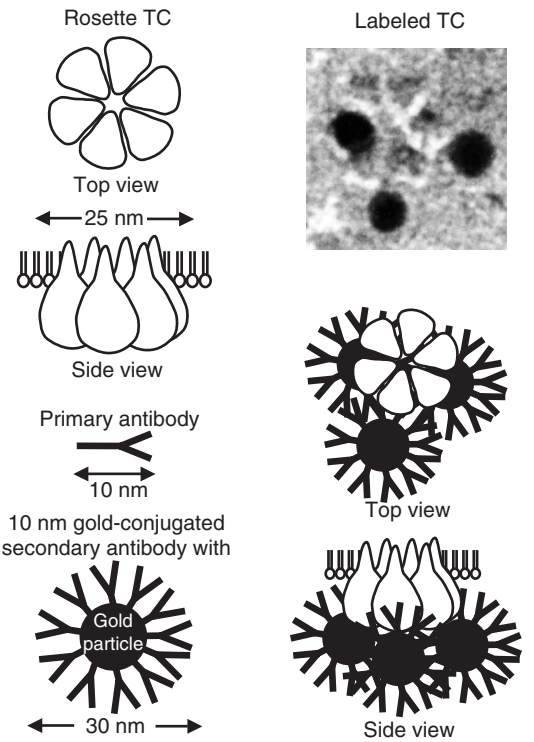

Figure 14-8. Scale model of the gold particle, antibodies, rosette TC, gold-conjugated antibody, and labeled rosette TC. The model of labeled rosette TC (*middle right*) closely resembles the actual image (*upper right*). (Figure 6 from: Itoh, T. 2002 Immunogold labeling of terminal cellulose-synthesizing complexes-demonstration coupled by freeze fracture and immunogold labeling techniques. Regulation of Plant Growth and Development (in Japanese) 37:44–50. Reproduced with kind permission of The Japanese Society for Chemical Regulation of Plants.)

proteins that control the dimensions of the cellulose microfibril (Saxena et al. 1994) using SDS-FRL.

The application of this technique will also probe the localization of other proteins which are hypothesized to be components of rosette TCs in plant cells (Doblin et al. 2002; Joshi et al. 2004), the membrane-anchored glucanase (Lane et al. 2001; Mølhøj et al. 2001; Sato et al. 2001; Szyjanowicz et al. 2004; Rober et al. 2005), sucrose synthase (Amor et al. 1995; Salnikov et al. 2001), and callose synthase (Cui et al. 2001; Zonglie et al. 2001a, b). A number of these proteins are important for cellulose synthesis. Recently, an *Arabidopsis* mutant defective in the COBRA protein was isolated (Roudier et al. 2005). This mutant exhibits disorganization of the orientation of cellulose microfibrils and subsequent reduction of crystalline cellulose. It is suggested that the COBRA protein is a GPI-anchored protein localized on the plasma membrane. This means that

COBRA protein is involved in the regulation of cellulose microfibril arrays and in the future it may be possible to determine the localization of this protein by SDS-FRL.

Generally speaking, SDS-FRL is a superb technique to visualize the localization of any kind of protein that resides not only in the plasma membrane but also the membranes of cell organelles. The authors hope that SDS-FRL will be applied in different fields to understand the function of not only plant cells but also other organisms in general.

Acknowledgments

This work was supported, in part by Welch Grant F-1217 and DOE Grant DE-FG-02–03ER15396 to RMB.

REFERENCES

Amor Y., Haigler C.H., Johnson S., Wainscott M., and Delmer D.P. 1995. A membrane-associated form of sucrose synthase and its potential role in synthesis of cellulose and callose in plants. Proc Natl Acad Sci USA 92:9353–9357.

Arioli T., Peng L., Betzner A.S., Burn J., Wittke W., Herth W., Camilleri C., Hofte H., Planzinski J., Birch R., Cork A., Glover J., Redmond J., and Williamson R.E. 1998. Molecular analysis of cellulose biosynthesis in *Arabidopsis*. Science 279:717–720.

Beveridge T.J. 1999. Structures of gram-negative cell walls and their derived membrane vesicles. J Bacteriol 181:4725–4733.

Brown, Jr. R.M., 1978. Biogenesis of natural polymer systems with special reference to cellulose assembly and deposition. The Third Philip Morris Science Symposium pp. 52–123.

Brown, Jr. R. M. 1996. The biosynthesis of cellulose. J Macromol Sci 10:1345–1373.

Brown, Jr. R. M., Willison J.H.M., and Richardson C.L. 1976. Cellulose synthesis in *A. xylinum*: Visualization of the site of synthesis and direct measurements of the *in vivo* process. Proc Natl Acad Sci USA 73:4565–4569.

Brown, Jr. R.M., and Montezinos D. 1976. Cellulose microfibrils: visualization of biosynthetic and orienting complexes in association with the plasma membrane. Proc Natl Acad Sci USA 73:143–147.

Cui X., Shin H., Song C., Laosinchai W., Amano Y., and Brown, Jr. R.M. 2001. A putative plant homolog of the yeast β-1,3-glucan synthase subunit FKS1 from cotton (*Gossypium hirsutum* L.) fibers. Planta 213:223–230.

Delmer D.P. and Amor Y. 1995. Cellulose biosynthesis. Plant Cell 7:987–1000.

Dobberstein B. and Kiermayer O. 1972. Das Auftreten eines bosonderen Typs von Golgivesikeln warend der Sekundarwandbildung von *Micrasterias denticulate* Breb. Protoplasma 75:185–194.

Doblin M.S., Kurek I., Jacob-Wilk D., and Delmer D.P. 2002. Cellulose biosynthesis in plants: From genes to rosettes. Plant Cell Physiol 43:1407–1420.

Emons A.M.C. 1991. Role of particle rosettes and terminal globules in cellulose synthesis. In: Haigler C.H. and Weimer P.J. (eds.), Biosynthesis and Biodegradation of Cellulose. Marcel Dekker, New York, pp. 71–98.

Emons A.M.C. 1994. Winding threads around plant cells: a geometrical model for microfibril deposition. Plant Cell Environ 17:3–14.

Fujimoto K. 1995. Freeze-fracture replica electron microscopy combined with SDS digestion for cytochemical labeling of integral membrane proteins. J Cell Sci 108:3443–3449.

Fujimoto K., Umeda M., and Fujimoto T. 1996. Transmembrane phospholipid distribution revealed by freeze-fracture replica labeling. J Cell Sci 109:2453–2460.

Giddings T.H., Brower D.L., and Staehelin L.A. 1980. Visualization of particle complexes in the plasma membrane of *Micrasterias denticulata* associated with the formation of cellulose fibrils in primary and secondary cell walls. J Cell Biol 84:327–339.

Grimson M.J., Haigler C.H., and Blanton R.L. 1996. Cellulose microfibrils, cell motility, and plasma membrane protein organization change in parallel during culmination in *Dictyostelium discoideum*. J Cell Sci 109:3079–3087.

Herth W. 1984. Oriented "rosette" alignment during cellulose formation in mung bean hypocotyls. Naturwissenschaften 71:216–217.

Herth W. 1985a. Plasma-membrane rosettes involved in localized wall thickening during xylem vessel formation of *Lepidium sativum* L. Planta 164:12–21.

Herth W. 1985b. Plant cell wall formation. In: Robards A.W. (ed.), Botanical Microscopy 1985. Oxford University Press, Oxford, pp. 285–310.

Herth W. 1987. Effects of 2,6-DCB on plasma membrane rosettes of wheat root cells. Naturwissenschaften 74:556–557.

Herth W. 1989. Inhibitor effects on putative cellulose synthetase complexes of vascular plants. In: Schuerch C. (ed.), Cellulose and Wood-Chemistry and Technology, Wiley, New York, pp. 795–810.

Herth W. and Weber, G. 1984. Occurrence of the putative cellulose-synthesizing "rosettes" in the plasma membrane of *Glycine max* suspension cultured cells. Naturwissenschaften 71:153–154.

Holland N., Holland D., Helentjaris T., Dhugga K.S., Xoconostle-Cazares B., and Delmer, D.P. 2000. A comparative analysis of the plant cellulose synthase (CesA) gene family. Plant Physiol 123:1313–1324.

Hotchkiss A.T., Jr. and Brown, Jr. R.M. 1987. The association of rosette and globule terminal complexes with cellulose microfibril assembly in *Nitella translucens* var. *axillaris* (Charophyceae). J Phycol 23:229–237.

Hotchkiss A.T. and Brown, Jr. R.M. 1988. Evolution of the cellulosic cell wall in the Charophyceae. In:Schuerch C (ed.) Cellulose and Wood-Chemistry and Technology, Wiley, NewYork, pp. 591–609.

Hotchkiss A.T., Jr., Gretz M.R., Hicks, K.B., and Brown, Jr. R.M. 1989. The composition and phylogenetic significance of the *Mougeotia* (Charophyceae) cell wall. J Phycol 25:646–654.

Itoh T. and Brown, Jr. R.M. 1984. The assembly of cellulose microfibrils in *Valonia macrophysa* Kutz. Planta 160:372–381.

Itoh T. 1990. Cellulose synthesizing complexes in some giant marine algae. J Cell Sci 95:309–319.

Itoh T. and Brown, Jr. R. M. 1988. Development of cellulose synthesizing complexes in *Borgesenia* and *Valonia*. Protoplasma 144:160–169.

Joshi C.P., Bhandari S., Ranjan P., Kalluri U.C., Liang X., Fujino T., and Samuga A. 2004. Genomics of cellulose biosynthesis in poplars. New Phytologist 164:53–61.

Kang M.S., Elango N., Mattie E., Au-Young J., Robbins P., and Cabib E. 1984. Isolation of chitin synthetase from *Saccharomyces cerevisiae*. Purification of an enzyme by entrapment in the reaction product. J Biol Chem 259:14966–14972.

Kimura S., and Itoh T. 1996. New cellulose synthesizing complexes (terminal complexes) involved in animal cellulose biosynthesis in the tunicate *Metandrocarpa uedai*. Protoplasma 194:151–163.

Kimura S., Chen H. P., Saxena I.M., Brown, Jr. R.M., and Itoh T. 2001. Localization of c-di-GMP-binding protein with the linear terminal complexes of *Acetobacter xylinus*. J Bacteriol 183:5668–5674.

Kimura S., Laosinchai W., Itoh T., Cui X., Linder C.R., and Brown, Jr. R.M. 1999. Immunogold labeking of rosette terminal cellulose-synthesizing complexes in the vascular plant, *Vigna angularis*. Plant Cell 11:2075–2085.

Lane D.R., Wiedemeier A., Peng L., Hofte H., Vernhettes S., Desprez T., Hocart C.H., Birch R.J., Baskin T.I., Burn J.E., Arioli T., Betzner A.S., and Williamson R.E. 2001. Temperature sensitive alleles of RSW2 link the KORRIGAN endo-1,4-β-glucanase to cellulose synthesis and cytokinesis in *Arabidopsis*. Plant Physiol 126:278–288.

Lin F.C., Brown, Jr. R.M., Drake R.P., Jr., and Haley B.E. 1990. Identification of the uridine 5′-diphosphoglucose (UDP-glc) binding subunit of cellulose synthase in *Acetobacter xylinus* using the photoaffinity probe 5-azido-UDP-glc. J Biol Chem 265:4782–4784.

Mayer R., Ross P., Weinhouse H., Amikam D., Volman G., Ohana P., Calhoon R.D., Wong H.G., Emerick A.W., and Bemziman M. 1991. Polypeptide composition of bacterial cyclic diguanylic acid-dependent cellulose synthase and the occurrence of immunologically cross-reacting proteins in higher plants. Proc Natl Acad Sci USA 88:5472–5476.

Mizuta S., Roberts E., and Brown, Jr. R.M. 1989. A new cellulose synthesizing complex in *Vaucheria hamata* and its relation to microfibril assembly. In Schuerch, C. (ed.), Cellulose and Wood-Chemistry and Technology. Wiley, New York, pp. 659–676.

Mølhøj M., Ulvskov P., and Dal Degan F. 2001. Characterization of the role of membrane-bound endo-beta-1,4-glucanases in cellulose biosynthesis. Plant Cell Physiol 43:1399–1406.

Mueller S.C. and Brown, Jr. R.M. 1980. Evidence for an intramembranous component associated with a cellulose microfibril synthesizing complex in higher plants. J Cell Biol 84:315–326.

Mueller S.C. and Brown, Jr. R.M. 1982. The control of cellulose microfibril deposition in the cell wall of higher plants. Planta 154:501–515.

Nobles D.R., Romanovicz D.K., and Brown, Jr. R.M. 2001. Cellulose in Cyanobacteria. Origin of vascular plant cellulose synthase? Plant Physiol 127:529–542.

Okuda K., Tsekos I., and Brown, Jr. R.M. 1994. Cellulose microfibril assembly in *Erythrocladia subintegra* Rosenv.: an ideal system for understanding the relationship between synthesizing complexes (TCs) and microfibril crystallization. Protoplasma 180:49–58.

Pear J.R., Kawagoe Y., Schreckengost W.E., Delmer D.P., and Stalker D.M. 1996. Higher plants contain homologs of the bacterial CesA genes encoding the catalytic subunit of cellulose synthase. Proc Natl Acad Sci USA 93:12637–12642.

Peer Y. Van-de, and Wachter R.D. 1997. Evolutionary relationships among the eukaryotic crown taxa taking into account site-to-site rate variation in 18S rRNA. J Mol Evol 45:619–630.

Peng L., Kawagoe Y., Hogan P., and Delmer D. 2002. Sitosterolbeta-glucoside as primer for cellulose synthesis in plants. Science 295:147–150.

Preston R.D. 1964. Structural and mechanical aspects of plant cell walls with particular reference to synthesis and growth. In: Zimmerman M.H. (ed.), Formation of Wood in Forest Trees. Academic Press, New York, pp. 169–188.

Richmond T. 2000. Higher plant cellulose synthases. Genome Biology 1(4):reviews 3001.1–3001.6.

Read S.M. and Basic T. 2002. Prime time for cellulose. Science 295:59–60.

Robert S., Bichet A., Grandjean O., Kierzkowski D., Satiat-Jeunema B., Pelletier S., Hauser M., Hofte H., and Vernhettesa S. 2005. An *Arabidopsis* endo-1,4-β-D-glucanase involved in cellulose synthesis undergoes regulated intracellular cycling. Plant Cell 17:3378–3389.

Roelofsen A. 1958. Cell wall structure as related to surface growth. Acta Bot Neerl 7:77–89.

Ross P., Mayer R., and Benziman M. 1991. Cellulose biosynthesis and function in bacteria. Microbiol Rev 55:35–58.

Ross P., Weinhouse H., Aloni Y., Michaeli D., Weinberger-Ohana P., Mayer R., Braun S., de Vroom E., van der Marel G.A., van Boom J.H., and Benziman M. 1987. Regulation of cellulose synthesis in *Acetobacter xylinus* by cyclic diguanylic acid. Nature 325:279–281.

Roudier F., Fernandez A.G., Fujita M., Himmelspach R., Borner G.H., Schindelman G., Song S., Baskin T.I., Dupree P., Wasteneys G.O., and Benfey P.N. 2005. COBRA, an *Arabidopsis* extracellular glycosyl-phosphatidyl inositol-anchored protein, specifically controls highly anisotropic expansion through its involvement in cellulose microfibril orientation. Plant Cell 17:1749–1763.

Rudolph U., Gross H., and Schnepf E. 1989. Investigation of the turnover of the putative cellulose-synthesizing particle 'rosettes' within the plasma membrane of *Funaria hygrometrica* protonema cells. Protoplasma 148:57–69.

Salnikov V.V., Grimson M.J., Delmer D.P., and Haigler C.H. 2001. Sucrose synthase localized to cellulose synthesis sites in tracheary elements. Phytochemistry 57:823–833.

Sarma V.R., Silverton E.W., Davies D.R., and Terry W.D. 1971. The three-dimensional structure at 6 A resolution of a human γG1 immunoglobulin molecule. J Biol Chem 216:3753–3759.

Sato S., Kato T., Kakegawa K., Ishii T., Liu YG., Awano T., Takabe K., NishiyamaY., Kuga S., Sato S., Nakamura Y., Tabata S., and Shibata D. 2001. Role of the putative membrane-bound endo-1,4-β-glucanase KORRIGAN in cell elongation and cellulose synthesis in *Arabidopsis thaliana*. Plant Cell Physiol 42:251–263.

Saunders G.W. 1997. Phylogenetic affinities of the Sarcinochrysidales and Chrysomeridales (Heterokonta) based on analyses of molecular and combined data. J Phycol 33:310–318.

Saxena I.M., Kudlicka K., Okuda K., and Brown, Jr. R.M. 1994. Characterization of genes in the cellulose synthesizing operon (acs operon) of *Acetobacter xylinus*: Implications for cellulose crystallization. J Bacteriology 176:5735–5752.

Saxena I.M., Brown, Jr. R.M., Fevre M., Geremia R., and Henrissat B. 1995. Multi-domain architecture of glycosyl transferases: Imprications for mechanism of actin. J Bacteriol 177:1419–1424.

Szyjanowicz P.M., McKinnon I., Taylor N.G., Gardiner J., Jarvis M.C., and Turner S.R. 2004. The irregular xylem 2 mutant is an allele of korrigan that affects the secondary cell wall of *Arabidopsis thaliana*. Plant J 37:730–740.

Tanaka K., Murata K., Yamazaki M., Onosato K., Miyao A., and Hirochika H. 2003. Three distinct rice cellulose synthase catalytic subunit genes required for cellulose synthesis in the secondary wall. Plant Physiol 133:73–83.

Taylor N.G., Scheible W.R., Culter S., Somerville C.R., and Turner S.R. 1999. The irregular xylem 3 locus of *Arabidopsis* encodes a cellulose synthase required for secondary cell wall synthesis. Plant Cell 11:769–780.

Taylor N.G., Howells R.M., Huttly A.K., Vickers K., and Turner S.R. 2003. Interactions among three distinct CesA proteins essential for cellulose synthesis. Proc Natl Acad Sci USA 100: 1450–1455.

Tsekos I. 1999. The sites of cellulose synthesis in algae:diversity and evolution of cellulose-synthesizing enzyme complexes. J Phycol 35:635–655.

Tsekos I. and Reiss H.-D. 1992. Occurrence of the putative microfibril-synthesizing complexes (linear terminal complexes) in the plasma membrane of the epiphytic marine alga *Erythrocladia subintegra* Rosenv. Protoplasma 169:57–67.

Zogaj X., Nimtzv M., Rohde M., Bokranz W., and Romling U. 2001. The multicellular morphotypes of *Salmonella typhimurium* and *Escherichia coli* produce cellulose as the second component of the extracellular matrix. Mol Microbiol 39:1452–1463.

Zonglie H., Delauney A.J., and Verma D.P.S. 2001a. A cell plate-specific callose synthase and its interaction with phragmoplastin. Plant Cell 13:755–768.

Zonglie H., Zhang Z., Olson J.M., and Verma D.P.S. 2001b. A novel UDP-glucose trasferase is part of the callose synthase complex and interacts with phragmoprastin at the forming cell plate. Plant Cell 13:769–779.

CHAPTER 15

CELLULOSE SHAPES

ALFRED D. FRENCH* AND GLENN P. JOHNSON

Southern Regional Research Center, Agricultural Research Service, US Department of Agriculture, 1100 Robert E. Lee Boulevard, New Orleans, LA 70124

Abstract

This chapter surveys the shapes of cellulose molecules. New, high-resolution experiments on the various crystalline polymorphs are reviewed, and their similar twofold helical shapes are compared. Conversion between cellulose I and II is discussed, including interdigitation and chain-folding as possible mechanisms. Information on molecular shape from cellotriose and tetraose is also reviewed along with data for derivatives and complexes. To convert crystallographic data from disaccharides such as cellobiose, the usual descriptors of disaccharides, the torsion angles φ and ψ, are converted to the helical polymer descriptors, *n* and *h*. Evidence is also gathered from crystals of complexes of proteins and cellodextrins. Once the experimental information is consolidated, it is shown how theoretically calculated energies for the various shapes can contribute to a coherent, overall picture of the possible shapes of the molecule in both crystalline and noncrystalline regions. Almost all of the studies of related molecules indicate that cellulose is a very extended molecule with between two and three residues per turn. Some of those molecules were slightly right-handed, but most were left-handed.

Keywords

conformation, diffraction, helix, molecular mechanics, quantum mechanics, screw axis, x-ray.

1 INTRODUCTION

The polysaccharides cellulose, starch, and callose all have equivalent chemical compositions, e.g., $C_6H_{11}O_5{-}(C_6H_{10}O_5)_{x\text{-}2}{-}C_6H_{11}O_6$, where *x* indicates the hundreds or thousands of glucose residues in each molecule. They differ in the details of the

* For correspondence: Tel: +1 (504) 286-4410; Fax: +1 (504) 286-4217; e-mail: afrench@srrc.ars.usda.gov

R.M. Brown, Jr. and I.M. Saxena (eds.), Cellulose: Molecular and Structural Biology, 257–284.

attachment of one glucose residue to the next with, respectively, β-(1,4)-, α-(1,4) and β-(1,3) linkages. Although molecular weight is also a factor, their different linkage geometries lead to individual three-dimensional shapes that are the basis for most of the properties that distinguish these molecules and their roles from each other. For example, we wear cellulose, in the form of cotton or rayon, and we eat starch, and not vice versa. In particular, the most frequently occurring shapes of these flexible molecules determine the way that the molecules associate to form larger structures that again will have specific properties. Knowledge of molecular shapes is useful in many ways because the shapes can be altered to change properties. Knowledge of shape is also vital to understanding cellulose biosynthesis because that process results in elaborate structures. These structures give important clues as to what occurs during biosynthesis.

This chapter provides an overview of the shapes of cellulose molecules. New, high-resolution experimental determinations of the shapes of cellulose in crystals are available, as well as many more experiments of varying quality for cellulose and its derivatives and related molecules. We will take advantage of this evidence. Once the experimental information is consolidated, we will show how theoretically calculated energies for the various shapes can contribute to a coherent, overall picture of the possible shapes of the molecule in both crystalline and noncrystalline regions.

2 CELLULOSE POLYMORPHY AND CRYSTAL STRUCTURES

It is not immediately obvious that most cellulose is crystalline, but its long chains of glucose residues associate in crystallites that consist of some 5,000 to as many as 300,000 glucose residues. This is in contrast to crystals of small compounds such as cellobiose that contain 10^{15} or more molecules. Those crystals yield very accurate structural information when studied with x-ray or neutron diffraction. However, even the small crystals of cellulose diffract such radiation, creating patterns of spots whose positions reveal the periodicity of the repeated arrays of atoms. The intensities of the spots contain information about the positions and types of atoms within the repeated unit. In Figure 15-1, we have superimposed six different chain segments that are composed of five glucose residues that have been replicated from the atomic coordinates in recent, high-resolution reports. Except for the O6 positions, the differences are not substantial.

Not all cellulose is crystalline. Less-ordered cellulose is more chemically reactive and has different physical properties. Therefore, it is necessary to understand both the crystalline and noncrystalline phases. Various treatments can be applied to destroy the crystallinity, but less-ordered cellulose also occurs naturally. For example, a given cellulose molecule will often pass through several crystallites, as in ramie (a bast fiber). In ramie, crystallites are long enough to accommodate approximately 300 glucose units (Nishiyama et al. 2003b), but the cellulose molecules in ramie are much longer than that.

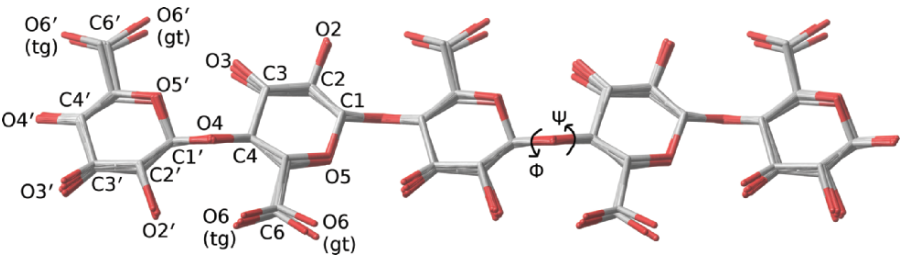

Figure 15-1. The six different chain shapes from the crystal structures of the cellulose polymorphs I, II, and III_I, superimposed at their C1, O4, and C4 atoms to show the differences in the molecular shapes. Indicated for the five-residue segments are the linkage torsion angles, φ and ψ. There are two unique chains in both the Iβ and II structures (with O6 ***tg***) and one each from Iα and III_I (with O6 ***gt***). The single-chain Iα structure has two sets of φ and ψ values because of its lower symmetry. Atomic numbering is indicated; the reducing end is to the right and the nonreducing end is on the left (*See Color Plate of this figure beginning on page 355*)

By definition, cellulose between the crystallites is noncrystalline, but the degree of disorder can vary. A fairly ordered but noncrystalline cellulose might have all chains aligned in the same direction and similar chain shapes. The noncrystallinity would arise from irregular spacing between the chains. On the other hand, a highly disordered, amorphous cellulose could have, within each molecule, randomly varied shapes, and similarly random relationships with other chains. Even in crystalline regions, the small crystallites have large fractions of the cellulose chains on the crystallite surfaces, and atoms on the surface may not conform to the internal periodicity. Distortions of the crystallites from outside forces also occur, such as curvature in the structure of the cell wall. Such departures from long-range order limit the diffraction data from celluloses of commercial importance, such as cotton or wood.

2.1 The polymorphs

Polysaccharides usually crystallize in numerous forms, or polymorphs, that depend on the history of the sample. At first glance the various cellulose forms give four different diffraction patterns, and the polymorphs were named I–IV. Now we know that, despite the similarities of patterns and overall molecular shape, there are important differences in chain-packing within these groups. Cellulose I is the predominant native structure. Cellulose made by bacteria and algae has a high proportion of the subgroup cellulose Iα, and cellulose from higher plants is mostly Iβ (Atalla and VanderHart 1984; Sugiyama et al. 1991).

Cellulose II can be obtained by dipping cotton, flax or other fibers in cold, concentrated NaOH with subsequent rinsing. Although that laboratory process is often called mercerization, commercial mercerization is done at higher temperatures and with dilute NaOH. It does not result in much, if any, conversion to

cellulose II. Cellulose also takes the II form after dissolution and regeneration, as in the manufacturing of rayon. Solutions of 65% nitric acid can also swell cellulose and convert it to cellulose II (Katz and Hess 1927; Chedin and Marsaudon 1954). Finally, there are instances of biosynthesis of cellulose II, e.g., by bacteria in low temperature surroundings (Hirai et al. 2002) or by bacteria that have undergone mutation (Kuga et al. 1993).

Cellulose III results from treatment of cellulose with amines of various sorts, with supercritical ammonia being especially effective. There are two different structures, one made from cellulose I, called III_I, and the other from cellulose II, called III_{II}. Although their structures apparently have similarities, they are different. They revert to their initial forms under certain conditions. Cellulose IV results from treatments at temperatures above 240°C. Again, there are two subgroups, IV_I and IV_{II}. The most recent information on IV_I is that it is very closely related to cellulose Iβ (Wada et al. 2004a).

2.2 High-resolution structure determinations

In the past few years, there have been advances in the detailed understanding of the crystalline structures through x-ray and neutron diffraction experiments. These advances were possible because synchrotron x-ray beams are much more powerful than ordinary laboratory beams, giving double or triple the amount of diffraction data. Neutron diffraction permits location of deuterium atoms so the "hydrogen bonding" systems can be worked out on samples that have had the hydroxyl hydrogen atoms substituted with deuterium atoms. Also, new methods have been used to prepare samples that are much more crystalline, also leading to more diffraction data.

So far, highly detailed structures have been published for cellulose Iα (Nishiyama et al. 2003a), Iβ (Nishiyama et al. 2002), mercerized II (Langan et al. 2001), and III_I (Wada et al. 2004b). Although it is fair to say that there is more to learn about these structures, and that controversies are not completely settled (Sternberg et al. 2003), the information presented on these structures so far is very strong. The cellulose I structures have an especially complex, disordered hydrogen bonding system. Besides the hydrogen bonding, strong van der Waals forces are in play to hold the crystals together (Ford et al. 2005). As mentioned above, superimposed chain segments for cellulose Iα, Iβ, II, and III_I are shown in Figure 15-1, and their crystal packing is displayed in Figure 15-2. Cellulose Iβ and II have two chain monoclinic unit cells. Cellulose Iα has a one-chain triclinic unit cell, and III_I has a one-chain monoclinic unit cell. All of the structures have an intramolecular hydrogen bond between O3-H and O5 of the preceding glucose residue.

2.3 The dominant twofold shape in crystals

When monomeric units in a molecular chain (e.g., the glucose residues in cellulose) are regularly repeated, i.e., in crystals, they form shapes that can be described mathematically as helices. Helices of cellulose in crystals are described

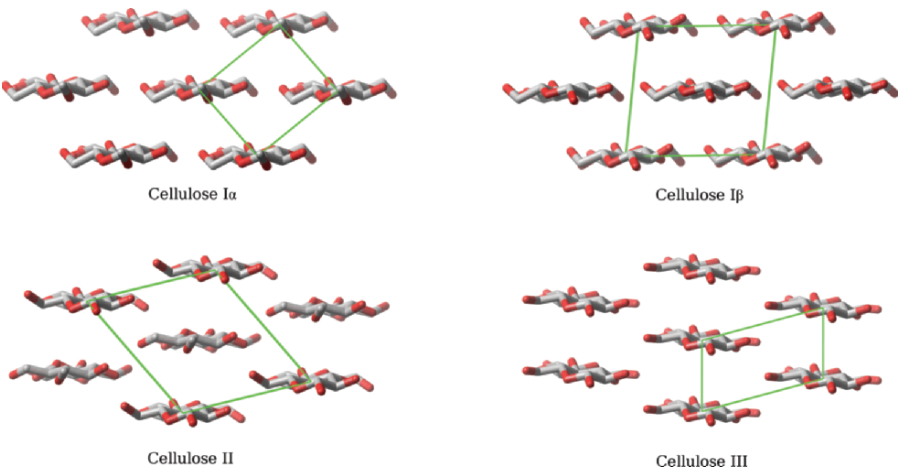

Figure 15-2. Views of the chain packing perpendicular to the molecular axes for cellulose Iα, Iβ, II, and III_I. The unit cells and seven chains are shown for each. Hydrogen atoms are not shown. The unit cells show the relationships of four chains and contain fractions of them; two-chain cells have an additional chain within their boundaries (*See Color Plate of this figure beginning on page 355*)

with *n*, the number of monomeric glucose units per turn of the helix, and *h*, the rise per glucose unit along the helix axis (see Figure 15-3). In the four main crystalline polymorphs, cellulose has approximate or exact twofold screw-axis symmetry, i.e., $n = 2$. From the highly detailed papers cited in the previous paragraph, the crystallographic repeats along the molecular axes (the helix pitch, $P = n \times h$), are 10.40 Å in Iα, 10.38 Å in Iβ and 10.31 Å in II and III_I. Therefore, the *h* values are 5.20 Å, 5.19 Å, and 5.155 Å, respectively. The chains have the shape of a flat ribbon that permits a very dense crystal packing similar to the packing of bricks in a wall. The densely packed crystallites appear to account for the strong and nearly insoluble nature of cellulose fibers. Twofold screw-axis symmetry relates successive glucose residues by rotation of 180° and simultaneous translation along the chain axis. Thus, the cellulose chain can be generated by repeatedly applying the twofold screw symmetry operator to a glucose residue *in these crystals*. As we will see below, twofold shapes are not the only likely ones for cellulose molecules.

If the chain symmetry is essentially the same in all polymorphs, what are the differences? One difference is the chain packing, with parallel (cellulose I and III_I) and antiparallel (cellulose II) arrangements. In Iα (see Figure 15-2), the central, horizontal sheet of three chains is shifted up towards the viewer by half a glucose residue compared to the bottom sheet of two chains, and the top sheet of two chains is shifted up another half glucose residue compared to the central sheet. These translations are different from the scheme in Iβ, in which the top and bottom rows of chains in the figure have no relative shift; only the central chain is shifted up by half a glucose residue. The similar hydrogen bonding schemes of Iα and Iβ are

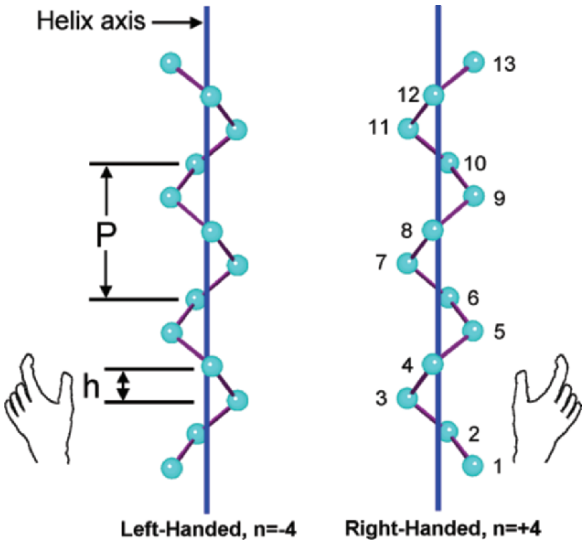

Figure 15-3. Schematic left- and right-handed helices with four monomeric units per turn and 13 units altogether in each. The pitch, ψ, of the helix is indicated, as is the rise per residue along the helix axis, *h* (*See Color Plate of this figure beginning on page 355*)

different from the scheme in cellulose II, which is close to that of III_I. Small variations in shapes of the glucose rings and the orientations of the $-CH_2OH$ groups are shown in Figure 15-1. Twofold or pseudo-twofold chain shapes are also known for III_{II}, IV_I, and IV_{II}, but high-resolution studies are as yet not available.

2.4 Topological nightmare

By far the most remarkable result from the above work has been the confirmation of parallel chain packing for both cellulose I structures and for cellulose III_I (Wada et al. 2001, 2004b), along with the finding that the chains are packed antiparallel in cellulose II. A crystal composed of parallel chains has all molecules pointed in the same direction, while antiparallel crystals have alternate chains in opposite directions. Thus, parallel structures have all the reducing ends of the molecules at one end of the crystal, and antiparallel structures have half the reducing groups at each end. Because laboratory mercerization converts parallel cellulose Iβ to antiparallel II despite retention of the fiber structure, there has been much controversy since these conclusions were first proposed based on much less data (Kolpak and Blackwell 1976; Stipanovic and Sarko 1976; Kolpak et al. 1978). Suspicion regarding fiber diffraction results is understandable. In the past, there have been several problematic determinations of cellulose structure. See, for example, a paper by one of the current authors, who found that parallel structures of cellulose did not fit literature x-ray data for ramie as well

as an antiparallel structure (French 1978) or the incorrect ***tg*** O6 positions in the above early proposals for cellulose II.

However, even prior to the new high-resolution diffraction work, there was corroboration by other techniques (Hieta et al. 1984; Chanzy and Henrissat 1985; Koyama et al. 1997) plus insight on the possible process of conversion (Nishiyama et al. 2000). Most researchers now agree that cellulose Iβ has parallel chains. Single-chain unit cells as found for Iα and III_I, by definition, characterize parallel chain structures. Therefore, the main question among those who have not accepted the parallel-to-antiparallel conversion is whether converted cellulose II could somehow retain the parallel packing of cellulose I (Kroon-Batenburg et al. 1996). That proposal avoids a necessity for the seemingly impossible parallel-to-antiparallel conversion with retention of the fibrous form.

There are several examples of structures where the antiparallel packing of cellulose II can be inferred without thorough crystal structure determination. Bacterial cellulose that was treated in concentrated NaOH for several days lost its long, fibrous form (Shibazaki et al. 1997). In the case of loosely packed, primary wall cellulose crystallites from parenchymal sugar beet cell walls, treatment with alkali >12% causes loss of the fibrous form. In both cases, the original long, needle-like crystallites became globular (Dinand et al. 2002). These conversions are consistent with chain-folding. Also, cellulose II formed by bacteria at low-temperature is in a "band" in which the cellulose molecular axis is perpendicular to the axis of the band (Hirai et al. 2002). The crystalline dense bands are narrower than the length of cellulose molecules, so such cellulose must be folded. At room temperature, the same bacterium produces cellulose I with the familiar fibrillar form. Another example of a folded cellulosic backbone is furnished by lamellar cellulose triacetate crystals grown from dilute solution (Manley 1960, 1963).

2.5 Interdigitation

The conversion of fibrous cellulose from Iβ to II is apparently special, occurring only for fibers that have substantial amounts of secondary cell wall material inside an intact primary wall such as found in seed (e.g., cotton) or bast (e.g., flax or ramie) fibers. Even keeping cotton or ramie fibers under tension while they are immersed in NaOH prevents the crystal structure change. These findings are consistent with the "interdigitation" hypothesis (see Shibazaki et al. 1997; for a recent paper) that has been advanced to explain the conversion. It is based on the idea that these dense secondary cell walls contain crystallites that are internally composed of parallel chains. In turn, the crystallites themselves are antiparallel to adjacent crystallites. Upon swelling in NaOH, the chains in the adjacent crystallites intermingle, producing crystallites that have antiparallel chains and lower potential energy. The constraints of an intact primary wall during NaOH treatment are thought to prevent massive folding of the cellulose but still allow the interdigitative movements of the extended molecules.

3 OTHER CELLULOSIC POLYMERS

Derivatizing or complexing cellulose sometimes results in other helical shapes. One complex, soda cellulose II, has a chain conformation with $n = 3^1$ (Whitaker et al. 1974). The crystal structures of the derivatives deviate from the twofold shape more often. These structures have not been determined with the same high resolution as the above recent studies but they have helices with two to three residues per turn. Among the structures are trinitrocellulose (Meader et al. 1978), with five glucose residues in two turns ($n = 2.5^1$), the nitromethane complex of cellulose triacetate (Zugenmaier 1985) which has 8 residues in 3 turns ($n = -2.67$) and triethylcellulose, which has $n = -3$ (Zugenmaier 1983, 1986). All are extended, with $h > 5$ Å. From this standpoint, then, the shapes in noncrystalline regions could range continuously between two and three residues per turn. Older literature (Hess and Trogus 1931) reports cellulose derivatives with four residues per turn but those proposals need to be re-evaluated in the light of current knowledge. One of the most interesting molecular shapes of a cellulose backbone is reported for xanthan, a gum that has a three-monosaccharide side chain on every other glucose unit in the backbone. In the native state, the molecule is reported to form a double helix, composed of strands that each repeat after five cellobiose units, in 47.4 Å (Chandrasekaran and Radha 1997). Other details are not known. The double helix can be disassociated, and a "onefold helix" has been proposed (Millane and Wang 1990) for interactions with other polysaccharides. In that proposed structure, the backbone has essentially the same shape as crystalline cellulose.

Very short cellulose chains, such as cellotetraose (Gessler et al. 1995), with four glucose residues, and methyl cellotrioside (Raymond et al. 1995), with just three glucose residues and a terminal methyl group on O1, have been crystallized and their structures determined. Based on their powder diffraction patterns, which are sharper but otherwise nearly identical to those of cellulose II, their structures (see Figure 15-4) should be similar to cellulose II. This is another observation that supports antiparallel cellulose II, as the short chains in these structures are also antiparallel.

4 INFORMATION FROM SMALL MOLECULES IN SELF-CRYSTALS AND PROTEIN–CARBOHYDRATE COMPLEXES

Another way to learn of the likely molecular shapes for cellulose depends on extrapolation of the shapes that are found in crystal structures of molecules such as cellobiose (Chu and Jeffrey 1968), α-cellobiose complexed with NaI and H_2O (Peralta-Inga et al. 2002), cellobiose octaacetate (Leung et al. 1976) and related compounds (French and Johnson 2004a). Similar, although less accurate,

[1] As will be discussed later, the Na cellulose II and trinitro structures are probably left-handed ($n = -3$ and -2.5, respectively), but were originally reported as right-handed.

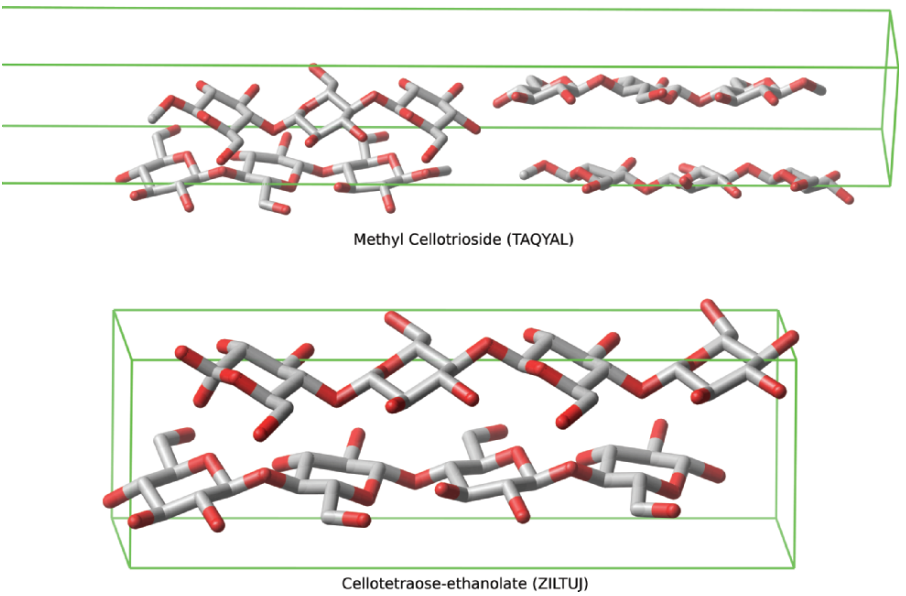

Figure 15-4. Views of the methyl cellotrioside (Raymond et al. 1995) and cellotetraose-ethanolate (Gessler et al. 1995) crystal structures. There are four unique cellotrioside molecules, with eight values of φ and ψ. Cellotetraose crystals contain two unique molecules, and have six values of φ and ψ. Only half of the trioside unit cell is shown. TAQYAL and ZILTUJ are the Cambridge Structural Database "refcodes" for these structures (*See Color Plate of this figure beginning on page 355*)

information can be obtained from complexes of molecules such as cellotetraose or lactose (4-*O*-β-D-galactopyranosyl-D-glucopyranose) with proteins. Through packing forces, crystals can distort similar molecules in different directions. However, our thinking is that the main determinants of the shape of a polysaccharide arise from intramolecular forces that are essentially the same as those for a disaccharide. Many short molecules are suitable for extrapolation. Small molecule atomic coordinates are contained in the Cambridge Structural Database (Allen 2002) and the protein–carbohydrate complexes are in the freely accessible Protein Data Bank (Berman et al. 2002), making it feasible to perform comprehensive searches.

So far, we have been describing the cellulose shapes in terms of the polymeric descriptors, *n* and *h*. These parameters do not apply to small molecules that are not helices. Instead, the most important shape variables for the small molecules are φ and ψ, the linkage torsion angles indicated in Figures 15-1 and Figure 15-5. To proceed, we need to present a conversion of φ and ψ to *n* and *h*,[2] after which

[2] The conversion is performed using equations developed by Shimanouchi and Mizushima (1955).

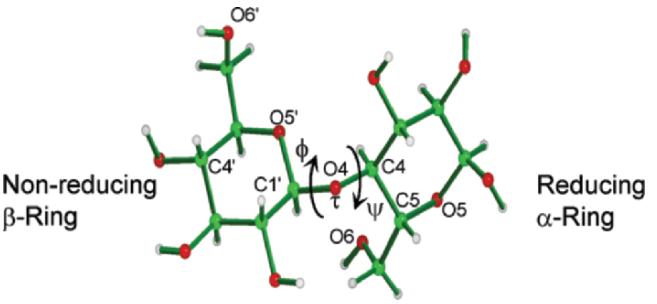

Figure 15-5. The α-cellobiose disaccharide with the geometry found in the crystal structure of the hydrated NaI complex (Peralta-Inga et al. 2002). The O6 and O6′ atoms are in *gg* positions. No intramolecular hydrogen bonds are formed in this structure (*See Color Plate of this figure beginning on page 355*)

we will operate primarily in φ,ψ space. Another reason to operate in φ,ψ space is that it is not convenient to calculate the energy based on *n* and *h*. We will return to the extrapolations from small molecules after we discuss the conversion and examine the cellulose, methyl cellotrioside and cellotetraose structures in terms of φ,ψ space.

5 THE φ,ψ TO *n,h* CONVERSION MAP

For a specific set of atomic coordinates for the glucose residue and a fixed linkage bond angle, τ, there is an exact conversion from φ, and ψ to values of *n* and *h*, as shown in Figure 15-6[3] (similar maps were presented in 1968 by Rees and Skerrett). The reverse conversion is ambiguous at best. Figure 15-6 shows that for a given *n* and *h*, there are two values of φ and ψ.

The generalized shape of the ring of β-D-glucose is a chair with carbon atom 4 high and carbon 1 low, denoted $^4C_1$ (see the nonreducing ring in Figure 15-5). However, all experimentally determined rings vary from the ideal shape to one

[3] Figure 15-6 shows a two-dimensional representation of ϕ,ψ space. Each axis encompasses a full 360º, but the starting and ending values are shifted from what the reader might expect. We do this because much of the previous and current work defines the ϕ and ψ torsion angles based on the hydrogen atoms, e.g. ϕ_H = H1′-C1′-O4-C4, and ψ_H = C1′-O4-C4-H4. Further, the values of those torsion angles are usually −180º to +180º. That convention places most of the observed structures of all disaccharides in a more-or-less central region of the ϕ,ψ map. In our case, however, we are going to plot the ϕ,ψ values found in crystal structures. The most common technique for determining the structure of molecules in crystals is x-ray diffraction, and the positions of hydrogen atoms in many x-ray studies are not accurately determined. Therefore, we define the torsion angles based on only carbon and oxygen atoms, i.e. ϕ_{O5} = O5′-C1′-O4-C4, and ψ_{C5} = C1′-O4-C4-C5. The numeric values (−300º to +60º) that we have used permit the favored regions of ϕ,ψ space to be located in the same position as when the axes were defined based on ϕ_H and ψ_H, ranging from −180º to +180º. Also, the important *n* = 2 line crosses ϕ,ψ space through the middle of the diagram.

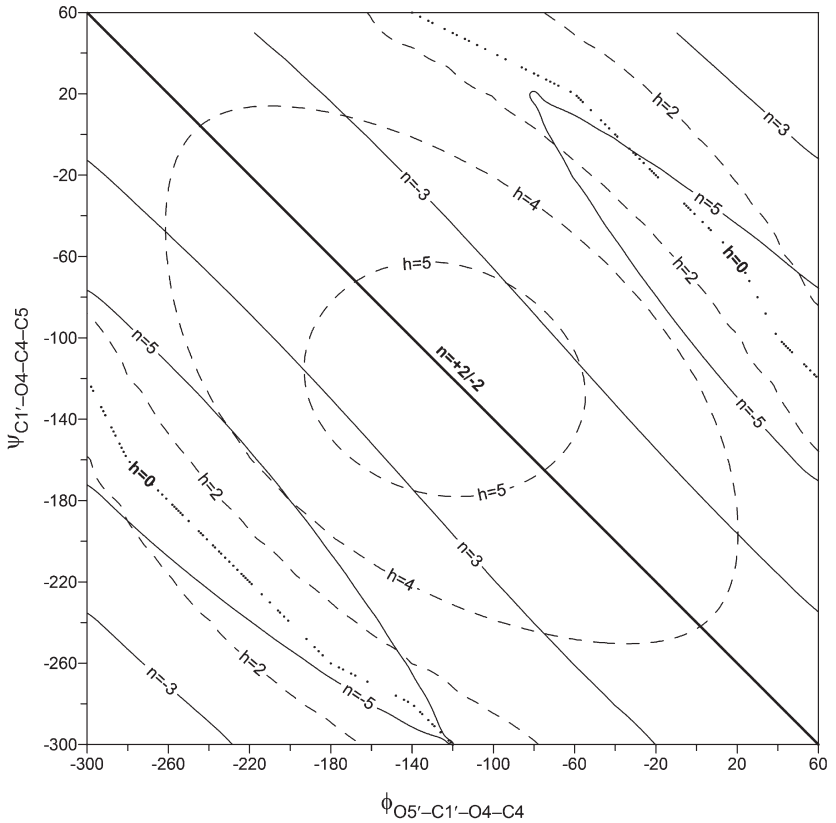

Figure 15-6. A conversion between φ and ψ and *n* and *h*. This plot was obtained with the geometry of the nonreducing ring of crystalline β-cellobiose (Chu and Jeffrey 1968) and a covalent bond angle of 116°. Models constructed of four glucose residues were stepped through all of φ and ψ space in 20° increments and the *n* and *h* values were calculated with the equations of Shimanouchi and Mitsushima (1955). A spreadsheet for those calculations is provided by French and Johnson 2004a, who also discuss helix theory in greater detail. Lines of constant *n*, ranging from −5 to +5 residues per turn, are solid, and the lines of iso-*h*, which range from 0 to 5, are dashed (several lines are omitted for clarity). Negative values of *n* denote left-handed helices, and positive values are for right-handed structures. Structures with $n = 2$ can be described as neutral. There are transitions in helix handedness when crossing the $n = 2$ line and when crossing the $h = 0$ line

degree or another, and τ values in small molecules range from 113.7° to 117.7° (French and Johnson 2004a). The interpretation in Figure 15-6 of φ and ψ to give *n* and *h* values is done with purely geometric manipulations based on a selected glucose ring geometry (the nonreducing ring of β-cellobiose) and an assumed glycosidic bond angle (116°). In terms of an overall conversion, it is only a qualitative picture, because of the variations in ring geometry and τ that are found in the different crystal structures. (Examples of conversion to *n* and *h*

from experimentally observed φ, ψ, τ and exact monomeric geometries are provided in French and Johnson (2004a)).

The variations in the values of *n* and *h* due to the variations in ring shape and τ are one reason that these conversion maps have seen little use in recent work. Still, because of the similarity of the ring shapes and the limited range of τ, these approximations are reasonable.

A key feature of Figure 15-6 is the corner-to-corner diagonal line that denotes structures having twofold symmetry. Structures close to that line, but above or to the right of it have left-handed shapes, denoted by negative values of *n*, and those below or to the left of the line are right-handed. (French and Johnson 2004a, explain why the value of *n* changes from positive to negative at 2 instead of 0.) In the central region, the values of *n* are generally low and *h* is near the maximum. Helices with high *h* are "extended," and those with minimal values are "collapsed."

There is another interesting situation in Figure 15-6. Moving in either direction from the central diagonal, the absolute values of *n* increase and the values of *h* decrease. At the point where *h* becomes zero, the helix deteriorates into a circle. Just as is the case along the center diagonal $n = 2$ line, there is a reversal of helix handedness when crossing the lines of $h = 0$. For longer chains, $h = 0$ is not possible because it would cause severe atomic overlap, but such structures could occur for short chains or in a short segment of the molecule that otherwise has linkages that lead to extended shapes.

One way to produce a fold in a cellulose chain is to give a short segment of the chain the shape that results in a helix with a small *h*, while the glucose residues on either side of that section have linkages that give an extended shape, as shown in Figure 15-7. Any structures near the $h = 0$ lines could lead to folding. Such bulb-shaped folds may, however, not fit well with neighboring folds, and more study is needed.

6 CRYSTAL STRUCTURES IN φ, ψ SPACE

6.1 Cellulose and its oligomers

Figure 15-8 shows the locations of φ and ψ values for cellulose Iα, Iβ, II, and III_I. Also indicated are the values from the crystal structures of methyl cellotrioside (Raymond et al. 1995) and an ethanol complex of cellotetraose (Gessler et al. 1995).

The distribution of the crystal structures slightly off the $n = 2$ line reflects minor variations in the monomeric geometry as well as slightly different glycosidic bond angles for cellulose Iβ, II, and III_I. The deviations do not indicate an absence of twofold screw symmetry. Cellulose Iα, cellotrioside and cellotetraose structures also fall near the $n = 2$ line despite the absence of exact twofold screw-axis symmetry. In the cellulose I structures, the O6 atoms are in the ***tg*** position (see Figure 15-1), allowing an intramolecular hydrogen bond with O2 in the next residue. All of the other structures in Figure 15-8 have O6 in the ***gt*** position (see Figure 15-1). All make O3–O5′ hydrogen bonds, and the structures with O6′ in the ***gt*** position also have long O3–O6′ hydrogen bonds.

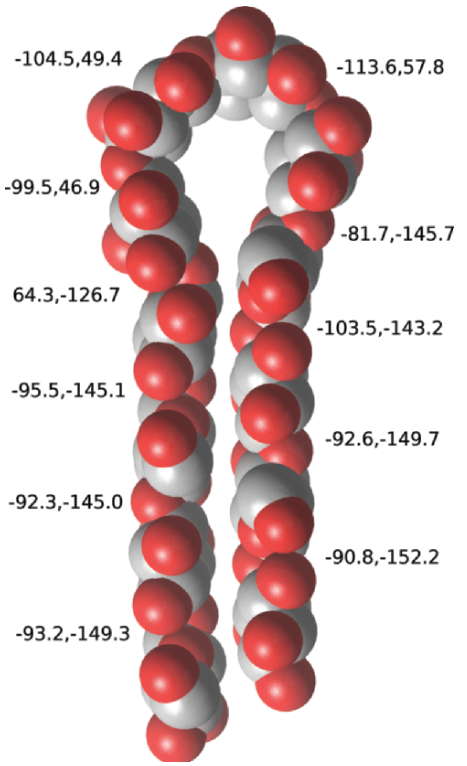

Figure 15-7. Drawing of a cellulose chain segment in a folding conformation. The φ and ψ values are indicated. This bend was energy minimized with MM3. The lower portions retain the linkage geometries of crystalline cellotetraose (Gessler et al. 1995) (*See Color Plate of this figure beginning on page 355*)

6.2 Small molecules

The range of linkage conformations from small molecule crystal structures (Figure 15-9) is greater than in Figure 15-8. A few of these structures are as close to the twofold line as are the linkages in Figure 15-8, but most are somewhat farther away from the line. The most distant are above and to the right, indicating left-handed helices with up to nearly three residues per turn. There is also one linkage geometry (Ernst and Vasella 1996) that would fall near the bottom edge of the full map in Figure 15-6 (not shown). It has a hydrogen bond between O3 and O2′ and could also correspond to the shape in a fold. This geometry, applied to three successive linkages, was the basis for the folding in Figure 15-7. The small-molecule based structures are discussed in more detail in French and Johnson (2004a). Structures that have hydroxyl groups and that have ψ values lower than −122° on Figure 15-9 have O6 in the ***gt*** position, at least on the nonreducing ring. Like cellulose II, they also form intramolecular, interresidue hydrogen bonds, with O3 donating simultaneously to O5′ and O6′. In group of seven structures above −122°, there are no intramolecular, interresidue hydrogen bonds. Some of those molecules possess the requisite hydroxyl groups but form inter- instead of intramolecular hydrogen

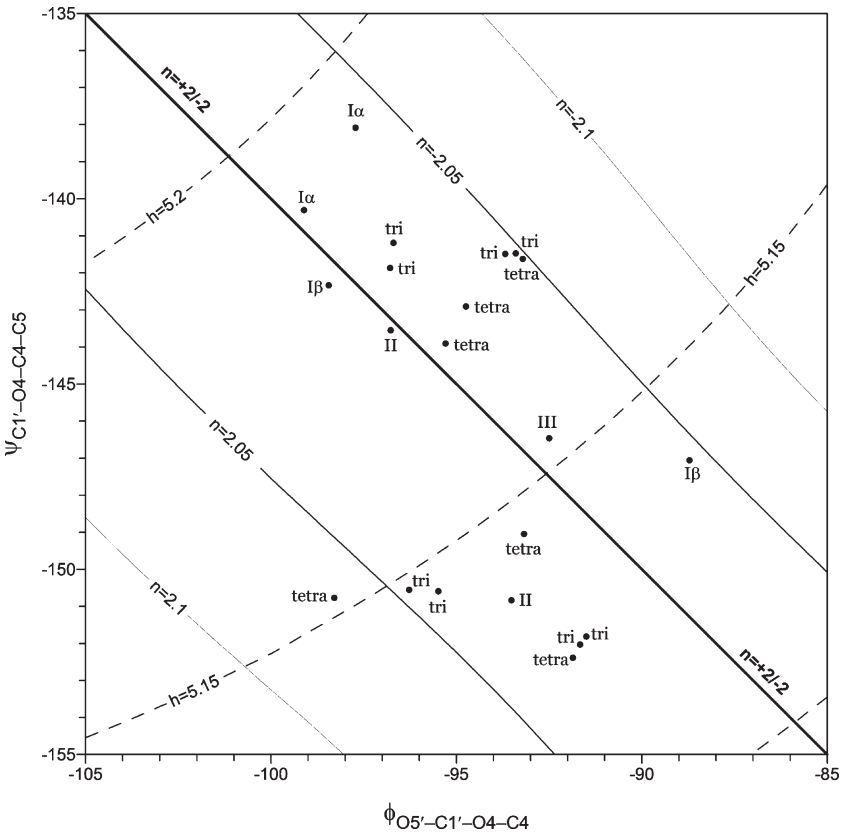

Figure 15-8. The locations in φ,ψ space of the linkage torsion angles from diffraction studies of cellulose Iα, Iβ, II, and III_I. Also shown are the lines of approximate conversion of φ and ψ to *n* and *h* from Figure 15-6. Only the small, occupied portion of φ,ψ space is shown. There are two sets of φ and ψ values for each structure except III_I. Also included are the eight conformations for the methyl cellotrioside (tri) and the six for cellotetraose (tetra). All fall near the idealized twofold ($n = 2$) line

bonds. Other molecules in that group were chemically substituted and could not form hydrogen bonds.

6.3 Protein–cellodextrin complexes

More structural data for cellulose-type linkage geometries are available from crystals of proteins that are complexed with either cellulose fragments or molecules that contain a lactose moiety. Figure 15-10 shows a complex of cellotetraose and an endoglucanase (Sakon et al. 1996), as well as the structure of the fragment in more detail. That protein is an enzyme that catalyzes the hydrolysis of cellulose molecules, but it also has nonhydrolytic binding sites. Other proteins do

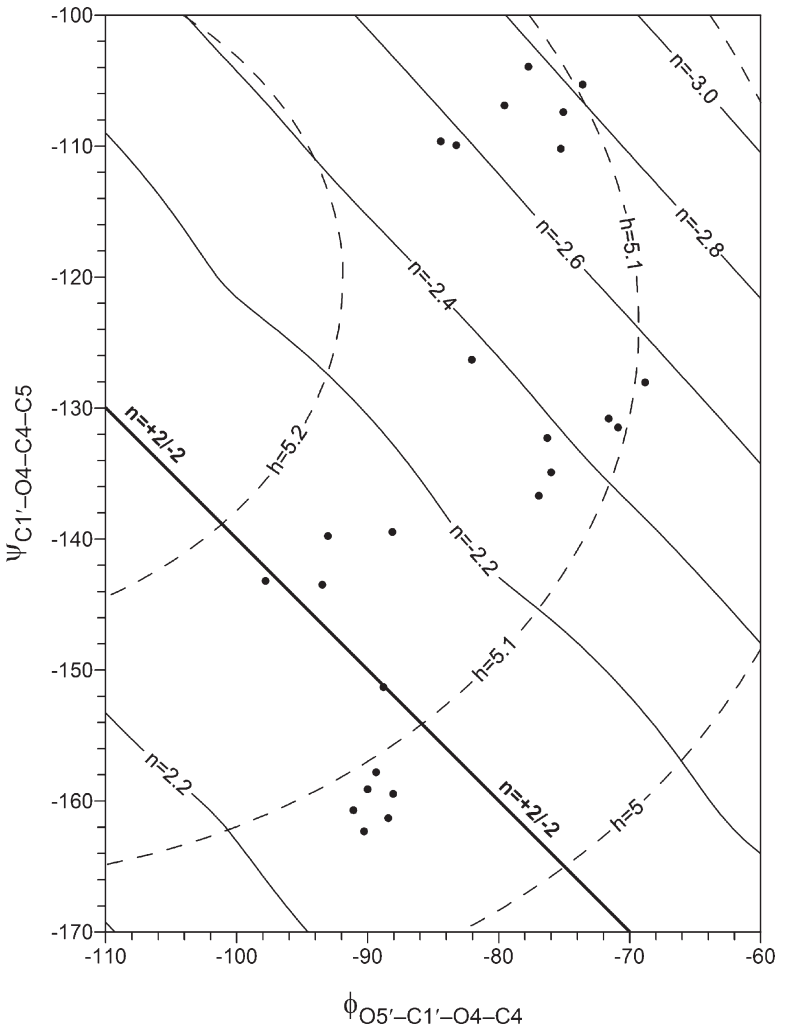

Figure 15-9. The locations of the small molecule crystal structures in φ,ψ space, along with the iso-*n* and iso-*h* contours from Figure 15-6

not break down cellulose but do bind it. Because the carbohydrate in these structures is surrounded by amino acid residues and water molecules, it is in a very different environment than when it is crystallized with like molecules in the small molecule crystals of the previous paragraph. While linkage distortion may be a feature of catalytic action (French et al. 2001b), we imagine that the various proteins mostly accommodate either a very low-energy form of an isolated cellulose molecule or can bind to a part of a cellulose crystal. Even well-determined protein crystal structures are generally less accurate than the small molecule structures

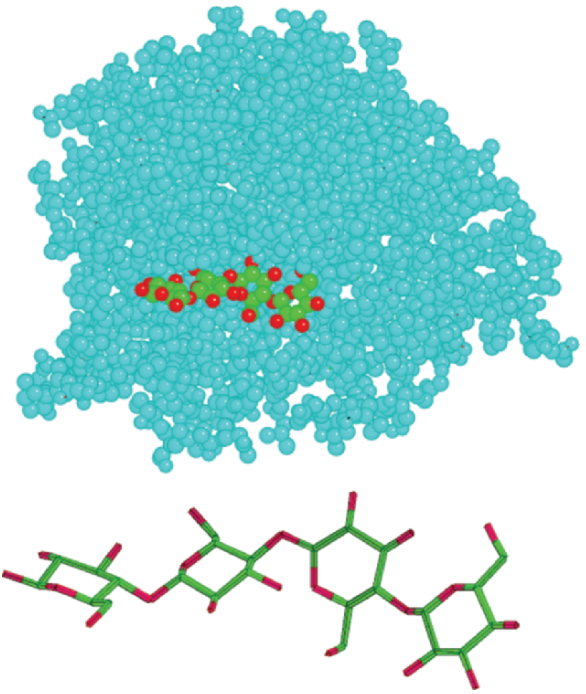

Figure 15-10. A cellotetraose fragment complexed with one of the two halves of an endoglucanase, 1ECE, plotted from the coordinates in the Protein Databank. Also shown is a stick representation of the tetraose without the surrounding protein. Two of its linkages have a twofold conformation, but the central linkage corresponds to a threefold helix with $h < 5$ Å, an unusual conformation (*See Color Plate of this figure beginning on page 355*)

but comparable to the best cellulose structures from fiber diffraction studies. Hydrogen positions are not usually reported.

Figure 15-11 shows the locations in φ,ψ and *n*,*h* space of the cellodextrin molecule linkages in protein complexes. The range of structures is quite similar to the range of the small molecule structures, but some of the structures are further away from the twofold axis line. Some of these linkage conformations correspond to helices with just over three residues per helix turn. Only one of these structures has a linkage with a pronounced (more than 2.5 residues per turn) right-handed character.

6.4 Lactose–protein complexes

Figure 15-12 shows the distribution of the geometries of lactose moieties from protein complexes. There is a much wider range of these structures (notice the difference in values on the axes), although most are in the same location as the above small-molecule and protein complex structures.

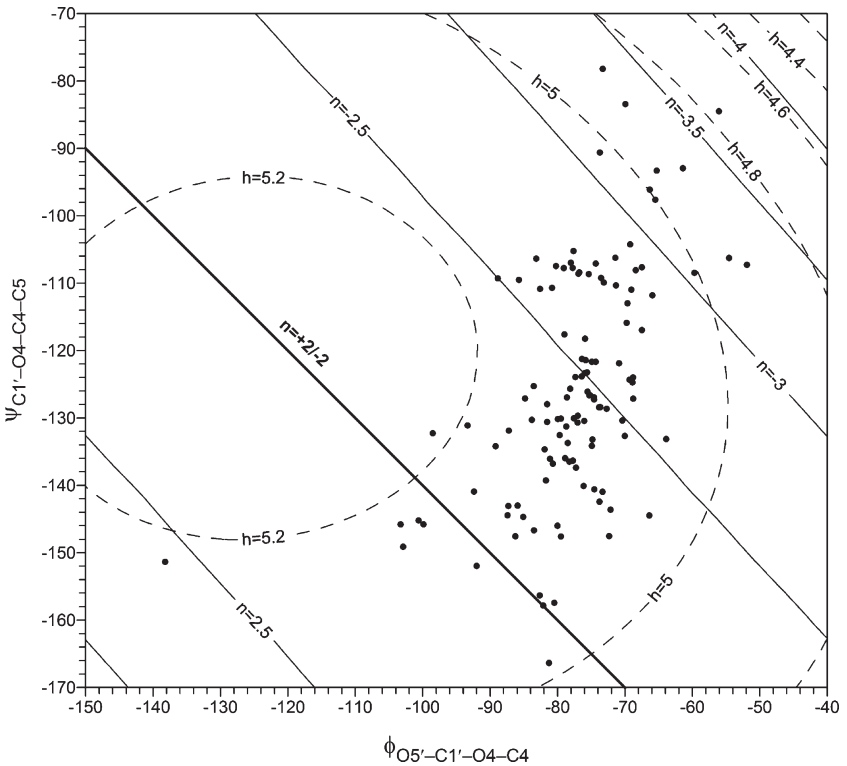

Figure 15-11. The locations of the conformations of cellodextrins in protein complexes in φ,ψ space, along with the approximate iso-*n* and iso-*h* contours from Figure 15-6

Several of these geometries correspond to right-handed helices with between 2 and 3 residues per turn, but most lead to left-handed cellulosic structures. Further, this same majority has a distribution of positions that is very similar to that of the small molecule conformations and the conformations in the protein cellodextrin complexes. Whether the lactose–protein complexes are less accurately determined or there are special causes for the wider spread of the data is under study as this is written.

7 COMPUTERIZED ENERGY CALCULATIONS BASED ON MOLECULAR MODELS

The surveys above include 315 experimental determinations of the linkage geometry, so the question of the shape of the cellulose molecule might be considered to be answered. Almost all of the linkage geometries are in a small region of φ,ψ space that corresponds to cellulose molecules with two to three residues per helix

turn and *h* values of 5 Å or more. The latter value indicates that helices are extended to nearly the length of the glucose molecule (5.42–5.57 Å). What can computerized theoretical determinations add to this story? In fact, there are several areas of input. An issue is whether new shapes are likely to be discovered. Also, what is the magnitude, in terms of energy, of any distortions caused by different condensed phase environments? A particularly important question regards the shapes of cellulose in solution. One way to resolve these questions is to calculate the energy of cellulose molecules distorted into the different shapes. These distortions are not unlike stretching a spring. The stretched spring shape has higher potential energy, and is therefore less likely to occur without the application of an external force. For example, some time ago, it was proposed that folding conformations for cellulose chains have such high energies that they would be unlikely (Simon et al. 1988). Our calculated energies for folded chains are lower than the energies of Simon et al., suggesting that folds are plausible after all.

The conformations from protein–lactose complexes in Figure 15-12 illustrate two ways that theoretical energy calculations can be useful. The observed points are literally sprinkled all over the map, while the other β-1,4 linkages were in a much smaller region of φ,ψ space. Because of possible inaccuracies or even errors in the determinations of carbohydrate structures in protein complexes,[4] it would be useful to have a tool for checking the plausibility for the structures that are distant (in φ,ψ space) from the other structures. In deciding whether an experimentally determined structure is a reasonable result, it should have a relatively low energy, perhaps slightly higher than the more frequently found structures. Secondly, if a correctly determined conformation does truly have a high energy, there may be special features of these complexes, such as catalytic sites in hydrolytic enzymes, that are distorting the molecules.

Looking further at Figure 15-12, it would be useful to have some idea of other low-energy regions that are not populated by observed structures, and the barriers between a particular isolated structure and the majority conformation. Finally, computerized models are an important aide to thinking about why observed structures occur. For example, is the twofold conformation found in all of the pure cellulose polymorphs an intrinsically ideal form, or is it the result of intermolecular forces resulting from crystallization?

One approach to these questions is to construct an energy surface or map. Such maps show the relative value of calculated potential energy at all locations in φ,ψ space. The regions of lowest energy, e.g., within the 1 kcal/mol contours, should contain a large fraction, perhaps the majority, of structures that are already observed if the maps are to be considered predictive. To make such a map, the values of φ and ψ for the molecule in question are stepped over a grid

[4] We do not know why the lactose–protein complex structures have a much wider range of conformations. At this time we cannot say that they are less accurately determined than the complexes of proteins and cellodextrins.

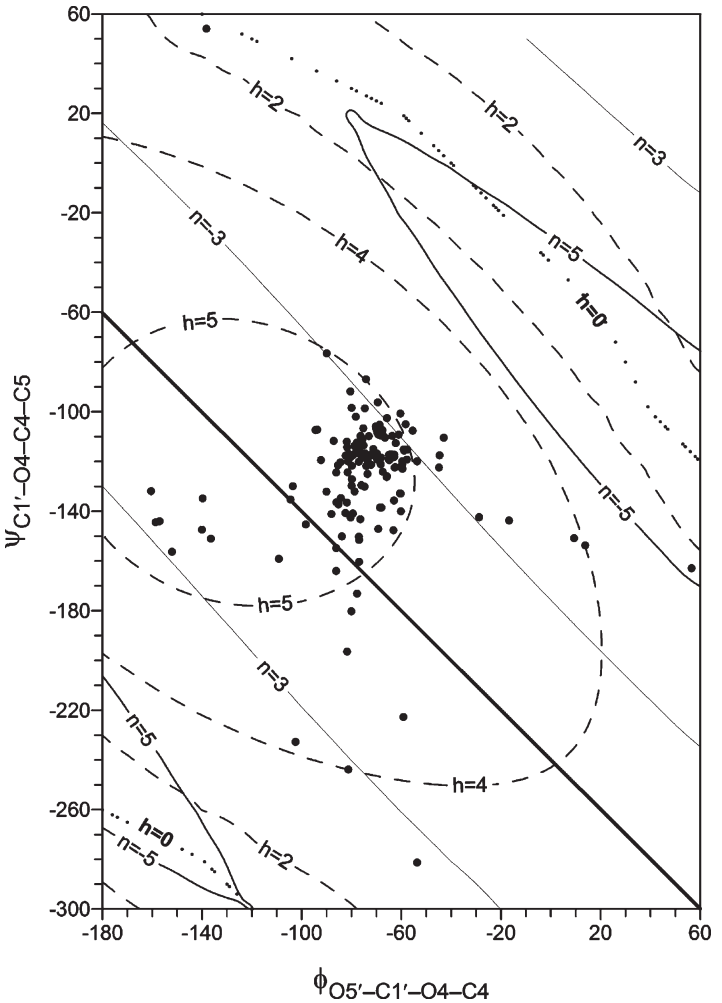

Figure 15-12. The locations in φ,ψ space of the conformations of the lactose linkages in protein complexes along with the approximate iso-*n* and iso-*h* contours from Figure 15-6

based on increments of some size, say 20°. In modern work, the geometry of the cellobiose molecule is optimized (except for the values of φ and ψ) by automatically adjusting the atomic positions until the energy is a minimum for each φ,ψ point. The energy depends substantially on the orientations of the exo-cyclic groups (−OH and $-CH_2OH$). To be confident that the lowest possible energy is achieved at each φ,ψ point, it is necessary to calculate the energy for numerous likely combinations of orientations of these groups. A thorough check of all possible orientational combinations would increase the required computer time

for such analyses to the point that it has been a barrier for even simple methods of calculating the energy.

For the maps to be useful, the energy calculations must accurately account for all important interactions. We recently discussed a number of approaches that we have exploited over the past few years (French and Johnson 2004b). The underlying foundation in our preferred methods is provided by electronic structure theory, also called quantum mechanics, or QM. QM energies are based on such fundamental properties as the speed of light and the mass of an electron, as well as on defined restrictions on the spatial distribution of the electrons (called the basis set). Because the methods are based on fundamental constants, they are often described by the Latin phrase, *ab initio*. At higher levels of QM calculations, there are fewer restrictions on the electron distribution and more complete descriptions of the electron–electron interactions are used. The problem with the really high levels of theory is that molecules as large as disaccharides demand more computational resources (time and memory) than are available.

One affordable way to use high level QM is to study only a characteristic fragment of the molecule in question. Herein, we have used a fragment that starts with cellobiose (itself a fragment of cellulose) but has all of the hydroxyl and hydroxymethyl groups replaced with just hydrogen atoms. The resulting structure consists of two tetrahydropyran rings, with a linkage oxygen atom. This is advantageous because it reduces the number of electrons in the model, substantially shortening the computation time. Because there are no $-OH$ and $-CH_2OH$ groups, only one structure must be considered at each φ,ψ point, an even bigger reduction in required time compared to cellobiose.

The energy surfaces for the analog have some important traits. The first, as shown in Figure 15-13, is that they are quite predictive for the experimental crystal structures, despite the inability of the analog to form any hydrogen bonds. Most of the structures fall within the 1 kcal/mol contour, roughly corresponding to the probability for a Boltzmann distribution at room temperature in which 82% of the structures will have an energy[5] less than 1 kcal/mol. Further, there is relatively little unoccupied space within the large area surrounded by the 1 kcal/mol contour. The fair amount of unoccupied space in this case, given the large number of experimentally observed conformations, is evidence of the importance of the missing hydrogen bonding and steric interactions in the simplified analog model (French and Johnson 2004b).

---

[5] Technically, the Boltzmann distribution applies to particles in an ideal gas, not to molecules in crystal structures. However, we have considered the group of related molecules in crystals to be subject to random distortions from crystal packing effects in each separate crystal structure. The energies of the particles in the ideal gas depend on the temperature through Boltzmann's constant or the ideal gas constant. If a Boltzmann-type distribution holds for distortions in crystal structures, the actual value of the constant, or the effective temperature, is unknown. This subject is discussed further in French et. al. (2000).

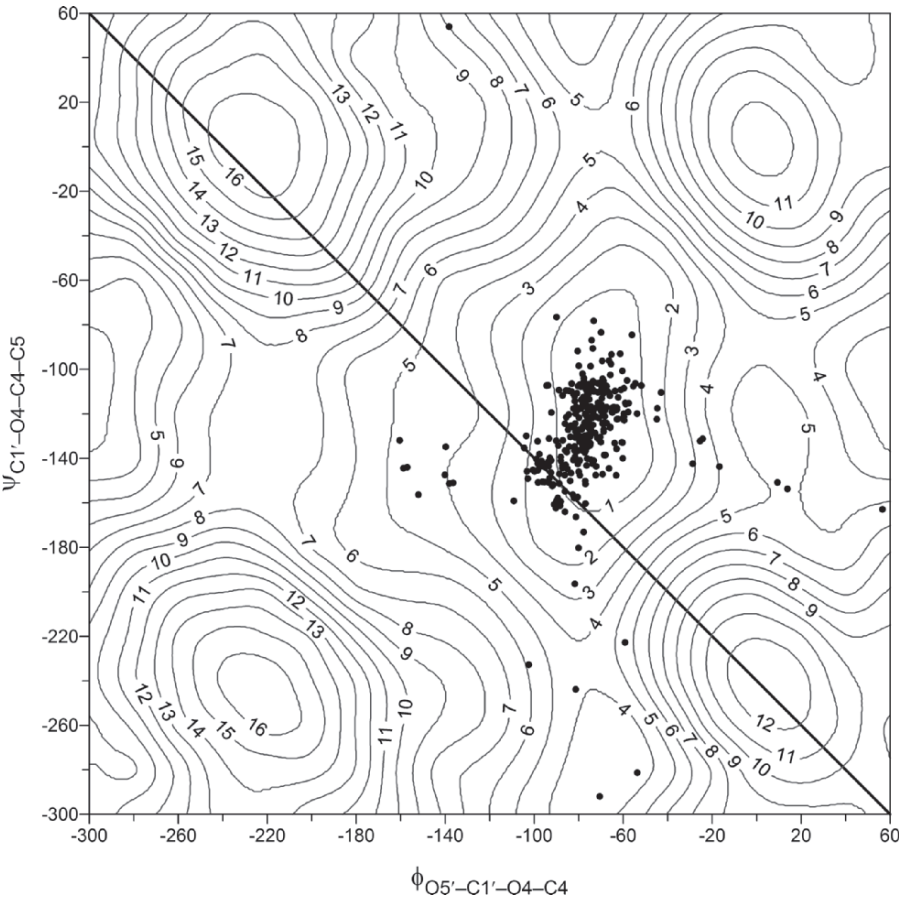

Figure 15-13. A QM energy surface covering φ,ψ space for the cellobiose analog, THP-O-THP (see text). Also shown are all of the observed linkage conformations in Figures 15-8, 15-9, 15-11, and 15-12, as well as the conformation of a heavily modified cellobiose (Ernst and Vasella 1996) at the bottom of the map. This surface was calculated with B3LYP/6-311++G** theory based on B3LYP/6-31G* geometries (see French and Johnson 2004b)

A second point of interest of these QM analog surfaces is that they are relatively invariant with different levels of QM theory. The map shown in Figure 15-13 is quite similar to the map in our earlier work (French et al. 2001a) that was based on a lower level of theory. Therefore, the size and shape of the lower energy contours are not expected to change much if even higher levels of theory were to be used. That is not the case for the full disaccharide, in which the hydrogen bonding and steric effects are rather dependent on the level of theory (French et al. 2002). Thirdly, these QM analog maps are being used to test empirical force fields that can carry out conformational analyses thousands of times faster.

Despite the apparent simplicity of these analogs, reproduction of these analog QM surfaces with general empirical force fields is difficult (Lii et al. 2005).

Finally, these QM analog energy surfaces can be used in a simple hybrid modeling method. Hybrid methods use a higher level of theory for the most critical parts of a molecule, and a lower level theory for the remainder of the molecule. In our nonintegral hybrid method (French et al. 2001b), QM theory is used for the tetrahydropyran-based analog, and the MM3 molecular mechanics program (Allinger et al. 1990) was used for the interactions of the hydroxyl and hydroxymethyl groups. A dielectric constant of 3.5 was used in the MM3 calculations to simulate a condensed phase. The main effect of increasing the dielectric constant is the reduction of the strength of hydrogen bonding (French and Johnson 2004b). The QM::MM3 hybrid energy surface with all the crystal structures except the protein-lactosyl moiety complex structures is shown in Figure 15-14. The same map with the protein–lactosyl complexes is plotted in Figure 15-15. Other hybrid maps for cellobiose have a somewhat larger 1 kcal/mol contour (French et al. 2005).

These particular hybrid surfaces have a much smaller 1 kcal/mol contour than Figure 15-13, principally because of the presence of the C6 group in the model. In contrast to Figure 15-13, there is no low-energy, but lightly populated, space at the top of the 1 kcal/mol contour. Despite the smaller area within the 1 kcal/mol contour of Figure 15-14, many of the structures still fit within the 1 kcal/mol contour. The major group outside of the 1 kcal/mol contour in Figure 15-14 is located along the twofold screw-axis line. That group is composed of cellulose and cellotetraose (see Figure 15-8) as well as a few of the small molecule structures, most of which do not have O1 hydroxyl groups. This suggests that crystal packing is responsible for the twofold conformation found for a number of the cellulosic structures, but that the energy of deformation for twofold screw symmetry is relatively low. The experimental φ,ψ points in Figure 15-15 are more randomly dispersed and some correspond to such high energies as to be interesting from the view point of either being substantially deformed or erroneously determined.

The 1 kcal/mol contours in Figures 15-14 and 15-15 are to the right of the twofold screw-axis line, as are most crystal structures. Thus, based on both experiment and theory, it is reasonable to expect that most cellulose structures that are deviate from twofold symmetry will be left-handed helices.

8 SUMMARY

The shapes of pure, crystalline cellulose in several polymorphs are now known in substantial detail, thanks to the experimental efforts of Chanzy, Langan, Nishiyama, Sugiyama, and Wada, who of course, benefitted from the work of many predecessors over the years. The details of the hydrogen bonding are in their original publications. Despite the many possible shapes for the cellulose molecule, only small variations occur in known crystals that contain only

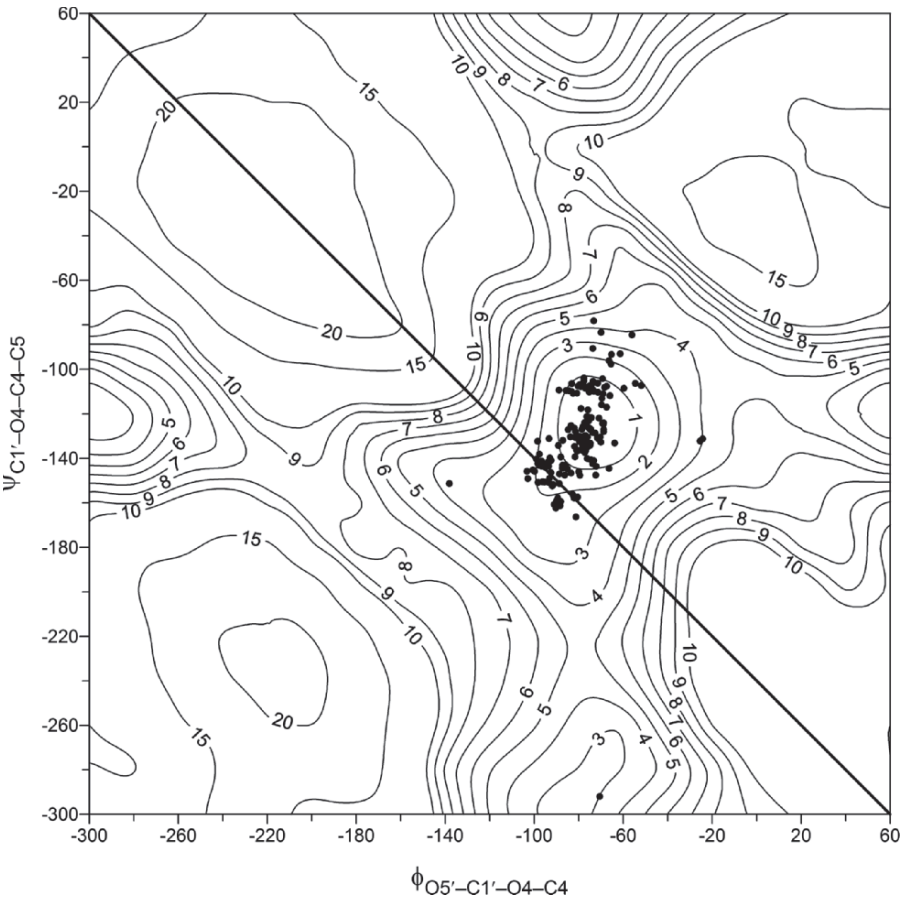

Figure 15-14. A QM::MM3 hybrid energy surface for cellobiose (see text). The dielectric constant was set to 3.5, reducing the strength of the hydrogen bond in the water dimer to about 2.35 kcal/mol each. Plotted in the φ,ψ space are the conformations of all of the above crystal structures except the lactose–protein complexes

cellulose. This conclusion includes the cellodextrins whose crystal structures are also known, i.e., methyl cellotrioside and cellotetraose. All of these structures have very dense packing that is permitted by the ability of the cellulose chain to take a twofold structure, even when the symmetry is not exact.

This extremely narrow distribution of structures is expanded considerably when the cellulose chain is considered to be a collection of β-1,4-linked glucose residues that have one of the geometries found in our survey of related small molecule crystals, such as cellobiose or cellobiose acetate. These extrapolated structures compare well with the experimentally determined cellulose derivatives and complexes if the latter are taken to be left-handed. Previously, we calculated

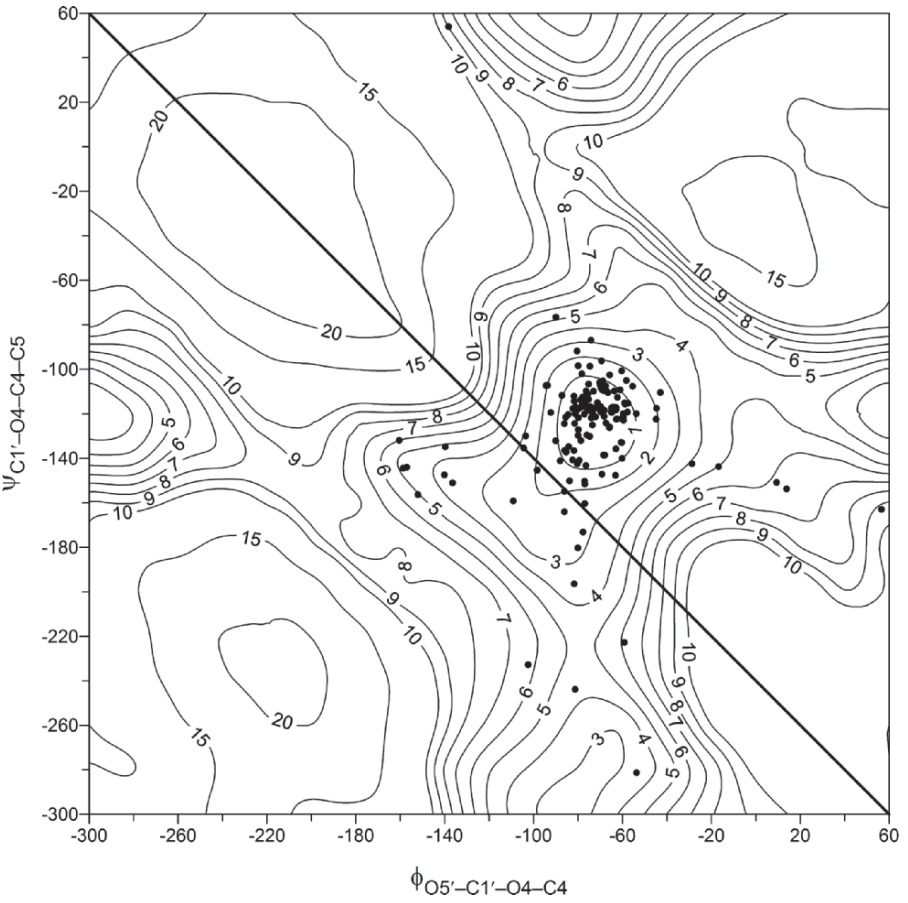

Figure 15-15. The same energy surface as in 15–13, but with the lactose–protein complexes plotted instead

the exact helical parameters for the extrapolated structures, and in the present work we show a general, approximate conversion from the φ and ψ values. In some cases, there is twofold screw symmetry in the polymer chains, and pseudo twofold screw symmetry in the disaccharide, but in other cases $n = -3$ or something intermediate, such as $n = -2.67$ or -2.5. The only known exception to the population of extended molecules comes from a model based on extrapolation of a very heavily substituted cellobiose molecule. It has a conformation that could account for chain folding, a phenomenon documented in several experiments. That structure falls in a low-energy minimum at the bottom of our maps.

The data on likely linkage conformation in cellulose were expanded considerably by including the less accurately determined linkage geometries from

carbohydrate molecules that are complexed with proteins. It might have been expected that the cellobiose linkage geometry would be different when it exists in interactions with amino acid residues and water molecules. A major difference was that there are relatively few conformations in protein complexes near the twofold screw-axis line, an indication that twofold structures might be slightly distorted. However, other questions arise with these structures, including the much larger range of the φ and ψ values, especially for the complexes of lactose moieties.

These issues are brought into focus by studies of the theoretically calculated conformational energy. Based on our energy calculations, it appears that some lactose linkages do have rather high energies, compared to the many geometries that fall inside the 1 kcal/mol contour. Other insights from the energy surfaces include the feasibility of chain folding. Minima near the centers of the map edges have relatively low energy, and the minimum at the top or bottom of our map is populated by one experimental example from the small molecule single crystals. A somewhat analogous example of folding occurs in cyclic molecules made from amylose (Gessler et al. 1999). In crystals of a cycloamylose with 26 glucose residues, 24 of the linkages have conformations in the central, lowest minimum on an energy map for its disaccharide fragment, maltose. The remaining two linkages are in a secondary minimum at the bottom of the energy surface. Those two linkages permit folds.

If an isolated cellulose molecule is under conditions where each linkage can take the lowest energy conformation, then the molecule might appear as in Figure 15-16. It is made by extrapolating the linkage geometry found in crystalline β-cellobiose (Chu and Jeffrey 1968), which happens to be at the overall minimum on our hybrid energy surface. It also is in the center of the range of conformations found in the various crystal structures. This model has about 2.4 glucose residues per turn, O6 in the ***gt*** position, and substantial hydrogen bonding from the O3 hydroxyl hydrogen atom to O5′ and O6′ on the adjacent residue. This particular hydrogen bonding arrangement was very common in our study of disaccharides (French and Johnson 2004a). Similarly,

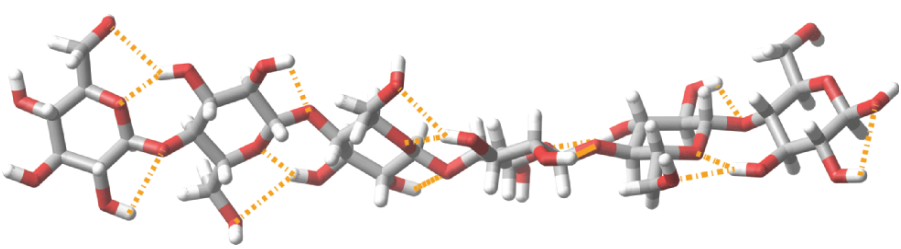

Figure 15-16. A cellulose segment with the lowest energy, as indicated by the combined information from the crystal structure surveys and the point of minimum energy on the QM::MM3 hybrid energy surface (*See Color Plate of this figure beginning on page 355*)

from the agreement among the small molecules, the protein complexes and the energy surface, we can predict that the linkage geometries in either the solid but noncrystalline state or in various kinds of solutions would have a statistical distribution of the conformations. These conformations would individually extrapolate to left-handed helices with two to three residues per turn, with the occasional right-handed or folding example. These results are consistent with the results of Umemura et al. (2004) who found average n values of −2.61 to −2.65 for cellotetra- to cellohexaose in aqueous solution by computerized molecular dynamics simulations.

It is often said that cellulose has a cellobiose repeating unit. In the minds of some workers, that statement conveys the shape that results from twofold screw-axis symmetry. In this work, we propose that the ideal shape for cellulose does not have a twofold structure and that a range of shapes should occur. To the extent that the cellulose molecule can take various shapes, it is unjustifiably limiting to define cellulose in terms of a particular shape.

Acknowledgments

Brenda Lauterbach and Professor Peter Reilly, Department of Chemical Engineering, Iowa State University, assisted with the analysis of the protein–carbohydrate complexes and Ms Lauterbach read the manuscript. Dr. Alexander Lambert, Southern Regional Research Center, and Mary An Godshall, Sugar Processing Research Institute, also commented on the paper.

REFERENCES

Allen F.H. 2002. The Cambridge structural database: a quarter of a million crystal structures and rising. Acta Crystallogr Sect B 58:380–388.

Allinger N.L., Rahman M., and Lii J.-H. 1990. A molecular mechanics force field (MM3) for alcohols and ethers. J Amer Chem Soc 112:8293–8307.

Atalla R.H. and VanderHart D.L. 1984. Native cellulose: a composite of two distinct crystalline forms. Science 223:283–285.

Berman H.M., Battistuz T., Bhat T.N., Bluhm W.F., Bourne P.E., Burkhardt K., Feng Z., Gilliland G.L., Iype L., Jain S., Fagan P., Marvin J., Padilla D., Ravichandran V., Schneider B., Thanki N., Weissig H., Westbrook J.D., and Zardecki, C. 2002. The protein data bank. Acta Crystallogr Sect D 58:899–907.

Chandrasekaran R. and Radha A. 1997. Molecular modeling of xanthan:galactomannan interactions. Carbohydr Polym 32:201–208.

Chanzy H. and Henrissat B. 1985. Undirectional degradation of valonia cellulose microcrystals subjected to cellulase action. FEBS Lett 184:285–288.

Chedin J. and Marsaudon A. 1954. Progress in the understanding of liquid reaction mediums, and interpretation of their reactions with cellulosic fibers: mercerization-nitration. Chim Ind (Paris) 71:55–68.

Chu S.S.C. and Jeffrey G.A. 1968. The refinement of the crystal structures of β-D-glucose and cellobiose. Acta Crystallogr Sect C (Cryst. Struct. Commun.) 42:177–179.

Dinand E., Vignon M., Chanzy H., and Heux L. 2002. Mercerization of primary wall cellulose and its implication for the conversion of cellulose I6cellulose II. Cellulose 9:7–18.

Ernst A. and Vasella A. 1996. Oligosaccharide analogs of polysaccharides. Part 8. Orthogonally protected cellobiose-derived dialkynes. A convenient method for the regioselective bromo- and

protodegermylation of trimethylgermyl- and trimethylsilyl-protected dialkynes. Helv Chim Acta 79:1279–1294.
Ford Z.M., Stevens E.D., Johnson G.P., and French A.D. 2005. Determining the crystal structure of cellulose III_I by modeling. Carbohyr Res, 2005. Carbohydr Res 340:827–833.
French A.D. 1978. The crystal structure of native ramie cellulose. Carbohydr Res 61:67–80.
French A.D., Kelterer A.-M., Johnson G.P., Dowd M.K., and Cramer C.J. 2000. Constructing and evaluating energy surfaces of crystalline disaccharides. J Mol Graph Model 18:95–107.
French A.D., Kelterer A.-M., Johnson G.P., Dowd M.K., and Cramer C.J. 2001a. HF/6-31G* energy surfaces for disaccharide analogs. J Comput Chem 22:65–78.
French A.D., Johnson G.P., Kelterer A.-M., Dowd M.K., and Cramer C.J. 2001b. QM/MM distortion energies in di- and oligosaccharides complexed with proteins. Int J Quant Chem 84:416–425.
French A.D., Johnson G.P., Kelterer A.-M., Dowd M.K., and Cramer C.J. 2002. Quantum mechanics studies of the intrinsic conformation of trehalose. J Phys Chem A 106:4988–4997.
French A.D. and Johnson G.P. 2004a. What crystals of small analogs are trying to tell us about cellulose structure. Cellulose 11:5–22.
French A.D. and Johnson G.P. 2004b. Advanced conformational energy surfaces for cellobiose. Cellulose 11:449–462.
French A.D., Johnson G.P., Kelterer A.-M., and Csonka G.I. 2005. Fluorinated cellobiose and maltose as stand-ins for energy surface calculations. Tetrahedron Asymmetry, 2005. Tetrahedron Asymmetry 16:577–586.
Gessler K., Krauss N., Steiner T., Betzel C., Sarko A., and Saenger W. 1995. β-D-Cellotetraose hemihydrate as a structural model for cellulose II. An x-ray diffraction study. J Am Chem Soc 117:11397–11406.
Gessler K., Usón I., Takaha T., Krauss N., Smith S.M., Okada S., Sheldrick G.M., and Saenger W. 1999. V-Amylose at atomic resolution: x-ray structure of a cycloamylose with 26 glucose residues (cyclomaltohexaicosaose). Proc Natl Acad Sci USA 96:4246–4251.
Hess K. and Trogus C. 1931. Zur Kenntis der Faserperiode bei Cellulosederivaten. Röntgenographische Untersuchungen an Cellulosederivaten X. Z Physikal Chem Bodenstein-Festband 11:385–391.
Hieta K., Kuga S., and Usuda M. 1984. Electron staining of reducing ends evidences a parallel-chain structure in Valonia cellulose. Biopolymers 23:1807–1810.
Hirai A., Tsuji M., and Horii F. 2002. TEM study of band-like cellulose assemblies produced by Acetobacter xylinum at 4°C. Cellulose 9:105–113.
Katz J.R. and Hess K. 1927. The swelling and mercerizing of natural cellulose fibers in nitric acid "philanized" cotton. I. Röntgen spectrographic research. Z Phys Chem-Leipzig 122:126–136.
Kolpak F. and Blackwell J. 1976. Determination of the structure of cellulose II. Macromolecules 9:273–278.
Kolpak F., Weih M., and Blackwell J. 1978. Mercerization of cellulose. 1. Determination of the structure of mercerized cotton. Polymer 19:123–131.
Koyama M., Helbert W., Imai T., Sugiyama J., and Henrissat B. 1997. Parallel-up structure evidences the molecular directionality during biosynthesis of bacterial cellulose. Proc Natl Acad Sci USA 94:9091–9095.
Kroon-Batenburg L.M.K., Bouma B., and Kroon J. 1996. Stability of cellulose structures studied by MD simulations. Could mercerized cellulose II be parallel? Macromolecules 29:5695–5699.
Kuga S., Takagi S., and Brown, Jr. R.M. 1993. Native folded-chain cellulose II. Polymer 34:3293–3297.
Langan P., Nishiyama Y., and Chanzy H. 2001. X-ray structure of mercerized cellulose II at 1 Å resolution. Biomacromolecules 2:410–416.
Leung F., Chanzy H.D., Perez S., Marchessault R.H. 1976. Crystal structure of β-D-acetyl cellobiose. Canad J Chem 54:1365–1371.
Lii J.-H., Chen K.-H., Johnson G.P., French A.D., and Allinger N.L. 2005. The external-anomeric torsional effect. Carbohydr Res, 2005. Carbohydr Res 340:832–862.
Manley St., R.J. 1960. Crystallization of cellulose triacetate from solution. J Poly Sci 47:509–512.
Manley St., R.J. 1963. Growth and morphology of single crystals of cellulose triacetate. J Poly Sci A 1:1875–1892.

Meader D., Atkins E.D.T., and Happey F. 1978. Cellulose trinitrate. Molecular conformation and packing considerations. Polymer 19:1371–1374.

Millane R.P. and Wang B. 1990. A cellulose-like conformation accessible to the xanthan backbone and implications for xanthan synergism. Carbohydr Poly 13:57–68.

Nishiyama Y., Kuga S., and Okano T. 2000. Mechanism of mercerization revealed by x-ray diffraction. J Wood Sci 46:452–457.

Nishiyama Y., Langan P., and Chanzy H. 2002. Crystal structure and hydrogen-bonding system in cellulose Iβ from synchrotron x-ray and neutron fiber diffraction. J Am Chem Soc 124:9074–9082.

Nishiyama Y., Sugiyama J., Chanzy H., and Langan P. 2003a. Crystal structure and hydrogen bonding system in cellulose Iα from synchrotron x-ray and neutron fiber diffraction. J Amer Chem Soc 125:14300–14306.

Nishiyama Y., Kim U.-J., Kim D.-Y., Katsumata K.S., May R.P., and Langan P. 2003b. Periodic disorder along ramie cellulose microfibrils. Biomacromolecules 4:1013–1017.

Peralta-Inga Z., Johnson G.P., Dowd M.K., Rendleman J.A., Stevens E.D., and French A.D. 2002. The crystal structure of the α-cellobioseθ2 NaIθ2 H_2O complex in the context of related structures and conformational analysis. Carbohydr Res 337:851–861.

Raymond S., Henrissat B., Qui D.T., Kvick A., and Chanzy H. 1995. The crystal structure of methyl β-cellotrioside monohydrate 0.25 ethanolate and its relationship to cellulose II. Carbohydr Res 277:209–229.

Rees D.A. and Skerrett R.J. 1968. Conformational analysis of cellobiose, cellulose and xylan. Carbohydr Res 7:334–348.

Sakon J., Adney W.S., Himmel M.E., Thomas S.R. and Karplus P.A. 1996. Crystal structure of thermostable family 5 endocellulase E1 from *Acidothermus cellulolyticus* in complex with cellotetraose. Biochemistry 35:10648–10660.

Shibazaki H., Kuga S., and Okano T. 1997. Mercerization and acid hydrolysis of bacterial cellulose. Cellulose 4:75–87.

Shimanouchi T. and Mizushima S.-I. 1955. On the helical configuration of a polymer chain. J Chem Phys 33:707–711.

Simon I., Scheraga H.A., and Manley St., R.J. 1988. Structure of cellulose. 1. Low-energy conformations of single chains. Macromolecules 21:983–990.

Sternberg U., Koch F.-T., Prieß W., and Witter R. 2003. Crystal structure refinements of cellulose polymorphs using solid state 13C chemical shifts. Cellulose 10:189–199.

Stipanovic A.J. and Sarko A. 1976. Packing analysis of carbohydrates and polysaccharides. 6. Molecular and crystal structure of regenerated cellulose II. Macromolecules 9:851–857.

Sugiyama J., Vuong R., and Chanzy H. 1991. Electron diffraction study on the two crystalline phases occurring in native cellulose from an algal cell wall. Macromolecules 24:4168–4175.

Umemura M., Yuguchi Y., and Hirotsu T. 2004. J Phys Chem A 108:7063–7070.

Wada M., Heux L., Isogai A., Nishiyama Y., Chanzy H., and Sugiyama J. 2001. Improved structural data of cellulose III_I prepared in supercritical ammonia. Macromolecules 34:1237–1243.

Wada M., Heux L., and Sugiyama J. 2004a. Polymorphism of cellulose I family: reinvestigation of cellulose IV_I. Biomacromolecules 5:1385–1391.

Wada M., Nishiyama Y., Sugiyama J., Chanzy H., and Langan P. 2004b. Cellulose III_I crystal structure and hydrogen bonding by synchrotron x-ray and neutron fiber diffraction. Macromolecules 37:8548–8555.

Whitaker P.M., Nieduszynski I.A., and Atkins E.D.T. 1974. Structural aspects of sodacellulose II. Polymer 15:125–127.

Zugenmaier P. 1983. Structural investigations on cellulose derivatives. J Appl Polym Sci: Appl Polym Symp 37:223–238.

Zugenmaier P. 1985. In Burchard W. (ed.) Polysaccharide. Springer, Berlin, p. 271.

Zugenmaier P. 1986. Structural investigations on some cellulose derivatives in the crystalline and liquid crystalline state. In Young R.A. and Rowell R.M. (eds.), Cellulose: Structure, Modification and Hydrolysis. Wiley, New York, pp. 221–245.

CHAPTER 16

NEMATIC ORDERED CELLULOSE: ITS STRUCTURE AND PROPERTIES

TETSUO KONDO*

Bio-Architecture Center (KBAC) and Graduate School of Bioresource and Bioenvironmental Sciences, Kyushu University, 6-10-1, Hakozaki, Higashi-ku, Fukuoka 812-8581, Japan

Abstract

The authors developed a unique form of β-glucan association, "nematic ordered cellulose" (NOC) that is molecularly ordered, yet noncrystalline. NOC has unique characteristics; in particular, its surface properties provide with a function of tracks or scaffolds for regulated movements and fiber production of *Acetobacter xylinum (=Gluconacetobacter xylinus)*, which produces cellulose ribbon-like nanofibers with 40–60 nm in width and moves due to the inverse force of the secretion of the fibers (Kondo et al. 2002). This review attempts to reveal the exclusive superstructure-property relationship in order to extend the usage of this nematic-ordered cellulose film as a functional template. In addition, this describes the other carbohydrate polymers with a variety of hierarchical nematic-ordered states at various scales, the so-called nano/micro hierarchical structures, which would allow development of new functional-ordered scaffolds.

Keywords

cellulose, hierarchical structure, nematic order, orientation, template.

1 INTRODUCTION

Interfacial surface structure and interaction of materials at the nanoscale have attracted much attention in the field of nanotechnology (Drexler 1992). Microbiological systems have been investigated as a microscale process (Zhao et al. 1998); however, recent studies showing the unique interaction of biological systems with entirely synthetic molecular assemblies have prompted

* For correspondence: Tel: +81-(0)92-642-2997; Fax: +81-(0)92-642-2997; e-mail: tekondo@agr.kyushu-u.ac.jp

R.M. Brown, Jr. and I.M. Saxena (eds.), Cellulose: Molecular and Structural Biology, 285–305.

consideration of a new generation of approaches for controlled nanoassembly (Whaley et al. 2000).

In biological systems, skeletal materials such as cell walls, bones, and shells are made primarily of a nanoscale building block of polysaccharides, proteins, and inorganic salts. The assembly of these building blocks facilitates the production of a hierarchical framework structure. Materials with hierarchical structures produced by organisms are mainly based on how the comprising components are biosynthesized and subsequently how they would be self-assembled. Once the structures are established, it is difficult to modify them into another form with a different function for an appropriate purpose.

In this sense, it is of importance in cellulose science including cell wall formation to understand various states on how molecules can be associated, and thereby how the higher hierarchical structure can be organized from molecular scales to micrometer scales through nanometer scales. In particular, interfacial surface structures and interactions are greatly important in fabrication of a hierarchical structure for 3D-materials built up from the molecules.

Cellulose comprises the major polymer of plant cell walls and has had a long history as a natural polymer material. The biomacromolecule, which is a β-1,4-glucan homopolymer, normally is classified according to how the β-glucan chains associate. We expand the concept how various states of molecular association can be categorized in cellulose. A major consideration is that the predominant crystalline state of cellulose is included as a component in the ordered state. This means that the ordered state also contains noncrystalline ordered states. The category "ordered" is in contrast to the "nonordered" state which to date has been considered as "amorphous cellulose" for lack of a useful way to characterize the product. It should be noted that in our concept, the amorphous state being categorized as the "nonordered" state, should be distinguished from the "noncrystalline" state of cellulose. Thus, in this classification, it becomes crucial whether the state is "ordered" or "nonordered." Namely, it may be advantageous to first prioritize whether or not the cellulose is in the ordered or nonordered domain, rather than determine if it is crystalline or noncrystalline. Figure 16-1 demonstrates the schematic representation of our concept. In this idea, a noncrystalline state in the ordered domain should have intermediates from amorphous to crystalline states, and these are important in determining further states of aggregation, which may lead to the crystalline state. Of course, the crystalline states are important, but so far, too much attention has been paid only for crystalline structures. A key concept here is that we should consider crystalline states as a subdivision of the broader concept of ordered domains.

Based on the above concept, we developed a new supramolecular associated form of glucan chains, nematic ordered cellulose (NOC), which is highly ordered, but not crystalline (Kondo et al. 2001). NOC has unique characteristics; in particular, its surface properties provide with a function of tracks or scaffolds for regulated movements due to the inverse force in production of nanocellulose fibers of *Acetobacter xylinum* (Kondo et al. 2002). When the

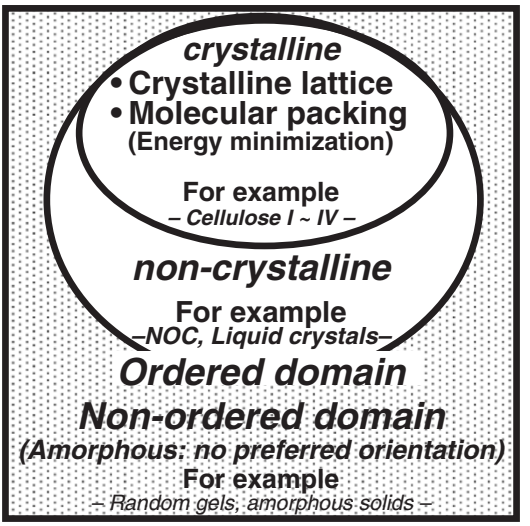

Figure 16-1. Our concept of glucan chain association for cellulose

interaction between the produced cellulose fibers called "bacteria cellulose ribbons" and specific sites of the oriented molecules on the unique surface of NOC is very strong, such ordered cellulose can be used as a template for the construction of nanocomposites, and the growth direction of the secreted cellulose is controlled by the epitaxial deposition of the microfibrils. Our proposed method is predicted to provide a novel type of nanotechnology using biological systems with molecular nanotemplates to design 3D-regulated structures. In order to extend the usage of this NOC film as a functional template, the present article will review the unique structure in relation to the exclusive surface properties of NOC, starting from how β-glucan association is initiated and established by uniaxial stretching of water swollen cellulose gel films (Kondo et al. 2004).

2 STRUCTURE OF NEMATIC ORDERED CELLULOSE

2.1 What is nematic ordered cellulose; NOC?

Prior to NOC, it will be required to know the characteristic feature of a cellulose molecule (Figure 16-2): cellulose owns an extended structure with a 2_1 screw axis composed by the β-1,4-glucosidic linkages between anhydroglucose units. Thus, it would be natural to accept the dimer called "cellobiose" as a repeating unit. The present three kinds of hydroxyl groups within an anhydroglucose unit exhibit different polarities, which contribute to formation of various kinds of inter- and intramolecular hydrogen bonds among secondary OH at the C-2,

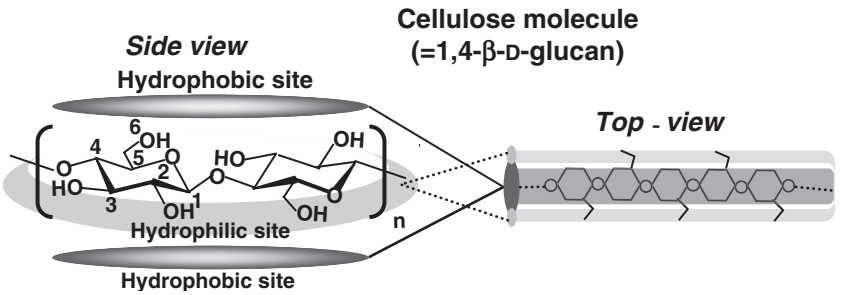

Figure 16-2. Site specific, amphiphilic nature in cellulose chemical structure

secondary OH at the C-3 and primary OH at the C-6 position. In addition, all the hydroxyl groups are bonded to a glucopyranose ring equatorially. This causes appearance of hydrophilic site parallel to the ring plane. On the contrary, the CH groups are bonded to a glucopyranose ring axially, causing hydrophobic site perpendicular to the ring as shown in Figure 16-2. These effects lead to formation of hydrogen bonds in parallel direction to a glucopyranose ring, and to Van der Waars interaction perpendicular to the ring.

Another important feature for the hydroxyl groups is the type of hydroxymethyl conformation at the C-6 position, because the conformation of C(5)–C(6) and the resulting interactions including inter- and intramolecular hydrogen bonds in the present cellulose structure may differ from that in crystallites and also it is assumed to make up the extent of crystallization, as well as the final morphology of cellulose. In the noncrystalline regions, the rotational position of hydroxymethyl groups at the C-6 position may be considered as indeterminate or totally nonoriented, which are not identical with those in the crystallites. Therefore, it was important to confirm the type of O(6) rotational position with respect to the O(5) and C(4) in a β-glucan chain, by employing CP/MAS ^{13}C NMR (Horii et al. 1983). The type of hydroxymethyl conformations is *gauche-trans* (***gt***), *trans-gauche* (***tg***), or *gauche- gauche* (***gg***) at the C-6 positions in carbohydrates. As for the noncrystalline states, they are considered as the *gg* conformation (see Figure 16-8).

Now, when the dissolved cellulose molecules are self-aggregated in water to form a gel presumably by a minimum amount of restricted engagements among hydrophobic sites of the ring above described, then it is stretched to reach NOC. Figure 16-3 illustrates structural characteristics of NOC in relation to the situation of OH groups explained in the following: NOC is prepared by uniaxial stretching of water-swollen cellulose from the *N*, *N*-dimethylacetamide (DMAc)/LiCl solution (the details are described in Section 5), and thereby, the cellulose molecular chains tend to be oriented toward the stretching axis (Togawa and Kondo 1999). Further, the hydroxymethyl groups at the C-6 position that are equatorial-bonded to the anhydroglucose unit are vertically stuck up against

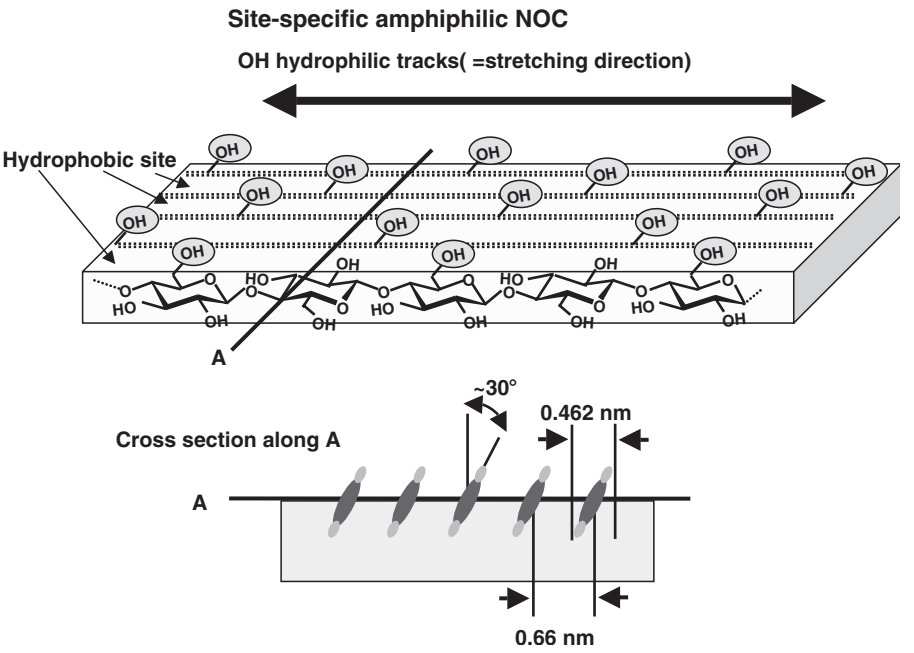

Figure 16-3. Schematic NOC surface structure and the cross section along the perpendicular A (=lateral direction) to the stretching direction

the surface, which indicates that the neighboring anhydroglucose ring planes are facing with each other. Simultaneously the stuck up OH groups in the individual molecular chains are also aligned like tracks along the stretching axis. On the contrary, the lateral order of the OH groups among the neighboring chains is not well coordinated because of the slipped molecular chain situation with each other. The uniaxial stretching also caused this situation. Therefore, the hydrophilic and polarized OH groups are totally to be oriented as molecular tracks only in the stretching direction across the entire NOC surface. Between the hydrophilic molecular tracks, the hydrophobic site due to the anhydroglucose plane was also appeared, resulting in both hydrophilic and hydrophobic tracks next to each other across the NOC surface. These amphiphilic molecular tracks enhance the unique surface properties of NOC as described later.

The NOC structure was basically indicated by the high-resolution transmission electron microscope (TEM) image. The NOC template with molecular ordering was shown in Figure 16-4 (Kondo et al. 2001). The high-resolution image obtained from the TEM shows a preferentially oriented direction on the surface. These observations confirmed the mean width of a single glucan chain corresponding to its known dimensions as viewed from its narrow axis of the anhydroglucose ring. The average chain width was 0.462 nm (standard

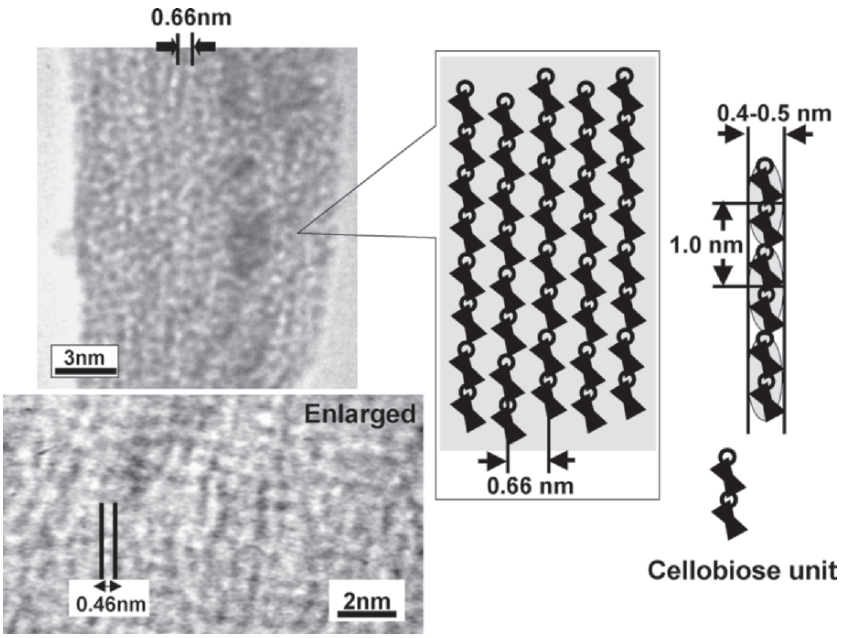

Figure 16-4. High-resolution TEM of NOC, the molecular ordering template (*left*). The film was negatively stained by uranyl acetate and spans a region of the copper support grid. Note the individual glucan chains that are separated by an average distance of 0.66 nm (*arrows*). In the enlarged image, the arrangement of glucan chains are clearly resolved with 0.46 nm in width. (*right*) Schematic diagram of NOC showing the arrangement of glucan chains and the linear spacing of the cellobiose units (*circled*). The polymer chains lie on their narrow axes

deviation = ±0.0517 nm). Thus, the true width seems to be ~0.4–0.5 nm when taking into account the negative stain. The average distance between two parallel chains was 0.660 nm (standard deviation = ±0.068 nm), which is wider than values for any crystalline cellulose. The average width of 0.462 nm from the top view is wider than that of 0.45 nm of the narrow axis in the anhydroglucose ring predicted from the space-filling model. This suggests tilting of the glucose planes of a cellulose molecule with a angle of 29.3° to the vertical axis against the surface of NOC as shown in the bottom image of Figure 16-3. It should be noted that the contact angle of a water drop of water on the NOC surface is ~72°, indicating fairly hydrophobic (Togawa and Kondo, unpublished). Prior to stretching for NOC preparation, the water-swollen cellulose exhibits ~50° as the contact angle. Thus, the surface condition of it is totally altered by stretching to provide tilting of the glucose planes for exposure of the specific hydrophobic site as shown in Figure 16-3.

The atomic force microscope (AFM) image analyses of the NOC surface without the negative stain demonstrate that well-aligned molecular aggregates

with a width of 4–6 nm and a height of ~6 nm in average are oriented uniaxially (Figure 16-5). The AFM resolution of the image is not at the molecular level. Without negative staining with uranyl acetate, it may be difficult to obtain a high resolution AFM image of the NOC surface, particularly the glucan chain images shown in the TEM micrograph of Figure 16-4, because of the surface flexibility when the AFM tip approaches close enough to observe the NOC surface.

The orientation parameter calculated from wide-angle x-ray diffraction (WAXD) photographs (Figure 16-6) became 0.88, which indicated a high degree of orientation. This means that the deviation (γ) angle of molecular orientation to the stretching direction was $0.0° < \gamma < 10.5°$. However under these conditions, the crystallinity did not significantly follow the increase of the orientation by the stretching (Togawa and Kondo 1999). Simultaneous orientation and crystallization did not occur as often seen with crystalline polymers (Ward 1997). The crystallinity was ~14.8 and 16.8% before and after stretching, respectively. Infrared spectra of deuterated samples also supported a low crystallinity of the film based on the ratio of the remaining hydroxyl groups in the drawn films that corresponds to the crystallinity index.

Figure 16-6 shows wide-angle x-ray diffraction (WAXD) intensity curves in both equatorial and meridional directions of NOC together with cellulose II fibers. In the equatorial diffraction of NOC, typical crystalline diffraction patterns representing cellulose II (Figure 16-6a) were not observed. The diffuse intensity equatorial profile for NOC (Figure 16-6b) indicated that it contains considerably more "amorphous" regions. The meridional scan of WAXD was employed to analyze the order along the stretching direction for NOC. Meridional intensities of cellulose are affected by the disorder of the neighboring chains that is symmetrical for the chain axis. In general, cellulose polymorphs provide almost the same meridional patterns; namely two strong distinct reflections of the (002) and (004) planes ($2\theta = 17.2°$, $d = 0.516$ nm; $2\theta = 34.7°$, $d = 0.259$ nm, respectively; see the right of Figure 16-6a).

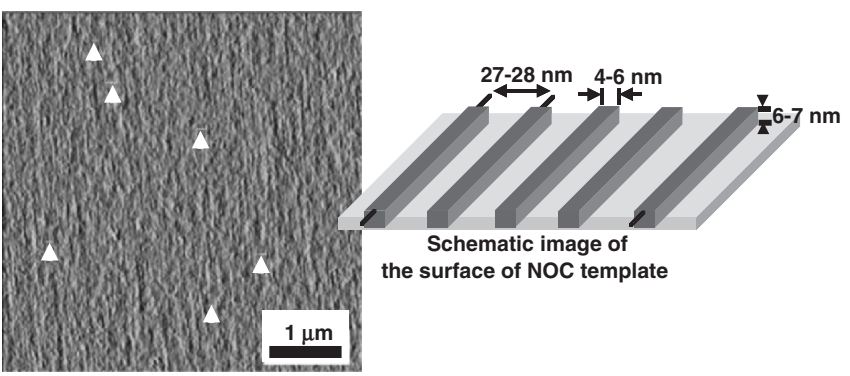

Figure 16-5. Atomic force micrographs showing the surface of the nematic ordered cellulose (NOC) template with a schematic representation

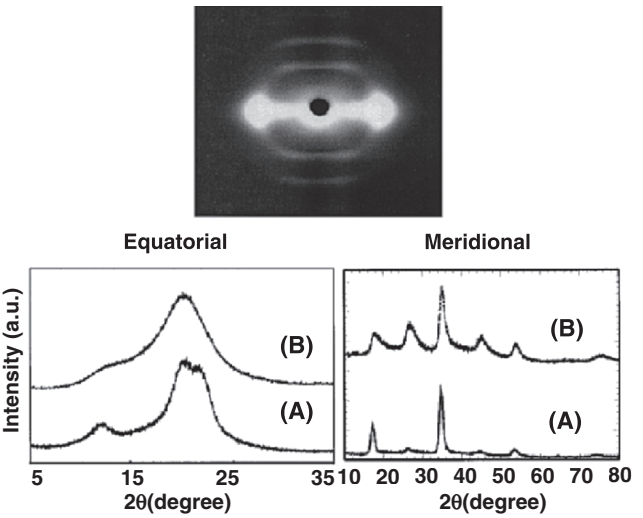

Figure 16-6. WAXD photograph of NOC together with equatorial (*left*) and meridional (*right*) intensity curves of the WAXD for cellulose II fibers (**a**) and NOC (**b**). The term, "a.u." indicates arbitrary unit

The present results demonstrate that NOC, which is highly ordered but noncrystalline, gives a totally different profile for the meridional scan as shown in Figure 16-6b. More reflections were found in the meridional direction when compared with cellulose II crystals. The characteristics are considerable line broadening of the meridional reflections in the profile of NOC. This indicates that the structure of the NOC film along the chain direction may have a certain disorder that causes the ordered, but noncrystalline regions. It may be considered that the situation is not a perfect disorder in the molecular chain direction, but some registrations may exist. Considering the crystallinity of the film sample (16.8%), the meridional direction profile should contain the contribution due to cellulose II crystals. When the contribution of the crystallite is subtracted from the meridional direction profile in Figure 16-6b, each reflection in the same figure would tend to have the similar shape and intensity as shown in Figure 16-7. Thus, we should consider the states of the structure for NOC to be ordered states that are neither crystalline nor amorphous.

Parallel to the x-ray diffraction, NOC also exhibited a diffuse pattern in the TEM electron diffraction mode, similar to that from x-ray diffraction of Figure 16-6 (not shown here).

As already described, the type of hydroxymethyl conformation at the C-6 position is assumed to provide the extent of crystallization, as well as the final morphology of cellulose (Horii et al. 1983; Kondo and Sawatari 1996; Togawa and Kondo 1999). The conformation of C(5)–C(6) and the resulting interactions including hydrogen bonds in NOC differ from that in crystallites.

CP/MAS ^{13}C NMR may suggest the type of hydroxymethyl conformations, ***gt***, ***tg***, or ***gg*** at the C-6 positions in carbohydrates as shown in Figure 16-8. Horii

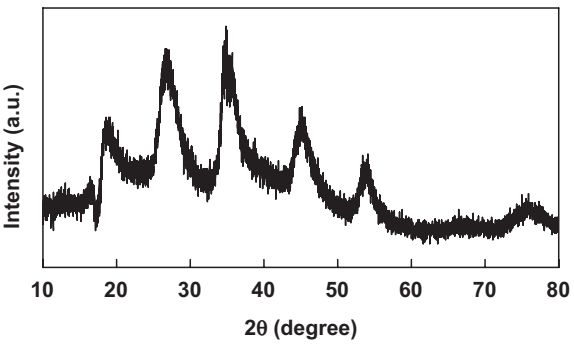

Figure 16-7. Calibrated meridional intensity curve of the WAXD for NOC. The term, "a.u." indicates arbitrary unit

et al. (1983) indicated that C-6 carbon resonance occurs only as a singlet near 64 ppm in the case of the *gt* conformation whereas a resonance band near 66 ppm appears when the ***tg*** conformation is present within the crystalline structures. According to these researchers, the chemical shifts fall into three groups of 60–62.6, 62.5–64.5, and 65.5–66.5 ppm, which are related to ***gg***, ***gt***, and ***tg*** conformations, respectively. The chemical shift of the C-6 for cellulose II (Dudley et al. 1983; Horii et al. 1985; Isogai et al. 1989) indicated the ***gt*** conformation,

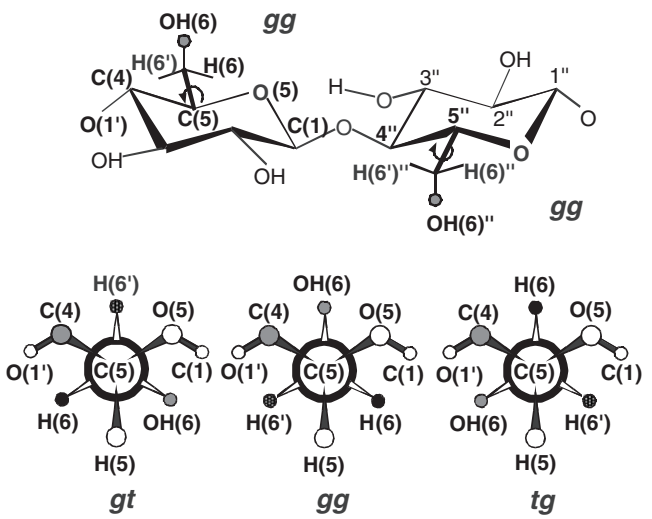

Figure 16-8. Schematic diagram of the hydroxymethyl conformations at the C-6 position, namely the orientation of the C6–O6 bond, *gauche-trans* (***gt***), *trans-gauche* (***tg***) or *gauche-gauche* (***gg***) with a cellobiose unit

which may agree with recent results from the neutron fiber diffraction analysis (Langan et al. 1999). As for the noncrystalline states, they are considered in the *gg* conformation. Therefore, it is easy to predict that NOC could have ***gg*** conformation of the hydroxymethyl group at the C(6) position.

In Figure 16-9, the CP/MAS ^{13}C NMR spectra for our NOC sample, as well as amorphous (a noncrystalline state without any preferred orientation) cellulose prepared from cellulose-SO_2-dimethylamine-dimethyl sulfoxide solution (Isogai and Atalla 1991) and CF11 cellulose powder (Whatman International Ltd.) are shown in the range from 50 to 80 ppm where chemical shifts at the C (6) position appear.

The chemical shift of CF11 appears at 65 ppm, corresponding to ***tg*** conformation, indicating that CF11 is native cellulose. Our NOC sample exhibits a broader signal similar to amorphous cellulose within the range of the type of the hydroxymethyl conformation, ***gg***, which also supports our suggestion that NOC is noncrystalline even though it is well ordered.

2.2 Nematic ordered α-chitin and cellulose/α-chitin blends

2.2.1 Nematic ordered α-chitin

Figure 16-10 shows high-resolution TEM(CHRTEM) images of molecular assembly in the stretched samples of α-chitin and cellulose/α-chitin blend with a composition of 25/75 that were prepared by the same manner for NOC and subsequently negatively stained with uranium acetate. They exhibited occurrence of the orientation of molecular aggregation as seen in white lines, but were not resolved at the individual molecular chain scale, unlike the high-resolution TEM image of NOC (Kondo et al. 2001). By image analyses of the two TEM

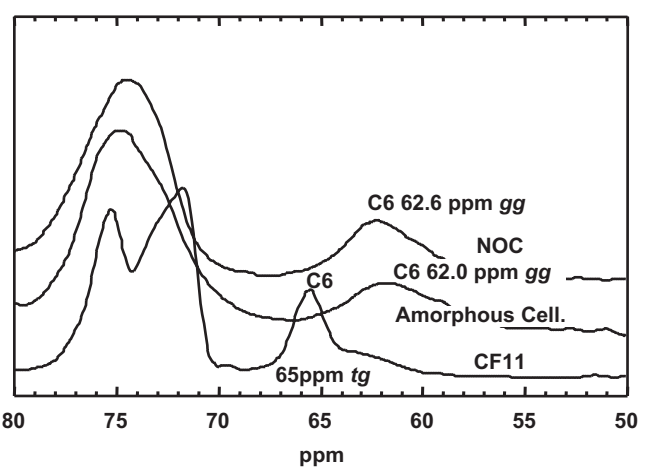

Figure 16-9. CP/MAS ^{13}C NMR spectra of NOC, amorphous cellulose, and native cellulose powder (Whatman CF11)

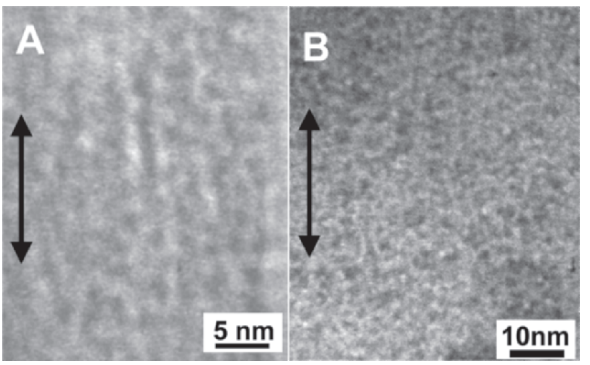

Figure 16-10. HRTEM images of single molecular chains in the order structure of the stretched water-swollen gel films at the drawing ratio of 2.0 of (**a**) α-chitin and (**b**) cellulose/α-chitin (25/75) blend. The double arrows indicate the stretching direction

photographs in Figure 16-10, the average width and distance between two parallel lines were obtained as listed in Table 16-1 in comparison of NOC data.

The crystal lattice parameters for native crystalline α-chitin were reported as $a = 0.474$ nm, $b = 1.886$ nm, $c = 1.032$ nm, and $\alpha = \beta = \gamma = 90°$, respectively (Minke and Blackwell 1978). Since the average distance between any two lines in well-ordered states in Figure 16-10a was 1.88 ± 0.27 nm, this value coincides with the lattice dimension of *b*-axis. Therefore, considering that the stretching direction corresponds to the molecular chain axis (*c*-axis), the top view of the TEM image of Figure 16-10a indicates that the b-c plane of α-chitin microfibril may be aligned parallel as white lines with a distance of 1.62 ± 0.21 nm on the surface. In other words, by the same preparation method for NOC, α-chitin molecules may be self-assembled to form a microfibril, and further the individual microfibrils tend to be arranged parallel with the distance of 1.62 ± 0.21 nm. This indicates presence of another nematic ordered state with a different scale in α-chitin.

2.2.2 Nematic ordered cellulose/α-chitin blends

Figure 16-10b and the corresponding data in Table 16-1 exhibit a case of the stretched film of the cellulose/α-chitin blend with a composition of 75/25 (w/w) in the same manner for NOC.

Table 16-1. The average width and distance between two parallel lines analyzed by TEM images

			(nm)
	Cellulose (NOC)*	α-Chitin	Cellulose/α-Chitin 75/25
Line width	0.46 ± 0.05 (chain width)	1.88 ± 0.27	1.38 ± 0.18
Distance between two lines	0.66 ± 0.07	1.62 ± 0.21	1.65 ± 0.27

*From Kondo et al. (2001).

The white dots or lines in Figure 16-10b indicate molecular chains or molecular aggregates. Some parts are well oriented parallel to the stretching direction, and the molecular aggregates are entirely ordered along the stretching axis. The average line width as shown in Table 16-1 is narrower than that for nematic ordered pure α-chitin, indicating that the intermolecular interaction between cellulose and α-chitin may be engaged. Possibly each molecular chain is facing with each other against the surface by a hydrophobic interaction such as a van der Waals force. On the other hand, the average distance between two parallel lines was not significantly different between the two stretched films from α-chitin and the cellulose/α-chitin blend. Therefore, it is considered that the cellulose/α-chitin molecular aggregates in the stretched film are aligned similarly to nematic ordered α-chitin.

To deal with the above case in comparison of the NOC, we employed WAXD measurements in order to understand the molecular ordering occurring during stretching of the blended films of the water swollen cellulose/α-chitin (50/50) gel. Water-swollen gel-like cellulose films formed after slow coagulation and the subsequent solvent-exchange were transparent and composed of ~93 wt% of water and 7 wt% of cellulose prior to stretching. When stretching the water-swollen film uniaxially, drops of water extruded from the film as the orientation of the film increased. The films stretched at the changing drawing ratio were provided for WAXD measurements.

Figure 16-11 shows WAXD photographs of the fiber structure. It suggests that the undrawn cellulose films after dried in a stretching device showed some orientation by natural shrinking, and with increase in drawing ratio of the samples, the rings were becoming arcs at the equatorial direction. Figure 16-12 shows WAXD photographs for the stretched cellulose/α-chitin (50/50) films at the desired drawn ratio.

When compared with that for cellulose shown in Figure 16-11, clearer Debye rings appeared even in undrawn films after dried. Like the cellulose case, with increase in drawing ratio of the samples, the rings were becoming arcs at the equatorial direction. Similarly, such arcs appeared also at the meridional direction. WAXD intensity curves in both directions indicate more clearly that some ordered crystallites, to some extent, were formed prior to stretching (data not shown, see Kondo et al. 2004). Through the stretching, the two peaks at $2\theta = 9.3$ and 19.5 in the equatorial direction were becoming narrower and sharper, while the meridional reflections were not significantly changed after the stretching. These results indicate that the intermolecular interaction between cellulose and α-chitin may cause molecular aggregations leading to some crystallization, and as a result, crystallites with a certain size were formed. Then, by stretching, the crystallites tend to be ordered parallel to the drawing axis.

The series of α-chitin used as a component for preparation of nematic ordered states have indicated that unlike NOC, at first the molecules tend to be aggregated prior to stretching, and then by the stretching the nematic ordered states of the aggregates were formed (Kondo et al. 2004). Namely, the nano/micro-hierarchical structures are supposed to be built up.

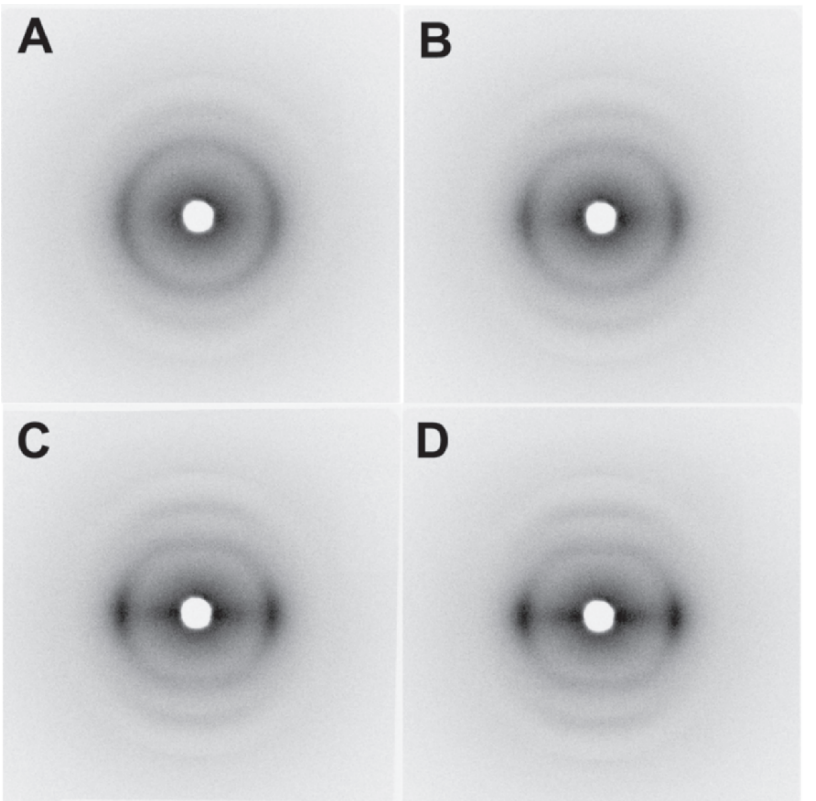

Figure 16-11. WAXD photographs for stretched cellulose films at the desired drawn ratio: (**a**) undrawn water-swollen film after dried at a fixed state; (**b**) draw ratio 1.5; (**c**) draw ratio 1.7, and (**d**) draw ratio 2.0

2.3 Another type of nematic ordered cellulose: honeycomb-patterned cellulose

Recently, a honeycomb-patterned cellulose triacetate film was successfully fabricated by casting of water-in-oil (W/O) emulsion on the substrate, and the subsequent deacetylation yielded a honeycomb-patterned cellulose film without deformation as shown in Figure 16-13 (Kasai and Kondo 2004). In the film forming process, when cellulose triacetate started to be precipitated as a honeycomb-patterned film, the honeycomb frames were supposed to be simultaneously stretched by natural drying of water droplets as a mold. This stretching effect of natural dry presumably resulted in an alignment of cellulose molecular chains along the honeycomb frames, similarly to formation of NOC-typed form (Kasai et al., unpublished).

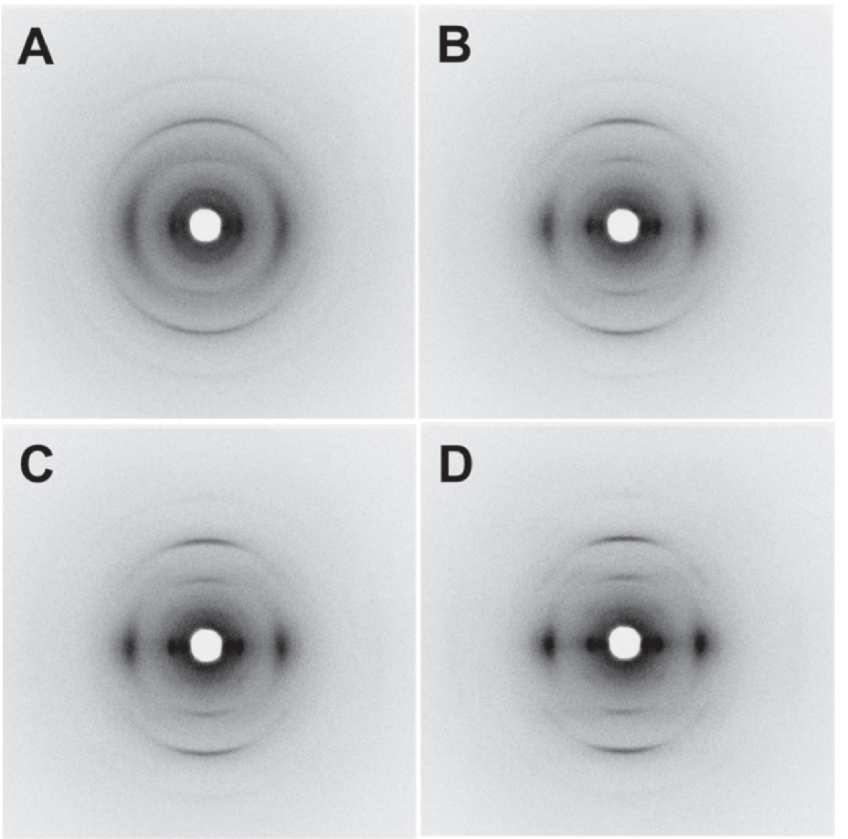

Figure 16-12. WAXD photographs for stretched cellulose/α-chitin (50/50) blended films at the desired drawn ratio: (**a**) undrawn water-swollen film after dried at a fixed state; (**b**) draw ratio 1.5; (**c**) draw ratio 1.7; and (**d**) draw ratio 2.0

3 PROPERTIES OF NEMATIC ORDERED CELLULOSE

3.1 The exclusive surface property of NOC and its unique application

As already described, NOC is considered as the template having the exclusive surface of a certain nano/micro structure. Namely, the OH groups together with the neighboring hydrophobic sites tend to be oriented as molecular tracks only in one direction across the entire NOC surface. These amphiphilic ordering tracks on the NOC surface were expected to induce an epitaxial deposition of substances such as organic and inorganic compounds. This is a unique application of NOC with a specific surface property to induce other substances to be oriented.

The ordering amphiphilic tracks of hydrophilic OH groups and hydrophobic polarity in NOC, for example, could induce an epitaxial deposition of biosynthesized

cellulose nanofibers secreted from the gram-negative bacterium, *A. xylinum* (=*Gluconacetobacter xylinus*), along the same axis of the tracks in NOC (Kondo et al. 2002). When active *A. xylinum* cells are transferred to the oriented surface, they synthesize cellulose ribbons parallel to the molecular orientation of the substrate. This is evidenced by direct video imaging of the motion of the bacteria as they synthesize the cellulose ribbon. The movement of *A. xylinum* in relation to cellulose biosynthesis was reported (Brown, Jr. et al. 1976). The cell movement (at a constant rate of 4.5 μm/min at 24°C) is the result of an inverse force imposed by the directed polymerization and crystallization of the cellulose. It is also well known that the bacterium rotates on its own axis.

This bio-directed epitaxial nanodeposition can be studied over time and under varied conditions including different substrates. For example, in Figure 16-14, a time-course analysis of an NOC template shows a bacterium moving in contact with a stretched NOC substrate.

Midway through this series, the cell, "jumps off" of the oriented substrate, and continues to secrete its cellulose ribbon but now in the form of a spiral that is the normal pattern of formation when not in contact with any organized substrate (Thompson et al. 1988). When the interaction between the bacterium and the surface of NOC is strong enough, the bacterium follows the track of the molecular template. As the polymer orientation of the NOC is not necessarily perfect, the bacterium may jump off the track at a structural defect (Figure 16-14 stage 3). After the bacterium leaves the track (Figure 16-14 stages 3–6), two forces, the inverse force of the secretion and the close interaction of adjacent microfibrils, affect the bacterium, possibly resulting in the synthesis of a spiral ribbon of microfibrils. In addition, the bacterium begins to rotate on its own axis. This rotation is the visible result of ribbon twisting which occurs to relieve strain induced by the absence of interaction with the substrate. When the ribbon is assembled in direct contact

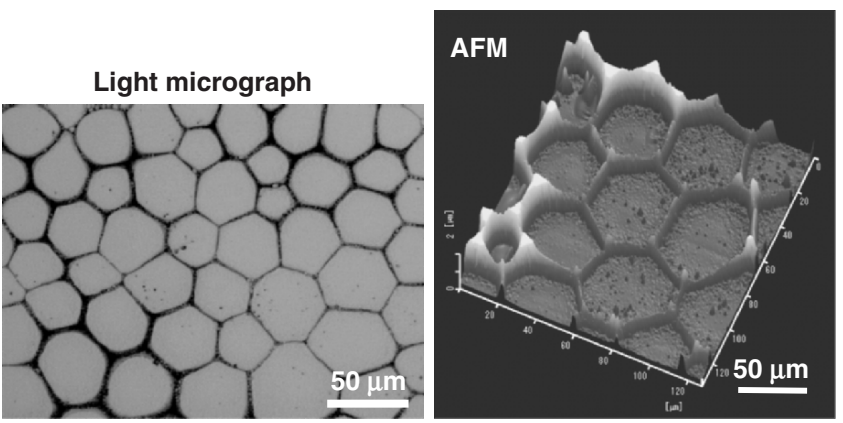

Figure 16-13. Light micrograph of honeycomb-patterned cellulose films from cellulose triacetate together with the surface topographic AFM image. (Scale bars are 50 μm.)

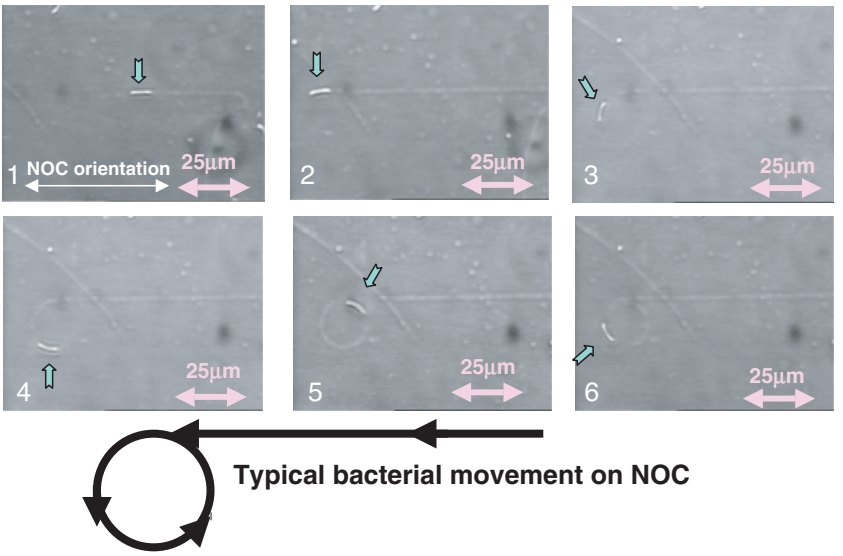

Figure 16-14. Successive images showing the motion of a bacterium as it secretes a cellulose ribbon using real-time video analysis. In (1), the bacterium is attached to and synthesizing its cellulose on the monomolecular rail track. In (2), the bacterium has jumped the track and is beginning to change its orientation. (3) to (5), the bacterium is generating the first complete spiral. In (6), the bacterium is on the second rotation of a spiral

with the oriented molecular NOC substrate, ribbon twisting is prevented, thus suggesting a control of this oriented solid surface over the final physical interaction of polymer chains immediately after synthesis and during the early stages of crystallization.

Cellulose ribbon interaction is more clearly shown by field emission scanning electron microscopy (FE-SEM) in Figure 16-15. In this experiment, the motion of the same sample is observed using light microscopy and then the sample is prepared for FE-SEM observations. In Figure 16-14 stage 1–2, the time-course sequence demonstrates an intense, directed nanodeposition that is exclusively linear and without cell rotation as the bacterium follows the track. This is confirmed by the ribbon structure shown by the FE-SEM images in Figure 16-15, a–c which reveal no twisting and a more perfect alignment with the substrate. Likewise, when the bacterium "jumps off" the track, the cellulose ribbon is twisted. On the other hand, when *Acetobacter* is cultured on the surface of a nonstretched cellulose swollen gel substrate (precursor for NOC), it moves in a random manner including spirals (data not shown). An FE-SEM image on the nonoriented substrate is shown in Figure 16-15e. The image suggests a random of microfibrils with the substrate surface. When *Acetobacter* cells are placed on an agar surface as a control, their interaction seems to be reduced, and twisted ribbons are always deposited, also in a random fashion (Figure 16-15f). It should be noted that this regulated movement of the bacterium was not observed in the synthetic polymers

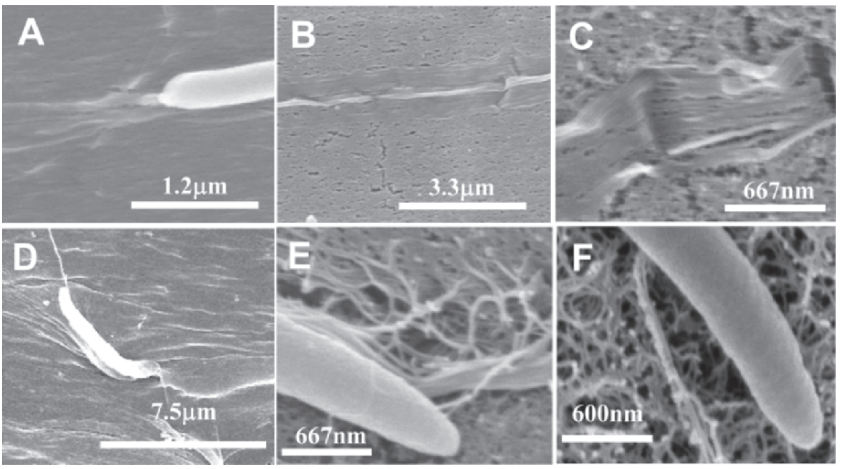

Figure 16-15. FE-SEM images of the cellulose ribbon deposition process. (**a**–**c**) examples of bacteria synthesizing cellulose ribbons on the oriented molecular track of NOC. In 15A, a bacterium shows a flat ribbon immediately behind its site of synthesis. (**b**) and (**c**) demonstrate the tight association between the molecular track and the cellulose ribbon. (**d**) is an example where the bacterium has just jumped off the track and following a spiral path. (**e**) demonstrates random cellulose deposition on the surface of a nonstretched NOC precursor. (**f**) shows random cellulose deposition on the surface of agar

having OH groups such as poly (vinyl alcohol), but only in nematic ordered states of carbohydrate polymers (Kondo et al. 2002). The authors have been recently successful to have the bacterium followed on the honeycomb-patterned cellulose frame having NOC states, resulting in 3D honeycomb cellulose structure (Kasai et al. unpublished).

The rate and direction of the movement correspond to those of the fiber production. The fibers were reported to produce at a rate of 2 μm/min at 25°C (Brown, Jr. et al. 1976). However, *A. xylinum* produced the fiber faster on NOC templates at a rate of 4.5 μm/min at 24 °C. This gap was considered due to difference of the strength of the interaction between the biosynthesized fiber and the NOC surface. This also indicated that the NOC surface promoted the secretion rate of the fibers. More to importance, the regulated movement of the bacteria due to the ordered surface of NOC may trigger the development a 3D structure of hierarchical architecture from the nano to the microlevels. Therefore, we have been attempting to regulate the 3D architecture of materials using the nanofibers secreted by *A. xylinum* as a building block.

4 THE FUTURE

In biological systems, skeletal materials such as cell walls, bones, and shells are made primarily of a nanoscale building block of polysaccharides, proteins, and inorganic salts. The assembly of these building blocks facilitates the production

of a hierarchical framework structure. The formation dynamics observed in this study could be applicable to the design of nanoscale controlled, hierarchically structured materials with specific properties. We have employed a biological system combined with a polymer platform having NOC-like surface in order to directly fabricate hierarchically ordered materials from the nanolevel up to the micron level. Therefore, such a surface property would greatly extend the possibilities of usage of cellulose to new areas. Thus, if a micropatterned film having a similar characteristic as NOC can be fabricated, the obtained 3D cellulose materials will be widely appreciated and used.

5 MATERIALS AND METHODS

5.1 Materials

Bleached cotton linters with a degree of polymerization (DP) of 1,300 were used as the starting cellulose sample. The cellulose was first dried under vacuum at 40°C. *N*,*N*-dimethylacetamide (DMAc) purchased from Katayama Chemicals Co. Ltd. (99+%) was dehydrated with molecular sieve 3A and used without further purification. Lithium chloride (LiCl) powder (Katayama Chemicals Co. Ltd.) was oven-dried at least for 3 days at 105°C. Methylcellulose with a degree of substitution (DS) of 1.6 and polyvinyl alcohol (PVA) with a DP of 2,000 were purchased from Shin-Etsu Chemical Co. Ltd. and Katayama Chemicals Co. Ltd., respectively. Cellulose acetate with a DS of 2.45 (L-70) and purified chitin were provided by Daicel Chemicals Co. Ltd. and Katakura Chikkarin, respectively.

NOC was prepared by stretching a water-swollen cellulose film which had been coagulated from a DMAc /LiCl solution. Dissolution of cellulose and preparation of the template was accomplished by a previously described procedure using a solvent exchange technique (Togawa and Kondo 1999).

5.2 Water-swollen cellulose film from the DMAc/LiCl solution

LiCl dried at 105°C was dissolved in anhydrous DMAc to give a concentration of 5% (w/w) solution. Dissolution of cellulose was basically followed by a previous swelling procedure using a solvent exchange technique (Togawa and Kondo 1999). Prior to swelling, the cellulose sample was disintegrated into fragments or small pieces by a mechanical disintegrator and dispersed into water which increased the surface area making it easier to dissolve. The treated cellulose was soaked in water overnight, then squeezed and filtered to remove the water. The cellulose was then immersed in methanol, and again squeezed and filtered to remove excess methanol. After four repetitions of the methanol treatments, an exchange with acetone was performed once. Following the treatments with water, methanol, and acetone described above, the sample was solvent-exchanged with DMAc twice in the same procedure and soaked in the same solvent overnight.

Another two repetitions of the above soaking and squeezing treatments with DMAc treatments were performed on the sample. Following the final squeeze, the cellulose was ready to be dissolved. The cellulose swollen by DMAc was dissolved in the DMAc/LiCl solution with constant stirring at room temperature for 3 weeks at most. As the viscosity of the solution depends on the DP of the polymer, ~1% cellulose with a DP of 1,300 was suitable for handling. After a week, when no change in viscosity was noted in the solution, 1–3% LiCl was added to the solution, and then it was heated up to 50–60°C for several hours. The resulting solution was then centrifuged and filtered to remove any insoluble portion. The actual concentration (wt%) of cellulose in the solution was determined by weighing a small portion of the dried cellulose film. At this stage, the molecules are almost completely dispersed.

The slow coagulation to prepare the gel-like film from a DMAc/LiCl solution was carried out according to the following manner. The solution was poured into a surface-cleaned glass Petri dish with a flat bottom and placed in a closed box containing saturated water vapor at room temperature. In this manner, saturated water vapor slowly diffused into the solution and precipitated the cellulose. The sample was allowed to stand at room temperature for several days until the precipitation under a saturated water vapor atmosphere was sufficiently complete to obtain the gel-like film. The precipitated gel-like film was washed with running distilled water for several days to remove the solvent, and a water-swollen transparent gel-like film was obtained. The films were stored in water until needed. It should be also noted that in the entire procedure from preparation of the solution until starting the slow coagulation with water vapor, rapid operation was required, otherwise the water vapor in the atmosphere would easily penetrate into the solution and cause precipitation of cellulose II crystals.

5.3 Preparation of NOC from water-swollen cellulose films

Drawn cellulose films were prepared by stretching water-swollen gel-like films. These films were cut into strips ~30 mm long and ~5 mm wide. These water-swollen strips then were clamped in a manual stretching device and elongated uniaxially to a draw ratio of 2.0 at room temperature. As the water-swollen films were gel-like, they could neither be clamped too tightly nor too loosely in the first stage of stretching. The entire drawing process was completed while the specimen was still in a wet state. Following air-drying, the drawn specimen in the stretching device was vacuum-dried at 40–50°C for more than 24 hours. The thickness of the dried films was about 80 μm.

5.4 Preparation of NOC template in Schramm-Hestrin (SH) medium

The never-dried NOC template was put into Schramm-Hestrin (SH) medium (Hestrin and Schramm 1954) at pH 6.0, and the solvent was exchanged and finally maintained in a Petri dish until used for the study.

Other noncrystalline ordered substrates were prepared in the same manner from different polymers. Nematic ordered blend films of cellulose and its derivatives were prepared as follows: DMAc/LiCl was used as the common solvent for all samples to be mixed. Solution concentrations were 1 wt% for cellulose and 5 wt% for the cellulose derivatives. All solutions were filtered and stored in a closed container. Separately prepared solutions of the cellulose and its derivatives were mixed at room temperature in the desired proportions. The relative composition of the two polymers in the mixed solutions was 70/30, 50/50, and 30/70 by weight (cellulose/the derivatives). After stirring for more than 3 days, the mixed solutions were used to prepare nematic ordered blend films by coagulation. The slow coagulation to prepare the gel-like film from a DMAc/LiCl solution was carried out according to the above. The solution was poured into a surface-cleaned glass Petri dish with a flat bottom and placed in a closed box containing saturated ethanol vapor at room temperature. In the blend solution, saturated ethanol vapor slowly diffusing into the solution was employed to precipitate the cellulose/cellulose derivative blend gel, instead of water vapor for NOC. It was allowed to stand at room temperature for a few days until precipitation under a saturated ethanol vapor atmosphere was complete to obtain the gel-like film. The precipitated gel-like film (at this stage fixation of the film appeared to be complete) was washed thoroughly with ethanol to remove the solvent, and then the film was put in water to exchange the solvent in order to obtain a water-swollen transparent gel-like film. This water-swollen cellulose/the derivative blended film was stretched in the same manner for NOC to be formed into nematic ordered blended films.

Acknowledgments

The author thanks Professor R.M. Brown, Jr. at University of Texas, Austin for the research collaboration and his valuable comment. Mr. Togawa and Ms. Hishrikawa at FFPRI are acknowledged by the long-term research collaboration. Dr. W. Kasai and Ms. Y. Tomita in my laboratory at Kyushu University are also acknowledged by their valuable comment on the text. This research was supported partly by a Grant-in-Aid for Scientific Research (No. 14360101), Japan Society for the Promotion of Science (JSPS).

REFERENCES

Brown, Jr. R.M., Willison J.H.M., and Richardson C.L. 1976. Cellulose biosynthesis in *Acetobacter xylinum*: visualization of the site of synthesis and direct measurement of the *in vivo* process. Proc Natl Acad Sci USA 73:4565–4569.

Drexler K.E. 1992. Nanosystems: Molecular Machinery, Manufacturing, and Computation. Wiley, Interscience, New York.

Dudley R.L., Fyfe C.A., Stephenson P.J., Deslandes Y., Hamer G.K., and Marchessault R.H. 1983. High-resolution carbon-13 CP/MAS NMR spectra of solid cellulose oligomers and the structure of cellulose II. J Am Chem Soc 105:2469–2472.

Hestrin S. and Schramm M. 1954. Synthesis of cellulose by *Acetobacter xylinum*. 2. Preparation of freeze-dried cells capable of polymerizing glucose to cellulose. Biochem J 58:345–352.

Horii F., Hirai A., and Kitamaru R. 1983. Solid-state ^{13}C-NMR study of conformations of oligosaccharides and cellulose conformation of CH_2OH group about the exo-cyclic C–C bond. Polym Bull 10:357–361.

Horii F., Hirai A., Kitamaru R., and Sakurada I. 1985. Cell Chem Technol 19:513.

Isogai A. and Atalla R.H. 1991. Amorphous celluloses stable in aqueous media: regeneration from SO_2-amine solvent systems. J Polym Sci Polym Chem 29:113–119.

Isogai A., Usuda M., Kato T., Uryu T., and Atalla R.H. 1989. Solid-state CP/MAS carbon-13 NMR study of cellulose polymorphs. Macromolecules 22:3168–3173.

Kasai W. and Kondo T. 2004. Fabrication of honeycomb-patterned cellulose films. Macromol Biosci 4:17–21.

Kasai W., Morita M., and Kondo T. unpublished.

Kondo T. and Sawatari C. 1996. A Fourier transform infra-red spectroscopic analysis of the character of hydrogen bonds in amorphous cellulose. Polymer 37:393–399.

Kondo T., Togawa E., and Brown, Jr. R.M. 2001. "Nematic ordered cellulose": a concept of glucan chain association. Biomacromolecules 2:1324–1330.

Kondo T., Nojiri M., Hishikawa Y., Togawa E., Romanovicz D., and Brown, Jr. R.M. 2002. Biodirected epitaxial nanodeposition of polymers on oriented macromolecular templates. Proc Natl Acad Sci USA 99:14008–14013.

Kondo T., Kasai W., and Brown, Jr. R.M. 2004. Formation of nematic ordered cellulose and chitin. Cellulose 11:463–474.

Langan P., Nishiyama Y., and Chanzy H. 1999. A revised structure and hydrogen bonding system in cellulose II from a neutron fiber diffraction analysis. J Am Chem Soc 121:9940–9946.

Minke R. and Blackwell J. 1978. The structure of α-chitin. J Mol Biol 120:167–181.

Togawa E. and Kondo T. 1999. Change of morphological properties in drawing water-swollen cellulose films prepared from organic solutions. a view of molecular orientation in the drawing process. J Polym Sci B: Polym Phys 37:451–459.

Thompson N.S., Kaustinen H.M., Carlson J.A., and Uhlin K.I. 1988. Tunnel structures in *Acetobacter xylinum*. Intl J Biol Macromol 10:126–127.

Whaley S.R., English D.S., Hu E.L., Barbara P.F., and Belcher A.M. 2000. Selection of peptides with semiconductor binding specificity for directed nanocrystal assembly. Nature 405:665–668.

Ward I.M. (ed.) 1997. Structure and Properties of Oriented Polymers. Chapman & Hall, London, p. 1.

Zhao X.-M., Whitesides G.M., Qin D., Xia Y., Rogers J.A., and Jackman R.J. 1998. Microfabrication, microstructures and microsystems. In Manz A. and Becker H. (eds.) Microsystem Technology in Chemistry and Life Sciences, Vol.194. Springer, Berlin, p. 1–20.

CHAPTER 17

BIOMEDICAL APPLICATIONS OF MICROBIAL CELLULOSE IN BURN WOUND RECOVERY

WOJCIECH CZAJA[1]*, ALINA KRYSTYNOWICZ[1], MAREK KAWECKI[2], KRZYSZTOF WYSOTA[2], STANISŁAW SAKIEL[2], PIOTR WRÓBLEWSKI[2], JUSTYNA GLIK[2], MARIUSZ NOWAK[2], AND STANISŁAW BIELECKI[1]

[1]*Institute of Technical Biochemistry, Technical University of Lodz, Stefanowskiego 4/10, Lodz, Poland;*
[2]*Center of Burn Healing, Jana Pawla II 2, Siemianowice Śląskie, Poland*

Abstract

Microbial cellulose (MC) is a very versatile biomaterial. Even though it has already been successfully deployed in such diverse scientific endeavors as electronics, acoustics, and fuel cells, it is particularly well suited for the creation of unique biomedical devices which can significantly improve the healing process. Because of the increased interest in tissue engineered products for the regeneration of damaged or diseased organs, microbial cellulose may become an essential material for a diverse array of medical treatments. Microbial cellulose from *Acetobacter xylinum* recently has been shown to be very beneficial in the treatment of superficial second degree and deep dermal second degree burns. In a clinical study performed on 34 patients, the MC wound dressing materials were directly applied on fresh burns covering up to 9–18% of the body surface. The following analyses were considered during the trials: macroscopic observations of the wound and wound exudates, epidermal growth, microbiological tests, and histopathological studies. The wounds are all very well isolated from the outside environment by application of the MC membranes. Due to the unique 3-D nanostructure, MC membranes virtually replicate the wound surface at the nano-scale level and create optimal moist conditions for wound healing and skin regeneration. In shallow wounds, MC dressing promoted growth of the epidermis and in deep wounds shortened the period of scab demarcation. Factors for this success include but are not limited to the following: (a) a moist environment for tissue regeneration; (b) significant pain reduction; (c) the specific microbial cellulose nano-morphology which appears to promote cell interaction and, tissue re-growth; (d) significant reduction of scar formation; and, (e) easy and safe release of wound care materials from the burn site during treatment. Microbial Cellulose promises to have many new applications in wound

* For correspondence: Tel: (+4842)6313442; Fax (+4842)6366618; e-mail: czajawoj@mail.p.lodz.pl

R.M. Brown, Jr. and I.M. Saxena (eds.), Cellulose: Molecular and Structural Biology, 307–321.

care that extend beyond burn applications including, but not limited to, the following: surgical wounds, bedsores, ulcers, tissue, and organ engineering.

Keywords

Acetobacter xylinum, bacterial cellulose, burns, microbial cellulose, wound dressing, wound healing.

1 INTRODUCTION

Burns of the skin are complicated injuries often resulting in extensive damage to the skin layers. Burns are classified according to depth and identified by three degrees (Latarjet 1995): first-degree burn – usually superficial, affects only the outer layer of skin (epidermis); second-degree burn – either superficial, with damage to the epidermis layer of the skin (second-degree A), or deep when penetrating into the dermis (second-degree B); third-degree burn – a total destruction of all the epidermis and dermis, extending into subcutaneous tissue (skin grafting is recommended). The major goal during treatment of burn patients is to quickly accomplish effective wound closure to increase the rate of healing and significantly reduce pain (Demling and DeSanti 1999; Jones et al. 2002; Prasanna et al. 2004).

The process of healing of burn tissues involves both regeneration of the epidermis and repair of the dermis resulting in formation of scar tissue (Balasubramani et al. 2001). There are several key factors regarding a present standard procedure of burn wound management in order to enhance healing while minimizing or preventing scarring (Latarjet 1995; Gallin and Hepperle 1998): (1) prevention of excessive loss of fluids from wounds (which increases up to 70 times in comparison with normal skin); (2) prevention of wound infection; and, (3) fast and effective closure of the wound, optimally with skin graft or other skin substitutes. The general design of an effective burn procedure relies on its immediate change into the surgical wound which is accomplished by the fast excision of necrotic tissues and closure of the wound with skin substitutes which are either split-thickness autografts (these would be optimal, due to immunological issues), allografts (these are considered as biological wound dressings and cannot replace autogenic skin), or xenografts (Balasubramani et al. 2001).

There is still a need for development of wound care dressing material, which could sufficiently protect wounds against infection or excessive loss of fluid. It is a well-known fact that limitation of these processes significantly reduces metabolic effects associated with burn injury and generally facilitates and accelerates the entire process of the burn treatment. Burns are always associated with serious metabolic and immunological disorders commonly called burn sickness. There are three major phases occurring during burn injury: the shock phase (up to 48 h after the burn event); the catabolic phase (up to several weeks) when a process of wound cleansing from necrotic tissues takes place; and, the anabolic phase, which occurs when the actual process of healing and tissue regeneration takes place. The shorter the period of the catabolic phase, the better are the chances to rescue patients with large area skin burns.

Due to recent advances in the field of biomedical materials, scientists have developed a variety of natural and synthetic polymers which can be used for wound

closure, drug delivery systems, novel vascular grafts, or as scaffolds for the creation of tissue engineered constructs. With respect to wound closure and wound care, many different biological and synthetic wound dressings already have been developed and introduced in the market, and many are still in the development phase. The criteria for an ideal wound care dressing material require it to display the structural and functional characteristics of autograft skin (Quinn et al. 1985; Balasubramani et al. 2001). The present status of a modern, successful wound care dressing material indicates several requisite characteristics: absence of toxicity, creation of a moist environment in the wound, high mechanical strength, elasticity, control of fluid loss, significant reduction of pain during treatment, and absorption of secretions from the wound. Additionally, material should be easy to store and ready for immediate usage, provide easy, close wound coverage, allow for painless removal from the wound, should display an optional shape and surface area, and it should enable the introduction or transfer of medicines into the wound (Quinn et al. 1985; Wu et al. 1995; Ruiz-Cardona et al. 1996; Delatte et al. 2001; Walker et al. 2003; Park et al. 2004).

In our experience, we have clinically investigated a novel biomaterial which meets the requirements for an ideal wound dressing system. Microbial cellulose (MC), which is synthesized and secreted by the GRAM negative bacterium, *Acetobacter xylinum*, displays unique physical, chemical, and mechanical properties including a high crystallinity (70–90%), a high water holding capacity (up to 200 times of its dry mass), a well-developed surface area comprised of nanofibers (3–8 nm), elasticity, mechanical strength (a Young's modulus of ~30 GPa), and biocompatibility (Ross et al. 1991; Brown, Jr. 1996; Watanabe et al. 1998; Bielecki et al. 2002; Krystynowicz et al. 2002; Czaja et al. 2004). Due to its unique nanostructure and remarkable properties, MC has been of great interest for many medical applications including artificial blood vessels, scaffolding for tissue engineering of cartilage, and a wound dressing material for chronic wounds (Ring et al. 1986; Fontana et al. 1990; Klemm et al. 2001; Alvarez et al. 2004; Svensson et al. 2005).

In our study, we describe the use of a modern wound dressing material synthesized by *A. xylinum*. This product, MC, is a new system for wound healing. The objective of our research was to clinically compare the wound healing effects of never-dried MC membranes with conventional cotton gauze wound dressings. We wanted to investigate its applicability as a new wound care dressing material in the treatment of large area, partial thickness skin burns (second-degree A/B).

2 EXPERIMENTAL DESIGN

2.1 Never-dried MC membranes preparation

MC produced by the vinegar fermentation bacterium *A. xylinum* is synthesized in the form of twisting ribbons, which in stationary culture forms a thick, gelatinous membrane on the surface of a liquid medium. The membrane formed in such conditions is characterized by the 3D structure made of an ultrafine network of

cellulose nano and microfibrils. This particular structure of the never-dried MC pellicle determines the remarkable and unique physical and mechanical properties of the wound dressing material which can hold a large amount of liquid and displays high mechanical strength (Table 17-1) *A. xylinum* E_{25} from the collection of Institute of Technical Biochemistry, Technical University of Lodz, Poland, was used in this study.

It is a typical GRAM-negative rod that is an obligate aerobe and it produces a thick membrane of pure cellulose at the gas/liquid interface of a static culture (Hestrin and Schramm 1954). Schramm–Hestrin medium (SH medium) (Hestrin and Schramm 1954) enriched with 1% (v/v) ethanol, with a pH adjustment to 5.7 was used in all experiments unless otherwise specified. The cells for the inoculum were grown in liquid SH medium in 250 ml Erlenmeyer flasks either statically or on a rotary shaker, for 2 days at 30°C. The thick gelatinous membrane that formed in the flask after 2 days was squeezed aseptically to remove the cells embedded inside it. The cell suspension was then transferred as the inoculum for the primary culture. The primary cultures were grown statically in plastic stacking trays of different sizes for 7 days at 30°C. The synthesized cellulose was harvested from the medium and washed with 2% sodium hydroxide (overnight) followed by several changes of distilled water in order to remove cells and any residual culture medium embedded in the cellulose material. The final product, in the form of a transparent, wet membrane, was packaged, sealed, and sterilized by γ-radiation. MC wound dressings used in the clinical study had the following sizes: 18 × 25 cm, 40 × 60 cm.

2.2 Clinical trials

Controlled, randomized clinical trials were conducted on 34 patients. The experimental group of individuals who received the MC consisted of 22 patients in the testing group (5 females with an average age of 49, and 17 males with an average age of 35). The control group consisted of 12 patients. All patients, both from testing and control groups, suffered from severe thermal burns (second-degree A/B) covering 9–18% of the total body surface area (TBSA). The research study protocol was approved by the Bioethical Committee of the Medical University of Silesia (Katowice, Poland) prior to the commencement of the study. Written consent of all patients was taken after presenting them appropriate information about the research project. Patients who were included in the study were between 18 and 70 years of age, had second-degree A/B burns covering 9–18% TBSA, did not have diabetes,

Table 17-1. Physical and mechanical characteristics of the MC wound dressing

Thickness (mm)	Crystallinity degree (%)	Young's modulus (GPa)	Water holding capacity (g water/g cellulose)	Cellulose content in the dressing (%)	Relative total deformation index (%)	Tensile strength (MPa)
3	65	2.7	79	0.6	30.1	92

collagenosis, uraemia, mental disease, cancer, immunosupression, or any blood transfusions for a year prior to the beginning of the clinical study, nor did they have any cytostatic or radiant energy treatments. Patients who did not sign the written consent form, did not understand the objectives and methods of the study, were pregnant, or who incurred serious side effects during treatment were excluded from the study.

After cleansing and disinfecting the wound, MC dressing materials were directly applied on fresh burns (second-degree A/B) closely covering up to 9–18% of the body surface of the experimental patients, and then covered with gauze wraps containing a 3% Braunol (B. Braun Medical) solution. The control group was treated with a standard procedure using gauze wound dressings with a 3% Braunol solution, silver sulfadiazine, povdone-iodine, or flammacerium ointment. The normal wound treatment period for both groups of patients (testing and control) was 10 days. The Parkland formula of fluid replacement with crystalloids was applied to all patients on the first day of hospitalization: body weight (kilograms) × the body surface area burned (percentage) × 4, yielding the intravenous crystaloid volume (in milliliters) to be administered over 24 h. One-half of this volume was given during the first 8 h of the burn treatment, followed by administering the remaining half of the volume over the next 16 h. Starting from the second day of hospitalization, the loss of fluid was determined using the hematocrit value, which is the proportion, by volume, of the blood that consists of red blood cells and is expressed as a percentage by volume.

During clinical evaluations the following diagnoses were considered: (a) macroscopic observations of the wound; (b) epidermal growth; (c) microbiological tests of blood (on the tenth day of the treatment); (d) wound exudates (on the first, fifth, and tenth day of the treatment); (e) urine (on the first and tenth day of the treatment); and, histopathological studies (on the first and tenth day of the treatment). Antibiotics were not used in any cases during the studies. Color photographs of the wounds were taken on the first, fifth, and tenth day of the treatment. Tissue specimens from experimental patients and control patients were obtained for examination by excising the wound during periodic changes of the MC dressing. Tissue specimens were fixed in 10% formalin solution, dehydrated and embedded in paraffin wax. Sections were mounted on plain glass slides and stained with hematoxylin and eosin in a conventional manner. Observations were carried out using bright field light microscopy.

3 CLINICAL OUTCOMES

3.1 High conformability, moisture donation, and faster healing

The medical tests conducted *in vivo* on the rat animal model showed that MC membranes successfully protected the surface of large-area skin burns from an excessive external fluid loss and significantly accelerated the process of healing

(Krystynowicz et al. 2000). These early promising results allowed permission from the Bioethical Committee to perform the clinical trials on humans.

During clinical trials, the MC wound dressing was applied on the fresh wound under sterile conditions. Because of its high conformability, the adherence of MC membrane to the wound surface was excellent (Figure 17-1). In all clinical cases, the dressings adhered very well to the wound sites during treatment, thus avoiding any dead spaces. In order to enhance the patient's mobility, MC dressings were additionally covered with gauze wraps, which helped to keep them in place. The large size of the cellulose membranes employed in this study (e.g., 40 × 60 cm) displayed a full adherence to the variable surfaces throughout the wound. This seemed to be very helpful in accelerating the healing of large area wounds. The applied, never-dried cellulose membrane allowed both: (a) maintenance of a proper moist environment around the wound and (b) due to its highly porous structure, absorbance of the wound's exudates. None of the patients treated during the trial developed any kind of hypersensitive reactions to the applied MC wound dressing.

In the general procedure used during our clinical trials, the MC dressing remained in contact with the wound for about 24 h or until it had become "almost dry". The dressing was then replaced with a new one. Due to the moisture still present in the never-dried cellulose structure, the release of the dressing from the wound was an entirely painless operation. However, in the beginning phase of our study, a single MC dressing was kept on the wound for more than 24 h, even up to 5 days, with or without its periodic rewetting by 0.9% NaCl. Later on, the completely or partly dried membrane was rewetted in order to achieve a painless removal from the wound (Figure 17-2b). An interesting preliminary observation was made during the extended treatment of burns with dry MC membranes. We observed that under completely dried MC dressings (that

Figure 17-1. Application of a large size MC dressing on a second-degree burn (*See Color Plate of this figure beginning on page 355*)

Figure 17-2. A second-degree A/B burn of both forearms. MC dressing applied on the wound (**a**); MC dressing dried on the wound in the second day of the treatment; left hand has been treated with the control technique (**b**); dry MC dressing removed from the wound after 4 days of treatment revealed a clean area with a fully regenerated epidermis underneath; left forearm treated with control procedure displayed presence of necrotic tissues (**c**); wound after 3 weeks upon burning shows a complete re-epithelialization on the healed right forearm whereas on the left forearm granulation tissues have just been formed (**d**) (*See Color Plate of this figure beginning on page 355*)

were not changed for up to 5 days), the process of healing was accompanied by the entire removal of necrotic tissues and wound exudates (Figure 17-2c). On the other hand, the negative effects of such a treatment included a painful dressing release from the wound and slight damage to the fresh epidermis or even deeper parts of the skin caused by the dry dressing removal. In several cases, the effect of wound squeezing generated by the continuously rewetted MC membrane has been found to be very helpful in the reduction of swelling.

The patient shown in Figure 17-2 suffered from second-degree A/B burn of the both forearms caused by exposure to flames. During clinical studies, the patient's right arm was treated with MC wound dressing and the patient's left arm (the control), with treatment consisting of moist gauze and ointment. In this particular case, the MC membrane was not changed daily, so the process of healing was carried out both in moist (for the first 18 h) and dry (during next 3 days) environments. Despite this fact, an entirely regenerated epidermis was revealed upon removal of the MC dressing from the wound after 4 days of treatment

(Figure 17-2c). At the same time, the left, control forearm still displayed the presence of the necrotic tissue, which finally started to separate from the wound during the next 2 days. Three weeks after burning, the right forearm was completely healed, whereas the left, control forearm had just initiated the formation of red granulation tissues (Figure 17-2d). This particular case shows that even under unfavorable, dry conditions during the longer periods of treatment, the MC provided rapid wound healing without the necessity for frequent dressing changes. More research is needed to elucidate the specific interactions between skin cells and the unique MC nanostructure in order to draw any more conclusions about the treatment with dry MC dressing.

Table 17-2 summarizes the healing process in the testing group of patients, treated with MC dressing and in the control group, treated with the standard technique over the period of 10 days. Analysis of these data clearly shows that the specific moist environment created in the wound upon application of MC membrane promotes its rapid self-cleaning. A significant decrease in the presence of necrotic tissue at the bottom of the wound was observed for patients treated with MC dressing. The data from the table shows that at the fifth day of the treatment, the presence of necrotic tissue at the bottom of the wound was clearly observed only in 3 patients from the testing group (a decrease of 75%) in comparison with 8 patients (a decrease of 33%) continuously displaying necrosis in the control group. Consequently, the formation of pink and red granular tissue in the wound took place much earlier in the group of patients treated with MC dressing than in the control group. Finally, it was proven that by the tenth day of the treatment period, the process of reepithelialization had begun in 7 patients from the testing group (58.3%) in comparison with 4 patients (33.3%) from the control group. These results show that the application of MC burn dressing in the treatment of partial thickness burns promotes the creation of a favorable

Table 17-2. The progress (A–E) of wound healing in the testing (treated with microbial cellulose dressings) and control group over the period of 10 days. The data points are number of patients and percentage of the group that fit in the particular progress category

		A	B	C	D	E
Day of observation	Group of patients	Necrotic tissue at the bottom of the wound	Bottom of the wound covered with pus or wound exudate	Pink granular tissue	Red granular tissue	Epidermis growth
1	Testing	12(100%)	–	–	–	–
	Control	12(100%)	–	–	–	–
5	Testing	3 (25%)	5 (41.7%)	4 (33.3%)	–	–
	Control	8 (66.7%)	–	1 (8.3%)	1 (8.3%)	2 (16.7%)
10	Testing	–	2 (16.7%)	3 (25%)	–	7 (58.3%)
	Control	–	6 (50%)	2 (16.7%)	–	4 (33.3%)

environment for fast wound cleansing, and consequently its rapid healing. No clinical signs of wound infections were noted at any time during treatment. For all patients included in the trials, there were generally no significant differences in the incidence of positive bacterial cultures from the MC and control dressing-treated wounds at days 1, 5, and 10 of treatment. Swabs typically grew organisms including *Pseudomonas aeruginosa*, *Staphylococcus aureus*, *Escherichia coli*, *Klebsiella pneumoniae*, and *Acinetobacter baumani*.

3.2 MC is particularly useful in the treatment of facial burns

It is a well-known fact that deep, large facial burns are difficult to heal and often require hospital care (Demling and DeSanti 1999). Facial burn injuries very often result in cosmetic disfigurement. Two factors, which play a key role in minimizing disfigurements are: (1) a fast and timely wound closure; and (2) application of pressure to maturing facial scars (Manigandan and Dhanaraj 2004). Due to its unique nanostructure the MC dressing can hold a large amount of liquid, and this makes it quite heavy, but at the same time it is still a highly conformable material. When applied on the face in the form of a mask (Figure 17-3b) the MC dressing initiates a positive pressure on the maturing scars, thus preventing extensive collagen overproduction. In deep burns, pressure therapy to limit collagen formation and reduce scarring normally is recommended as soon as healing allows (Roques 2002). By applying MC dressing on fresh burns, this positive effect of pressure can be achieved from the beginning of the healing process. Figure 17-3, images a–f show a patient with the severe deep second-degree burns of the facial surface caused by exposure to flame. In this particular case, closure of the entire face was achieved with a single sheet of MC membrane in which the holes for eyes, nose, and mouth were made after placement. By comparison, most of the commercially available, standard skin dressings and substitutes usually are too small to cover the entire facial surface, so two or three sheets attached to each other with staples must be normally applied. Shortly after application of the moist dressing on the wounded face, the swelling gradually decreased, and the feeling of pressure on the facial surface had subsided. Seventeen days after the burns, the process of wound healing had significantly progressed (Figure 17-3c). The epithelialization in the regions of wound edges and from the deep epidermal appendages was clearly observed at that time. After 44 days, the wounded face was entirely healed with no need for skin grafting and no significant signs of extensive scarring (Figure 17-3d). The same patient was examined for scar tissue formation after about 20 months post burning. The patient displayed several shallow, nonovergrowing (nonhypertrophic) scar tissues on the facial surface where a third-degree burn occurred (Figure 17-3e). Additionally, the lack of tissue fragments on the right ear was also observed (Figure 17-3f).

One of the positive effects of treatment with MC dressing was a significant reduction of scar tissue formation on the facial surface affected by partial and

Figure 17-3. A deep second-degree facial burn caused by the exposure to flame (**a**); a highly conformable mask of the MC dressing with holes on eyes, nose, and mouth was tightly applied on the wounded face (**b**); the epithelialization in the regions of wound edges and from the deep epidermal appendages has been clearly observed at 17 days upon burning (**c**); the entirely healed face after next 28 days (**d**); examination after about 20 months upon burning showed the shallow, nonhypertrophic scar tissues on the facial surface where third-degree burn occurred (*front*) (**e**); and the lack of tissue fragments on the right ear (**f**) (*See Color Plate of this figure beginning on page 355*)

deep thickness burns. Another positive effect was the character of the remaining scars, which were not overgrown and did not cause any contractions, especially in the region of eyelids. Based on our observations, we can conclude that MC dressing appreciably improved the management and healing rate for deep

second-degree facial burns compared to a standard technique with moist gauze dressing and ointment.

A significant decrease of pain has been observed throughout the treatments with MC material. After daily patient interviews, there were only two cases in which patients terminated treatment with the MC dressing, explaining that they could not withstand the psychological effect of wearing the mask on their wounded faces.

To date, the standard procedure of care for facial burns remains that of an open technique, using topical antibiotics (Hartford 1997; Demling and DeSanti 1999). This is mostly due to the difficulty of using occlusive dressings or skin substitutes on facial burns (Hartford 1997; Demling and DeSanti 1999). Application of the MC dressing, which can be easily formed in the shape of a face mask, could entirely overcome those obstacles. Its physical properties allow excellent molding to all facial contours, displaying a high degree of conformability even to moving facial parts. The histological appearance of the typical wound tissue in Figure 17-4 clearly shows how tightly the MC membrane adhered to the surface of the wound during the overall process of healing.

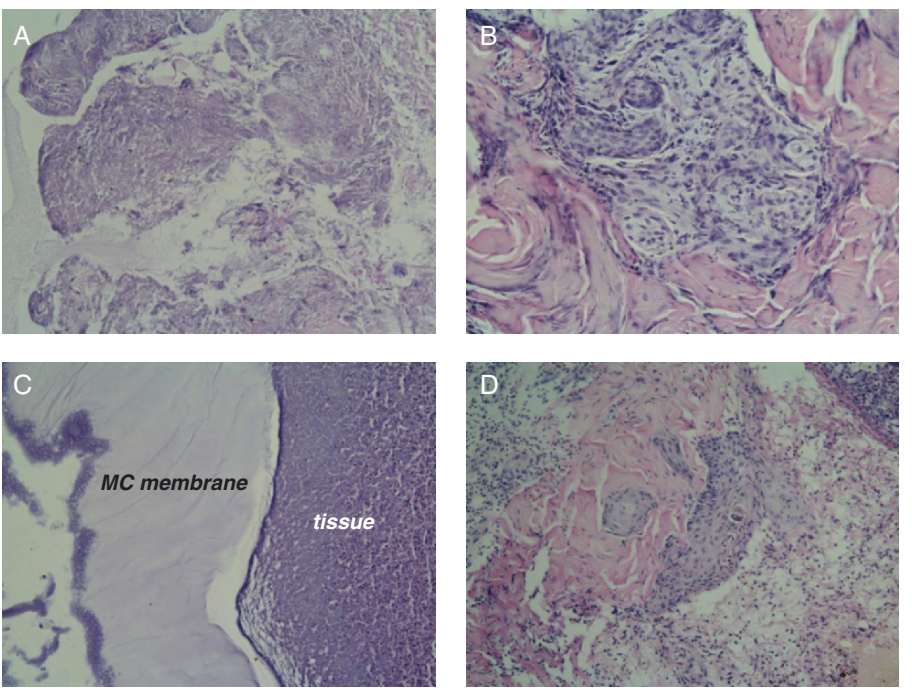

Figure 17-4. Photomicrographs of a biopsy specimen from a wound treated with MC dressing. (**a**) Necrosis of wound tissues; (**b**) growth of granulation tissue and keratinocytes from the appendages of skin (fifth day of treatment with MC dressing); (**c**) fragment of MC dressing tightly adhered to the wound tissue (fifth day of treatment with MC dressing); and (**d**) a fresh epidermis growing in the wound after 10 days of treatment with MC dressing (*See Color Plate of this figure beginning on page 355*)

A similar situation can be observed during application of the MC dressing on the burn wounds of ears. Most ear burns cause a partial loss of some parts of the ear cartilage, and consequently reconstruction is required (Manigandan and Dhanaraj 2004). Generally, the process of ear healing faces many difficulties during the treatment due to the weak blood supply of ears and a shallow position of the cartilage. Another difficulty is the anatomical shape of the ear, which does not allow for easy coverage. Application of MC membrane, which easily and tightly adheres to the ear's contours, creates a specific close contact of a moist layer that entirely isolates the wound from the external environment (data not shown). Another interesting and important advantage of the MC dressing includes its transparency, which allows for continuous clinical observation of the healing progress.

The unique 3D nanostructure of MC seems to be a key factor, which determines its usefulness as a wound dressing material (Figure 17-5). A specific occlusive, moist environment created upon close contact application of the MC membrane significantly facilitated the process of necrotic debris removal (autolytic debridement) in comparison with the control group of patients. In addition, this environment improved the development of granulation tissue and accelerated the entire process of re-epithelialization. It also created an optimal healing environment by maintaining a moisture layer for new cell migration and growth. A significant decrease in daily wound care needs, degree of pain, and the overall time of healing was observed in the treatment with MC dressing in comparison with the control procedures. Many other studies have shown that wound healing of partial-thickness burns can be successfully obtained with appropriate dressing material. Promising results have been obtained using different membranous, occlusive materials like Allevyn, Aquacel, OrCel, Biobrane-L, TransCyte, Integra, and other materials (Demling and DeSanti 1999; Loss et al. 2000; Innes et al. 2001; Vloemans et al. 2001; Still et al. 2003). All of the above dressings provided a moist healing environment, which was associated with a short healing time. Generally, the transparent films and colloids which resulted in a smooth

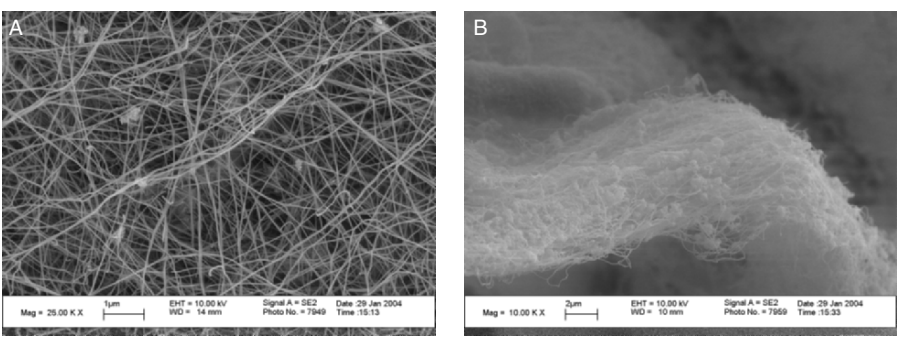

Figure 17-5. Ultrafine net of microbial cellulose (**a**) has a very smooth network of micro- and nanofibrils and (**b**) the cross-section of MC membrane with multilayer architecture

epithelial surface and lowest donor site pain have been shown to be the closest to meet the ideal conditions for fast and stable healing (Innes et al. 2001). The ideal dressing, which possesses all of the qualities of the wound dressing discussed in the introductory chapter of this report, has not yet been developed. However, we believe that the MC dressing, which fulfills all these requirements has the potential to become an ideal wound dressing, particularly for treatment of partial-thickness burns.

4 CONCLUSIONS

In conclusion, our results have shown that wounds are very well isolated from the outside environment by application of the MC membranes. Due to its unique 3D nanostructure, the MC membrane can virtually replicate the wound surface at the nanoscale level and create optimal moist conditions for wound healing and skin regeneration. During the clinical trials, MC dressings were very well tolerated by patients, significantly reducing pain during treatment and allowing for painless removal of the dressing from the wound. In shallow wounds, MC dressing promoted growth of the epidermis and in deep wounds shortened the period of scab demarcation. In our opinion, treatment with MC dressings should be continued until an entirely new epidermis appears, otherwise a second necrosis can take place. The MC dressing needs to be changed every day or rewetted to maintain the desired moist environment. Drying of the dressing on the wound causes the effect of squeezing (pressing). The results to date suggest that MC dressing might be effective in reducing scar formation. In our opinion, cellulose dressings should be applied to fresh wounds immediately after burn injury. Considering this and the capability to produce MC dressing of different sizes and shapes, we think that, in addition to hospitals and ambulatories, MC should be widely used in all emergency responding units such as police, emergency, firemen, army, etc. The unique features of the MC have been demonstrated to be effective in the burn wound healing response.

Acknowledgments

This work has been financially supported by the Grants No. 4 TO9B 056 24 and PBZ-MIN-007/PO4/2003 from the Polish State Committee for Scientific Research. The authors are grateful to Professor R.M. Brown, Jr. and D. Nobles from the Section of Molecular Genetics and Microbiology, University of Texas at Austin, USA for helpful discussions during preparation of this manuscript.

REFERENCES

Alvarez O.M., Patel M., Booker J., and Markowitz L. 2004. Effectiveness of biocellulose wound dressing for the treatment of chronic venous leg ulcers: results of a single center randomized study involving 24 patients. Wounds 16:224–233.

Balasubramani M., Kumar T.R., and Babu M. 2001. Skin substitutes: a review. Burns 27:534–544.

Bielecki S., Krystynowicz A., Turkiewicz M., and Kalinowska H. 2002. Bacterial cellulose. In: Steinbuchel A. (ed.) Biopolymers: Vol. 5. Polysaccharides I. Wiley-VCH Verlag GmbH, Munster, Germany, pp. 37–90.

Brown, Jr. R.M. 1996. The biosynthesis of cellulose. Pure Appl Chem 10:1345–1373.

Czaja W., Romanovicz D., and Brown, Jr. R.M. 2004. Structural investigations of microbial cellulose produced in stationary and agitated culture. Cellulose 11:403–411.

Delatte S.J., Evans J., Hebra A., Adamson W., Othersen H.B., and Tagge E.P. 2001. Effectiveness of beta-glucan collagen for treatment of partial-thickness burns in children. J Pediatr Surg 36:113–118.

Demling R.H. and DeSanti L. 1999. Management of partial thickness facial burns (comparison of topical antibiotics and bio-engineered skin substitutes). Burns 25:256–261.

Fontana J.D., de Sousa A.M., Fontana C.K., Torriani I.L., Moreschi J.C., Gallotti B.J., de Sousa S.J., Narcisco G.P., Bichara J.A., and Farah L.F. 1990. *Acetobacter* cellulose pellicle as a temporary skin substitute. Appl Biochem Biotechnol 24/25:253–264.

Gallin W.J. and Hepperle B. 1998. Burn healing in organ cultures of embryonic chicken skin: a model system. Burns 24:613–620.

Hartford C.F. 1997. Care of outpatient burns. In: Herndon D. (ed.) Total Burn Care. Saunders, Philadelphia, p. 71.

Hestrin S. and Schramm M. 1954. Synthesis of cellulose by *Acetobacter xylinum*: II. Preparation of freeze-dried cells capable of polymerizing glucose to cellulose. Biochem J 58:345–352.

Innes M.E., Umraw N., Fish J.S., Gomez M., and Cartotto R.C. 2001. The use of silver coated dressings on donor site wounds: a prospective, controlled matched pair study. Burns 27:621–627.

Jones I., Currie L., and Martin R. 2002. A guide to biological skin substitutes. Br J Plast Surg 55:185–193.

Klemm D., Schumann D., Udhardt U., and Marsch S. 2001. Bacterial synthesized cellulose – artificial blood vessels for microsurgery. Progr Polym Sci 26:1561–1603.

Krystynowicz A., Czaja W., Pomorski L., Kołodziejczyk M., and Bielecki S. 2000. The evaluation of usefulness of microbial cellulose as wound dressing material. 14th Forum for Applied Biotechnology, Proceedings Part I, Meded Fac Landbouwwet-Rijksuniv Gent, Gent, Belgium, pp. 213–220.

Krystynowicz A., Czaja W., Wiktorowska-Jezierska A., Gonçalves-Mi kiewicz M., Turkiewicz M., and Bielecki S. 2002. Factors affecting the yield and properties of bacterial cellulose. J Ind Microbiol Biotechnol 29:189–195.

Latarjet J. 1995. A simple guide to burn treatment. Burns 21:221–225.

Loss M., Wedler V., Künzi W., Meuli-Simmen C., and Meyer V.E. 2000. Artificial skin, split-thickness autograft and cultured autologous keratinocytes combined to treat a severe burn injury of 93% of TBSA. Burns 26:644–652.

Manigandan C. and Dhanaraj P. 2004. An innovative, cost-effective, pressure-relieving device for burned ears. Burns 30:269–271.

Park S.N., Kim J.K., and Suh H. 2004. Evaluation of antibiotic-loaded collagen-hyaluronic acid matrix as a skin substitute. Biomaterials 25:3689–3698.

Prasanna M., Mishra P., and Thomas C. 2004. Delayed primary closure of the burn wounds. Burns 30:169–175.

Quinn K.J., Courtney J.M., Evans J.H., Gaylor J.D.S., and Reid W.H. 1985. Principles of burn dressings. Biomaterials 6:369–377.

Ring D., Nashed W., and Dow T. 1986. Liquid loaded pad for medical applications. US Patent No. 4588400.

Roques C. 2002. Pressure therapy to treat burn scars. Wound Repair Regen 10:122–125.

Ross P., Mayer R., and Benziman M. 1991. Cellulose biosynthesis and function in bacteria. Microbiol Rev 55:35–58.

Ruiz-Cardona L., Sanzgiri Y.D., Benedetti L.M., Stella V.J., and Topp E.M. 1996. Application of benzyl hyaluronate membranes as potential wound dressings: evaluation of water vapour and gas permeabilities. Biomaterials 17:1639–1643.

Still J., Glat P., Silverstein P., Griswold J., and Mozingo D. 2003. The use of a collagen sponge/living cell composite material to treat donor sites in burn patients. Burns 29:837–841.

Svensson A., Nicklasson E., Harrah T., Panilaitis B., Kaplan D.L., Brittberg M., and Gatenholm P. 2005. Bacterial cellulose as a potential scaffold for tissue engineering of cartilage. Biomaterials 26:419–431.

Vloemans A.F.P.M., Soesman A.M., Kreis R.W., and Middelkoop E. 2001. A newly developed hydrofibre dressing, in the treatment of partial-thickness burns. Burns 27:167–173.

Walker M., Hobot J.A., Newman G.R., and Bowler P.G. 2003. Scanning electron microscopic examination of bacterial immobilization in a carboxymethyl cellulose (AQUACEL) and alginate dressings. Biomaterials 24:883–890.

Watanabe K., Tabuchi M., Morinaga Y., and Yoshinaga F. 1998. Structural features and properties of bacterial cellulose produced in agitated culture. Cellulose 5:187–200.

Wu P., Fisher A.C., Foo P.P., Queen D., and Gaylor J.D.S. 1995. *In vitro* assessment of water vapour transmission of synthetic wound dressings. Biomaterials 16:171–175.

CHAPTER 18

CELLULOSE AS A SMART MATERIAL

JAEHWAN KIM*

Center for EAPap Actuator, Department of Mechanical Engineering, Inha University, 253 Yonghyun-Dong, Nam-Ku, Incheon 402-751, South Korea

Abstract

Cellulose-based electroactive papers (EAPap) are studied as a smart material. Various kinds of paper fibers are tested and cellulose paper is found to be a possible candidate for EAPap. The performance of cellulose-based EAPap actuators is investigated. Regenerated cellulose papers exhibit remarkable performance; 4 mm of tip displacement and 1.11 mN blocking force are observed from the 30 mm EAPap in the presence of 0.25 kV/μm excitation voltage. This actuation voltage per unit thickness is quite low compared to other electronic EAP materials. The electrical power consumption was 10 mW/cm^2. This power usage is promising since it can be operated with microwave power, which is attractive for many applications.

The environmental effects of humidity and temperature on the performance of EAPap are studied. As humidity increases, the displacement increases due to the increase of mobility and the decrease of stiffness. At 30°C, the best performance is observed. This temperature may be associated with the ion mobility of EAPap samples. The mechanical properties of EAPap are tested for cellulose-based papers. In the mechanical test, the typical Young's modulus of EAPap ranges from 4 to 9 GPa, which is quite high compared to other EAP materials.

The role of inherent polarization and ionic transport effects in actuation mechanism of EAPap actuators are investigated. To physically investigate the actuation mechanism, several tests are performed. X-ray diffraction (XRD) spectra are compared before and after electrical activation and the possibility of crystalline structure change is observed. Dielectric property measurement indicates a dependence of the dielectric constant on fiber direction, as well as on frequency, humidity, and temperature. Thus, we conclude that piezoelectric effect and ionic migration effect are in the EAPap at the same time associated with dipole moment of cellulose paper ingredients. The amount of these effects may depend on environmental condition.

Since cellulose-based EAPaps are quite simple to fabricate, lightweight, and utilize low-excitation voltage, a number of applications including flapping wing for flying

* For correspondence: Tel: +82-32-860-78326; Fax: +82-32-868-1716; e-mail: jaehwan@inha.ac.kr

R.M. Brown, Jr. and I.M. Saxena (eds.), Cellulose: Molecular and Structural Biology, 323–343.

objects, flexible speakers, active sound absorbing materials, and smart shape control devices may be accrued within a foreseeable future. Possible applications are addressed with some challenges in EAPap research.

Keywords

electroactive paper (EAPap), ion migration effect, piezoelectric effect, regenerated cellulose, smart material.

1 INTRODUCTION

Smart materials can sense changes in the environment and generate a useful response. In such materials both sensing and actuating functions with the appropriate controls must be integrated and comprise the central control points of the material (Spillman et al. 1996). Smart materials provide "smartness," a functionality that adds significant value to such materials, technologies, or end products. Smartness enables system performance enhancements that are not possible with traditional nonsmart approaches. The applications of smart materials are numerous and varied.

In the last 10 years, the field of smart materials has received much attention as a result of the development of new electroactive polymer (EAP) materials that exhibit a large displacement (Bar-Cohen 2004). This characteristic is a valuable attribute that has enabled a myriad of potential applications, and it has evolved to offer functional similarity to biological muscles. The potential to operate biologically inspired mechanisms driven by EAP will offer capabilities that are currently considered science fiction. EAP materials are able to offer a range of performance and characteristics that may not be reproduced by other technologies. Therefore, it is certain that EAP materials have a promising future for applications such as biologically inspired actuators driving various mechanisms for manipulation and mobility including microrobots, microflying objects, and animatronic devices. The field of EAP is broad and offers enormous potential for many applications. Much of the ongoing EAP research tends to focus on the development and understanding of the new polymer materials.

Generally, EAP materials are divided into two major categories based on their activation mechanism: electronic (driven by electric field or Coulomb forces) and ionic (involving mobility or diffusion of ions). Electronic polymers, such as electrostrictive, electrostatic, piezoelectric, and ferroelectric, require a high activation field close to the breakdown level. An exceptionally high electrostrictive response has been found in electron-irradiated poly(vinylidene fluoride-trifluoroethylene) [P(VDF-TrFE)] copolymer (Zhang et al. 1998). It is the electric field-induced change between nonpolar and polar regions that are responsible for the large electrostriction observed in this polymer. As large as 4% electrostrictive strains can be achieved at low frequency drive fields having amplitudes of about 150 V/μm. Dielectric elastomer-based EAPs have been under investigation for the last 10 years (Perline et al. 2000). Dielectric elastomer transducers are rubbery polymer materials with compliant electrodes that have a large electromechanical response to

an applied electric field. The induced strain is proportional to the square of electric field, multiplied by the dielectric constant and inversely proportional to the elastic modulus. A graft-elastomer EAP was developed that exhibits not only large electric field-induced strain (4%) but also a relatively high elastic modulus (560 MPa) (Su et al. 1999). By combining this graft elastomer with a piezoelectric polymer, an electrostrictive-piezoelectric multifunctional polymer blend system has been developed. *The critical problem of these electronic EAPs is that they need high voltage for activation*, which results in high electrical strain-related difficulties, such as voltage breakdown shielding, packaging, miniaturization, and driver configuration in device implementations.

In contrast, ionic EAP materials, such as gels, polymer-metal composites, conductive polymers, and carbon nanotubes require low drive voltage. However, their wetness must be maintained, and except for conductive polymers, it is difficult to sustain DC-induced displacements. Ionic polymer gels can be synthesized to produce strong actuators having the potential that matches or is comparable to the force and energy density of biological muscles. Muscle-like actuators have been made from bilayers of cross-linked polyacrylamide and polyacrylic acid hydrogels sandwiched between electrodes (Calvert and Liu 1998). The polyacrylic acid responds to applied positive polarity field by contracting and expelling water which is taken up by the polyacrylamide layer. When activated, these gels bend as the cathode side becomes more alkaline and the anode side more acidic. However, the response of this multilayered gel structure is relatively slow because of the need to diffuse ions through the gel. Ionomeric polymer-metal composites (IPMCs) are a well-known EAP that bends in response to an electrical activation as a result of mobility of cations in the polymer network (Shahinpoor et al. 1998; Tadokoro et al. 2000). A relatively low voltage is required to stimulate bending in IPMCs, whereas the base polymer provides channels for mobility of positive ions in a fixed network of negative ions on interconneted clusters. However, the slow response and the need of wetness restrict the applications. Conducting polymers (CP) typically function via a reversible counterion insertion and expulsion that occurs during redox cycling (Madden 1999). Most studies to date have investigated the contractile properties of either two CPs, polypyrrole or polyaniline. Researchers have reported the construction and characterization of a linear actuator prototype made of polyaniline fibers, a solid polymer electrolyte, and a spiral-shaped copper wire as counterelectrode (Otero and Sansina 1995). CP actuators have been used to develop a microrobotic arm with individual controllable hinges for an elbow, a wrist and 2–4 fingers by using CP actuators (Jager et al. 2000). Single-walled carbon nanotubes (SWNTs) were shown to generate higher stresses than natural muscle and higher strains than high-modulus ferroelectrics (Baughman et al. 1999). Like natural muscles, the macroscopic actuators are assemblies of billions of individual nanoscale actuators.

A bold departure from the current direction of EAP research is required to overcome the current challenges facing these materials, while still using the valuable accomplishments already attained. This is especially true for microinsect robots,

microflying objects, and animatronic devices, all of which require a new and innovative EAP material that is ultralightweight and operates using low power levels. Thus, it is necessary to develop a new EAP actuator with an ultralightweight, fast response, robustness, and low power consumption.

An interesting actuation phenomenon in cellulose-based papers has been reported (Kim et al. 2002). When an electric field was applied on paper, a large displacement with low force was produced. This was the first discovery of the electroactive paper (EAPap) actuator. After a period of research effort, the actuation principle has been partially understood, and cellulose papers have been found to be good candidates for EAPap actuators (Figure 18-1a). When 0.25 V/μm of excitation voltage was applied, more than 4 mm of tip displacement was observed out of the 30 mm long EAPap beam. This excitation voltage is low compared with other electronic EAP materials. These characteristics are very promising for many applications in ultralightweight and micro devices since they can surpass technical barriers of currently available EAPs.

The electrical power requirement of cellulose EAPap actuators is less than 15 mW/cm^2. This low electrical power consumption is promising for achieving a microwave-driven actuator. Cellulose EAPap can be integrated with a microstrip antenna, so called rectenna (rectifying antenna). When microwaves arrive at the rectenna, the microwave power is converted into DC power, and distributed to the EAPap actuator via power allocation device (PAD) circuit. Since rectenna and PAD are thin film based, they can be integrated onto cellulose EAPap, which comprise a remotely-driven EAPap actuator. Since this remote power supply capability does not require any battery, an ultralightweight EAP actuator can be achieved. In addition, the wireless power supply will improve agility

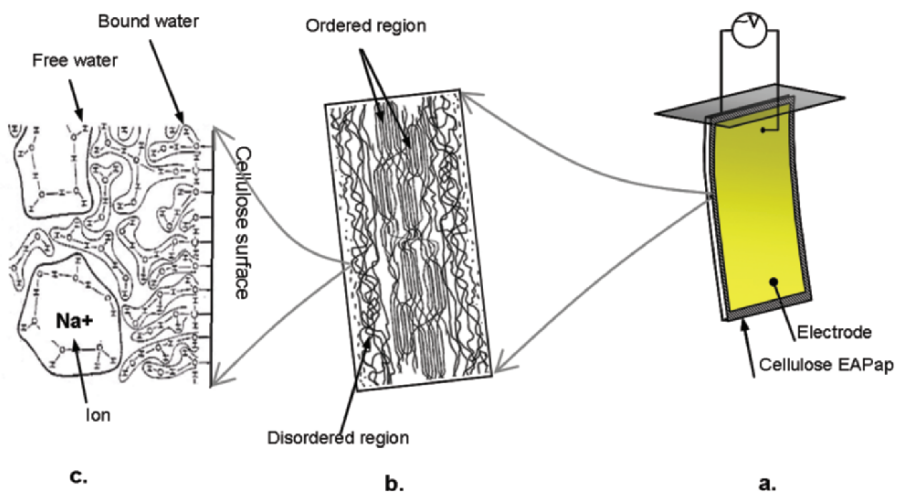

Figure 18-1. Configuration of EAPap bending actuator (Kim et al. 2006c) [Courtesy of ACS] (*See Color Plate of this figure beginning on page 355*)

and allow for longer operational distances of the actuator applied devices. This idea is useful for specific applications that require multifunctional capabilities such as smart skin, ultralightweight space structures, microrobots, flapping wing for insect-like flying objects, and smart wall paper. This chapter describes the development story of EAP actuators, their performance evaluation, the actuation principle, mechanical testing, and potential applications.

2 EXPERIMENTS

2.1 EAPap sample preparation

EAPap is made by depositing thin electrodes on both sides of cellulose paper. Figure 18–1 shows the configuration of cellulose EApap actuator. Paper is a chemically and physically processed composite material derived from vascular and structural tissues of higher plants. The building blocks of this composite material are lignin (a hydrophobic cross-linked polymer), cellulose (a linear partially crystalline polysaccharide), and a collection of other polysaccharides (hemicelluloses, which are very hydrophillic, and extractives). Cellulose consists of unbranched polymers of linked glucose residues arranged in linear chains, where every other glucose residue is rotated ~180° (Brown, Jr. et al. 1996). In nature, cellulose never occurs as a single chain, but exists from the moment of its synthesis as a crystalline array of many parallel, oriented chains called microfibrils, which are its fundamental structural units. The glucan chain length (degree of polymerization) varies from about 2,000 to more than 25,000 glucose residues. Microfibril size can vary from "element fibril," which has approximately 36 chains, to the large microfibrils of cellulosic algae which contain more than 1,200 chains, and are so highly organized that they can diffract as a single crystal (Atalla and Vanderhart 1984).

In the beginning of EAPap research, several kinds of papers with different fibrous natures were selected to investigate their electroactive characteristics: hardwood paper, softwood paper, kraft paper, electrolyte paper, Korean paper, carbon paper and cellophane film. Hardwood paper is made with deciduous trees that have broad leaves, and soft wood paper is from conifers. Kraft paper is made with a chemical pulp that is obtained from wood by placing a chip of it in a pressurized vessel in the presence of hot caustic soda and sodium sulfide. Electrolyte paper is a capacitor tissue paper made with kraft paper immersed in an electrolyte. Korean traditional paper is made of bast fibers of the Korean paper mulberry. Carbon paper is an electroconductive paper made by mixing carbon fibers into chemical pulp. Carbon fibers size is ~8 μm. Cellophane is a regenerated cellulose made by dissolving cellulose fibers into a solution and cast it, which is well-known cellulose xanthate process. Before testing the electrical actuation of EAPaps, SEM picture were taken to examine their surface structure (Figure 18–2). In the preparation of EAPap actuators, a gold electrode is deposited on both sides of paper sheets by means of physical vapor deposition.

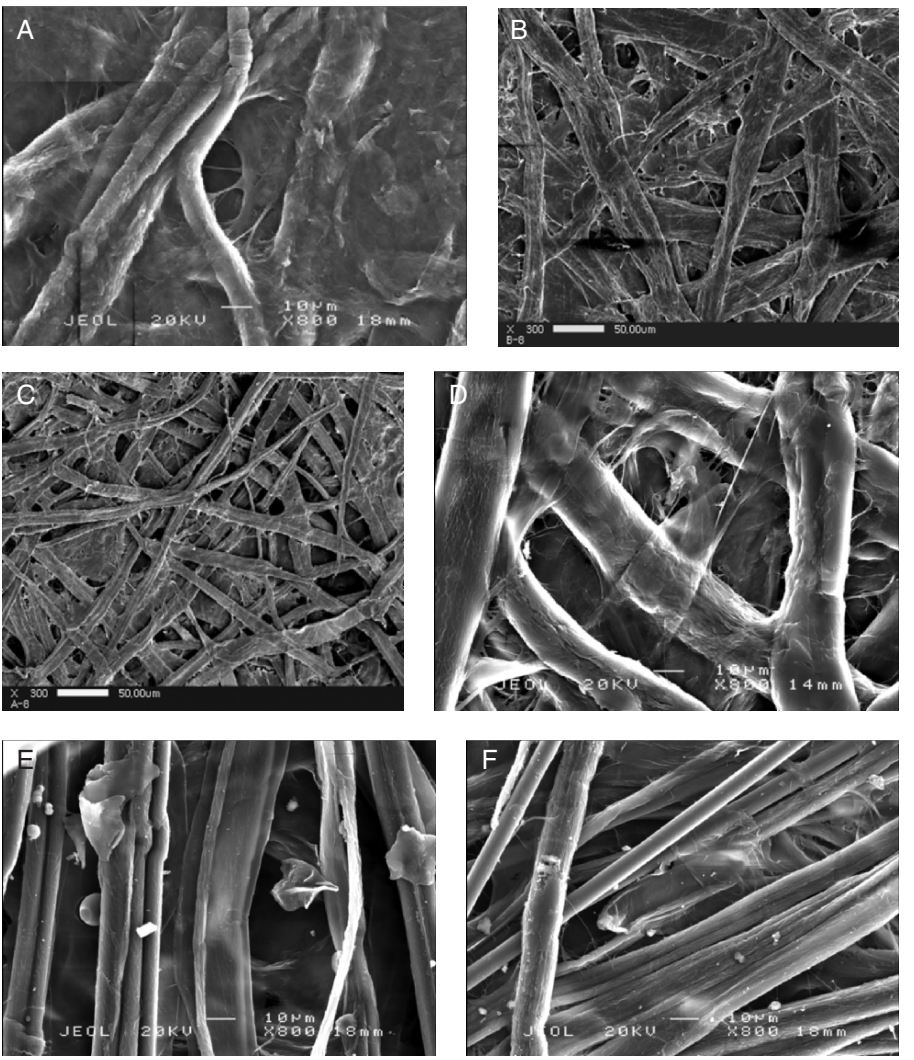

Figure 18-2. SEM of paper samples (×800) B,C: (Kim et al. 2002) [Courtesy of IOP]

The thickness of gold electrodes is about 0.1?μm, which is so thin that its bending stiffness is negligible. The size of sample is 10 × 40 mm and the thickness ranges from 14 to 25 μm.

When the samples were actuated by applying electric field across the electrodes, small bending displacements were observed. Especially, the cellophane EAPap exhibited the best displacement output. Thus, we have focused on regenerated cellulose. For further study, the fabrication process of regenerated cellulose EAPap was setup at our laboratory. Figure 18–3 shows the xanthate cellulose

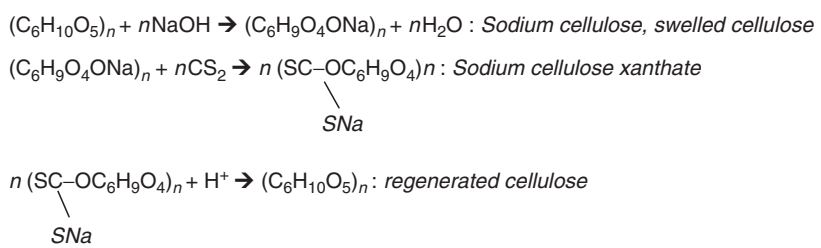

Figure 18-3. Regenerated cellulose process with xanthate cellulose solution

process for regenerated cellulose (Woodings 2001). Cotton pulp was beaten by a beater with water for 1 h and the water was removed by a sand filter. The sodium hydroxide was mixed with the beaten pulp in a three-hole round bottom flask. A stirrer was used to mix them maintaining 70°C with heating mantle. After cooling it, carbon disulphide was added to them and agitated again with nitrogen purging. After aging, a treacle-like yellow solution was obtained. This solution was coated on a glass plate using spin coater (Laurell Technology). The cellulose coated glass was put in the H_2SO_4 bath, and the sample was washed with fresh water. The washed sample was baked at a vacuum dried oven, and gold electrodes were deposited on both sides of it.

2.2 EAPap actuator performance

The performance of EAPap actuators was evaluated in terms of free tip displacement and blocked force. In order to simultaneously acquire the tip displacement signal while an electrical field is applied across the electrodes, a computerized set-up was made (Figure 18–4). An EAPap actuator was supported vertically in an environment chamber that can be controlled the humidity and temperature. Function generator (Agilent 33220A) controlled by a computer sent the excitation voltage to the actuator, and it produced a bending deformation. The tip displacement of the EAPap actuator was measured by the high precision Laser Doppler Vibrometer (Ometron VS100) mounted on an optical table and the signal was converted to the displacement through the Labview software in the computer. To measure the tip blocked force, a microbalance was used. Blocked force is the maximum tip force when the tip of EAPap actuator is fixed. An EAPap actuator was fixed vertically in the environmental chamber by using tongs and the microbalance (Precisa XT220A, micro Newton resolution) was mounted on an optical table. A vertical fixture was placed on the balance and the tip of the actuator was contacted with the fixture. Since the tip of EAPap actuator was contacted by the top of the fixture, a horizontal pushing force on the fixture was converted to the vertical force due to the moment equilibrium of the fixture structure. The pure vertical force was measured by pushed down the balance and the balance after nullifying the initial weight of the vertical fixture.

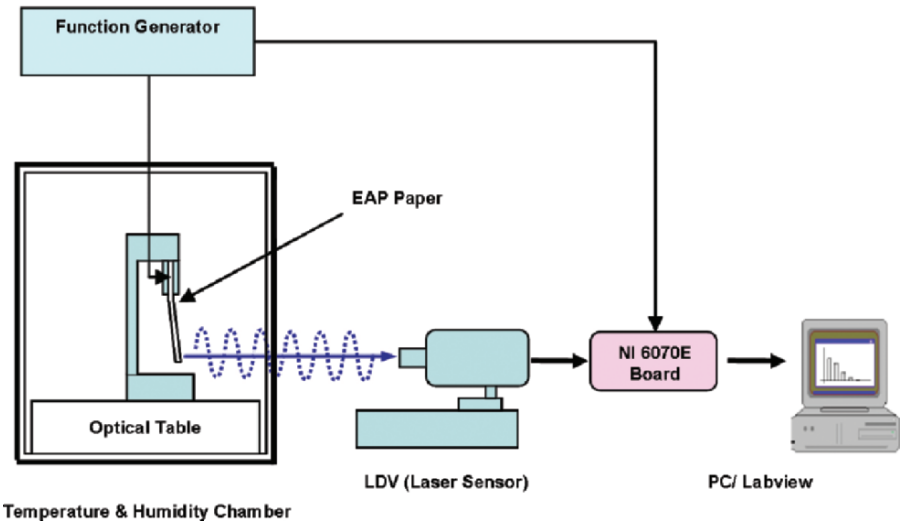

Figure 18-4 .Tip displacement measurement setup (Kim et al. 2004) [Courtesy of SPIE] (*See Color Plate of this figure beginning on page 355*)

Table 18–1 represents the tip displacement of EAPap actuator made with six different papers. Here, "-" means that no significant displacement was observed. Hardwood and softwood paper exhibited a small displacement less than 1 mm. Meanwhile, cellophane EAPap exhibited very large displacement output. Detailed displacement measurements were conducted on the cellophane EAPap actuator.

Figure 18–5 shows the displacement output of the actuator as a function of voltage (V_{p-p}) and relative humidity (%) at 4 Hz. At 5 V, it exhibited the maximum displacement of 4.3 mm. This value corresponds to the electric field strength of 0.25 V/μm, which is very low comparing with other electronic electroactive polymers (150 V/μm) (Su et al. 1999). This low actuation voltage is an advantage of the EAPap actuautor. The tip displacement result shows that the displacement increases with the humidity. Normally, there is a decrease in the elastic modulus of paper when the

Table 18–1. Tip displacement output of EAPap actuator with different papers

Paper	Displacement output
Hardwood paper	0.08 mm (5 Hz)
Softwood paper	0.10 mm (5 Hz)
Kraft paper	–
Electrolyte paper	–
Korean paper	–
Carbon paper	–
Cellophane	4.3 mm (4 Hz)

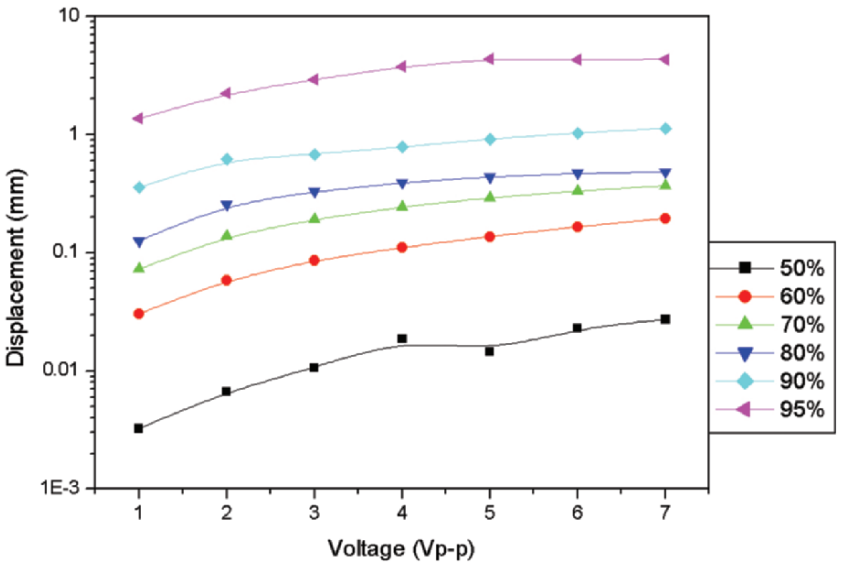

Figure 18-5. Tip displacement of cellophane EAPap actuator with voltage and relative humidity (Kim et al. 2006c) [Courtesy of ACS] (*See Color Plate of this figure beginning on page 355*)

relative humidity is increased. According to O'sullivan's observation, the conductivity of cellophane paper is increased when the relative humidity is increased (Mark 1989). This is due to the increase of mobility in the cellulose. Comparing with other papers that have random fiber orientation, cellophane has its orientation effect. In other words, the elastic moduli in mechanical and transverse directions are different. The cellophane EAPap sample made with 45° from the mechanical direction showed the best tip displacement output. This angle might be associated with the crystal structure for the actuation mechanism of the EAPap actuator.

2.3 EAPap actuation principle

To successfully transit cellulose EAPap actuators into these applications, it is crucial to ascertain the actuation principle responsible for the performance parameters. Based on the cellulose structure and our processing of the cellulose-based EAPap, we believe that the actuation is due to a combination of two mechanisms: ion migration and piezoelectric effect associated with dipolar orientation. In the remainder of this report, we present experimental evidence of both.

Cellulose EAPap material is composed of molecular chains with a dipolar nature. In particular, the crystal structure of cellulose II is monoclinic, which is noncentro-symmetric and exhibits piezoelectric and pyroelectric properties. To investigate the dipole effects in EAPap, thermally stimulated current (TSC) measurement was conducted (Hongo et al. 1996). The classical procedure in TSC includes (1) heating the sample to a given temperature (200°C); (2) applying

the electric field at this temperature for a time *t*; (3) cooling the sample down to room temperature with the field on to freeze-in any dipolar alignment; (4) reheating the sample at a slow rate while monitoring the current to quantify any dipolar alignment that took place in step (2) (350°C); and (5) finally, the sample is reheated one last time while current is monitored once again (350°C). This last step may differentiate between current discharge due to dipolar alignment and real charge injection (space charge); real charge injection may not fully escape the material in one heating. Figure 18–6a shows the depolarized current with temperature with different poling electric fields and (b) does the peak current values as a function of the poling electric field. The depolarization current increases linearly as the poling electric field increases. This behavior is usually indicative of dipole orientation (Turnhout 1999).

Generally, the polarizability of dielectric materials may be separated into several parts. An electronic contribution arises from a displacement of the electron shell relative to a nucleus and an ionic contribution from the displacement of a charged ion with respect to other ions. In cellulose materials that possess molecular groups having permanent dipole moments such as water, the hydroxyl, and carboxyl groups will also make a contribution (Mark 1989). At low frequency all of these parts contribute to the polarizability, as will any free ions (space charges) in the material. As the frequency increases, the space charges and permanent dipoles relax. Space charges are usually the first to relax, followed by the permanent dipole groups. In the cellulose EAPap, the presence of disordered region gives rise to localized states associated with hydrogen bonding of cellulose chains. Since there are many localized states, the release or excitation of the carriers in these states may dominate the charge transfer process. Thus, disordered region mainly contribute to the dipolar orientation, by stabilizing dipoles and leading to a permanent polarization, resulting in a piezoelectric behavior.

Further investigation of the actuation behavior of EAPap material, x-ray diffraction (XRD) was tested on the cellophane EAPap sample before and after the electrical actuation. The cellophane EAPap actuator was activated for several hours, then it was removed from the power source and XRD was performed on the surface of the EAPap sample. XRD was measured with an x-ray diffractometer (D/MAX-2500, Rigaku). XRD patterns using Cu-Ka radiation at 40 kV and 30 mA were recorded using $2\theta = 5–80°$. Figure 18–7 shows the XRD results. Table 18–2 summarizes the XRD peaks before and after the actuation. After actuation, the (110) peak at 12.26° decreased to 12.08° while the (200) peak at 21.64° increased slightly to 22.02°. It is clear that the (110) peak sharpened after the actuation while the (200) peak was changed to blunt. This confirms that the first peak increased and the second peak decreased.

Notice that the small peak at 16.78° started to appear after the electrical activation. This means that some structural change took place during the electrical actuation, which might be associated with the crystallization of disordered region. In other words, recrystallization of disordered cellulose of EAPap sample could be accelerated by molecular rearrangement during the electrical

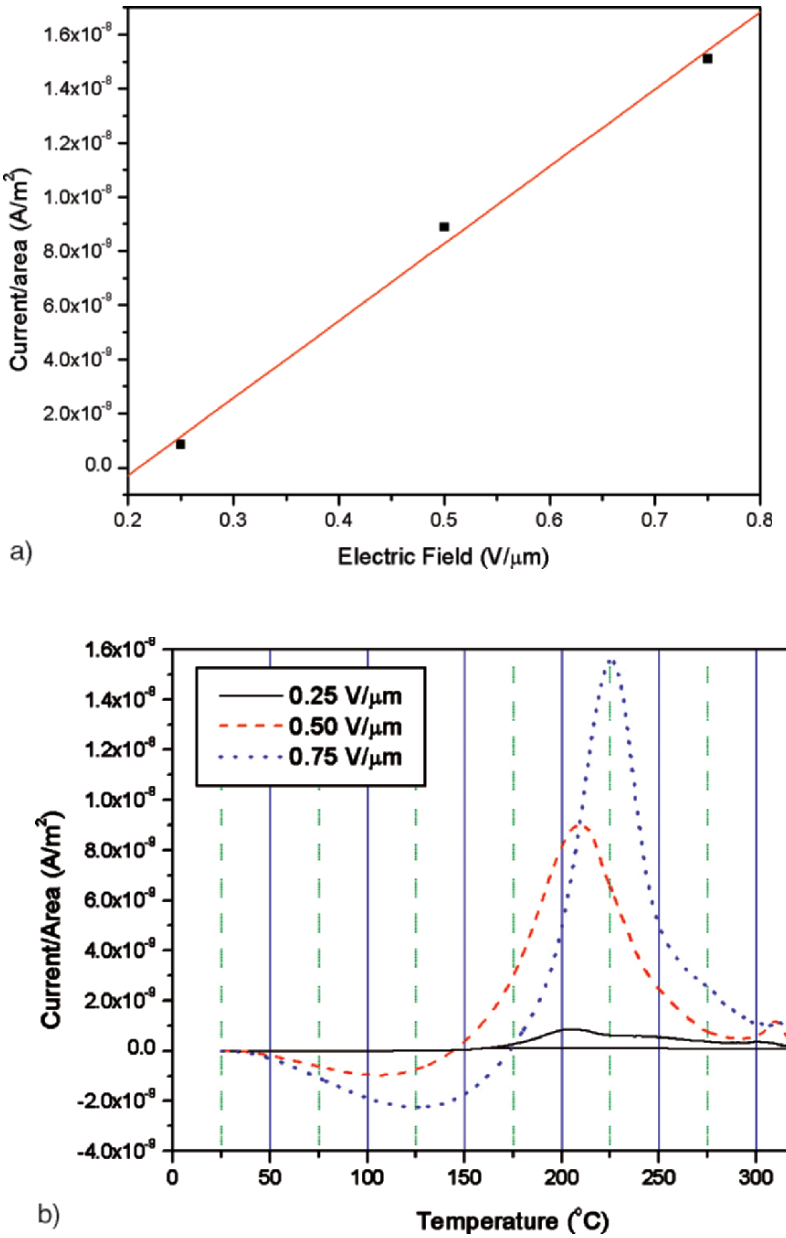

Figure 18-6. TSC results of cellulose EAPap. (**a**) The depolarized current with temperature and different poling electric field. (**b**) The peak current values as a function of the poling electric field (Kim et al. 2006c) [Courtesy of ACS] (*See Color Plate of this figure beginning on page 355*)

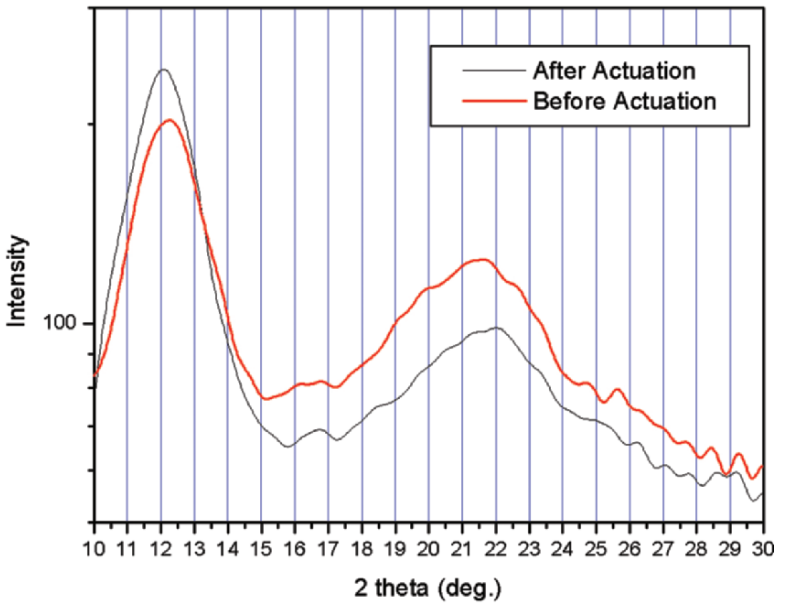

Figure 18-7. XRD of EAPap samples before and after the actuation tests (Kim et al. 2006c) [Courtesy of ACS] (*See Color Plate of this figure beginning on page 355*)

activation, leading to a structure closer to that of cellulose II allomorph. Structural changes of native cellulose crystals have been made by annealing in aqueous alkaline and acid solutions in high temperature (Yamamoto et al. 1989). However, there has not been any report that the cellulose polymorphs can be changed in the presence of electric fields. Our observation may be the first report on the structural change of cellulose by applying electric field. The electrical activation is believed to enhance the recrystallization, which might improve the piezoelectricity of EAPap material.

For the dielectric constant measurement of cellophane EAPap, LCR (inductance, capacitance and resistance) meter (HP4282A) was used, and the frequency ranged from 20 Hz to 10 MHz. EAPap samples were prepared parallel (mechanical), perpendicular (transverse), and 45° to the fiber orientation. Figure 18–8 shows

Table 18–2. X-ray peaks of cellulose EAPap material before and after electrical actuation (the last two columns show the peaks for Cellulose I and II for comparison (Klemm et al. 2005))

Peaks	Before actuation	After actuation	Cellulose I	Cellulose II
(110)	12.26	12.08	14.80	12.10
($1\bar{1}0$)	16.78	16.74	16.30	19.8
(200)	21.46	22.02	22.60	22.0

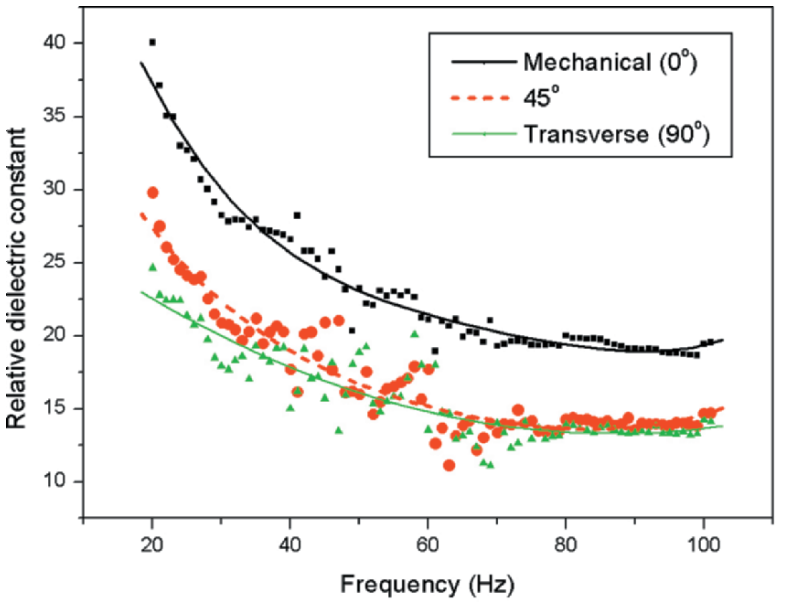

Figure 18-8. Dielectric constant test results (*See Color Plate of this figure beginning on page 355*)

the measured dielectric constants versus frequency for three different orientations of cellulose paper. The dielectric constants decreased as the frequency increased. Regarding the directional effect, the mechanical direction value is greater than other directions. This is due to the microfibril alignment along the mechanical direction. A remarkable result is that the range of dielectric constants is higher than that of ordinary papers. This high dielectric property might be associated with piezoelectric effect.

Generally, papers are known as ionic conductors. Cellophane EAPap material is a sheet of regenerated cellulose. Morphologically, regenerated cellulose has ordered and disordered regions, in which the ordered domains are mostly crystalline (Eichhorn 2005). The disordered molecules retain preferential direction parallel to the chains in the microfibrils, and they form surface disorder on the microfibrils. Figure 18–9b shows the concept of microfibril. The cellophane EAPap material has large regions of disordered cellulose chains, where water molecules can be found attached to hydroxyl groups (Figure 18–9c). During the paper making process, some sodium ions could remain in the paper fiber. We observed that large amount of sodium ion (nearly 1,700 ppm) remained in the cellulose film used for the EAPap actuator. When an external electric field is applied, these ions can be mobile and migrate to the negative electrode. In addition, the molecular motion of free water in disordered region is less restricted by the cellulose molecules, and the water molecules can be interacted with ions in the cellulose.

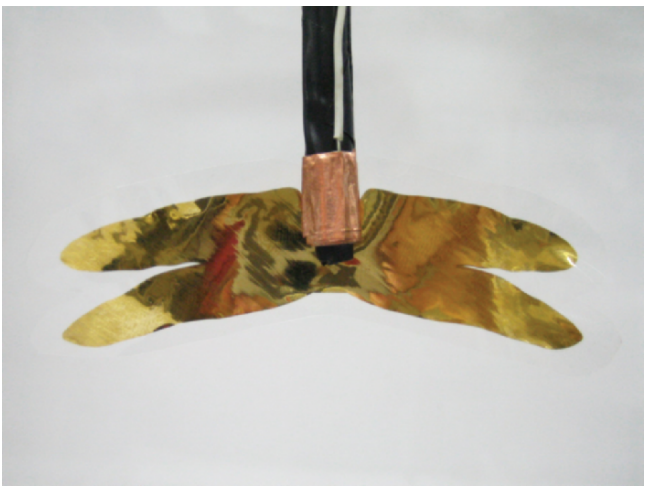

Figure 18-9. Photograph of EAPap actuator (*See Color Plate of this figure beginning on page 355*)

In the presence of an electric field, the sodium ions surrounded with free water molecules can move to the cathode. Selective ionic and water transport across the polymer under an electric field results in volumetric changes, which in turn lead to bending. When a DC electric field was applied, the cellulose EAPap actuator was bent to the positive electrode, which confirmed the above explanation. The ambient humidity effect on the EAPap actuator performance is further evidence, where ion transport is facilitated when humidity intake is higher. Thus, the actuation principle of cellulose EAPap might be a combination of piezoelectric and ionic migration effects associated with the dipole moment of cellulose material.

2.4 Mechanical test of EAPap

Cellulose film (cellophane) used for EAPap was mechanically tested under ASTM Standard D 882–97, the standard for measuring tenisle elastic properties of this plastic sheeting. The testing machine used was the SATEC T1000 tension test machine. This film has an easily identifiable mechanical direction, labeled 0°-direction, on which cellulose fibers are oriented. The three directions tested are defined relative to the 0° direction as 0°, 45°, and 90°. Thickness of the cellulose film was 16 μs. The graph in Figure 18–10 shows a typical test results for the cellulose film in 0° direction. The initial elastic modulus was determined from the high, initial slope of the stress-strain curve. Its value is 9.2 GPa, which is an order of magnitude higher than other EAP materials. This result is very promising for high force output of EAPap actuators. A second quite pronounced quasiconstant slope was found beginning at ~20% of the failure strain or at ~70% of the failure stress. This modulus was dubbed the plastic

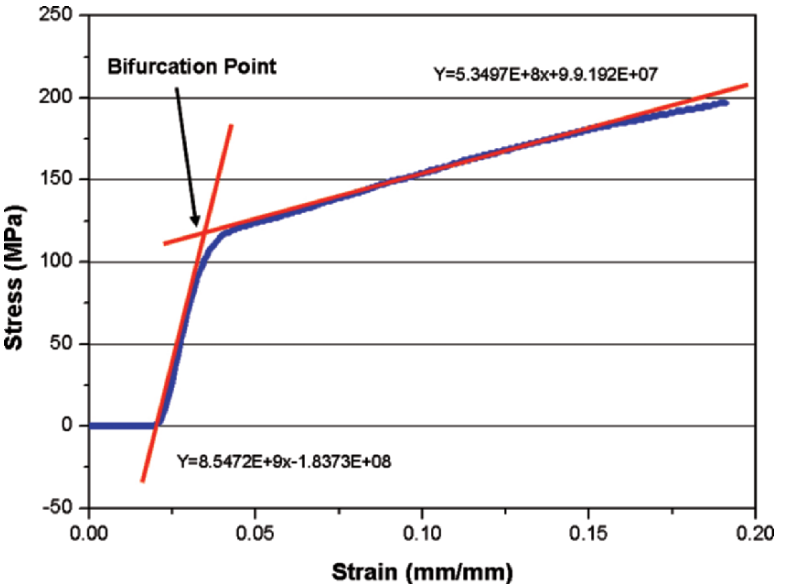

Figure 18-10. Pull test result of cellulose based EAPap (*See Color Plate of this figure beginning on page 355*)

modulus, E_p. The bifurcation point (σ_b,ε_b) was determined by passing a best fit straight line along the initial portion of the stress-strain curve and a second straight line along the secondary portion of the stress-strain curve and finding the intersection point. The first slope may be associated with the strength of cellulose microfibrils, while the mechanical strength of amorphous part of cellulose is dominantly related with the second slope. The strength at the bifurcation point is termed as yield strength and the strength before rupture is ultimate strength. Table 18–3 shows the elastic modulus, plastic modulus, yield strength, and ultimate strength of a cellulose film that is used for EAPap in the 0°, 45°, and 90° orientations.

The cellulose film used for EAPap is anisotropic, decreasing its strength from the mechanical direction to the transverse direction.

When cellulose EAPap material is used in its specific applications, the cellulose paper may experience either extended periods of constant loading or constant strain. A transient response where deformation occurs due to constant loading for an extended period of time is called creep. A transient response that occurs due to constant deformation is called relaxation. Figure 18–11 contains the creep plot for the cellulose film oriented at 0°. The load ranged from 30–75% of the yield strength of the cellulose film. As is noted in the graph, when the load values approached to 60 MPa, the viscoelastic response changed from one with a decreasing strain rate to one where the strain rate was constant. This material behavior is possibly linearly viscoelastic. Microfibrils provide the primary elastic properties of the cellulose film

Table 18–3. Static mechanical properties of cellulose film: elastic modulus (E_1), plastic modulus (E_2), yield strength (σ_b), ultimate strength (σ_u) (MPa)

Orientation	E_1	E_2	σ_b	σ_u
0	9,213	444	132	199
45	5,971	110	106	136
90	5,682	35	86	96

material. Although microfibril failure may occur at any load, there may be a critical load where there is no longer enough intact microfibrils to decrease the strain rate to zero. However, this load may still not apply enough stress to sufficiently increase the strain rate beyond some constant value and bring the cellulose film to failure.

Figure 18–12 contains the relaxation plots for the cellulose film oriented at 0°. The strains applied are 1% and 2%. These strain values were up to 60% of the ultimate strains determined from previous testing. Unlike the creep data analysis, there appears to be no change in the viscoelastic behavior as the strain values increased. The responses appear to be linearly viscoelastic and do not vary according to load level. These results were in line with expectations. Relaxation at the microstructure level may be a result of rearrangement of hydroxyl groups in amorphous regions of cellulose. Also, bonding between microfibrils or

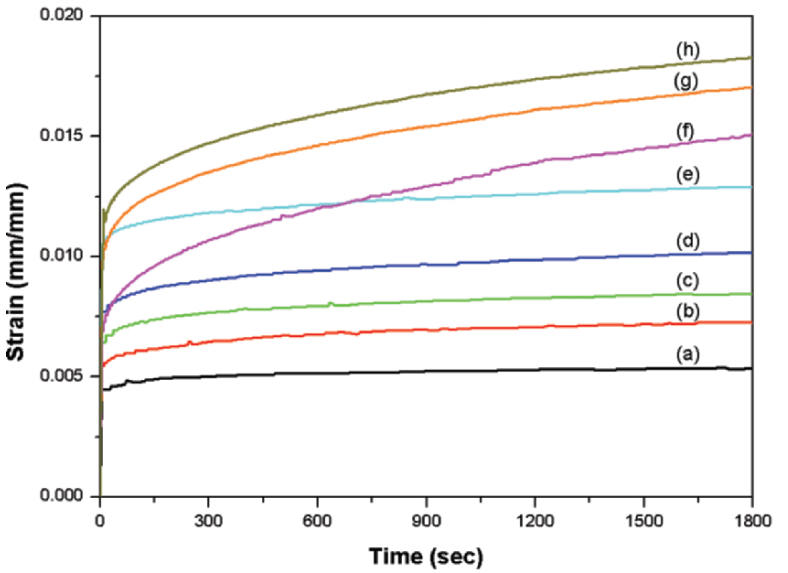

Figure 18-11. Strain response under the constant stress. (**a**) 10 MPa, (**b**) 15 MPa, (**c**) 20 MPa, (**d**) 22.5 MPa (**e**) 25 MPa, (**f**) 27.5 MPa, (**g**) 30 MPa, and (**h**) 32.5 MPa (*See Color Plate of this figure beginning on page 355*)

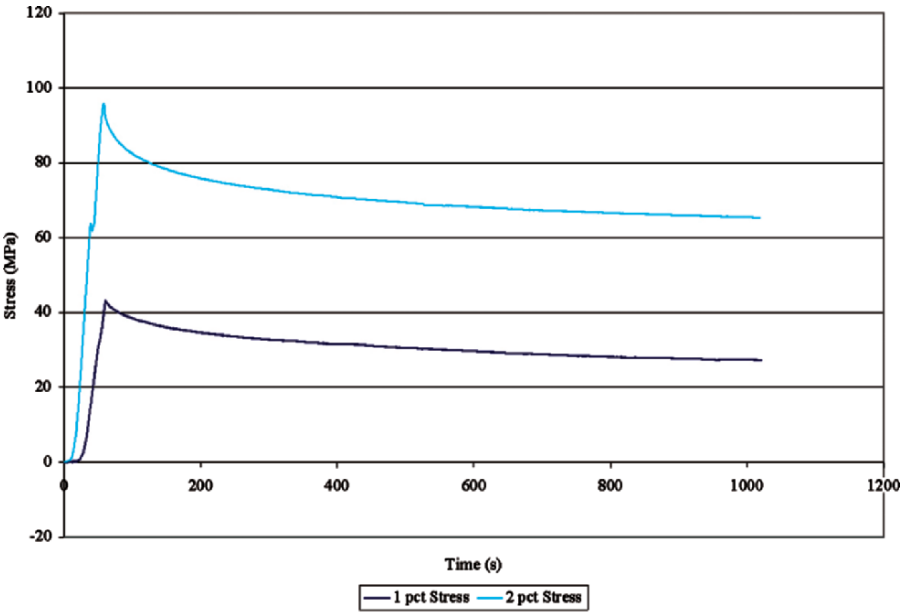

Figure 18-12. Stress response under the constant strain: 1% and 2% strains (*See Color Plate of this figure beginning on page 355*)

between microfibrils and the matrix could be slipping or breaking. As the strain approached the ultimate load for the cellulose paper, permanent damage had occurred. Therefore, relaxation was rapid and there was no residual strength.

3 POTENTIAL APPLICATIONS

In exploiting many of the unique capabilities of EAPap actuators for applications, innovative actuators and devices should include not only the features that exceed the shortcomings of existing EAP materials, but also address other relevant issues such as device-specific configuration design, power, and control. The low electrical power consumption of cellulose EAPap material is promising for achieving a microwave-driven actuator. Figure 18–13 shows the concept of microwave-driven EAPap actuator. Cellulose EAPap can be integrated with a microstrip antenna, so called rectenna (rectifying antenna). When the microwave arrives at the rectenna, it converts the microwave power into DC power, and this power is distributed to the EAPap actuator via PAD circuit. Since rectenna and PAD are thin film based, they can be integrated onto cellulose EAPap, which comprise a remotely driven EAPap actuator. This idea is useful for specific applications that require multifunctional capabilities such as smart skin, ultralightweight space structures, microrobots, flapping wing for insect-like flying objects, and smart wall. So far, rectennas have

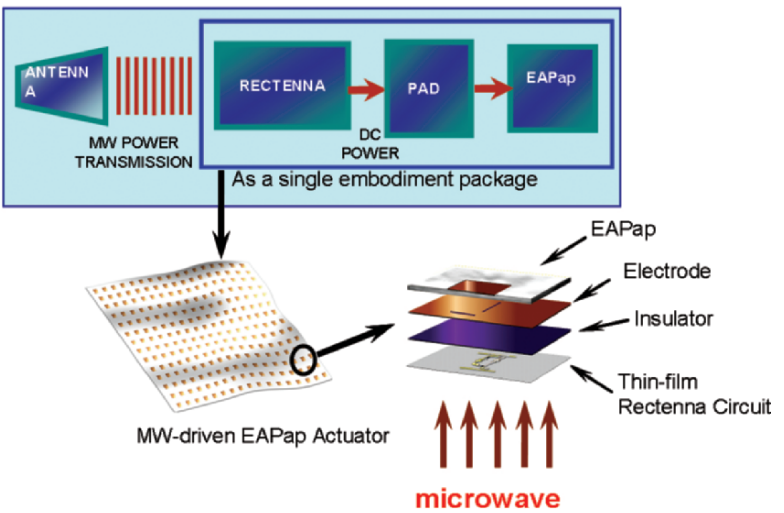

Figure 18-13. Concept of microwave-driven EAPap actuator (*See Color Plate of this figure beginning on page 355*)

been fabricated on a flexible membrane, and microwave power transmission has been successfully demonstrated in a laboratory level experiment, which is sufficient to activate EAPap actuators. Since Heinrich Hertz first tested the concept of microwave power transmission, significant tests have already been completed using microwave power transmission (Kim et al. 2006b).

Microwave power transmission is an off-board source of power such that the weight of target system can be ultimately reduced by eliminating the need of a battery. The thin-film technology developed for semiconductor microfabrication enables the fabrication of rectennas in a miniaturized scale and at low cost. The use of high frequency microwaves, such as K-band (30 GHz) and W-band (90 GHz), allows a dense population rectenna array that can increase the efficiency of the receiving electrical power.

The development of niche applications is important because they will bring rapid revolutionary improvements that propel the capabilities of EAPaps and nurture a wide range of technology transfer. Based upon the unique capabilities of EAPap actuators and utilizing microwave power transmission, niche applications such as a microwave-driven linear actuator, smart wall paper, animatronics, microrobots, flapping wing for microflying objects, and smart membrane skin for ultralightweight space structures can be developed. Table 18–4 shows some the microwave-driven EAPap applications and the potential advantages.

Some of the applications appear to be exotic in that they are based on devices or systems that do not yet commonly exist or are simply not feasible with traditional actuator technologies (Figure 18–14).

Table 18–4. Representative applications for microwave-driven EAPap

Application	Potential advantages of EAPap	Current EAP materials and disadvantages
Robotic, or prosthetic actuators	Reconfigurable ability in novel shape; direct drive; lightweight; ability to integrate actuators and structure	Conducting polymers Wetness
Loud speaker, smart wall paper	Flat-paper loudspeakers on walls	Dielectric elastomers
	Active/semiactive noise suppression	High voltage
Smart skin	Can enable new functionality in large area arrays Allows large out-of-plane motions Lighter and cost effective	Shape alloy film, carbon nanotubes Microfabrication difficulty
Flapping wing	Light weight, low power consumption, remote power supply, cheap	IPMC, Dielectric elastomers Wetness, high voltage
Entertainment industry	Offering attractive characteristics to produce more realistic models of living creatures at lower cost	Dielectric elastomers High voltage
MEMS	Paper-MEMS Biodegradable, cheap	None

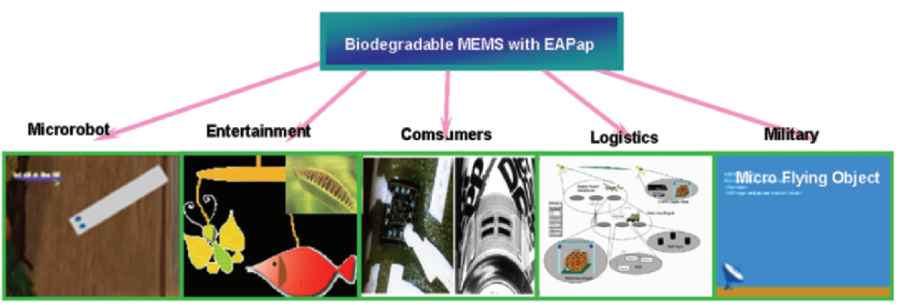

Figure 18-14. Applications of microwave-driven EAPap actuators (*See Color Plate of this figure beginning on page 355*)

4 SUMMARY

In this report, cellulose has been investigated as a smart material. Various kinds of paper fibers were tested, and cellulose paper was found to be a good candidate for EAPap. The performance of cellulose EAPap actuators was investigated. Regenerated cellulose exhibited a remarkable displacement output. When 0.25 V/μm

of excitation voltage was applied to the paper actuator, 4.3 mm of tip displacement was observed. This actuation voltage per unit thickness is quite low compared to other electronic EAP materials. The environmental effects of humidity and temperature on the performance of EAPap actuator were studied. As humidity increased, the displacement increased due to the mobility increase and the stiffness decrease. The best displacement output was shown at 30°C. This temperature may be associated with the ion mobility of EAPap samples.

The actuation principle of EAPap actuators was investigated in terms of ion migration and piezoelectric effects. To physically investigate the actuation mechanism, several tests were performed. TSC measurement showed a linear relationship of depolarized current with the applied electric field, indicating dipolar orientation. By comparing XRD spectra before and after electrical activation, the possibility of recrystallization in the cellulose material was observed. Dielectric property measurement indicated a dependence of the dielectric constant on fiber direction. Thus, we conclude that the combination of piezoelectric effect and ionic migration effect might be the actuation principle.

By optimizing the piezoelectric effect and the ion migration of cellulose material, oriented EAPap will enable inexpensive and lightweight biomimetic actuators and MEMS devices. Cellulose EAPap material also is promising as biosensors since it is biodegradable, biocompatible, sustainable, capable of broad chemical modification, and has high mechanical stiffness and strength. Control of the disordered regions, recrystallization and orientation of cellulose are all issues that need to be addressed in order for cellulose EAPap to fulfill its promise as a smart material. It is true that there is plenty still to discover and cellebrate in cellulose (Ball 2005).

Acknowledgment

This work was supported by the Creative Research Initiatives (EAPap Actuator) of KOSEF/MOST. The author also would like to thank graduate students, Sungryul Yun, Woochul Jung, Yukeun Kang, and Chunseok Song who worked at the Research Center for EAPap Actuator.

REFERENCES

Atalla R.H. and Vanderhart D.L. 1984. Native cellulose: a composite of two distinct crystalline forms. Science 223:283–285.

Ball P. 2005. In praise of wood. Nat Mater 4:515.

Bar-Cohen Y. 2004. EAP history, current status, and infrastructure. In Bar-Cohen Y. (ed.) Electroactive Polymer (EAP) Actuators as Artificial Muscles. SPIE Press, Washington, pp. 3–42.

Baughman R.H., Cui C., Zakhidov A.A., Iqbal Z., Barisci J.N., Spinks G.M., Wallace G.G., Mazzoldi A., Rosei D.D., Rinzler A.G., Jaschinski O., Roth S., and Kertesz M. 1999. Carbon nanotube actuators. Science 284:1340–1344.

Brown, Jr. R.M., Saxena I.M., and Kudlicka K. 1996. Cellulose biosynthesis in higher plants. Trends Plant Sci 1:149–156.

Calvert P. and Liu Z. 1998. Free form fabrication of hydrogels. Acta Mater 46:2565–2571.

Eichhorn S.J., Young R.J., and Davies G.R. 2005. Modeling crystal and molecular deformation in regenerated cellulose fibers. *Biomacromolecules* 6:507–513.

Hongo T., Koizumi T., Yamane C., and Okajima K. 1996. Thermally stimulated depolarized current (TSDC) analysis on the structural change of regenerated cellulose membranes caused by the change in water content. Polym J 28:1077–1083.

Jager E.W., Inganas O., and Lundstorm I. 2000. Microrobots for micrometer-size object in aqueous media: potential tools for single cell manipulation. Science 288:2335–2338.

Kim J., Song C.S., and Yun S.R. 2006a. Cellulose based electro-active papers: performance and environmental effects. Smart Mater Struct 15:719–723.

Kim J., Seo Y-B. 2002. Electro-active paper actuators. Smart Mater Struct 11:355–360.

Kim J., Park J-H., and Jeong W-C. 2004. Temperature and humidity effects on electro-active paper actuators. SPIE's 11th Annual Symposium on Smart Structures and Materials:EAPAD, 5385: 508–512.

Kim J., Yang S.Y., Song K., Jones S., and Choi S.H. 2006b. Performance characterization of flexible dipole rectennas for smart actuators. Smart Mater Struct 15:809–815.

Kim J., Yeen S., and Ounaies Z. 2006c. Discovery of cellulose as a smart material. Macromolecules 39:4202–4206.

Klemm D., Heublein B., Fink H.-P., and Bohn A. 2005. Cellulose: fascinating biopolymer and sustainable raw material. Angwe Chem Int Ed 44:3358–3393.

Madden J.D. 1999. Encapsulated polypyrrole actuators. Synthetic Metals 105:61–64.

Mark R.E. 1989. Handbook of Physics and Mechanical Testing of Paper and Paperboard. Marcel Dekker, New York, pp. 171–195.

Otero T.F. and Sansina J.M. 1995. Artificial muscles based on conducting polymers. J Bioelectrochem Bioenergy 38:411–414.

Perline R.E., Kornbluh R.D., Pei Q., and Joseph J.P. 2000. High-speed electrically actuated elastomers with over 100% strain. Science 287:836–839.

Shahinpoor M., Bar-Cohen Y., Simson J.O., and Smith J. 1998. Ionic polymer-metal composites (IPMCs) as biomimetic sensors, actuators and artificial muscles-a review. Smart Mater Struct 7:R15–R30.

Spillman Jr., W.B., Sirkis J.S., and Gardiner P.T. 1996. Smart materials and structures: what are they? Smart Mater Struct 5:247–254.

Su J., Harrison J.S., Clair St. T., Bar-Cohen Y., and Leary S. 1999. Electrostrictive graft elastomers and applications. MRS Symposium Proceedings. Warrendale, PA, 600:131–136.

Tadokoro S., Fukuhara M., Bar-Cohen Y., Oguro K., and Takamori T. 2000. CAE approach in application of Nafion-Pt composite (ICPF) actuators: analysis for surface wipers of NASA MUSES-CN nanorover. SPIE's 7th Annual Symposium on Smart Structures and Materials. Newport Beach, CA.

Turnhout J. 1999. Thermally stimulated discharge of electrets. In Sessler G.M. (ed.), Electrets, Vol. I. Laplacian Press, Morgan Hill, CA, pp. 81–163.

Woodings C. 2001. A brief history of regenerated cellulose. In Woodings C. (ed.), Regenerated Cellulose Fibres. Woodhead Publishing, Cambridge, pp. 5–6.

Yamamoto H., Horii F., and Odani H. 1989. Structural changes of native cellulose crystals induced by annealing in aqueous alkaline and acidic solutions at high temperature. Macromolecules 22:4130–4132.

Zhang Q.M., Bharti V., and Zhao X. 1998. Giant electrostriction and relaxor ferroelectric behavior in electron-irradiated poly(vinylidene fluoride -trifloroethylene) copolymer. Science 280:2101–2104.

INDEX

COLOR PLATES

The Color Plates are indexed by the CHAPTER NO. followed by the FIGURE NO.

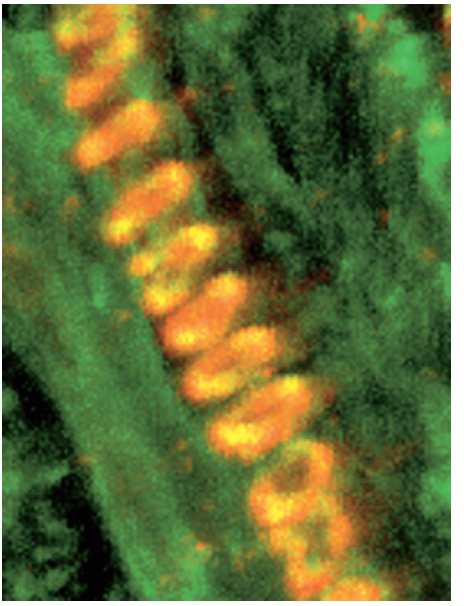

Figure 4-3. Colocalization of IRX3 with microtubules. Project of a series of images obtained from confocal microscopy from immunolabeling on developing xylem. The orange color represents the colocalization of IRX3 (red) with the cortical microtubules (green)

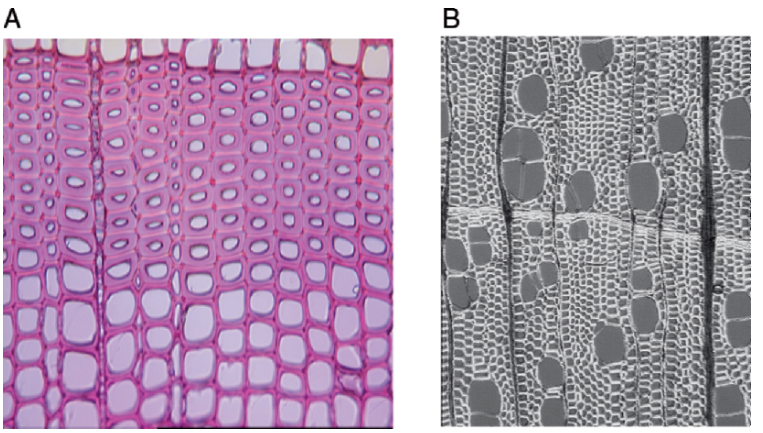

Figure 6-1. Transverse sections of woody tissues in softwood (pine, **a**) and hardwood (birch, **b**). The majority of softwood tracheids occur in organized rows (**a**) while hardwood contains rows of fibers interrupted by large vessels (**b**). Seasonal variation of the cell wall thickness in the softwood tracheids is clearly visible in (**a**). Reproduced from Daniel 2003. With permission

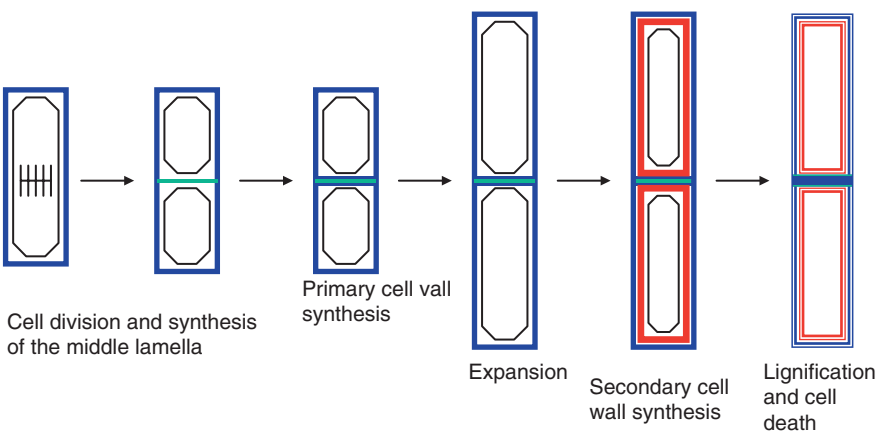

Figure 6-2. A schematic representation of cell wall synthesis during plant cell development

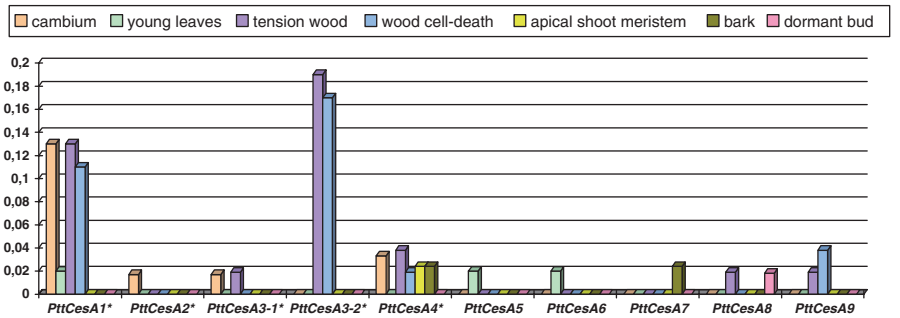

Figure 6-4. Relative abundance of the ten different PttCesA clones in the different tissue specific EST libraries from *Populus tremula* (L.) × *tremuloides* (Michx.). Data from Djerbi et al. 2003

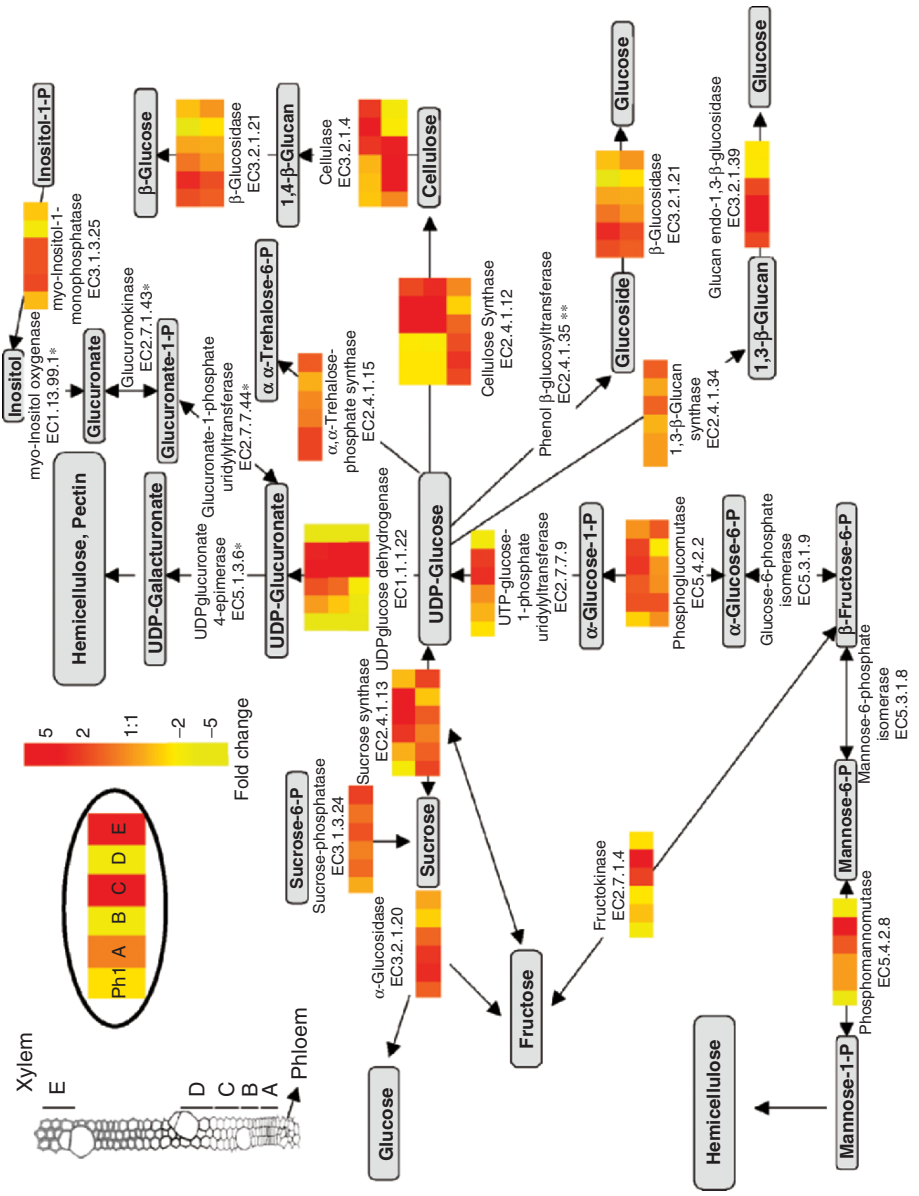
Xylem
Phloem
E
D
C
B
A
Ph1 A B C D E
5
2
1:1
−2
−5
Fold change
Inositol
myo-Inositol oxygenase
EC1.13.99.1*
Inositol-1-P
myo-Inositol-1-monophosphatase
EC3.1.3.25
Glucuronate
Glucuronokinase
EC2.7.1.43*
Glucuronate-1-P
Glucuronate-1-phosphate uridylyltransferase
EC2.7.7.44*
UDP-Galacturonate
UDPglucuronate 4-epimerase
EC5.1.3.6*
UDP-Glucuronate
Hemicellulose, Pectin
α,α-Trehalose-phosphate synthase
EC2.4.1.15
α α-Trehalose-6-P
β-Glucose
β-Glucosidase
EC3.2.1.21
1,4-β-Glucan
Cellulase
EC3.2.1.4
Cellulose
Cellulose Synthase
EC2.4.1.12
UDP-Glucose
UDPglucose dehydrogenase
EC1.1.1.22
UTP-glucose-1-phosphate uridylyltransferase
EC2.7.7.9
α-Glucose-1-P
Phosphoglucomutase
EC5.4.2.2
α-Glucose-6-P
Glucose-6-phosphate isomerase
EC5.3.1.9
β-Fructose-6-P
Mannose-6-phosphate isomerase
EC5.3.1.8
Mannose-6-P
Phosphomannomutase
EC5.4.2.8
Mannose-1-P
Hemicellulose
Fructokinase
EC2.7.1.4
Fructose
Sucrose synthase
EC2.4.1.13
Sucrose
α-Glucosidase
EC3.2.1.20
Sucrose-6-P
Sucrose-phosphatase
EC3.1.3.24
Glucose
Phenol β-glucosyltransferase
EC2.4.1.35 **
Glucoside
β-Glucosidase
EC3.2.1.21
Glucose
1,3-β-Glucan synthase
EC2.4.1.34
1,3-β-Glucan
Glucan endo-1,3-β-glucosidase
EC3.2.1.39
Glucose

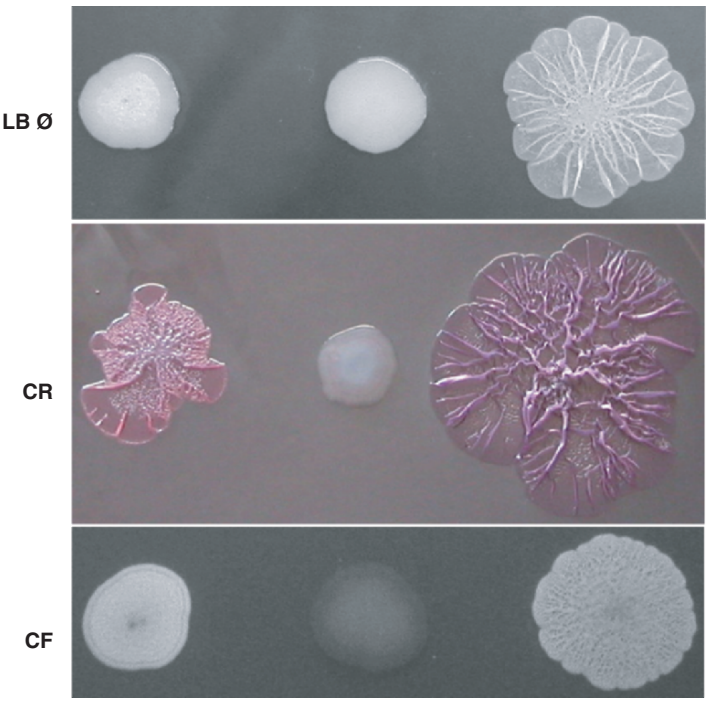

Figure 7-1. Salmonella typhimurium expressing cellulose. (**a**) *S. Typhimurium* colonies grown for 48 h on a regular Luria Bertani agar plate without salt (LBØ), a Congo Red plate (CR) and a Calcofluor plate (CF). *Left*: strain that expresses cellulose; *middle*: strain that does not express cellulose. *Right*: strain that expresses cellulose and curli fimbriae.

Figure 6-6. Expression profiles of selected genes encoding enzymes influencing cellulose synthesis in *Populus tremula* (L.) × *tremuloides* (Michx.) (data from Hertzberg et al. 2001). The tissues sampled were: Ph, phloem; A, cambium; B, early expansion; C, late expansion, early secondary wall synthesis; D, secondary wall synthesis; and E, programmed cell death. In each zone, the expression level of selected genes is given relative to the average expression in the combined zones (A–E). The color code indicates expression levels ranging from fivefold downregulation (*yellow*) to fivefold upregulation (*deep orange*). The metabolites of each pathway are shown in the *gray boxes*. The enzymatic reactions are indicated by *arrows* accompanied by the name and the EC number of the relevant enzyme. If more than one gene has been identified for a given enzyme, the expression level of each gene is shown separately. *No genes have been cloned coding for a protein involved in this reaction. **No plant genes have been found representing a protein involved in this reaction

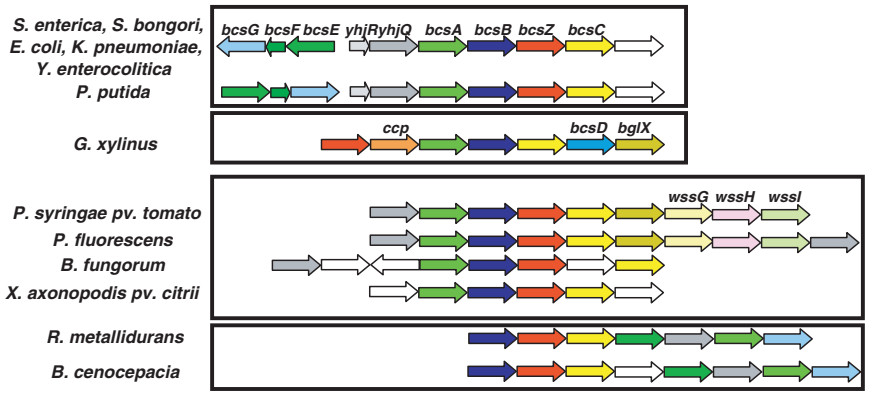

Figure 7-3. Comparison of the cellulose biosynthesis operons *bcs* of *Enterobacteriaceae* with organisatorically closely related *bcs* operons. ORFs that encode homologous genes involved in cellulose biosynthesis have the same color. *White arrows* indicate genes with no apparent association with cellulose production. Sequences: *Salmonella typhimurium* (AJ315148); *Escherichia coli* (NC 000913); *Pseudomonas putida* KT2440 (NC 002947); *Gluconacetobacter xylinus* (AB015802); *Pseudomonas fluorescens* SJW25 (AY074776); *Xanthomonas axonopodis* pv. *citrii* (NC_003919). Preliminary sequence data for *Pseudomonas syringae* pv. *tomato* were obtained from The Institute for Genomic Research at http://www.tigr.org, for *Burkholderia fungorum* LB400 and *Ralstonia metallidurans* CH34 from the DOE Joint Genome Institute at http://www.jgi.doe.gov/JGI_microbial/html/index.html, for *Burkholderia cenocepacia* J2315, *Salmonella bongori* and *Yersinia enterocolitica* 0:8 from the Sanger center at http://www.sanger.ac.uk/Projects/Microbes/ and for *Klebsiella pneumoniae* from the University of Washington at http://genome.wustl.edu/projects/bacterial/

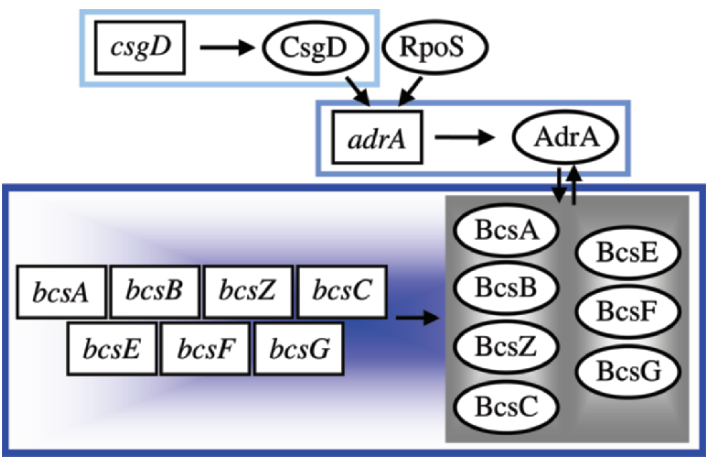

Figure 7-4. (**a**) The cellulose biosynthesis module with regulatory units. Cellulose biosynthesis is activated by the direct or indirect interaction of the AdrA protein with gene products from the *bcs* operons. Transcription of *adrA* is conducted by CsgD together with the second principal sigma factor in stationary phase, RpoS.

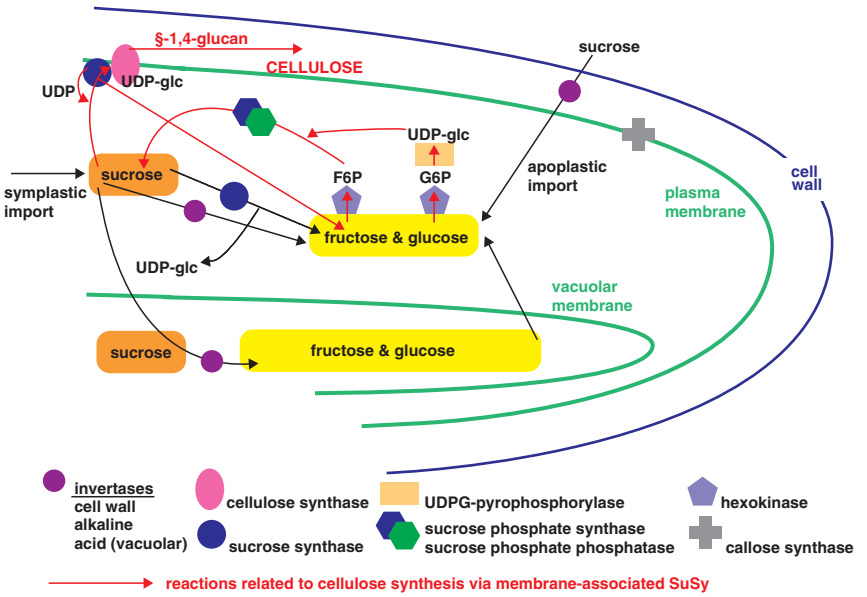

Figure 9-1. Diagram of key enzymes, metabolites, and pathways associated with cellulose synthesis in secondary wall stage cotton fibers. (Figure 10 from: Haigler et al. 2001. Carbon partitioning to cellulose synthesis. Plant Mol Biol 47:29–51. Reproduced with kind permission from Springer Science and Business Media.)

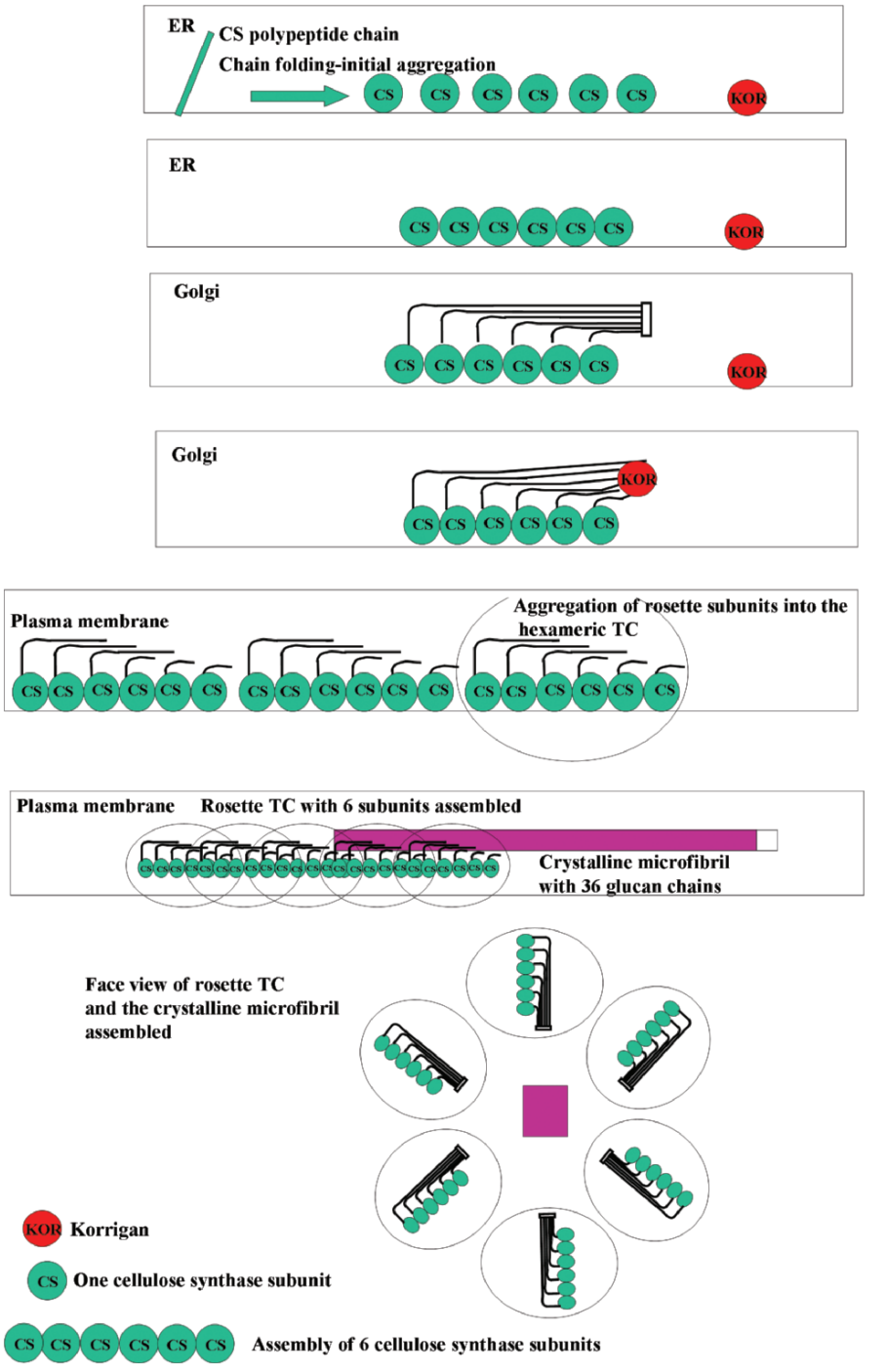
ER
CS polypeptide chain
Chain folding-initial aggregation
CS
KOR
ER
Golgi
Plasma membrane
Aggregation of rosette subunits into the hexameric TC
Plasma membrane
Rosette TC with 6 subunits assembled
Crystalline microfibril with 36 glucan chains
Face view of rosette TC and the crystalline microfibril assembled
KOR Korrigan
CS One cellulose synthase subunit
Assembly of 6 cellulose synthase subunits

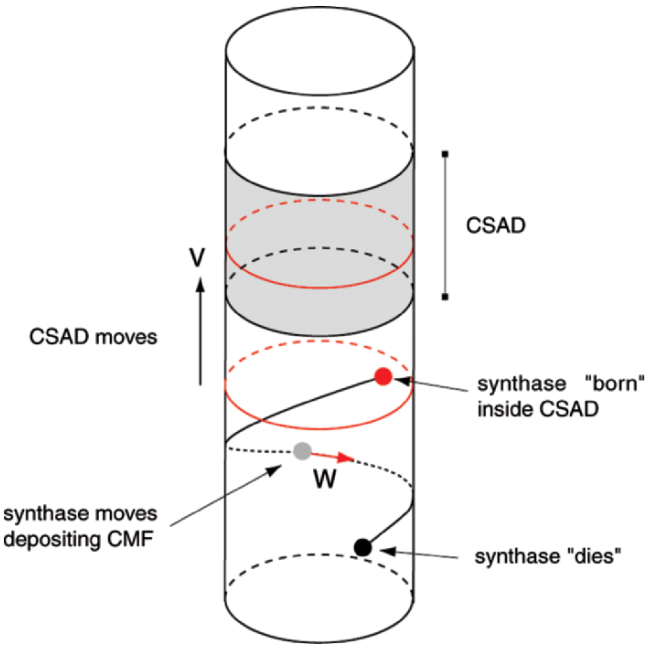

Figure 11-1. The cellulose synthase life cycle. After being inserted into the plasma membrane within a cellulose synthase activation domain (CSAD: located between the red circles at the time of deposition) the synthase moves with an average speed w within the plasma membrane, leaving a cellulose microfibril in its wake. The direction of motion and hence the angle the deposited CMF makes with the cell axis is determined by the local density of other synthases. The CMF synthase becomes inactive after a characteristic lifetime $t^{\dagger}$, which determines the length of the microfibrils. The CSAD itself, here shown in grey, moves with a speed v in the direction opposite to that of the CMF synthases

Figure 10-1. Two-step assembly of the rosette terminal complex (TC) in plants. In the first stage, a cellulose synthase particle complex containing six cellulose synthase molecules is assembled in the ER by protein–protein interactions. Single rosette particles synthesize glucan chains that will stay attached as noncrystalline cellulose in the ER and other intracellular compartments. KOR is also synthesized in the ER and it may be transported from the Golgi apparatus in vesicles with or without the rosette particles. The vesicles carrying the rosette particles and/or KOR may be directed to sites of cellulose synthesis by the microtubules. Once the vesicles carrying the cellulose synthases and KOR fuse with the plasma membrane and the rosette particles are present in the plasma membrane, KOR is able to digest the noncrystalline cellulose. In the second stage, the assembly of the individual rosette particles into a hexameric rosette TC structure is favored by the assembly of glucan chains into a crystalline cellulose product. KOR can also digest the noncrystalline cellulose while in the Golgi apparatus, and under these circumstances assembly of the rosette can take place in the Golgi apparatus itself. KOR does not digest crystalline cellulose. The assembled rosette TC continues to synthesize cellulose microfibril and the movement of the cellulose synthase in the plasma membrane is governed by the rate of cellulose synthesis. The rosette particles, KOR, and in some cases even the rosette TC may be recycled from the plasma membrane

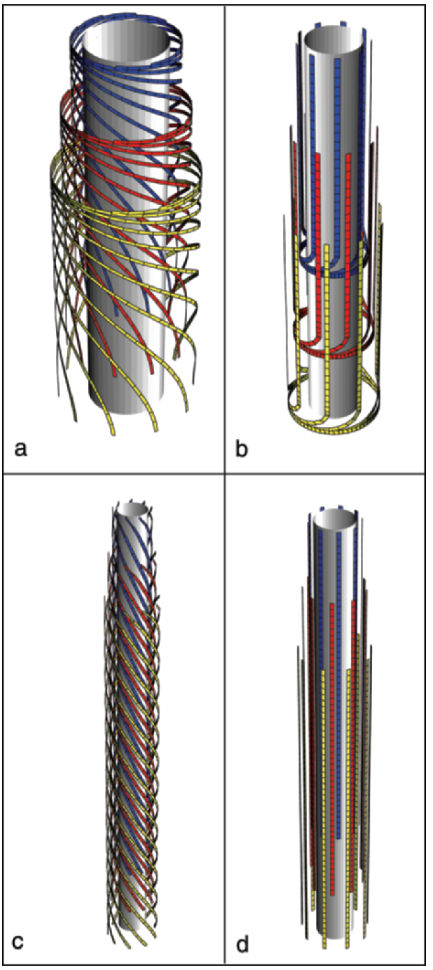

Figure 11-2. Different cell wall textures as predicted by the geometrical model. The ribbons shown represent the tracks of CMFs, obtained from the explicit solutions to the CMF evolution equation. (**a**) The helicoidal texture in which the angle of orientation between subsequent lamellae changes by a constant amount. (**b**) A crossed polylamellate texture with alternate lamellae with transverse and axial oriented CMFs. (**c**) A purely axial texture. (**d**) A helical texture in which the CMFs have an almost constant winding angle

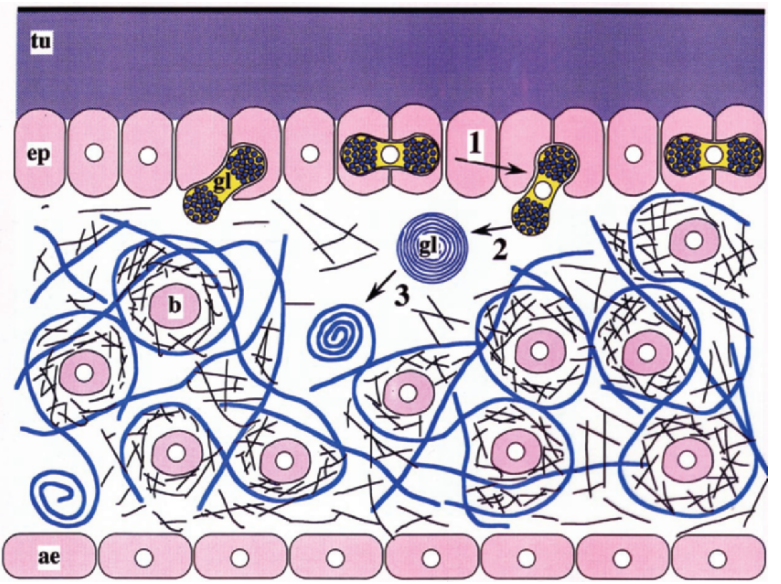

Figure 13-7. A schematic illustration showing the step-wise involvement of glomerulocytes in the formation of a cellulose network in the hemocoel: (**1**) glomerulocytes are transferred into hemocoel; (**2**) bundles of cellulose skeleton are released in the hemocoel; (**3**) cellulose microfibrils of the skeleton are untied to make cellulose network. Tu = tunic, ep = epidermis, gl = glomerulocyte, ae =atrial epitherium, b = blood cell

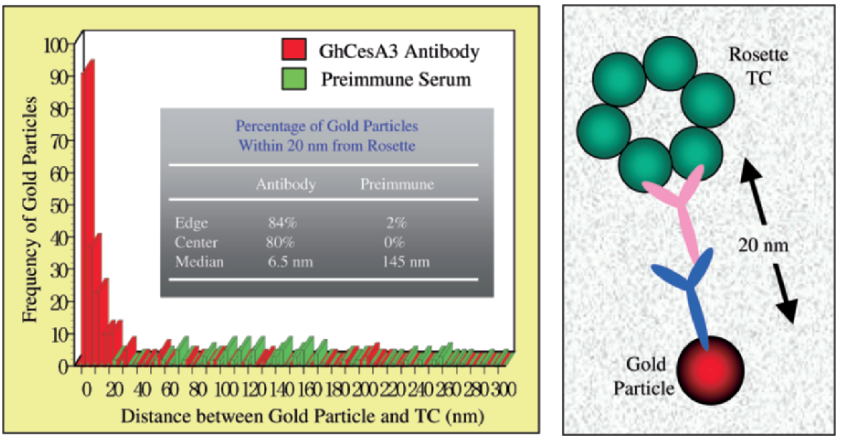

Figure 14-6. Frequency distributions of the number of gold particles associated with the immune serum containing antibodies to cellulose synthase and the preimmune control serum as a function of the measured distance to the center and the edge of the nearest rosette TC (*left*). Schematic diagram for the measurement of the distance between gold particles and rosette TC (*right*) is also shown (green:rosette, pink:primary antibody to cellulose synthase, blue:secondary antibody, red: gold particle the 93 kDa antibody-labeled particles. (**a**) Schematic diagram for the measurement of the distance between gold particles and linear TCs. The distance (double arrowheads) between the edge of gold particles and the linear TCs is indicated by the dotted line. (**b**) Frequency distribution of the number of gold particles associated with the 93 kDa protein antibody is shown as a function of the measured distance (nanometers) to the linear TC. Total number of gold particles measured was 277, taken from 30 different cells

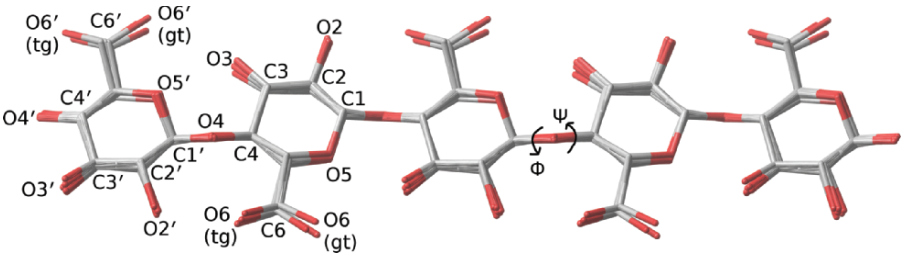

Figure 15-1. The six different chain shapes from the crystal structures of the cellulose polymorphs I, II, and III_I, superimposed at their C1, O4, and C4 atoms to show the differences in the molecular shapes. Indicated for the five-residue segments are the linkage torsion angles, N and P. There are two unique chains in both the Iβ and II structures (with O6 tg) and one each from Iα and III_I (with O6 *gt*). The single-chain Iα structure has two sets of N and P values because of its lower symmetry. Atomic numbering is indicated; the reducing end is to the right and the nonreducing end is on the left

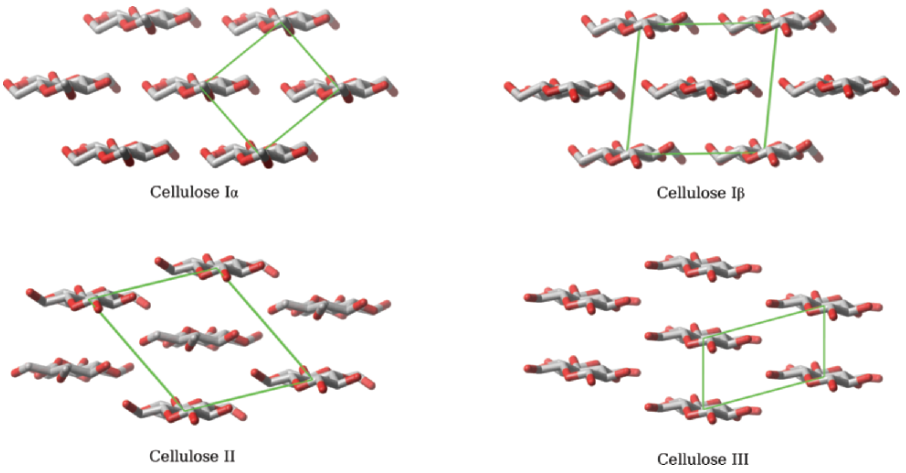

Figure 15-2. Views of the chain packing perpendicular to the molecular axes for cellulose Iα, Iβ, II, and III_I. The unit cells and seven chains are shown for each. Hydrogen atoms are not shown. The unit cells show the relationships of four chains and contain fractions of them; two-chain cells have an additional chain within their boundaries

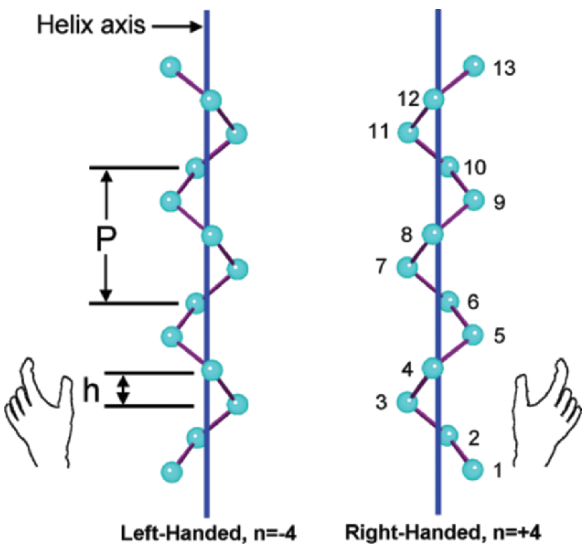

Figure 15-3. Schematic left- and right-handed helices with four monomeric units per turn and 13 units altogether in each. The pitch, P, of the helix is indicated, as is the rise per residue along the helix axis, *h*

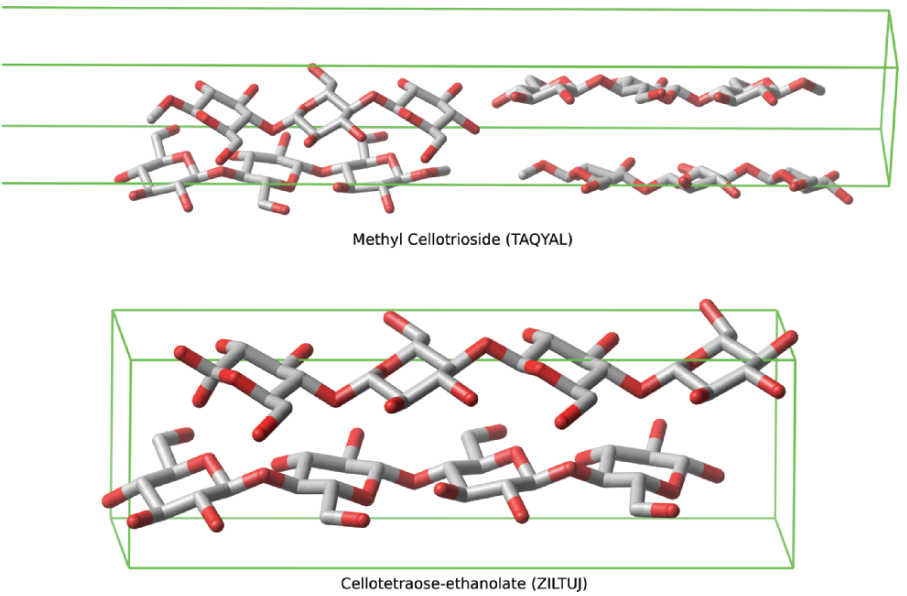

Figure 15-4. Views of the methyl cellotrioside (Raymond et al. 1995) and cellotetraose-ethanolate (Gessler et al. 1995) crystal structures. There are four unique cellotrioside molecules, with eight values of N and P. Cellotetraose crystals contain two unique molecules, and have six values of N and P. Only half of the trioside unit cell is shown. TAQYAL and ZILTUJ are the Cambridge Structural Database "refcodes" for these structures

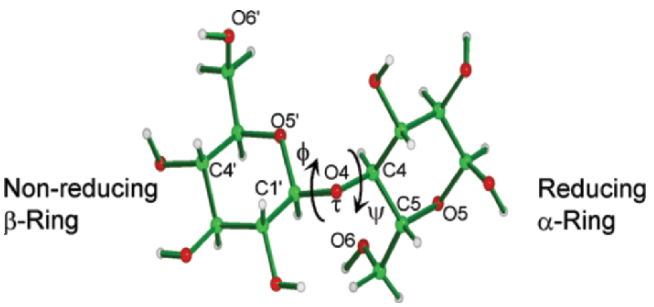

Figure 15-5. The α-cellobiose disaccharide with the geometry found in the crystal structure of the hydrated NaI complex (Peralta-Inga et al. 2002). The O6 and O6′ atoms are in *gg* positions. No intramolecular hydrogen bonds are formed in this structure

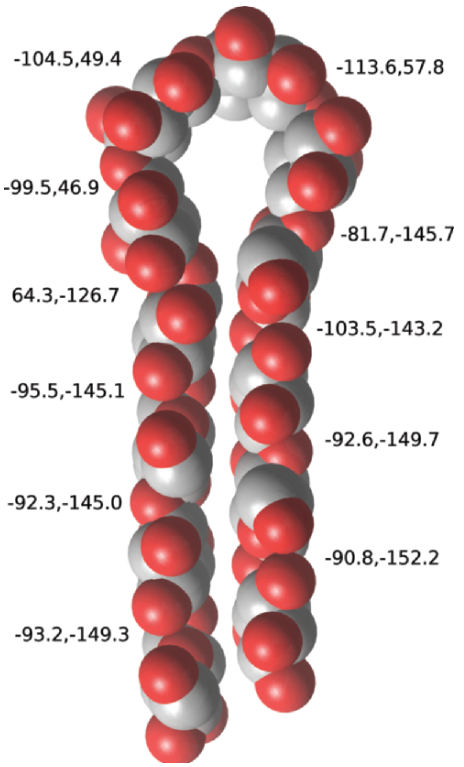

Figure 15-7. Drawing of a cellulose chain segment in a folding conformation. The N and P values are indicated. This bend was energy minimized with MM3. The lower portions retain the linkage geometries of crystalline cellotetraose (Gessler et al. 1995)

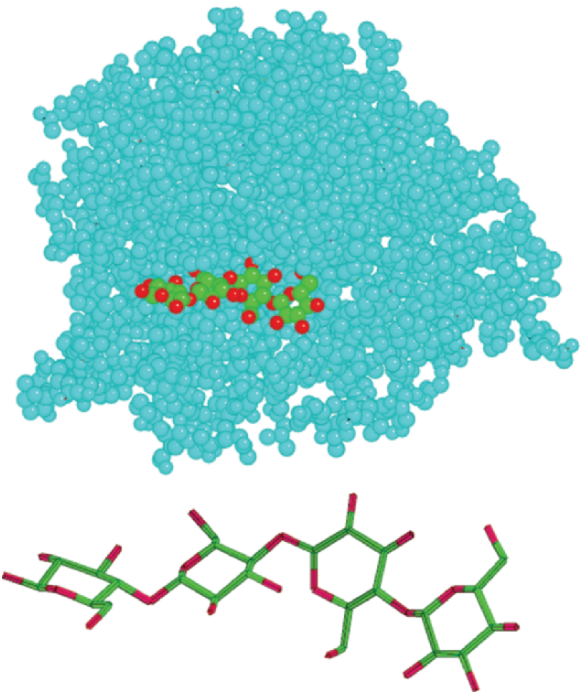

Figure 15-10. A cellotetraose fragment complexed with one of the two halves of an endoglucanase, 1ECE, plotted from the coordinates in the Protein Databank. Also shown is a stick representation of the tetraose without the surrounding protein. Two of its linkages have a twofold conformation, but the central linkage corresponds to a threefold helix with $h < 5$ Å, an unusual conformation

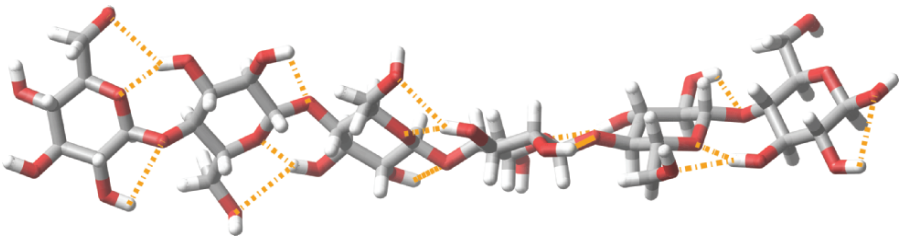

Figure 15-16. A cellulose segment with the lowest energy, as indicated by the combined information from the crystal structure surveys and the point of minimum energy on the QM::MM3 hybrid energy surface

Figure 17-1. Application of a large size MC dressing on a second-degree burn

Figure 17-2. A second-degree A/B burn of both forearms. MC dressing applied on the wound (**a**); MC dressing dried on the wound in the second day of the treatment; left hand has been treated with the control technique (**b**); dry MC dressing removed from the wound after 4 days of treatment revealed a clean area with a fully regenerated epidermis underneath; left forearm treated with control procedure displayed presence of necrotic tissues (**c**); wound after 3 weeks upon burning shows a complete re-epithelialization on the healed right forearm whereas on the left forearm granulation tissues have just been formed (**d**)

Figure 17-3. A deep second-degree facial burn caused by the exposure to flame (**a**); a highly conformable mask of the MC dressing with holes on eyes, nose, and mouth was tightly applied on the wounded face (**b**); the epithelialization in the regions of wound edges and from the deep epidermal appendages has been clearly observed at 17 days upon burning (**c**); the entirely healed face after next 28 days (**d**); examination after about 20 months upon burning showed the shallow, nonhypertrophic scar tissues on the facial surface where third-degree burn occurred (*front*) (**e**); and the lack of tissue fragments on the right ear (**f**)

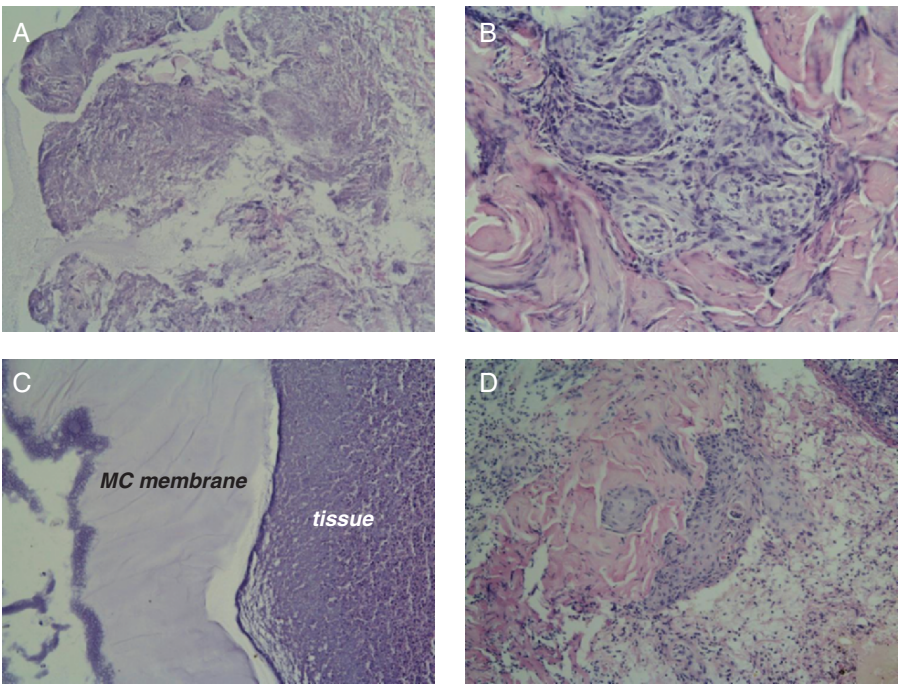

Figure 17-4. Photomicrographs of a biopsy specimen from a wound treated with MC dressing. (**a**) Necrosis of wound tissues; (**b**) growth of granulation tissue and keratinocytes from the appendages of skin (fifth day of treatment with MC dressing); (**c**) fragment of MC dressing tightly adhered to the wound tissue (fifth day of treatment with MC dressing); and (**d**) a fresh epidermis growing in the wound after 10 days of treatment with MC dressing

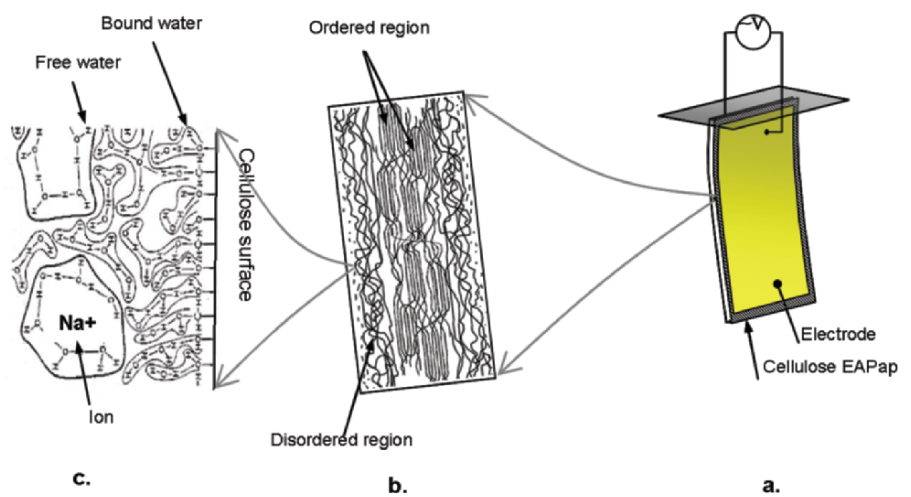

Figure 18-1. Configuration of EAPap bending actuator

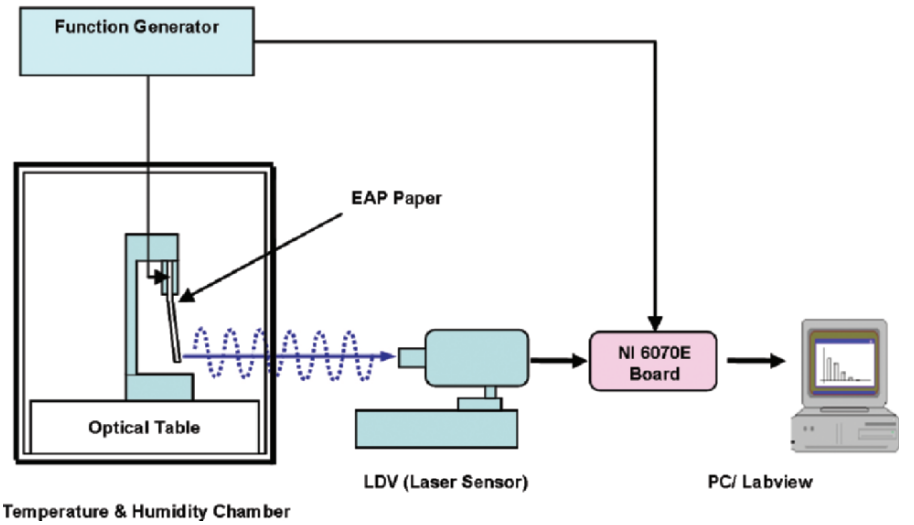

Figure 18-4 .Tip displacement measurement setup

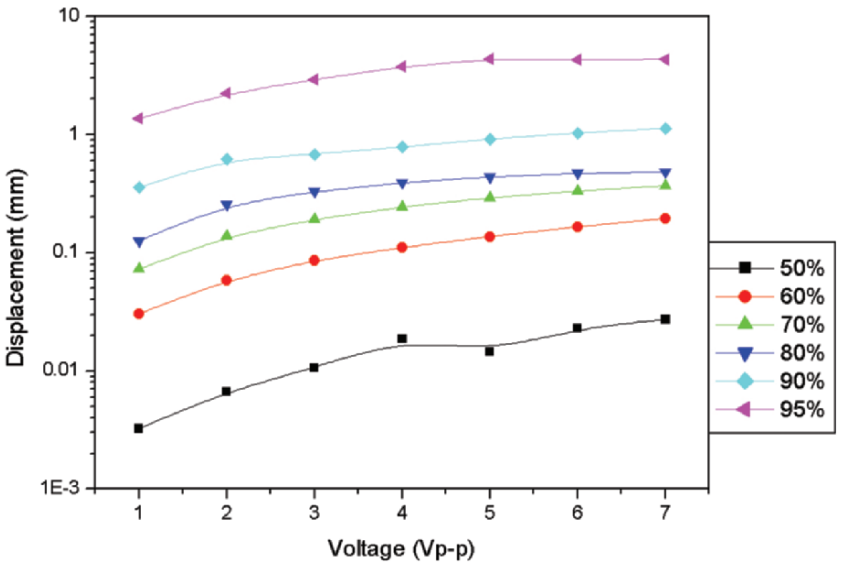

Figure 18-5. Tip displacement of cellophane EAPap actuator with voltage and relative humidity.

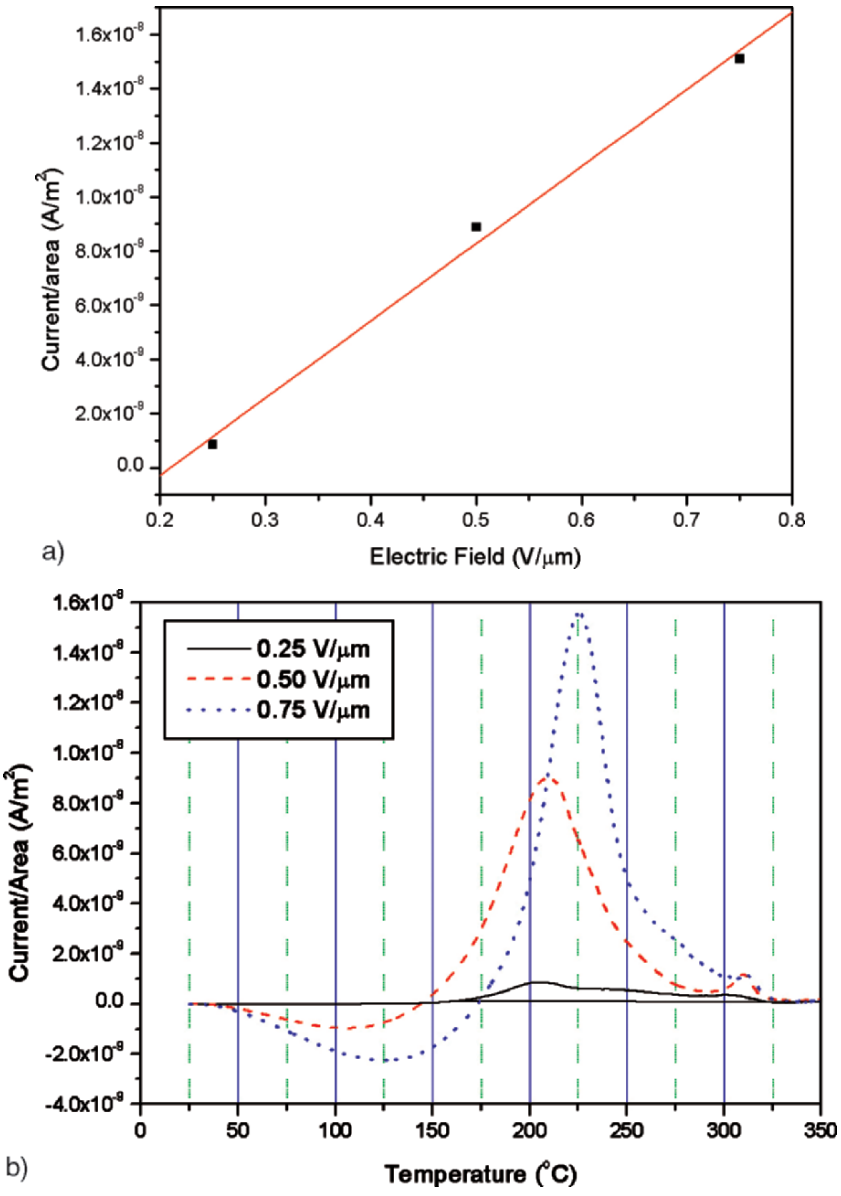

Figure 18-6. TSC results of cellulose EAPap. (**a**) The depolarized current with temperature and different poling electric field. (**b**) The peak current values as a function of the poling electric field

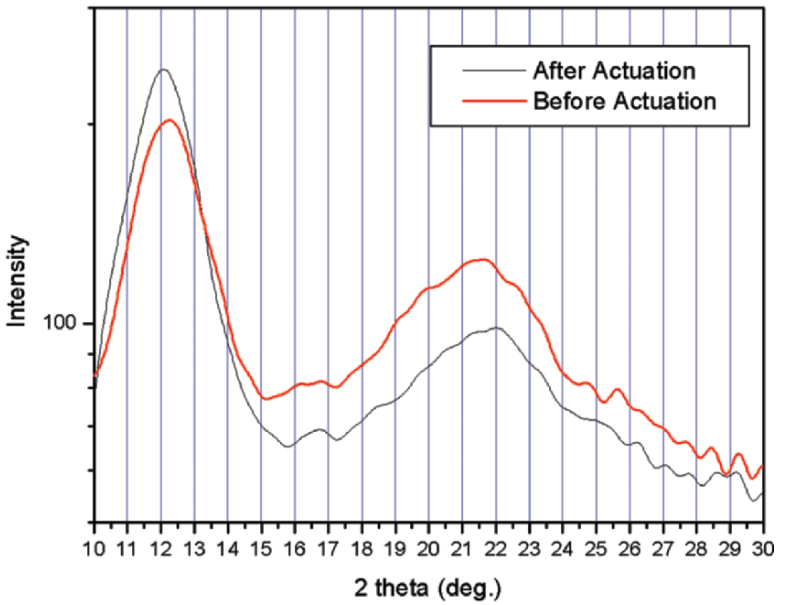

Figure 18-7. XRD of EAPap samples before and after the actuation tests

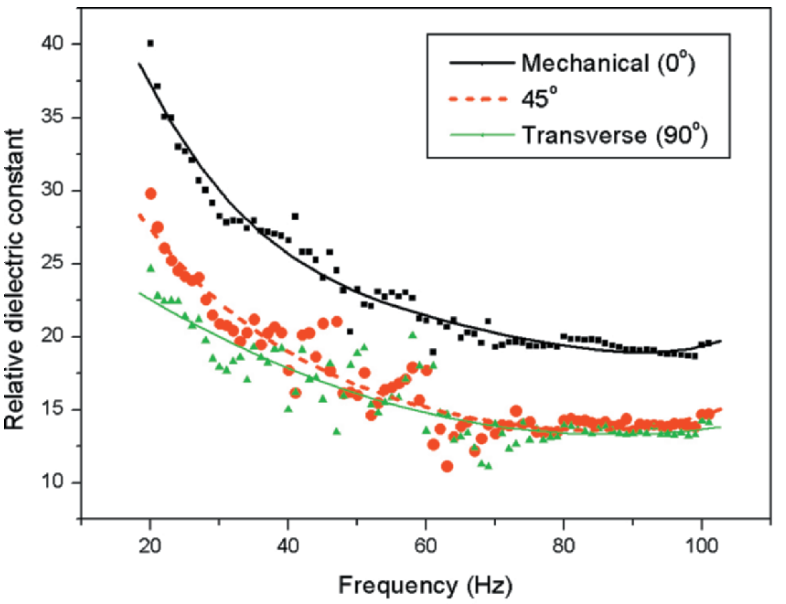

Figure 18-8. Dielectric constant test results

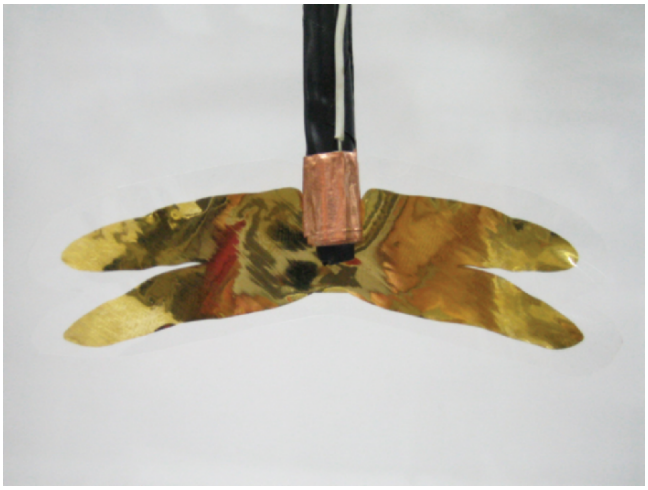

Figure 18-9. Photograph of EAPap actuator

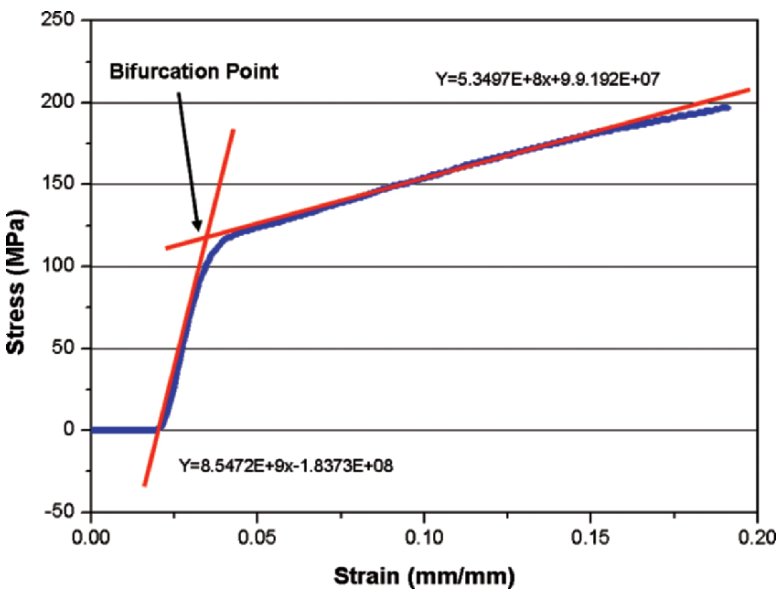

Figure 18-10. Pull test result of cellulose based EAPap

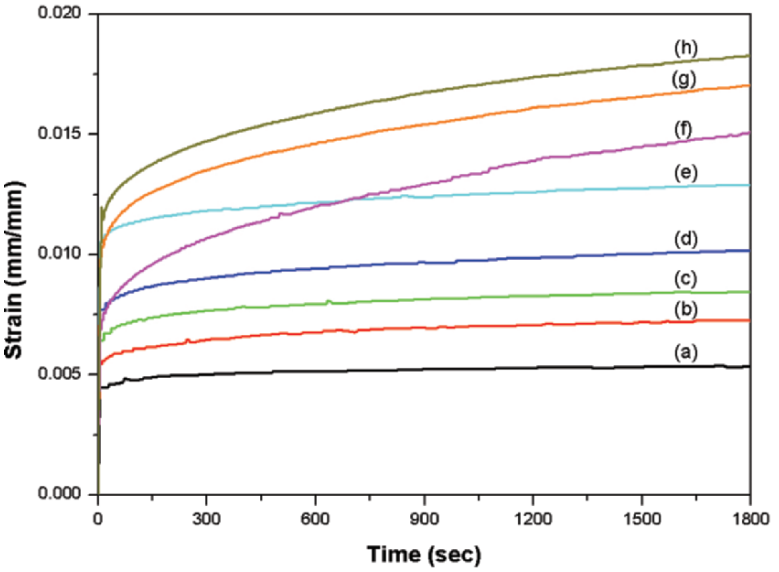

Figure 18-11. Strain response under the constant stress. (**a**) 10 MPa, (**b**) 15 MPa, (**c**) 20 MPa, (**d**) 22.5 MPa (**e**) 25 MPa, (**f**) 27.5 MPa, (**g**) 30 MPa, and (**h**) 32.5 MPa

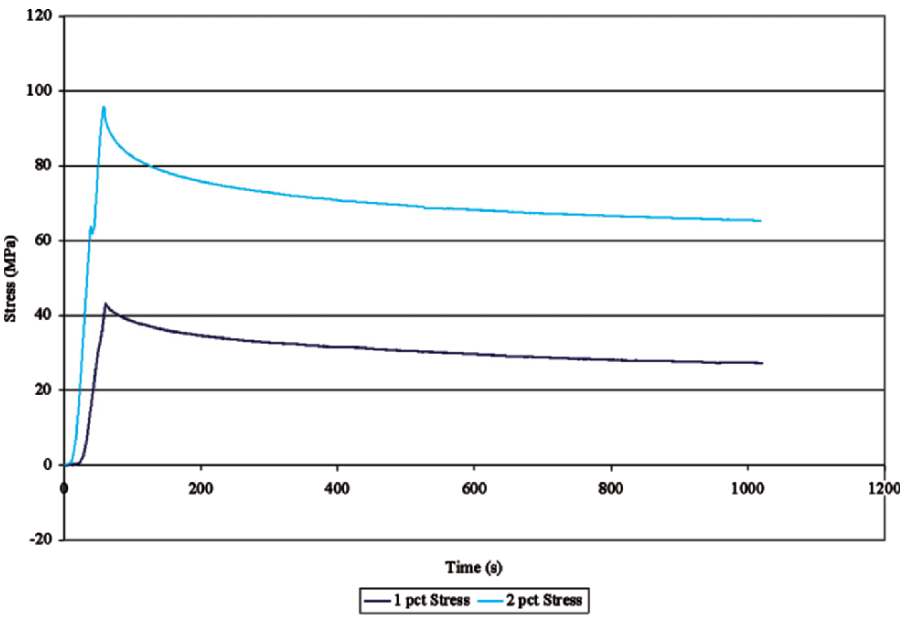

Figure 18-12. Stress response under the constant strain: 1% and 2% strains

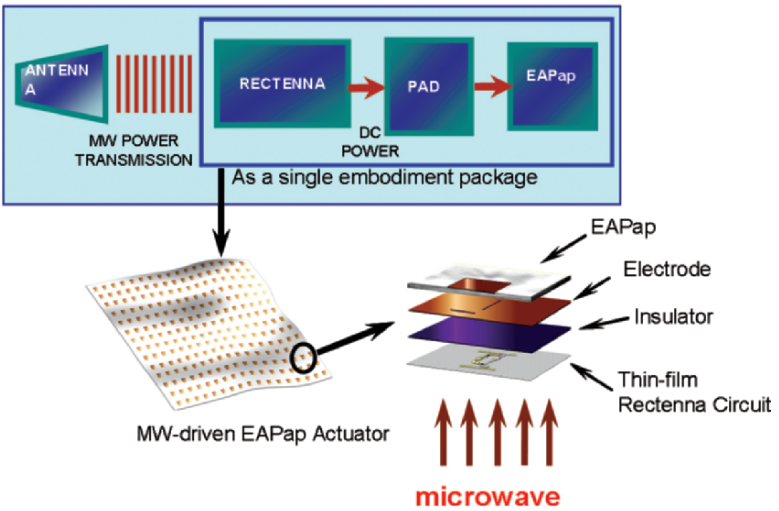

Figure 18-13. Concept of microwave-driven EAPap actuator

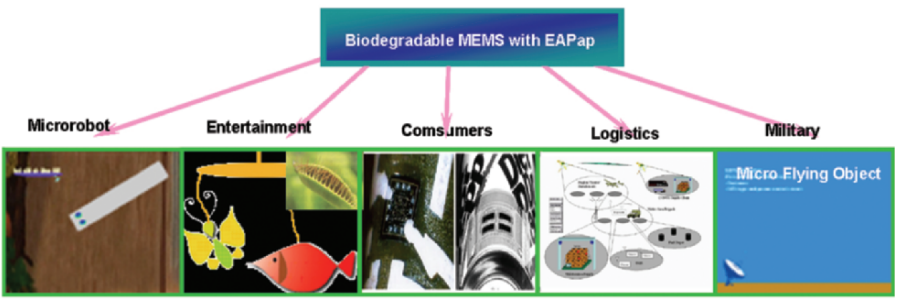

Figure 18-14. Applications of microwave-driven EAPap actuators